CELL BIOLOGY, PHYSIOLOGY AND MOLECULAR PHARMACOLOGY OF G PROTEIN COUPLED RECEPTORS

EDITED BY: Sameer Mohammad, Muheeb Beg and Manveen Kaur Gupta
PUBLISHED IN: Frontiers in Cell and Developmental Biology

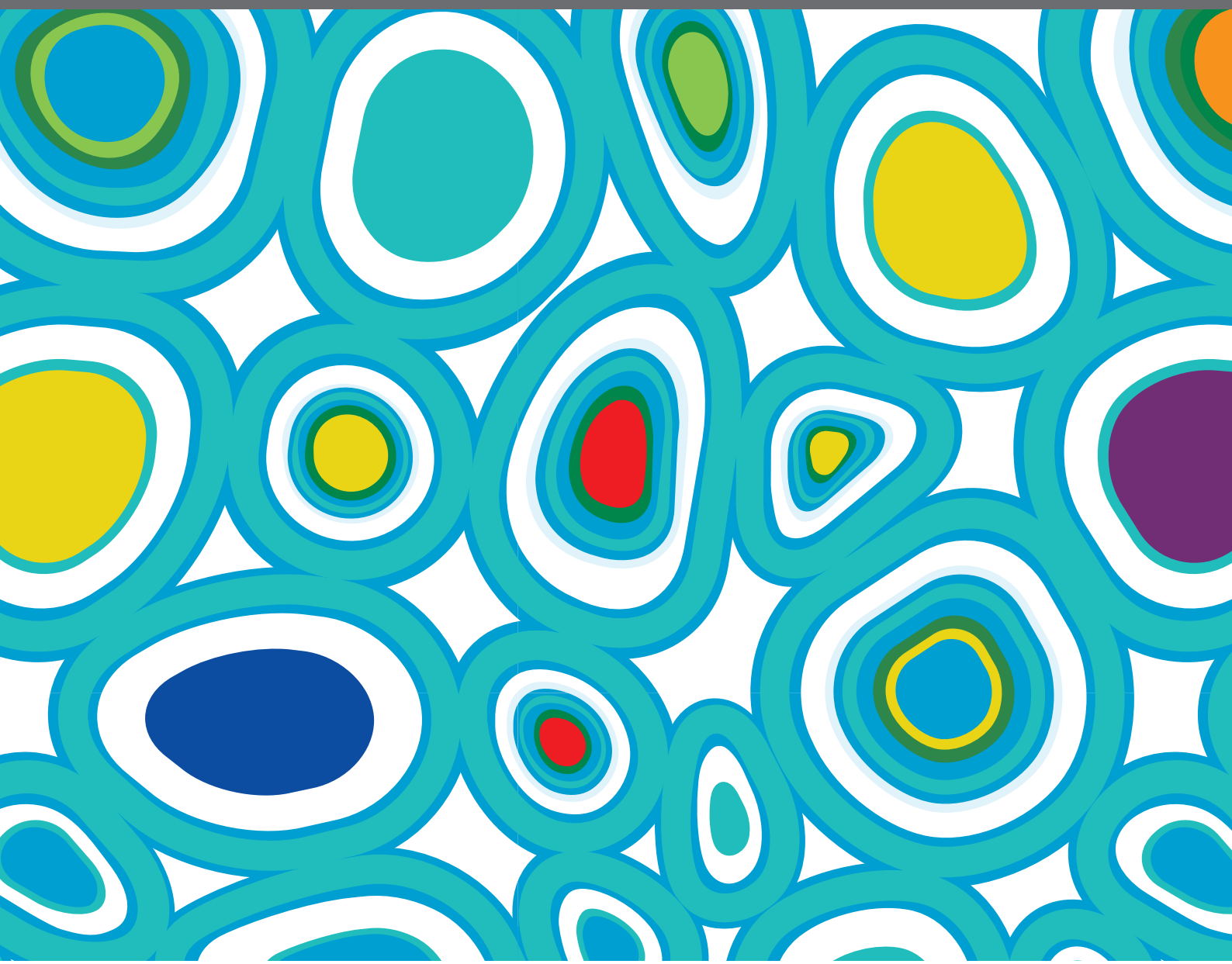

frontiers Research Topics

ISSN 1664-8714
ISBN 978-2-88974-213-4
DOI 10.3389/978-2-88974-213-4

About Frontiers

Frontiers is more than just an open-access publisher of scholarly articles: it is a pioneering approach to the world of academia, radically improving the way scholarly research is managed. The grand vision of Frontiers is a world where all people have an equal opportunity to seek, share and generate knowledge. Frontiers provides immediate and permanent online open access to all its publications, but this alone is not enough to realize our grand goals.

Frontiers Journal Series

The Frontiers Journal Series is a multi-tier and interdisciplinary set of open-access, online journals, promising a paradigm shift from the current review, selection and dissemination processes in academic publishing. All Frontiers journals are driven by researchers for researchers; therefore, they constitute a service to the scholarly community. At the same time, the Frontiers Journal Series operates on a revolutionary invention, the tiered publishing system, initially addressing specific communities of scholars, and gradually climbing up to broader public understanding, thus serving the interests of the lay society, too.

Dedication to Quality

Each Frontiers article is a landmark of the highest quality, thanks to genuinely collaborative interactions between authors and review editors, who include some of the world's best academicians. Research must be certified by peers before entering a stream of knowledge that may eventually reach the public - and shape society; therefore, Frontiers only applies the most rigorous and unbiased reviews.
Frontiers revolutionizes research publishing by freely delivering the most outstanding research, evaluated with no bias from both the academic and social point of view. By applying the most advanced information technologies, Frontiers is catapulting scholarly publishing into a new generation.

What are Frontiers Research Topics?

Frontiers Research Topics are very popular trademarks of the Frontiers Journals Series: they are collections of at least ten articles, all centered on a particular subject. With their unique mix of varied contributions from Original Research to Review Articles, Frontiers Research Topics unify the most influential researchers, the latest key findings and historical advances in a hot research area! Find out more on how to host your own Frontiers Research Topic or contribute to one as an author by contacting the Frontiers Editorial Office: frontiersin.org/about/contact

CELL BIOLOGY, PHYSIOLOGY AND MOLECULAR PHARMACOLOGY OF G PROTEIN COUPLED RECEPTORS

Topic Editors:
Sameer Mohammad, King Abdullah International Medical Research Center, Saudi Arabia
Muheeb Beg, University of Gothenburg, Sweden
Manveen Kaur Gupta, Case Western Reserve University, United States

Citation: Mohammad, S., Beg, M., Gupta, M. K., eds. (2022). Cell Biology, Physiology and Molecular Pharmacology of G Protein Coupled Receptors. Lausanne: Frontiers Media SA. doi: 10.3389/978-2-88974-213-4

Table of Contents

frontiers in Cell and Developmental Biology

EDITORIAL
published: 09 December 2021
doi: 10.3389/fcell.2021.815291

Editorial: Cell Biology, Physiology and Molecular Pharmacology of G Protein Coupled Receptors

Manveen Kaur Gupta[1], *Muheeb Beg*[2] *and Sameer Mohammad*[3]*

[1]Cardiovascular and Metabolic Sciences, Lerner Research Institute, Cleveland Clinic & Case Western Reserve University, Cleveland, OHIO, United States, [2]Department of Medical Biochemistry and Cell Biology, Institute of Biomedicine, Sahlgrenska Academy, University of Gothenburg, Gothenburg, Sweden, [3]Experimental Medicine, King Abdullah International Medical Research Center (KAIMRC), King Saud Bin Abdulaziz University for Health Sciences (KSAU-HS), Ministry of National Guard Health Affairs (NGHA), Riyadh, Saudi Arabia

Keywords: GPCR (G protein coupled receptor), adrenergic receptor (AR), GPCR drug discovery, GRK (G protein receptor kinase), Incretin – Based therapy

Editorial on the Research Topic

Cell Biology, Physiology and Molecular Pharmacology of G protein Coupled Receptors

G protein-coupled receptors (GPCRs) are the largest family of cell-surface proteins. They are characterized by seven transmembrane domains; a cytoplasmic C-terminus, and an extracellular N-terminal domain. GPCRs respond to a wide variety of signaling molecules and signal through the trimeric G-protein complex. GPCRs are expressed essentially on all cells, facilitating cellular responses to external stimuli and are involved in nearly every biological process (Pierce et al., 2002; Strange, 2008; Hanyaloglu and Grammatopoulos, 2017; Pavlos and Friedman, 2017; Wang et al., 2018). There are ~800 members of the GPCR family, of them more than 400 are sensory receptors (olfactory, vision, and taste receptors (Alexander et al., 2019). The remaining ~350 are non-sensory receptors and are activated by physical ligands, which include peptide hormones, large polypeptides, amino acids and small metabolites, free fatty acids and many others (Okuno et al., 2006; Mohammad, 2015; Wolf and Grünewald, 2015; Husted et al., 2017; Al Mahri et al., 2020; Davenport et al., 2020). Based on sequence homology, GPCRs are divided into different families: Class A (rhodopsin), Class B (secretin, adhesion), Class C (Glutamate), and frizzled receptors (Alexander et al., 2019). Most of these receptors have a known physical ligand, which activates the receptor to elicit the signaling cascade and the downstream effect on physiological function. GPCRs are substantially involved in human pathophysiology and are pharmacologically tractable, making them the most intensely studied drug targets. Nearly one-third of all drugs approved by the US Food and Drug administration involve GPCR target sites. In addition, several GPCR based drugs are currently undergoing clinical trials (Nieto Gutierrez and McDonald, 2018; Sriram and Insel, 2018). However, only about 100 GPCRs have been extensively studied and successfully targeted while the functional relevance of a significant number of GPCRs remains to be studied. Therefore, intense efforts are on to expansively study the rest of the members of the GPCR family to unearth additional therapeutic possibilities.

This research topic comprises of research papers and review articles on diverse GPCRs and their regulators. The collection of articles highlights the role of GPCRs in physiology, pathophysiology, and explores the possibility of exploiting their therapeutic potential. Perez (2021) reviews current developments on the role of α1-Adrenergic Receptors (α1-ARs) in cognition, cardioprotection, and metabolism. α1-ARs belong to the family of adrenergic receptors and have been extensively studied for their role in blood pressure regulation, cardiac hypertrophy, and muscle contraction. α1-ARs are

OPEN ACCESS

Edited and reviewed by:
Ana Cuenda,
Spanish National Research Council (CSIC), Spain

***Correspondence:**
Sameer Mohammad
mohammadsa1@ngha.med.sa

Specialty section:
This article was submitted to Signaling, a section of the journal Frontiers in Cell and Developmental Biology

Received: *15 November 2021*
Accepted: *18 November 2021*
Published: *09 December 2021*

Citation:
Gupta MK, Beg M and Mohammad S (2021) Editorial: Cell Biology, Physiology and Molecular Pharmacology of G Protein Coupled Receptors. Front. Cell Dev. Biol. 9:815291. doi: 10.3389/fcell.2021.815291

also highly expressed in the cognitive centers of the brain and their activation has a profound effect on learning and memory function. The review highlights the potential of α1A-AR agonists or positive allosteric modulators to treat Alzheimer's disease and to protect the heart at the same time.

Lin et al. (2021) in their paper demonstrate the role of Adenosine Receptor (AdoR) signaling and its downstream targets in *Drosophila*. They demonstrate that AdoR signaling represents an important pathway in response to stress conditions such as cytotoxicity, oxidative damage, and thermal stress in *Drosophila*. The paper provides important insights into the molecular mechanism of Ado regulation of stress response that could help understand how Ado signaling affects disease pathogenesis.

An interesting paper by Chou et al. (2021) shows how G-Protein-Coupled Estrogen Receptor-1 (GPER-1) positively regulates chondrocyte proliferation at the growth plate during early puberty and contributes to the longitudinal growth of long bones. GPER-1 is widely expressed in both mouse and human tissues including bone and cartilage. Interestingly, during pubertal progression, the expression of GPER-1 shows a significant decrease suggesting its involvement in the modulation of pubertal bone growth. Previous studies have investigated the expression of GPER-1 in bone and cartilage but the functional significance of GPER-1 in bone growth remains unclear. Using chondrocyte-specific GPER-1 knockdown mice, the authors demonstrate that GPER-1 positively regulates chondrocyte proliferation at the growth plate during early puberty and contributes to the longitudinal growth of long bones.

In a comprehensive review (Morrow et al., 2021), critically assess the role of incretin receptors, GIP receptor (GIPR), GLP-1 receptor (GLP-1R), and GLP-2 receptor (GLP-2R) in intestinal physiology. Incretin hormones (GIP and GLP-1) are gut peptides that are released from intestinal L- and K-cells respectively in response to food intake. Once released into the bloodstream, they bind to incretin receptors (GIPR. GLP-1R and GLP-2R) in pancreatic β-cells and enhance insulin releases in a glucose-dependent manner. In subjects with type 2 diabetes, this incretin effect is diminished or no longer present. Therefore, incretin-based therapies have been successfully used in diabetic patients. The authors in this paper highlight the biology and paracrine roles of GLP-1, GIP, and GLP-2 in integrating the response to food intake with the maintenance of the structure and function of the gut as it relates to nutrient absorption. A thought-provoking paper included in this research topic is by Kizilkaya et al. (2021) on incretin receptor GIPR. The authors functionally characterized two missense GIPR variants, R190Q (rs139215588) and E288G (rs143430880) that are associated with lower body mass index (BMI). The authors show that two naturally occurring rare GIPR variants, R190Q and E288G (rs139215588 and rs143430880, respectively), result in impaired GIPR function at the molecular level which in turn seems to impact human physiology and pathophysiology regarding adiposity, bone health, and cardiovascular system. These results indicate that GIPR antagonists could protect from diet-induced obesity and improve glycemic and insulinotropic effects, which is in contrast to other studies that have shown the beneficial effect of GIPR agonists on adipose metabolism. Previous studies show that how a single amino acid substitution in the GIPR receptor (E354Q) leads to enhanced agonist induced desensitization that impairs the ability of the GIP to control adipose insulin sensitivity (Mohammad et al., 2014). The data from these studies add to the interesting debate whether GIPR activation or GIPR inhibition is the right strategy to treat metabolic abnormalities associated with Type-2 diabetes.

It is widely documented that GPCR signaling involves cross-regulation of many pathways including cross-talks between different GPCRs as well as with other signaling pathways. Besides the acute signaling, GPCR, in direct or through crosstalk, also regulate the development of addictive diseases. In this area (Maccioni et al., 2021), in their paper demonstrate that treatment with non-sedative doses of the novel positive-allosteric modulator (PAM) of the GABA-B receptor, KK-92A ([(4-(cycloheptylamino)-5-(4-(trifluoromethyl)phenyl)pyrimidin-2-yl)methanol]) potently and effectively suppressed operant oral alcohol self-administration and cue-induced reinstatement of alcohol-seeking in alcohol-preferring Sp rats. KK-92A has high potency and selectivity for GABA-B. Besides, KK-92A has high bioavailability in the brain and a remarkable *in vivo* efficacy. The data from this study add to the earlier experimental data on the ability of KK-92A to reduce nicotine self-administration and cue-induced reinstatement of nicotine seeking in rats and therefore, broadening the anti-addictive profile of KK-92A.

Matthees et al. (2021) elucidate the role of GPCR Kinases (GRKs) in the regulation of GPCR signaling. GRKs and β-arrestins interact with activated GPCRs and regulate their intracellular trafficking. The authors discuss how the expression levels of GRKs, arrestins, and GPCRs play a crucial role in the development of pathological conditions. They analyzed expression data for GRKs and β-arrestins in 61 tissues annotated in the Human Protein Atlas and presented their analysis in the context of pathophysiological dysregulation of the GPCR/GRK/β-arrestin system. This tissue-specific point of view might be the key to unraveling the individual impact of different GRK isoforms on GPCR regulation.

The review by Tian et al. (2020) highlights recent progress regarding the critical components of the JAK2-STAT5 pathway and its crosstalk with G-protein coupled receptor (GPCR) signaling. Hormones are crucial for ductal morphogenesis in the mammary gland. During puberty, estrogen, growth hormone (GH), and prolactin are required for the development of the mammary gland. GH and prolactin regulate mammary gland function through the phosphorylation of Janus kinase 2 (JAK2) and activation of its downstream regulator signal transducers and activators of transcription 5 (STAT5). The authors evaluate recent data to demonstrate that GPCR activation has a profound impact on the JAK2-STAT5 signaling pathway.

Finally (Li et al., 2021), describe Identification and Functional Analysis of G Protein-Coupled Receptors in steroid hormone, 20-Hydroxyecdysone (20E) signaling from the Helicoverpa armigera Genome. The authors show that 20-hydroxyecdysone signals through multiple GPCRs including prolactin-releasing peptide receptor (PRRPR), smoothened (SMO), adipokinetic hormone receptor (AKHR), 5-hydroxytryptamine receptor (HTR),

Frizzled 7 (FZD7), and tachykinin-like peptides receptor 86C (TKR86C) to regulate growth and development of Helicoverpa armigera.

CONCLUSION

In conclusion, the research topic contains a fascinating collection of original research papers and review articles encompassing cell biology, physiology, and molecular pharmacology of G-protein coupled receptors. We hope that the data and information conveyed through this research topic will be beneficial to the scientific community in general and researchers in this exciting research area, in particular. We believe the research ideas presented will push more studies to further understand the physiological significance of GPCRs and unearth additional therapeutic possibilities.

AUTHOR CONTRIBUTIONS

All authors listed have made a substantial, direct, and intellectual contribution to the work and approved it for publication. SM, MKG and MB wrote, edited and finalized the paper.

FUNDING

The work was supported by King Abdullah International Medical Research Center (Grant # RC20/385 to SM).

ACKNOWLEDGMENTS

We thank all authors and reviewers for their contribution to the Research Topic.

REFERENCES

Alexander, S. P. H., Christopoulos, A., Davenport, A. P., Kelly, E., Mathie, A., Peters, J. A., et al. (2019). The Concise Guide to Pharmacology 2019/20: G Protein-Coupled Receptors. *Br. J. Pharmacol.* 176, S21–S141. doi:10.1111/bph.14748

Chou, Y.-S., Chuang, S.-C., Chen, C.-H., Ho, M.-L., and Chang, J.-K. (2021). G-Protein-Coupled Estrogen Receptor-1 Positively Regulates the Growth Plate Chondrocyte Proliferation in Female Pubertal Mice. *Front. Cel Dev. Biol.* 9, 710664. doi:10.3389/fcell.2021.710664

Davenport, A. P., Scully, C. C. G., de Graaf, C., Brown, A. J. H., and Maguire, J. J. (2020). Advances in Therapeutic Peptides Targeting G Protein-Coupled Receptors. *Nat. Rev. Drug Discov.* 19, 389–413. doi:10.1038/s41573-020-0062-z

Hanyaloglu, A. C., and Grammatopoulos, D. K. (2017). Pleiotropic GPCR Signaling in Health and Disease. *Mol. Cell Endocrinol.* 449, 1–2. doi:10.1016/j.mce.2017.05.013

Husted, A. S., Trauelsen, M., Rudenko, O., Hjorth, S. A., and Schwartz, T. W. (2017). GPCR-mediated Signaling of Metabolites. *Cel Metab.* 25, 777–796. doi:10.1016/j.cmet.2017.03.008

Kizilkaya, H. S., Sørensen, K. V., Kibsgaard, C. J., Gasbjerg, L. S., Hauser, A. S., Sparre-Ulrich, A., et al. (2021). Loss of Function Glucose-dependent Insulinotropic Polypeptide Receptor Variants Are Associated with Alterations in BMI, Bone Strength and Cardiovascular Outcomes. *Front. Cel Dev. Biol.* 9, 749607. doi:10.3389/fcell.2021.749607

Li, Y.-L., Li, Y.-X., Wang, X.-P., Kang, X.-L., Guo, K.-Q., Dong, D.-J., et al. (2021). Identification and Functional Analysis of G Protein-Coupled Receptors in 20-Hydroxyecdysone Signaling from the Helicoverpa Armigera Genome. *Front. Cel Dev. Biol.* 9, 753787. doi:10.3389/fcell.2021.753787

Lin, Y.-H., Maaroufi, H. O., Kucerova, L., Rouhova, L., Filip, T., and Zurovec, M. (2021). Adenosine Receptor and its Downstream Targets, Mod(mdg4) and Hsp70, Work as a Signaling Pathway Modulating Cytotoxic Damage in Drosophila. *Front. Cel Dev. Biol.* 9, 651367. doi:10.3389/fcell.2021.651367

Maccioni, P., Kaczanowska, K., Lawrence, H., Yun, S., Bratzu, J., Gessa, G. L., et al. (2021). The Novel Positive Allosteric Modulator of the GABAB Receptor, KK-92A, Suppresses Alcohol Self-Administration and Cue-Induced Reinstatement of Alcohol Seeking in Rats. *Front. Cel Dev. Biol.* 9, 727576. doi:10.3389/fcell.2021.727576

Mahri, S. A., Ghamdi, A. A., Akiel, M., Aujan, M. A., Mohammad, S., and Aziz, M. A. (2020). Free Fatty Acids Receptors 2 and 3 Control Cell Proliferation by Regulating Cellular Glucose Uptake. *Wjgo* 12, 514–525. doi:10.4251/WJGO.V12.I5.514

Matthees, E. S. F., Haider, R. S., Hoffmann, C., and Drube, J. (2021). Differential Regulation of GPCRs-Are GRK Expression Levels the Key? *Front. Cel Dev. Biol.* 9, 687489. doi:10.3389/fcell.2021.687489

Mohammad, S., Patel, R. T., Bruno, J., Panhwar, M. S., Wen, J., and McGraw, T. E. (2014). A Naturally Occurring GIP Receptor Variant Undergoes Enhanced Agonist-Induced Desensitization, Which Impairs GIP Control of Adipose Insulin Sensitivity. *Mol. Cell Biol.* 34, 3618–3629. doi:10.1128/mcb.00256-14

Mohammad, S. (2015). Role of Free Fatty Acid Receptor 2 (FFAR2) in the Regulation of Metabolic Homeostasis. *Cdt* 16, 771–775. doi:10.2174/1389450116666150408103557

Morrow, N. M., Hanson, A. A., and Mulvihill, E. E. (2021). Distinct Identity of GLP-1R, GLP-2R, and GIPR Expressing Cells and Signaling Circuits within the Gastrointestinal Tract. *Front. Cel Dev. Biol.* 9, 703966. doi:10.3389/fcell.2021.703966

Nieto Gutierrez, A., and McDonald, P. H. (2018). GPCRs: Emerging Anti-cancer Drug Targets. *Cell Signal.* 41, 65–74. doi:10.1016/j.cellsig.2017.09.005

Okuno, Y., Yang, J., Taneishi, K., Yabuuchi, H., and Tsujimoto, G. (2006). GLIDA: GPCR-Ligand Database for Chemical Genomic Drug Discovery. *Nucleic Acids Res.* 34, D673–D677. doi:10.1093/nar/gkj028

Pavlos, N. J., and Friedman, P. A. (2017). GPCR Signaling and Trafficking: The Long and Short of it. *Trends Endocrinol. Metab.* 28, 213–226. doi:10.1016/j.tem.2016.10.007

Perez, D. M. (2021). Current Developments on the Role of α1-Adrenergic Receptors in Cognition, Cardioprotection, and Metabolism. *Front. Cel Dev. Biol.* 9, 652152. doi:10.3389/fcell.2021.652152

Pierce, K. L., Premont, R. T., and Lefkowitz, R. J. (2002). Seven-transmembrane Receptors. *Nat. Rev. Mol. Cel Biol.* 3, 639–650. doi:10.1038/nrm908

Sriram, K., and Insel, P. A. (2018). G Protein-Coupled Receptors as Targets for Approved Drugs: How many Targets and How many Drugs? *Mol. Pharmacol.* 93, 251–258. doi:10.1124/mol.117.111062

Strange, P. G. (2008). Signaling Mechanisms of GPCR Ligands. *Curr. Opin. Drug Discov. Dev.* 11, 196–202.

Tian, M., Qi, Y., Zhang, X., Wu, Z., Chen, J., Chen, F., et al. (2020). Regulation of the JAK2-STAT5 Pathway by Signaling Molecules in the Mammary Gland. *Front. Cel Dev. Biol.* 8, 604896. doi:10.3389/fcell.2020.604896

Wang, J., Gareri, C., and Rockman, H. A. (2018). G-protein-coupled Receptors in Heart Disease. *Circ. Res.* 123, 716–735. doi:10.1161/CIRCRESAHA.118.311403

Wolf, S., and Grünewald, S. (2015). Sequence, Structure and Ligand Binding Evolution of Rhodopsin-like G Protein-Coupled Receptors: A crystal Structure-Based Phylogenetic Analysis. *PLoS One* 10, e0123533. doi:10.1371/journal.pone.0123533

Conflict of Interest: The authors declare that the research was conducted in the absence of any commercial or financial relationships that could be construed as a potential conflict of interest.

Publisher's Note: All claims expressed in this article are solely those of the authors and do not necessarily represent those of their affiliated organizations, or those of the publisher, the editors and the reviewers. Any product that may be evaluated in this article, or claim that may be made by its manufacturer, is not guaranteed or endorsed by the publisher.

frontiers in Cell and Developmental Biology

REVIEW
published: 17 November 2020
doi: 10.3389/fcell.2020.604896

Regulation of the JAK2-STAT5 Pathway by Signaling Molecules in the Mammary Gland

Min Tian[1], Yingao Qi[1], Xiaoli Zhang[1], Zhihui Wu[1], Jiaming Chen[1], Fang Chen[1,2,3], Wutai Guan[1,2,3] and Shihai Zhang[1,2,3]**

[1] Guangdong Province Key Laboratory of Animal Nutrition Control, College of Animal Science, South China Agricultural University, Guangzhou, China, [2] College of Animal Science and National Engineering Research Center for Breeding Swine Industry, South China Agricultural University, Guangzhou, China, [3] Guangdong Laboratory for Lingnan Modern Agriculture, South China Agricultural University, Guangzhou, China

OPEN ACCESS

Edited by:
Sameer Mohammad, King Abdullah International Medical Research Center (KAIMRC), Saudi Arabia

Reviewed by:
Jurgen Muller, University of Bradford, United Kingdom
Serge Roche, Institut National de la Santé et de la Recherche Médicale (INSERM), France

***Correspondence:**
Wutai Guan
wutaiguan1963@163.com; wtguan@scau.edu.cn
Shihai Zhang
zhangshihai@scau.edu.cn

Specialty section:
This article was submitted to Signaling, a section of the journal Frontiers in Cell and Developmental Biology

Received: *10 September 2020*
Accepted: *29 October 2020*
Published: *17 November 2020*

Citation:
Tian M, Qi Y, Zhang X, Wu Z, Chen J, Chen F, Guan W and Zhang S (2020) Regulation of the JAK2-STAT5 Pathway by Signaling Molecules in the Mammary Gland. Front. Cell Dev. Biol. 8:604896. doi: 10.3389/fcell.2020.604896

Janus kinase 2 (JAK2) and signal transducers and activators of transcription 5 (STAT5) are involved in the proliferation, differentiation, and survival of mammary gland epithelial cells. Dysregulation of JAK2-STAT5 activity invariably leads to mammary gland developmental defects and/or diseases, including breast cancer. Proper functioning of the JAK2-STAT5 signaling pathway relies on crosstalk with other signaling pathways (synergistically or antagonistically), which leads to normal biological performance. This review highlights recent progress regarding the critical components of the JAK2-STAT5 pathway and its crosstalk with G-protein coupled receptor (GPCR) signaling, PI3K-Akt signaling, growth factors, inflammatory cytokines, hormone receptors, and cell adhesion.

Keywords: Stat5, JAK2, signaling molecules, milk production, mammary gland development

INTRODUCTION

The mammary gland is a critical organ in mammals and is involved in milk production and delivery. The mammary gland is a derivative of the skin, develops early during the embryonic stage and further develops and differentiates into a functional mammary gland during pubertal and adult stages (Gjorevski and Nelson, 2011). The development of the embryonic mammary gland starts with the formation of placodes, which then invaginate the mesenchyme and form mammary gland buds (Robinson, 2008). These buds continue to elongate and bifurcate, developing into a rudimentary gland prior to birth. Subsequently, the rudimentary mammary gland enters a quiescent phase and grows isomorphic with the body. The second stage of mammary gland development is initiated at puberty. During this period, mammary gland development is regulated and sustained by hormones, growth factors and cytokines. The tips of the rudimentary ducts transform into terminal end buds (TEBs) and penetrate into the mammary fat pad (Hinck and Silberstein, 2005). The mature mammary duct is mainly composed of myoepithelial cells (outer layer) and luminal epithelial cells (inner layer). During gestation, these mammary epithelial cells differentiate into milk-producing secretory alveoli, which synthesize the majority of milk fat, protein and lactose (Brisken et al., 1999; Oakes et al., 2008). The mammary gland rapidly undergoes involution after weaning, and approximately 80% of the epithelium is removed via apoptosis (Alexander et al., 2001; Watson, 2006).

Hormones are crucial for ductal morphogenesis in the mammary gland. During puberty, estrogen, growth hormone (GH) and prolactin are required for the development of the mammary gland (McNally and Martin, 2011). Estrogens are mainly secreted by the ovary and sensed by estrogen receptors (ERs), which are nuclear receptors. ERs regulate the transcription of multiple genes with a variety of coregulators [such as steroid receptor coactivator 1 (SRC-1) and Cbp/p300-interacting transactivator 1 (CITED1)] in the mammary gland (Howlin et al., 2006a,b). In contrast to estrogen, GH and prolactin regulate mammary gland function through the phosphorylation of Janus kinase 2 (JAK2) and activation of its downstream regulator signal transducers and activators of transcription 5 (STAT5) (Ihle, 1996). JAK2-STAT5 is proposed to be a critical signaling pathway in the mammary gland. In addition to the abovementioned hormones, JAK2-STAT5 is also regulated by cytokines such as IL-12, INF-γ, IL-4, IL-13, and IL-6. Recent studies have provided additional evidence that other prominent cellular signaling pathways (GPCR, PI3K/Akt and cell adhesion) might also be involved in crosstalk with JAK2-STAT5. The signaling pathways that interact with JAK2-STAT5 are overwhelmingly complex. In this review, we focus on the constitutive and extensive communication between JAK2-STAT5 and other signaling pathways.

STATS AND JAKS IN THE MAMMARY GLAND

In the mammary gland, five STATs (STAT1, 3, 5a,b, and 6) have been identified (Watson and Neoh, 2008). STAT1 and STAT6 have been reported to play minor roles in the mammary gland. Although STAT1 is highly activated in the mammary gland, STAT1 knockout does not significantly affect ductal or alveolar morphogenesis (Klover et al., 2010). STAT6 is downstream of IL-4 and IL-3 and partially regulates the development of the alveoli. However, mice lacking STAT6 are still able to lactate (Khaled et al., 2007). In contrast to STAT1 and STAT6, STAT5, and STAT3 are the key STATs in the mammary gland. STAT5 promotes the proliferation of mammary gland epithelial cells, while STAT3 regulates the process of apoptosis during involution (Chapman et al., 2000). During late pregnancy and lactation, STAT5 is highly activated, as high levels of STAT5 can be detected in the nucleus in epithelial cells of the mammary gland, whereas STAT5 levels are undetectable during the involution period (Bednorz et al., 2011). STAT5 is involved in the side branching and maturation of alveolar cells (Vafaizadeh et al., 2010). Conditional inhibition of STAT5 in the mammary gland at different times further reveals its roles during specific periods of lactation (Reichenstein et al., 2011). Knocking out STAT5 during the first 3 days of lactation affects the expression of ER and connexin 32 (C × 32, a gap junction protein). STAT5 knockout during the first 10 days of lactation decreases neonatal body weight by 30–40% due to changes in mammary gland morphology and a reduction in milk production. Two isoforms of STAT5 (STAT5a and STAT5b) have been identified in the mammary gland (Liu et al., 1996). STAT5a and STAT5b are encoded by two separate genes located on chromosome 11 (mouse) and chromosome 17 (human). These genes are highly homologous (96% conserved at the protein level) and contain different C-terminal regions (Rani and Murphy, 2016). Knocking out STAT5a inhibits the normal development and differentiation of the mammary gland during pregnancy, whereas deletion of STAT5B only impairs body growth (Cui et al., 2004). After weaning, the phosphorylation of STAT5 is significantly decreased with increased phosphorylation of STAT3 (Watson and Neoh, 2008). The switch from the activation of STAT5 to STAT3 indicates the triggering of mammary gland involution. Activated STAT5 and STAT3 can enter the nucleus and regulate related gene expression. STAT5 is thought to regulate genes related to milk protein synthesis (α-casein) and other genes with unclear biological functions (kallikrein-8, prosaposin and Grb10) (Clarkson et al., 2006). In addition, activated STAT5 also regulates ACC1 expression by binding to its promoter and initiating *de novo* synthesis of fatty acids (Mao et al., 2002). Consistently, knocking down STAT5 decreases the expression of ACC1 (Li et al., 2019). It is still not clear whether STAT5 also regulates ACC2. This evidence indicates that STAT5 plays a vital role in milk synthesis. As expected, STAT3 regulates apoptosis by targeting the apoptosis regulator genes CCAAT enhancer binding protein-δ and c-Fos and regulating the PI3K/Akt signaling pathway (Clarkson et al., 2006).

Two isoforms of JAK (JAK1 and JAK2) are expressed in the mammary gland, and these factors are upstream of STAT. The biological functions of these two JAKs are somewhat different. Briefly, prolactin mainly regulates STAT5 activation through JAK2, while JAK1 is primarily regulates STAT3 activation (Xie et al., 2002). It is worth noting that JAK2 not only binds to the prolactin receptor but can also enter the nucleus. The potential mechanisms by which JAK2 regulates nuclear gene expression in the mammary gland are by modulating tyrosine kinase activity and preventing protein degradation. For example, JAK2 interacts with transcription factor nuclear factor 1-C2 (NF1-C) and enhances its stability, which further regulates the expression of genes involved in milk synthesis (Nilsson et al., 2006).

NOVEL FACTORS IN JAK2-STAT5 ACTIVATION

The JAK2-STAT5 signaling pathway was identified long ago in the mammary gland. Recent studies have shown that additional components are required for the activation of JAK2-STAT5 (**Figure 1**). A prolyl isomerase called cyclophilin A (CypA) has been found to be an essential component for JAK2-STAT5 activation. CypA knockout disrupts mammary gland morphogenesis and differentiation by inhibiting the JAK2-STAT5 pathway (Volker et al., 2018). CUB and zona pellucida-like domain-containing protein 1 (CUZD1) is the other component involved in the regulation of mammary gland differentiation. CUZD1 knockout abolishes STAT5 phosphorylation and impairs mammary ductal branching and alveolar development. However, CUZD1 overexpression in mammary epithelial cells increases STAT5 phosphorylation (Mapes et al., 2017). Immunoprecipitation results show that CUZD1 forms a complex with JAK2 and STAT5, and CUZD1

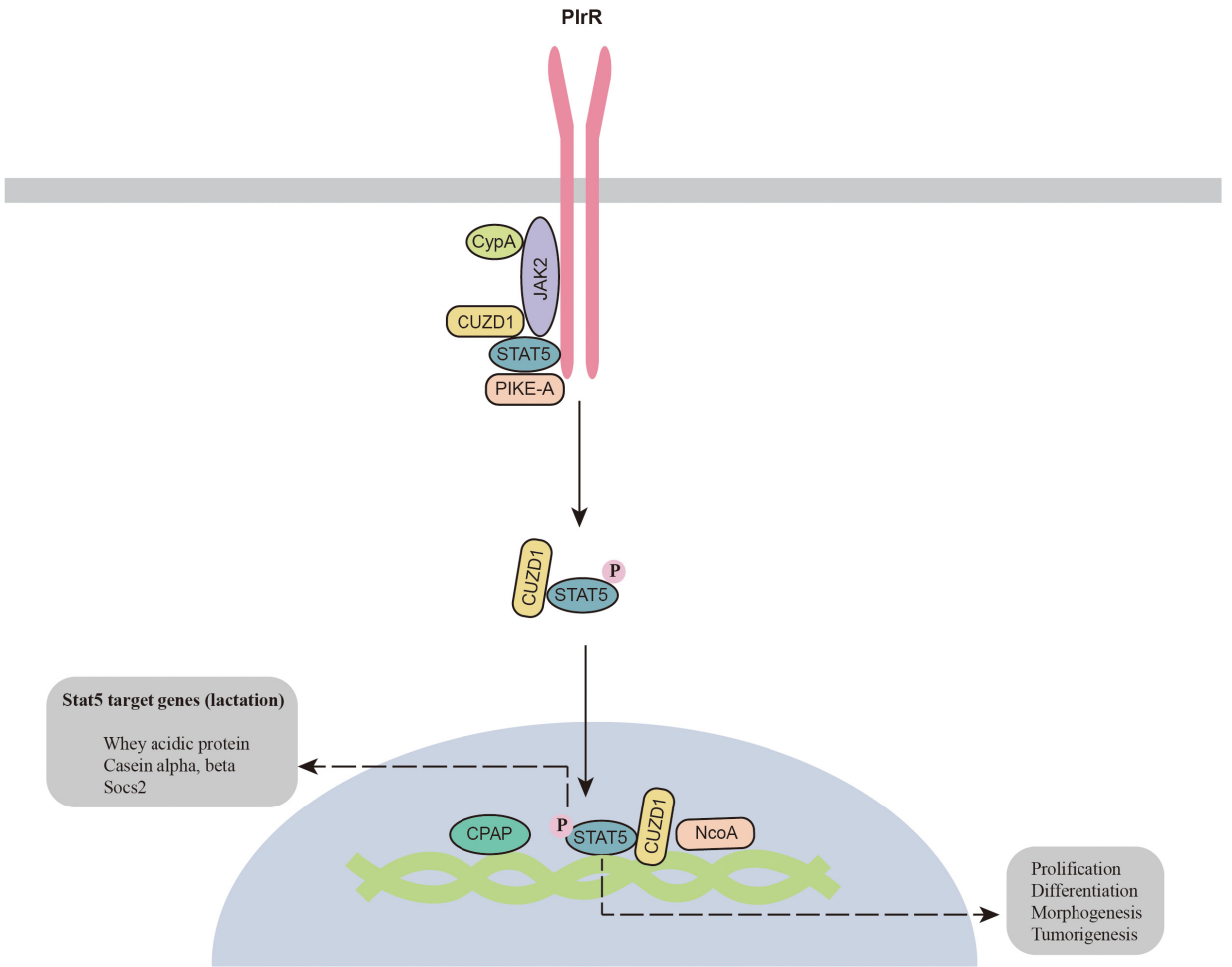

FIGURE 1 | Novel components of the JAK2-STAT5 signaling pathway. CPAP, centrosomal P4.1-associated protein; CypA, cyclophilin A; CUZD1, zona pellucida-like domain-containing protein 1; JAK2, Janus kinase 2; NcoA, nuclear receptor co-activator; PIKE-A, PI 3-kinase enhancer A; PlrR, prolactin receptor; STAT5, signal transducers and activators of transcription 5.

knockout disrupts the connection between JAK2 and STAT5 (Mapes et al., 2017). In addition, PIKE-A has also been reported to participate in complex formation with PRLR and STAT5, which is required for activation of the PRLR and STAT5 signaling pathways (Chan et al., 2010). Knockout of PIKE-A in HC11 mammary gland epithelial cells attenuates cell proliferation by inhibiting STAT5 activation and cyclin D1 expression. The other critical protein for STAT5 activation is zinc finger homeobox 3 (ZFHX3), which is highly expressed during lactation (Zhao et al., 2016). ZFHX3 knockout results in underdevelopment of the mammary gland with decreased PRLR expression and STAT5 phosphorylation. The underlying mechanism by which ZFHX3 regulates the STAT5 signaling pathway is still unknown. The zinc finger transcription factor Miz1, which contains an N-terminal POZ domain and zinc finger motifs, has also been reported to maintain the normal function of the mammary gland. Knockout of Miz1 disrupts the activation of STAT5 signaling through by disrupting intracellular transport and localization of PRLR and ERBB4 (Sanz-Moreno et al., 2014).

In addition, a number of cofactors for p-STAT5 have also been identified in the mammary gland. For example, centrosomal P4.1-associated protein (CPAP) interacts with STAT5 and enhances its activity (Peng et al., 2002). NCoA-1 is another coactivator of STAT5a that regulates the synergistic effects of glucocorticoid receptor and STAT5a on beta-casein expression (Litterst et al., 2003). In summary, JAK2-STAT5 is a complicated signaling pathway, as a number of proteins are required for its activation in the mammary gland. More studies are required to clarify how these components function to regulate the JAK2-STAT5 signaling pathway.

JAK2-STAT5 CROSSTALK WITH THE GPCR SIGNALING PATHWAY

G protein-coupled receptors (GPCRs) are crucial pharmaceutical targets that account for 33% of the targets of Food and Drug Administration (FAD)-approved drugs (Hauser et al., 2017).

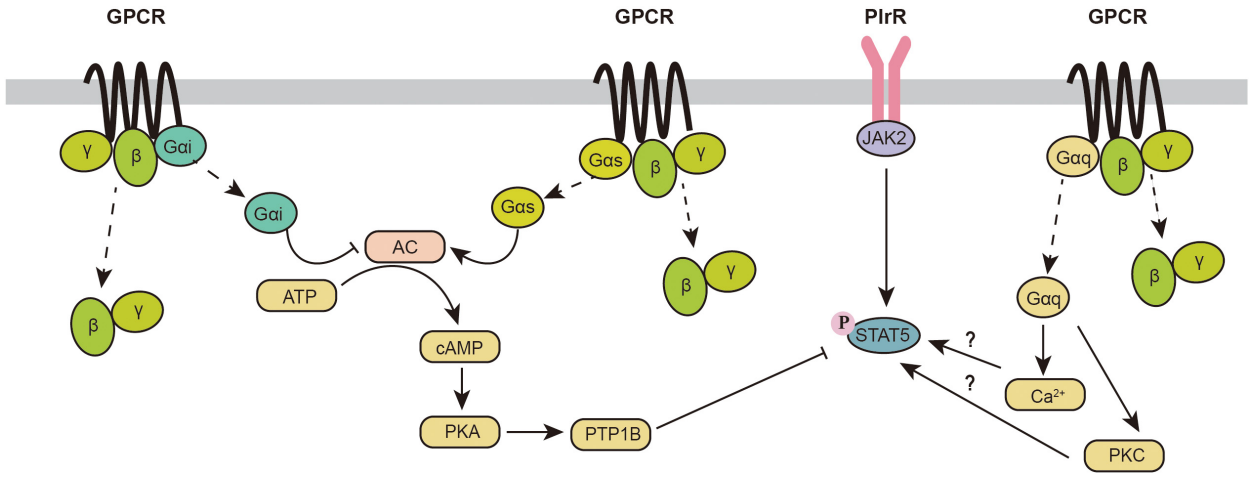

FIGURE 2 | Crosstalk between the GPCR and JAK2-STAT5 signaling pathways. AC, adenylyl cyclase; cAMP, cellular adenosine 3',5'-cyclic monophosphate; GPCR, G protein-coupled receptor; JAK2, Janus kinase 2; PKA, protein kinase A; PKC, protein kinase C; PIrR, prolactin receptor; PTP1B, protein-tyrosine phosphatase 1B; STAT5, signal transducers and activators of transcription 5.

GPCRs are activated by small carboxylic acid metabolites (GPR41, GPR43, GPR81, GPR109A, GPR109B, and GPR84), triglyceride metabolites (GPR40, GPR120, and GPR119), bile acids (GPBAR1), and amino acid and amino acid metabolites (GPR142, CasR, GPR35, TAAR1, and FBR1/2) (Husted et al., 2017). Dietary nutrients and their metabolites can regulate the development and lactation of the mammary gland through the activation of GPCR signaling pathways. In addition, a number of hormones (glucagon, luteinizing hormone, and epinephrine) and neurotransmitters (acetylcholine, dopamine, and serotonin) can also trigger the activation of corresponding GPCRs (Neves et al., 2002). Previously, glucagon, epinephrine and dopamine have been reported to be involved in the regulation of breast cancer (Wang et al., 2002; Ligumsky et al., 2012; Cui et al., 2019), while serotonin controls the development of the mammary gland (Matsuda et al., 2004). These receptors control multiple signaling cascades and regulate various physiological functions. Therefore, understanding the interplay between GPCRs and JAK2-STAT5 is crucial.

GPCRs are 7-transmembrane proteins that are coupled to heterotrimeric G proteins on the intracellular side of the membrane (Thal et al., 2018). The G protein contains G_{α} (binds to GTP/GDP), G_{β} and G_{γ} subunits (Wettschureck and Offermanns, 2005). The unique downstream signal activation of different GPCRs mainly relies on the classification of the G_{α} subunits. To date, four G_{α} subunits ($G_{\alpha s}$, $G_{\alpha i}$, $G_{\alpha q/11}$, and $G_{\alpha\ 12/13}$) have been identified in cells (Syrovatkina et al., 2016). $G_{\alpha i}$ and $G_{\alpha s}$ mainly participate in the regulation of cellular adenosine 3′,5′-cyclic monophosphate (cAMP) through adenylyl cyclase (AC) (Neves et al., 2002). cAMP is a critical second messenger that mainly regulates cellular biological functions through protein kinase A (PKA) and exchange proteins directly activated by PKA and cAMP (EPAC). $G_{\alpha q}$ can increase cellular Ca^{2+} signaling and activate protein kinase C (PKC)-dependent signaling pathways (Neves et al., 2002; Winzell and Ahrén, 2007).

Originally, it was reported that GPCR activation has minor effects on the JAK2-STAT5 signaling pathway. However, recent evidence indicates an intimate relationship between GPCR and JAK2-STAT5 signaling pathways (**Figure 2**). Activation of GPCRs coupled to the $G_{\alpha q}$ subunit has been reported to increase the phosphorylation of STAT5. The oxytocin receptor (OXTR) is a G protein-coupled receptor that binds to $G_{\alpha q}$. Overexpression of OXTR in the mouse mammary gland increases phosphorylation of STAT5 and induces lactation during the early lactation period, whereas OXTR-induced phosphorylation of STAT5 is decreased with attenuated milk production during the peak lactation period (Li et al., 2018). Furthermore, knockout of OXTR can impair milk ejection (Li et al., 2018). This finding indicates that the effect of the $G_{\alpha q}$ signaling pathway in the mammary gland may be dependent on different lactation periods. GPR54 is another GPCR coupled to $G_{\alpha q}$, which can be activated by kisspeptins (Kps). GPR54 is highly expressed during the lactation period. Activation of GPR54 increases β-casein synthesis in the mammary gland with activation of the mTOR, ERK1/2, and STAT5 signaling pathways (Kobayashi et al., 2016). In summary, these data provide some primary evidence for a potential link between the $G_{\alpha q}$ signaling pathway and JAK2-STAT5. However, the underlying mechanism involved in this process is not clear.

In addition to $G_{\alpha q}$, $G_{\alpha s}$- and $G_{\alpha i}$-related signaling pathways also participate in the phosphorylation of STAT5. As a direct downstream target of the $G_{\alpha s/\alpha i}$ signaling pathway, increased cellular cAMP significantly decreases STAT5 phosphorylation and β-casein synthesis through an increase in protein-tyrosine phosphatase 1B (PTP1B) (Chiba et al., 2016). In addition, it has been reported that PKA inhibition inhibits the secretion of newly synthesized caseins (Clegg et al., 1998). PKA inhibits the vesicular structure of the Golgi body and inhibits casein production mainly through exocytosis (Clegg et al., 1998). Furthermore,

PKA is also known to decrease protein synthesis through the inhibition of the mTORC1 signaling pathway (phosphorylation of raptor on Ser792) (Jewell et al., 2019). Because $G_{\alpha s}$ is a positive regulator of cAMP and $G_{\alpha i}$ is a negative regulator of cAMP, activation of the $G_{\alpha s}$ signaling pathway inhibits the stat5 signaling pathway, while triggering $G_{\alpha i}$ signaling can activate the STAT5 signaling pathway.

It is worth noting that many GPCRs are not coupled to a unique G_{α} protein, which makes the situation more complicated. For example, melatonin regulates mammary gland function through the melatonin receptors MT1 and MT2. MT2 is only coupled to a $G_{\alpha i}$ subunit, while MT1 is coupled to both $G_{\alpha i}$ and $G_{\alpha q}$ subunits (Tosini et al., 2014). Although $G_{\alpha i}$ and $G_{\alpha q}$ are thought to individually activate STAT5 in the mammary gland, overexpression of MT1 in the mammary gland surprisingly inhibits mammary gland development and milk synthesis, which is consistent with the decrease in STAT5 phosphorylation and the expression of estrogen and progesterone receptors (Xiang et al., 2012). One possible reason for this contradictory finding might be that the activation of GPCRs activates not only the G_{α} signaling pathway but also $G_{\beta\gamma}$ subunits, regulating many downstream effector targets. At present, the effects of $G_{\beta\gamma}$ on the phosphorylation of STAT5 in the mammary gland are still unclear. In more complicated situations, some GPCRs might be coupled to $G_{\alpha s}$ and $G_{\alpha q}$. Recent studies indicate that the activation of GPCRs could be biased (Qiao et al., 2020; Suomivuori et al., 2020). Thus, it is unrealistic to hypothesize which G_{α} subunits will be dominantly activated. More studies are needed to identify the effects of different GPCRs on the phosphorylation of STAT5.

JAK2-STAT5 CROSSTALK WITH THE PI3K-AKT SIGNALING PATHWAY

During puberty, branching morphogenesis is initiated by GH, estrogen, and IGF1. Intriguingly, GH, estrogen and IGF-1 are all involved in the activation of the PI3K/Akt signaling pathway. Breast cancer is the most common health risk for women. Approximately two-thirds of breast cancers are hormone-dependent (Subramani et al., 2017). Estrogen and GH dysregulation are also closely related to breast cancer. Specifically, genetic ablation of p110α (a catalytic subunit of PI3K) inhibits tumor formation, while knocking out p110β enhances ductal branching and tumorigenesis (Utermark et al., 2012). This evidence suggests that PI3K/Akt signaling is involved in the regulation of normal mammary gland growth and breast cancer development.

Akt is an important regulator of mammary gland development and milk synthesis. During the gestation and lactation periods, total and phosphorylated Akt are significantly increased in the mammary gland and are significantly decreased during the involution period (Schwertfeger et al., 2001; Boxer et al., 2006). Three isoforms of Akt have been identified in the mammary gland. Different Akt subtypes seem to execute different functions. Knockout of Akt1 but not Akt2 or Akt3 interferes with the activation of STAT5, delays differentiation and promotes apoptosis in the mammary gland (Maroulakou et al., 2008). However, Chen et al. (2010) found that knocking out either Akt1 or Akt2 in mice still resulted in normal mammary epithelial differentiation and STAT5 activation. Knockout of one allele of Akt2 in Akt1-deficient mice significantly blocks the phosphorylation of STAT5, which leads to defects in mammary gland differentiation and milk production. This evidence indicates that Akt isoforms might play overlapping regulatory roles and are critical in the mammary gland. Importantly, activation of the PI3K-Akt pathway triggers autocrine-mediated prolactin secretion, which indirectly activates the JAK2-STAT5 signaling pathway. This process is required for the initiation of lactation (Oliver and Watson, 2013). Future studies are needed to verify whether Akt1 and Akt2 are both required for the activation of the JAK2-STAT5 signaling pathway.

In the mammary gland, JAK2 deficiency decreases mammary gland cell proliferation, which can be partially recused by the overexpression of Akt1 (Sakamoto et al., 2007), suggesting a potential link between JAK2 and Akt1. In addition, activation of STAT5 can also directly regulate PI3K-Akt1 signaling through the mechanism described below (**Figure 3**). First, Stat5 directly binds to consensus sites within Akt1 and enhances its transcriptional activation (Creamer et al., 2010; Schmidt et al., 2014). Second, stat5 increases the transcription of two subunits (p85α and p110α) of phosphatidylinositol 3-kinase (PI3K) in the mammary gland (Schmidt et al., 2014). Third, STATs can regulate the activity of PI3K by binding to the p85 regulatory subunit (Rosa Santos et al., 2000; Nyga et al., 2005). This evidence indicates strong crosstalk between the PI3K-Akt and JAK2-STAT5 signaling pathways.

JAK2-STAT5 CROSSTALK WITH GROWTH FACTORS AND INFLAMMATORY CYTOKINES

Growth factors are crucial elements involved in JAK2/STAT5 regulation in the mammary gland (**Figure 4**). Transforming growth factor-β (TGF-β) is considered a crucial factor in the regulation of mammary gland development, as well as mammary tumorigenesis. TGF-β regulates mammary gland epithelial cells through an autocrine mechanism. Three isoforms of TGF-β (TGF-β1, TGF-β2, and TGF-β3) have been identified in mammals. All isoforms negatively regulate the development of the mammary gland (Daniel and Robinson, 1992). TGF-β3 is significantly increased during the involution process in the mouse mammary gland (Faure et al., 2000). A high concentration of TGF-β inhibits the branching process of the mammary gland (Nelson et al., 2006), whereas ductal proliferation and lateral branching are highly increased in TGF-β-mutant mice (Joseph et al., 1999; Crowley et al., 2005). The imbalance between non-canonical and canonical TGF-β signaling leads to mammary tumorigenesis (Parvani et al., 2011). The canonical downstream targets of TGF-β signaling are Smads, which are a group of transcription factors. TGFβ-induced Smad signaling (smad2/3/4 complex) antagonizes prolactin-mediated JAK/STAT signaling by blocking STAT5 transactivation of its target genes

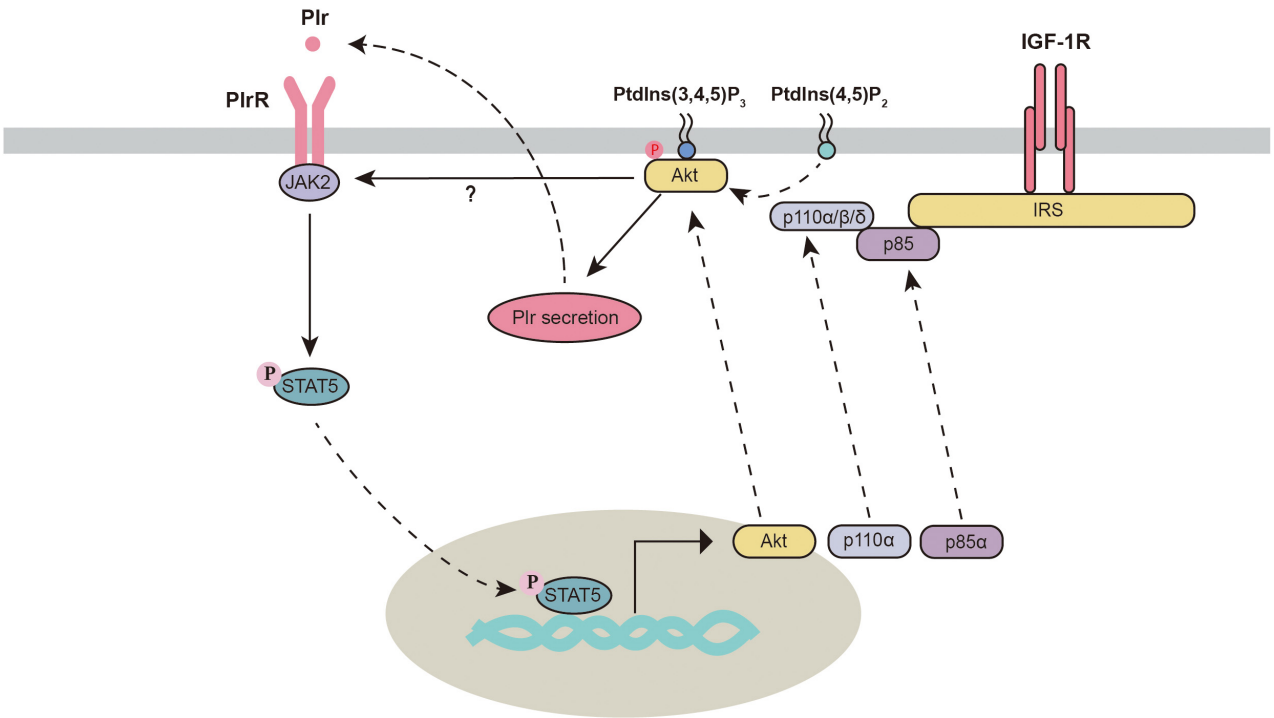

FIGURE 3 | Crosstalk between the PI3K/Akt and JAK2-STAT5 signaling pathways. Akt, protein kinase B; IGF-1R, insulin-like growth factor 1 receptor; IRS, insulin receptor substrate; JAK2, Janus kinase 2; Plr, prolactin; PlrR, prolactin receptor; PtdIns(3,4,5)P_3, phosphatidylinositol 3,4,5-trisphosphate; PtdIns(4,5)P_2, phosphatidylinositol-4,5-bisphosphate; STAT5, signal transducers and activators of transcription 5.

(Cocolakis et al., 2008). Intriguingly, TGFβ is usually highly expressed during the middle of lactation. The antagonistic effect of TGFβ is partially reduced by SnoN, which is an inhibitor of smad proteins (Jahchan et al., 2012). In addition, TGF-β might also regulate the function of the mammary gland via the activation of the non-canonical WNT5A pathway (Roarty and Serra, 2007).

Epidermal growth factor (EGF) is an important factor for mammary gland development (Long et al., 2003). EGF receptors (ERBBs) belong to the tyrosine kinase family, and four ERBBs have been identified (ERBB1, ERBB2, ERBB3, and ERBB4) in the mammary gland. ERBB1 and ERBB4 have been reported to participate in the regulation of mammary gland development. When ERBB1 is knocked out, alveolar development is severely impaired (Fowler et al., 1995). Intriguingly, it has been proposed that ERBB1 is mainly located in the stroma but not in the epithelium (Wiesen et al., 1999; Gallego et al., 2001). These findings suggest an intimate reciprocal stromal-epithelial interaction in the mammary gland. In contrast to ERBB1, the absence of ERBB4 leads to a deficiency in milk secretion (Tidcombe et al., 2003). Specifically, knocking out ERBB4 in mammary epithelial cells significantly impairs the differentiation and proliferation of cells in the mammary gland (Long et al., 2003). ERBB4 tyrosine kinases might also act as scaffold proteins that interact with JAK2 and STAT5 (Muraoka-Cook et al., 2008). When activated, ERBB4 is cleaved at Val-675 and releases a soluble 80-kDa intracellular domain (s80HER4). The kinase activity of s80HER4 is also required for the nuclear translocation of STAT5A (Muraoka-Cook et al., 2006). Thus, similar to PRLR, stimulation of ERBB4 triggers the activation of STAT5. Although some studies indicate cooperative crosstalk between prolactin and EGF (Darcy et al., 1995), other studies showed an antagonistic relationship between these factors (Fenton and Sheffield, 1997; Huang et al., 2006). EGF might inhibit PRL-induced mammary gland functions by modifying STAT5-mediated gene expression. In addition, EGF blocks the STAT5-induced pathway through growth factor receptor-bound protein 2 (Grb2), which is a positive regulator of cell proliferation during morphogenesis (Brummer et al., 2006).

In the context of mammary gland infection by pathogens during lactation, multiple inflammatory cytokines (TNF-α, IL-1β, and IL-6) are released by immune cells in the mammary gland and impair milk production (Shuster et al., 1996; Quesnell et al., 2012). IL-1β and TNF-α have been reported to inhibit milk protein production (β-casein expression) through activation of the NF-κB signaling pathway (Bonizzi and Karin, 2004). NF-κB and AMPK are two critical downstream signals of inflammatory cytokines (TNF-α, IL-1β, and IL-6). To date, JAK2 has been demonstrated to induce the phosphorylation of the inhibitor of NF-κB (Digicaylioglu and Lipton, 2001). However, no evidence indicates that NF-κB can regulate the activation of AMPK, which indicates that this field still needs further research. Interestingly, some experimental clues in non-mammary gland epithelial cells suggest that P38/ERK MAPK signaling pathways might

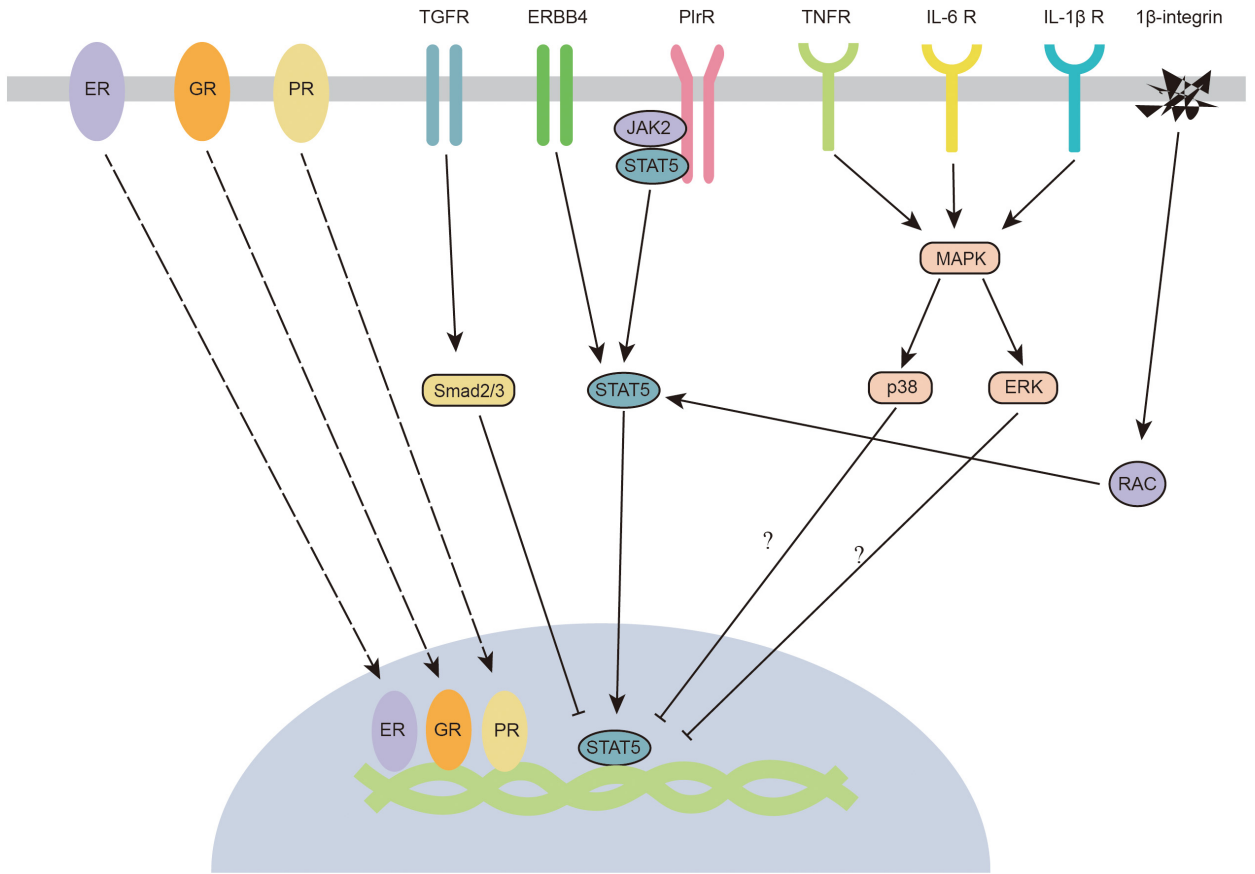

FIGURE 4 | Crosstalk between JAK2-STAT5 and hormone receptors, growth factors, inflammatory cytokines, and integrins. ER, estrogen receptor; ERBB4, epidermal growth factor receptor 4; ERK, extracellular signal-regulated kinase; GR, glucocorticoid receptor; IL-1β R, interleukin-1beta receptor; IL-6 R, interleukin-6 receptor; JAK2, janus kinase 2; MAPK, mitogen-activated protein kinases; PlrR, prolactin receptor; PR, progestinreceptor; Smad2/3, STAT5, signal transducers and activators of transcription 5; TGFR, transforming growth factor receptor; TNFR, tumour necrosis factor receptor.

be involved in the regulation of STAT5 (**Figure 4**). ERK has been reported to inhibit the transcriptional activity of STAT (Krasilnikov et al., 2003). Furthermore, the phosphorylation of p38 is negatively correlated with the phosphorylation of STAT5 (Gaoxia et al., 2018). The potential effects of P38/ERK MAPK of STAT5 in mammary gland epithelial cells still require further study. Recently, TNF-α has been shown to significantly inhibit lactose synthesis by inactivating JAK2 in the mammary gland (Kobayashi et al., 2016). It would be interesting to know if other inflammatory cytokines also affect the activation of the JAK2-STAT5 signaling pathway.

JAK2-STAT5 CROSSTALK WITH HORMONE RECEPTORS

As we previously mentioned in the "JAK2-STAT5 and PI3K-Akt" section, numerous hormones indirectly regulate JAK2-STAT5 through the PI3K/Akt signaling pathway. In this section, we summarize certain hormone receptors that can directly regulate the JAK2-STAT5 signaling pathway. Prolactin is one of the most predominant hormones that regulates mammary gland development (Saunier et al., 2003). The prolactin receptor-dependent signaling pathway is critical for the proliferation and differentiation of mammary alveoli during gestation (Miyoshi et al., 2001). It is widely known that prolactin is mainly responsible for the activation of JAK2-STAT5. In addition to the prolactin receptor, glucocorticoid, estrogen, and progestin receptors have also been reported to directly regulate the JAK2-STAT5 signaling pathway (**Figure 4**). In the mammary gland, glucocorticoid administration can increase milk protein synthesis through glucocorticoid receptors. The glucocorticoid receptor has been reported to interact with STAT5a and enhance STAT5a-mediated gene transcription. Both glucocorticoid receptor and STAT5a recruit the histone acetyltransferase (HAT) p300 coactivator (Pfitzner et al., 1998; Kabotyanski et al., 2006). Intriguingly, a recent study indicated that glucocorticoid receptors regulate beta-casein gene expression by directly interacting with a proximal promoter and a distal enhancer, forming a chromatin loop that connects the promoter and enhancer (Kabotyanski et al., 2009). This chromatin loop is important in regulating milk synthesis gene

expression. Similar to glucocorticoid receptors, estrogen and progestin receptors have also been proposed to regulate STAT5 by interacting with the DNA domain. Estrogen receptor-α and -β enhance prolactin-induced STAT5 activation by directly binding to the STAT5 DNA-binding domain (Björnström et al., 2001; Faulds et al., 2001). The crosstalk between the progestin receptor and the PRLR/STAT5 signaling pathway occurs at the β-casein promoter. Progestin-induced activation of progestin receptor leads to direct binding of progestin receptor to the beta-casein promoter and blocks its activation, which might lead to an inactivated form of STAT5a (Richer et al., 1998).

Recently, some preliminary evidence has indicated that hormones such as insulin, serotonin and leptin also participate in the regulation of the JAK2-STAT5 signaling pathway. Insulin plays an important role in enhancing milk synthesis by phosphorylating STAT5 in the mammary gland (Menzies et al., 2010). The insulin receptor can directly interact with STAT5 and induce its phosphorylation (Chen et al., 1997). In addition, one of the critical downstream signaling pathways of insulin is thought to increase the activity of the PI3K/KAT signaling pathway, which is a critical signaling pathway that crosstalks with JAK2-STAT5. Serotonin inhibits the phosphorylation of STAT5 and decreases β-casein expression (Chiba et al., 2014). Although leptin has not been reported to directly crosstalk with the STAT5 signaling pathway in the mammary gland, it is thought to synergize with prolactin to enhance the expression of beta-casein in the mammary gland through the inactivation of STAT3 (Motta et al., 2007).

INTEGRINS AND JAK2-STAT5

Cell adhesion is a critical factor that determines the fate of epithelial cells (Schmidt et al., 1993). As major receptors associated with cell adhesion, integrins have been reported to regulate cell proliferation, differentiation and migration (Díaz-Coránguez et al., 2019). β1-integrin is thought to maintain the function of the mammary gland via the integrin-containing adhesion complex protein ILK (integrin-linked kinase). ILK regulates STAT5 signaling through Rac1 (Akhtar et al., 2009), which (RAS-related C3 botulinum substrate 1) is a critical downstream factor of integrins (Akhtar and Streuli, 2006; **Figure 4**). Mechanistically, Rac1 recruits STAT5 to kinase complexes and enhances its phosphorylation (Xu et al., 2010). Knocking out β1-integrin decreases the activation of STAT5, impairs the differentiation of secretory epithelial cells, and inhibits the mRNA expression of beta-casein and whey acidic protein (Faraldo et al., 2002).

OTHER SIGNALING PATHWAYS AND THE ACTIVATION OF JAK2-STAT5

In addition to the abovementioned pathways that interact with JAK2-STAT5, other signaling pathways are involved in the regulation of JAK2-STAT5. (1) The Hedgehog signaling pathway negatively regulates mammary gland development. Overexpressing the Hedgehog effector protein GLI1 attenuates the expression of STAT5 through snail and inhibits mammary gland lactation (Fiaschi et al., 2007). (2) Peroxisome proliferator-activated receptor γ (PPARγ) has been shown to regulate STAT5A protein expression (Olsen and Haldosen, 2006). (3) NF-kappa B functions as a negative regulator of the JAK2-STAT5 pathway by interfering with STAT5 tyrosine phosphorylation (Geymayer and Doppler, 2000). However, more evidence is required to support the interplay between JAK2-STAT5 and these signaling pathways.

CONCLUSION AND PERSPECTIVE

Signal transducers and activators of transcription 5 is a crucial transcription factor that directly regulates multiple genes that participate in proliferation, differentiation, and milk secretion in the mammary gland. The current understanding of the crosstalk between JAK2-STAT5 and other signals includes the following: (1) activation of the $G_{\alpha i}$ or $G_{\alpha q}$ GPCR signaling pathway is thought to increase the phosphorylation of STAT5, and the effects of different types of GPCRs could be different due to the bias of agonists; (2) Akt1 activates STAT5 phosphorylation, which can increase the expression of Akt1 and PI3K subunits (p85α and p110α); (3) TGF-β, TNF-α, IL-6, and IL-1β are negative regulators of STAT5 activation, while the effects of EGF on the mammary gland are still controversial; (4) ER, GR and PR are positive regulators of the JAK2-STAT5 signaling pathway by directly interacting with the DNA domain; and (5) cell adhesion is crucial in maintaining the PrlR/STAT5 signaling cascade through β1-integrin.

It is worth noting that in addition to its function in mammary gland epithelial cells, the STAT5 signaling pathway also plays an important role in macrophages in the mammary gland and is required for normal mammary gland development. STAT5 knockout in macrophages leads to decreased ductal elongation but increased epithelial cell proliferation. Mechanistically, STAT5 deletion induces the expression of the proliferative factors Cyp19a1/aromatase and IL-6, which enhance ER signaling in the mammary gland (Brady et al., 2017). It would be interesting to know whether the STAT5 signaling pathway also plays a crucial role in other cell types (fibroblasts, adipocytes, blood vessels, nerves, and various immune cells) in the mammary gland. With the development of single-cell RNA sequencing, it would be possible to identify the potential signals that crosstalk with JAK-STAT5 in individual cells in the mammary gland. More research on the crosstalk among different types of cells in the mammary gland would help us to better understand the signaling networks in the whole mammary gland.

Mammary gland development and lactation are complicated processes that are accompanied by magnificent changes in reproductive hormones. During lactation, mastitis occurs widely and causes inflammatory injury of the mammary gland. Although various signaling interactions have been identified between JAK2-STAT5 and reproductive hormones, growth factors and inflammatory cytokines, the potential challenge in the future is

to precisely predict the biological modifications in the mammary gland mediated by these combinatorial signaling activities.

AUTHOR CONTRIBUTIONS

MT and SZ initiated the idea, the scope, and the outline of this review manuscript. MT, SZ, YQ, XZ, ZW, JC, and FC studied and analyzed all of the publications cited in this manuscript and were involved in the manuscript preparation. SZ and WG conducted the final editing and proofreading. All authors read and approved the final manuscript.

FUNDING

This work was supported by the National Natural Science Foundation of China (nos. 31802067 and 31872364) and the Natural Science Foundation of Guangdong Province (no. 2018A030310201).

REFERENCES

Akhtar, N., Marlow, R., Lambert, E., Schatzmann, F., Lowe, E. T., Cheung, J., et al. (2009). Molecular dissection of integrin signalling proteins in the control of mammary epithelial development and differentiation. *Development* 136, 1019–1027. doi: 10.1242/dev.028423

Akhtar, N., and Streuli, C. H. (2006). Rac1 links integrin-mediated adhesion to the control of lactational differentiation in mammary epithelia. *J. Cell Biol.* 173, 781–793. doi: 10.1083/jcb.200601059

Alexander, C. M., Selvarajan, S., Mudgett, J., and Werb, Z. (2001). Stromelysin-1 regulates adipogenesis during mammary gland involution. *J. Cell Biol.* 152, 693–703. doi: 10.1083/jcb.152.4.693

Bednorz, N. L., Brill, B., Klein, A., Gäbel, K., and Groner, B. (2011). Tracking the activation of Stat5 through the expression of an inducible reporter gene in a transgenic mouse line. *Endocrinology* 152, 1935–1947. doi: 10.1210/en.2011-0053

Björnström, L., Kilic, E., Norman, M., Parker, M. G., and Sjöberg, M. (2001). Cross-talk between Stat5b and estrogen receptor-alpha and -beta in mammary epithelial cells. *J. Mol. Endocrinol.* 27, 93–106. doi: 10.1677/jme.0.0270093

Bonizzi, G., and Karin, M. (2004). The two NF-kappaB activation pathways and their role in innate and adaptive immunity. *Trends Immunol.* 25, 280–288. doi: 10.1016/j.it.2004.03.008

Boxer, R. B., Stairs, D. B., Dugan, K. D., Notarfrancesco, K. L., Portocarrero, C. P., Keister, B. A., et al. (2006). Isoform-specific requirement for Akt1 in the developmental regulation of cellular metabolism during lactation. *Cell Metab.* 4, 475–490. doi: 10.1016/j.cmet.2006.10.011

Brady, N. J., Farrar, M. A., and Schwertfeger, K. L. (2017). STAT5 deletion in macrophages alters ductal elongation and branching during mammary gland development. *Dev. Biol.* 428, 232–244. doi: 10.1016/j.ydbio.2017.06.007

Brisken, C., Kaur, S., Chavarria, T. E., Binart, N., Sutherland, R. L., Weinberg, R. A., et al. (1999). Prolactin controls mammary gland development via direct and indirect mechanisms. *Dev. Biol.* 210, 96–106. doi: 10.1016/j.ydbio.2017.06.007

Brummer, T., Schramek, D., Hayes, V. M., Bennett, H. L., Caldon, C. E., Musgrove, E. A., et al. (2006). Increased proliferation and altered growth factor dependence of human mammary epithelial cells overexpressing the Gab2 docking protein. *J. Biol. Chem.* 281, 626–637. doi: 10.1074/jbc.M509567200

Chan, C. B., Liu, X., Ensslin, M. A., Dillehay, D. L., Ormandy, C. J., Sohn, P., et al. (2010). PIKE-A is required for prolactin-mediated STAT5a activation in mammary gland development. *EMBO J.* 29, 956–968. doi: 10.1038/emboj.2009.406

Chapman, R. S., Lourenco, P., Tonner, E., Flint, D., Selbert, S., Takeda, K., et al. (2000). The role of Stat3 in apoptosis and mammary gland involution. Conditional deletion of Stat3. *Adv. Exp. Med. Biol.* 480, 129–138. doi: 10.1007/0-306-46832-8_16

Chen, C. C., Boxer, R. B., Stairs, D. B., Portocarrero, C. P., Horton, R. H., Alvarez, J. V., et al. (2010). Akt is required for Stat5 activation and mammary differentiation. *Breast Cancer Res.* 12:R72. doi: 10.1186/bcr2640

Chen, J., Sadowski, H. B., Kohanski, R. A., and Wang, L. H. (1997). Stat5 is a physiological substrate of the insulin receptor. *Proc. Natl. Acad. Sci. U.S.A.* 94, 2295–2300. doi: 10.1073/pnas.94.6.2295

Chiba, T., Kimura, S., Takahashi, K., Morimoto, Y., Sanbe, A., Ueda, H., et al. (2014). Serotonin suppresses β-casein expression via inhibition of the signal transducer and activator of transcription 5 (STAT5) protein phosphorylation in human mammary epithelial cells MCF-12A. *Biol. Pharm. Bull.* 37, 1336–1340. doi: 10.1248/bpb.b14-00723

Chiba, T., Maeda, T., Sanbe, A., and Kudo, K. (2016). Serotonin suppresses β-casein expression via PTP1B activation in human mammary epithelial cells. *Biochem. Biophys. Res. Commun.* 473, 323–328. doi: 10.1016/j.bbrc.2016.03.103

Clarkson, R. W. E., Boland, M. P., Kritikou, E. A., Lee, J. M., Freeman, T. C., Tiffen, P. G., et al. (2006). The genes induced by signal transducer and activators of transcription (STAT)3 and STAT5 in mammary epithelial cells define the roles of these STATs in mammary development. *Mol. Endocrinol.* 20, 675–685. doi: 10.1210/me.2005-0392

Clegg, R. A., Gardner, R. A., Lavialle, F., Boisgard, R., and Ollivier-Bousquet, M. (1998). Casein secretion in mammary tissue: tonic regulation of basal secretion by protein kinase A. *Mol. Cell. Endocrinol.* 141, 163–177. doi: 10.1016/s0303-7207(98)00080-x

Cocolakis, E., Dai, M., Drevet, L., Ho, J., Haines, E., Ali, S., et al. (2008). Smad signaling antagonizes STAT5-mediated gene transcription and mammary epithelial cell differentiation. *J. Biol. Chem.* 283, 1293–1307. doi: 10.1074/jbc.M707492200

Creamer, B. A., Sakamoto, K., Schmidt, J. W., Triplett, A. A., Moriggl, R., and Wagner, K.-U. (2010). Stat5 promotes survival of mammary epithelial cells through transcriptional activation of a distinct promoter in Akt1. *Mol. Cell. Biol.* 30, 2957–2970. doi: 10.1128/MCB.00851-09

Crowley, M. R., Bowtell, D., and Serra, R. (2005). TGF-beta, c-Cbl, and PDGFR-alpha the in mammary stroma. *Dev. Biol.* 279, 58–72. doi: 10.1016/j.ydbio.2004.11.034

Cui, B., Luo, Y., Tian, P., Peng, F., Lu, J., Yang, Y., et al. (2019). Stress-induced epinephrine enhances lactate dehydrogenase A and promotes breast cancer stem-like cells. *J. Clin. Invest.* 129, 1030–1046. doi: 10.1172/JCI121685

Cui, Y., Riedlinger, G., Miyoshi, K., Tang, W., Li, C., Deng, C. X., et al. (2004). Inactivation of Stat5 in mouse mammary epithelium during pregnancy reveals distinct functions in cell proliferation, survival, and differentiation. *Mol. Cell. Biol.* 24, 8037–8047.doi: 10.1128/MCB.24.18.8037-8047.2004

Daniel, C. W., and Robinson, S. D. (1992). Regulation of mammary growth and function by TGF-β. *Mol. Reprod. Dev.* 32, 145–151. doi: 10.1002/mrd.1080320210

Darcy, K. M., Shoemaker, S. F., Lee, P. P., Vaughan, M. M., Black, J. D., and Ip, M. M. (1995). Prolactin and epidermal growth factor regulation of the proliferation, morphogenesis, and functional differentiation of normal rat mammary epithelial cells in three dimensional primary culture. *J. Cell. Physiol.* 163, 346–364. doi: 10.1002/jcp.1041630216

Díaz-Coránguez, M., Liu, X., and Antonetti, D. A. (2019). Tight Junctions in Cell Proliferation. *Int. J. Mol. Sci.* 20:5972. doi: 10.3390/ijms232345972

Digicaylioglu, M., and Lipton, S. A. (2001). Erythropoietin-mediated neuroprotection involves cross-talk between Jak2 and NF-κ B signalling cascades. *Nature* 412, 641–647. doi: 10.1038/35088074

Faraldo, M. M., Deugnier, M. A., Tlouzeau, S., Thiery, J. P., and Glukhova, M. A. (2002). Perturbation of beta 1-integrin mammary gland results in function in involuting premature dedifferentiation of secretory epithelial cells. *Mol. Biol. Cell* 13, 3521–3531. doi: 10.1091/mbc.E02-02-0086

Faulds, M. H., Pettersson, K., Gustafsson, J. A., and Haldosén, L. A. (2001). Cross-talk between ERs and signal transducer and activator of transcription 5 is E2 dependent and involves two functionally separate mechanisms. *Mol. Endocrinol.* 15, 1929–1940. doi: 10.1210/mend.15.11.0726

Faure, E., Heisterkamp, N., Groffen, J., and Kaartinen, V. (2000). Differential expression of TGF-β isoforms during postlactational mammary gland involution. *Cell Tissue Res.* 300, 89–95. doi: 10.1007/s004410000183

Fenton, S. E., and Sheffield, L. G. (1997). Prolactin inhibits EGF-induced DNA synthesis in mammary epithelium via early signaling mechanisms: possible involvement of protein kinase C. *Exp. Cell Res.* 236, 285–293. doi: 10.1006/excr.1997.3727

Fiaschi, M., Rozell, B., Bergstrom, A., Toftgard, R., and Kleman, M. I. (2007). Targeted expression of GLI1 in the mammary gland disrupts pregnancy-induced maturation and causes lactation failure. *J. Biol. Chem.* 282, 36090–36101. doi: 10.1074/jbc.M704280200

Fowler, K. J., Walker, F., Alexander, W., Hibbs, M. L., Nice, E. C., Bohmer, R. M., et al. (1995). A mutation in the epidermal growth factor receptor in waved-2 mice has a profound effect on receptor biochemistry that results in impaired lactation. *Proc. Natl. Acad. Sci. U.S.A.* 92, 1465–1469. doi: 10.1073/pnas.92.5.1465

Gallego, M. I., Binart, N., Robinson, G. W., Okagaki, R., Coschigano, K. T., Perry, J., et al. (2001). Prolactin, growth hormone, and epidermal growth factor activate Stat5 in different compartments of mammary tissue and exert different and overlapping developmental effects. *Dev. Biol.* 229, 163–175. doi: 10.1006/dbio.2000.9961

Gaoxia, D., Ying, T., and Xinqin, L. (2018). adiponectin participates in preeclampsia by regulating the biological function of placental trophoblasts through P38 MAPK-STAT5 Pathway. *Iran J. Public Health* 47:1838.

Geymayer, S., and Doppler, W. (2000). Activation of NF-kappaB p50/p65 is regulated in the developing mammary gland and inhibits STAT5-mediated beta-casein gene expression. *FASEB J.* 14, 1159–1170. doi: 10.1096/fasebj.14.9.1159

Gjorevski, N., and Nelson, C. M. (2011). Integrated morphodynamic signalling of the mammary gland. *Nat. Rev. Mol. Cell Biol.* 12, 581–593. doi: 10.1038/nrm3168

Hauser, A. S., Attwood, M. M., Rask-Andersen, M., Schiöth, H. B., and Gloriam, D. E. (2017). Trends in GPCR drug discovery: new agents, targets and indications. *Nat. Rev. Drug Discov.* 16, 829–842. doi: 10.1038/nrd.2017.178

Hinck, L., and Silberstein, G. B. (2005). Key stages in mammary gland development: the mammary end bud as a motile organ. *Breast Cancer Res.* 7, 245–251. doi: 10.1186/bcr1331

Howlin, J., McBryan, J., and Martin, F. (2006a). Pubertal mammary gland development: insights from mouse models. *J. Mamm. Gland Biol. Neoplasia* 11, 283–297. doi: 10.1007/s10911-006-9024-2

Howlin, J., McBryan, J., Napoletano, S., Lambe, T., McArdle, E., Shioda, T., et al. (2006b). CITED1 homozygous null mice display aberrant pubertal mammary ductal morphogenesis. *Oncogene* 25, 1532–1542. doi: 10.1038/sj.onc.1209183

Huang, Y., Li, X., Jiang, J., and Frank, S. J. (2006). Prolactin modulates phosphorylation, signaling and trafficking of epidermal growth factor receptor in human T47D breast cancer cells. *Oncogene* 25, 7565–7576. doi: 10.1038/sj.onc.1209740

Husted, A. S., Trauelsen, M., Rudenko, O., Hjorth, S. A., and Schwartz, T. W. (2017). GPCR-mediated signaling of metabolites. *Cell Metab.* 25, 777–796. doi: 10.1016/j.cmet.2017.03.008

Ihle, J. N. (1996). STATs: signal transducers and activators of transcription. *Cell* 84, 331–334. doi: 10.1016/s0092-8674(00)81277-5

Jahchan, N. S., Wang, D., Bissell, M. J., and Luo, K. (2012). SnoN regulates mammary gland alveologenesis and onset of lactation by promoting prolactin/Stat5 signaling. *Development* 139, 3147–3156. doi: 10.1242/dev.079616

Jewell, J. L., Fu, V., Hong, A. W., Yu, F. X., Meng, D., Melick, C. H., et al. (2019). GPCR signaling inhibits mTORC1 via PKA phosphorylation of raptor. *eLife* 8:e43038. doi: 10.7554/eLife.43038

Joseph, H., Gorska, A. E., Sohn, P., Moses, H. L., and Serra, R. (1999). Overexpression of a kinase-deficient transforming growth factor-beta type II receptor in mouse mammary stroma results in increased epithelial branching. *Mol. Biol. Cell* 10, 1221–1234. doi: 10.1091/mbc.10.4.1221

Kabotyanski, E. B., Huetter, M., Xian, W., Rijnkels, M., and Rosen, J. M. (2006). Integration of prolactin and glucocorticoid signaling at the beta-casein promoter and enhancer by ordered recruitment of specific transcription factors and chromatin modifiers. *Mol. Endocrinol.* 20, 2355–2368. doi: 10.1210/me.2006-0160

Kabotyanski, E. B., Rijnkels, M., Freeman-Zadrowski, C., Buser, A. C., Edwards, D. P., and Rosen, J. M. (2009). Lactogenic hormonal induction of long distance interactions between beta-casein gene regulatory elements. *J. Biol. Chem.* 284, 22815–22824. doi: 10.1074/jbc.M109.032490

Khaled, W. T., Read, E. K., Nicholson, S. E., Baxter, F. O., Brennan, A. J., Came, P. J., et al. (2007). The IL-4/IL-13/Stat6 signalling pathway promotes luminal mammary epithelial cell development. *Development* 134, 2739–2750. doi: 10.1242/dev.003194

Klover, P. J., Muller, W. J., Robinson, G. W., Pfeiffer, R. M., Yamaji, D., and Hennighausen, L. (2010). Loss of STAT1 from mouse mammary epithelium results in an increased Neu-induced tumor burden. *Neoplasia* 12, 899–905. doi: 10.1593/neo.10716

Kobayashi, K., Kuki, C., Oyama, S., and Kumura, H. (2016). Pro-inflammatory cytokine TNF-α is a key inhibitory factor for lactose synthesis pathway in lactating mammary epithelial cells. *Exp. Cell Res.* 340, 295–304. doi: 10.1016/j.yexcr.2015.10.030

Krasilnikov, M., Ivanov, V. N., Dong, J., and Ronai, Z. E. (2003). ERK and PI3K negatively regulate STAT-transcriptional activities in human melanoma cells: implications towards sensitization to apoptosis. *Oncogene* 22, 4092–4101.

Li, D., Ji, Y., Zhao, C., Yao, Y., Yang, A., Jin, H., et al. (2018). OXTR overexpression leads to abnormal mammary gland development in mice. *J. Endocrinol.* 239, 121–136. doi: 10.1530/JOE-18-0356

Li, T., Weng, J., Zhang, Y., Liang, K., Fu, G., Li, Y., et al. (2019). mTOR direct crosstalk with STAT5 promotes de novo lipid synthesis and induces hepatocellular carcinoma. *Cell Death Dis.* 10, 1–11.

Ligumsky, H., Wolf, I., Israeli, S., Haimsohn, M., Ferber, S., Karasik, A., et al. (2012). The peptide-hormone glucagon-like peptide-1 activates cAMP and inhibits growth of breast cancer cells. *Breast Cancer Res. Treat.* 132, 449–461. doi: 10.1007/s10549-011-1585-0

Litterst, C. M., Kliem, S., Marilley, D., and Pfitzner, E. (2003). NCoA-1/SRC-1 is an essential coactivator of STAT5 that binds to the FDL motif in the alpha-helical region of the STAT5 transactivation domain. *J. Biol. Chem.* 278, 45340–45351. doi: 10.1074/jbc.M303644200

Liu, X., Robinson, G. W., and Hennighausen, L. (1996). Activation of Stat5a and Stat5b by tyrosine phosphorylation is tightly linked to mammary gland differentiation. *Mol. Endocrinol.* 10, 1496–1506. doi: 10.1210/mend.10.12.8961260

Long, W., Wagner, K. U., Lloyd, K. C., Binart, N., Shillingford, J. M., Hennighausen, L., et al. (2003). Impaired differentiation and lactational failure of Erbb4-deficient mammary glands identify ERBB4 as an obligate mediator of STAT5. *Development* 130, 5257–5268. doi: 10.1242/dev.00715

Mao, J., Molenaar, A. J., Wheeler, T. T., and Seyfer, H. M. (2002). STAT5 binding contributes to lactational stimulation of promoter III expressing the bovine acetyl-CoA carboxylase alpha-encoding gene in the mammary gland. *J. Mol. Endocrinol.* 29, 73–88. doi: 10.1677/jme.0.0290073

Mapes, J., Li, Q., Kannan, A., Anandan, L., Laws, M., Lydon, J. P., et al. (2017). CUZD1 is a critical mediator of the JAK/STAT5 signaling pathway that controls mammary gland development during pregnancy. *PLoS Genet.* 13:e1006654. doi: 10.1371/journal.pgen.1006654

Maroulakou, I. G., Oemler, W., Naber, S. P., Klebba, I., Kuperwasser, C., and Tsichlis, P. N. (2008). Distinct roles of the three Akt isoforms in lactogenic differentiation and involution. *J. Cell. Physiol.* 217, 468–477. doi: 10.1002/jcp.21518

Matsuda, M., Imaoka, T., Vomachka, A. J., Gudelsky, G. A., Hou, Z., Mistry, M., et al. (2004). Serotonin regulates mammary gland development via an autocrine-paracrine loop. *Dev. Cell* 6, 193–203. doi: 10.1016/s1534-5807(04)00022-x

McNally, S., and Martin, F. (2011). Molecular regulators of pubertal mammary gland development. *Ann Med.* 43, 212–234. doi: 10.3109/07853890.2011.554425

Menzies, K. K., Lee, H. J., Lefevre, C., Ormandy, C. J., Macmillan, K. L., and Nicholas, K. R. (2010). Insulin, a key regulator of hormone responsive milk protein synthesis during lactogenesis in murine mammary explants. *Funct. Integr. Genom.* 10, 87–95. doi: 10.1007/s10142-009-0140-0

Miyoshi, K., Shillingford, J. M., Smith, G. H., Grimm, S. L., Wagner, K. U., Oka, T., et al. (2001). Signal transducer and activator of transcription (Stat) 5 controls the proliferation and differentiation of mammary alveolar epithelium. *J. Cell Biol.* 155, 531–542. doi: 10.1083/jcb.200107065

Motta, M., Accornero, P., Taulli, R., Bernabei, P., Desrivieres, S., and Baratta, M. (2007). Leptin enhances STAT-3 phosphorylation in HC11 cell line: effect on cell differentiation and cell viability. *Mol. Cell. Endocrinol.* 263, 149–155. doi: 10.1016/j.mce.2006.09.010

Muraoka-Cook, R. S., Sandahl, M., Husted, C., Hunter, D., Miraglia, L., Feng, S. M., et al. (2006). The intracellular domain of ErbB4 induces differentiation of mammary epithelial cells. *Mol. Biol. Cell* 17, 4118–4129. doi: 10.1091/mbc.e06-02-0101

Muraoka-Cook, R. S., Sandahl, M., Hunter, D., Miraglia, L., and Earp, H. S. (2008). Prolactin and ErbB4/HER4 signaling interact via Janus kinase 2 to induce mammary epithelial cell gene expression differentiation. *Mol. Endocrinol.* 22, 2307–2321. doi: 10.1210/me.2008-0055

Nelson, C. M., Vanduijn, M. M., Inman, J. L., Fletcher, D. A., and Bissell, M. J. (2006). Tissue geometry determines sites of mammary branching morphogenesis in organotypic cultures. *Science* 314, 298–300. doi: 10.1126/science.1131000

Neves, S. R., Ram, P. T., and Iyengar, R. (2002). G protein pathways. *Science* 296, 1636–1639.

Nilsson, J., Bjursell, G., and Kannius-Janson, M. (2006). Nuclear Jak2 and transcription factor NF1-C2: a novel mechanism of prolactin signaling in mammary epithelial cells. *Mol. Cell. Biol.* 26, 5663–5674. doi: 10.1128/MCB.02095-05

Nyga, R., Pecquet, C., Harir, N., Gu, H., Dhennin-Duthille, I., Regnier, A., et al. (2005). Activated STAT5 proteins induce activation of the PI 3-kinase/Akt and Ras/MAPK pathways via the Gab2 scaffolding adapter. *Biochem. J.* 390, 359–366. doi: 10.1042/BJ20041523

Oakes, S. R., Rogers, R. L., Naylor, M. J., and Ormandy, C. J. (2008). Prolactin regulation of mammary gland development. *J. Mamm. Gland Biol. Neoplasia* 13, 13–28. doi: 10.1007/s10911-008-9069-5

Oliver, C. H., and Watson, C. J. (2013). Making milk: a new link between STAT5 and Akt1. *Jakstat* 2, 2154–2168. doi: 10.4161/jkst.23228

Olsen, H., and Haldosen, L. A. (2006). Peroxisome proliferator-activated receptor gamma regulates expression of signal transducer and activator of transcription 5A. *Exp. Cell Res.* 312, 1371–1380. doi: 10.1016/j.yexcr.2005.12.023

Parvani, J. G., Taylor, M. A., and Schiemann, W. P. (2011). Noncanonical TGF-β signaling during mammary tumorigenesis. *J. Mamm. Gland Biol. Neoplasia* 16, 127–146. doi: 10.1007/s10911-011-9207-3

Peng, B., Sutherland, K. D., Sum, E. Y. M., Monilola, O., Sergio, W., and Tang, T. K. (2002). CPAP is a novel stat5-interacting cofactor that augments stat5-mediated transcriptional activity. *Mol. Endocrinol.* 16, 2019–2033. doi: 10.1210/me.2002-0108

Pfitzner, E., Jähne, R., Wissler, M., Stoecklin, E., and Groner, B. (1998). p300/CREB-binding protein enhances the prolactin-mediated transcriptional induction through direct interaction with the transactivation domain of Stat5, but does not participate in the Stat5-mediated suppression of the glucocorticoid response. *Mol. Endocrinol.* 12, 1582–1593. doi: 10.1210/mend.12.10.0180

Qiao, A., Han, S., Li, X., Li, Z., Zhao, P., Dai, A., et al. (2020). Structural basis of G(s) and G(i) recognition by the human glucagon receptor. *Science* 367, 1346–1352. doi: 10.1126/science.aaz5346

Quesnell, R. R., Klaessig, S., Watts, J. L., and Schukken, Y. H. (2012). Bovine intramammary *Escherichia coli* challenge infections in late gestation demonstrate a dominant antiinflammatory immunological response. *J. Dairy Sci.* 95, 117–126. doi: 10.3168/jds.2011-4289

Rani, A., and Murphy, J. J. (2016). STAT5 in cancer and immunity. *J. Interf. Cytokine Res.* 36, 226–237. doi: 10.1089/jir.2015.0054

Reichenstein, M., Rauner, G., and Barash, I. (2011). Conditional repression of STAT5 expression during lactation reveals its exclusive roles in mammary gland morphology, milk-protein gene expression, and neonate growth. *Mol. Reprod. Dev.* 78, 585–596. doi: 10.1002/mrd.21345

Richer, J. K., Lange, C. A., Manning, N. G., Owen, G., Powell, R., and Horwitz, K. B. (1998). Convergence of progesterone with growth factor and cytokine signaling in breast cancer. Progesterone receptors regulate signal transducers and activators of transcription expression and activity. *J. Biol. Chem.* 273, 31317–31326. doi: 10.1074/jbc.273.47.31317

Roarty, K., and Serra, R. (2007). Wnt5a is required for proper mammary gland development and TGF-beta-mediated inhibition of ductal growth. *Development* 134, 3929–3939. doi: 10.1242/dev.008250

Robinson, G. W. (2008). Cooperation of signalling pathways in embryonic mammary gland development. *Nat. Rev. Genet.* 8, 963–972. doi: 10.1038/nrg2227

Rosa Santos, S. C., Dumon, S., Mayeux, P., Gisselbrecht, S., and Gouilleux, F. (2000). Cooperation between STAT5 and phosphatidylinositol 3-kinase in the IL-3-dependent survival of a bone marrow derived cell line. *Oncogene* 19, 1164–1172.

Sakamoto, K., Creamer, B. A., Triplett, A. A., and Wagner, K. U. (2007). The Janus Kinase 2 Is required for expression and nuclear accumulation of Cyclin D1 in proliferating mammary epithelial cells. *Mol. Endocrinol.* 21, 1877–1892. doi: 10.1210/me.2006-0316

Sanz-Moreno, A., Fuhrmann, D., Wolf, E., von Eyss, B., Eilers, M., and Elsässer, H. P. (2014). Miz1 deficiency in the mammary gland causes a lactation defect by attenuated Stat5 expression and phosphorylation. *PLoS One* 9:e89187. doi: 10.1371/journal.pone.0089187

Saunier, E., Dif, F., Kelly, P. A., and Edery, M. (2003). Targeted expression of the dominant-negative prolactin receptor in the mammary gland of transgenic mice results in impaired lactation. *Endocrinology* 144, 2669–2675. doi: 10.1210/en.2002-221038

Schmidt, J. W., Piepenhagen, P. A., and Nelson, W. J. (1993). Modulation of epithelial morphogenesis and cell fate by cell-to-cell signals and regulated cell adhesion. *Semin Cell Biol.* 4, 161–173. doi: 10.1006/scel.1993.1020

Schmidt, J. W., Wehde, B. L., Sakamoto, K., Triplett, A. A., Anderson, S. M., Tsichlis, P. N., et al. (2014). Stat5 regulates the phosphatidylinositol 3-kinase/Akt1 pathway during mammary gland development and tumorigenesis. *Mol. Cell. Biol.* 34, 1363–1377. doi: 10.1128/MCB.01220-13

Schwertfeger, K. L., Richert, M. M., and Anderson, S. M. (2001). Mammary gland involution is delayed by activated Akt in transgenic mice. *Mol. Endocrinol.* 15, 867–881. doi: 10.1210/mend.15.6.0663

Shuster, D. E., Lee, E. K., and Kehrli, M. E. Jr. (1996). Bacterial growth, inflammatory cytokine production, and neutrophil recruitment during coliform mastitis in cows within ten days after calving, compared with cows at midlactation. *Am. J. Vet. Res.* 57, 1569–1575.

Subramani, R., Nandy, S. B., Pedroza, D. A., and Lakshmanaswamy, R. (2017). Role of growth hormone in breast cancer. *Endocrinology* 158, 1543–1555. doi: 10.1210/en.2016-1928

Suomivuori, C. M., Latorraca, N. R., Wingler, L. M., Eismann, S., King, M. C., Kleinhenz, A. L. W., et al. (2020). Molecular mechanism of biased signaling in a prototypical G protein-coupled receptor. *Science* 367, 881–887. doi: 10.1126/science.aaz0326

Syrovatkina, V., Alegre, K. O., Dey, R., and Huang, X. Y. (2016). Regulation, signaling, and physiological functions of G-Proteins. *J. Mol. Biol.* 428, 3850–3868. doi: 10.1016/j.jmb.2016.08.002

Thal, D. M., Glukhova, A., Sexton, P. M., and Christopoulos, A. (2018). Structural insights into G-protein-coupled receptor allostery. *Nature* 559, 45–53. doi: 10.1038/s41586-018-0259-z

Tidcombe, H., Jackson-Fisher, A., Mathers, K., Stern, D. F., Gassmann, M., and Golding, J. P. (2003). Neural and mammary gland defects in ErbB4 knockout mice genetically rescued from embryonic lethality. *Proc. Natl. Acad. Sci. U.S.A.* 100, 8281–8286. doi: 10.1073/pnas.1436402100

Tosini, G., Owino, S., Guillaume, J. L., and Jockers, R. (2014). Understanding melatonin receptor pharmacology: latest insights from mouse models, and their relevance to human disease. *Bioessays* 36, 778–787. doi: 10.1002/bies.201400017

Utermark, T., Rao, T., Cheng, H., Wang, Q., Lee, S. H., Wang, Z. C., et al. (2012). The p110α and p110β isoforms of PI3K play divergent roles in mammary gland development and tumorigenesis. *Genes Dev.* 26, 1573–1586. doi: 10.1101/gad.191973.112

Vafaizadeh, V., Klemmt, P., Brendel, C., Weber, K., Doebele, C., Britt, K., et al. (2010). Mammary epithelial reconstitution with gene-modified stem cells assigns roles to Stat5 in luminal alveolar cell fate decisions, differentiation, involution, and mammary tumor formation. *Stem Cells* 28, 928–938. doi: 10.1002/stem.407

Volker, S. E., Hedrick, S. E., Feeney, Y. B., and Clevenger, C. V. (2018). Cyclophilin A function in mammary epithelium impacts Jak2/Stat5 signaling, morphogenesis, differentiation, and tumorigenesis in the mammary gland. *Cancer Res.* 78, 3877–3887. doi: 10.1158/0008-5472.CAN-17-2892

Wang, P. S., Walker, A. M., Tsuang, M. T., Orav, E. J., Glynn, R. J., Levin, R., et al. (2002). Dopamine antagonists and the development of breast cancer. *Arch. Gen. Psychiatry* 59, 1147–1154. doi: 10.1001/archpsyc.59.12.1147

Watson, C. J. (2006). Involution: apoptosis and tissue remodelling that convert the mammary gland from milk factory to a quiescent organ. *Breast Cancer Res.* 8:203. doi: 10.1186/bcr1401

Watson, C. J., and Neoh, K. (2008). The Stat family of transcription factors have diverse roles in mammary gland development. *Semin. Cell Dev. Biol.* 19, 401–406. doi: 10.1016/j.semcdb.2008.07.021

Wettschureck, N., and Offermanns, S. (2005). Mammalian G proteins and their cell type specific functions. *Physiol. Rev.* 85, 1159–1204. doi: 10.1152/physrev.00003.2005

Wiesen, J. F., Young, P., Werb, Z., and Cunha, G. R. (1999). Signaling through the stromal epidermal growth factor receptor is necessary for mammary ductal development. *Development* 126, 335–344.

Winzell, M. S., and Ahrén, B. (2007). G-protein-coupled receptors and islet function-implications for treatment of type 2 diabetes. *Pharmacol. Ther.* 116, 437–448. doi: 10.1016/j.pharmthera.2007.08.002

Xiang, S., Mao, L., Yuan, L., Duplessis, T., Jones, F., Hoyle, G. W., et al. (2012). Impaired mouse mammary gland growth and development is mediated by melatonin and its MT1 G protein-coupled receptor via repression of ERα, Akt1, and Stat5. *J. Pineal Res.* 53, 307–318. doi: 10.1111/j.1600-079X.2012.01000.x

Xie, J., LeBaron, M. J., Nevalainen, M. T., and Rui, H. (2002). Role of tyrosine kinase Jak2 in prolactin-induced differentiation and growth of mammary epithelial cells. *J. Biol. Chem.* 277, 14020–14030. doi: 10.1074/jbc.M112399200

Xu, R., Spencer, V. A., Groesser, D. L., and Bissell, M. J. (2010). Laminin regulates PI3K basal localization and activation to sustain STAT5 activation. *Cell Cycle* 9, 4315–4322. doi: 10.4161/cc.9.21.13578

Zhao, D., Ma, G., Zhang, X., He, Y., Li, M., Han, X., et al. (2016). Zinc finger homeodomain factor Zfhx3 is essential for mammary lactogenic differentiation by maintaining prolactin signaling activity. *J. Biol. Chem.* 291, 12809–12820. doi: 10.1074/jbc.M116.719377

Conflict of Interest: The authors declare that the research was conducted in the absence of any commercial or financial relationships that could be construed as a potential conflict of interest.

frontiers in Cell and Developmental Biology

ORIGINAL RESEARCH
published: 12 March 2021
doi: 10.3389/fcell.2021.651367

Adenosine Receptor and Its Downstream Targets, Mod(mdg4) and Hsp70, Work as a Signaling Pathway Modulating Cytotoxic Damage in *Drosophila*

Yu-Hsien Lin[1,2†], Houda Ouns Maaroufi[1,2], Lucie Kucerova[1], Lenka Rouhova[1,2], Tomas Filip[1,2] and Michal Zurovec[1,2*]*

[1] Biology Centre of the Czech Academy of Sciences, Institute of Entomology, Ceske Budejovice, Czechia, [2] Faculty of Science, University of South Bohemia, Ceske Budejovice, Czechia

OPEN ACCESS

Edited by:
Sameer Mohammad,
King Abdullah International Medical Research Center (KAIMRC), Saudi Arabia

Reviewed by:
Rodrigo A. Cunha,
University of Coimbra, Portugal
Pavel Hyršl,
Masaryk University, Czechia

***Correspondence:**
Yu-Hsien Lin
r99632012@gmail.com
Michal Zurovec
zurovec@entu.cas.cz

†Present address:
Yu-Hsien Lin,
Department of Plant Physiology, Swammerdam Institute for Life Sciences, University of Amsterdam, Amsterdam, Netherlands

Specialty section:
This article was submitted to Signaling, a section of the journal Frontiers in Cell and Developmental Biology

Received: 09 January 2021
Accepted: 22 February 2021
Published: 12 March 2021

Citation:
Lin Y-H, Maaroufi HO, Kucerova L, Rouhova L, Filip T and Zurovec M (2021) Adenosine Receptor and Its Downstream Targets, Mod(mdg4) and Hsp70, Work as a Signaling Pathway Modulating Cytotoxic Damage in Drosophila. Front. Cell Dev. Biol. 9:651367. doi: 10.3389/fcell.2021.651367

Adenosine (Ado) is an important signaling molecule involved in stress responses. Studies in mammalian models have shown that Ado regulates signaling mechanisms involved in "danger-sensing" and tissue-protection. Yet, little is known about the role of Ado signaling in *Drosophila*. In the present study, we observed lower extracellular Ado concentration and suppressed expression of Ado transporters in flies expressing mutant huntingtin protein (mHTT). We altered Ado signaling using genetic tools and found that the overexpression of Ado metabolic enzymes, as well as the suppression of Ado receptor (AdoR) and transporters (ENTs), were able to minimize mHTT-induced mortality. We also identified the downstream targets of the AdoR pathway, the modifier of mdg4 (Mod(mdg4)) and heat-shock protein 70 (Hsp70), which modulated the formation of mHTT aggregates. Finally, we showed that a decrease in Ado signaling affects other *Drosophila* stress reactions, including paraquat and heat-shock treatments. Our study provides important insights into how Ado regulates stress responses in *Drosophila*.

Keywords: heat-shock protein 70, modifier of mdg4, mutant huntingtin, cytotoxicity, neurodegeneration, equilibrative nucleoside transporter

INTRODUCTION

Tissue injury, ischemia, and inflammation activate organismal responses involved in the maintenance of tissue homeostasis. Such responses require precise coordination among the involved signaling pathways. Adenosine (Ado) represents one of the key signals contributing to the orchestration of cytoprotection, immune reactions, and regeneration, as well as balancing energy metabolism (Borea et al., 2016). Under normal conditions, the Ado concentration in blood is in the nanomolar range; however, under pathological circumstances the extracellular Ado (e-Ado) level may dramatically change (Moser et al., 1989). Ado has previously been considered a retaliatory metabolite, having general tissue protective effects. Prolonged adenosine signaling, however, can exacerbate tissue dysfunction in chronic diseases (Antonioli et al., 2019). As suggested for the nervous system in mammals, Ado seems to act as a high pass filter for injuries by sustaining viability with low insults and bolsters the loss of viability with more intense insults (Cunha, 2016).

Adenosine signaling is well-conserved among phyla. The concentration of Ado in the *Drosophila melanogaster* hemolymph is maintained in the nanomolar range, as in mammals, and increases dramatically in adenosine deaminase mutants or during infections (Dolezelova et al., 2005; Novakova and Dolezal, 2011). Unlike mammals, *D. melanogaster* contains only a single Ado receptor (AdoR) isoform (stimulating cAMP) and several proteins that have Ado metabolic and transport activities involved in the fine regulation of adenosine levels. *D. melanogaster* adenosine deaminase-related growth factors (ADGFs), which are related to human ADA2, together with adenosine kinase (AdenoK) are the major metabolic enzymes converting extra- and intra-cellular adenosine to inosine and AMP, respectively (Zurovec et al., 2002; Maier et al., 2005; Stenesen et al., 2013). The transport of Ado across the plasma membrane is mediated by three equilibrative and two concentrative nucleoside transporters (ENTs and CNTs, respectively) similar to their mammalian counterparts. Ado signaling in *Drosophila* has been reported to affect various physiological processes, including the regulation of synaptic plasticity in the brain, proliferation of gut stem cells, hemocyte differentiation, and metabolic adjustments during the immune response (Knight et al., 2010; Mondal et al., 2011; Bajgar et al., 2015; Xu et al., 2020).

The present study examined the role of *Drosophila* Ado signaling on cytotoxic stress and aimed to clarify the underlying mechanism. Earlier reports have shown that expression of the expanded polyglutamine domain from human mutant huntingtin protein (mHTT) induces cell death in both *Drosophila* neurons and hemocytes (Marsh et al., 2000; Lin et al., 2019). In our study, we confirmed the low-viability phenotype of mHTT-expressing larvae and observed that such larvae display a lower level of e-Ado in the hemolymph. Furthermore, we used genetic tools and altered the expression of genes involved in Ado metabolism and transport to find out whether changes in Ado signaling can modify the phenotype of mHTT-expressing flies. Finally, we uncovered a downstream mechanism of the *Drosophila* Ado pathway, namely *mod(mdg4)* and heat-shock protein 70 (Hsp70), which modify both the formation of mHTT aggregates and the stress response to heat-shock and paraquat treatments.

RESULTS

Decreased Hemolymph Ado Titer in mHTT-Expressing Larvae

To characterize the involvement of Ado signaling in the stress response, we used mHTT-expressing flies as a well-characterized genetic model for neurodegeneration and cytotoxic stress (Rosas-Arellano et al., 2018). We initially examined flies overexpressing normal exon 1 from human huntingtin (Q20 HTT), or its mutant pathogenic form (Q93 mHTT), driven by the ubiquitous *daughterless-Gal4* (*da-Gal4*) and pan-neuron driver (*elav-Gal4*). We observed that 100% of Q93-expressing larvae driven by *da-Gal4* died during the wandering stage. In contrast, those driven by *elav-Gal4* displayed no impact on larval development (**Supplementary Figure 1A**) but with a reduced adult eclosion rate (**Supplementary Figure 1B**) and lifespan (**Supplementary Figure 1C**). These results are consistent with previous observations (Song et al., 2013).

Measurement of the extracellular Ado (e-Ado) concentration in the hemolymph of Q93-expressing larvae (3rd instar) showed that its level was significantly lower compared to larvae expressing Q20 or control *da-GAL4* only (**Figure 1A**). Since e-Ado concentration may be associated with the level of extracellular ATP (e-ATP), we also examined its titer in larval hemolymph. However, as shown in **Figure 1B**, there was no significant difference in e-ATP levels between Q20, Q93, and control *da-GAL4* larvae.

We thus postulated that the lower level of e-Ado in Q93 larvae might be caused by changes in genes involved in Ado metabolism or transport. Therefore, we compared the expression of *adgf* genes (*adgf-a*, *adgf-c*, and *adgf-d*), adenosine kinase (*adenoK*), adenosine transporters (*ent1*, *ent2*, *ent3*, and *cnt2*), and *adoR* in the brains of Q93- and Q20-expressing larvae driven by *elav-Gal4* (**Figure 1C**). The results showed that the expression levels of *adgf-a* and *adgf-d*, as well as transporters *ent1*, *ent2*, and *ent3*, in the brain of Q93 larvae were significantly lower than in Q20 larvae. There was no difference in the expression of *cnt2* and *adoR* between Q93 and Q20 larvae.

Enhanced e-Ado Signaling Increased Mortality of mHTT Flies

To study the effect of e-Ado signaling on mHTT-induced cytotoxicity, we compared the survival of transgenic lines that co-express RNAi constructs of Ado metabolic, transport and receptor genes together with Q93 and Q20 driven by *elav-GAL4*. The results showed that knocking down *adgf-D*, *ent1*, *ent2*, and *adoR* resulted in a significantly increased eclosion rate (**Figure 1D**), and silencing *adgf-A* and *adenoK*, *ent1*, *ent2*, and *adoR* significantly extended the adult lifespan of mHTT-expressing flies (**Figure 1E**). Notably, the RNAi silencing of *ent2* and *adoR* extended the lifespan of mHTT-expressing flies to 30 and 40 days, respectively, which is about 1.5∼2 times longer than that of control *gfp*-RNAi-expressing mHTT flies. To ensure that the mortality of the Q93 flies was mainly caused by mHTT expression and not by the RNAi constructs, we examined the survival of flies co-expressing normal htt Q20 together with RNAi transgenes until all corresponding experimental flies (expressing Q93 together with RNAi constructs) died. We did not observe a significant effect for any of the RNAi transgenes on adult survival (**Supplementary Figure 2**).

It is generally assumed that gain- and loss-of-function manipulations of functionally important genes should lead to the opposite phenotypes. We therefore tested whether the overexpression of *adgf-A*, *adenoK*, *ent2*, and *adoR* would rescue mHTT phenotypes. As shown in **Figure 1F**, increasing either the intra- or extracellular Ado metabolism by overexpressing *adenoK* and *adgf-A* in Q93 flies extended their lifespan in comparison to control Q93 flies overexpressing GFP protein. In contrast, the overexpression of *ent2* and *adoR* significantly decreased the lifespan of mHTT-expressing flies. Therefore, the overexpression

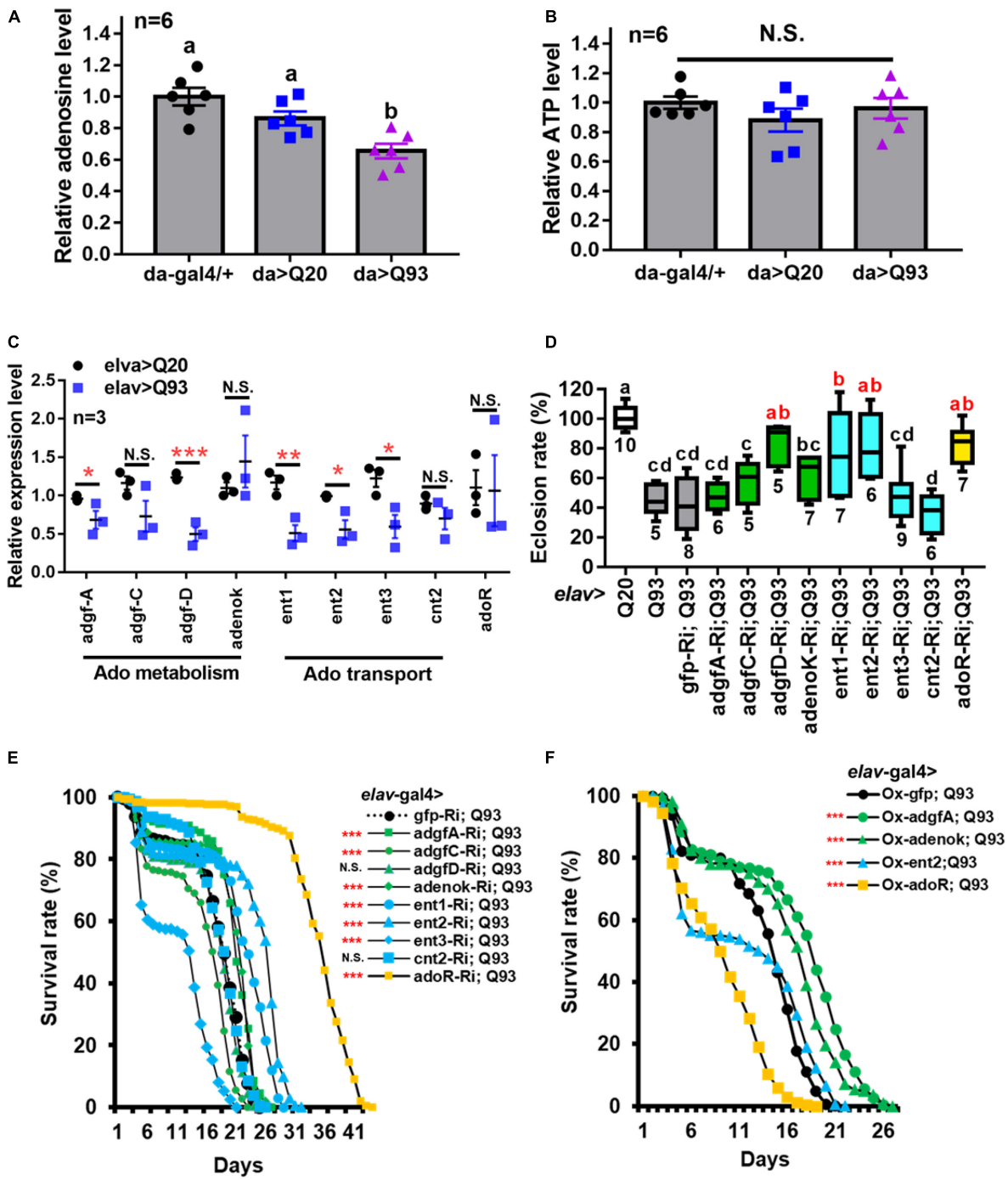

FIGURE 1 | Reduced extracellular Ado transport and receptor suppress mHTT induced lethality. **(A,B)** Relative level of extracellular Ado **(A)** and ATP **(B)** titers in Q93-expressing (da > Q93), Q20-expressing (da > Q20), and control *da*-GAL4 (da/+) larvae. Ado and ATP concentration are normalized to control larvae. Significance was analyzed by ANOVA; significant differences ($P < 0.05$) among treatment groups are marked with different letters; N.S., not significant; $n = 6$. Error bars are presented as mean ± SEM. **(C)** Transcription levels of genes involved in regulating Ado homeostasis in Q93-expressing (elav > Q93) and control Q20-expressing (elav > Q20) larval brains. Significance was analyzed by Student's *t*-test and labeled as follows: $^{*}P < 0.05$, $^{**}P < 0.01$, $^{***}P < 0.001$; N.S., not significant. $n = 3$. Error bars are presented as mean ± SEM. **(D)** Eclosion rate of mHTT-expressing adult females (elav > Q93) with RNAi silencing (Ri) Ado metabolic enzymes, transporters, *adoR*, and control *gfp*. Numbers below each column indicate the number of replicates (n). Significance was analyzed by ANOVA; significant differences ($P < 0.05$) among treatment groups are marked with different letters. **(E)** Survival of mHTT-expressing adult females (elav > Q93) with RNAi silencing (Ri) Ado metabolic enzymes, transporters, *adoR*, and control *gfp*. Significance was analyzed by weighted log-rank test; significant differences between each treatment group and control (*gfp*-Ri) are labeled as follows: $^{***}P < 0.001$; N.S., not significant. $n > 200$. **(F)** Survival of mHTT-expressing adult females (elav > Q93) overexpressing (Ox) Ado metabolic enzymes (*adgf-A* and *adenok*), transporters (*ent2*), *adoR*, and control *gfp*. Significance was analyzed by a weighted log-rank test; significant differences between each treatment group to control (*gfp*-Ri) are labeled as $^{***}P < 0.001$. $n > 200$.

of *adoR* and *ent2* genes resulted in a phenotype opposite to that observed in the knockdowns, thus supporting the importance of these genes as key regulators of mHTT phenotypes.

Knocking Down *ent2* and *adoR* Reduced Cell Death and mHTT Aggregate Formation

To determine whether the reduction of Ado signaling could affect other phenotypes of Q93 flies, we examined the effect of knocking down genes involved in Ado signaling and metabolism on *Drosophila* rhabdomere degeneration and mHTT aggregate formation. We expressed RNAi transgenes in the eyes of Q93 flies using the *gmr-GAL4* driver (Mugat et al., 2008; Kuo et al., 2013) and compared the levels of retinal pigment cell degeneration (**Figure 2A**). The results revealed that silencing Ado metabolic enzymes did not significantly influence the level of retinal pigment cell degeneration; however, retinal pigment cell degeneration was significantly reduced in *ent2* knockdown flies. Surprisingly we did not observe a significant rescue of cell death by silencing *adoR* (**Supplementary Figure 3**). We therefore assumed that it might be due to insufficient RNAi efficiency for suppressing AdoR signaling in the eye. To test this, we examined two combinations: mHTT-expressing flies with the adoR RNAi transgene under an adoR heterozygous mutant background ($AdoR^1/+$), and mHTT-expressing flies under an $AdoR^1$ homozygous mutant background. As shown in **Figure 2A**, both had significantly rescued retinal pigment cell degeneration, similar to that of *ent2* RNAi flies.

To examine the level of mHTT aggregate formation in the *Drosophila* brain, we drove the expression of transgenes using *elav-GAL4* and stained the brains with mHTT antibody (MW8), which exclusively stains mHTT inclusions (Ko et al., 2001). The results showed that mHTT inclusions were reduced to 50% in 10-day-old Q93 *adoR* RNAi flies (**Figures 2B,C**), with 20-day-old Q93 *adoR* RNAi flies exhibiting a similar level of suppression (**Supplementary Figure 4**). Our results demonstrate that decreased e-Ado signaling by either knocking down the transporter *ent2* or *adoR* has a strong influence on reducing mHTT-induced cell cytotoxicity and mHTT aggregate formation.

Epistatic Interaction of *adoR* and *ent2* on mHTT-Induced Mortality

The above results indicated that knockdown of *adoR*, *ent1*, or *ent2* expression significantly extended the adult longevity of mHTT files (**Figure 1E**). Therefore, we next tested whether there is a synergy between the effects of *adoR* and both transporters. First, we co-expressed *adoR* RNAi constructs with *ent1* RNAi in Q93-expressing flies. As shown in **Figure 3A**, the double knockdown of *ent1* and *adoR* shows a sum of individual effects on lifespan which is greater than the knockdown of *adoR* alone. There seems to be a synergy between *ent1* and *adoR*, suggesting that *ent1* may have its own effect which is partially independent from *adoR* signaling. In contrast, when we performed a double knockdown of *adoR* and *ent2* RNAi in Q93-expressing flies, the silencing of both had the same effect as silencing *adoR* only, indicating that they are involved in the same pathway.

Identification of Potential Downstream Targets of the AdoR Pathway

Our results indicate that *ent2* and *adoR* modify mHTT cytotoxicity and belong to the same pathway. To identify their potential downstream target genes, we compared the gene expression profiles of larvae carrying mutations in *adoR* or *ent2* as well as adult *adoR* mutants by using microarrays (Affymetrix). The data are presented as Venn diagrams, which show the intersection between differentially expressed genes for individual mutants in all three data sets, including six upregulated (**Figure 3B**) and seven downregulated mRNAs (**Figure 3C**). According to Flybase annotations[1], four of these genes were expressed in the nervous system (*ptp99A* was upregulated, while *CG6184*, *cindr*, and *mod(mdg4)* were downregulated) (**Supplementary Table 1**).

In order to examine the potential roles of these four genes in the interaction with mHTT, we co-expressed RNAi constructs of these candidate genes with mHTT and assessed the adult lifespan (**Figure 3D**). The results showed that only the knockdown of *mod(mdg4)* extended the lifespan of mHTT-expressing flies, and that the survival curve was not significantly different from that of *adoR* RNAi Q93 flies. Furthermore, *mod(mdg4)* RNAi was the only one of these constructs that significantly reduced retinal pigment cell degeneration (**Figure 3E**) and decreased the formation of mHTT inclusions (**Figures 3F,G**).

We next examined the possible epistatic relationship between *ent2*, *adoR*, and *mod(mdg4)* by combining the overexpression of *ent2* or *adoR* with *mod(mdg4)* RNAi in mHTT-expressing flies (**Figure 3H**). The results showed that the knockdown of *mod(mdg4)* RNAi was able to minimize the lethal effects caused by *ent2* and *adoR* overexpression in mHTT flies. This indicated that *mod(mdg4)* is a downstream target of the AdoR pathway. In addition, we found that increasing the e-Ado concentration by microinjecting Ado significantly increased *mod(mdg4)* expression in GAL4 control flies but not in the flies with *adoR* knockdown (**Figure 3I**). *mod(mdg4)* expression in the brain of mHTT Q93 larvae was lower than in control Q20 HTT larvae (**Figure 3J**). This result is consistent with a lower e-Ado level in Q93 mHTT larvae (**Figure 1A**).

Taken together, our results demonstrate that *mod(mdg4)* serves as a major downstream target of the AdoR pathway, modulating the process of mHTT inclusion formation and mHTT-induced cytotoxicity.

AdoR Pathway With Mod(mdg4) as Regulators of Hsp70 Protein Production

Earlier studies on *Drosophila* protein two-hybrid screening have indicated that Mod(mdg4) is able to interact with six proteins from the Hsp70 family (Giot et al., 2003; Oughtred et al., 2019). In addition, Hsp70 family proteins are known to contribute to suppressing mHTT aggregate formation (Warrick et al., 1999; Chan et al., 2000). In the present study, we compared the levels of Hsp70 protein in *adoR* and *mod(mdg4)* RNAi flies (**Figures 4A,B** and **Supplementary Figure 5**); the results showed that both

[1]http://flybase.org

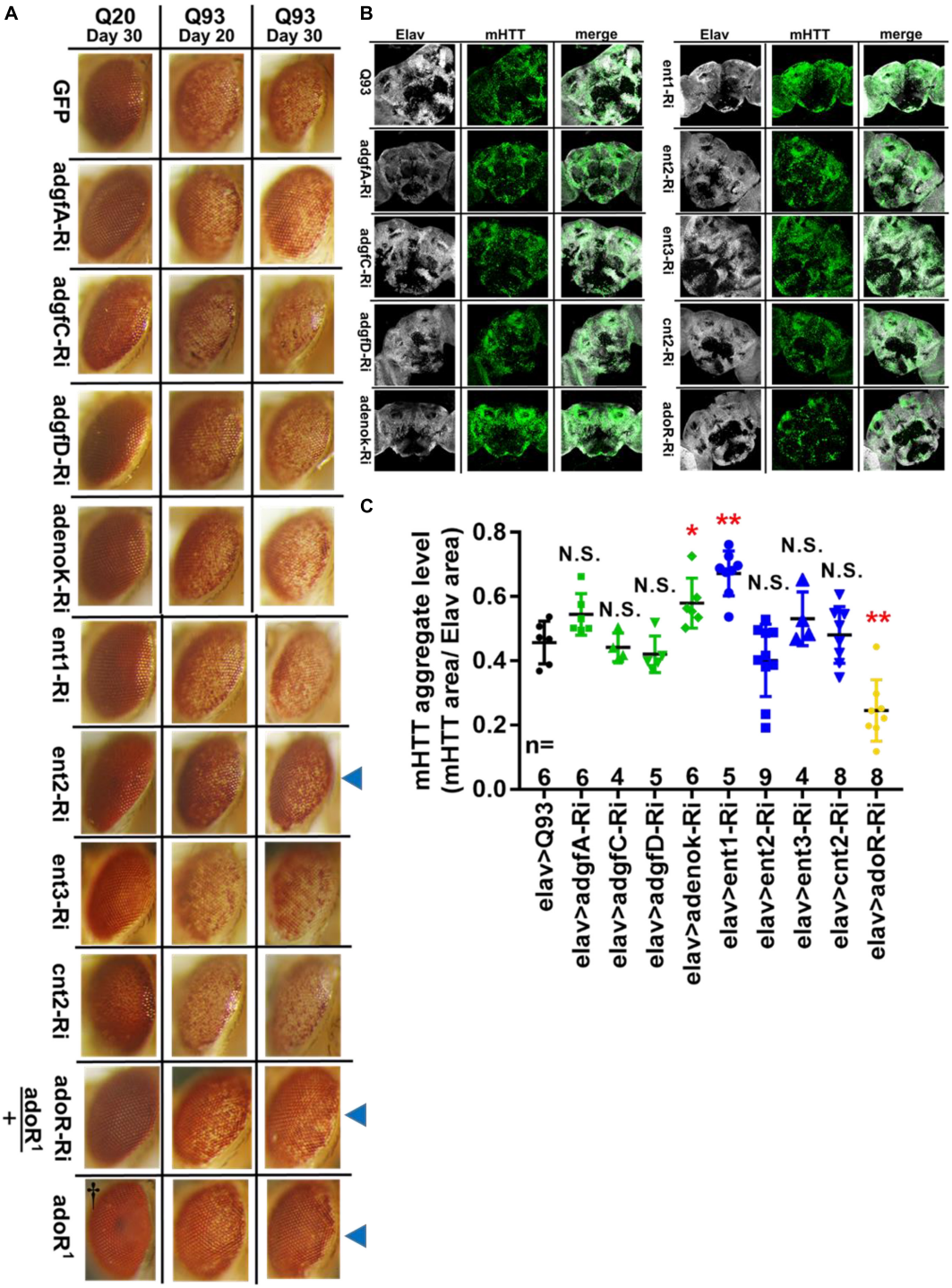

FIGURE 2 | Suppression of *ent2* and *adoR* decreased mHTT-induced cytotoxicity and mHTT aggregate formation. **(A)** Retinal pigment cell degeneration in mHTT-expressing adult females (gmr > Q93) with RNAi silencing Ado metabolic enzymes, transporters, *adoR* (*adoR* heterozygous mutant background), and mHTT-expressing flies under *adoR* homozygous mutant background. Blue arrows indicate treated groups showing a significantly reduced loss of pigment. †Eye image of control homozygous $adoR^1$ mutant without *htt* expression. Detailed methodologies for sample collection and eye imaging are described in section "Materials and Methods." **(B)** Representative confocal images of the brains of 10-day-old mHTT-expressing adult females (elav > Q93) with RNAi silencing Ado metabolic enzymes, transporters, and *adoR*. Neuronal cells were detected with anti-Elav; mHTT aggregates were detected with anti-HTT (MW8). **(C)** Level of mHTT aggregate formation was calculated by normalizing the area of mHTT signal to the area of Elav signal. Significance in mHTT aggregate levels was analyzed using a Mann–Whitney *U*-test; significant differences between control Q93 flies and each RNAi treatment group are labeled as follows: $*P < 0.05$; $**P < 0.01$; N.S., not significant. Error bars are presented as mean ± SEM. The number (n) of examined brain images are shown below each bar.

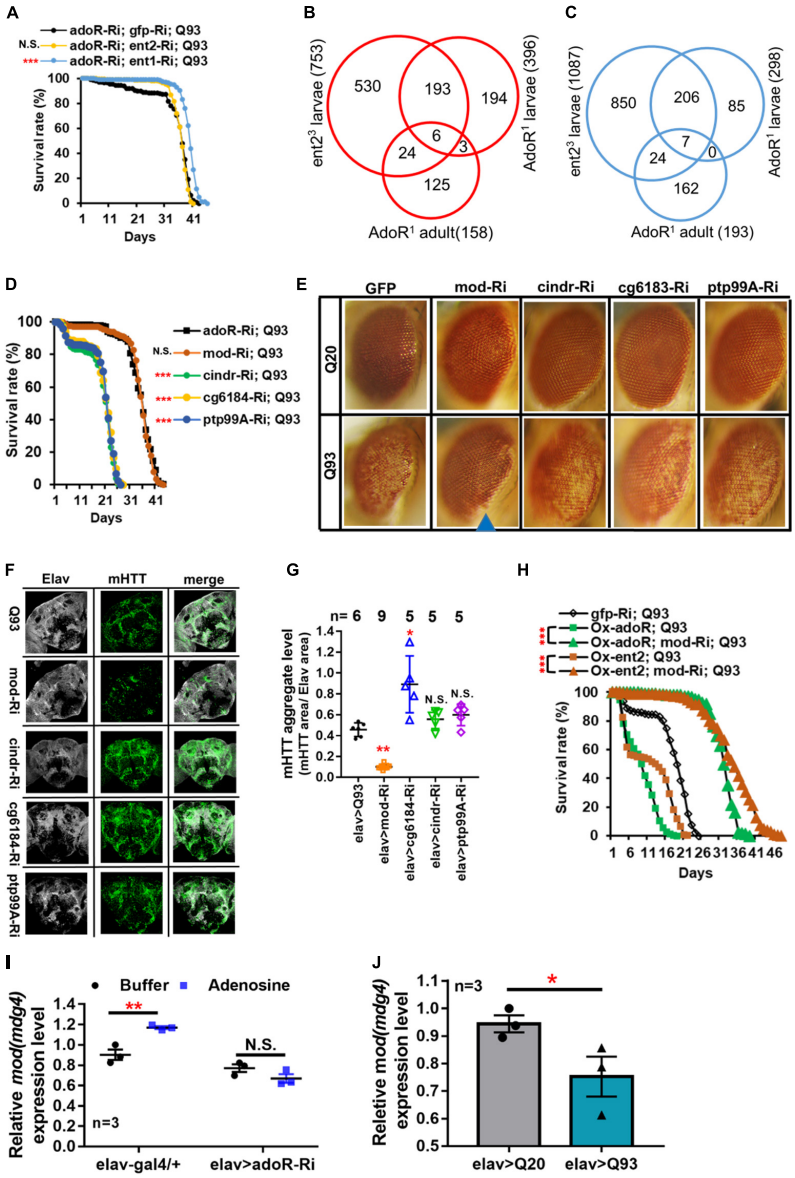

FIGURE 3 | Mod(mdg4) as a downstream target of ENT2/AdoR pathway modulated mHTT effects and aggregate formation. **(A)** Survival of mHTT-expressing adult females (elav > Q93) with RNAi co-silencing (Ri) transporters (*ent1* or *ent2*), and *adoR*. Significance was analyzed by a weighted log-rank test; significant differences between each treatment group and control (*gfp*-Ri) are labeled as follows: ***$P < 0.001$; N.S., not significant. $n > 200$. **(B,C)** Microarray analysis of the transcriptomes of *ent2* and *adoR* mutants. Venn diagram shows the number of common genes (in intersect region) which were upregulated **(B)** or downregulated **(C)** among the *adoR* mutant larvae vs. control (w^{1118}), *adoR* mutant adults vs. control (w^{1118}), and ent2 mutant larvae vs. control (w^{1118}). The cutoff values for expression differences were set at $Q < 0.05$ (false discovery rate, FDR). **(D)** Survival of mHTT-expressing adult females (elav > Q93) with RNAi co-silencing (Ri) of potential downstream genes of the ENT2/AdoR pathway. Significance was analyzed by a weighted log-rank test; significant differences between each treatment group to control (*adoR*-Ri) are labeled as follows: ***$P < 0.001$; N.S., not significant. $n > 200$. **(E)** Retinal pigment cell degeneration in mHTT-expressing adult females (gmr > Q93) with RNAi silencing potential downstream genes of the ENT2/AdoR pathway. Blue arrows indicate treated groups showing a significantly reduced loss of pigment. Detailed methodologies for sample collection and eye imaging are described in section "Materials and Methods." **(F)** Representative confocal images of the brains of 10-day-old mHTT-expressing adult females (elav > Q93) with RNAi silencing potential downstream genes of the ENT2/AdoR pathway. Neuronal cells were detected with anti-Elav and mHTT aggregates were detected with anti-HTT (MW8). **(G)** The level of mHTT aggregate formation was calculated by normalizing the area of mHTT signal to the area of Elav signal. Significance in mHTT aggregate levels was analyzed using a Mann–Whitney *U*-test; significant differences between control Q93 flies and each RNAi treatment group are labeled as follows: *$P < 0.05$; **$P < 0.01$; N.S., not significant. Error bars are presented as mean ± SEM. The number (n) of examined brain images are indicated above each bar. **(H)** Survival of mHTT-expressing adult females (elav > Q93) with co-RNAi silencing *mod(mdg4)* and co-overexpressing *adoR* or *ent2*. Significance was analyzed by a weighted log-rank test; significant differences are labeled as ***$P < 0.001$. $n > 200$. **(I)** Transcription level of *mod(mdg4)* 2 h after Ado injection into the whole body of 3- to 5-day old control adult females (elav-gal4/+) and *adoR* RNAi females (elav > adoR-Ri). Significance was analyzed by Student's *t*-test and labeled as follows: **$P < 0.01$; N.S., not significant. $n = 3$. Error bars are presented as mean ± SEM. **(J)** Transcription levels of *mod(mdg4)* in Q93-expressing (elav > Q93) and control Q20-expressing (elav > Q20) larval brains. Significance was analyzed by Student's *t*-test and labeled as *$P < 0.05$. $n = 3$. Error bars are presented as mean ± SEM.

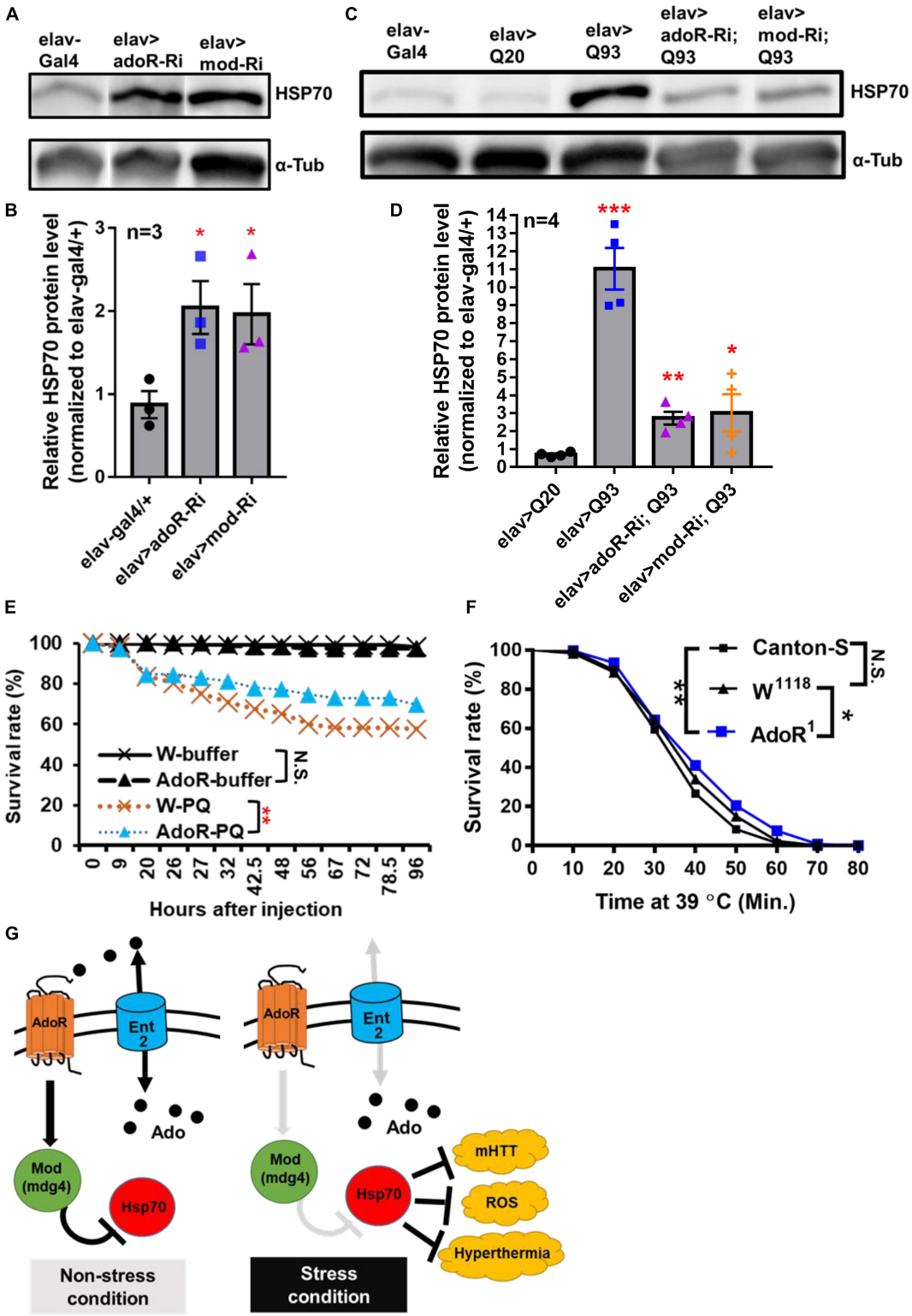

FIGURE 4 | AdoR regulated the Hsp70 protein level and influenced the stress response to paraquat and heat-shock treatments. **(A,B)** Representative images of western blot analysis. **(A)** Hsp70 protein level in the head of 10-day-old adult females with RNAi Silencing of (elav > adoR-Ri), *mod(mdg4)* (elav > mod-Ri), and control (elav-gal4/+). **(B)** The Hsp70 protein level was quantified by normalizing the intensity of the Hsp70 band to the α-tubulin band using ImageJ; values of RNAi treatment groups were further normalized to the elav-gal4 control. Significance was analyzed by Student's *t*-test; significant differences between the control

(Continued)

FIGURE 4 | Continued
and each RNAi treatment group are labeled as $^{*}P < 0.05$. $n = 3$. Error bars are presented as mean ± SEM. Original gel images are presented in the **Supplementary Figure 6**. **(C,D)** Representative images of western blot analysis. **(C)** Hsp70 protein level in the head of 10-day-old HTT (elav > Q20) or mHTT expressing (elav > Q93) adult females with RNAi silencing *adoR* and *mod(mdg4)*. **(D)** The Hsp70 protein level was quantified by normalizing the intensity of the Hsp70 band to the α-tubulin band by using ImageJ; values of each treatment group were further normalized to the elav-gal4 control. Significance was analyzed by Student's *t*-test; significant differences between HTT-expressing flies (elav > Q20) and each RNAi treatment of Q93-expressing flies are labeled as follows: $^{*}P < 0.05$, $^{**}P < 0.01$, $^{***}P < 0.001$. $n = 4$. Error bars are presented as mean ± SEM. Original gel images are presented in the **Supplementary Figure 7**. **(E)** Survival of w^{1118} and homozygous *adoR* mutant adult males after paraquat (PQ) injection. Control groups were injected with ringer buffer. Significance was analyzed by weighted log-rank test; significant differences are labeled as follows: $^{**}P < 0.01$, N.S., not significant. W-ringer, $n = 116$; $AdoR^{1}$-ringer, $n = 118$; W-PQ, $n = 118$; and $AdoR^{1}$-PQ, $n = 119$. **(F)** Survival of Cantons-S, w^{1118} and homozygous *adoR* mutant ($AdoR^{1}$) adult males during heat-shock treatment. Significance was analyzed by weighted log-rank test; significant differences are labeled as follows: $^{*}P < 0.05$, $^{**}P < 0.01$. Cantons-S and W^{1118}, $n = 300$; $AdoR^{1}$, $n = 370$. **(G)** Summary model of Ado signaling under stress response. Under a non-stress condition, the activated AdoR and Mod(mdg4) reduce Hsp70 production. In contrast, decreased Ado signaling under a stress condition resulted in Hsp70 production, which in turn enhanced stress tolerance.

knockdowns doubled the level of Hsp70 compared to *elav-Gal4* control flies under a non-stress condition (i.e., without mHTT expression). We next compared the level of Hsp70 in flies co-expressing mHTT with each RNAi construct (**Figures 4C,D** and **Supplementary Figure 6**). Interestingly, both *adoR* and *mod(mdg4)* RNAi flies co-expressing Q93 mHTT again showed levels around two-fold higher than the Q20 HTT-expressing control, although it was around ten times higher in Q93 mHTT-only flies. These results indicate that *adoR* and *mod(mdg4)* are able to suppress Hsp70 protein production under a non-stress condition. The knockdown of *adoR* and *mod(mdg4)* leads to an increase of Hsp70 production, thus preventing mHTT aggregate formation and decreasing mHTT cytotoxicity.

Decreased Susceptibility to Oxidative and Heat-Shock Stresses in *adoR* Mutant Flies

Since Hsp70 proteins are also involved in the response against oxidative stress (Azad et al., 2011; Shukla et al., 2014; Donovan and MarrII, 2016) and heat-shock stress (Gong and Golic, 2006; Bettencourt et al., 2008; Shilova et al., 2018) in *Drosophila*, we postulated that increased Hsp70 production by decreased e-Ado signaling may also enhance the resistance against both stresses. To test this, we treated flies with either paraquat (a potent oxidative stress inducer; **Figure 4E**) or a higher temperature (to induce heat-shock; **Figure 4F**). We then compared the survival rate between the mutant flies and w^{1118} or Canton-S control flies. The results showed that *adoR* mutant flies were more resistant to paraquat and heat-shock treatment. Our results therefore demonstrate that the *Drosophila* AdoR pathway with its downstream gene *mod(mdg4)* suppresses Hsp70 protein production under a non-stress condition. Thus, the knockdown of *ent2*, *AdoR*, and *mod*(*mdg4*) results in increased levels of Hsp70, which in turn helps flies to respond to various stresses, including mHTT cytotoxicity, oxidative, and heat-shock stresses (**Figure 4G**).

DISCUSSION

Adenosine signaling represents an evolutionarily conserved pathway affecting a diverse array of stress responses (Fredholm, 2007). As a ubiquitous metabolite, Ado has evolved to become a conservative signal among eukaryotes. In previous studies, *Drosophila adoR* mutants (Dolezelova et al., 2007; Wu et al., 2009) and mice with a knockout of all four *adoRs* (Xiao et al., 2019) both displayed minor physiological alteration under normal conditions. This is consistent with the idea that Ado signaling more likely regulates the response to environmental changes (stresses) rather than being involved in maintaining fundamental homeostasis in both insect and mammalian models (Cunha, 2019). Our study examined the impact of altering the expression of genes involved in Ado signaling and metabolism on the cytotoxicity and neurodegeneration phenotype of Q93 mHTT-expressing flies. We discovered a novel downstream target of this pathway, *mod(mdg4)*, and showed its effects on the downregulation of Hsp70 proteins, a well-known chaperone responsible for protecting cells against various stress conditions, including mHTT cytotoxicity, as well as thermal or oxidative stress (Soares et al., 2019).

The low level of Ado observed in our *da-Gal4* mHTT flies suggests that it might have a pathophysiological role; lowering of the Ado level might represent a natural response to cytotoxic stress. Consistently, our experimentally decreased Ado signal rescued the mHTT phenotype, while an increased Ado signal had deleterious effects. Interestingly, a high level of Ado in the hemolymph has previously been observed in *Drosophila* infected by a parasitoid wasp (Novakova and Dolezal, 2011; Bajgar et al., 2015). A raised e-Ado titer has not only been shown to stimulate hemocyte proliferation in the lymph glands (Mondal et al., 2011), but also to trigger metabolic reprogramming and to switch the energy supply toward hemocytes (Bajgar et al., 2015). In contrast, our experiments show that a lowered e-Ado titer results in increased Hsp70 production. Increased Hsp70 has previously been shown to protect the cells from protein aggregates and cytotoxicity caused by mHTT expression, as well as some other challenges including oxidative stress (paraquat treatment) or heat-shock (Garbuz, 2017). The fine regulation of extracellular Ado in *Drosophila* might mediate the differential Ado responses via a single receptor isoform. Our earlier experiments on *Drosophila* cells also suggested that different cell types have different responses to Ado signaling (Fleischmannova et al., 2012).

Our data also showed that altered adenosine signaling through the receptor is closely connected to Ado transport, especially to ent2 transporter function. We observed that *adoR* and *ent2*

knockdowns provide the most prominent rescue of mHTT phenotypes. In addition, the overexpression of *adoR* and *ent2* genes results in effects that are opposite to their knockdowns, thus supporting the importance of these genes as key regulators of mHTT phenotypes. Our previous report showed that responses to *adoR* and *ent2* mutations cause identical defects in associative learning and synaptic transmission (Knight et al., 2010). In the present study, we show that the phenotypic response of mHTT flies to *adoR* and *ent2* knockdowns are also identical. Our results suggest that the source of e-Ado for inducing AdoR signaling is mainly released by *ent2*. Consistently, the knockdown of *ent2* has previously been shown to block Ado release from *Drosophila* hemocytes upon an immune challenge (Bajgar et al., 2015), as well as from wounded cells stimulated by *scrib*-RNAi (Poernbacher and Vincent, 2018) or bleomycin feeding (Xu et al., 2020). These data support the idea that both *adoR* and *ent2* work in the same signaling pathway.

Our results revealed that lower AdoR signaling has a beneficial effect on mHTT-expressing flies, including increasing their tolerance to oxidative and heat-shock stresses. The effect of lower Ado signaling in mammals has been studied by pharmacologically blocking AdoRs, especially by the non-selective adenosine receptor antagonist caffeine. Interestingly, caffeine has beneficial effects on both neurodegenerative diseases and oxidative stress in humans (Rivera-Oliver and Diaz-Rios, 2014; Martini et al., 2016). In contrast, higher long-term Ado concentrations have cytotoxic effects by itself in both insect and mammalian cells (Schrier et al., 2001; Merighi et al., 2002). Chronic exposure to elevated Ado levels has a deleterious effect, causing tissue dysfunction, as has been observed in a mammalian system (Antonioli et al., 2019). Extensive disruption of nucleotide homeostasis has also been observed in mHTT-expressing R6/2 and Hdh150 mice (Toczek et al., 2016).

We identified a downstream target of the AdoR pathway, *mod(mdg4)*, which modulates mHTT cytotoxicity and aggregations. This gene has previously been implicated in the regulation of position effect variegation, chromatin structure, and neurodevelopment (Dorn and Krauss, 2003). The altered expression of *mod(mdg4)* has been observed in flies expressing untranslated RNA containing CAG and CUG repeats (Mutsuddi et al., 2004; Van Eyk et al., 2011). In addition, *mod(mdg4)* has complex splicing, including *trans*-splicing, producing at least 31 isoforms (Krauss and Dorn, 2004). All isoforms contain a common N-terminal BTB/POZ domain which mediates the formation of homomeric, heteromeric, and oligomeric protein complexes (Bardwell and Treisman, 1994; Albagli et al., 1995; Espinas et al., 1999). Among these isoforms, only two [including *mod(mdg4)*-56.3 (isoform H) and *mod(mdg4)*-67.2 (isoform T)] have been functionally characterized. *mod(mdg4)*-56.3 is required during meiosis for maintaining chromosome pairing and segregation in males (Thomas et al., 2005; Soltani-Bejnood et al., 2007). *mod(mdg4)*-67.2 interacts with suppressor of hairy wing [Su(Hw)] and Centrosomal protein 190 kD (CP190) forming a chromatin insulator complex which inhibits the action of adjacent enhancers on the promoter, and is important for early embryo development and oogenesis (Buchner et al., 2000; Soshnev et al., 2013; Melnikova et al., 2018). In the present study, we showed that *mod(mdg4)* is controlled by AdoR which consecutively works as a suppressor of Hsp70 chaperone. The downregulation of *adoR* or *mod(mdg4)* leads to the induction of Hsp70, which in turn suppresses mHTT aggregate formation and other stress phenotypes. Although our results showed that silencing all *mod(mdg4)* isoforms decreases cytotoxicity and mHTT inclusion formation, we could not clarify which of the specific isoforms is involved in such effects, since AdoR seems to regulate the transcriptions of multiple isoforms (**Supplementary Figure 7**). Further study will be needed to identify the specific *mod(mdg4)* isoform(s) connected to Hsp70 production.

In summary, our data suggest that the cascade (*ent2*)-*AdoR-mod(mdg4)-Hsp70* might represent an important general Ado signaling pathway involved in the response to various stress conditions, including reaction to mHTT cytotoxicity, oxidative damage, or thermal stress in *Drosophila* cells. The present study provides important insights into the molecular mechanisms of how Ado regulates mHTT aggregate formation and stress responses in *Drosophila*; this might be broadly applicable for understanding how the action of Ado affects disease pathogenesis.

MATERIALS AND METHODS

Fly Stocks

Flies were reared at 25°C on standard cornmeal medium. The following RNAi lines were acquired from the TRiP collection (Transgenic RNAi project) at Harvard Medical School: adgfA-Ri (BL67233), adgfC-Ri (BL42915), adgfD-Ri (BL56980), adenoK-Ri (BL64491), ent1-Ri (BL51055), adoR-Ri (BL27536), gfp-Ri (BL41552), mod(mdg4)-Ri (BL32995), cindr-Ri (BL38976), and ptp99A-Ri (BL57299). The following RNAi lines were acquired from the Vienna Drosophila RNAi Center (VDRC): ent2-Ri (ID100464), ent3-Ri (ID47536), cnt2-Ri (ID37161), and cg6184-Ri (ID107150).

Flies overexpressing human normal huntingtin (HTT) exon 1, Q20Httexon^{1111F1L}, mutant pathogenic fragments (mHTT), Q93Httexon^{14F132} and elav^{C155}-GAL4 were obtained from Prof. Lawrence Marsh (UC Irvine, United States) (Steffan et al., 2001). The UAS-overexpression lines, Ox-adenoK and Ox-adoR, were obtained from Dr. Ingrid Poernbacher (The Francis Crick Institute, United Kingdom) (Poernbacher and Vincent, 2018). gmr-GAL4 was obtained from Dr. Marek Jindra (Biology Centre CAS, Czechia). da-GAL4 was obtained from Dr. Ulrich Theopold (Stockholm University). The UAS overexpression strains Ox-adgfA, Ox-ent2, adoR^{1} and ent2^{3} mutant flies, were generated in our previous studies (Dolezal et al., 2003, 2005; Dolezelova et al., 2007; Knight et al., 2010).

Eclosion Rate and Adult Lifespan Assay

For assessing the eclosion rate, male flies containing the desired RNAi or overexpression transgene (RiOx) in the second chromosome with genotype w^{1118}/Y; RiOx/CyO; UAS-Q93/MKRS were crossed with females of *elav-GAL4*; +/+; +/+. The ratio of eclosed adults between *elav-GAL4*/+; RiOx/+; UAS-Q93/+ and *elav-GAL4*/+; RiOx/+; +/MKRS was then calculated.

If the desired RiOx transgene was in the third chromosome, female flies containing *elav-GAL4*; +/+; RiOx were crossed with male w^{1118}/Y; +/+; UAS-Q93/MKRS, and the ratio of eclosed adults between *elav-GAL4*; +/+; RiOx/UAS-Q93 and *elav-GAL4*; +/+; RiOx/MKRS was calculated. If the ratio showed higher than 100%, it indicated that the number of Q93 or Q20 flies containing RiOx was higher than the flies containing only RiOx construct without Q93 or Q20 expression.

For the adult survival assay, up to 30 newly emerged female adults were placed in each cornmeal-containing vial and maintained at 25°C. At least 200 flies of each genotype were tested and the number of dead flies was counted every day. Flies co-expressing RiOx and HTT Q20 were used for evaluating the effect of RNAi or overexpression of the desired transgenes.

Extracellular Adenosine and ATP Level Measurements

To collect the hemolymph, 6 third-instar larvae (96 h post-oviposition) were torn in 150 μl of 1× PBS containing thiourea (0.1 mg/ml) to prevent melanization. The samples were then centrifuged at 5000 × *g* for 5 min to separate the hemocytes and the supernatant was collected for measuring the extracellular adenosine or ATP level. For measuring the adenosine titer, 10 μl of hemolymph was mixed with the reagents of an adenosine assay kit (Biovision) following the manufacturer's instructions. The fluorescent intensity was then quantified (Ex/Em = 533/587 nm) using a microplate reader (BioTek Synergy 4). For measuring the ATP level, 10 μl of hemolymph was incubated with 50 μl of CellTiter-Glo reagent (Promega) for 10 min. Then, the luminescent intensity was quantified using an Orion II microplate luminometer (Berthold). To calibrate the standard curve of ATP concentration, 25 μM ATP standard solution (Epicenter) was used for preparing a concentration gradient (0, 2, 4, 6, 8, and 10 μM) of ATP solution and the luminescent intensity was measured for each concentration. The protein concentration of the hemolymph sample was determined by a Bradford assay. The adenosine and ATP concentrations were first normalized to protein concentration. Then, the values of Q20 and Q93 samples were normalized to values of the *GAL4* control sample. Six independent replicates for each genotype were performed for the analysis of adenosine and ATP levels.

RNA Extraction

The brains of 10 third-instar larvae (96 h post-oviposition) or 15 whole female flies were pooled for each replicate. The samples were first homogenized in RiboZol (VWR) and the RNA phase was separated by chloroform. For brain samples, the RNA was precipitated by isopropanol, washed in 75% ethanol, and dissolved in nuclease-free water. For whole fly samples, the RNA phase was purified using NucleoSpin RNA columns (Macherey-Nagel) following the manufacturer's instructions. All purified RNA samples were treated with DNase to prevent genomic DNA contamination. cDNA was synthesized from 2 μg of total RNA using a RevertAid H Minus First Strand cDNA Synthesis Kit (Thermo Fisher Scientific).

Adenosine Injection

Three- to five-day-old female adults were injected with 50 nl of 10 mM adenosine solution using a NANOJECT II (Drummond Scientific); control flies were injected with 50 nl of 1× PBS. Two hours post-injection, 15 injected flies for each replicate were collected for RNA extraction.

Microarray Analysis

The Affymetrix GeneChip® *Drosophila* genome 2.0 array system was used for microarray analysis following the standard protocol: 100 ng of RNA was amplified with a GeneChip 3′ express kit (Affymetrix), and 10 μg of labeled cRNA was hybridized to the chip according to the manufacturer's instructions. The statistical analysis of array data was as described in our previous studies (Arefin et al., 2014; Kucerova et al., 2016). Storey's *q* value [false discovery rate (FDR)] was used to select significantly differentially transcribed genes ($q < 0.05$). Transcription raw data are shown in **Supplementary Table 2** and have been deposited in the ArrayExpress database[2] (accession No. E-MTAB-8699 and E-MTAB-8704).

qPCR and Primers

5× HOT FIREPol® EvaGreen® qPCR Mix Plus with ROX (Solis Biodyne) and an Eco Real-Time PCR System (Illumina) were used for qPCR. Each reaction contained 4 μl of EvaGreen qPCR mix, 0.5 μl each of forward and reverse primers (10 μM), 5 μl of diluted cDNA, and ddH2O to adjust the total volume to 20 μl. The list of primers is shown in **Supplementary Table 3**. The expression level was calculated using the $2^{-\Delta\Delta Ct}$ method with the ct values of target genes normalized to a reference gene, ribosomal protein 49 (*rp49*).

Imaging of Retinal Pigment Cell Degeneration

Twenty- and thirty-day-old female adults were collected and their eye depigmentation phenotypes were recorded. At least 30 individuals for each genotype were examined under a microscope, and at least five representative individuals were chosen for imaging. Pictures were taken with an EOS 550D camera (Canon) mounted on a SteREO Discovery V8 microscope (Zeiss).

Brain Immunostaining

Brains dissected from 10- or 20-day-old adult females were used for immunostaining. The brains were fixed in 4% PFA, permeabilized with PBST (0.1% Triton X-100), blocked in PAT (PBS, 0.1% Triton X-100, 1% BSA), and stained with antibodies in PBT (PBS, 0.3% Triton X-100, 0.1% BSA). Primary antibodies used in this study were mouse anti-HTT; MW8, which specifically binds to mHTT aggregates (1:40, DSHB); and rat anti-Elav (1:40, DSHB), which is a pan-neuronal antibody. Secondary antibodies were Alexa Fluor 488 anti-mouse and Alexa Fluor 647 anti-rat (1:200, Invitrogen). The samples were mounted in Fluoromount-G (Thermo Fisher Scientific) overnight, prior to image examination.

[2]www.ebi.ac.uk/arrayexpress

Quantification of mHTT Aggregates

Images of aggregates were taken using a FluoView 100 confocal microscope (Olympus). The intensity of mHTT aggregates detected by anti-HTT antibody (MW8) or anti-Elav was quantified using ImageJ software. The level of mHTT aggregates was determined by calculating the ratio between areas of mHTT to the Elav signal. At least six brain images from each genotype were analyzed.

Western Blot

Twenty heads, collected from 10-day-old adult females, were pooled for each replicate. The samples were homogenized in 100 μl of RIPA buffer with 1 μl of Halt^{TM} proteinase inhibitor cocktail (Thermo Fisher Scientific). From each sample, 80 μl of supernatant was collected after 10 min of centrifugation at 12000 × *g*, which was then mixed with 16 μl of 6× loading buffer. After boiling at 95°C for 3 min, 10 μl were then loaded for running an SDS-PAGE gel. Proteins were then transfered to an Immobilon-E PVDF membrane (Millipore), which was then washed with 1× PBS containing 0.05% Tween 20 (three washes, each 15 min) and blocked in 5% BSA for 1 h at room temperature before staining. The membrane was subsequently stained with primary antibodies overnight at 4°C and secondary antibody for 1 h at room temperature. After immunostaining, the membrane was treated with 2 ml of SuperSignal^{TM} West Pico PLUS Chemiluminescent Substrate (Thermo Fisher Scientific) for 10 min at room temperature, and images were recorded using a Fujifilm LAS-3000 Imager. The primary antibodies used for staining were rat anti-Hsp70 (7FB) (1:2000, Thermo Fisher Scientific) and mouse anti-Tub (1:500, DSHB). The secondary antibodies were donkey anti-rat IgG (H + L) HRP (1:5000, Thermo Fisher Scientific) and donkey anti-Mouse IgG (H + L) HRP (1:5000, Thermo Fisher Scientific).

Paraquat Injection

Three- to five-day-old males were collected for paraquat injection. Each fly was injected with 50 nl of 3 mM paraquat ringer solution using a NANOJECT II (Drummond Scientific). Control flies were injected with ringer buffer. 70–20 of injected flies were pooled into one vial for each replicate, and six replicates were performed for each treatment.

Heat-Shock Treatment

The heat-shock procedure followed a previous study (Gong and Golic, 2006) with few modifications. Newly emerged males (0 or 1 day old) were collected and maintained on a standard cornmeal diet. The following day, 10 flies were transferred into each empty vial and given a mild heat-shock at 35°C for 30 min, then transferred to a circulating water bath at 39°C. The number of surviving flies was checked every 10 min; flies which did not move any part of their body were considered dead.

Statistical Analysis

A Shapiro–Wilk test was applied to determine data normality. For data which were not normally distributed ($P < 0.05$), statistical significance was analyzed using the Mann–Whitney *U*-test. For normally distributed data ($P > 0.05$), statistical significance was established using Student's *t*-test or one-way ANOVA with Tukey's HSD *post hoc* test. For the statistical analysis of survival curves, we used OASIS 2 to perform a weighted log-rank test (Han et al., 2016).

DATA AVAILABILITY STATEMENT

The datasets presented in this study can be found in online repositories. The names of the repository/repositories and accession number(s) can be found in the article/ **Supplementary Material**.

AUTHOR CONTRIBUTIONS

Y-HL performed the experiments and prepared the manuscript. HM assisted in recording the adult lifespan and eye phenotypes, and also as performed the brain dissection, immunochemistry, and confocal microscopy imaging. LK performed the microarray sample preparation, analyzed the microarray data and paraquat injection. LR assisted in recording the adult lifespan and eye phenotypes, prepared the fly strains, and performed the heat-shock treatment. TF established the methodologies for recording the eclosion rate and survival, and prepared the fly strains. MZ conceived the project and supervised the manuscript preparation. All authors contributed to the article and approved the submitted version.

FUNDING

This work was supported by the grant agency of the University of South Bohemia (065/2017/P to Y-HL), junior grant project GACR (19-13784Y to LK), and European Community's Program Interreg Österreich-Tschechische Republik (REGGEN/ATCZ207 to MZ).

ACKNOWLEDGMENTS

We thank Dr. Ingrid Poernbacher (The Francis Crick Institute, United Kingdom), Prof. Lawrence Marsh (UC Irvine, United States), Dr. Marek Jindra (Biology Centre CAS, Czechia), Dr. Tomas Dolezal (University of South Bohemia, Czechia), Dr. Ulrich Theopold (Stockholm University), Bloomington *Drosophila* Stock Center, and Vienna *Drosophila* Resource Center for providing us with fly strains.

SUPPLEMENTARY MATERIAL

The Supplementary Material for this article can be found online at: https://www.frontiersin.org/articles/10.3389/fcell.2021.651367/full#supplementary-material

REFERENCES

Albagli, O., Dhordain, P., Deweindt, C., Lecocq, G., and Leprince, D. (1995). The BTB/POZ domain: a new protein-protein interaction motif common to DNA- and actin-binding proteins. *Cell Growth Differ.* 6, 1193–1198.

Antonioli, L., Fornai, M., Blandizzi, C., Pacher, P., and Hasko, G. (2019). Adenosine signaling and the immune system: when a lot could be too much. *Immunol. Lett.* 205, 9–15. doi: 10.1016/j.imlet.2018.04.006

Arefin, B., Kucerova, L., Dobes, P., Markus, R., Strnad, H., Wang, Z., et al. (2014). Genome-wide transcriptional analysis of *Drosophila* larvae infected by entomopathogenic nematodes shows involvement of complement, recognition and extracellular matrix proteins. *J. Innate Immun.* 6, 192–204. doi: 10.1159/000353734

Azad, P., Ryu, J., and Haddad, G. G. (2011). Distinct role of Hsp70 in *Drosophila* hemocytes during severe hypoxia. *Free Radic. Biol. Med.* 51, 530–538. doi: 10.1016/j.freeradbiomed.2011.05.005

Bajgar, A., Kucerova, K., Jonatova, L., Tomcala, A., Schneedorferova, I., Okrouhlik, J., et al. (2015). Extracellular adenosine mediates a systemic metabolic switch during immune response. *PLoS Biol.* 13:e1002135. doi: 10.1371/journal.pbio.1002135

Bardwell, V. J., and Treisman, R. (1994). The POZ domain: a conserved protein-protein interaction motif. *Genes Dev.* 8, 1664–1677. doi: 10.1101/gad.8.14.1664

Bettencourt, B. R., Hogan, C. C., Nimali, M., and Drohan, B. W. (2008). Inducible and constitutive heat shock gene expression responds to modification of Hsp70 copy number in *Drosophila melanogaster* but does not compensate for loss of thermotolerance in Hsp70 null flies. *BMC Biol.* 6:5. doi: 10.1186/1741-7007-6-5

Borea, P. A., Gessi, S., Merighi, S., and Varani, K. (2016). Adenosine as a multi-signalling guardian angel in human diseases: when, where and how does it exert its protective effects? *Trends Pharmacol. Sci.* 37, 419–434. doi: 10.1016/j.tips.2016.02.006

Buchner, K., Roth, P., Schotta, G., Krauss, V., Saumweber, H., Reuter, G., et al. (2000). Genetic and molecular complexity of the position effect variegation modifier mod(mdg4) in *Drosophila*. *Genetics* 155, 141–157.

Chan, H. Y., Warrick, J. M., Gray-Board, G. L., Paulson, H. L., and Bonini, N. M. (2000). Mechanisms of chaperone suppression of polyglutamine disease: selectivity, synergy and modulation of protein solubility in *Drosophila*. *Hum. Mol. Genet.* 9, 2811–2820. doi: 10.1093/hmg/9.19.2811

Cunha, R. A. (2016). How does adenosine control neuronal dysfunction and neurodegeneration? *J. Neurochem.* 139, 1019–1055. doi: 10.1111/jnc.13724

Cunha, R. A. (2019). Signaling by adenosine receptors-homeostatic or allostatic control? *PLoS Biol.* 17:e3000213. doi: 10.1371/journal.pbio.3000213

Dolezal, T., Dolezelova, E., Zurovec, M., and Bryant, P. J. (2005). A role for adenosine deaminase in *Drosophila* larval development. *PLoS Biol.* 3:e201. doi: 10.1371/journal.pbio.0030201

Dolezal, T., Gazi, M., Zurovec, M., and Bryant, P. J. (2003). Genetic analysis of the ADGF multigene family by homologous recombination and gene conversion in *Drosophila*. *Genetics* 165, 653–666.

Dolezelova, E., Nothacker, H. P., Civelli, O., Bryant, P. J., and Zurovec, M. (2007). A *Drosophila* adenosine receptor activates cAMP and calcium signaling. *Insect Biochem. Mol. Biol.* 37, 318–329.

Dolezelova, E., Zurovec, M., Dolezal, T., Simek, P., and Bryant, P. J. (2005). The emerging role of adenosine deaminases in insects. *Insect Biochem. Mol. Biol.* 35, 381–389. doi: 10.1016/j.ibmb.2004.12.009

Donovan, M. R., and Marr, M. T. II (2016). dFOXO activates large and small heat shock protein genes in response to oxidative stress to maintain proteostasis in *Drosophila*. *J. Biol. Chem.* 291, 19042–19050. doi: 10.1074/jbc.M116.723049

Dorn, R., and Krauss, V. (2003). The modifier of mdg4 locus in *Drosophila*: functional complexity is resolved by trans splicing. *Genetica* 117, 165–177. doi: 10.1023/A:1022983810016

Espinas, M. L., Jimenez-Garcia, E., Vaquero, A., Canudas, S., Bernues, J., and Azorin, F. (1999). The N-terminal POZ domain of GAGA mediates the formation of oligomers that bind DNA with high affinity and specificity. *J. Biol. Chem.* 274, 16461–16469. doi: 10.1074/jbc.274.23.16461

Fleischmannova, J., Kucerova, L., Sandova, K., Steinbauerova, V., Broz, V., Simek, P., et al. (2012). Differential response of *Drosophila* cell lines to extracellular adenosine. *Insect Biochem. Mol. Biol.* 42, 321–331. doi: 10.1016/j.ibmb.2012.01.002

Fredholm, B. B. (2007). Adenosine, an endogenous distress signal, modulates tissue damage and repair. *Cell Death Differ.* 14, 1315–1323. doi: 10.1038/sj.cdd.4402132

Garbuz, D. G. (2017). Regulation of heat shock gene expression in response to stress. *Mol. Biol.* 51, 352–367. doi: 10.1134/S0026893317020108

Giot, L., Bader, J. S., Brouwer, C., Chaudhuri, A., Kuang, B., Li, Y., et al. (2003). A protein interaction map of *Drosophila melanogaster*. *Science* 302, 1727–1736. doi: 10.1126/science.1090289

Gong, W. J., and Golic, K. G. (2006). Loss of Hsp70 in *Drosophila* is pleiotropic, with effects on thermotolerance, recovery from heat shock and neurodegeneration. *Genetics* 172, 275–286. doi: 10.1534/genetics.105.048793

Han, S. K., Lee, D., Lee, H., Kim, D., Son, H. G., Yang, J. S., et al. (2016). OASIS 2: online application for survival analysis 2 with features for the analysis of maximal lifespan and healthspan in aging research. *Oncotarget* 7, 56147–56152. doi: 10.18632/oncotarget.11269

Knight, D., Harvey, P. J., Iliadi, K. G., Klose, M. K., Iliadi, N., Dolezelova, E., et al. (2010). Equilibrative nucleoside transporter 2 regulates associative learning and synaptic function in *Drosophila*. *J. Neurosci.* 30, 5047–5057. doi: 10.1523/JNEUROSCI.6241-09.2010

Ko, J., Ou, S., and Patterson, P. H. (2001). New anti-huntingtin monoclonal antibodies: implications for huntingtin conformation and its binding proteins. *Brain Res. Bull.* 56, 319–329. doi: 10.1016/S0361-9230(01)00599-8

Krauss, V., and Dorn, R. (2004). Evolution of the trans-splicing *Drosophila* locus mod(mdg4) in several species of Diptera and Lepidoptera. *Gene* 331, 165–176. doi: 10.1016/j.gene.2004.02.019

Kucerova, L., Broz, V., Arefin, B., Maaroufi, H. O., Hurychova, J., Strnad, H., et al. (2016). The *Drosophila* chitinase-like protein IDGF3 is involved in protection against nematodes and in wound healing. *J. Innate Immun.* 8, 199–210. doi: 10.1159/000442351

Kuo, Y., Ren, S., Lao, U., Edgar, B. A., and Wang, T. (2013). Suppression of polyglutamine protein toxicity by co-expression of a heat-shock protein 40 and a heat-shock protein 110. *Cell Death Dis.* 4:e833. doi: 10.1038/cddis.2013.351

Lin, Y. H., Maaroufi, H. O., Ibrahim, E., Kucerova, L., and Zurovec, M. (2019). Expression of human mutant huntingtin protein in *Drosophila* hemocytes impairs immune responses. *Front. Immunol.* 10:2405. doi: 10.3389/fimmu.2019.02405

Maier, S. A., Galellis, J. R., and Mcdermid, H. E. (2005). Phylogenetic analysis reveals a novel protein family closely related to adenosine deaminase. *J. Mol. Evol.* 61, 776–794. doi: 10.1007/s00239-005-0046-y

Marsh, J. L., Walker, H., Theisen, H., Zhu, Y.-Z., Fielder, T., Purcell, J., et al. (2000). Expanded polyglutamine peptides alone are intrinsically cytotoxic and cause neurodegeneration in *Drosophila*. *Hum. Mol. Genet.* 9, 13–25. doi: 10.1093/hmg/9.1.13

Martini, D., Del Bo, C., Tassotti, M., Riso, P., Del Rio, D., Brighenti, F., et al. (2016). Coffee consumption and oxidative stress: a review of human intervention studies. *Molecules* 21:979. doi: 10.3390/molecules21080979

Melnikova, L., Kostyuchenko, M., Parshikov, A., Georgiev, P., and Golovnin, A. (2018). Role of Su(Hw) zinc finger 10 and interaction with CP190 and Mod(mdg4) proteins in recruiting the Su(Hw) complex to chromatin sites in *Drosophila*. *PLoS One* 13:e0193497. doi: 10.1371/journal.pone.0193497

Merighi, S., Mirandola, P., Milani, D., Varani, K., Gessi, S., Klotz, K. N., et al. (2002). Adenosine receptors as mediators of both cell proliferation and cell death of cultured human melanoma cells. *J. Invest. Dermatol.* 119, 923–933. doi: 10.1046/j.1523-1747.2002.00111.x

Mondal, B. C., Mukherjee, T., Mandal, L., Evans, C. J., Sinenko, S. A., Martinez-Agosto, J. A., et al. (2011). Interaction between differentiating cell- and niche-derived signals in hematopoietic progenitor maintenance. *Cell* 147, 1589–1600. doi: 10.1016/j.cell.2011.11.041

Moser, G. H., Schrader, J., and Deussen, A. (1989). Turnover of adenosine in plasma of human and dog blood. *Am. J. Physiol.* 256, C799–C806. doi: 10.1152/ajpcell.1989.256.4.C799

Mugat, B., Parmentier, M. L., Bonneaud, N., Chan, H. Y., and Maschat, F. (2008). Protective role of engrailed in a *Drosophila* model of Huntington's disease. *Hum. Mol. Genet.* 17, 3601–3616. doi: 10.1093/hmg/ddn255

Mutsuddi, M., Marshall, C. M., Benzow, K. A., Koob, M. D., and Rebay, I. (2004). The spinocerebellar ataxia 8 noncoding RNA causes neurodegeneration and associates with staufen in *Drosophila*. *Curr. Biol.* 14, 302–308. doi: 10.1016/j.cub.2004.01.034

Novakova, M., and Dolezal, T. (2011). Expression of *Drosophila* adenosine deaminase in immune cells during inflammatory response. *PLoS One* 6:e17741. doi: 10.1371/journal.pone.0017741

Oughtred, R., Stark, C., Breitkreutz, B. J., Rust, J., Boucher, L., Chang, C., et al. (2019). The BioGRID interaction database: 2019 update. *Nucleic Acids Res.* 47, D529–D541. doi: 10.1093/nar/gky1079

Poernbacher, I., and Vincent, J. P. (2018). Epithelial cells release adenosine to promote local TNF production in response to polarity disruption. *Nat. Commun.* 9:4675. doi: 10.1038/s41467-018-07114-z

Rivera-Oliver, M., and Diaz-Rios, M. (2014). Using caffeine and other adenosine receptor antagonists and agonists as therapeutic tools against neurodegenerative diseases: a review. *Life Sci.* 101, 1–9. doi: 10.1016/j.lfs.2014.01.083

Rosas-Arellano, A., Estrada-Mondragon, A., Pina, R., Mantellero, C. A., and Castro, M. A. (2018). The tiny *Drosophila Melanogaster* for the biggest answers in Huntington's disease. *Int. J. Mol. Sci.* 19:2398. doi: 10.3390/ijms19082398

Schrier, S. M., Van Tilburg, E. W., Van Der Meulen, H., Ijzerman, A. P., Mulder, G. J., and Nagelkerke, J. F. (2001). Extracellular adenosine-induced apoptosis in mouse neuroblastoma cells: studies on involvement of adenosine receptors and adenosine uptake. *Biochem. Pharmacol.* 61, 417–425. doi: 10.1016/S0006-2952(00)00573-6

Shilova, V. Y., Zatsepina, O. G., Garbuz, D. G., Funikov, S. Y., Zelentsova, E. S., Schostak, N. G., et al. (2018). Heat shock protein 70 from a thermotolerant Diptera species provides higher thermoresistance to *Drosophila* larvae than correspondent endogenous gene. *Insect Mol. Biol.* 27, 61–72. doi: 10.1111/imb.12339

Shukla, A. K., Pragya, P., Chaouhan, H. S., Tiwari, A. K., Patel, D. K., Abdin, M. Z., et al. (2014). Heat shock protein-70 (Hsp-70) suppresses paraquat-induced neurodegeneration by inhibiting JNK and caspase-3 activation in *Drosophila* model of Parkinson's disease. *PLoS One* 9:e98886. doi: 10.1371/journal.pone.0098886

Soares, T. R., Reis, S. D., Pinho, B. R., Duchen, M. R., and Oliveira, J. M. A. (2019). Targeting the proteostasis network in Huntington's disease. *Ageing Res. Rev.* 49, 92–103. doi: 10.1016/j.arr.2018.11.006

Soltani-Bejnood, M., Thomas, S. E., Villeneuve, L., Schwartz, K., Hong, C. S., and Mckee, B. D. (2007). Role of the mod(mdg4) common region in homolog segregation in *Drosophila* male meiosis. *Genetics* 176, 161–180. doi: 10.1534/genetics.106.063289

Song, W., Smith, M. R., Syed, A., Lukacsovich, T., Barbaro, B. A., Purcell, J., et al. (2013). Morphometric analysis of Huntington's disease neurodegeneration in *Drosophila*. *Methods Mol. Biol.* 1017, 41–57. doi: 10.1007/978-1-62703-438-8_3

Soshnev, A. A., Baxley, R. M., Manak, J. R., Tan, K., and Geyer, P. K. (2013). The insulator protein Suppressor of Hairy-wing is an essential transcriptional repressor in the *Drosophila* ovary. *Development* 140, 3613–3623. doi: 10.1242/dev.094953

Steffan, J. S., Bodai, L., Pallos, J., Poelman, M., Mccampbell, A., Apostol, B. L., et al. (2001). Histone deacetylase inhibitors arrest polyglutamine-dependent neurodegeneration in *Drosophila*. *Nature* 413, 739–743. doi: 10.1038/35099568

Stenesen, D., Suh, J. M., Seo, J., Yu, K., Lee, K. S., Kim, J. S., et al. (2013). Adenosine nucleotide biosynthesis and AMPK regulate adult life span and mediate the longevity benefit of caloric restriction in flies. *Cell Metab.* 17, 101–112. doi: 10.1016/j.cmet.2012.12.006

Thomas, S. E., Soltani-Bejnood, M., Roth, P., Dorn, R., Logsdon, J. M. Jr., and Mckee, B. D. (2005). Identification of two proteins required for conjunction and regular segregation of achiasmate homologs in *Drosophila* male meiosis. *Cell* 123, 555–568. doi: 10.1016/j.cell.2005.08.043

Toczek, M., Zielonka, D., Zukowska, P., Marcinkowski, J. T., Slominska, E., Isalan, M., et al. (2016). An impaired metabolism of nucleotides underpins a novel mechanism of cardiac remodeling leading to Huntington's disease related cardiomyopathy. *Biochim. Biophys. Acta* 1862, 2147–2157. doi: 10.1016/j.bbadis.2016.08.019

Van Eyk, C. L., O'keefe, L. V., Lawlor, K. T., Samaraweera, S. E., Mcleod, C. J., Price, G. R., et al. (2011). Perturbation of the Akt/Gsk3-beta signalling pathway is common to *Drosophila* expressing expanded untranslated CAG, CUG and AUUCU repeat RNAs. *Hum. Mol. Genet.* 20, 2783–2794. doi: 10.1093/hmg/ddr177

Warrick, J. M., Chan, H. Y., Gray-Board, G. L., Chai, Y., Paulson, H. L., and Bonini, N. M. (1999). Suppression of polyglutamine-mediated neurodegeneration in *Drosophila* by the molecular chaperone HSP70. *Nat. Genet.* 23, 425–428. doi: 10.1038/70532

Wu, M. N., Ho, K., Crocker, A., Yue, Z., Koh, K., and Sehgal, A. (2009). The effects of caffeine on sleep in *Drosophila* require PKA activity, but not the adenosine receptor. *J. Neurosci.* 29:11029–11037. doi: 10.1523/JNEUROSCI.1653-09.2009

Xiao, C., Liu, N., Jacobson, K. A., Gavrilova, O., and Reitman, M. L. (2019). Physiology and effects of nucleosides in mice lacking all four adenosine receptors. *PLoS Biol.* 17:e3000161. doi: 10.1371/journal.pbio.3000161

Xu, C., Franklin, B., Tang, H. W., Regimbald-Dumas, Y., Hu, Y., Ramos, J., et al. (2020). An in vivo RNAi screen uncovers the role of AdoR signaling and adenosine deaminase in controlling intestinal stem cell activity. *Proc. Natl. Acad. Sci. U.S.A.* 117, 464–471. doi: 10.1073/pnas.1900103117

Zurovec, M., Dolezal, T., Gazi, M., Pavlova, E., and Bryant, P. J. (2002). Adenosine deaminase-related growth factors stimulate cell proliferation in *Drosophila* by depleting extracellular adenosine. *Proc. Natl. Acad. Sci. U.S.A.* 99, 4403–4408. doi: 10.1073/pnas.062059699

Conflict of Interest: The authors declare that the research was conducted in the absence of any commercial or financial relationships that could be construed as a potential conflict of interest.

frontiers in Cell and Developmental Biology

REVIEW
published: 24 May 2021
doi: 10.3389/fcell.2021.687489

Differential Regulation of GPCRs—Are GRK Expression Levels the Key?

Edda S. F. Matthees†, Raphael S. Haider†, Carsten Hoffmann and Julia Drube*

Institut für Molekulare Zellbiologie, CMB – Center for Molecular Biomedicine, Universitätsklinikum Jena, Friedrich-Schiller-Universität Jena, Jena, Germany

G protein-coupled receptors (GPCRs) comprise the largest family of transmembrane receptors and their signal transduction is tightly regulated by GPCR kinases (GRKs) and β-arrestins. In this review, we discuss novel aspects of the regulatory GRK/β-arrestin system. Therefore, we briefly revise the origin of the "barcode" hypothesis for GPCR/β-arrestin interactions, which states that β-arrestins recognize different receptor phosphorylation states to induce specific functions. We emphasize two important parameters which may influence resulting GPCR phosphorylation patterns: (A) direct GPCR–GRK interactions and (B) tissue-specific expression and availability of GRKs and β-arrestins. In most studies that focus on the molecular mechanisms of GPCR regulation, these expression profiles are underappreciated. Hence we analyzed expression data for GRKs and β-arrestins in 61 tissues annotated in the Human Protein Atlas. We present our analysis in the context of pathophysiological dysregulation of the GPCR/GRK/β-arrestin system. This tissue-specific point of view might be the key to unraveling the individual impact of different GRK isoforms on GPCR regulation.

Keywords: GPCR, GRK, β-arrestin, IDP, tissue-specific expression, barcode hypothesis

OPEN ACCESS

Edited by:
Sameer Mohammad, King Abdullah International Medical Research Center (KAIMRC), Saudi Arabia

Reviewed by:
Attila Remenyi, Hungarian Academy of Sciences (MTA), Hungary
Uwe Lendeckel, University of Greifswald, Germany

****Correspondence:***
Carsten Hoffmann
carsten.hoffmann@med.uni-jena.de

† These authors have contributed equally to this work

Specialty section:
This article was submitted to Signaling, a section of the journal Frontiers in Cell and Developmental Biology

Received: *29 March 2021*
Accepted: *29 April 2021*
Published: *24 May 2021*

Citation:
Matthees ESF, Haider RS, Hoffmann C and Drube J (2021) Differential Regulation of GPCRs—Are GRK Expression Levels the Key? Front. Cell Dev. Biol. 9:687489. doi: 10.3389/fcell.2021.687489

INTRODUCTION

G protein-coupled receptors (GPCRs) constitute a family of over 800 membrane-localized receptors. They respond to a large variety of extracellular stimuli, among them, photons, odors, hormones, or neurotransmitters, to induce specific intracellular signaling (Marinissen and Gutkind, 2001). This is achieved by a vast diversity of ligand binding domains. Nevertheless, GPCRs share a seven-transmembrane architecture that undergoes large conformational changes during receptor activation in order to activate a common set of intracellular signaling proteins (Nygaard et al., 2013; Latorraca et al., 2017). Hence, G proteins, GPCR kinases (GRKs) and arrestins, as most prominent interaction partners of GPCRs, engage active receptors at their opened intracellular cavity in a similar fashion (Nygaard et al., 2013; Flock et al., 2017). This process usually involves the insertion

Abbreviations: AMP, adenosine monophosphate; AP2, adaptor protein 2; ARRDC, arrestin-domain-containing proteins, α-arrestins; ART, arrestin-related trafficking adaptors, α-arrestins; β2ADR, β2 adrenergic receptor; CXCL12, C-X-C motif chemokine 12, also known as stromal cell-derived factor 1 (SDF1); CXCR2, C-X-C chemokine receptor type 2, also known as Interleukin 8 receptor beta, IL8RB, CD182; CXCR4, C-X-C chemokine receptor type 4, also known as fusin or CD184; DAG, diacylglycerol; FANTOM5, Functional Annotation of Mammalian Genomes 5; FLR, finger loop region; GDP, guanosine diphosphate; GPCR, G protein-coupled receptor; GRK, GPCR kinase; GTEx, Genotype-Tissue Expression; GTP, guanosine triphosphate; HPA, Human Protein Atlas; IDR, intrinsically disordered regions; IL3, intracellular loop 3; MAPK, mitogen-activated protein kinase; MEK, mitogen-activated protein kinase kinase; NX, normalized expression; PBMC, peripheral blood mononuclear cells; PDB, Protein Data Bank; PKA, protein kinase A; PKC, protein kinase C; shRNA, short hairpin RNA; siRNA, short interfering RNA.

of small loop structures or alpha-helical domains into the GPCR cavity. The similarities between the C-terminal alpha helix of G_α subunits, the N-terminal domain of GRKs, and the finger loop region (FLR) of arrestins, which enable or enhance the interaction with active GPCRs, are highlighted in **Figure 1A**.

For the main signaling transducers, the trimeric G proteins, this interaction leads to a guanosine diphosphate (GDP)—guanosine triphosphate (GTP) exchange followed by dissociation of G_α and $G_{\beta\gamma}$ subunits (Oldham and Hamm, 2008; Flock et al., 2015). The now activated G protein subunits are able to individually regulate levels of second messengers [e.g., cyclic adenosine monophosphate (cAMP), calcium, or diacylglycerol (DAG)] to induce a cellular response. Subsequently, intracellular peptide stretches of active GPCRs are phosphorylated by GRKs. In turn, this accumulation of negative charges enables high affinity binding of arrestins (Gurevich and Gurevich, 2019), initiating the desensitization and internalization of receptors. As arrestins and G proteins utilize at least overlapping binding interfaces (DeWire et al., 2007), arrestin-bound receptors are canonically unable to further induce their primary signaling. Moreover, arrestins have been shown to serve as scaffolds for more than 100 intracellular proteins (Xiao et al., 2007; Crepieux et al., 2017), that enable the formation of specific effector-hubs, regulating intracellular trafficking and signaling of active GPCRs. In this review, we want to discuss the current state of research regarding the phosphorylation-dependent processes that underlie GPCR regulation. Moreover, we want to highlight the potential influence of tissue specific expression levels of GPCR-regulating genes on signaling outcomes.

ARRESTINS AND GRKs FACILITATE TARGETED DOWNSTREAM FUNCTIONS FOR HUNDREDS OF GPCRs

Human physiology features a sizeable amount of G_α and $G_{\beta\gamma}$ subunits (Milligan and Kostenis, 2006). Thus, the diversity of primary GPCR signaling is adequately explained as different receptors preferably couple to specific combinations of G protein trimers (Inoue et al., 2019). However, the downregulation of most GPCRs is tightly controlled by only four ubiquitously expressed GRKs (GRK2, 3, 5, and 6) and two arrestin isoforms, namely β-arrestin1 and β-arrestin2. Still, the processes enabled by these proteins are highly diverse and seem specific for each GPCR. For some receptors, the interactions with GRKs and arrestins lead to desensitization and immediate recycling, redirecting the receptor back to the membrane after initial internalization (Claing et al., 2002). In contrast, certain GPCRs exhibit prolonged intracellular trafficking which localizes the receptors to specific intracellular compartments and may give rise to a second wave of endosomal signaling (Godbole et al., 2017).

GRKs have been shown to be allosterically activated via binding to active GPCRs (Palczewski et al., 1991; Chen et al., 1993; Huang and Tesmer, 2011). This binding mechanism has not been fully understood yet, but possibly features the insertion of a N-terminal α-helix into the cytoplasmic cavity of the GPCR. Although structural evidence is not necessarily conclusive (Cato et al., 2021), this mode of GRK-binding is highly attractive, as G proteins and arrestins probe for active GPCR conformations in a similar fashion (**Figure 1A**). In a cellular context, GRK-binding leads to the phosphorylation of active GPCRs at their intracellular sites. Notably, GRKs have also been shown to phosphorylate non-GPCR substrates (Palczewski et al., 1991; McCarthy and Akhtar, 2002), albeit with higher efficiency in the presence of active GPCRs. Thus, GRKs most likely also regulate other cellular processes in a phosphorylation-dependent manner, but in this review, we will predominantly discuss their impact on GPCR signaling. Non-visual GRKs are classified into two families (Gurevich et al., 2012; Mushegian et al., 2012; Homan and Tesmer, 2014). GRK2 and GRK3 constitute the GRK2 family and are expressed in the cytosol. Subsequent to GPCR activation, GRK2 and 3 are recruited to the membrane, facilitated by GPCR complex formation and stabilizing interactions with $G_{\beta\gamma}$-subunits (Tesmer et al., 2005). In contrast, GRK4 family kinases, namely GRK4, 5, and 6, are generally membrane-associated. In this review, we will further focus on effects of GRK2, 3, 5, and 6. Some of these GRK isoforms have been shown to preferentially phosphorylate different residues at the intracellular side of GPCRs (Nobles et al., 2011), to induce receptor internalization and desensitization.

Upon binding to the active and phosphorylated GPCR, arrestins undergo conformational changes that involve the disruption of the polar core and three element interaction site, the two main auto-inhibitory intramolecular interactions. This renders the arrestin C-terminus and phosphate-sensing N-domain solvent-exposed, accompanied by a ∼18° interdomain rotation. Especially, since arrestins have no enzymatic function, these conformational changes can be seen as hallmarks of arrestin activation. The release of the arrestin C-terminus is furthermore hypothesized to play a central role in the mediation of arrestin-dependent downstream functions. It harbors binding motifs for the adaptor protein 2 (AP2) complex and clathrin (Goodman et al., 1996; Krupnick et al., 1997; Laporte et al., 2000), in addition to a mitogen-activated protein kinase kinase (MEK) phosphorylation site (Cassier et al., 2017) that enables scaffolding of mitogen-activated protein kinases (MAPKs). Hence, arrestins are able to facilitate clathrin-dependent GPCR internalization and enhance G protein-induced MAPK signaling. In recent years arrestins have been shown to assume distinct conformational states, accommodating not only the active structure of a GPCR but also its specific intracellular phosphorylation. Depending on the overall geometry of the resulting GPCR–arrestin complex, a certain set of effector proteins may then be recruited to orchestrate specific functions.

Crystal structures (Shukla et al., 2013; Kang et al., 2015) and cryo-electron microscopy (Thomsen et al., 2016; Huang et al., 2020; Lee et al., 2020; Staus et al., 2020) studies have shown that these GPCR–arrestin complexes can occur in different configurations. Although they are most probably not mutually exclusive but rather present in a certain equilibrium, different GPCRs make use of distinct binding interfaces when coupling to arrestins. The two main interaction sites on the receptor are constituted by the opened intracellular cavity of the active GPCR and phosphorylated peptide stretches like

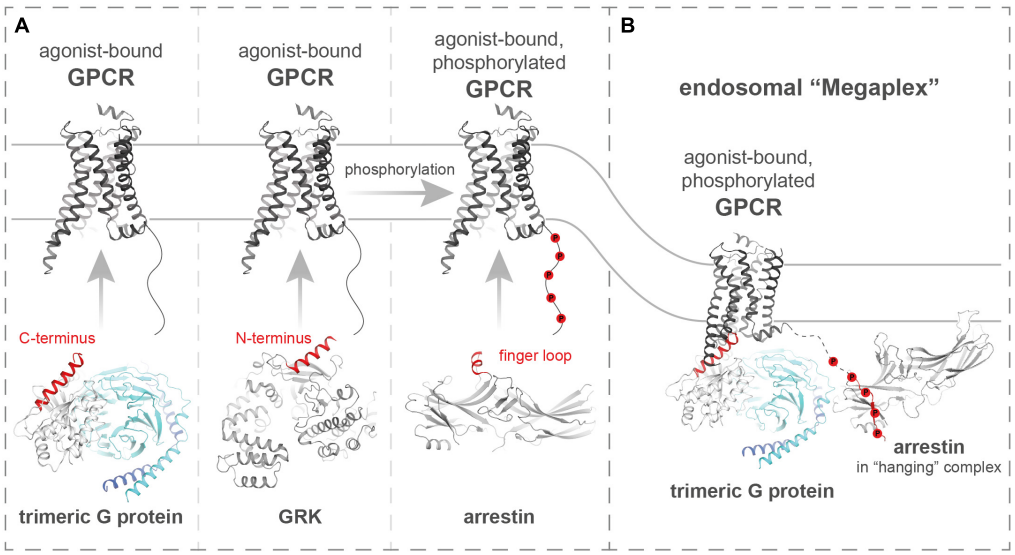

FIGURE 1 | G proteins, GRKs, and arrestins share similar structural features to engage active GPCR folds. **(A)** Schematic depiction of how active GPCRs (PDB: 3SN6) interact with trimeric G proteins (PDB: 3SN6), GRKs (PDB: 3NYN), and arrestins (PDB: 5DGY), as most prominent mediators and regulators of GPCR signaling. On the cartoon structures of the intracellular effector proteins, helices that interact with active GPCR folds are highlighted in red. **(B)** Structure of the endosomal complex (PDB: 6NI2) between an active GPCR, a trimeric G protein, and β-arrestin1.

the C-terminus or intracellular loop 3 (IL3). Arrestins bind to these phosphorylated regions via positive charges buried in their N-domain. Subsequently, the active GPCR cavity is engaged by the arrestin FLR, which is inserted into the receptor transmembrane helix bundle and might assume an alpha-helical structure to stabilize this interaction (Kang et al., 2015). GPCR–arrestin complexes that make use of both binding interfaces were termed either "core," "tight," or "snuggly" and are usually characterized by high affinity binding and uncoupling of G proteins. Recently, GPCR–arrestin complexes were discovered that only rely on the interaction between the arrestin N-domain and the phosphorylated GPCR C-terminus (Thomsen et al., 2016; Nguyen et al., 2019). This complex configuration is independent of the FLR and does not utilize the transmembrane helix bundle binding interface, therefore still allowing further activation of G proteins (**Figure 1B**). Moreover, arrestins that associate with GPCRs in this "hanging" configuration can still assume active conformations and have been shown to functionally increase receptor internalization (Kumari et al., 2017). Thus, GRK-mediated receptor phosphorylation is crucial for the formation of "core" and "hanging" GPCR–arrestin complexes. Phosphorylation is often also hypothesized to be the starting point of arrestin complex formation, however, the precise determination of succession of these binding events is still occluded, as arrestins also have an affinity for active, yet unphosphorylated GPCRs (Gurevich and Gurevich, 2006; Haider et al., 2019; Drube et al., 2021).

Differential spacing of negative charges at the receptor C-terminus has been shown to induce specific conformational changes in arrestins (Lee et al., 2016; Nuber et al., 2016; Mayer et al., 2019). Furthermore, these conformational states have been linked with distinct functional outcomes (Yang et al., 2015; Lee et al., 2016). As these findings suggest that every GPCR–arrestin complex is formed in a specific configuration, this could explain how only two β-arrestin isoforms are able to mediate targeted processes for more than 800 different GPCRs. Based on this argumentation, the "barcode" hypothesis was put forward, stating that the arrestin N-domain is capable of recognizing a plethora of different GPCR phosphorylation states. Different phosphorylation patterns ("barcodes") would then only induce certain conformational changes that dictate arrestin functions for the interaction with a given GPCR (**Figure 2A**).

HOW ARRESTINS INTERPRET DIFFERENT PHOSPHORYLATION PATTERNS: THE "BARCODE" HYPOTHESIS

In its most straightforward interpretation, the "barcode" hypothesis states that arrestins react to different phosphorylation patterns via specific conformational changes in order to fulfill targeted functions (**Figure 2A**). This adequately explains how different GPCRs can experience divergent arrestin-mediated regulation, and constitutes a solid foundation for the investigation of these phosphorylation-dependent processes. In line with this hypothesis, arrestins have been shown to undergo specific conformational changes for the coupling with different GPCRs (Lee et al., 2016; Nuber et al., 2016).

Multiple studies showed that different GRK isoforms preferentially phosphorylate specific sites of the same GPCR (Nobles et al., 2011; Doll et al., 2012; Miess et al., 2018). These findings expand the "barcode" hypothesis, as they suggest

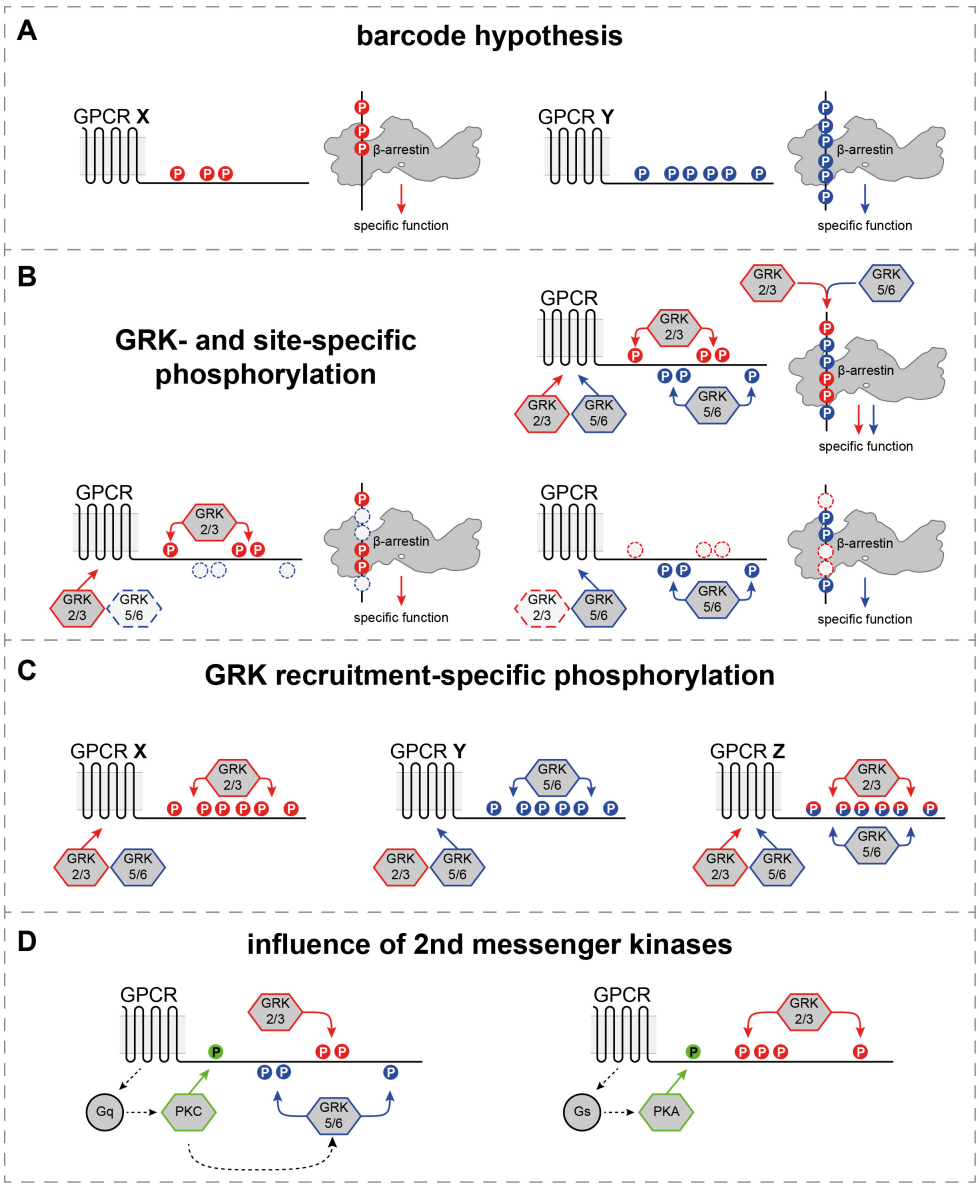

FIGURE 2 | Differential and GRK-specific GPCR phosphorylation induces distinct β-arrestin mediated functions. **(A)** The most straightforward way to interpret the "barcode" hypothesis, as different GPCRs feature different C-terminal phosphorylation patterns to induce distinct β-arrestin functions. **(B)** Individual GRK isoforms or families (GRK2/3 or GRK5/6) have been shown to preferentially phosphorylate specific sites at different GPCR C-termini (Nobles et al., 2011; Doll et al., 2012; Miess et al., 2018). Depending on the availability of kinases in a cellular system, the same GPCR could be phosphorylated by GRK2/3 or GRK5/6 only, to induce specific functions, or by all GRK isoforms to achieve the activation of all possible β-arrestin functions. **(C)** Certain GPCRs have been shown to be functionally phosphorylated by GRK2/3 only, or GRK2/3/5/6 (Drube et al., 2021). This might constitute another layer of coupling preference at the foundation of the "barcode" hypothesis. **(D)** Second messenger kinases, like PKC and PKA are activated by the primary G protein signaling and have been shown to phosphorylate GPCRs directly. Additionally, they are able to modulate the activity of certain GRK isoforms or families (Chuang et al., 1995; Winstel et al., 1996; Pronin and Benovic, 1997).

that one receptor may feature different phosphorylation states depending on the cellular context and the availability of kinases. For example, the β2 adrenergic receptor (β2ADR) has been shown to be differentially phosphorylated by GRK2 or GRK6, resulting in kinase-specific C-terminal phosphorylation patterns (Nobles et al., 2011). From these results, a "site-specific barcode" hypothesis emerged, which suggests that GRK2/3 or GRK5/6 phosphorylate the receptor at different sites to induce divergent functions (**Figure 2B**). Thus, depending on the available kinases, a GPCR could be phosphorylated at GRK2/3- or GRK5/6-specific sites only, or fully phosphorylated by all four GRK isoforms to induce all possible arrestin-mediated functions.

Indeed, there is evidence that supports this hypothesis as specific phosphorylation patterns have been linked with distinct conformational changes in β-arrestins and downstream functions (Yang et al., 2015). Interestingly, GRK2/3 phosphorylation

was proposed to be the driver of receptor internalization, whereas GRK5/6-mediated GPCR phosphorylation was linked with increased ERK signaling (Kim et al., 2005; Ren et al., 2005; Yang et al., 2015). In contrast to these reports, overlapping or even opposing effects for individual GRK isoforms were identified, depending on the used cellular system and the investigated receptor (Tran et al., 2004; Zhu et al., 2013).

The mentioned studies rely on siRNA/shRNA approaches or GRK inhibitors to investigate the impact of individual GRK isoforms on GPCR regulation. These methods bear the risk of co-analyzing a remaining expression of targeted GRK(s) in knockdown approaches, or potential off-target effects of pharmacological intervention. Furthermore, the impact of these methods depends on the initial endogenous GRK expression levels, which were not assessed in these studies. As an example, the knockdown or inhibition of GRK2 would have less pronounced effects in a cellular system that genuinely features a low expression of GRK2. Non-visual GRKs are usually thought of as ubiquitously expressed and their actual tissue distribution is underappreciated in most studies that focus on molecular mechanisms of GPCR regulation. Additionally, no clear consensus sequences have been identified for specific GRK isoforms, although efforts were made to fill this gap (Pinna and Ruzzene, 1996; Asai et al., 2014; Kang et al., 2020).

Recent studies which utilize the CRISPR/Cas9 technology to achieve a partial (Moller et al., 2020) or complete genetic ablation (Drube et al., 2021) of GRK2, 3, 5, and/or 6 suggest that GPCR-specific GRK-coupling preferences might determine which isoforms regulate a given receptor (**Figure 2C**). Using β-arrestin recruitment as a read-out for GRK-mediated receptor regulation, two subsets of GPCRs have been identified (Drube et al., 2021): receptors that are functionally phosphorylated by GRK2, 3, 5, and 6 and those for which arrestin recruitment could only be mediated by GRK2 and 3. By analysis of the β2ADR, this study shows that even though GRK2 and GRK6 preferentially phosphorylate distinct C-terminal sites (Nobles et al., 2011), the individual overexpression of either kinase mediates β-arrestin recruitment to the same extent. These findings indicate that different GRK isoforms might be able to induce identical GPCR regulation on a molecular level, but specific contributions to these processes are ultimately defined by the relative tissue expression of GRK2, 3, 5, and 6.

GPCR phosphorylation patterns are also influenced by second messenger kinases like protein kinase A (PKA) or protein kinase C (PKC) (**Figure 2D**). Those kinases are activated via the primary G_s or G_q signaling pathways, respectively, and have been shown to phosphorylate GPCRs directly. Interestingly, PKC also phosphorylates GRKs and is able to modulate their activity (Chuang et al., 1995; Winstel et al., 1996; Pronin and Benovic, 1997). Thus, the resulting phosphorylation "barcode" of a GPCR might be changed by direct phosphorylation or via increasing or decreasing the activity of specific GRK isoforms, depending on the individual G protein-coupling preference. This cross-talk between GPCR regulating kinases is largely underappreciated in recent literature and needs more elaboration to complete our understanding of phosphorylation-dependent GPCR regulation.

Additionally, there are more unanswered biological questions at the foundation of the "barcode" hypothesis. Given that GRK isoforms preferably phosphorylate different sites, how is it that specific GRK consensus sequences are still elusive? Can a receptor molecule be phosphorylated by more than one GRK? If so, does the sequence in which a GPCR is phosphorylated by multiple GRK isoforms change the resulting phosphorylation pattern? These questions still need to be answered by future experiments in order to unravel the intricate details of GPCR regulation.

HOW THE "BARCODE" HYPOTHESIS CAN BE INTERPRETED STRUCTURALLY: INTRINSICALLY DISORDERED REGIONS

One possible extension to explain the "barcode" hypothesis structurally, which goes beyond pure electrostatic interactions of negatively charged phosphate groups on the receptor with basic amino acid side chains of arrestin, might be intrinsically disordered regions (IDRs) of the GPCR itself. IDRs are longer protein regions which do not show a persistent traditional secondary structure of an α-helix or β-sheet (van der Lee et al., 2014; Shammas et al., 2016). Such disordered regions are frequently found in proteins which are involved in signaling cascades (Wright and Dyson, 2015). Intriguingly, IDRs can form different secondary structures when interacting with specific binding partners. An impressive example is the protein p53 which was crystallized with 14 different binding partners and depending on the complex partner, the IDRs of p53 exhibited very different structures (Oldfield and Dunker, 2014). The analysis of GPCR sequences identified IDRs with >50 amino acids in three major receptor regions, namely the N-terminus, the third intracellular loop (IL3), and the receptor C-terminus (Jaakola et al., 2005; Venkatakrishnan et al., 2014). Not surprisingly, the two intracellular regions are well known to be involved in the signal transduction of GPCRs. Due to their flexibility, they frequently need to be truncated or substituted to increase receptor stability in structural biology approaches (Fonin et al., 2019). Furthermore, IDRs are frequently subject to post-translational modifications which help to support structural stabilization of such regions (Venkatakrishnan et al., 2014). Most commonly IDRs are stabilized by phosphorylation, followed by less common ubiquitination (Bah and Forman-Kay, 2016). Both are well known post-translational modifications for GPCRs occurring within IL3 and the C-terminus of the receptor (Patwardhan et al., 2021). Since IDRs are characterized by a lack of persistent structure (Shammas et al., 2016), their folding state may greatly influence the kinetics of interactions with other partners. For example, increasing the proportion of IDRs with a structure that resembles the bound state might enhance the binding affinity for the partner protein (Shammas et al., 2016). This might be due to effects either on the binding on-rate (k_{on}) or off-rate (k_{off}) of the complex.

If we now carefully consider these possibilities, we can envision that a given GPCR interacts with a GRK and depending on their relative complex geometry, this event will add the first phosphate group to the receptor stretch which is closest to the

active site of the GRK. Early experimental evidence for such a scenario was demonstrated for rhodopsin 30 years ago when even exogenous peptides in the vicinity of GRK1 were phosphorylated (Palczewski et al., 1991). This initial phosphorylation could have local structural consequences and allow or disallow certain residues of the receptor to be phosphorylated next. Depending on the GRK subtype, this can have different consequences for the phosphorylation pattern of a given GPCR. In the case that a GPCR is phosphorylated by more than one GRK, even the relative sequence of GRKs phosphorylating the receptor might have differential consequences. This relative order could be dominated by either different GRK expression levels or accessibility of the GPCR. Such a scenario could help to explain the apparent lack of consensus sequences for GRKs and account for altered GPCR signaling when certain GRKs are up- or downregulated under pathophysiological conditions.

GRKs and β-arrestins are often stated to be ubiquitiously expressed (Nogues et al., 2018). However, a detailed comparative analysis of the tissue and cell-type specific expression pattern of β-arrestins or GRKs is currently not available (Nogues et al., 2018). Therefore, to understand the GRK/arrestin regulatory system in more detail, we analyzed the Human Protein Atlas (HPA)[1] (Thul et al., 2017) for reported expression levels of GRK2, 3, 5, 6, and the two β-arrestins. Furthermore, we included five human arrestin-domain-containing (ARRDC) proteins, also called α-arrestins, based on similarities in mechanistic substrate recognition (Aubry et al., 2009; Kang et al., 2014): Their yeast homolog proteins named ART (arrestin related trafficking adaptors as synonym for ARRDCs in yeast) are reported to use a basic patch in their arrestin domain to recognize the exposed acidic sorting motive of their substrate, for instance a nutrient transporter. To be recognized, the transporter must exist in a conformation that exposes the acidic sorting motif. This exposure occurs during the substrate transport process (active protein state) and is further assisted by phosphorylation (Kahlhofer et al., 2021). Interestingly, ARRDCs lack the auto-inhibitory polar core region seen in visual and β-arrestins and might therefore resemble more of an active arrestin state. Although little is currently known on the function of human ARRDCs, these proteins were reported to interact with GPCRs (Tian et al., 2016). In combination with the mechanistic similarities from their yeast homologs, this observation encouraged us to assemble the information on ARRDC expression besides the β-arrestins.

THE TISSUE PERSPECTIVE: ARE GRK EXPRESSION LEVELS THE KEY?

To evaluate the composition of GPCR-regulating systems for different tissues, we accessed the HPA and analyzed the relative tissue-specific expression levels for various GRK and arrestin isoforms. The HPA is a largescale project, aiming to elucidate human gene expression and localization in cells, tissues, and organs (Uhlen et al., 2015). Since its first publication in 2005, the website has been updated multiple times to include an increasing amount of data generated by different techniques and to combine information from various sources. To compare expression levels of the four ubiquitously expressed GRK isoforms, the two β-arrestins, and ARRDC1-5, we utilized the consensus transcriptomics data of the HPA, the Genotype-Tissue Expression (GTEx), and the Functional Annotation of Mammalian Genomes 5 (FANTOM5) project, made available on the HPA website[2] (HPA version 20.1, Ensembl version 92.38, last accessed March 10th, 2021). Although mRNA expression levels do not always equate to protein levels in the cells, we nevertheless assume that the mRNA levels somewhat reflect the resulting protein levels. Therefore, we used the available mRNA expression data for our analysis, as it is more detailed than the existing protein expression data. For each gene, the consensus normalized RNA expression (NX) value is calculated via normalization to the maximum expression value found in the three sources (**Table 1**). By comparing the consensus NX values, different expression patterns within distinct tissues can be identified.

With this approach, we found tissues that predominantly express one GRK, with all other isoforms being comparatively lower expressed [e.g., GRK5 in heart muscle (23) or GRK2 in skin (46)]. The database also reveals tissues in which two GRK isoforms are comparably high expressed [e.g., GRK2 and 6 in bone marrow (7) or GRK2 and 5 in gallbladder (21)] or tissues with similar NX values for all GRKs [e.g., smooth muscle (48)]. Interestingly, some functional groups of tissues, categorized according to the HPA, share common expression patterns. For example, GRK2 is the predominant isoform expressed in all assessed tissues of the brain, whereas GRK3 is the most abundant isoform in adipose tissue. Bone marrow and lymphoid tissues feature high expression levels of GRK2 and GRK6. Furthermore, GRK6 is highly expressed in all assessed blood cells. Some of them express GRK6 and GRK2 at similar levels [dendritic cells (14) and total peripheral blood mononuclear cells (PBMC; 59)], or feature GRK2 as the second highest expressed isoform [e.g., granulocytes (22) and monocytes (31)]. In contrast, B- (5) and T-cells (52) show similar expression levels of GRK6 and GRK5.

These different GRK expression patterns occur alongside distinct expression levels of β-arrestins. Some tissues express the two β-arrestin isoforms at similar levels [e.g., colon (12) or lung (28)], while other tissues feature a predominant expression of one isoform [e.g., β-arrestin2 in bone marrow (7) or β-arrestin1 in pancreas (35)]. Considering the expression levels of ARRDC1-5 adds another layer of complexity to this system of GRK-mediated GPCR regulation. To visualize the respective protein-specific expression profiles for all listed tissues in the HPA, we prepared radar plots of β-arrestin1 and 2, GRK2, 3, 5, and 6 (**Figure 3**). Using a clustering heatmap [generated with R package *pheatmap* (Kolde, 2013. pheatmap: Pretty Heatmaps. R package version 1.0.12[3])], we analyzed the relative expression of these genes, normalized to the respective maximal expression (**Figure 4A**). The clustering algorithm identified the highest degree of similarity for the relative expression profiles of GRK2, 6, and β-arrestin2, according to the Euclidean distance. Following

[1]http://proteinatlas.org/humanproteome/cell

[2]https://www.proteinatlas.org/

[3]http://CRAN.R-project.org/package=pheatmap

TABLE 1 | Relative tissue expression of GRK2, 3, 5, and 6, β-arrestin1 and -2, and ARRDC1-5.

Index	Tissue	GRK2	GRK3	GRK5	GRK6	βarr-1	βarr2	ARRDC1	ARRDC2	ARRDC3	ARRDC4	ARRDC5
1	Adipose tissue	13.1	28.0	15.9	6.8	20.9	21.6	8.4	26.7	40.4	9.2	0.2
2	Adrenal gland	10.7	6.0	8.3	5.5	5.4	15.6	8.9	5.3	37.9	9.3	0.0
3	Amygdala	24.5	11.9	3.4	7.8	27.7	23.7	5.3	10.4	9.3	11.4	0.2
4	Appendix	35.8	12.4	16.8	26.8	14.7	47.8	16.9	12.5	12.3	11.5	0.7
5	B-cells	4.1	6.2	9.3	9.2	0.1	2.2	9.9	5.9	4.7	0.5	2.6
6	Basal ganglia	17.0	10.8	7.8	7.3	31.7	18.3	7.0	34.6	14.6	18.4	0.2
7	Bone marrow	78.2	7.0	2.7	68.1	9.6	102.8	22.1	39.3	68.7	6.7	2.2
8	Breast	17.0	11.3	10.2	10.2	15.9	10.0	10.7	27.7	40.8	14.8	0.2
9	Cerebellum	32.9	7.9	6.5	7.7	24.4	28.1	4.2	3.2	17.9	3.3	0.2
10	Cerebral cortex	35.3	18.9	5.0	10.9	36.7	26.3	8.0	19.5	13.8	16.3	0.6
11	Cervix, uterine	12.8	4.7	12.5	5.9	6.9	8.7	11.1	10.9	25.6	9.4	0.2
12	Colon	17.2	4.0	18.8	9.2	17.8	16.1	21.4	9.6	18.6	27.4	0.2
13	Corpus callosum	12.2	3.1	3.9	6.6	11.2	20.4	6.0	28.3	14.8	67.3	0.2
14	Dendritic cells	6.0	3.7	2.2	5.7	12.7	18.0	32.1	3.1	3.4	2.4	3.9
15	Ductus deferens	12.6	0.7	4.5	5.0	2.0	1.9	23.2	7.3	9.4	11.6	0.2
16	Duodenum	17.5	3.0	12.4	10.9	15.4	23.0	24.2	6.9	4.5	11.2	0.1
17	Endometrium	11.4	5.7	13.4	8.0	7.6	7.4	6.9	7.6	30.0	10.7	0.2
18	Epididymis	9.9	3.1	12.2	6.0	4.5	7.8	12.5	4.7	14.6	11.9	0.2
19	Esophagus	20.2	2.7	8.1	11.0	13.8	7.1	22.4	8.1	28.5	11.8	0.2
20	Fallopian tube	12.6	9.1	7.7	6.6	12.1	10.8	8.5	8.5	13.3	10.8	0.1
21	Gallbladder	17.6	5.0	19.5	9.3	9.2	14.8	20.6	13.1	17.4	14.7	0.3
22	Granulocytes	21.0	5.6	6.5	32.1	14.7	52.9	52.7	3.7	43.1	3.1	3.3
23	Heart muscle	13.6	4.6	45.4	6.2	12.2	10.2	7.1	8.5	16.0	9.7	0.2
24	Hippoc. formation	21.9	15.7	4.2	8.0	25.0	27.3	6.0	14.1	9.5	18.7	0.2
25	Hypothalamus	17.4	8.3	4.2	7.3	16.0	20.9	4.8	8.2	8.6	9.2	0.1
26	Kidney	13.0	3.0	4.3	5.7	9.1	10.5	13.9	10.7	23.5	14.1	0.2
27	Liver	14.1	3.4	5.7	6.6	7.4	15.6	14.6	9.8	33.4	21.8	0.2
28	Lung	19.1	9.4	27.6	11.1	37.3	35.0	19.6	22.6	32.3	14.1	0.5
29	Lymph node	42.8	14.1	8.8	37.6	9.7	31.3	19.3	19.0	14.6	6.4	2.2
30	Midbrain	13.4	9.7	3.7	7.1	19.1	20.1	5.9	47.5	14.6	18.1	0.2
31	Monocytes	18.3	8.0	3.7	22.6	37.5	32.8	33.9	6.3	7.7	5.1	1.2
32	NK-cells	3.8	0.0	0.2	17.4	3.9	5.9	6.6	7.2	5.3	0.1	1.7
33	Olfactory region	19.0	9.8	2.5	10.7	25.7	19.6	7.6	9.0	5.7	15.2	0.2
34	Ovary	9.8	4.1	16.5	6.1	12.5	8.7	4.7	4.9	57.9	7.4	0.2
35	Pancreas	10.4	8.4	3.5	12.1	28.8	8.3	30.4	6.2	14.4	25.0	0.2
36	Parathyroid gland	9.7	4.4	26.2	3.5	1.8	6.6	6.9	18.7	20.5	3.7	0.0
37	Pituitary gland	12.2	8.2	6.3	5.6	3.3	10.2	12.0	5.7	15.4	6.5	0.2
38	Placenta	12.7	4.5	24.0	4.9	17.7	16.0	15.9	8.1	44.7	13.0	0.2
39	Pons and medulla	15.7	9.6	4.5	6.7	21.8	19.7	7.9	20.1	13.4	29.4	0.2
40	Prostate	17.8	8.2	7.5	8.1	12	7.4	16	10.1	26.7	8.3	0.2
41	Rectum	16.2	4.3	6.4	5.5	16.9	13.2	6.4	7.2	12.6	17	0.1
42	Retina	9.3	4.8	5.6	5	10.1	10.7	9.3	6	17.8	4.6	0.2
43	Salivary gland	17.4	3.7	5	10.8	8.5	8.7	22.1	15.3	43.2	6.5	0.2
44	Seminal vesicle	20.8	1.9	6.7	5.2	7.5	6.2	26.7	11.6	18.1	13.5	0.2
45	Skeletal muscle	20.8	1.4	12.8	7.4	7.2	5.5	9.1	60.7	58.4	10.1	0.2
46	Skin	23.5	4.1	4.7	7.7	11.6	5.8	15.2	9.4	24.6	25.3	0
47	Small intestine	26.3	6.1	10.4	14.5	18.5	21	28.4	13.3	10.3	15.3	1
48	Smooth muscle	12.2	6.2	10.8	7.8	15.9	13.7	6.2	6.7	16.6	14	0.2
49	Spinal cord	12.5	4.9	4.8	5.4	6.4	21.7	4.7	16.8	19.9	48.7	0.3
50	Spleen	59.6	23.2	17	34.3	26.5	66.6	21.5	18.7	16	5.9	2.3
51	Stomach	17.4	4	13.9	9.1	23.1	12.5	30.7	12.1	11.7	18.1	0.2
52	T-cells	5.3	0.4	11.3	11.7	3.6	11.4	12.4	16	15.4	0.1	3.5

(Continued)

TABLE 1 | Continued

Index	Tissue	GRK2	GRK3	GRK5	GRK6	βarr-1	βarr2	ARRDC1	ARRDC2	ARRDC3	ARRDC4	ARRDC5
53	Testis	6.8	14.8	3.5	10.5	3.1	5	6.9	3.2	12.7	10.2	29.1
54	Thalamus	11.1	2.7	4.7	5.1	19	18.3	4.5	32.9	15.2	41.9	0.2
55	Thymus	35.9	11.6	9.8	32.3	3.8	23.5	16.6	10.5	15.6	1.9	0.2
56	Thyroid gland	10.1	4.5	8.9	5.3	6.4	6.4	14.4	14.3	59	14.9	0.2
57	Tongue	13.6	1.3	10.7	6.4	3.9	3.2	11.6	4.9	17.2	4.5	0.2
58	Tonsil	37.5	15.2	8.6	26.5	7.2	17	21.2	19.1	24.1	3.5	0.8
59	Total PBMC	7.4	1.6	4.2	9.1	10.9	16	13.4	4.7	6.4	0.8	0.9
60	Urinary bladder	17.1	6.7	9.5	11.4	13.2	15.7	11.4	9.3	47.7	11.7	0.2
61	Vagina	15.5	2.5	13.6	6.5	7.9	7.1	12.6	11.3	26	12.4	0.2

Consensus transcriptomics data of the Human Protein Atlas, the Genotype-Tissue Expression, and the Functional Annotation of Mammalian Genomes 5 project as normalized expression (NX) calculated in relation to the maximum NX value in the three sources for each gene. The data are based on the Human Protein Atlas version 20.1 (https://www.proteinatlas.org/), last accessed March 10th, 2021.

this analysis, we depicted the relative expression data for these three genes as an overlay radar chart (**Figure 4B**). This overlay reveals stunningly similar tissue expression patterns for these three proteins. It is tempting to speculate that GRK2, 6, and β-arrestin2 constitute an intricate system, in which disbalance is unfavorable and might lead to dysfunctional GPCR regulation under pathological conditions.

PATHOPHYSIOLOGICAL EFFECTS OF DYSREGULATED GRK EXPRESSION CHANGES

As every cell of the human body expresses GPCRs, the regulated expression levels of GRKs and β-arrestins are crucial to maintain healthy cellular and organ functions. In the following section, we highlight selected examples where a dysregulation of this delicate regulatory system might contribute to the development or progress of different pathological conditions.

The role of dysregulated GRK expression in the development of tumors was subject to extensive work and we refer to excellent reviews for further reading (Nogues et al., 2017; Nogues et al., 2018; Sun et al., 2018; Yu et al., 2018). All non-visual GRKs have been found to be dysregulated in at least one tumor model where they can act either as oncogenes or as tumor suppressors. As one example, the mean mRNA expression level of GRK5 for all analyzed tissues (**Figure 3** and **Table 1**) is 9.7 NX. In brain tissues (indices 3, 6, 9, 10, 13, 24, 25, 30, 33, 39, 49, and 54 of **Table 1**), the expression levels of GRK5 range from 2.5 to 7.8 NX. Similarly low expression levels are also seen in prostate (**Table 1**, index 40) with a relative expression of 7.5 NX. In these naturally low GRK5 expressing tissues, upregulation of GRK5 is increasing aggressiveness of glioma (Kaur et al., 2013) and is associated with increased proliferation of prostate cancer (Kim et al., 2012; Chakraborty et al., 2014; DeRita et al., 2017). In contrast, downregulation of GRK5 expression in colon (**Table 1**, index 12), a tissue with a high expression of 18.8 NX, leads to promoted proliferation in colorectal cancer (Wu et al., 2011). GRKs cannot be generally classified as either tumor suppressors or promotors, since their influence on tumor progression is highly specific for individual cancer entities or tested cell lines (Sun et al., 2018). It is tempting to speculate that upregulation of GRK levels in tissues that naturally feature a low expression level of that given GRK, or downregulation of GRK levels in high expressing tissues might allow a prediction of the impact on cancer progression. This again strengthens the idea that the balance of different players in the given cellular context is the key for physiological regulation of cell growth.

GRKs are important regulators of cell migration, which is crucial for the formation of metastases. Hence, dysregulated GRK levels influence the migratory potential of cancer cells. Changes in GRK2 expression lead to different outcomes depending on the used stimuli and cell type and were extensively discussed elsewhere (Penela et al., 2014). Again, a general association of up- or downregulation of GRK2 with reduction or promotion of migration cannot be made. GRK3 regulates CXCR4-mediated migration and metastasis in breast cancer cell models (Billard et al., 2016). It was shown that shRNA mediated downregulation of GRK3 in breast cancer cell lines led to an increased migration toward CXCL12, whereas overexpression of GRK3 diminished the chemotaxis.

A study using GRK6 knockout ($GRK6^{-/-}$) mice showed that the absence of GRK6 led to increased growth of subcutaneously injected Lewis lung cancer cells, and an increased formation of metastases formed by tail vain injected Lewis lung cancer cells (Raghuwanshi et al., 2013). In this model, CXCR2-mediated promotion of metastasis is regulated by GRK6, and the loss of this negative regulator promotes the malignant phenotype.

Besides the involvement of GRKs in cancer biology, the role of GRK2 in the cardiovascular system is also well studied (Huang et al., 2011; Schumacher and Koch, 2017; Murga et al., 2019). The importance of GRK2 in the heart is highlighted by the fact, that homozygous $GRK2^{-/-}$ mouse embryos exhibited a more than 70% decreased cardiac ejection fraction (Jaber et al., 1996), whereas heterozygous $GRK2^{+/-}$ mice showed increased contractile function compared to wild type mice (Huang et al., 2011). This again indicates that the balanced expression is important for physiological function of GRKs and that any change in this delicate system often lead to unpredictable outcomes.

Besides adaptive dysregulation by pathophysiological conditions, gene mutations can also lead to altered expression levels. Mutations in GRK2 were detected in patients suffering

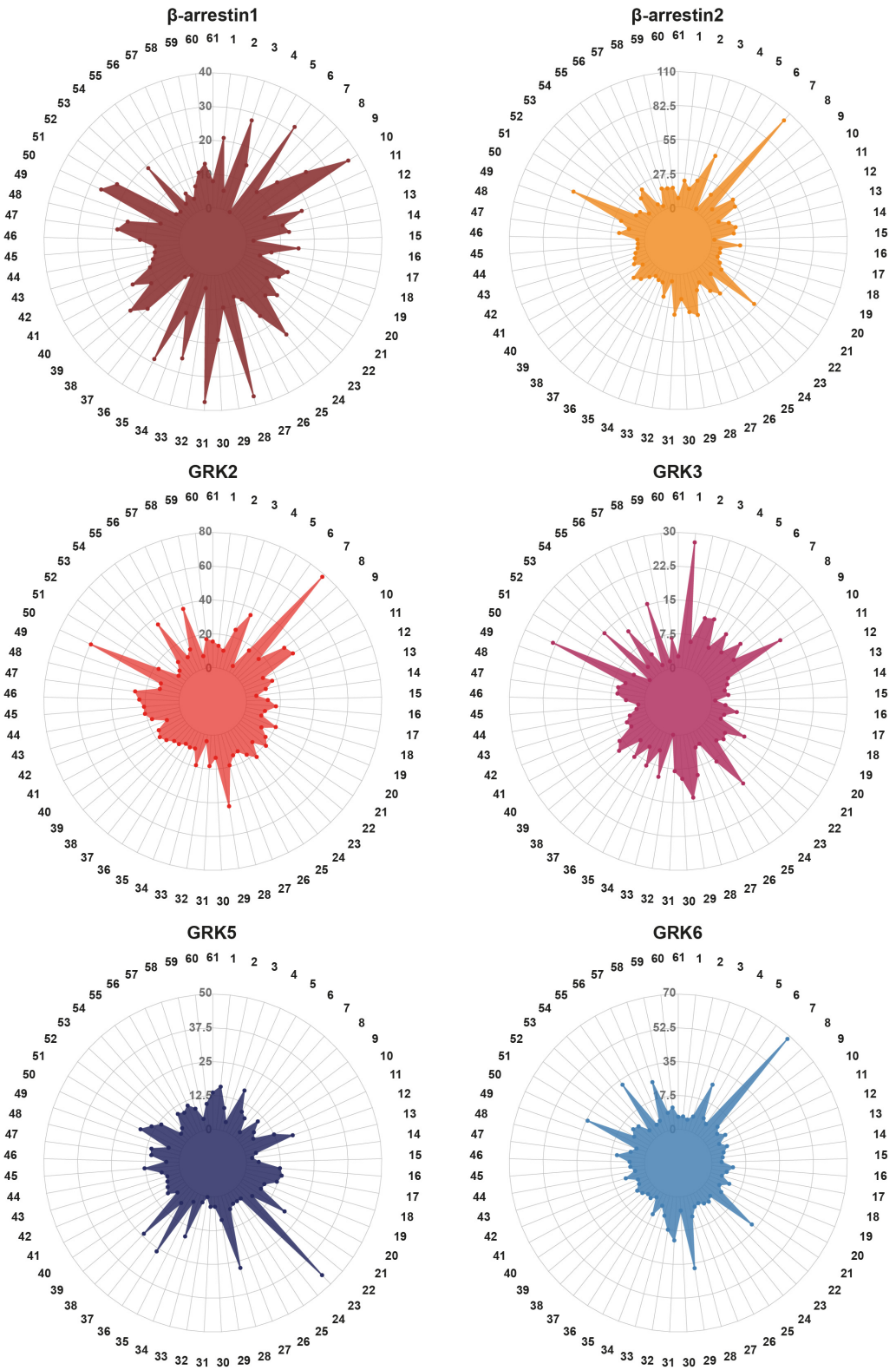

FIGURE 3 | Visualization of the tissue-specific expression levels of GRK2, 3, 5, and 6, β-arrestin1 and -2. The consensus expression data of **Table 1** are visualized in radar plots for each protein in 61 tissues. The numbers correspond to the assigned indices of tissues in **Table 1**. The data are based on the Human Protein Atlas version 20.1 (https://www.proteinatlas.org/), last accessed March 10th, 2021.

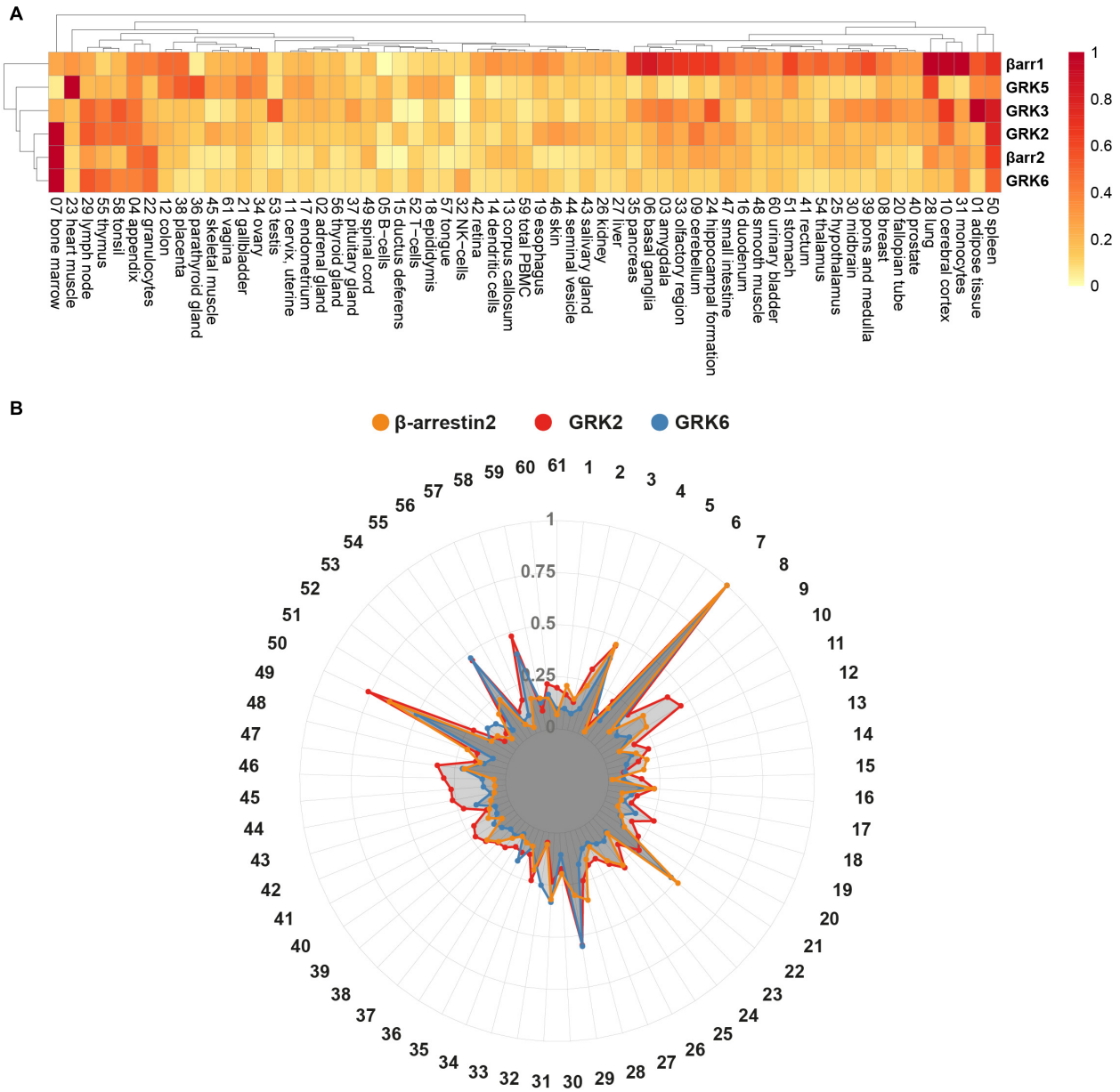

FIGURE 4 | Clustering of relative protein expression and overlay of GRK2, GRK6, and β-arrestin2 tissue expression. **(A)** Clustering of relative expression profiles of GRK2, 3, 5, 6, and β-arrestin1 and 2, according to Euclidean distance. The NX values of **Table 1** were normalized to the respective maximal tissue expression for each protein. The clustering heatmap was generated using the *pheatmap* R package (Kolde (2013). pheatmap: Pretty Heatmaps. R package version 1.0.12, http://CRAN.R-project.org/package=pheatmap). **(B)** Relative tissue expression of GRK2 (red), GRK6 (blue), and β-arrestin2 (yellow) are shown together. The data are based on the Human Protein Atlas version 20.1 (https://www.proteinatlas.org/), last accessed March 10th, 2021.

from Jeune syndrome (Bosakova et al., 2020). In one patient a mutation was identified to cause a functional loss of GRK2. Interestingly, this did not lead to expected embryonic lethality as seen in mice (Jaber et al., 1996), as the patient was born alive, but passed away 5 days after birth. GRK2 was identified as an essential regulator of skeletogenesis (Bosakova et al., 2020). The patient had a very small chest and suffered from pulmonary insufficiency, but did not show gross abnormalities in the central nervous system. Functional analyses in the same study revealed an impairment of Hedgehog and canonical Wnt signaling leading to the observed phenotype.

All described examples so far pointed out the importance to maintain physiological GRK expression levels to prevent pathophysiological conditions. Although this is not the immediate focus of this review, the GPCR–GRK–β-arrestin system is also influenced by changes of β-arrestin expression levels. In 60% of patients suffering from Sezary Syndrome (a rare cutaneous T cell lymphoma), a mono-allelic loss of the

β-arrestin2 gene was found (Cristofoletti et al., 2019). Cell culture experiments showed that downregulation of β-arrestin2 led to an impaired internalization of CXCR4 after CXCL12 stimulation, and it was hypothesized that this would lead to an increased migration toward high CXCL12 levels in skin. Another study found that, β-arrestin2 deficiency in dendritic cells promotes migration and cytokine production which contributes to autoimmune encephalomyelitis (Cai et al., 2019). The dysregulated expression of β-arrestin1 was found to be important in context of maternal-fetal tolerance in human pregnancies (Liu et al., 2021) where a strongly reduced mRNA expression of β-arrestin1 was found in villous samples of missed abortion.

CONCLUDING REMARKS

Taken together, there is surmounting evidence that the expression levels of GRKs, arrestins, and GPCRs play a crucial role in the development of pathological conditions. Literature suggests that the regulatory system of GPCRs is a common, yet fine-tuned machinery which is vital for the maintenance of healthy cellular functions. As different tissues express specific sets of GPCRs to properly react to extracellular stimuli, this regulatory system is adjusted via differential expression of GRKs and arrestins to service this exact set of GPCRs. Disturbance of this equilibrated regulation can then have differential consequences, especially considering that malignancies can also feature the overexpression or downregulation of GPCRs. This is highlighted by the seemingly unpredictable behavior of key players, as in cancer, they can act as both, tumor suppressors or oncogenes, depending on the pathological and cellular context. More work has to be done on mapping functional sets of GPCRs expressed by a given cell and understanding the individual impact of different GRK isoforms on their regulation. This tissue-specific point of view, in combination with further development and elaboration of the "barcode" hypothesis might be the key to unraveling the intricate details of GPCR regulation.

AUTHOR CONTRIBUTIONS

EM compiled and visualized the tissue expression data. RH and EM illustrated all figures. EM, RH, CH, and JD wrote the manuscript. All authors contributed to the article and approved the submitted version.

FUNDING

This research was supported by the European Regional Development Fund (Grant ID: EFRE HSB 2018 0019), the University Hospital Jena IZKF Grant No. MSP10, and the European Union's Horizon 2020 MSCA-ITN-2019 Program ONCORNET2.0 (Grant ID: 860229).

REFERENCES

Asai, D., Toita, R., Murata, M., Katayama, Y., Nakashima, H., and Kang, J. H. (2014). Peptide substrates for G protein-coupled receptor kinase 2. *FEBS Lett.* 588, 2129–2132. doi: 10.1016/j.febslet.2014.04.038

Aubry, L., Guetta, D., and Klein, G. (2009). The arrestin fold: variations on a theme. *Curr. Genom.* 10, 133–142. doi: 10.2174/138920209787847014

Bah, A., and Forman-Kay, J. D. (2016). Modulation of intrinsically disordered protein function by post-translational modifications. *J. Biol. Chem.* 291, 6696–6705. doi: 10.1074/jbc.R115.695056

Billard, M. J., Fitzhugh, D. J., Parker, J. S., Brozowski, J. M., McGinnis, M. W., Timoshchenko, R. G., et al. (2016). G protein coupled receptor kinase 3 regulates breast cancer migration, invasion, and metastasis. *PLoS One* 11:e0152856. doi: 10.1371/journal.pone.0152856

Bosakova, M., Abraham, S. P., Nita, A., Hruba, E., Buchtova, M., Taylor, S. P., et al. (2020). Mutations in GRK2 cause Jeune syndrome by impairing Hedgehog and canonical Wnt signaling. *EMBO Mol. Med.* 12, e11739. doi: 10.15252/emmm.201911739

Cai, Y., Yang, C., Yu, X., Qian, J., Dai, M., Wang, Y., et al. (2019). Deficiency of beta-Arrestin 2 in dendritic cells contributes to autoimmune diseases. *J. Immunol.* 202, 407–420. doi: 10.4049/jimmunol.1800261

Cassier, E., Gallay, N., Bourquard, T., Claeysen, S., Bockaert, J., Crepieux, P., et al. (2017). Phosphorylation of beta-arrestin2 at Thr(383) by MEK underlies beta-arrestin-dependent activation of Erk1/2 by GPCRs. *Elife* 6:e23777. doi: 10.7554/eLife.23777

Cato, M. C., Yen, Y. C., Francis, C. J., Elkins, K. E., Shareef, A., Sterne-Marr, R., et al. (2021). The open question of how GPCRs interact with GPCR kinases (GRKs). *Biomolecules* 11:447. doi: 10.3390/biom11030447

Chakraborty, P. K., Zhang, Y., Coomes, A. S., Kim, W. J., Stupay, R., Lynch, L. D., et al. (2014). G protein-coupled receptor kinase GRK5 phosphorylates moesin and regulates metastasis in prostate cancer. *Cancer Res.* 74, 3489–3500. doi: 10.1158/0008-5472.CAN-13-2708

Chen, C. Y., Dion, S. B., Kim, C. M., and Benovic, J. L. (1993). Beta-adrenergic receptor kinase. agonist-dependent receptor binding promotes kinase activation. *J. Biol. Chem.* 268, 7825–7831.

Chuang, T. T., LeVine, H. III, and De Blasi, A. (1995). Phosphorylation and activation of beta-adrenergic receptor kinase by protein kinase C. *J. Biol. Chem.* 270, 18660–18665. doi: 10.1074/jbc.270.31.18660

Claing, A., Laporte, S. A., Caron, M. G., and Lefkowitz, R. J. (2002). Endocytosis of G protein-coupled receptors: roles of G protein-coupled receptor kinases and beta-arrestin proteins. *Prog. Neurobiol.* 66, 61–79. doi: 10.1016/s0301-0082(01)00023-5

Crepieux, P., Poupon, A., Langonne-Gallay, N., Reiter, E., Delgado, J., Schaefer, M. H., et al. (2017). A comprehensive view of the beta-arrestinome. *Front. Endocrinol.* 8:32. doi: 10.3389/fendo.2017.00032

Cristofoletti, C., Bresin, A., Caprini, E., Russo, G., and Narducci, M. G. (2019). Loss of beta-arrestin-2 gene and possible functional consequences on Sezary Syndrome. *Cell Cycle* 18, 1292–1294. doi: 10.1080/15384101.2019.1617007

DeRita, R. M., Zerlanko, B., Singh, A., Lu, H., Iozzo, R. V., Benovic, J. L., et al. (2017). c-Src, insulin-like growth factor I Receptor, G-protein-coupled receptor kinases and focal adhesion kinase are enriched into prostate cancer cell exosomes. *J. Cell Biochem.* 118, 66–73. doi: 10.1002/jcb.25611

DeWire, S. M., Ahn, S., Lefkowitz, R. J., and Shenoy, S. K. (2007). Beta-arrestins and cell signaling. *Annu. Rev. Physiol.* 69, 483–510. doi: 10.1146/annurev.physiol.69.022405.154749

Doll, C., Poll, F., Peuker, K., Loktev, A., Gluck, L., and Schulz, S. (2012). Deciphering micro-opioid receptor phosphorylation and dephosphorylation in HEK293 cells. *Br. J. Pharmacol.* 167, 1259–1270. doi: 10.1111/j.1476-5381.2012.02080.x

Drube, J., Haider, R. S., Matthees, E. S. F., Reichel, M., Zeiner, J., Fritzwanker, S., et al. (2021). GRK2/3/5/6 knockout: the impact of individual GRKs on arrestin-binding and GPCR regulation. *bioRxiv* [Preprint]. doi: 10.1101/2021.02.12.430971

Flock, T., Hauser, A. S., Lund, N., Gloriam, D. E., Balaji, S., and Babu, M. M. (2017). Selectivity determinants of GPCR-G-protein binding. *Nature* 545, 317–322. doi: 10.1038/nature22070

Flock, T., Ravarani, C. N. J., Sun, D., Venkatakrishnan, A. J., Kayikci, M., Tate, C. G., et al. (2015). Universal allosteric mechanism for Galpha activation by GPCRs. *Nature* 524, 173–179. doi: 10.1038/nature14663

Fonin, A. V., Darling, A. L., Kuznetsova, I. M., Turoverov, K. K., and Uversky, V. N. (2019). Multi-functionality of proteins involved in GPCR and G protein signaling: making sense of structure-function continuum with intrinsic disorder-based proteoforms. *Cell Mol. Life Sci.* 76, 4461–4492. doi: 10.1007/s00018-019-03276-1

Godbole, A., Lyga, S., Lohse, M. J., and Calebiro, D. (2017). Internalized TSH receptors en route to the TGN induce local Gs-protein signaling and gene transcription. *Nat. Commun.* 8:443. doi: 10.1038/s41467-017-00357-2

Goodman, O. B. Jr., Krupnick, J. G., Santini, F., Gurevich, V. V., Penn, R. B., Gagnon, A. W., et al. (1996). Beta-arrestin acts as a clathrin adaptor in endocytosis of the beta2-adrenergic receptor. *Nature* 383, 447–450. doi: 10.1038/383447a0

Gurevich, E. V., Tesmer, J. J., Mushegian, A., and Gurevich, V. V. (2012). G protein-coupled receptor kinases: more than just kinases and not only for GPCRs. *Pharmacol. Ther.* 133, 40–69. doi: 10.1016/j.pharmthera.2011.08.001

Gurevich, V. V., and Gurevich, E. V. (2006). The structural basis of arrestin-mediated regulation of G-protein-coupled receptors. *Pharmacol. Ther.* 110, 465–502. doi: 10.1016/j.pharmthera.2005.09.008

Gurevich, V. V., and Gurevich, E. V. (2019). GPCR signaling regulation: the role of GRKs and arrestins. *Front. Pharmacol.* 10:125. doi: 10.3389/fphar.2019.00125

Haider, R. S., Wilhelm, F., Rizk, A., Mutt, E., Deupi, X., Peterhans, C., et al. (2019). Arrestin-1 engineering facilitates complex stabilization with native rhodopsin. *Sci. Rep.* 9:439. doi: 10.1038/s41598-018-36881-4

Homan, K. T., and Tesmer, J. J. (2014). Structural insights into G protein-coupled receptor kinase function. *Curr. Opin. Cell Biol.* 27, 25–31. doi: 10.1016/j.ceb.2013.10.009

Huang, C. C., and Tesmer, J. J. G. (2011). Recognition in the face of diversity: interactions of heterotrimeric G proteins and G protein-coupled receptor (GPCR) kinases with activated GPCRs. *J. Biol. Chem.* 286, 7715–7721. doi: 10.1074/jbc.R109.051847

Huang, W., Masureel, M., Qu, Q., Janetzko, J., Inoue, A., Kato, H. E., et al. (2020). Structure of the neurotensin receptor 1 in complex with beta-arrestin 1. *Nature* 579, 303–308. doi: 10.1038/s41586-020-1953-1

Huang, Z. M., Gold, J. I., and Koch, W. J. (2011). G protein-coupled receptor kinases in normal and failing myocardium. *Front. Biosci.* 16:3047–3060. doi: 10.2741/3898

Inoue, A., Raimondi, F., Kadji, F. M. N., Singh, G., Kishi, T., Uwamizu, A., et al. (2019). Illuminating G-protein-coupling selectivity of GPCRs. *Cell* 177, 1933–1947.e25. doi: 10.1016/j.cell.2019.04.044

Jaakola, V. P., Prilusky, J., Sussman, J. L., and Goldman, A. (2005). G protein-coupled receptors show unusual patterns of intrinsic unfolding. *Protein Eng. Des. Sel.* 18, 103–110. doi: 10.1093/protein/gzi004

Jaber, M., Koch, W. J., Rockman, H., Smith, B., Bond, R. A., Sulik, K. K., et al. (1996). Essential role of beta-adrenergic receptor kinase 1 in cardiac development and function. *Proc. Natl. Acad. Sci. U.S.A.* 93, 12974–12979. doi: 10.1073/pnas.93.23.12974

Kahlhofer, J., Leon, S., Teis, D., and Schmidt, O. (2021). The alpha-arrestin family of ubiquitin ligase adaptors links metabolism with selective endocytosis. *Biol. Cell* 113, 183–219. doi: 10.1111/boc.202000137

Kang, D. S., Tian, X., and Benovic, J. L. (2014). Role of beta-arrestins and arrestin domain-containing proteins in G protein-coupled receptor trafficking. *Curr. Opin. Cell Biol.* 27, 63–71. doi: 10.1016/j.ceb.2013.11.005

Kang, J. H., Toita, R., Kawano, T., Murata, M., and Asai, D. (2020). Design of substrates and inhibitors of G protein-coupled receptor kinase 2 (GRK2) based on its phosphorylation reaction. *Amino Acids* 52, 863–870. doi: 10.1007/s00726-020-02864-x

Kang, Y., Zhou, X. E., Gao, X., He, Y., Liu, W., Ishchenko, A., et al. (2015). Crystal structure of rhodopsin bound to arrestin by femtosecond X-ray laser. *Nature* 523, 561–567. doi: 10.1038/nature14656

Kaur, G., Kim, J., Kaur, R., Tan, I., Bloch, O., Sun, M. Z., et al. (2013). G-protein coupled receptor kinase (GRK)-5 regulates proliferation of glioblastoma-derived stem cells. *J. Clin. Neurosci.* 20, 1014–1018. doi: 10.1016/j.jocn.2012.10.008

Kim, J. I., Chakraborty, P., Wang, Z., and Daaka, Y. (2012). G-protein coupled receptor kinase 5 regulates prostate tumor growth. *J. Urol.* 187, 322–329. doi: 10.1016/j.juro.2011.09.049

Kim, J., Ahn, S., Ren, X. R., Whalen, E. J., Reiter, E., Wei, H., et al. (2005). Functional antagonism of different G protein-coupled receptor kinases for beta-arrestin-mediated angiotensin II receptor signaling. *Proc. Natl. Acad. Sci. U.S.A.* 102, 1442–1447. doi: 10.1073/pnas.0409532102

Kolde, R. (2013.) Available online at: https://cran.r-project.org/web/packages/pheatmap/index.html

Krupnick, J. G., Goodman, O. B. Jr., Keen, J. H., and Benovic, J. L. (1997). Arrestin/clathrin interaction. localization of the clathrin binding domain of nonvisual arrestins to the carboxy terminus. *J. Biol. Chem.* 272, 15011–15016. doi: 10.1074/jbc.272.23.15011

Kumari, P., Srivastava, A., Ghosh, E., Ranjan, R., Dogra, S., Yadav, P. N., et al. (2017). Core engagement with beta-arrestin is dispensable for agonist-induced vasopressin receptor endocytosis and ERK activation. *Mol. Biol. Cell* 28, 1003–1010. doi: 10.1091/mbc.E16-12-0818

Laporte, S. A., Oakley, R. H., Holt, J. A., Barak, L. S., and Caron, M. G. (2000). The interaction of beta-arrestin with the AP-2 adaptor is required for the clustering of beta 2-adrenergic receptor into clathrin-coated pits. *J. Biol. Chem.* 275, 23120–23126. doi: 10.1074/jbc.M002581200

Latorraca, N. R., Venkatakrishnan, A. J., and Dror, R. O. (2017). GPCR dynamics: structures in motion. *Chem. Rev.* 117, 139–155. doi: 10.1021/acs.chemrev.6b00177

Lee, M. H., Appleton, K. M., Strungs, E. G., Kwon, J. Y., Morinelli, T. A., Peterson, Y. K., et al. (2016). The conformational signature of beta-arrestin2 predicts its trafficking and signalling functions. *Nature* 531, 665–668. doi: 10.1038/nature17154

Lee, Y., Warne, T., Nehme, R., Pandey, S., Dwivedi-Agnihotri, H., Chaturvedi, M., et al. (2020). Molecular basis of beta-arrestin coupling to formoterol-bound beta1-adrenoceptor. *Nature* 583, 862–866. doi: 10.1038/s41586-020-2419-1

Liu, T., Ma, Y., Yin, Q., Zhou, H., and Fang, Y. (2021). Association of beta-arrestin1 and p53-Mdm2 signaling in the development of missed abortion. *J. Obstet. Gynaecol. Res.* 47, 1675–1685. doi: 10.1111/jog.14643 ,

Marinissen, M. J., and Gutkind, J. S. (2001). G-protein-coupled receptors and signaling networks: emerging paradigms. *Trends Pharmacol. Sci.* 22, 368–376. doi: 10.1016/s0165-6147(00)01678-3

Mayer, D., Damberger, F. F., Samarasimhareddy, M., Feldmueller, M., Vuckovic, Z., Flock, T., et al. (2019). Distinct G protein-coupled receptor phosphorylation motifs modulate arrestin affinity and activation and global conformation. *Nat. Commun.* 10:1261. doi: 10.1038/s41467-019-09204-y

McCarthy, N. E., and Akhtar, M. (2002). Activation of rhodopsin kinase. *Biochem. J.* 363(Pt. 2), 359–364. doi: 10.1042/0264-6021:3630359

Miess, E., Gondin, A. B., Yousuf, A., Steinborn, R., Mosslein, N., Yang, Y., et al. (2018). Multisite phosphorylation is required for sustained interaction with GRKs and arrestins during rapid mu-opioid receptor desensitization. *Sci. Signal.* 11:eaas9609. doi: 10.1126/scisignal.aas9609

Milligan, G., and Kostenis, E. (2006). Heterotrimeric G-proteins: a short history. *Br. J. Pharmacol.* 147(Suppl. 1), S46–S55. doi: 10.1038/sj.bjp.0706405

Moller, T. C., Pedersen, M. F., van Senten, J. R., Seiersen, S. D., Mathiesen, J. M., Bouvier, M., et al. (2020). Dissecting the roles of GRK2 and GRK3 in mu-opioid receptor internalization and beta-arrestin2 recruitment using CRISPR/Cas9-edited HEK293 cells. *Sci. Rep.* 10:17395. doi: 10.1038/s41598-020-73674-0

Murga, C., Arcones, A. C., Cruces-Sande, M., Briones, A. M., Salaices, M., and Mayor, F. Jr. (2019). G protein-coupled receptor kinase 2 (GRK2) as a potential therapeutic target in cardiovascular and metabolic diseases. *Front. Pharmacol.* 10:112. doi: 10.3389/fphar.2019.00112

Mushegian, A., Gurevich, V. V., and Gurevich, E. V. (2012). The origin and evolution of G protein-coupled receptor kinases. *PLoS One* 7:e33806. doi: 10.1371/journal.pone.0033806

Nguyen, A. H., Thomsen, A. R. B., Cahill, T. J. III, Huang, R., Huang, L. Y., Marcink, T., et al. (2019). Structure of an endosomal signaling GPCR-G protein-beta-arrestin megacomplex. *Nat. Struct. Mol. Biol.* 26, 1123–1131. doi: 10.1038/s41594-019-0330-y

Nobles, K. N., Xiao, K., Ahn, S., Shukla, A. K., Lam, C. M., Rajagopal, S., et al. (2011). Distinct phosphorylation sites on the beta(2)-adrenergic receptor establish a barcode that encodes differential functions of beta-arrestin. *Sci. Signal.* 4:ra51. doi: 10.1126/scisignal.2001707

Nogues, L., Palacios-Garcia, J., Reglero, C., Rivas, V., Neves, M., Ribas, C., et al. (2018). G protein-coupled receptor kinases (GRKs) in tumorigenesis and cancer progression: GPCR regulators and signaling hubs. *Semin. Cancer Biol.* 48, 78–90. doi: 10.1016/j.semcancer.2017.04.013

Nogues, L., Reglero, C., Rivas, V., Neves, M., Penela, P., and Mayor, F. Jr. (2017). G-protein-coupled receptor kinase 2 as a potential modulator of the hallmarks of cancer. *Mol. Pharmacol.* 91, 220–228. doi: 10.1124/mol.116.107185

Nuber, S., Zabel, U., Lorenz, K., Nuber, A., Milligan, G., Tobin, A. B., et al. (2016). beta-Arrestin biosensors reveal a rapid, receptor-dependent activation/deactivation cycle. *Nature* 531, 661–664. doi: 10.1038/nature17198

Nygaard, R., Zou, Y., Dror, R. O., Mildorf, T. J., Arlow, D. H., Manglik, A., et al. (2013). The dynamic process of beta(2)-adrenergic receptor activation. *Cell* 152, 532–542. doi: 10.1016/j.cell.2013.01.008

Oldfield, C. J., and Dunker, A. K. (2014). Intrinsically disordered proteins and intrinsically disordered protein regions. *Annu. Rev. Biochem.* 83, 553–584. doi: 10.1146/annurev-biochem-072711-164947

Oldham, W. M., and Hamm, H. E. (2008). Heterotrimeric G protein activation by G-protein-coupled receptors. *Nat. Rev. Mol. Cell Biol.* 9, 60–71. doi: 10.1038/nrm2299

Palczewski, K., Buczylko, J., Kaplan, M. W., Polans, A. S., and Crabb, J. W. (1991). Mechanism of rhodopsin kinase activation. *J. Biol. Chem.* 266, 12949–12955.

Patwardhan, A., Cheng, N., and Trejo, J. (2021). Post-translational modifications of G protein-coupled receptors control cellular signaling dynamics in space and time. *Pharmacol. Rev.* 73, 120–151. doi: 10.1124/pharmrev.120.000082

Penela, P., Nogues, L., and Mayor, F. Jr. (2014). Role of G protein-coupled receptor kinases in cell migration. *Curr. Opin. Cell Biol.* 27, 10–17. doi: 10.1016/j.ceb.2013.10.005

Pinna, L. A., and Ruzzene, M. (1996). How do protein kinases recognize their substrates? *Biochim. Biophys. Acta* 1314, 191–225. doi: 10.1016/s0167-4889(96)00083-3

Pronin, A. N., and Benovic, J. L. (1997). Regulation of the G protein-coupled receptor kinase GRK5 by protein kinase C. *J. Biol. Chem.* 272, 3806–3812. doi: 10.1074/jbc.272.6.3806

Raghuwanshi, S. K., Smith, N., Rivers, E. J., Thomas, A. J., Sutton, N., Hu, Y., et al. (2013). G protein-coupled receptor kinase 6 deficiency promotes angiogenesis, tumor progression, and metastasis. *J. Immunol.* 190, 5329–5336. doi: 10.4049/jimmunol.1202058

Ren, X. R., Reiter, E., Ahn, S., Kim, J., Chen, W., and Lefkowitz, R. J. (2005). Different G protein-coupled receptor kinases govern G protein and beta-arrestin-mediated signaling of V2 vasopressin receptor. *Proc. Natl. Acad. Sci. U.S.A.* 102, 1448–1453. doi: 10.1073/pnas.0409534102

Schumacher, S. M., and Koch, W. J. (2017). Noncanonical roles of G protein-coupled receptor kinases in cardiovascular signaling. *J. Cardiovasc. Pharmacol.* 70, 129–141. doi: 10.1097/FJC.0000000000000483

Shammas, S. L., Crabtree, M. D., Dahal, L., Wicky, B. I., and Clarke, J. (2016). Insights into coupled folding and binding mechanisms from kinetic studies. *J. Biol. Chem.* 291, 6689–6695. doi: 10.1074/jbc.R115.692715

Shukla, A. K., Manglik, A., Kruse, A. C., Xiao, K., Reis, R. I., Tseng, W. C., et al. (2013). Structure of active beta-arrestin-1 bound to a G-protein-coupled receptor phosphopeptide. *Nature* 497, 137–141. doi: 10.1038/nature12120

Staus, D. P., Hu, H., Robertson, M. J., Kleinhenz, A. L. W., Wingler, L. M., Capel, W. D., et al. (2020). Structure of the M2 muscarinic receptor-beta-arrestin complex in a lipid nanodisc. *Nature* 579, 297–302. doi: 10.1038/s41586-020-1954-0

Sun, W. Y., Wu, J. J., Peng, W. T., Sun, J. C., and Wei, W. (2018). The role of G protein-coupled receptor kinases in the pathology of malignant tumors. *Acta Pharmacol. Sin.* 39, 1699–1705. doi: 10.1038/s41401-018-0049-z

Tesmer, V. M., Kawano, T., Shankaranarayanan, A., Kozasa, T., and Tesmer, J. J. (2005). Snapshot of activated G proteins at the membrane: the Galphaq-GRK2-Gbetagamma complex. *Science* 310, 1686–1690. doi: 10.1126/science.1118890

Thomsen, A. R. B., Plouffe, B., Cahill, T. J. III, Shukla, A. K., Tarrasch, J. T., Dosey, A. M., et al. (2016). GPCR-G protein-beta-arrestin super-complex mediates sustained G protein signaling. *Cell* 166, 907–919. doi: 10.1016/j.cell.2016.07.004

Thul, P. J., Akesson, L., Wiking, M., Mahdessian, D., Geladaki, A., Ait Blal, H., et al. (2017). A subcellular map of the human proteome. *Science* 356:eaal3321. doi: 10.1126/science.aal3321

Tian, X., Irannejad, R., Bowman, S. L., Du, Y., Puthenveedu, M. A., von Zastrow, M., et al. (2016). The alpha-arrestin ARRDC3 regulates the endosomal residence time and intracellular signaling of the beta2-adrenergic receptor. *J. Biol. Chem.* 291, 14510–14525. doi: 10.1074/jbc.M116.716589

Tran, T. M., Friedman, J., Qunaibi, E., Baameur, F., Moore, R. H., and Clark, R. B. (2004). Characterization of agonist stimulation of cAMP-dependent protein kinase and G protein-coupled receptor kinase phosphorylation of the beta2-adrenergic receptor using phosphoserine-specific antibodies. *Mol. Pharmacol.* 65, 196–206. doi: 10.1124/mol.65.1.196

Uhlen, M., Fagerberg, L., Hallstrom, B. M., Lindskog, C., Oksvold, P., Mardinoglu, A., et al. (2015). Proteomics. tissue-based map of the human proteome. *Science* 347:1260419. doi: 10.1126/science.1260419

van der Lee, R., Buljan, M., Lang, B., Weatheritt, R. J., Daughdrill, G. W., Dunker, A. K., et al. (2014). Classification of intrinsically disordered regions and proteins. *Chem. Rev.* 114, 6589–6631. doi: 10.1021/cr400525m

Venkatakrishnan, A. J., Flock, T., Prado, D. E., Oates, M. E., Gough, J., and Madan Babu, M. (2014). Structured and disordered facets of the GPCR fold. *Curr. Opin. Struct. Biol.* 27, 129–137. doi: 10.1016/j.sbi.2014.08.002

Winstel, R., Freund, S., Krasel, C., Hoppe, E., and Lohse, M. J. (1996). Protein kinase cross-talk: membrane targeting of the beta-adrenergic receptor kinase by protein kinase C. *Proc. Natl. Acad. Sci. U.S.A.* 93, 2105–2109. doi: 10.1073/pnas.93.5.2105

Wright, P. E., and Dyson, H. J. (2015). Intrinsically disordered proteins in cellular signalling and regulation. *Nat. Rev. Mol. Cell Biol.* 16, 18–29. doi: 10.1038/nrm3920

Wu, C. C., Tsai, F. M., Shyu, R. Y., Tsai, Y. M., Wang, C. H., and Jiang, S. Y. (2011). G protein-coupled receptor kinase 5 mediates Tazarotene-induced gene 1-induced growth suppression of human colon cancer cells. *BMC Cancer* 11:175. doi: 10.1186/1471-2407-11-175

Xiao, K., McClatchy, D. B., Shukla, A. K., Zhao, Y., Chen, M., Shenoy, S. K., et al. (2007). Functional specialization of beta-arrestin interactions revealed by proteomic analysis. *Proc. Natl. Acad. Sci. U.S.A.* 104, 12011–12016. doi: 10.1073/pnas.0704849104

Yang, F., Yu, X., Liu, C., Qu, C. X., Gong, Z., Liu, H. D., et al. (2015). Phospho-selective mechanisms of arrestin conformations and functions revealed by unnatural amino acid incorporation and (19)F-NMR. *Nat. Commun.* 6:8202. doi: 10.1038/ncomms9202

Yu, S., Sun, L., Jiao, Y., and Lee, L. T. O. (2018). The role of G protein-coupled receptor kinases in cancer. *Int. J. Biol. Sci.* 14, 189–203. doi: 10.7150/ijbs.22896

Zhu, W., Tilley, D. G., Myers, V. D., Coleman, R. C., and Feldman, A. M. (2013). Arginine vasopressin enhances cell survival via a G protein-coupled receptor kinase 2/beta-arrestin1/extracellular-regulated kinase 1/2-dependent pathway in H9c2 cells. *Mol. Pharmacol.* 84, 227–235. doi: 10.1124/mol.113.086322

Conflict of Interest: The authors declare that the research was conducted in the absence of any commercial or financial relationships that could be construed as a potential conflict of interest.

frontiers in Cell and Developmental Biology

REVIEW
published: 25 May 2021
doi: 10.3389/fcell.2021.652152

Current Developments on the Role of α_1-Adrenergic Receptors in Cognition, Cardioprotection, and Metabolism

*Dianne M. Perez**

The Lerner Research Institute, The Cleveland Clinic Foundation, Cleveland, OH, United States

OPEN ACCESS

Edited by:
Muheeb Beg,
University of Gothenburg, Sweden

Reviewed by:
Alan Bush,
Massachusetts General Hospital and Harvard Medical School, United States
Gianluigi Pironti,
Karolinska Institutet (KI), Sweden
Van Doze,
University of North Dakota, United States

***Correspondence:**
Dianne M. Perez
Perezd@ccf.org

Specialty section:
This article was submitted to Signaling, a section of the journal Frontiers in Cell and Developmental Biology

Received: *11 January 2021*
Accepted: *29 April 2021*
Published: *25 May 2021*

Citation:
Perez DM (2021) Current Developments on the Role of α_1-Adrenergic Receptors in Cognition, Cardioprotection, and Metabolism. Front. Cell Dev. Biol. 9:652152. doi: 10.3389/fcell.2021.652152

The α_1-adrenergic receptors (ARs) are G-protein coupled receptors that bind the endogenous catecholamines, norepinephrine, and epinephrine. They play a key role in the regulation of the sympathetic nervous system along with β and α_2-AR family members. While all of the adrenergic receptors bind with similar affinity to the catecholamines, they can regulate different physiologies and pathophysiologies in the body because they couple to different G-proteins and signal transduction pathways, commonly in opposition to one another. While α_1-AR subtypes (α_{1A}, α_{1B}, α_{1C}) have long been known to be primary regulators of vascular smooth muscle contraction, blood pressure, and cardiac hypertrophy, their role in neurotransmission, improving cognition, protecting the heart during ischemia and failure, and regulating whole body and organ metabolism are not well known and are more recent developments. These advancements have been made possible through the development of transgenic and knockout mouse models and more selective ligands to advance their research. Here, we will review the recent literature to provide new insights into these physiological functions and possible use as a therapeutic target.

Keywords: adrenergic receptor, G-protein coupled receptor, cognition, cardioprotection, metabolism

INTRODUCTION

α_1-Adrenergic receptors (ARs) regulate the sympathetic nervous system by binding and transducing the effects of the endogenous catecholamines, epinephrine, and norepinephrine (Graham and Lanier, 1986). ARs are members of the G-protein-coupled receptor (GPCR) superfamily and are composed of nine adrenergic receptor subtypes (α_{1A}, α_{1B}, α_{1D}, α_{2A}, α_{2B}, α_{2C}, β_1, β_2, and β_3) from the three distinct families (α_1, α_2, β) which are activated by the same catecholamines and are related as paralogs.

The α_1-AR subtype cDNAs were cloned in the late 1980s and early 1990s (Cotecchia et al., 1988; Schwinn et al., 1990; Lomasney et al., 1991; Perez et al., 1991, 1994; Laz et al., 1994). They have distinct pharmacological properties which helped to determine their classification and

characterization. Before the cloning of the receptors, α_1-ARs were already subdivided into the α_{1A}- and α_{1B}-AR subtypes based upon radioligand binding data in various tissues which showed two-site competition binding curves to the antagonists WB4101 and phentolamine. The α_{1A}-AR subtype was defined as having a 10–100-fold higher binding affinity for these two antagonists while the α_{1B}-AR subtype was defined as having the weaker binding affinity (Morrow and Creese, 1986). The α_{1C}-AR designation is missing from the α_1-AR subtype lineage because of a misclassification early on in the cloning of the receptors[1].

α_1-ARs are mainly coupled to the heterotrimeric Gq/11 (Gαq) family of G-proteins to activate phospholipase Cβ1 (PLCβ1), resulting in the hydrolysis of membrane-bound phosphatidylinositol 4,5-bisphosphate and the cytosolic release of inositol triphosphate (IP3) and diacylglycerol (DAG) (Piascik and Perez, 2001; **Table 1**). The IP3 plays a key role in calcium regulation by binding to IP3 receptors located on the endoplasmic reticulum resulting in calcium channel opening and the release of intracellular calcium. The DAG activates protein kinase C (PKC) which can phosphorylate many other types of proteins and signals downstream in the signaling cascade. There are also reports that α_1-ARs can couple to G_i G-proteins under overexpressed conditions or in certain cell lines (Akhter et al., 1997; Melien et al., 2000; Snabaitis et al., 2005) but this has not been shown to occur *in vivo*. α_1-ARs can also signal through G-protein-independent mechanisms involving β-arrestins which act as scaffolds to recruit and activate other second messengers such as ERK 1/2, p38, and Src (Perez-Aso et al., 2013; Segura et al., 2013). α_1-ARs can also couple to phospholipase A_2 and calcium channels though this may not be direct coupling (Perez et al., 1993).

While the α_1-AR subtypes display differences in internalization resulting in spatio-temporal changes in signaling (Stanasila et al., 2008; Perez-Aso et al., 2013; Segura et al., 2013), there is some evidence that the α_1-AR subtypes differentially couple to different signaling proteins, such as Regulators of G-protein Signaling (RGS) (Hague et al., 2005). These G-protein modulators can interact with the alpha subunits of large G-proteins to increase the rate of GTP hydrolysis and to stop the receptor signaling process. RGS2 can directly bind to the third intracellular loop of the α_{1A}-AR to inhibit its signaling process but does not bind at the α_{1B}- or α_{1D}-AR subtypes (Hague et al., 2005). As RGS2 plays a prominent role in regulating GPCR cardiovascular functions (Tang et al., 2003; Zou et al., 2006) and GPCR G_{11} signaling pathways (Cunningham et al., 2001), α_{1A}-AR coupling to RGS2 may regulate many of its subtype-specific functions. Another way that α_1-ARs create differential signaling pathways is through biased agonism (Wootten et al., 2018). Cirazoline or A61603, imidazolines which are α_{1A}-AR selective agonists, can bias the receptor toward cAMP signaling rather than Ca^{+2} release or ERK phosphorylation (Evans et al., 2011; da Silva et al., 2017) or can enhance the α_{1A}-AR desensitization and internalization process (Akinaga et al., 2013) leading to differential coupling to β-arrestin-mediated signaling.

TRANSGENIC AND KNOCKOUT MOUSE MODELS

Due to the lack of sufficiently selective pharmacological agents to use in order to distinguish subtype-specific effects, a number of transgenic and knockout (KO) mouse models were developed that were used to determine long-term *in vivo* stimulatory or inhibitory effects of the α_1-AR subtypes on physiology and pathophysiology (**Table 2**). KOs of the α_{1A}-AR (Rokosh and Simpson, 2002; Zhang et al., 2020), α_{1B}-AR (Cavalli et al., 1997), and α_{1D}-AR (Tanoue et al., 2002) were developed using traditional insertion of the β-galactosidase or neomycin resistance gene in place of the first exon of the receptor. Recently, a cardiac-conditional KO of the α_{1A}-AR was developed (Zhang et al., 2020). There is also a double KO model created by mating together the α_{1A} and α_{1B}-AR KO mice (O'Connell et al., 2003) and a triple KO of all three subtypes (Sanbe et al., 2007). Transgenic mice overexpressing α_1-ARs were designed to either target to the myocyte using the α myosin heavy chain promoter to drive only cardiac expression of wild-type (WT) or constitutively active mutations (CAMs) in the receptor (Milano et al., 1994; Grupp et al., 1998; Eckhart et al., 2000; Lin et al., 2001) or used CAMs in the receptors that were driven by large fragments of the endogenous mouse promoters to generate systemic expression (Zuscik et al., 2000, 2001; Ross et al., 2003; Rorabaugh et al., 2005). The systemic expression of the CAMs also allows assessment of cardiovascular effects due to chronic α_1-AR expression outside of the myocyte as well as in the brain or other organ systems. There is also only mild overexpression of the receptor in the heart and brain (2–3 fold) and throughout the body in using the endogenous promoters as compared to using the α myosin heavy chain promoter which caused very high amounts of receptor overexpression, often exceeding 100-fold. The use of CAMs instead of the WT receptor results in continuously activated receptors that do not need an agonist to be present and can be representative of a chronically stimulated condition, but this is still debated. In both overexpressed and KO mouse models, there is always the possibility of changes in the expression of other genes and receptors in compensation or as a result of additional insertion or deletion of genetic material, a widespread phenomenon that is hard to decipher and under reported (El-Brolosy and Stainier, 2017). Recognizing these limitations and seeing if general phenotypes repeat in the various mouse models of particular receptor subtypes is suggested. These different types of mouse models will be referred to throughout this review.

COGNITION

Localization in the Brain

The expression of the specific α_1-AR subtypes in the brain was previously difficult to determine because of the lack of

[1]The α_{1C}-AR was first designated novel but more detailed analysis revealed that it was a bovine analog of the α_{1A}-AR (Schwinn et al., 1990; Laz et al., 1994; Perez et al., 1994). To avoid confusion, an actual novel α_1-AR subtype discovered through molecular cloning was designated the α_{1D}-AR (Perez et al., 1991) and the α_{1C} designation was dropped from the classification scheme.

TABLE 1 | Properties of the α_1-AR subtypes.

Subtype	α_{1A}	α_{1B}	α_{1D}
Signal transduction	G_q/G_{11}/PLC/PKC/ DAG/IP3/Ca^{+2} RGS2	G_q/G_{11}/PLC/PKC/ DAG/IP3/Ca^{+2}	G_q/G_{11}/PLC/PKC/ DAG/IP3/Ca^{+2}
Selective Agonists	A61603, cirazoline	None	None
Selective Antagonists	Niguldipine, 5-Methylurapidil,	None	BMY-7378
Allosteric	Amilorides (NAMs) 9-aminoacridine (NAM)	Conopeptide rho-TIA (NAM) 9-aminoacridine (NAM)	None
Tissue distribution	Hippocampus, amygdala, cerebral cortex, neural stem and progenitor cells, interneurons, hypothalamus, myocyte, smooth muscle, vascular, mesenteric arteries	Cerebral cortex, myocyte, smooth muscle, vascular	Reticular thalamic nuclei, hippocampus, spinal cord, aorta, smooth muscle, vascular, coronary arteries
Physiological function	Cognition, neurogenesis, LTP, spatial memory, blood pressure, positive inotropy, contraction smooth muscle, blood pressure, cardiac hypertrophy, cardiac adaptive, cardiac ischemic protection, glucose uptake (all tissues), glycolysis (cardiac, adipocytes, skeletal muscle), glucose tolerance, whole body fatty acid oxidation.	Memory consolidation, fear-motivated exploration, spatial learning-novelty, contraction smooth muscle, blood pressure, negative inotropy, cardiac hypertrophy, cardiac maladaptive, baroreflex, glucose uptake (non-cardiac tissues), glycolysis (adipocytes, skeletal muscle), glucose tolerance, whole body fatty acid oxidation.	Contraction smooth muscle, contraction-mesenteric beds, blood pressure.

high avidity antibodies to the α_1-ARs (Jensen et al., 2009c; Böhmer et al., 2014). Initial autoradiography studies used non-selective radiolabels that could not distinguish between the α_1-ARs subtypes but did demonstrate high abundance throughout the rat brain (Unnerstall et al., 1985). Eventually, more specific and sensitive techniques were developed to determine the α_1-AR subtype localization in the brain such as using the full-length cDNA sequence of the α_{1A}-AR in hybridization studies (Domyancic and Morilak, 1997) or transgenic and knock-out (KO) mouse models of the α_1-AR subtypes with the α_1-ARs tagged with endogenous promoter-driven expression of EGFP or use of the β-galactosidase gene to KO the receptor (Papay et al., 2004, 2006). Using these approaches, the α_{1A}- and α_{1B}-ARs were shown to be expressed in similar areas of the brain, but the relative expression was different (Papay et al., 2004, 2006). The α_{1A}-AR subtype was more noticeably expressed in the cognitive areas such as the hippocampus, amygdala, and particular cortical areas (**Table 1**; Papay et al., 2006), while the α_{1B}-AR appeared more prominent throughout the cortex and thalamus (Drouin et al., 2002; Papay et al., 2004). The α_{1A}-AR subtype was also more prominently expressed in neural progenitors and stem cells (Papay et al., 2006; Gupta et al., 2009). Using long sequences of antisense to the α_{1D}-AR to assess brain localization, the α_{1D}-AR although of low overall abundance, was present in the reticular thalamic nuclei, hippocampus, cortex and spinal cord (Harasawa et al., 2003). Using the α_1-AR KO mice and comparing the total amount of α_1-AR radioligand receptor binding to normal wild-type mice, it was concluded that the brain contains the highest amount of the α_{1A}-AR subtype at ∼55% (Rokosh and Simpson, 2002), followed by the α_{1B}-AR at 35% (Cavalli et al., 1997) but only 10% of the total α_1-AR pool for the α_{1D}-AR subtype (Tanoue et al., 2002; Sadalge et al., 2003).

The localization of the α_1-ARs in the brain may have some species variation (Palacios et al., 1987; Zilles et al., 1991), but the cognitive areas appear similar in humans with high expression in the hippocampus and prefrontal cortex and the lowest expression in the caudate and putamen (Shimohama et al., 1986; Szot et al., 2005). The α_{1A}-AR subtype appears to be prominent in expression in the hippocampus as assessed by RNA (Szot et al., 2005), single cell PCR (Hillman et al., 2005), protein localization using the EGFP-tagged transgenics (Papay et al., 2006) and functionally by regulating the CA1 hippocampal interneurons (Jurgens et al., 2009). In addition, the α_{1A}-AR subtype regulated adult neurogenesis in the mouse subgranular and subventricular zones (Gupta et al., 2009; Jurgens et al., 2009; Collette et al., 2010) as assessed by increased BrdU incorporation and co-localization studies of EGFP-tagged α_{1A}-ARs with stem cell and neural progenitor markers (**Table 2**). In addition, when normal WT mice were given the α_{1A}-AR selective agonist, cirazoline, they also displayed increased neurogenesis (Gupta et al., 2009). The regulation of neurogenesis by the α_{1A}-AR and its regulation of hippocampal function and translation to human brain domains may potentially play a therapeutic role to increase synaptic plasticity and cognition in diseases of dementia.

General Cognition

The α_1-ARs have been previously associated with general roles in learning and memory functions (Sirviö and MacDonald, 1999) but these studies were not well characterized nor assigned to specific AR subtypes because of the lack of subtype-specific ligands. A few early studies suggested that α_1-AR stimulation inhibits memory functions in monkeys (Arnsten and Jentsch, 1997; Mao et al., 1999) or in chickens (Gibbs and Summers, 2001) but used very low replicates, very high concentrations of ligands rendering them non-selective or attributed to species variation.

TABLE 2 | Genetic animal models of the α_1-AR subtypes.

Animal model	Genotype	Cognitive phenotype	Cardiac phenotype	Metabolic phenotype	References
α_{1A}-AR	CAM, systemic overexpression expression (2–3 fold)	Increased spatial memory, learning, LTP, paired pulse, neurogenesis	Adaptive-ischemic preconditioning, increased contractility, no changes in BP	Higher whole-body FAO, increased glucose uptake in cardiac and other tissues, cardiac glucose oxidation, glucose tolerance, leptin secretion	Ross et al., 2003; Rorabaugh et al., 2005; Gupta et al., 2009; Shi et al., 2016, 2017; Papay and Perez, 2020; Perez, 2021
α_{1A}-AR	αMHC, heart-targeted overexpression (66-fold)		Adaptive-increased inotropy, protects after TAC and MI, no hypertrophy, angiogenesis		Lin et al., 2001; Du et al., 2004, 2006; Zhao et al., 2015
α_{1A}-AR	αMHC, heart-targeted overexpression (170-fold)		Maladaptive-increased mortality, fibrosis in aged mice		Chaulet et al., 2006
α_{1A}-AR (rats)	αMHC, heart-targeted overexpression		Adaptive-protects against MI, ischemic preconditioning		Zhao et al., 2012, 2015
α_{1B}-AR	αMHC, heart-targeted overexpression (26 and 46-fold)		Maladaptive-negative inotropy, dilated cardiomyopathy, no hypertrophy		Akhter et al., 1997; Grupp et al., 1998; Lemire et al., 2001
α_{1B}-AR	CAM, αMHC, heart-targeted overexpression (3-fold)		Maladaptive-hypertrophy, increased progression to HF, no preconditioning		Milano et al., 1994; Gao et al., 2000; Wang et al., 2000
α_{1B}-AR	CAM, systemic overexpression expression (2-3 fold)	Autonomic failure; Parkinson's Disease Plus neurodegeneration	Maladaptive-negative inotropy, hypertrophy in older mice, fibrosis, hypotension	Higher whole-body FAO, increased glucose tolerance and uptake in non-cardiac tissues, leptin secretion	Zuscik et al., 2000, 2001; Ross et al., 2003; Papay et al., 2013; Shi et al., 2016, 2017
α_{1AB}-AR	CAM double systemic overexpression		No basal hypertrophy but induced when either α_{1A}- or α_{1B}-ARs are individually stimulated		Papay et al., 2013
α_{1A}-AR	KO	Poor cognitive behavior	Maladaptive-increased pathology after MI, normal heart size	Higher whole-body carbohydrate oxidation, decreased cardiac glucose uptake, glucose intolerance	Doze et al., 2011; Shi et al., 2016, 2017; Yeh et al., 2017
α_{1A}-AR	Conditional heart-targeted KO		Maladaptive-increased mortality; increased pathology after MI		Zhang et al., 2020
α_{1B}-AR	KO	Locomotor, decreased addiction, memory consolidation, novelty/fear memory	No changes in basal BP, decreased induced BP; loss of NE-induced hypertrophy, decreased baroreflex response	Insulin resistance, higher whole-body carbohydrate oxidation, glucose intolerance and decreased glucose uptake in non-cardiac tissues and leptin secretion	Knauber and Müller, 2000a; Spreng et al., 2001; Drouin et al., 2002; Vecchione et al., 2002; Auclair et al., 2004; Burcelin et al., 2004; Townsend et al., 2004
α_{1D}-AR	KO	Decreased locomotion, attention	Decrease basal and induced BP		Sadalge et al., 2003; Hosoda et al., 2005
$\alpha_{1A/B}$-AR	Double KO		Maladaptive- loss of heart growth, decreased survival and contractility after TAC, fibrosis, apoptosis		McCloskey et al., 2003; O'Connell et al., 2003; Turnbull et al., 2003
$\alpha_{1A/B/D}$-AR	Triple KO		Hypotension		Sanbe et al., 2007

BP, blood pressure; CAM, constitutively active mutation(s); FAO, fatty acid oxidation; HF, heart failure; KO, knockout; LTP, long-term potentiation; MHC, myosin heavy chain promoter; MI, myocardial infarction; TAC, transverse aortic constriction.

However, as will be discussed, most of the recent studies indicate that α_1-AR stimulation increases various types of memory in both formation and storage.

Long-Term Potentiation

Long-term potentiation (LTP) is a type of long-lasting synaptic plasticity that increases the strength of synaptic transmission over a long period of time (i.e., mins-hours) (Hopkins and Johnston, 1984; Kandel, 2001). LTP is considered a major mechanism of learning and memory, particularly in the hippocampus (Bliss and Collingridge, 1993). α_1-AR stimulation can induce LTP in the hippocampus (Izumi and Zorumski, 1999; Sirviö and MacDonald, 1999; Lv et al., 2016) and there is one report in the neocortex (Pankratov and Lalo, 2015) which is also a center for neuronal spatial and recognition memory (Vann and Albasser, 2011). Interestingly, the α_1-ARs can also stimulate ATP release on astrocytes to induce LTP via ATP receptors on the pyramidal neurons in the neocortex, suggesting that glial cell regulation by α_1-ARs may also be involved in memory formation. Glia communicate through calcium signaling to neurons, causing the release of ATP and its subsequent increase in synaptic plasticity and LTP (Pascual et al., 2005). LTP stimulation by α_1-ARs may be α_{1A}-AR-specific as the CAM α_{1A}-AR transgenic mice significantly increased LTP at hippocampal synapses (Doze et al., 2011; **Table 2**). The CAM α_{1A}-AR mice also increased cognitive scores in a series of behavioral tests while the α_{1A}-AR KO mice performed poorly compared to normal controls (Doze et al., 2011). The α_{1A}-AR selective agonist, cirazoline also increased cognitive scores in normal mice when administered for 2 months. While the α_{1B}-AR KO mice had impaired cognition in some behavior tests (Knauber and Müller, 2000a,b; Spreng et al., 2001), there was no assessment of effects of α_{1B}- or α_{1D}-AR KO on LTP.

Long-term depression (LTD) is also a form of long-term synaptic plasticity that can contribute to cognitive functions by increasing the flexibility of the synapse to store information (Heynen et al., 1996), such as remembering the exposure to novel objects (Manahan-Vaughan and Braunewell, 1999). Novelty exposure can reverse LTP in the hippocampus (Xu et al., 1998), suggesting a correlation between LTD and LTP that may impart different forms of synaptic information during spatial learning (Kemp and Manahan-Vaughan, 2004). There are reports that α_1-AR mediated LTD required co-activation with a number of partners such as β-ARs (Katsuki et al., 1997), NMDA (Scheiderer et al., 2004) and the M1 muscarinic receptor (Scheiderer et al., 2008). α_1-ARs have been shown to induce LTD at excitatory CA3–CA1 synapses in the rat hippocampus (Dyer-Reaves et al., 2019) through ERK signaling in the pyramidal neurons (Vanhoose et al., 2002; Scheiderer et al., 2008) and had characteristics of a novel form of synaptic plasticity (Hebb, 1949). However, there is no evidence of which α_1-AR subtype(s) mediate LTD. This Hebbian LTD requires coincident presynaptic and postsynaptic NMDAR activity (Scheiderer et al., 2004) and is different and independent of the "classical" LTD which is induced by low frequency synaptic stimulation that is repetitive (Mulkey and Malenka, 1992). The mechanism of the Hebbian LTD also involves postsynaptic activation of the α_1-AR as the paired pulse facilitation ratio did not change (Scheiderer et al., 2004). Paired pulse facilitation is a measurement of synaptic enhancement observed under a short period of time (i.e., milliseconds). For a pulse facilitation effect, a second evoked excitatory postsynaptic potential is increased when it follows immediately after a first evoked excitatory postsynaptic potential (Foster and McNaughton, 1991) and is used as evidence of an increase in the probability of neurotransmitter release. Increases in paired pulse facilitation that occur with LTP suggest a presynaptic mechanism (Schultz et al., 1994), because potentiated presynaptic neurons must increase neurotransmitter release.

Spatial Memory

The hippocampus also regulates spatial and associative learning functions (Mahmoodi et al., 2010) in addition to long-term memory functions. α_1-AR blockage using the α_1-AR antagonist prazosin in the hippocampus demonstrated impaired spatial learning (Petrasek et al., 2010) while stimulation of the α_1-AR improved spatial memory (Puumala et al., 1998; Torkaman-Boutorabi et al., 2014). Transgenic mice overexpressing CAM α_{1A}-ARs, or WT mice given the α_{1A}-AR selective agonist cirazoline, displayed increased learning and memory using several spatial memory behavioral tests such as the Barnes, dry multi-T, and Morris water mazes (Doze et al., 2011), while α_{1A}-AR KO mice showed decreased learning and memory compared to normal controls in the same cognitive tests (Doze et al., 2011; Collette et al., 2014; **Table 2**). The α_{1B}-AR KO mice also had impaired spatial learning to novelty and exploration (Spreng et al., 2001) and a decrease in non-spatial memory functions such as memory consolidation, fear-motivated exploration (Knauber and Müller, 2000a), and short and long-term latency in a passive avoidance test (Knauber and Müller, 2000b). α_{1D}-AR KO mice did not show changes in several different behavioral cognitive tests (Sadalge et al., 2003) but did show changes in locomotion and attention (Mishima et al., 2004). Together with enhancement of LTP and paired pulse facilitation (a type of short-term synaptic plasticity) in the CAM α_{1A}-AR transgenic mice (Doze et al., 2011), these studies suggest that the α_{1A}- and perhaps the α_{1B}-AR to a lesser degree but not the α_{1D}-AR are involved in spatial learning and memory processes.

Spatial Working Memory

Spatial working memory involves executive-type or motivational-related types of memory and relies more on the prefrontal cortex than the hippocampus as the task is more complex (Robbins, 1996). α_1-AR stimulation increases while α_1-AR blockade inhibits working memory (Pussinen et al., 1997; Puumala et al., 1998; Lapiz and Morilak, 2006; Hvoslef-Eide et al., 2015) by promoting both focused and flexible attention (Berridge et al., 2012; Berridge and Spencer, 2016). There is also an improvement in working memory with the cognitive-enhancing, wake-promoting neurochemical modafinil that is hypothesized to be mediated by α_1-ARs since effects are blocked by prazosin (Duteil et al., 1990; Stone et al., 2002; Winder-Rhodes et al., 2010).

α_1-ARs regulate spatial working memory through the release of glutamate in the prefrontal cortex due to a sustained excitatory

effect on the pyramidal neurons increasing synaptic plasticity (Marek and Aghajanian, 1999; Zhang et al., 2013). When the ventral hippocampus was lesioned *in vivo* and α_1-AR function was impaired, there was a decrease in glutamatergic synaptic plasticity within the prefrontal cortex which caused memory and learning dysfunction (Bhardwaj et al., 2014). Glutamatergic synaptic plasticity mediated through α_1-ARs signals through PKC-dependent pathways in various cortical areas (Mouradian et al., 1991; Marek and Aghajanian, 1996; Chen et al., 2006; Kobayashi et al., 2008; Velásquez-Martinez et al., 2012; Luo et al., 2014, Luo et al., 2015a,b) and may require the co-signaling from both glutamate and the N-type Ca^{2+} channels (Luo et al., 2015a). PKC can increase synaptic plasticity and associated memory processes through the phosphorylation of synaptic proteins or enhancing the sensitivity to calcium which promotes the exocytosis of the synaptic vesicles, increasing neurotransmitter release (Shimazaki et al., 1996; Stevens and Sullivan, 1998; Hilfiker and Augustine, 1999; Wu and Wu, 2001).

Besides glutamatergic mechanisms, the disruption of GABAergic transmission in the prefrontal cortex can also cause a decrease in working memory (Enomoto et al., 2011; Bañuelos et al., 2014). α_1-AR stimulation in the medial prefrontal cortex inhibits the inwardly rectifying potassium channels (Kirs) located on the interneuron, leading to depolarization and an increased calcium influx through calcium channels resulting in increased GABAergic transmission onto the pyramidal neurons (Luo et al., 2015b). The excitation can be enhanced when the α_1-ARs stimulation is facilitated by postsynaptic α_2-ARs decreasing the hyperpolarization of cyclic nucleotide-gated cation channels (Zhang et al., 2013). Therefore, α_1-ARs may work to improve spatial working memory through both glutamatergic and GABAergic mechanisms which suggests that α_1-AR agonists could be used to target enhancement of spatial working memory.

Memory Consolidation

α_1-AR activation can enhance memory recall and consolidation. The process of memory consolidation changes recent and labile memories into long-lasting ones. The process starts in the hippocampus but as time passes and the memory is reorganized, the long-lasting memory is then distributed in the neocortex (Squire et al., 2015). The α_1-AR antagonist, prazosin, blocked the norepinephrine-facilitated reconsolidation of memory during fear conditioning (Gazarini et al., 2013) and the consolidation of both short-term and intermediate-term memory in chickens (Gibbs and Bowser, 2010). The mechanism for α_1-ARs to consolidate memories was suggested to be mediated through an increase in free cytosolic calcium in astrocytes as effects were blocked with glycolytic inhibitors (Gibbs and Bowser, 2010). Astrocytes, unlike neurons, mediate learning and memory utilizing glycogenolysis, which the astrocyte needs for the synthesis of glutamate (Gibbs et al., 2008; Newman et al., 2011).

The basolateral nucleus of the amygdala (BLA) can also be involved in the storage and consolidation of memory (Ferry and McGaugh, 2000). As cAMP signaling is mainly involved in mediating the effects of norepinephrine on memory consolidation, the β-ARs were previously considered the main AR to transduce those effects (Ikegaya et al., 1997; Ferry and McGaugh, 2000; Ferry and Quirarte, 2012). However, both β- and α_1-ARs may be needed together to mediate memory storage in the BLA. The stimulation of cAMP through a β-AR agonist in the BLA can be blocked with an α_1-AR antagonist and memory storage is increased with use of a synthetic cAMP analog (Ferry et al., 1999a,b). Similarly, stimulation of α_1-ARs can potentiate β-AR-mediated cAMP formation in the BLA to enhance memory storage (Ferry et al., 1999a,b). α_{1B}-AR KO mice had a decrease in latency in the passive avoidance test suggesting deficits in memory consolidation *in vivo* (Knauber and Müller, 2000b; **Table 2**). Research performed in amnesia patients developed the concept of memory consolidation as time was needed for this process to occur and greater memory deficits were seen in retrograde amnesia patients with loss of information from recent memory (Brown, 2002). α_1-AR stimulation can reverse cannabinoid-induced (Moshfegh et al., 2011) and scopolamine-induced amnesia (Azami et al., 2010) and enhance recall when α_1-AR agonists were administered before electroconvulsive shocks (Anand et al., 2001).

Dementia-Related Diseases

α_1-AR functions may change and contribute to the aging process in the loss of memory function. α_1-AR protein is increased in the aging mouse brain and with improved learning, supporting a role for these receptors in age-related cognitive decline (Knauber and Müller, 2000b). In patients suffering from Alzheimer's Disease (AD), α_1-AR protein and mRNA is reduced in the prefrontal cortex (Shimohama et al., 1986; Kalaria, 1989; Szot et al., 2007). The mRNA levels of the α_{1A}-AR were significantly decreased in the prefrontal cortex with AD with no changes in the mRNA of the α_2-AR (Szot et al., 2007). There is also an α_{1A}-AR polymorphism that associates with AD (Hong et al., 2001). Decreases in spatial memory that are due to the aging process were improved in rats when the α_1-AR was stimulated (Riekkinen et al., 1997).

The 3xTG (Transgenic) is a widely used AD mouse model that contains three genetic mutations associated with familial AD (APP Swedish, MAPT P301L, and PSEN1 M146V) (Oddo et al., 2003). This AD mouse model displays β-amyloid deposits, tau immunoreactivity, cognitive impairment, and decreases in LTP and basal synaptic transmission (Oddo et al., 2003). When the 3xTG AD mouse model was given a selective α_{1A}-AR positive allosteric modulator, spatial memory as assessed in the Barnes maze was improved along with LTP (Perez, 2021). These results suggest that selective agonists that increase α_{1A}-AR functions may be able to improve cognitive decline in AD.

Another cognitive disease is vascular dementia which is the second-most frequent form of dementia after AD. α_1-AR autoantibodies with agonistic function were found in 50% of people with dementia (Karczewski et al., 2010, 2012, 2018; Hempel et al., 2016; Thyrian et al., 2018). While these agonistic autoantibodies may also cause vascular damage, shown for several neurotransmitters (Wu and Li, 2016), one interpretation of the data consistent with the role of the α_{1A}-AR in improving cognition, but also speculative, is that they may develop during dementia to compensate for the loss in receptor density as documented by Shimohama et al. (1986) and Szot et al. (2007).

CARDIOPROTECTION

The heart expresses both the α_{1A} and α_{1B}-AR subtypes with relative expression levels depending upon the species (Steinfath et al., 1992; Michel et al., 1994; Jensen et al., 2009a). The α_{1D}-AR is weakly expressed if at all in the myocyte (Price et al., 1994; Scofield et al., 1995) but is present in vascular smooth muscle, particularly in the coronary arteries, mesenteric beds and the aorta (**Table 1**; Hrometz et al., 1999; Gisbert et al., 2002; Chalothorn et al., 2003; Turnbull et al., 2003; Hosoda et al., 2005; Jensen et al., 2009b; Methven et al., 2009; Martínez-Salas et al., 2011). A KO mouse model of the α_{1B}-AR was created with a human placental alkaline phosphatase inserted into the first exon to facilitate reporting (Myagmar et al., 2017). Using this new KO model and the conventional α_{1A}-KO which has the β-galactosidase reporter, the authors report a heterogenous population of the α_{1B} and α_{1A}-AR subtypes in the myocytes. The α_{1B} was present in all of the myocytes but the α_{1A} was present in only 60% of the myocytes and 20% of those had very high expression levels. This intermittent variable expression of the α_{1A}-AR subtype was also observed in the mesenteric arteries in the $\alpha_{1B/D}$ double KO and in the transgenic systemically expressing α_1-AR WT mice that were tagged with the green fluorescent protein (Papay et al., 2004; McGrath, 2015). Since this intermittent expression is only present in genetically altered mouse models, this suggests that intermittent expression may be an artifact. However, the current lack of highly avid α_1-AR antibodies that can be used for *in vivo* localization (Jensen et al., 2009c; Böhmer et al., 2014), precludes using immunoassays to determine if intermittent expression is an artifact. A potential experiment that may confirm intermittent expression in a WT mouse would be to perform autoradiography with and without selective α_1-AR blockers such as niguldipine to block the α_{1A}-AR subtype.

It is generally accepted that α_1-AR stimulation can regulate a positive inotropic response in the heart, although the response can be variable and display negative inotropy depending upon the species and the region in the heart analyzed (Endoh et al., 1991; Nishimaru et al., 2001; Endoh, 2016). The α_{1A}- and not the α_{1B}-AR is suggested to play a role in positive inotropy (Lin et al., 2001; Ross et al., 2003; Luo et al., 2007; Janssen et al., 2018). The systemically over-expressed CAM α_{1B}-AR mice had no changes in basal cardiac parameters but had autonomic failure (Zuscik et al., 2001). The autonomic failure in the CAM α_{1B}-AR mice indicated reduced circulating catecholamine levels, bradycardia, reproductive problems and weight loss. Together with the widespread neurodegeneration and a phenotype that was consistent with a Parkinson Disease plus syndrome, the basal hypotension seen in these mice was likely due to the autonomic failure rather than a direct effect on the ability to contract vascular smooth muscle. The CAM α_{1B}-AR mice also had a negative inotropic response to phenylephrine (Ross et al., 2003). Radioligand binding analysis revealed that there was decreased α_{1A}-AR density which was likely causing the negative inotropic effect (Ross et al., 2003). This functional antagonism of the positive inotropy of the α_{1A}-AR by the α_{1B}-AR was also found in a mouse model of right ventricular failure (Cowley et al., 2015). The heart-targeted WT α_{1B}-AR also displayed negative inotropy (Grupp et al., 1998). In contrast, both the cardiac-targeted WT and systemically expressed CAM α_{1A}-AR mediated a positive inotropic response in the mouse heart (Lin et al., 2001; Rorabaugh et al., 2005; **Table 2**). In human myocardium, the α_{1A}-AR selective agonist, A61603, had a strong positive inotropic response representing about 70% of the β-AR response (Janssen et al., 2018).

Heart Failure

In human heart failure, radioligand binding indicates that β_1-ARs are downregulated (Bristow et al., 1982, 1986; Rockman et al., 2002) while α_1-AR are either unchanged (Bristow et al., 1988; Jensen et al., 2009a) or decreased (Limas et al., 1989; Zhao et al., 1996; Fischer et al., 2008; Shi et al., 2013). MicroRNA-133 was found to be a key control in the downregulation of the β_1-AR and several components of its signal transduction cascade in the heart (Castaldi et al., 2014), opening up new avenues of therapeutics in addition to β-blockers. Radioligand binding of human hearts with end-stage dilated cardiomyopathy versus non-failing controls revealed that while β_1-ARs are downregulated as previously reported (Bristow et al., 1982, 1986), there was also a loss in the α_{1A}-AR subtype receptor levels (Shi et al., 2013). The differences in these studies of the density of α_1-ARs could be the severity of the heart failure (Limas et al., 1989), the level of sympathetic overdrive (Zhao et al., 1996) or the etiology of heart failure studied (ischemic versus non-ischemic) as α_1-ARs are known to increase in density during ischemia (Corr et al., 1981; Maisel et al., 1987; Kurz et al., 1991) and could have masked the decrease in α_{1A}-ARs during failure.

α_1-ARs also can mediate cardiac hypertrophy, an increase in protein mass of the myocyte through an increase in protein synthesis which remodels the heart in response to various physiological and pathophysiological stimuli (Simpson, 1983; Fuller et al., 1990; Ikeda et al., 1991; Perez-Aso et al., 2013; Cotecchia et al., 2015). While both the α_{1A} and α_{1B}-ARs are involved in hypertrophy, the α_{1A}-AR seems better coupled to enhance hypertrophic signaling pathways. The α_{1A}-AR agonist, A-61603, increased the size of the myocyte by increasing the rate of protein synthesis (Autelitano and Woodcock, 1998). The various transgenic mouse models showed variable degrees of cardiac hypertrophy but have never been as robust as seen in cell cultures (**Table 2**). Cardiac hypertrophy can be a normal physiological response which is adaptive and improves function while hypertrophy that is associated with fibrosis or apoptosis is maladaptive and can lead to heart failure. Both the α_{1A}- and α_{1B}-AR subtypes are required for physiological cardiac hypertrophy (O'Connell et al., 2003) as single KO do not have decreased heart size (Vecchione et al., 2002; **Table 2**). The systemic-expressing CAM α_{1A} displayed adaptive cardiac hypertrophy without increasing blood pressure (Papay et al., 2013). The heart-targeted CAM α_{1B} mouse induced hypertrophy (Milano et al., 1994) but displayed maladaptive remodeling after pressure overload (Wang et al., 2000). The systemically expressing CAM α_{1B} also induces cardiac hypertrophy (Zuscik et al., 2001) but was more pronounced when the mouse aged

(Papay et al., 2013). A systemically expressing WT α_{1B}-AR also displayed a lower degree of hypertrophy that only manifested in aged mice with fibrosis indicating a maladaptive cardiac hypertrophy (Zuscik et al., 2001). KO of the α_{1B}-AR had a loss of NE-induced hypertrophy but not a decrease in heart size at birth (Vecchione et al., 2002). While a heart-targeted WT α_{1B} with high overexpression did not induce hypertrophy, it did induce a maladaptive dilated cardiomyopathy (Akhter et al., 1997; Grupp et al., 1998; Lemire et al., 2001). The α_{1B}-AR has been suggested to regulate cardiac hypertrophy differently than the α_{1A}-AR and the two AR subtypes may need to be co-activated to regulate hypertrophy (Papay et al., 2013). The CAM α_{1A}-AR mice selectively secreted interleukin-6 (IL-6) and atrial naturietic factor while the CAM α_{1B}-AR mice activated nuclear factor-kB (Papay et al., 2013). The α_{1AB}-AR double KO mice also failed to develop hypertrophy when stimulated with IL-6 but WT mice developed hypertrophy when given IL-6. These hypertrophic signals were blocked in each mouse model and no increase in heart weight observed when the other AR was coactivated or when the two transgenic mouse models were crossbred, resulting in a CAM $\alpha_{1A/B}$-AR double transgenic mouse model (Papay et al., 2013). Hypertrophy became apparent in the CAM α_{1AB}-AR double transgenic when either the α_{1A}-AR or α_{1B}-AR were independently stimulated (Papay et al., 2013). These results suggest that both the AR subtypes can increase hypertrophy through different signaling pathways. Increased α_{1A}-AR signaling can induce an adaptive hypertrophy consistent with its postulated role of cardiac protection while increased α_{1B}-AR signaling induces a maladaptive hypertrophy in the heart. These differences between adaptive versus maladaptive hypertrophy may be due to differences in α_1-AR mediation of IL-6, ANF, and NF-kB signaling pathways.

α_{1A}-AR Mediated Protection in Heart Failure

It is postulated that selective α_{1A}-AR stimulation may be a potential therapeutic in heart failure (Perez and Doze, 2011; Janssen et al., 2018) while α_{1B}-AR stimulation, on the other hand, is maladaptive. This is evidenced by the heart-targeted WT α_{1B}-AR mice induced dilated cardiomyopathy (Lemire et al., 2001) while heart-targeted CAM α_{1B}-AR progressed to heart failure after pressure-overload (Wang et al., 2000; **Table 2**). In contrast, the heart-targeted WT α_{1A}-AR mice were protected against pressure-overload induced heart failure (Du et al., 2004) or dysfunction due to myocardial infarction (Du et al., 2006) compared to non-transgenic controls. This mouse model also showed increased vascular endothelial growth factor-A expression which induced angiogenesis and resulted in increased capillary density and blood flow to the heart, postulated to be a contributing mechanism for cardioprotection (Zhao et al., 2015). This phenotype of induced angiogenesis could be reproduced when WT mice were given the α_{1A}-AR agonist, A61603. A61603 or dabuzalgron also increased survival and prevented the damage due to the cardiotoxic agent, doxorubicin (Beak et al., 2017; Montgomery et al., 2017) and increased contraction in a mouse model of right heart failure (Cowley et al., 2015).

Preconditioning and Ischemia

The high metabolic rate of the heart can cause the heart to be sensitive to the lack of oxygen (i.e., ischemia) resulting in injury to the muscle. α_1-AR have long been known to mediate protective effects against ischemia or preconditioning in ischemia in several species (Banerjee et al., 1993; Kitakaze et al., 1994; Tsuchida et al., 1994; Salvi, 2001; Rorabaugh et al., 2005; Zhao et al., 2012; Nazari et al., 2019; Papay and Perez, 2020). In preconditioning, short periods of ischemia can stimulate signaling in the heart that protects the cardiac muscle from subsequent ischemic injury. The mechanism has been multi-faceted and attributed to PKC (Tsuchida et al., 1994; Mitchell et al., 1995; Rehring et al., 1996; Rorabaugh et al., 2005), mitochondrial potassium channels (Nazari et al., 2019), mitochondrial permeability transition pore (Naderi et al., 2010), 5′-nucleotidase activity (Tsuchida et al., 1994) or angiogenesis (Zhao et al., 2012). In recent studies, the ischemic protective effect of the α_1-AR observed in primary cardiomyocytes was also proposed to be through the metabolic effects of glucose (Papay and Perez, 2020). Most models of ischemic preconditioning and particularly those by α_1-ARs converge first on PKC, then diverge to other downstream effectors (Downey and Cohen, 1997; Simkhovich et al., 2013) and are postulated to also do so in the human heart (Speechly-Dick et al., 1995).

α_{1A}-AR Mediated Protection in Ischemia

The α_{1A}-AR subtype has been shown to mediate the cardioprotective effects of α_1-ARs in ischemic preconditioning. These studies have been performed in transgenic or KO mouse models as blocking one subtype is still not specific enough to perform with antagonists. The systemically expressed CAM α_{1A} mice were inherently preconditioned against ischemia while the CAM α_{1B} was not (Rorabaugh et al., 2005; **Table 2**). The heart-targeted CAM α_{1B}-AR also did not show ischemic preconditioning (Gao et al., 2000). In corroboration, the heart-targeted WT α_{1A}-AR transgenic rat exhibited preconditioning that appeared during the second window of protection that occurs days (and not minutes) after ischemia (Du et al., 2006; Zhao et al., 2012, 2015). There are also two reports that α_{1B}-AR stimulation in WT mice can induce ischemic preconditioning involving PKC but used sensitivity to chloroethylclonidine as a criteria to block α_{1B}-ARs selectively (Hu and Nattel, 1995; Gao et al., 2007). However, chloroethylclonidine was shown to not be selective against the α_{1B}-AR but can block all the α_1-AR subtypes (Xiao and Jeffries, 1998). Transgenic rats with myocyte-specific α_{1A}-AR overexpression protected the heart from permanent coronary occlusion and during preconditioning (Zhao et al., 2012, 2015). The α_{1A}-AR KO or conditional cardiac KO of the α_{1A}-AR also had more pathological injury from myocardial infarction after left anterior descending ligation (Yeh et al., 2017; Zhang et al., 2020). Together, these results strongly suggest that the α_{1A}-AR subtype mediates ischemic protection in the heart.

Hypertension

α_1-ARs are highly expressed in vascular smooth muscle (Hussain and Marshall, 1997; Martí et al., 2005). The rise in calcium

upon stimulation of α_1-ARs in the vasculature activates myosin light chain kinase and actin/myosin cross-bridge formation to induce vascular muscle contraction and increased blood pressure (Somlyo and Somlyo, 2003). The smaller resistance arteries play a more important role in blood pressure regulation and are under stronger control from the sympathetic nervous system. Signals mediated through α_1-AR activation have been shown to be involved in blood pressure regulation through their control of calcium release and sensitization and signaling through mechanisms involving PKC, PI3K, Rho Kinase, and MAPK (Woo and Lee, 1999; Wier and Morgan, 2003; Villalba et al., 2007; Gutiérrez et al., 2019).

While α_1-AR antagonists are effective blockers to treat hypertension, they are used as a second line of defense (Chobanian et al., 2003) because of the side effects, poorer outcomes, and worsening or increased risk of heart failure (ALLHAT Collaborative Research Group, 2000). Using KO mice, the α_{1A} was found to decrease blood pressure upon deletion, but only by 15% of the full phenylephrine effect (Rokosh and Simpson, 2002; **Table 2**). However, the α_{1B}-AR KO mediated 45% of the phenylephrine response (Cavalli et al., 1997; Vecchione et al., 2002). Similar minor effects on blood pressure were observed in the α_{1D}-AR KO compared to the α_{1A}-AR or α_{1B}-AR KOs (Cavalli et al., 1997; Hosoda et al., 2005). Only the α_{1D}-AR KO decreased basal resting levels of blood pressure (Vecchione et al., 2002; Hosoda et al., 2005).

Since all of the α_1-ARs appear to regulate blood pressure to a certain degree, specific blockage of the α_{1D}-AR may provide better therapeutics to treat hypertension with less overall side effects on other organ systems. This is because the α_{1B}-AR appears to have the strongest effect on blood pressure while α_{1D}-AR blockage would still lower blood pressure but is not expressed or minimally expressed in the heart (Price et al., 1994; Scofield et al., 1995) or the brain (Tanoue et al., 2002; Sadalge et al., 2003), thereby reducing potential side effects. The α_{1D}-AR is also expressed and regulates contraction in the small resistance mesenteric beds which is an important contributor to total peripheral resistance (Christensen and Mulvany, 1993; Hrometz et al., 1999; Gisbert et al., 2002; Methven et al., 2009). The α_{1B}-AR subtype controls the neuroeffector junction and sympathetic regulation of the baroreflex response (Townsend et al., 2004) and both the α_{1A}- and α_{1B}-AR subtypes regulate physiological hypertrophy (O'Connell et al., 2003). The α_{1A}-AR as reviewed above is a major regulator of neurotransmission and cognition; thus, blockage of α_{1A}- or α_{1B}-ARs would affect more off targets than vascular smooth muscle. Therefore, antagonists against the α_{1D}-AR subtype might be more effective therapeutically against hypertension by avoiding negative side effects on the heart and brain but may focus effects better on blood pressure regulation.

METABOLISM

The sympathetic nervous system is known to regulate many aspects of metabolism. α_1-ARs stimulation has long been known to regulate gluconeogenesis in the liver (Chan and Exton, 1978; Hue et al., 1978; García-Sáinz and Hernández-Sotomayor, 1985; de Oliveira et al., 2013). α_1-ARs also regulate somatostatin-induced gluconeogenesis in the kidney (Dileepan et al., 1982; Dileepan and Wagle, 1985). Gluconeogenesis generates the synthesis of glucose from non-carbohydrate sources while glycolysis breaks down glucose to yield energy (i.e., ATP). Gluconeogenesis becomes important during fasting or starvation when glucose is needed by the cell after glycogen is depleted. α_1-AR agonists also stimulate glycogen phosphorylase activity, the rate limiting step in glycogen breakdown, which inhibits glycogen synthesis, and increases the breakdown of glycogen (Assimacopoulos-Jeannet et al., 1977; Aggerbeck et al., 1980; Thomas et al., 1985; Ballou et al., 2001; de Oliveira et al., 2013) and stimulates the release of glucagon from the pancreas (Ahrén and Lundquist, 1987; Skoglund et al., 1987; Vieira et al., 2004). However, recent studies have indicated that α_1-ARs regulate metabolism at a much more systemic level as reviewed below.

α_1-AR Stimulation Increases Glucose Tolerance

α_1-AR stimulation is known to increase glucose uptake in the heart or in primary myocytes (Doenst and Taegtmeyer, 1999; Egert et al., 1999; Shi et al., 2016, 2017; Sato et al., 2018; Papay and Perez, 2020). The systemically expressing CAM α_{1A} but not the CAM α_{1B}-AR mice increased glucose uptake into the heart and only the α_{1A}-AR KO mice displayed decreased glucose uptake into the heart (Shi et al., 2017). In corroboration, the α_{1A}-selective agonist, A61603 increased glucose uptake into primary cardiomyocytes or human α_{1A}-AR transfected Chinese hamster ovary (CHO) cells (Sato et al., 2018). While glucose uptake into the heart appears α_{1A}-AR specific, both the α_{1A}- and α_{1B}-AR subtypes mediate glucose uptake into other tissues. The systemically expressing CAM α_{1A} and α_{1B}-AR mice both increased glucose uptake into adipose tissue and skeletal muscle while KO of the respective subtype decreased glucose uptake into those same tissues (Shi et al., 2017). The mechanism of α_{1A}-AR mediated glucose uptake in the myocyte was through PKCδ signaling that resulted in GLUT 1/4 translocation which causes their activation to transport glucose into the cell (Shi et al., 2016).

The KO and CAM mice also displayed effects on glucose utilization and homeostasis. Both the systemically expressing CAM α_{1A}- and α_{1B}-AR mice had an increased tolerance for glucose, lower fasting glucose levels while KO mice had poor tolerance and high blood glucose after fasting (Shi et al., 2017). α_1-AR stimulation also increased glucose absorption in the intestines (Mourad and Saadé, 2011). Hypothalamic central administration of prazosin increased plasma glucose levels (Murashita et al., 2007; Ikegami et al., 2013b) and glucose intolerance (Ikegami et al., 2013a). When fatty acid oxidation was suppressed centrally in the brain, α_1-ARs stimulated the counter-regulatory increases in plasma glucose levels (Sajapitak et al., 2008). A metabolomic analysis in a neuronal cell culture also showed that α_1-AR stimulation results in lower levels of carbohydrates (Wenner et al., 2016).

These results are consistent with other studies in the α_{1B}-AR KO mice which displayed insulin resistance and dysfunctional glucose homeostasis (Burcelin et al., 2004) and the use of prazosin treatment, an α_1-AR antagonist, which increases risk of metabolic syndrome and high fasting plasma glucose levels in patients with benign prostatic hyperplasia (Lee et al., 2013). The mechanism of the increase in glucose tolerance and lowering of plasma glucose levels is likely due to the increased utilization of glucose through uptake and oxidation in various organs.

α_1-AR Mediated Glucose Oxidation in the Heart

α_1-AR stimulation can also directly increase glucose oxidation in both normal and ischemic primary adult myocytes performed by measuring the rate of ^{14}C-CO_2 production using ^{14}C-glucose as a substrate (Papay and Perez, 2020). This study confirmed that the glucose uptake into the heart also drives the oxidation of glucose for energy utilization to the heart. Stimulation of glucose oxidation in the heart improves the recovery from damage during ischemia (Dyck et al., 2006; Ussher et al., 2012; Masoud et al., 2014; Li Y. et al., 2017). Ischemia in the heart can increase glucose uptake by increasing the translocation of GLUT 1/4 (Egert et al., 1999), as this was also shown to be mediated by the α_{1A}-AR (Shi et al., 2016). The α_1-AR mediated glucose oxidation in primary myocytes was also blocked by PKC and AMPK inhibitors (Papay and Perez, 2020) consistent with the role of PKCδ in translocating the glucose transporters in the heart by the α_{1A}-AR (Shi et al., 2016). α_1-AR stimulation increased glucose uptake in the L6 skeletal muscle cell line also through an AMPK pathway (Hutchinson and Bengtsson, 2006). AMPK is an energy sensor that can regulate the rate of glucose and fatty acid uptake and oxidation according to the needs of the cell. AMPK signaling is cardioprotective during heart failure by switching the energy production in the heart from fatty acid oxidation to glucose oxidation (Kim et al., 2012). AMPK also can increase glucose uptake during ischemia to prevent post-ischemic cardiac damage and dysfunction (Russell et al., 2004; Kim et al., 2011). While α_{1A}-AR mediated ischemic preconditioning was mediated through PKC (Rorabaugh et al., 2005), PKC was also shown to mediate its protection against ischemic damage through AMPK (Wang et al., 2011). These results suggest that glucose uptake and subsequent oxidation in the heart may be α_{1A}-AR specific, signal through PKC/AMPK activation and may mediate α_{1A}-AR's cardioprotective effects during ischemia and heart failure.

α_1-AR Mediated Glucose Metabolism in Other Tissues

α_1-ARs are the main receptors that regulate the control of hepatic glucose metabolism in mice (Chu et al., 2000; Miyamoto et al., 2012; de Oliveira et al., 2013). α_1-AR stimulation increased glucose uptake into L6 muscle cells (Hutchinson and Bengtsson, 2005, 2006) and C2C12 skeletal myoblasts (Liu et al., 2001). α_1-AR stimulation also increases glucose uptake into brown and white adipocytes (Faintrenie and Géloën, 1998; Cheng et al., 2000; Boschmann et al., 2002; Flechtner-Mors et al., 2002, 2004; Chernogubova et al., 2005). The sympathetic nervous system enhances glucose uptake into human adipocytes independently of insulin action through the α_1-AR (Flechtner-Mors et al., 2002, 2004; McCarty, 2004). In obese people that have insulin resistance, α_1-AR stimulation may provide a critical alternative pathway for glucose uptake.

α_1-ARs Mediated Fatty Acid Oxidation

The KO and transgenic mice of the α_1-AR subtypes were used to discern effects of the specific subtypes on general whole-body metabolism. Systemically expressing CAM mice were assessed by indirect calorimetry and found that both CAM α_{1A}- and α_{1B}-AR mice decreased the respiratory exchange ratio (RER) (ratio of CO_2 production and O_2 consumption) which indicated an increase in whole body preference to metabolize fatty acids as a substrate (i.e., fatty acid oxidation) while the KO mice from both subtypes preferred to burn carbohydrates and increased the RER (Shi et al., 2017). It is likely that α_1-AR stimulation increases fatty acid oxidation in the skeletal muscle as that muscle utilizes 40–50% of a body's whole energy metabolism. While there is a report that prazosin can increase angiogenesis in skeletal muscle resulting in increased capillarization to improve the diffusion of glucose into the muscle and may increase glucose oxidation due to substrate availability (Akerstrom et al., 2014), prazosin's effect was due to improved blood flow and not to GLUT 1/4 translocation.

Both systemically expressing CAM α_{1A}- and α_{1B}-AR mice displayed increased plasma levels of leptin while KO mice decreased leptin levels (Shi et al., 2017). In obese humans, α_1-AR blockade reduces leptin levels (Ihara et al., 2006). While leptin can also directly increase glucose oxidation in the absence of insulin in skeletal muscle through a neural hypothalamic β-AR mechanism (Nevzorova et al., 2006; Glund et al., 2007; Shiuchi et al., 2009; Minokoshi et al., 2012; Cadaret et al., 2017), leptin mainly increases fatty acid oxidation in skeletal muscle and the liver through α_1-AR stimulation of AMPK activity (Minokoshi et al., 2002, 2012; Miyamoto et al., 2012).

α_1-ARs can also couple to peroxisome proliferator-activated receptor-delta (PPARs) to regulate fatty acid oxidation and utilization (Tanaka et al., 2003). PPAR subtypes β/δ are nuclear receptors and serve as sensors of fatty acid levels. They bind and are activated by fatty acids and their derivatives and activate transcription factors to regulate metabolism (Poulsen et al., 2012). Using midodrine to non-selectively stimulate α_1-ARs, α_1-ARs activated PPARs and AMPK to increase oxidative phosphorylation in rat skeletal muscle or in C2C12 skeletal muscle cells (Lee et al., 2020). PPARs are crucial to maintain normal cardiac function and its energy requirements. Cardiac-targeted KO of PPARδ decreases basal fatty acid oxidation leading to cardiac dysfunction, lipid accumulation and heart failure (Cheng et al., 2004). Overexpression of a CAM PPARβ/δ leads to increased levels of fatty acid oxidation (Barak et al., 2002).

Tissue transglutaminase (TG2) is an ubiquitous and multi-functional protein and enzyme with regulatory crosslinking

functions in cell adhesion and the cytoskeleton but also has GTP hydrolyzing activities (Fesus and Piacentini, 2002; Eckert et al., 2014). Phenylephrine, an α_1-AR non-selective agonist was injected into TG2 KO mice and resulted in a lowering of the RER indicating that the mice were burning more whole-body fatty acids than glucose when compared to normal mice with intact TG2 (Lénárt et al., 2020). α_1-AR stimulation also resulted in lower organ damage particularly in the heart but also in the lung, liver, kidney, and skeletal muscle and a weaker vasoconstriction response compared to normal mice (Lénárt et al., 2020). When the same mice were given a β_3-AR agonist, the RER was lowered and organ damage was changed to the same extent in both TG2 KO or normal mice (Lénárt et al., 2020). A β_3 agonist lowers the RER because of its high density in adipose tissue (Ferrer-Lorente et al., 2005). These results concur with the whole-body indirect calorimetry studies that showed that the systemically expressing CAM α_1-AR mice burned more fatty acids (Shi et al., 2017) and protected the heart from ischemic damage (Rorabaugh et al., 2005; Shi et al., 2016). TG2 is a protein ubiquitously found in cells and can function in both protein cross-linking and bind GTP to act as a G-protein transducer at α_1-ARs (Nakaoka et al., 1994; Baek et al., 1996; Feng et al., 1996; Kang et al., 2004).

α_1-AR stimulation can increase the rate of lipolysis in obese individuals (Flechtner-Mors et al., 2002) increasing the availability of fatty acids. α_1-ARs stimulation also increase fatty acid oxidation in the liver or in hepatocytes (Sugden et al., 1980; Kosugi et al., 1983; Oberhaensli et al., 1985; de Oliveira et al., 2013) and during a high-fat diet can reduce hepatic steatosis (i.e., fatty liver disease) (Nakade et al., 2020). Using a metabolomic analysis, the α_{1A}-AR selective agonist, A61603, produced a reduction in cardiac polyunsaturated fatty acids (Willis et al., 2016). The systemically expressed CAM α_{1A}-AR mice displayed significantly decreased fasting plasma triglycerides while α_{1A}-AR KO displayed increased levels of triglycerides (Shi et al., 2017). In contrast, α_1-AR blockers such as prazosin or doxazosin have been reported to lower triglycerides and cholesterol but increase high density lipoproteins in humans (Ferrara et al., 1986; Weinberger, 1986; Trost et al., 1987). The reason for this discordance is unknown. However, α_1-AR quinazoline-based antagonists and particularly prazosin and doxazosin have known non-α_1-AR mediated off-target effects (Benning and Kyprianou, 2002; Lin et al., 2007; Isgor and Isgor, 2012).

PHARMACOLOGICAL INTERVENTIONS

Development of α_1-AR Subtype-Selective Ligands

Development of selective α_1-AR subtype ligands has not been a focus in the pharmaceutical industry because of the ALLHAT Collaborative Research Group (2000) clinical trials and the major cardiovascular events that occur when α_1-AR antagonists are used. There are still no selective blockers or agonists for the α_{1B}-AR, and while BMY 7378 is somewhat selective for the α_{1D}-AR (Goetz et al., 1995), there is no clear clinical target. α_{1A}-AR antagonists have fared better in drug development because they target prostate and lower urinary tract problems which often affect men with increasing age and who also have high blood pressure; thus, tackling two problems with one therapeutic (Van Asseldonk et al., 2015). However, these therapeutics, as are all α_1-AR antagonists, are contraindicated in people with heart problems (O'Connell et al., 2013). Recent studies also suggest that α_1-AR antagonists increase mortality rates in hospitalized patients with Covid-19 (Rose et al., 2020).

The above review indicates that the α_{1A}-AR subtype may be a target for drug development for cardioprotection and cognitive enhancement in dementia-type diseases. The potential for α_{1A}-AR agonists to be used to treat these diseases has a major problematic side effect of increasing blood pressure (Woo and Lee, 1999; Wier and Morgan, 2003; Villalba et al., 2007; Gutiérrez et al., 2019). This drawback has limited the development of α_1-AR-based therapeutics by pharmaceutical companies (Fordyce et al., 2015). However, there are two avenues of development that are recently being used to circumvent the blood pressure effect of α_{1A}-AR agonists. The first one is the use of the imidazoline pharmacophore instead of the endogenous phenethylamine pharmacophore that is possessed by norepinephrine, epinephrine and several other α_1-AR agonists (**Figure 1**).

Imidazolines

In general, imidazolines have better binding and functional agonistic selectivity for α_2-ARs and reduce blood pressure by decreasing norepinephrine release at the α_{2A}-AR autoreceptor (Ruffolo et al., 1983). However, in the early days of α_1-AR agonist drug development, it was noted imidazolines interacted with the α_1-ARs in a different way structurally than with α_2-ARs. The Easson-Stedman hypothesis states that adrenergic agonists that are chiral by possessing an asymmetric hydroxyl-substituted benzylic carbon atom will have higher binding affinity and potency for the R(−) (i.e., right hand) isomer when compared to the S(+) (i.e., desoxy) isomer (Easson and Stedman, 1933). Imidazoline binding to α_1-ARs did not adhere to the Easson-Stedman hypothesis that held with phenethylamines, such as norepinephrine (Patil et al., 1974; Ruffolo et al., 1980, 1983; Hieble et al., 1986). While most imidazolines that selectively bind to the α_2-AR are agonists, they become weak antagonists at the α_1-AR (Ruffolo and Waddell, 1982). During drug development, specific substitutions off the imidazoline pharmacophore can convert imidazolines from α_2-AR agonists to α_1-AR agonists (Ruffolo et al., 1980; Hieble et al., 1986; Knepper et al., 1995). Furthermore, subsequent studies indicated that imidazolines that had higher affinity for the α_1-AR than the α_2-AR had agonist-selectivity for the α_{1A}-AR subtype in both binding affinity and function compared to the other two α_1-AR subtypes, the α_{1B}- or α_{1D}-AR (Minneman et al., 1994). Structure-function analysis revealed that imidazolines, while agonists at the α_{1A}-AR, interact with amino acid residues closer to the cell surface in the α_{1A}-AR binding pocket, similar to α_1-AR antagonists, confirming the differences seen with the Easson-Stedman hypothesis (Waugh et al., 2001). These differences in binding also explained why most imidazolines are partial and not full agonists at the α_1-ARs.

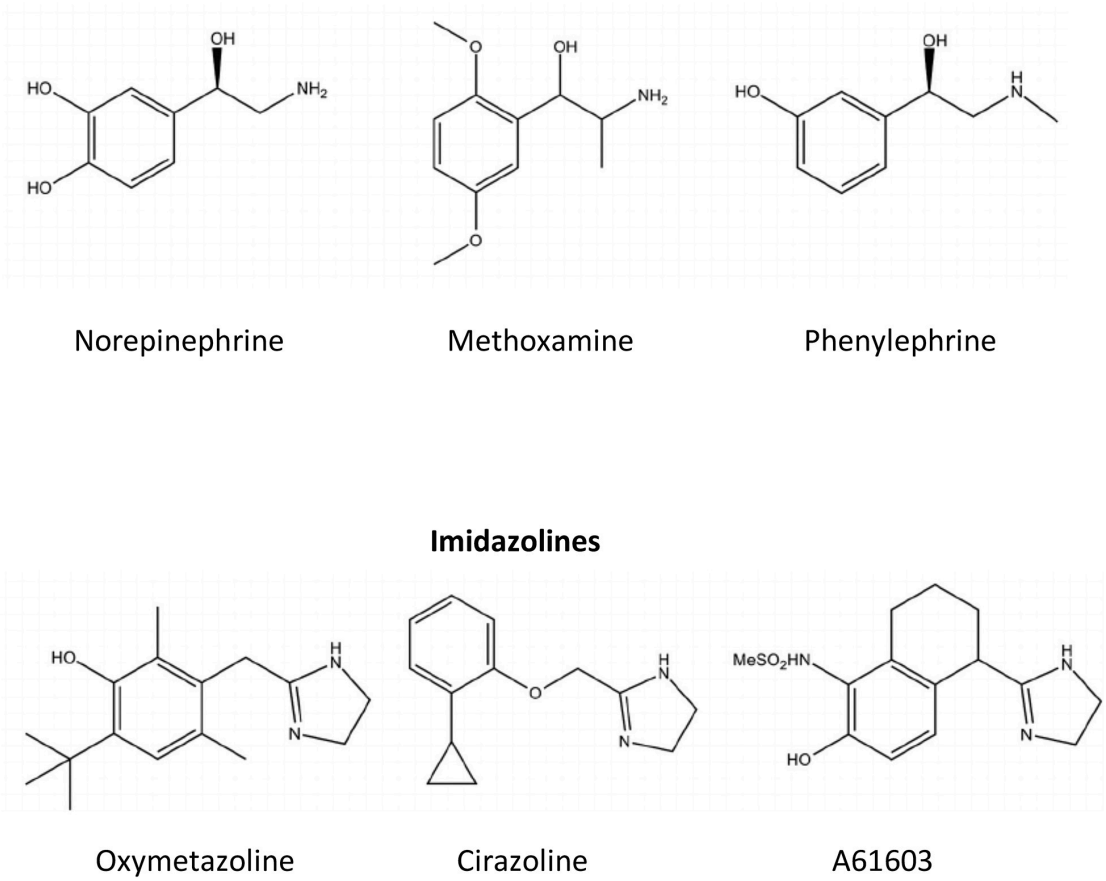

FIGURE 1 | Chemical structures for common α_1-AR agonists. Ligands such as norepinephrine that contain a phenyl, two-carbon ethyl, and amine group in their structural backbone are referred to as phenethylamines. Ligands that contain an imidazole ring in its structural backbone instead of the phenyl ring are referred to as imidazolines.

There are several commercially available imidazolines, such as cirazoline and A61603, that are selective for the α_{1A}-AR versus the α_{1B}- and α_{1D}-AR subtypes and with lower affinity against the α_2-AR. An analog of cirazoline and an α_{1A}-AR partial agonist, RO 115–1240 and later by the commercial product dabuzalgron, was shown to reduce stress urinary incontinence without increasing blood pressure (Blue et al., 2004; Musselman et al., 2004). The therapeutic index is wide enough that R0 115–1240 can contract bladder smooth muscle at a much lower dose than required to contract vascular smooth muscle by the α_{1A}-AR. This is possible because of the higher receptor density of the α_{1A}-AR in the urinary tract compared with vascular smooth muscle and its partial agonist activity that allows reflex mechanisms to control changes in blood pressure (Ford et al., 1996; Walden et al., 1997; Kava et al., 1998; Musselman et al., 2004; Michel and Vrydag, 2006). While all of the above are indeed possible mechanisms for α_{1A}-AR agonists to avoid increasing blood pressure, imidazolines were subsequently shown to have bias signaling or agonist trafficking which can lead to lower efficacy of the signaling pathways known to increase blood pressure. Imidazolines induce a more robust cAMP signaling response versus the inositol phosphate signal which increases calcium release to cause the vascular smooth muscle contraction (Evans et al., 2011; da Silva et al., 2017). Confirming the role of α_{1A}-AR-selective imidazolines in cardioprotection, dabuzalgron was shown to protect against cardiac damage induced by doxorubicin (Beak et al., 2017; Montgomery et al., 2017) and A61603 increased inotropy in a mouse model of right heart failure (Cowley et al., 2015), but blood pressure was not assessed at the dosage used in these experiments. Confirming the role of α_{1A}-AR-selective imidazolines in enhancing cognition, cirazoline, which crosses the blood brain barrier, was shown to increase cognition in normal mice (Doze et al., 2011).

Allosteric Modulators

A second avenue of drug development for α_{1A}-AR agonists with a wide therapeutic index to avoid increases in blood pressure are allosteric modulators. Allosteric modulators offer greater selectivity in both binding and signaling than conventional ligands which bind to the natural endogenous site on the receptor (i.e., orthosteric) (Christopoulos, 2002). Besides greater selectivity because they bind in a different place than orthosteric

agonists that is non-conserved between subtypes of the receptor, allosteric modulators offer many other benefits in therapeutics. These are the saturability of its binding site (i.e., ceiling effect) and conformational or probe bias that can alter the receptor to induce a bias in signaling and activation properties but only when the receptor is already occupied with a specific ligand or probe (Christopoulos, 2002).

Allosteric modulators are classified by their ability to modulate function. Positive allosteric modulators (PAMs) increase a receptor's functional response while negative allosteric modulators (NAMs) decrease the functional response. There are also neutral or silent allosteric modulators (SAMs) that bind to the receptor and display no measurable changes in function (Lindsley et al., 2016) but can block the effects of PAMs or NAMS (Rodriguez et al., 2005). There are now many GPCR allosteric modulators that have been developed (Chen et al., 2008; Wold et al., 2019; Zhou and Cunningham, 2019; Fasciani et al., 2020) with several in clinical trials or with FDA approval (Wold et al., 2019). The HIV entry inhibitor maraviroc is the most known clinically used GPCR allosteric modulator against the CCR5 receptor (Maeda et al., 2012).

There are a few NAMs that have been characterized for the α_1-AR but have not been developed for clinical use (Leppik et al., 2000; Sharpe et al., 2003; Chen et al., 2004; Lima et al., 2005; Ragnarsson et al., 2013; Campbell et al., 2017). We have developed the first PAM of the α_1-ARs with selectivity at the α_{1A}-AR subtype. It has the imidazoline pharmacophore and can cross the blood brain barrier in sufficient concentration to cause neurological effects without increased blood pressure (Perez, 2021). We have demonstrated its ability to significantly increase LTP in a mouse model of AD along with increases in cognitive behavior using the Barnes maze and fear-conditioning tests. This was achieved using a 10-month dosing scheme and studies are underway to test effects of this compound in a dose-efficacy preclinical trial for 3 months (Perez, 2021).

Therapeutic Autoantibodies and Vaccines Against α_1-ARs

There has been recent work in therapeutic vaccines directed at the α_1-AR subtypes and their roles in hypertension and cardiovascular disease. Autoantibodies against the α_1-ARs were first found in patients over 20 years ago with severe hypertension (Fu et al., 1994; Luther et al., 1997; Wenzel et al., 2008). A vaccine made against the second extracellular loop of the α_{1D}-AR was found to have antagonistic behavior (Li et al., 2019). The vaccine was injected into spontaneously hypertensive rats (SHR) with or without pre-treatment with NG-nitro-L-arginine methyl ester (L-NAME) to generate NO and to reduce blood pressure (Li et al., 2019). This α_{1D}-AR vaccine reduced the systolic blood pressure up to 15 mmHg in the SHR group and up to 29 mmHG in the SHR + L-NAME group. This vaccine also prevented cardiac hypertrophy and fibrosis, vascular remodeling, and renal injury even better than compared to treatment with prazosin, suggesting that the antibody has blocking activity. There is one commercially available α_{1D}-AR antagonist, BMY7378 (Goetz et al., 1995), but is not sufficiently selective to avoid blocking the other α_1-AR subtypes for therapeutic use. Because of the unique amino acid sequence used in a non-conserved region of the second extracellular loop of the receptor, vaccines against the α_{1D}-AR subtype would be highly selective and avid to regulate the blood pressure response and avoid blocking the other α_1-AR subtypes.

However, the vast majority of autoantibodies are associated with agonistic activity resulting from a rise in intracellular calcium, and postulated to result in a vasoconstrictive effect (Bkaily et al., 2003; Karczewski et al., 2010; Yan et al., 2014). However, one controlled clinical study indicated that hypertensive patients with α_1-AR autoantibodies displayed normal cardiovascular responses to α_1-AR stimulation and removal of α_1-AR autoantibodies by immunoadsorption did not alter that response (Schroeder et al., 2012).

While the autoantibody against the α_{1D}-AR appears antagonistic, several autoantibodies have been developed or discovered against the first or second extracellular loop of the α_1-AR appear to be agonistic in behavior (Zhou et al., 2008; Karczewski et al., 2012; Hempel et al., 2016; Wallukat et al., 2020). While developing these autoantibodies for cardioprotective effects for the α_{1A}-AR may be tempting, they may not be regulated by the normal desensitization and negative feedback mechanisms common in GPCRs to turn off or wane the signal, resulting in abnormal and non-physiological signaling and proliferation (Zhou et al., 2008; Karczewski et al., 2018; Becker et al., 2019; Wallukat et al., 2020). This abnormal signaling and proliferation may account for the vascular damage that many autoantibodies also impart (Zhou et al., 2008; Karczewski et al., 2012, 2018; Becker et al., 2019; Wallukat et al., 2020). Autoantibodies against the α_1-AR have also been associated with coronary heart disease (Thyrian et al., 2018), cardiac remodeling and dysfunction (Zhou et al., 2005; Li T. et al., 2017), pre-eclampsia (Ma et al., 2013), thromboangiitis obliterans (Buerger's Disease) (Klein-Weigel et al., 2014), AD and vascular dementia (Karczewski et al., 2012, 2018; Hempel et al., 2016), and prostate cancer (Wallukat et al., 2020). Therefore, both agonistic and antagonistic autoantibodies against the α_1-AR subtypes would need to be thoroughly analyzed for off target effects.

SUMMARY

α_1-ARs are part of the adrenergic family of sympathetic control and have long been known to regulate blood pressure, smooth muscle contraction and cardiac hypertrophy. In recent work, α_{1A}-AR stimulation also mediates adaptive effects and signals in the heart that lead to protective outcomes against ischemia and heart failure. They are also highly expressed in the cognitive centers of the brain and stimulation of α_1-ARs, particularly the α_{1A}-AR, can increase both short-term as well as LTP leading to increased learning and memory functions. With its ability to increase adult neurogenesis, there is a potential for α_{1A}-AR agonists or positive allosteric modulators to treat AD and to protect the heart at the same time. α_1-AR stimulation also mediates several aspects of whole-body and organ-specific

metabolism to regulate glucose uptake, gluconeogenesis, glucose breakdown, lipolysis, and fatty acid oxidation for energy production. The regulation of cardiac metabolism by the α_{1A}-AR is likely a contributing factor for its protective effects in the heart. For pharmacological interventions, it is suggested that therapeutics that focus on α_{1A}-AR agonism be developed. To avoid the potential side effects on blood pressure, the imidazoline rather than the phenethylamine pharmacophore should be of primary focus for drug discovery. Several α_{1A}-AR imidazoline-based agonists have been used in preclinical studies and allosteric agonists that will not increase blood pressure are now in development for heart failure and AD.

AUTHOR CONTRIBUTIONS

DP performed all of the research, writing, and editing of this manuscript.

FUNDING

This manuscript was funded through grants from the National Institute on Aging (RO1-AG066627) and The Edward N. and Della L. Thome Memorial Foundation (award Program in Alzheimer's Drug Discovery Research).

REFERENCES

Aggerbeck, M., Guellaen, G., and Hanoune, J. (1980). Adrenergic receptor of the alpha1-subtype mediates the activation of the glycogen phosphorylase in normal rat liver. *Biochem. Pharmacol.* 29, 643–645. doi: 10.1016/0006-2952(80)90389-5

Ahrén, B., and Lundquist, I. (1987). Alpha-adrenoceptor blockade by phentolamine inhibits beta-adrenergically and cholinergically induced glucagon secretion in the mouse. *Horm. Metab. Res.* 19, 600–603. doi: 10.1055/s-2007-1011889

Akerstrom, T., Laub, L., Vedel, K., Brand, C. L., Pedersen, B. K., Lindqvist, A. K., et al. (2014). Increased skeletal muscle capillarization enhances insulin sensitivity. *Am. J. Physiol. Endocrinol. Metab.* 307, E1105–E1116.

Akhter, S. A., Milano, C. A., Shotwell, K. F., Cho, M. C., Rockman, H. A., Lefkowitz, R. J., et al. (1997). Transgenic mice with cardiac overexpression of α1B-adrenergic receptors. In vivo α1-adrenergic receptor-mediated regulation of β-adrenergic signaling. *J. Biol. Chem.* 272, 21253–21259.

Akinaga, J., Lima, V., Kiguti, L. R., Hebeler-Barbosa, F., Alcántara-Hernández, R., García-Sáinz, J. A., et al. (2013). Differential phosphorylation, desensitization, and internalization of α1A-adrenoceptors activated by norepinephrine and oxymetazoline. *Mol. Pharmacol.* 83, 870–881. doi: 10.1124/mol.112.082313

ALLHAT Collaborative Research Group (2000). Major cardiovascular events in hypertensive patients randomized to doxazosin vs chlorthalidone: the antihypertensive and lipid-lowering treatment to prevent heart attack trial (ALLHAT). ALLHAT collaborative research group. *JAMA* 283, 1967–1975. doi: 10.1001/jama.283.15.1967

Anand, A., Andrade, C., Sudha, S., Guido, S., and Venkataraman, B. V. (2001). Phenylephrine and ECS-induced retrograde amnesia. *J. ECT* 17, 166–169. doi: 10.1097/00124509-200109000-00003

Arnsten, A. F., and Jentsch, J. D. (1997). The α1-adrenergic agonist, cirazoline, impairs spatial working memory performance in aged monkeys. *Pharmacol. Biochem. Behav.* 58, 55–59. doi: 10.1016/s0091-3057(96)00477-7

Assimacopoulos-Jeannet, F. D., Blackmore, P. F., and Exton, J. H. (1977). Studies on alpha-adrenergic activation of hepatic glucose output. Studies on role of calcium in alpha-adrenergic activation of phosphorylase. *J. Biol. Chem.* 252, 2662–2669. doi: 10.1016/s0021-9258(17)40509-6

Auclair, A., Drouin, C., Cotecchia, S., Glowinski, J., and Tassin, J. P. (2004). 5-HT2A and alpha1b-adrenergic receptors entirely mediate dopamine release, locomotor response and behavioural sensitization to opiates and psychostimulants. *Eur. J. Neurosci.* 20, 3073–3084. doi: 10.1111/j.1460-9568.2004.03805.x

Autelitano, D. J., and Woodcock, E. A. (1998). Selective activation of alpha1A-adrenergic receptors in neonatal cardiac myocytes is sufficient to cause hypertrophy and differential regulation of alpha1-adrenergic receptor subtype mRNAs. *J. Mol. Cell Cardiol.* 30, 1515–1523. doi: 10.1006/jmcc.1998.0717

Azami, N. S., Piri, M., Oryan, S., Jahanshahi, M., Babapour, V., and Zarrindast, M. R. (2010). Involvement of dorsal hippocampal alpha-adrenergic receptors in the effect of scopolamine on memory retrieval in inhibitory avoidance task. *Neurobiol. Learn. Mem.* 93, 455–462. doi: 10.1016/j.nlm.2010.01.003

Baek, K. J., Das, T., Gray, C. D., Desai, S., Hwang, K. C., Gacchui, R., et al. (1996). A 50 KDa protein modulates guanine nucleotide binding of transglutaminase II. *Biochemistry* 35, 2651–2657. doi: 10.1021/bi9522965

Ballou, L. M., Tian, P. Y., Lin, H. Y., Jiang, Y. P., and Lin, R. Z. (2001). Dual regulation of glycogen synthase kinase-3beta by the alpha1A-adrenergic receptor. *J. Biol. Chem.* 276, 40910–40916.

Banerjee, A., Locke-Winter, C., Rogers, K. B., Mitchell, M. B., Brew, E. C., Cairnes, C. B., et al. (1993). Preconditioning against myocardial dysfunction after ischemia and reperfusion by an α1-adrenergic mechanism. *Circ. Res.* 73, 656–670. doi: 10.1161/01.res.73.4.656

Bañuelos, C., Beas, B. S., McQuail, J. A., Gilbert, R. J., Frazier, C. J., Setlow, B., et al. (2014). Prefrontal cortical GABAergic dysfunction contributes to age-related working memory impairment. *J. Neurosci.* 34, 3457–3466. doi: 10.1523/jneurosci.5192-13.2014

Barak, Y., Liao, D., He, W., Ong, E. S., Nelson, M. C., Olefsky, J. M., et al. (2002). Effects of peroxisome proliferator-activated receptor delta on placentation, adiposity, and colorectal cancer. *Proc. Natl. Acad. Sci. U.S.A.* 99, 303–308. doi: 10.1073/pnas.012610299

Beak, J., Huang, W., Parker, J. S., Hicks, S. T., Patterson, C., et al. (2017). An oral selective alpha-1A adrenergic receptor agonist prevents doxorubicin cardiotoxicity. *JACC Basic Transl. Sci.* 2, 39–53. doi: 10.1016/j.jacbts.2016.10.006

Becker, N. P., Goettel, P., Mueller, J., Wallukat, G., and Schimke, I. (2019). Functional autoantibody diseases: basics and treatment related to cardiomyopathies. *Front. Biosci.* 24:14.

Benning, C. M., and Kyprianou, N. (2002). Quinazoline-derived alpha1-adrenoceptor antagonists induce prostate cancer cell apoptosis via an alpha1-adrenoceptor-independent action. *Cancer Res.* 62, 597–602.

Berridge, C., Shumsky, J. S., Andrzejewski, M. E., McGaughy, J., Spencer, R. C., Devilbiss, D., et al. (2012). Differential sensitivity to psychostimulants across prefrontal cognitive tasks: differential involvement of Noradrenergic α1- vs. α2-Receptors. *Biol. Psychiatry* 71, 467–473. doi: 10.1016/j.biopsych.2011.07.022

Berridge, C. W., and Spencer, R. C. (2016). Differential cognitive actions of norepinephrine α2 and α1 receptor signaling in the prefrontal cortex. *Brain Res.* 1641(Pt B), 189–196. doi: 10.1016/j.brainres.2015.11.024

Bhardwaj, S. K., Tse, Y. C., Ryan, R., Wong, T. P., and Srivastava, L. K. (2014). Impaired adrenergic-mediated plasticity of prefrontal cortical glutamate synapses in rats with developmental disruption of the ventral hippocampus. *Neuropsychopharmacology* 39, 2963–2973. doi: 10.1038/npp.2014.142

Bkaily, G., El-Bizri, N., Bui, M., Sukarieh, R., Jacques, D., and Fu, M. L. (2003). Modulation of intracellular Ca2+ via L-type calcium channels in heart cells by the autoantibody directed against the second extracellular loop of the alpha1-adrenoceptors. *Can. J. Physiol. Pharmacol.* 81, 234–246. doi: 10.1139/y03-044

Bliss, T. V., and Collingridge, G. L. (1993). A synaptic model of memory: long-term potentiation in the hippocampus. *Nature* 361, 31–39. doi: 10.1038/361031a0

Blue, D. R., Daniels, D. V., Gever, J. R., Jett, M. F., O'Yang, C., Tang, H. M., et al. (2004). Pharmacological characteristics of Ro 115-1240, a selective α1A/L-adrenoceptor partial agonist: a potential therapy for stress urinary incontinence. *BJU Int.* 93, 162–170. doi: 10.1111/j.1464-410x.2004.04577.x

Böhmer, T., Pfeiffer, N., and Gericke, A. (2014). Three commercial antibodies against α1-adrenergic receptor subtypes lack specificity in paraffin-embedded sections of murine tissues. *Naunyn. Schmiedebergs Arch. Pharmacol.* 387, 703–706. doi: 10.1007/s00210-014-0992-2

Boschmann, M., Krupp, G., Luft, F. C., Klaus, S., and Jordan, J. (2002). In vivo response to alpha(1)-adrenoreceptor stimulation in human white adipose tissue. *Obes. Res.* 10, 555–558. doi: 10.1038/oby.2002.75

Bristow, M. R., Ginsburg, R., Minobe, W., Cubicciotti, R. S., Sageman, W. S., Lurie, K., et al. (1982). Decreased catecholamine sensitivity and beta-adrenergic-receptor density in failing human hearts. *N. Engl. J. Med.* 307, 205–211. doi: 10.1056/nejm198207223070401

Bristow, M. R., Ginsburg, R., Umans, V., Fowler, M., Minobe, W., Rasmussen, R., et al. (1986). β1- and β2-adrenergic-receptor subpopulations in nonfailing and failing human ventricular myocardium: coupling of both receptor subtypes to muscle contraction and selective β1-receptor down-regulation in heart failure. *Circ. Res.* 59, 297–309. doi: 10.1161/01.res.59.3.297

Bristow, M. R., Minobe, W., Rasmussen, R., Hershberger, R. E., and Hoffman, B. B. (1988). Alpha-1 adrenergic receptors in the nonfailing and failing human heart. *J. Pharmacol. Exp. Ther.* 247, 1039–1045.

Brown, A. S. (2002). Consolidation theory and retrograde amnesia in humans. *Psychonom. Bull. Rev.* 9, 403–425. doi: 10.3758/bf03196300

Burcelin, R., Uldry, M., Foretz, M., Perrin, C., Dacosta, A., Nenniger-Tosato, M., et al. (2004). Impaired glucose homeostasis in mice lacking the α1b-adrenergic receptor subtype. *J. Biol. Chem.* 279, 1108–1115. doi: 10.1074/jbc.m307788200

Cadaret, C. N., Beede, K. A., Riley, H. E., and Yates, D. T. (2017). Acute exposure of primary rat soleus muscle to zilpaterol HCl (β2 adrenergic agonist), TNFα, or IL-6 in culture increases glucose oxidation rates independent of the impact on insulin signaling or glucose uptake. *Cytokine* 96, 107–113. doi: 10.1016/j.cyto.2017.03.014

Campbell, A. P., Wakelin, L. P., Denny, W. A., and Finch, A. M. (2017). Homobivalent conjugation increases the allosteric effect of 9-aminoacridine at the α1-adrenergic receptors. *Mol. Pharmacol.* 91, 135–144. doi: 10.1124/mol.116.105874

Castaldi, A., Zaglia, T., Di Mauro, V., Carullo, P., Viggiani, G., Borile, G., et al. (2014). MicroRNA-133 modulates the β1-adrenergic receptor transduction cascade. *Circ .Res.* 115, 273–283. doi: 10.1161/circresaha.115.303252

Cavalli, A., Lattion, A. L., Hummler, E., Nenniger, M., Pedrazzini, T., Aubert, J. F., et al. (1997). Decreased blood pressure response in mice deficient of the alpha1b-adrenergic receptor. *Proc. Natl. Acad. Sci. U.S.A.* 94, 11589–11594. doi: 10.1073/pnas.94.21.11589

Chalothorn, D., McCune, D. F., Edelmann, S. E., Tobita, K., Keller, B. B., Lasley, R. D., et al. (2003). Differential cardiovascular regulatory activities of the α_{1B}- and α_{1D}-adrenoceptor subtypes. *J. Pharmacol. Exp. Ther.* 305, 1045–1053. doi: 10.1124/jpet.102.048553

Chan, T. M., and Exton, J. H. (1978). Studies on α-adrenergic activation of hepatic glucose output. Studies on α-adrenergic inhibition of hepatic pyruvate kinase and activation of gluconeogenesis. *J. Biol. Chem.* 253, 6393–6400. doi: 10.1016/s0021-9258(19)46946-9

Chaulet, H., Lin, F., Guo, J., Owens, W. A., Michalicek, J., Kesteven, S. H., et al. (2006). Sustained augmentation of cardiac alpha1A-adrenergic drive results in pathological remodeling with contractile dysfunction, progressive fibrosis and reactivation of matricellular protein genes. *J. Mol. Cell Cardiol.* 40, 540–552. doi: 10.1016/j.yjmcc.2006.01.015

Chen, Q., Li, D. P., and Pan, H. L. (2006). Presynaptic alpha1-adrenergic receptors differentially regulate synaptic glutamate and GABA release to hypothalamic presympathetic neurons. *J. Pharmacol. Exp. Ther.* 316, 733–742. doi: 10.1124/jpet.105.094797

Chen, Y., Goudet, C., Pin, J. P., and Conn, P. J. (2008). N-{4-Chloro-2-[(1,3-dioxo-1,3-dihydro-2H-isoindol-2-yl) methyl]phenyl}-2-hydroxybenzamide (CPPHA) acts through a novel site as a positive allosteric modulator of group 1 metabotropic glutamate receptors. *Mol. Pharmacol.* 73, 909–918. doi: 10.1124/mol.107.040097

Chen, Z., Rogge, G., Hague, C., Alewood, D., Colless, B., Lewis, R. J., et al. (2004). Subtype-selective noncompetitive or competitive inhibition of human alpha1-adrenergic receptors by rho-TIA. *J. Biol. Chem.* 279, 35326–35333. doi: 10.1074/jbc.m403703200

Cheng, J. -T., Liu, I. -M., Yen, S. -T., and Chen, P. -C. (2000). Role of α1A-adrenoceptor in the regulation of glucose uptake into white adipocyte of rats in vitro. *Auton. Neurosci.* 84, 140–146. doi: 10.1016/s1566-0702(00)00197-1

Cheng, L., Ding, G., Qin, Q., Huang, Y., Lewis, W., He, N., et al. (2004). Cardiomyocyte-restricted peroxisome proliferator-activated receptor-δ deletion perturbs myocardial fatty acid oxidation and leads to cardiomyopathy. *Nat. Med.* 10, 1245–1250. doi: 10.1038/nm1116

Chernogubova, E., Hutchinson, D. S., Nedergaard, J., and Bengtsson, T. (2005). Alpha1- and beta1-adrenoceptor signaling fully compensates for beta3-adrenoceptor deficiency in brown adipocyte norepinephrine-stimulated glucose uptake. *Endocrinology* 146, 2271–2284. doi: 10.1210/en.2004-1104

Chobanian, A. V., Bakris, G. L., Black, H. R., Cushman, W. C., Green, L. A., Izzo, J. L. Jr., et al. (2003). The seventh report of the joint national committee on prevention, detection, evaluation, and treatment of high blood pressure: the JNC 7 report. *JAMA* 289, 2560–2571. doi: 10.1001/jama.289.19.2560

Christensen, K. L., and Mulvany, M. J. (1993). Mesenteric arcade arteries contribute substantially to vascular resistance in conscious rats. *J. Vasc. Res.* 30, 73–79. doi: 10.1159/000158978

Christopoulos, A. (2002). Allosteric binding sites on cell-surface receptors: novel targets for drug discovery. *Nat. Rev. Drug Discov.* 1, 198–210. doi: 10.1038/nrd746

Chu, C. A., Sindelar, D. K., Igawa, K., Sherck, S., Neal, D. W., Emshwiller, M., et al. (2000). The direct effects of catecholamines on hepatic glucose production occur via alpha(1)- and beta(2)-receptors in the dog. *Am. J. Physiol.* 279, E463–E473.

Collette, K., Fagerlie, R., Haselton, J., Perez, D. M., and Doze, V. (2010). Norepinephrine, through activation of α1A-ARs, stimulates production of new neurons, leading to an alleviation of depression and anxiety. *FASEB J.* 24, 1058–1057.

Collette, K. M., Zhou, X. D., Amoth, H. M., Lyons, M. J., Papay, R. S., Sens, D. A., et al. (2014). Long-term α1B-adrenergic receptor activation shortens lifespan, while α1A-adrenergic receptor stimulation prolongs lifespan in association with decreased cancer incidence. *Age* 36:9675.

Corr, P. B., Shayman, J. A., Kramer, J. B., and Kipnis, R. J. (1981). Increased α-adrenergic receptors in ischemic cat myocardium: a potential mediator of electrophysiological derangements. *J. Clin. Invest.* 67, 1232–1236. doi: 10.1172/jci110139

Cotecchia, S., Del Vescovo, C. D., Colella, M., Caso, S., and Diviani, D. (2015). The alpha1-adrenergic receptors in cardiac hypertrophy: signaling mechanisms and functional implications. *Cell Signal.* 27, 1984–1993. doi: 10.1016/j.cellsig.2015.06.009

Cotecchia, S., Schwinn, D. A., Randall, R. R., Lefkowitz, R. J., Caron, M. G., and Kobilka, B. K. (1988). Molecular cloning and expression of the cDNA for the hamster alpha 1-adrenergic receptor. *Proc. Natl. Acad. Sci. U.S.A.* 85, 7159–7163. doi: 10.1073/pnas.85.19.7159

Cowley, P. M., Wang, G., Chang, A. N., Makwana, O., Swigart, P. M., Lovett, D. H., et al. (2015). The alpha1A-adrenergic receptor subtype mediates increased contraction of failing right ventricular myocardium. *Am. J. Physiol. Heart Circ. Physiol.* 309, H888–H896.

Cunningham, M. L., Waldo, G. L., Hollinger, S., Hepler, J. R., and Harden, T. K. (2001). Protein kinase C phosphorylates RGS2 and modulates its capacity for negative regulation of Galpha 11 signaling. *J. Biol. Chem.* 276, 5438–5444. doi: 10.1074/jbc.m007699200

da Silva, E. D., Sato, M., Merlin, J., Broxton, N., Hutchinson, D. S., Ventura, S., et al. (2017). Factors influencing biased agonism in recombinant cells expressing the human α1A-adrenoceptor. *Br. J. Pharmacol.* 174, 2318–2333. doi: 10.1111/bph.13837

de Oliveira, A. L., de Paula, M. N., Comar, J. F., Vilela, V. R., Peralta, R. M., and Bracht, A. (2013). Adrenergic metabolic and hemodynamic effects of octopamine in the liver. *Int. J. Mol. Sci.* 14, 21858–21872. doi: 10.3390/ijms141121858

Dileepan, K. N., Khawaja, A. M., and Wagle, S. R. (1982). Studies on the mechanism of action of somatostatin on renal gluconeogenesis: evidence for the involvement of alpha 1-adrenergic stimuli. *Arch. Biochem. Biophys.* 213, 169–176. doi: 10.1016/0003-9861(82)90452-0

Dileepan, K. N., and Wagle, S. R. (1985). Somatostatin: a metabolic regulator. *Life Sci.* 37, 2335–2343. doi: 10.1016/0024-3205(85)90100-6

Doenst, T., and Taegtmeyer, H. (1999). α-adrenergic stimulation mediates glucose uptake through phosphatidylinositol 3-kinase in rat heart. *Circ. Res.* 84, 467–474. doi: 10.1161/01.res.84.4.467

Domyancic, A. V., and Morilak, D. A. (1997). Distribution of alpha1A adrenergic receptor mRNA in the rat brain visualized by in situ hybridization. *J. Comp. Neurol.* 386, 358–378. doi: 10.1002/(sici)1096-9861(19970929)386:3<358::aid-cne3>3.0.co;2-0

Downey, J. M., and Cohen, M. V. (1997). Signal transduction in ischemic preconditioning. *Adv. Exp. Med. Biol.* 430, 39–55.

Doze, V. A., Papay, R. S., Goldenstein, B. L., Gupta, M. K., Collette, K. M., Nelson, B. W., et al. (2011). Long-term α1A-adrenergic receptor stimulation improves synaptic plasticity, cognitive function, mood, and longevity. *Mol. Pharmacol.* 80, 747–758. doi: 10.1124/mol.111.073734

Drouin, C., Darracq, L., Trovero, F., Blanc, G., Glowinski, J., Cotecchia, S., et al. (2002). Alpha1b-adrenergic receptors control locomotor and rewarding effects of psychostimulants and opiates. *J. Neurosci.* 22, 2873–2884. doi: 10.1523/jneurosci.22-07-02873.2002

Du, X. J., Fang, L., Gao, X. M., Kiriazis, H., Feng, X., Hotchkin, E., et al. (2004). Genetic enhancement of ventricular contractility protects against pressure-overload-induced cardiac dysfunction. *J. Mol. Cell Cardiol.* 37, 979–987. doi: 10.1016/j.yjmcc.2004.07.010

Du, X. J., Gao, X. M., Kiriazis, H., Moore, X. L., Ming, Z., Su, Y., et al. (2006). Transgenic alpha1A-adrenergic activation limits post-infarct ventricular remodeling and dysfunction and improves survival. *Cardiovasc. Res.* 71, 735–743. doi: 10.1016/j.cardiores.2006.06.015

Duteil, J., Rambert, F. A., Pessonnier, J., Hermant, J. F., Gombert, R., and Assous, E. (1990). Central alpha 1-adrenergic stimulation in relation to the behaviour stimulating effect of modafinil; studies with experimental animals. *Eur. J. Pharmacol.* 180, 49–58. doi: 10.1016/0014-2999(90)90591-s

Dyck, J. R., Hopkins, T. A., Bonnet, S., Michelakis, E. D., Young, M. E., Watanabe, M., et al. (2006). Absence of malonyl coenzyme A decarboxylase in mice increases cardiac glucose oxidation and protects the heart from ischemic injury. *Circulation* 114, 1721–1728. doi: 10.1161/circulationaha.106.642009

Dyer-Reaves, K., Goodman, A. M., Nelson, A. R., and McMahon, L. L. (2019). Alpha1-adrenergic receptor mediated long-term depression at CA3-CA1 synapses can be induced viaaccumulation of endogenous norepinephrine and is preserved following noradrenergic denervation. *Front. Synaptic* 11:27. doi: 10.3389/fnsyn.2019.00027

Easson, L. H., and Stedman, E. (1933). Studies on the relationship between chemical constitution and physiological action: molecular dissymmetry and physiological activity. *Biochem. J.* 27, 1257–1266. doi: 10.1042/bj0271257

Eckert, R. L., Kaartinen, M. T., Nurminskaya, M., Belkin, A. M., Colak, G., Johnson, G. V., et al. (2014). Transglutaminase regulation of cell function. *Physiol. Rev.* 94, 383–417. doi: 10.1152/physrev.00019.2013

Eckhart, A. D., Duncan, S. J., Penn, R. B., Benovic, J. L., Lefkowitz, R. J., and Koch, W. J. (2000). Hybrid transgenic mice reveal in vivo specificity of G protein-coupled receptor kinases in the heart. *Circ. Res.* 86, 43–50. doi: 10.1161/01.res.86.1.43

Egert, S., Nguyen, N., and Schwaiger, M. (1999). Contribution of alpha-adrenergic and beta-adrenergic stimulation to ischemia-induced glucose transporter (GLUT) 4 and GLUT1 translocation in the isolated perfused rat heart. *Circ. Res.* 84, 1407–1415. doi: 10.1161/01.res.84.12.1407

El-Brolosy, M. A., and Stainier, D. (2017). Genetic compensation: a phenomenon in search of mechanisms. *PLoS Genet.* 13:e1006780. doi: 10.1371/journal.pgen.1006780

Endoh, M. (2016). Cardiac α1-adrenoceptors and inotropy: myofilament Ca2+ sensitivity, intracellular Ca2+ mobilization, signaling pathway, and pathophysiological relevance. *Circ. Res.* 119, 587–590. doi: 10.1161/circresaha.116.309502

Endoh, M., Hiramoto, T., Ishihata, A., Takanashi, M., and Inui, J. (1991). Myocardial alpha 1-adrenoceptors mediate positive inotropic effect and changes in phosphatidylinositol metabolism. Species differences in receptor distribution and the intracellular coupling process in mammalian ventricular myocardium. *Circ. Res.* 68, 1179–1190. doi: 10.1161/01.res.68.5.1179

Enomoto, T., Tse, M. T., and Floresco, S. B. (2011). Reducing prefrontal gamma-aminobutyric acid activity induces cognitive, behavioral, and dopaminergic abnormalities that resemble schizophrenia. *Biol. Psychiatry* 69, 432–441. doi: 10.1016/j.biopsych.2010.09.038

Evans, B. A., Broxton, N., Merlin, J., Sato, M., Hutchinson, D. S., Christopoulos, A., et al. (2011). Quantification of functional selectivity at the human α1A-adrenoceptor. *Mol. Pharmacol.* 79, 298–307. doi: 10.1124/mol.110.067454

Faintrenie, G., and Géloën, A. (1998). Alpha-1 adrenergic stimulation of glucose uptake in rat white adipocytes. *J. Pharmacol. Exp. Ther.* 1286, 607–610.

Fasciani, I., Petragnano, F., Aloisi, G., Marampon, F., Carli, M., Scarselli, M., et al. (2020). Allosteric modulators of G protein-coupled dopamine and serotonin receptors: a new class of atypical antipsychotics. *Pharmaceuticals.* 13:388. doi: 10.3390/ph13110388

Feng, J. F., Rhee, S. G., and Im, M. J. (1996). Evidence that phospholipase delta-1 is the effector in the Gh (transglutaminase II)-mediated signalling. *J. Biol. Chem.* 271, 16451–16454. doi: 10.1074/jbc.271.28.16451

Ferrara, L. A., Marotta, T., Rubba, P., de Simone, B., Leccia, G., Son, S., et al. (1986). Effects of alpha-adrenergic and beta-adrenergic receptor blockade on lipid metabolism. *Am. J. Med.* 80(Suppl. 2A), 104–108. doi: 10.1016/0002-9343(86)90168-3

Ferrer-Lorente, R., Cabot, C., Fernández-López, J. A., and Alemany, M. (2005). Combined effects of oleoyl-estrone and a beta3-adrenergic agonist (CL316,243) on lipid stores of diet-induced overweight male Wistar rats. *Life Sci.* 77, 2051–2058. doi: 10.1016/j.lfs.2005.04.008

Ferry, B., and McGaugh, J. L. (2000). Role of amygdala norepinephrine in mediating stress hormone regulation of memory storage. *Acta Pharmacol. Sin.* 21, 481–493.

Ferry, B., and Quirarte, G. (2012). "Role of norepinephrine in mediating inhibitory avoidance memory storage: a critical involvement of the basolateral amygdala," in *The Amygdala: A Discrete Multitasking Manager, 980-953-307-188-1*, ed. B. Ferry (London: In Tech – Open Science), 203–230.

Ferry, B., Roozendaal, B., and McGaugh, J. L. (1999a). Basolateral amygdala noradrenergic influences on memory storage are mediated by an interaction between beta- and alpha1-adrenoceptors. *J. Neurosci.* 19, 5119–5123. doi: 10.1523/jneurosci.19-12-05119.1999

Ferry, B., Roozendaal, B., and McGaugh, J. L. (1999b). Involvement of α1-adrenergic receptors in the basolateral amygdala in modulation of memory storage. *Eur. J. Pharmacol.* 372, 9–16. doi: 10.1016/s0014-2999(99)00169-7

Fesus, L., and Piacentini, M. (2002). Transglutaminase 2: an enigmatic enzyme with diverse functions. *Trends Biochem. Sci.* 27, 534–539. doi: 10.1016/s0968-0004(02)02182-5

Fischer, V., Gabauer, I., Tillinger, A., Novakova, M., Pechan, I., Krizanova, O., et al. (2008). Heart adrenoceptor gene expression and binding sites in the human failing heart. *Ann. N. Y. Acad. Sci.* 1148, 400–408. doi: 10.1196/annals.1410.013

Flechtner-Mors, M., Jenkinson, C. P., Alt, A., Biesalski, H. K., Adler, G., and Ditschuneit, H. H. (2004). Sympathetic regulation of glucose uptake by the alpha1-adrenoceptor in human obesity. *Obes. Res.* 12, 612–620. doi: 10.1038/oby.2004.70

Flechtner-Mors, M., Jenkinson, C. P., Alt, A., Adler, G., and Ditschuneit, H. H. (2002). In vivo alpha (1)-adrenergic lipolytic activity in subcutaneous adipose tissue of obese subjects. *J. Pharmacol. Exp. Ther.* 301, 229–233. doi: 10.1124/jpet.301.1.229

Ford, A. P., Arredondo, N. F., Blue, D. R. Jr., Bonhaus, D. W., Jasper, J., Kava, M. S., et al. (1996). RS-17053 (N-[2-(2-cyclopropylmethoxyphenoxy) ethyl]-5-chloro-alpha, alpha-dimethyl-1H-indole-3-ethanamine hydrochloride), a selective alpha 1A-adrenoceptor antagonist, displays low affinity for functional alpha 1-adrenoceptors in human prostate: implications for adrenoceptor classification. *Mol. Pharmacol.* 492, 209–215.

Fordyce, C. B., Roe, M. T., Ahmad, T., Libby, P., Borer, J. S., Hiatt, W. R., et al. (2015). Cardiovascular drug development: is it dead or just hibernating? *J. Am. Coll. Cardiol.* 65, 1567–1582.

Foster, T. C., and McNaughton, B. L. (1991). Long-term synaptic enhancement in CA1 is due to increased quanta1 size, not quanta1 content. *Hippocampus* 1, 79–79. doi: 10.1002/hipo.450010108

Fu, M. L., Herlitz, H., Wallukat, G., Hilme, E., Hedner, T., Hoebeke, J., et al. (1994). Functional autoimmune epitope on alpha 1-adrenergic receptors in patients with malignant hypertension. *Lancet* 344, 1660–1663. doi: 10.1016/s0140-6736(94)90456-1

Fuller, S. J., Gaitanaki, C. J., and Sugden, P. H. (1990). Effects of catecholamines on protein synthesis in cardiac myocytes and perfused hearts isolated from adult

rats. Stimulation of translation is mediated through the alpha 1-adrenoceptor. *Biochem. J.* 266, 727–736. doi: 10.1042/bj2660727

Gao, H., Chen, L., and Yang, H.-T. (2007). Activation of α1B-adrenoceptors alleviates ischemia/reperfusion injury by limitation of mitochondrial Ca2+ overload in cardiomyocytes. *Cardiovasc. Res.* 75, 584–595. doi: 10.1016/j.cardiores.2007.04.008

Gao, X. M., Wang, B. H., Woodcock, E., and Du, X. J. (2000). Expression of active alpha(1B)-adrenergic receptors in the heart does not alleviate ischemic reperfusion injury. *J. Mol. Cell Cardiol.* 32, 1679–1686. doi: 10.1006/jmcc.2000.1201

García-Sáinz, J. A., and Hernández-Sotomayor, S. M. (1985). Adrenergic regulation of gluconeogenesis: possible involvement of two mechanisms of signal transduction in alpha 1-adrenergic action. *Proc. Natl. Acad. Sci. U.S.A.* 82, 6727–6730. doi: 10.1073/pnas.82.20.6727

Gazarini, L., Stern, C. A., Carobrez, A. P., and Bertoglio, L. J. (2013). Enhanced noradrenergic activity potentiates fear memory consolidation and reconsolidation by differentially recruiting α1- and β-adrenergic receptors. *Learn. Mem.* 20, 210–219. doi: 10.1101/lm.030007.112

Gibbs, M. E., and Bowser, D. N. (2010). Astrocytic adrenoceptors and learning: alpha1-adrenoceptors. *Neurochem. Int.* 57, 404–410. doi: 10.1016/j.neuint.2010.03.020

Gibbs, M. E., and Summers, R. J. (2001). Stimulation of α1-adrenoceptors inhibits memory consolidation in the chick. *Eur. J. Neurosci.* 14, 1369–1376. doi: 10.1046/j.0953-816x.2001.01742.x

Gibbs, M. E., Hutchinson, D., and Hertz, L. (2008). Astrocytic involvement in learning and memory consolidation. *Neurosci. Biobehav. Rev.* 32, 927–944.

Gisbert, R., Ziani, K., Miquel, R., Noguera, M. A., Ivorra, M. D., Anselmi, E., et al. (2002). Pathological role of a constitutively active population of alpha (1D)-adrenoceptors in arteries of spontaneously hypertensive rats. *Br. J. Pharmacol.* 135, 206–216. doi: 10.1038/sj.bjp.0704447

Glund, S., Deshmukh, A., Long, Y. C., Moller, T., Koistinen, H. A., Caidahl, K., et al. (2007). Interleukin-6 directly increases glucose metabolism in resting human skeletal muscle. *Diabetes Metab. Res. Rev.* 56, 1630–1637. doi: 10.2337/db06-1733

Goetz, A. S., King, H. K., Ward, S. D., True, T. A., Rimele, T. J., and Saussy, D. L. Jr. (1995). BMY 7378 is a selective antagonist of the D subtype of alpha 1-adrenoceptors. *Eur. J. Pharmacol.* 272, R5–R6.

Graham, R. M., and Lanier, S. M. (1986). "Identification and characterization of alpha- adrenergic receptors," in *The Heart, and Cardiovascular System*, eds H. A. Fozzard, et al. (New York, NY: Raven Press), 1059–1095.

Grupp, I. L., Lorenz, J. N., Walsh, R. A., Boivin, G. P., and Rindt, H. (1998). Overexpression of α1B-adrenergic receptor induces left ventricular dysfunction in the absence of hypertrophy. *Am. J. Physiol.* 275(Pt 2), H1338–H1350.

Gupta, M. K., Papay, R. S., Jurgens, C. W., Gaivin, R. J., Shi, T., Doze, V. A., et al. (2009). α1-Adrenergic receptors regulate neurogenesis and gliogenesis. *Mol. Pharmacol.* 76, 314–326. doi: 10.1124/mol.109.057307

Gutiérrez, A., Contreras, C., Sánchez, A., and Prieto, D. (2019). Role of phosphatidylinositol 3-kinase (PI3K), mitogen-activated protein kinase (MAPK), and protein kinase C (PKC) in calcium signaling pathways linked to the α1-adrenoceptor in resistance arteries. *Front. Physiol.* 10:55. doi: 10.3389/fphys.2019.00055

Hague, C., Bernstein, L. S., Ramineni, S., Chen, Z., Minneman, K. P., and Hepler, J. R. (2005). Selective inhibition of α1A-adrenergic receptor signaling by RGS2 association with the receptor third intracellular loop. *J. Biol. Chem.* 280, 27289–27295. doi: 10.1074/jbc.m502365200

Harasawa, I., Honda, K., Tanoue, A., Shinoura, H., Ishida, Y., Okamura, H., et al. (2003). Responses to noxious stimuli in mice lacking α1D-adrenergic receptors. *Neuroreport* 14, 1857–1860. doi: 10.1097/00001756-200310060-00020

Hebb, D. O. (1949). *The Organization of Behavior*. New York, NY: Wiley.

Hempel, P., Heinig, B., Jerosch, C., Decius, I., Karczewski, P., Kassner, U., et al. (2016). Immunoadsorption of agonistic autoantibodies against α1-adrenergic receptors in patients with mild to moderate dementia. *Ther. Apher. Dial.* 20, 523–529. doi: 10.1111/1744-9987.12415

Heynen, A. J., Abraham, W. C., and Bear, M. F. (1996). Bidirectional modification of CA1 synapses in the adult hippocampus in vivo. *Nature* 381, 163–166. doi: 10.1038/381163a0

Hieble, J. P., DeMarinis, R. M., and Matthews, W. D. (1986). Evidence for and against heterogeneity of α1-adrenoceptors. *Life Sci.* 38, 1339–1350. doi: 10.1016/0024-3205(86)90466-2

Hilfiker, S., and Augustine, G. J. (1999). Regulation of synaptic vesicle fusion by protein kinase C. *J. Physiol.* 515:1. doi: .1111/j.1469-7793.1999.001ad.x

Hillman, K. L., Knudson, C. A., Carr, P. A., Doze, V. A., and Porter, J. E. (2005). Adrenergic receptor characterization of CA1 hippocampal neurons using real time single cell RT-PCR. *Brain Res. Mol. Brain Res.* 139, 267–276. doi: 10.1016/j.molbrainres.2005.05.033

Hong, C. J., Wang, Y. C., Liu, T. Y., Liu, H. C., and Tsai, S. J. (2001). A study of α-adrenoceptor gene polymorphisms and Alzheimer disease. *J. Neural Transm.* 108, 445–450. doi: 10.1007/s007020170065

Hopkins, W. F., and Johnston, D. (1984). Frequency-dependent noradrenergic modulation of long-term potentiation in the hippocampus. *Science* 226, 350–352. doi: 10.1126/science.6091272

Hosoda, C., Koshimizu, T. A., Tanoue, A., Nasa, Y., Oikawa, R., Tomabechi, T., et al. (2005). Two alpha1-adrenergic receptor subtypes regulating the vasopressor response have differential roles in blood pressure regulation. *Mol. Pharmacol.* 67, 912–922. doi: 10.1124/mol.104.007500

Hrometz, S. L., Edelmann, S. E., McCune, D. F., Olges, J. R., Hadley, R. W., Perez, D. M., et al. (1999). Expression of multiple α1-adrenoceptors on vascular smooth muscle: correlation with the regulation of contraction. *J. Pharmacol. Exp. Ther.* 290, 452–463.

Hu, K., and Nattel, S. (1995). Mechanisms of ischemic preconditioning in rat hearts. *Involvement of alpha* 1B-adrenoceptors, pertussis toxin-sensitive G proteins, and protein kinase C. *Circulation* 92, 2259–2265. doi: 10.1161/01.cir.92.8.2259

Hue, L., Felíu, J. E., and Hers, H. G. (1978). Control of gluconeogenesis and of enzymes of glycogen metabolism in isolated rat hepatocytes. A parallel study of the effect of phenylephrine and of glucagon. *Biochem. J.* 176, 791–797. doi: 10.1042/bj1760791

Hussain, M. B., and Marshall, I. (1997). Characterization of alpha1-adrenoceptor subtypes mediating contractions to phenylephrine in rat thoracic aorta, mesenteric artery and pulmonary artery. *Br. J. Pharmacol.* 122, 849–858. doi: 10.1038/sj.bjp.0701461

Hutchinson, D. S., and Bengtsson, T. (2005). α1A-adrenoceptors activate glucose uptake in L6 muscle cells through a phospholipase C-, phosphatidylinositol-3 kinase-, and atypical protein kinase C-dependent pathway. *Endocrinology* 146, 901–912. doi: 10.1210/en.2004-1083

Hutchinson, D. S., and Bengtsson, T. (2006). AMP-activated protein kinase activation by adrenoceptors in L6 skeletal muscle cells: mediation by alpha1-adrenoceptors causing glucose uptake. *Diabetes Metab. Res. Rev.* 55, 682–690. doi: 10.2337/diabetes.55.03.06.db05-0901

Hvoslef-Eide, M., Oomen, C. A., Fisher, B. M., Heath, C. J., Robbins, T. W., Saksida, L. M., et al. (2015). Facilitation of spatial working memory performance following intra-prefrontal cortical administration of the adrenergic alpha1 agonist phenylephrine. *Psychopharmacology* 232, 4005–4016. doi: 10.1007/s00213-015-4038-3

Ihara, S., Shimamoto, K., Watanabe, H., Sakai, R., and Kawana, M. (2006). An alpha1-receptor blocker reduces plasma leptin levels in hypertensive patients with obesity and hyperleptinemia. *Hypertens. Res.* 29, 805–811. doi: 10.1291/hypres.29.805

Ikeda, U., Tsuruya, Y., and Yaginuma, T. (1991). Alpha 1-adrenergic stimulation is coupled to cardiac myocyte hypertrophy. *Am. J. Physiol.* 260, H953–H956.

Ikegami, M., Ikeda, H., Ishikawa, Y., Ohsawa, M., Ohashi, T., Kai, M., et al. (2013a). Olanzapine induces glucose intolerance through the activation of AMPK in the mouse hypothalamus. *Eur. J. Pharmacol.* 718, 376–382. doi: 10.1016/j.ejphar.2013.08.006

Ikegami, M., Ikeda, H., Ohashi, T., Kai, M., Osada, M., Kamei, A., et al. (2013b). Olanzapine-induced hyperglycemia: possible involvement of histaminergic, dopaminergic and adrenergic functions in the central nervous system. *Neuroendocrinology* 98, 224–232. doi: 10.1159/000356119

Ikegaya, Y., Nakanishi, K., Saito, H., and Abe, K. (1997). Amygdala beta-noradrenergic influence on hippocampal long-term potentiation in vivo. *Neuroreport* 8, 3143–3146. doi: 10.1097/00001756-199709290-00027

Isgor, B. S., and Isgor, Y. G. (2012). Effect of alpha-1-adrenoceptor blocker on cytosolic enzyme targets for potential use in cancer chemotherapy. *Int. J. Pharmacol.* 8, 333–343. doi: 10.3923/ijp.2012.333.343

Izumi, Y., and Zorumski, C. F. (1999). Norepinephrine promotes long-term potentiation in the adult rat hippocampus in vitro. *Synapse* 31, 196–202. doi: 10.1002/(sici)1098-2396(19990301)31:3<196::aid-syn4>3.0.co;2-k

Janssen, P. M. L., Canan, B. D., Kilic, A., Whitson, B. A., and Baker, A. J. (2018). Human myocardium has a robust α1A-subtype adrenergic receptor inotropic response. *J. Cardiovasc. Pharmacol.* 72, 136–142. doi: 10.1097/fjc.0000000000000604

Jensen, B. C., Swigart, P. M., De Marco, T., Hoopes, C., and Simpson, P. C. (2009a). Alpha1-Adrenergic receptor subtypes in nonfailing and failing human myocardium. *Circ. Heart Fail.* 2, 654–663. doi: 10.1161/circheartfailure.108.846212

Jensen, B. C., Swigart, P. M., Laden, M. E., DeMarco, T., Hoopes, C., and Simpson, P. C. (2009b). The alpha-1D Is the predominant alpha-1-adrenergic receptor subtype in human epicardial coronary arteries. *J. Am. Coll. Cardiol.* 54, 1137–1145. doi: 10.1016/j.jacc.2009.05.056

Jensen, B. C., Swigart, P. M., and Simpson, P. C. (2009c). Ten commercial antibodies for alpha1-adrenergic receptor subtypes are nonspecific. *Naunyn. Schmiedebergs. Arch. Pharmacol.* 379, 409–412. doi: 10.1007/s00210-008-0368-6

Jurgens, C. W. D., Knudson, C. A., Carr, P. A., Perez, D. M., and Doze, V. A. (2009). α1-Adrenergic receptor regulation of interneuron function. *FASEB J.* 23:946.4.

Kalaria, R. N. (1989). Characterization of [125I]-HEAT binding to alpha 1-receptors in human brain: assessment in aging and Alzheimer's disease. *Brain Res.* 501, 287–294. doi: 10.1016/0006-8993(89)90645-8

Kandel, E. R. (2001). The molecular biology of memory storage: a dialogue between genes and synapses. *Science* 294, 1030–1038. doi: 10.1126/science.1067020

Kang, S. K., Yi, K. S., Kwon, N. S., Park, K. H., Kim, U. H., Baek, K. J., et al. (2004). Alpha1B-adrenoceptor signaling and cell motility: GTPase function of Gh/transglutaminase 2 inhibits cell migration through interaction with cytoplasmic tail of integrin alpha subunits. *J. Biol. Chem.* 279, 36593–36600.

Karczewski, P., Haase, H., Hempel, P., and Bimmler, M. (2010). Agonistic antibody to the alpha1-adrenergic receptor mobilizes intracellular calcium and induces phosphorylation of a cardiac 15-kDa protein. *Mol. Cell. Biochem.* 333, 233–242. doi: 10.1007/s11010-009-0224-0

Karczewski, P., Hempel, P., and Bimmler, M. (2018). Role of alpha1-adrenergic receptor antibodies in Alzheimer's disease. *Front. Biosci.* 23:2082–2089. doi: 10.2741/4691

Karczewski, P., Hempel, P., Kunze, R., and Bimmler, M. (2012). Agonistic autoantibodies to the α(1) -adrenergic receptor and the β(2) -adrenergic receptor in Alzheimer's and vascular dementia. *Scand. J. Immunol.* 75, 524–530. doi: 10.1111/j.1365-3083.2012.02684.x

Katsuki, H., Izumi, Y., and Zorumski, C. F. (1997). Noradrenergic regulation of synaptic plasticity in the hippocampal CA1 region. *J. Neurophysiol.* 77, 3013–3020. doi: 10.1152/jn.1997.77.6.3013

Kava, M. S., Blue, D. R. Jr., Vimont, R., Clarke, D. E., and Ford, A. P. D. W. (1998). α1L-Adrenoceptor mediation of smooth muscle contraction in rabbit bladder neck: a model for lower urinary tract tissues of man. *Br. J. Pharmacol.* 123, 1359–1366. doi: 10.1038/sj.bjp.0701748

Kemp, A., and Manahan-Vaughan, D. (2004). Hippocampal long-term depression and long-term potentiation encode different aspects of novelty acquisition. *Proc. Natl. Acad. Sci. U.S.A.* 101, 8192–8197. doi: 10.1073/pnas.0402650101

Kim, A. S., Miller, E. J., Wright, T. M., Li, J., Qi, D., Atsina, K., et al. (2011). A small molecule AMPK activator protects the heart against ischemia-reperfusion injury. *J. Mol. Cell. Cardiol.* 51, 24–32. doi: 10.1016/j.yjmcc.2011.03.003

Kim, M., Shen, M., Ngoy, S., Karamanlidis, G., Liao, R., and Tian, R. (2012). AMPK isoform expression in the normal and failing hearts. *J. Mol. Cell. Cardiol.* 52, 1066–1073. doi: 10.1016/j.yjmcc.2012.01.016

Kitakaze, M., Hori, M., Morioka, T., Minamino, T., Takashima, S., Sato, H., et al. (1994). Alpha 1-adrenoceptor activation mediates the infarct size-limiting effect of ischemic preconditioning through augmentation of 5'-nucleotidase activity. *J. Clin. Invest.* 93, 2197–2205. doi: 10.1172/jci117216

Klein-Weigel, P. F., Bimmler, M., Hempel, P., Schöpp, S., Dreusicke, S., Valerius, J., et al. (2014). G-protein coupled receptor auto-antibodies in thromboangiitis obliterans (Buerger's disease) and their removal by immunoadsorption. *Vasa* 43, 347–352. doi: 10.1024/0301-1526/a000372

Knauber, J., and Müller, W. E. (2000a). Decreased exploratory activity and impaired passive avoidance behaviour in mice deficient for the α1b-adrenoceptor. *Eur. Neuropsychopharmacol.* 10, 423–427. doi: 10.1016/s0924-977x(00)00100-0

Knauber, J., and Müller, W. E. (2000b). Subchronic treatment with prazosin improves passive avoidance learning in aged mice: possible relationships to alpha1-receptor up-regulation. *J. Neural. Transm.* 107, 1413–1426. doi: 10.1007/s007020070005

Knepper, S. M., Buckner, S. A., Brune, M. E., DeBernardis, J. F., Meyer, M. D., and Hancock, A. A. (1995). A-61603, a potent α1-adrenergic receptor agonist, selective for the α1A receptor subtype. *J. Pharmacol. Exp. Ther.* 274, 97–10.

Kobayashi, M., Sasabe, T., Shiohama, Y., and Koshikawa, N. (2008). Activation of alpha1-adrenoceptors increases firing frequency through protein kinase C in pyramidal neurons of rat visual cortex. *Neurosci. Lett.* 430, 175–180. doi: 10.1016/j.neulet.2007.10.047

Kosugi, K., Harano, Y., Nakano, T., Suzuki, M., Kashiwagi, A., and Shigeta, Y. (1983). Mechanism of adrenergic stimulation of hepatic ketogenesis. *Metabolism* 32, 1081–1087. doi: 10.1016/0026-0495(83)90081-1

Kurz, T., Yamada, K. A., DaTorre, S. D., and Corr, P. B. (1991). Alpha 1-adrenergic system and arrhythmias in ischaemic heart disease. *Eur. Heart J.* 12(Suppl. F), 88–98. doi: 10.1093/eurheartj/12.suppl_f.88

Lapiz, M. D., and Morilak, D. A. (2006). Noradrenergic modulation of cognitive function in rat medial prefrontal cortex as measured by attentional set shifting capability. *Neuroscience* 137, 1039–1049. doi: 10.1016/j.neuroscience.2005.09.031

Laz, T. M., Forray, C., Smith, K. E., Bard, J. A., Vaysse, P. J., Branchek, T. A., et al. (1994). The rat homologue of the bovine alpha 1c-adrenergic receptor shows the pharmacological properties of the classical alpha 1A subtype. *Mol. Pharmacol.* 46, 414–422.

Lee, Y. C., Liu, C. C., Juan, Y. S., Wu, W. J., Li, W. M., Yeh, H. C., et al. (2013). The impact of metabolic syndrome on the responsiveness to α1-blocker in men with BPH/LUTS. *Int. J. Clin. Pract.* 67, 356–362. doi: 10.1111/ijcp.12086

Lee, Y.-J., Kim, H. S., Seo, H. S., Na, J. O., Jang, Y.-N., Han, Y.-M., et al. (2020). Stimulation of Alpha1-Adrenergic receptor ameliorates cellular functions of multiorgans beyond vasomotion through PPARδ. *PPAR Res.* 2020:3785137.

Lemire, I., Ducharme, A., Tardif, J. C., Poulin, F., Jones, L. R., Allen, B. G., et al. (2001). Cardiac-directed overexpression of wild-type alpha1B-adrenergic receptor induces dilated cardiomyopathy. *Am. J. Physiol. Heart Circ. Physiol.* 281, H931–H938.

Lénárt, K., Pap, A., Pórszász, R., Oláh, V. A., Fésüs, L., and Mádi, A. (2020). Transglutaminase 2 has metabolic and vascular regulatory functions revealed by in vivo activation of alpha1-adrenergic receptor. *Int. J. Mol. Sci.* 21:3865. doi: 10.3390/ijms21113865

Leppik, R. A., Mynett, A., Lazareno, S., and Birdsall, N. J. (2000). Allosteric interactions between the antagonist prazosin and amiloride analogs at the human α1A-adrenergic receptor. *Mol. Pharmacol.* 57, 436–445. doi: 10.1124/mol.57.3.436

Li, C., Yan, X., Wu, D., Zhang, K., Liang, X., Pan, Y., et al. (2019). Vaccine targeted alpha 1D-adrenergic receptor for hypertension. *Hypertension* 74, 1551–1562. doi: 10.1161/hypertensionaha.119.13700

Li, T., Xu, J., Qin, X., Hou, Z., Guo, Y., Liu, Z., et al. (2017). Glucose oxidation positively regulates glucose uptake and improves cardiac function recovery after myocardial reperfusion. *Am. J. Physiol. Endocrinol. Metab.* 313, E577–E585.

Li, Y., Tian, J., Ma, X. R., Li, R. T., Zhang, S. L., Wang, P. L., et al. (2017). Increase in G protein-coupled receptor autoantibodies with decline of cardiac function in hypercholesterolemic rats. *Eur. Rev. Med. Pharmacol. Sci.* 21, 1065–1073.

Lima, V., Mueller, A., Kamikihara, S. Y., Raymundi, V., Alewood, D., Lewis, R. J., et al. (2005). Differential antagonism by conotoxin rho-TIA of contractions mediated by distinct alpha1-adrenoceptor subtypes in rat vas deferens, spleen and aorta. *Eur. J. Pharmacol.* 508, 183–192. doi: 10.1016/j.ejphar.2004.12.011

Limas, C. J., Limas, C., and Goldenberg, I. F. (1989). Intracellular distribution of adrenoceptors in the failing human myocardium. *Am. Heart J.* 117, 1310–1316. doi: 10.1016/0002-8703(89)90411-0

Lin, F., Owens, W. A., Chen, S., Stevens, M. E., Kesteven, S., Arthur, J. F., et al. (2001). Targeted alpha(1A)-adrenergic receptor overexpression induces enhanced cardiac contractility but not hypertrophy. *Circ. Res.* 89, 343–350. doi: 10.1161/hh1601.095912

Lin, S. C., Chueh, S. C., Hsiao, C. J., Li, T. K., Chen, T. H., Liao, C. H., et al. (2007). Prazosin displays anticancer activity against human prostate cancers: targeting DNA and cell cycle. *Neoplasia* 9, 830–839. doi: 10.1593/neo.07475

Lindsley, C. W., Emmitte, K. A., Hopkins, C. R., Bridges, T. M., Gregory, K. J., Niswender, C. M., et al. (2016). Practical strategies and concepts in GPCR

allosteric modulator discovery: recent advances with metabotropic glutamate receptors. *Chem. Rev.* 116, 6707–6741. doi: 10.1021/acs.chemrev.5b00656

Liu, I. M., Tsai, C. C., Lai, T. Y., and Cheng, J. T. (2001). Stimulatory effect of isoferulic acid on α1A-adrenoceptor to increase glucose uptake into cultured myoblast C2C12 cells of mice. *Auton. Neurosci.* 88, 175–180. doi: 10.1016/s1566-0702(01)00241-7

Lomasney, J. W., Cotecchia, S., Lorenz, W., Leung, W. Y., Schwinn, D. A., Yang-Feng, T. L., et al. (1991). Molecular cloning and expression of the cDNA for the alpha 1Aadrenergic receptor. The gene for which is located on human chromosome 5. *J. Biol. Chem.* 266, 6365–6369. doi: 10.1016/s0021-9258(18)38126-2

Luo, D. L., Gao, J., Fan, L. L., Tang, Y., Zhang, Y. Y., and Han, Q. D. (2007). Receptor subtype involved in alpha 1-adrenergic receptor-mediated Ca2+ signaling in cardiomyocytes. *Acta. Pharmacol. Sin.* 28, 968–974. doi: 10.1111/j.1745-7254.2007.00605.x

Luo, F., Li, S. H., Tang, H., Deng, W. K., Zhang, Y., and Liu, Y. (2015a). Phenylephrine enhances glutamate release in the medial prefrontal cortex through interaction with N-type Ca2+ channels and release machinery. *J. Neurochem.* 132, 38–50. doi: 10.1111/jnc.12941

Luo, F., Tang, H., and Cheng, Z. Y. (2015b). Stimulation of α1-adrenoceptors facilitates GABAergic transmission onto pyramidal neurons in the medial prefrontal cortex. *Neuroscience* 300, 63–74. doi: 10.1016/j.neuroscience.2015.04.070

Luo, F., Tang, H., Li, B. M., and Li, S. H. (2014). Activation of alpha1-adrenoceptors enhances excitatory synaptic transmission via a pre- and postsynaptic protein kinase C-dependent mechanism in the medial prefrontal cortex of rats. *Eur. J. Neurosci.* 39, 1281–1293. doi: 10.1111/ejn.12495

Luther, H. P., Homuth, V., and Wallukat, G. (1997). Alpha 1-adrenergic receptor antibodies in patients with primary hypertension. *Hypertension* 29, 678–682. doi: 10.1161/01.hyp.29.2.678

Lv, J., Zhan, S. Y., Li, G. X., Wang, D., Li, Y. S., and Jin, Q. H. (2016). α1-Adrenoceptors in the hippocampal dentate gyrus involved in learning-dependent long-term potentiation during active-avoidance learning in rats. *Neuroreport* 27, 1211–1216. doi: 10.1097/wnr.0000000000000679

Ma, G., Li, Y., Zhang, J., Liu, H., Hou, D., Zhu, L., et al. (2013). Association between the presence of autoantibodies against adrenoreceptors and severe pre-eclampsia: a pilot study. *PLoS One* 8:e57983. doi: 10.1371/journal.pone.0057983

Maeda, K., Das, D., Nakata, H., and Mitsuya, H. (2012). CCR5 inhibitors: emergence, success, and challenges. *Expert Opin. Emerg. Drugs* 17, 135–145. doi: 10.1517/14728214.2012.673584

Mahmoodi, G., Ahmadi, S., Pourmotabbed, A., Oryan, S., and Zarrindast, M. R. (2010). Inhibitory avoidance memory deficit induced by scopolamine: Interaction of cholinergic and glutamatergic systems in the ventral tegmental area. *Neurobiol. Learn. Mem.* 94, 83–90. doi: 10.1016/j.nlm.2010.04.004

Maisel, A. S., Motulsky, H. J., Ziegler, M. G., and Insel, P. A. (1987). Ischemia- and agonist-induced changes in alpha- and beta-adrenergic receptor traffic in guinea pig hearts. *Am. J. Physiol.* 253(5 Pt 2), H1159–H1166.

Manahan-Vaughan, D., and Braunewell, K. H. (1999). Novelty acquisition is associated with induction of hippocampal long-term depression. *Proc. Natl. Acad. Sci. U.S.A.* 96, 8739–8744. doi: 10.1073/pnas.96.15.8739

Mao, Z. M., Arnsten, A. F., and Li, B. M. (1999). Local infusion of an α1-adrenergic agonist into the prefrontal cortex impairs spatial working memory performance in monkeys. *Biol. Psychiatry* 46, 1259–1265. doi: 10.1016/s0006-3223(99)00139-0

Marek, G. J., and Aghajanian, G. K. (1996). Alpha1B-adrenoceptor-mediated excitation of piriform cortical interneurons. *Eur. J. Pharmacol.* 305, 95–100. doi: 10.1016/0014-2999(96)00158-6

Marek, G. J., and Aghajanian, G. K. (1999). 5-HT2A receptor or α1-adrenoceptor activation induces excitatory postsynaptic currents in layer V pyramidal cells of the medial prefrontal cortex. *Eur. J. Pharmacol.* 367, 197–206. doi: 10.1016/s0014-2999(98)00945-5

Martí, D., Miquel, R., Ziani, K., Gisbert, R., Ivorra, M. D., Anselmi, E., et al. (2005). Correlation between mRNA levels and functional role of alpha1-adrenoceptor subtypes in arteries: evidence of alpha1L as a functional isoform of the alpha1A-adrenoceptor. *Am. J. Physiol. Heart Circ. Physiol.* 289, H1923–H1932.

Martínez-Salas, S. G., Campos-Peralta, J. M., Pardo, J. P., Hernández-Muñoz, R., Ibarra, M., Tanoue, A., et al. (2011). α(1D)-Adrenoceptor regulates the vasopressor action of α(1A)-adrenoceptor in mesenteric vascular bed of α(1D)-adrenoceptor knockout mice. *Auton. Autacoid. Pharmacol.* 31, 64–71. doi: 10.1111/j.1474-8673.2011.00468.x

Masoud, W. G., Ussher, J. R., Wang, W., Jaswal, J. S., Wagg, C. S., Dyck, J. R., et al. (2014). Failing mouse hearts utilize energy inefficiently and benefit from improved coupling of glycolysis and glucose oxidation. *Cardiovasc. Res.* 101, 30–38. doi: 10.1093/cvr/cvt216

McCarty, M. F. (2004). Elevated sympathetic activity may promote insulin resistance syndrome by activating alpha-1 adrenergic receptors on adipocytes. *Med. Hypothes.* 62, 830–838. doi: 10.1016/j.mehy.2003.11.007

McCloskey, D. T., Turnbull, L., Swigart, P., O'Connell, T. D., Simpson, P. C., and Baker, A. J. (2003). Abnormal myocardial contraction in α_{1A}- and α_{1B}-adrenoceptor double-knockout mice. *J. Mol. Cell. Cardiol.* 35, 1207–1216. doi: 10.1016/s0022-2828(03)00227-x

McGrath, J. C. (2015). Localization of α-adrenoceptors: JR vane medal lecture. *Br. J. Pharmacol.* 172, 1179–1194. doi: 10.1111/bph.13008

Melien, O., Sandnes, D., Johansen, E. J., and Christoffersen, T. (2000). Effects of pertussis toxin on extracellular signal-regulated kinase activation in hepatocytes by hormones and receptor-independent agents: evidence suggesting a stimulatory role of G(i) proteins at a level distal to receptor coupling. *J. Cell Physiol.* 184, 27–36. doi: 10.1002/(sici)1097-4652(200007)184:1<27::aid-jcp3>3.0.co;2-q

Methven, L., Simpson, P. C., and McGrath, J. C. (2009). Alpha1A/B-knockout mice explain the native alpha1D-adrenoceptor's role in vasoconstriction and show that its location is independent of the other alpha1-subtypes. *Br. J. Pharmacol.* 158, 1663–1675. doi: 10.1111/j.1476-5381.2009.00462.x

Michel, M. C., Hanft, G., and Gross, G. (1994). Radioligand binding studies of alpha 1-adrenoceptor subtypes in rat heart. *Br. J. Pharmacol.* 111, 533–538. doi: 10.1111/j.1476-5381.1994.tb14770.x

Michel, M. C., and Vrydag, W. (2006). Alpha1-, alpha2- and beta-adrenoceptors in the urinary bladder, urethra and prostate. *Br. J. Pharmacol.* 147(Suppl. 2), S88–S119.

Milano, C. A., Dolber, P. C., Rockman, H. A., Bond, R. A., Venable, M. E., Allen, L. F., et al. (1994). Myocardial expression of a constitutively active alpha 1B-adrenergic receptor in transgenic mice induces cardiac hypertrophy. *Proc. Natl. Acad. Sci. U.S.A.* 91, 10109–10113. doi: 10.1073/pnas.91.21.10109

Minneman, K. P., Theroux, T. L., Hollinger, S., Han, C., and Esbenshade, T. A. (1994). Selectivity of agonists for cloned α1-adrenergic receptor subtypes. *Mol. Pharmacol.* 46, 929–936.

Minokoshi, Y., Kim, Y. B., Peroni, O. D., Fryer, L. G., Müller, C., Carling, D., et al. (2002). Leptin stimulates fatty-acid oxidation by activating AMP-activated protein kinase. *Nature* 415, 339–343. doi: 10.1038/415339a

Minokoshi, Y., Toda, C., and Okamoto, S. (2012). Regulatory role of leptin in glucose and lipid metabolism in skeletal muscle. *Indian J. Endocrinol. Metab.* 16(Suppl. 3), S562–S568.

Mishima, K., Tanoue, A., Tsuda, M., Hasebe, N., Fukue, Y., Egashira, N., et al. (2004). Characteristics of behavioral abnormalities in alpha1d-adrenoceptors deficient mice. *Behav. Brain Res.* 152, 365–373. doi: 10.1016/j.bbr.2003.10.038

Mitchell, M. B., Meng, X., Ao, L., Brown, J. M., Harken, A. H., and Banerjee, A. (1995). Preconditioning of isolated rat heart is mediated by protein kinase C. *Circ. Res.* 76, 73–81. doi: 10.1161/01.res.76.1.73

Miyamoto, L., Ebihara, K., Kusakabe, T., Aotani, D., Yamamoto-Kataoka, S., Sakai, T., et al. (2012). Leptin activates hepatic 5'-AMP-activated protein kinase through sympathetic nervous system and alpha1-adrenergic receptor: a potential mechanism for improvement of fatty liver in lipodystrophy by leptin. *J. Biol. Chem.* 287, 40441–40447. doi: 10.1074/jbc.m112.384545

Montgomery, M. D., Chan, T., Swigart, P. M., Myagmar, B. E., Dash, R., and Simpson, P. C. (2017). An alpha-1A adrenergic receptor agonist prevents acute doxorubicin cardiomyopathy in male mice. *PLoS ONE* 12:e0168409. doi: 10.1371/journal.pone.0168409

Morrow, A. L., and Creese, I. (1986). Characterization of alpha 1-adrenergic receptor subtypes in rat brain: a reevaluation of [3H]-WB4104 and [3H]-prazosin binding. *Mol. Pharmacol.* 29, 321–330.

Moshfegh, A., Babaei, P., Oryan, S., Soltani, B., Zarrindast, M. R., Moshfegh, A., et al. (2011). Involvement of dorsal hippocampal α1-adrenergic receptors in the effect of WIN55,212-2 on memory retrieval in inhibitory avoidance task. *Neurosci. Lett.* 489, 69–73. doi: 10.1016/j.neulet.2010.07.079

Mourad, F. H., and Saadé, N. E. (2011). Neural regulation of intestinal nutrient absorption. *Prog. Neurobiol.* 95, 149–162. doi: 10.1016/j.pneurobio.2011.07.010

Mouradian, R. D., Sessler, F. M., and Waterhouse, B. D. (1991). Noradrenergic potentiation of excitatory transmitter action in cerebrocortical slices: evidence for mediation by an alpha 1 receptor-linked second messenger pathway. *Brain Res.* 546, 83–95. doi: 10.1016/0006-8993(91)91162-t

Mulkey, R. M., and Malenka, R. C. (1992). Mechanisms underlying induction of homosynaptic long-term depression in area CA1 of the hippocampus. *Neuron* 9, 967–975. doi: 10.1016/0896-6273(92)90248-c

Murashita, M., Kusumi, I., Hosoda, H., Kangawa, K., and Koyama, T. (2007). Acute administration of clozapine concurrently increases blood glucose and circulating plasma ghrelin levels in rats. *Psychoneuroendocrinology* 32, 777–784. doi: 10.1016/j.psyneuen.2007.05.007

Musselman, D. M., Ford, A. P., Gennevois, D. J., Harbison, M. L., Laurent, A. L., et al. (2004). A randomized crossover study to evaluate Ro 115-1240, a selective α1A/L -adrenoceptor partial agonist in women with stress urinary incontinence. *BJU Int.* 93, 78–83. doi: 10.1111/j.1464-410x.2004.04560.x

Myagmar, B. E., Flynn, J. M., Cowley, P. M., Swigart, P. M., Montgomery, M. D., Thai, K., et al. (2017). Adrenergic receptors in individual ventricular myocytes: the beta-1 and alpha-1B are in all cells, the alpha-1A is in a subpopulation, and the beta-2 and beta-3 are mostly absent. *Circ. Res.* 120, 1103–1115. doi: 10.1161/circresaha.117.310520

Naderi, R., Imani, A., Faghihi, M., and Moghimian, M. (2010). Phenylephrine induces early and late cardioprotection through mitochondrial permeability transition pore in the isolated rat heart. *J. Surg. Res.* 164, e37–e42.

Nakade, Y., Kitano, R., Yamauchi, T., Kimoto, S., Sakamoto, K., Inoue, T., et al. (2020). Effect of adrenergic agonists on high-fat diet-induced hepatic steatosis in mice. *Int. J. Mol. Sci.* 21:9392. doi: 10.3390/ijms21249392

Nakaoka, H., Perez, D. M., Baek, K. J., Das, T., Husain, A., Misono, K., et al. (1994). Gh: A GTP binding protein with transglutaminase activity and receptor signaling function. *Science* 254, 1593–1596. doi: 10.1126/science.7911253

Nazari, A., Sedighi, M., Dalvand, P., Azizi, Y., Moghimian, M., and Boroujeni, S. N. (2019). Late cardiac perconditioning by phenylephrine in an isolated rat heart model is mediated by mitochondrial potassium channels. *Braz. J. Pharmac. Sci.* 55:e18075.

Nevzorova, J., Evans, B. A., Bengtsson, T., and Summers, R. J. (2006). Multiple signalling pathways involved in β2-adrenoceptor-mediated glucose uptake in rat skeletal muscle cells. *Br. J. Pharmacol.* 147, 446–454. doi: 10.1038/sj.bjp.0706626

Newman, L. A., Korol, D. L., and Gold, P. E. (2011). Lactate produced by glycogenolysis in astrocytes regulates memory processing. *PLoS One* 6:e28427. doi: 10.1371/journal.pone.0028427

Nishimaru, K., Kobayashi, M., Matsuda, T., Tanaka, Y., Tanaka, T., and Shigenobu, K. (2001). alpha-Adrenoceptor stimulation-mediated negative inotropism and enhanced Na(+)/Ca(2+) exchange in mouse ventricle. *Am. J. Physiol. Heart Circ. Physiol.* 280, H132–H141.

Oberhaensli, R. D., Schwendimann, R., and Keller, U. (1985). Effect of norepinephrine on ketogenesis, fatty acid oxidation, and esterification in isolated rat hepatocytes. *Diabetes Metab. Res. Rev.* 34, 774–779. doi: 10.2337/diabetes.34.8.774

O'Connell, T. D., Ishizaka, S., Nakamura, A., Swigart, P. M., Rodrigo, M. C., Simpson, G. L., et al. (2003). The α(1a/c)- and α(1b)-adrenergic receptors are required for physiological cardiac hypertrophy in the double-knockout mouse. *J. Clin. Invest.* 111, 1783–1791. doi: 10.1172/jci200316100

O'Connell, T. D., Jensen, B. C., Baker, A. J., and Simpson, P. C. (2013). Cardiac alpha1-adrenergic receptors: novel aspects of expression, signaling mechanisms, physiologic function, and clinical importance. *Pharmacol. Rev.* 66, 308–333. doi: 10.1124/pr.112.007203

Oddo, S., Caccamo, A., Shepherd, J. D., Murphy, M. P., Golde, T. E., Kayed, R., et al. (2003). Triple-transgenic model of Alzheimer's disease with plaques and tangles: intracellular Abeta and synaptic dysfunction. *Neuron* 39, 409–421.

Palacios, J. M., Hoyer, D., and Cortés, R. (1987). Alpha 1-Adrenoceptors in the mammalian brain: similar pharmacology but different distribution in rodents and primates. *Brain Res.* 419, 65–75. doi: 10.1016/0006-8993(87)90569-5

Pankratov, Y., and Lalo, U. (2015). Role for astroglial α1-adrenoreceptors in gliotransmission and control of synaptic plasticity in the neocortex. *Front. Cell Neurosci.* 9:230. doi: 10.3389/fncel.2015.00230

Papay, R., Gaivin, R., Jha, A., McCune, D. F., McGrath, J. C., Rodrigo, M. C., et al. (2006). Localization of the mouse alpha1A-adrenergic receptor (AR) in the brain: alpha1AAR is expressed in neurons, GABAergic interneurons, and NG2 oligodendrocyte progenitors. *J. Comp. Neurol.* 497, 209–222. doi: 10.1002/cne.20992

Papay, R., Gaivin, R., McCune, D. F., Rorabaugh, B. R., Macklin, W. B., McGrath, J. C., et al. (2004). Mouse alpha1B-adrenergic receptor is expressed in neurons and NG2 oligodendrocytes. *J. Comp. Neurol.* 478, 1–10. doi: 10.1002/cne.20215

Papay, R. S., and Perez, D. M. (2020). α1-Adrenergic receptors increase glucose oxidation under normal and ischemic conditions in adult mouse cardiomyocytes. *J. Recept. Signal Transduct. Res.* 5, 1–7.

Papay, R. S., Shi, T., Piascik, M. T., Naga Prasad, S. V., and Perez, D. M. (2013). α1A-adrenergic receptors regulate cardiac hypertrophy in vivo through interleukin-6 secretion. *Mol. Pharmacol.* 83, 939–948. doi: 10.1124/mol.112.084483

Pascual, O., Casper, K. B., Kubera, C., Zhang, J., Revilla-Sanchez, R., et al. (2005). Astrocytic purinergic signaling coordinates synaptic networks. *Science* 310, 113–116. doi: 10.1126/science.1116916

Patil, P. N., Miller, D. D., and Trendelenburg, U. (1974). Molecular geometry and adrenergic drug activity. *Pharmacol. Rev.* 26, 323–392.

Perez, D. M. (2021). Novel positive allosteric modulators of the α1A-adrenergic receptor to treat Alzheimer's disease. *Brain Connect.*. 11, A1–A8.

Perez, D. M., DeYoung, M. B., and Graham, R. M. (1993). Coupling of expressed alpha 1B- and alpha 1D-adrenergic receptor to multiple signaling pathways is both G protein and cell type specific. *Mol. Pharmacol.* 44, 784–795.

Perez, D. M., and Doze, V. A. (2011). Cardiac and neuroprotection regulated by α(1)-adrenergic receptor subtypes. *J. Recept. Signal Transduct. Res.* 31, 98–110. doi: 10.3109/10799893.2010.550008

Perez, D. M., Piascik, M. T., and Graham, R. M. (1991). Solution-phase library screening for the identification of rare clones: isolation of an alpha 1D-adrenergic receptor cDNA. *Mol. Pharmacol.* 40, 876–883.

Perez, D. M., Piascik, M. T., Malik, N., Gaivin, R., and Graham, R. M. (1994). Cloning, expression, and tissue distribution of the rat homolog of the bovine alpha 1C-adrenergic receptor provide evidence for its classification as the alpha 1A subtype. *Mol. Pharmacol.* 46, 823–831.

Perez-Aso, M., Segura, V., Monto, F., Barettino, D., Noguera, M. A., Milligan, G., et al. (2013). The three α1-adrenoceptor subtypes show different spatio-temporal mechanisms of internalization and ERK1/2 phosphorylation. *Biochim.. Biophys. Acta* 1833, 2322–2333. doi: 10.1016/j.bbamcr.2013.06.013

Petrasek, T., Doulames, V., Prokopova, I., Vales, K., Stuchlik, A., Petrasek, T., et al. (2010). Combined administration of alpha1-adrenoceptor antagonist prazosin and beta-blocker propranolol impairs spatial avoidance learning on a dry arena. *Behav. Brain Res.* 208, 402–407. doi: 10.1016/j.bbr.2009.12.025

Piascik, M. T., and Perez, D. M. (2001). Alpha1-adrenergic receptors: new insights and directions. *J. Pharmacol. Exp. Ther.* 298, 403–410.

Poulsen, L. L., Siersbæk, M., and Mandrup, S. (2012). PPARs: fatty acid sensors controlling metabolism. *Semin. Cell Dev. Biol.* 23, 631–639. doi: 10.1016/j.semcdb.2012.01.003

Price, D. T., Lefkowitz, R. J., Caron, M. G., Berkowitz, D., and Schwinn, D. A. (1994). Localization of mRNA for three distinct alpha 1-adrenergic receptor subtypes in human tissues: implications for human alpha-adrenergic physiology. *Mol. Pharmacol.* 45, 171–175.

Pussinen, R., Nieminen, S., Koivisto, E., Haapalinna, A., Riekkinen, P., and Sirvio, J. (1997). Enhancement of intermediate-term memory by an α-1 agonist or a partial agonist at the glycine site of the NMDA receptor. *Neurobiol. Learn. Mem.* 67, 69–74. doi: 10.1006/nlme.1996.3738

Puumala, T., Greijus, S., Narinen, K., Haapalinna, A., Riekkinen, P., and Sirviö, J. (1998). Stimulation of α-1 adrenergic receptors facilitates spatial learning in rats. *Eur. Neuropsychopharmacol.* 8, 17–26. doi: 10.1016/s0924-977x(97)00040-0

Ragnarsson, L., Wang, C. I., Andersson, Å, Fajarningsih, D., Monks, T., Brust, A., et al. (2013). Conopeptide ρ-TIA defines a new allosteric site on the extracellular surface of the α1B-adrenoceptor. *J. Biol. Chem.* 288, 1814–1827. doi: 10.1074/jbc.m112.430785

Rehring, T. F., Friese, R. S., Cleveland, J. C., Meng, X., Robertson, F. G., Harken, A. H., et al. (1996). Alpha-adrenergic preservation of myocardial pH during ischemia is PKC isoform dependent. *J. Surg. Res.* 63, 324–327. doi: 10.1006/jsre.1996.0269

Riekkinen, M., Kemppainen, S., Riekkinen, P. Jr. (1997). Effects of stimulation of alpha 1-adrenergic and NMDA/glycine-B receptors on learning defects in aged rats. *Psychopharmacology* 131, 49–56. doi: 10.1007/s002130050264

Robbins, T. W. (1996). Dissociating executive functions of the prefrontal cortex. *Philos. Trans. R. Soc. Lond. B Biol. Sci.* 351, 1463–1470. doi: 10.1098/rstb.1996.0131

Rockman, H., Koch, W., and Lefkowitz, R. (2002). Seven-transmembrane-spanning receptors and heart function. *Nature* 415, 206–212. doi: 10.1038/415206a

Rodriguez, A. L., Nong, Y., Sekaran, N. K., Alagille, D., Tamagnan, G. D., and Conn, P. J. (2005). A close structural analog of 2-methyl-6-(phenylethynyl)-pyridine acts as a neutral allosteric site ligand on metabotropic glutamate receptor subtype 5 and blocks the effects of multiple allosteric modulators. *Mol. Pharmacol.* 68, 1793–1802. doi: 10.1124/mol.105.016139

Rokosh, D. G., and Simpson, P. C. (2002). Knockout of the alpha1A/C-adrenergic receptor subtype: the alpha1A/C is expressed in resistance arteries and is required to maintain arterial blood pressure. *Proc. Natl. Acad. Sci. U.S.A.* 99, 9474–9479. doi: 10.1073/pnas.132552699

Rorabaugh, B. R., Ross, S. A., Gaivin, R. J., Papay, R. S., McCune, D. F., Simpson, P. C., et al. (2005). alpha1A- but not alpha1B-adrenergic receptors precondition the ischemic heart by a staurosporine-sensitive, chelerythrineinsensitive mechanism. *Cardiovasc. Res.* 65, 436–445. doi: 10.1016/j.cardiores.2004.10.009

Rose, L., Graham, L., Koenecke, A., Powell, M., Xiong, R., Shen, Z., et al. (2020). The association between Alpha-1 adrenergic receptor antagonists and in-hospital mortality from COVID-19. *medRxiv* doi: 10.1101/2020.12.18.20248346

Ross, S. A., Rorabaugh, B. R., Chalothorn, D., Yun, J., Gonzalez-Cabrera, P. J., McCune, D. F., et al. (2003). The alpha(1B)-adrenergic receptor decreases the inotropic response in the mouse Langendorff heart model. *Cardiovasc. Res.* 60, 598–607. doi: 10.1016/j.cardiores.2003.09.020

Ruffolo, R. R. Jr., Rice, P. J., Patil, P. N., Hamada, A., and Miller, D. D. (1983). Differences in the applicability of the Easson-Stedman hypothesis to the α1- and α2-adrenergic effects of phenethylamines and imidazolines. *Eur. J. Pharmacol.* 86, 471–475. doi: 10.1016/0014-2999(83)90199-1

Ruffolo, R. R. Jr., and Waddell, J. E. (1982). Receptor interactions of imidazolines. IX. Cirazoline is an alpha-1 adrenergic agonist and an alpha-2 adrenergic antagonist. *J. Pharmacol. Exp. Ther.* 222, 29–36.

Ruffolo, R. R. Jr., Yaden, E. L., Waddell, J. E., and Dillard, R. D. (1980). Receptor interactions of imidazolines. VI. Significance of carbon bridge separating phenyl and imidazoline rings of tolazoline-like α-adrenergic imidazolines. *J. Pharmacol. Exp. Ther.* 214, 535–540.

Russell, R. R. III, Li, J., Coven, D. L., Pypaert, M., Zechner, C., Palmeri, M., et al. (2004). AMP-activated protein kinase mediates ischemic glucose uptake and prevents postischemic cardiac dysfunction, apoptosis, and injury. *J. Clin. Invest.* 114, 495–503. doi: 10.1172/jci19297

Sadalge, A., Coughlin, L., Fu, H., Wang, B., Valladares, O., Valentino, R., et al. (2003). α1d Adrenoceptor signaling is required for stimulus induced locomotor activity. *Mol. Psychiatry.* 8, 664–672. doi: 10.1038/sj.mp.4001351

Sajapitak, S., Uenoyama, Y., Yamada, S., Kinoshita, M., Iwata, K., Bari, F. Y., et al. (2008). Paraventricular alpha1- and alpha2-adrenergic receptors mediate hindbrain lipoprivation-induced suppression of luteinizing hormone pulses in female rats. *J. Reprod. Dev.* 54, 198–202. doi: 10.1262/jrd.20024

Salvi, S. (2001). Protecting the myocardium from ischemic injury: a critical role for alpha(1)-adrenoreceptors? *Chest* 119, 1242–1249. doi: 10.1378/chest.119.4.1242

Sanbe, A., Tanaka, Y., Fujiwara, Y., Tsumura, H., Yamauchi, J., Cotecchia, S., et al. (2007). Alpha1-adrenoceptors are required for normal male sexual function. *Br. J. Pharmacol.* 152, 332–340. doi: 10.1038/sj.bjp.0707366

Sato, M., Evans, B. A., Sandström, A. L., Chia, L. Y., Mukaida, S., Thai, B. S., et al. (2018). α1A-Adrenoceptors activate mTOR signalling and glucose uptake in cardiomyocytes. *Biochem. Pharmacol.* 148, 27–40. doi: 10.1016/j.bcp.2017.11.016

Scheiderer, C. L., Dobrunz, L. E., and McMahon, L. L. (2004). Novel form of long-term synaptic depression in rat hippocampus induced by activation of α1-adrenergic receptors. *J. Neurophysiol.* 91, 1071–1077. doi: 10.1152/jn.00420.2003

Scheiderer, C. L., Smith, C. C., McCutchen, E., McCoy, P. A., Thacker, E. E., Kolasa, K., et al. (2008). Coactivation of M(1) muscarinic and alpha1 adrenergic receptors stimulates extracellular signal-regulated protein kinase and induces long-term depression at CA3-CA1 synapses in rat hippocampus. *J. Neurosci.* 14, 5350–5358. doi: 10.1523/jneurosci.5058-06.2008

Schroeder, C., Stabroth, C., Luft, F. C., and Jordan, J. (2012). Adrenergic cardiovascular control before and after removal of stimulatory α1-adrenoreceptor antibodies. *Hypertension* 59, e6–e7.

Schultz, P. E., Cook, E. P., and Johnston, D. (1994). Changes in paired-pulse facilitation suggest presynaptic involvement in long-term potentiation. *J. Neurosci.* 14, 5325–5337. doi: 10.1523/jneurosci.14-09-05325.1994

Schwinn, D. A., Lomasney, J. W., Lorenz, W., Szklut, P. J., Fremeau, R. T. Jr., Yang-Feng, T. L., et al. (1990). Molecular cloning and expression of the cDNA for a novel α1- adrenergic receptor subtype. *J. Biol. Chem.* 265, 8183–8189. doi: 10.1016/s0021-9258(19)39055-6

Scofield, M. A., Liu, F., Abel, P. W., and Jeffries, W. B. (1995). Quantification of steady state expression of mRNA for α1-adrenergic receptor subtypes using reverse transcription and a competitive polymerase chain reaction. *J. Pharmacol. Exp. Ther.* 275, 1035–1042.

Segura, V., Perez-Aso, M., Monto, F., Carceller, E., Noguera, M. A., Pediani, J., et al. (2013). Differences in the signaling pathways of α1A- and α1B-adrenoceptors are related to different endosomal targeting. *PLoS One* 8, e64996. doi: 10.1371/journal.pone.0064996

Sharpe, I. A., Thomas, L., Loughnan, M., Motin, L., Palant, E., Croker, D. E., et al. (2003). Allosteric α1-adrenoreceptor antagonism by the conopeptide ρ-TIA. *J. Biol. Chem.* 278, 34451–34457. doi: 10.1074/jbc.m305410200

Shi, T., Moravec, C. S., and Perez, D. M. (2013). Novel proteins associated with human dilated cardiomyopathy: selective reduction in α(1A)-adrenergic receptors and increased desensitization proteins. *J. Recept. Signal Transduct. Res.* 33, 96–106. doi: 10.3109/10799893.2013.764897

Shi, T., Papay, R. S., and Perez, D. M. (2016). α1A-Adrenergic receptor prevents cardiac ischemic damage through PKCδ/GLUT1/4-mediated glucose uptake. *J. Recept. Signal Transduct. Res.* 36, 261–270. doi: 10.3109/10799893.2015.1091475

Shi, T., Papay, R. S., and Perez, D. M. (2017). The role of α1-adrenergic receptors in regulating metabolism: increased glucose tolerance, leptin secretion and lipid oxidation. *J. Recept. Signal Transduct. Res.* 37, 124–132. doi: 10.1080/10799893.2016.1193522

Shimazaki, Y., Nishiki, T., Omori, A., Sekiguchi, M., Kamata, Y., Kozaki, S., et al. (1996). Phosphorylation of 25-kDa synaptosome-associated protein. Possible involvement in protein kinase C-mediated regulation of neurotransmitter release. *J. Biol. Chem.* 271, 14548–14553. doi: 1074/jbc.271.24.14548

Shimohama, S., Taniguchi, T., Fujiwara, M., and Kameyama, M. (1986). Biochemical characterization of α1-adrenergic receptors in human brain and changes in Alzheimer-type dementia. *J. Neurochem.* 47, 1295–1301.

Shiuchi, T., Haque, M. S., Okamoto, S., Inoue, T., Kageyama, H., Lee, S., et al. (2009). Hypothalamic orexin stimulates feeding-associated glucose utilization in skeletal muscle via sympathetic nervous system. *Cell Metab.* 10, 466–480. doi: 10.1016/j.cmet.2009.09.013

Simkhovich, B. Z., Przyklenk, K., and Kloner, R. A. (2013). Role of protein kinase C in ischemic "conditioning": from first evidence to current perspectives. *J. Cardiovasc. Pharmacol. Ther.* 18, 525–532. doi: 10.1177/1074248413494814

Simpson, P. (1983). Norepinephrine-stimulated hypertrophy of cultured rat myocardial cells is an alpha1-adrenergic response. *J. Clin. Invest.* 72, 732–738. doi: 10.1172/jci111023

Sirviö, J., and MacDonald, E. (1999). Central alpha1-adrenoceptors: their role in the modulation of attention and memory formation. *Pharmacol. Ther.* 83, 49–65.

Skoglund, G., Lundquist, I., and Ahren, B. (1987). Alpha 1- and alpha 2-adrenoceptor activation increases plasma glucagon levels in the mouse. *Eur. J. Pharmacol.* 143, 83–88. doi: 10.1016/0014-2999(87)90737-0

Snabaitis, A. K., Muntendorf, A., Wieland, T., and Avkiran, M. (2005). Regulation of the extracellular signal-regulated kinase pathway in adult myocardium: differential roles of G(q/11), Gi and G(12/13) proteins in signalling by alpha1-adrenergic, endothelin-1 and thrombin-sensitive protease-activated receptors. *Cell Signal.* 17, 655–664. doi: 10.1016/j.cellsig.2004.10.008

Somlyo, A. P., and Somlyo, A. V. (2003). Ca2+ sensitivity of smooth muscle and nonmuscle myosin II: modulated by G proteins, kinases, and myosin

phosphatase. *Physiol. Rev.* 83, 1325–1358. doi: 10.1152/physrev.00023.2003

Speechly-Dick, M. E., Grover, G. J., and Yellon, D. M. (1995). Does ischemic preconditioning in the human involve protein kinase C and the ATP-dependent K+ channel? Studies of contractile function after simulated ischemia in an atrial in vitro model. *Circ. Res.* 77, 1030–1035. doi: 10.1161/01.res.77.5.1030

Spreng, M., Cotecchia, S., and Schenk, F. (2001). A behavioral study of alpha-1b adrenergic receptor knockout mice: increased reaction to novelty and selectively reduced learning capacities. *Neurobiol. Learn Mem.* 75, 214–229. doi: 10.1006/nlme.2000.3965

Squire, L. R., Genzel, L., Wixted, J. T., and Morris, R. G. (2015). Memory consolidation. *Cold Spring Harb. Perspect. Biol.* 7:a021766.

Stanasila, L., Abuin, L., Dey, J., and Cotecchia, S. (2008). Different internalization properties of the alpha1a- and alpha1b-adrenergic receptor subtypes: the potential role of receptor interaction with beta-arrestins and AP50. *Mol. Pharmacol.* 74, 562–573. doi: 10.1124/mol.107.043422

Steinfath, M., Chen, Y. Y., Lavicky, J., Magnussen, O., Nose, M., Rosswag, S., et al. (1992). Cardiac alpha 1-adrenoceptor densities in different mammalian species. *Br. J. Pharmacol.* 107, 185–188. doi: 10.1111/j.1476-5381.1992.tb14484.x

Stevens, C. F., and Sullivan, J. (1998). Synaptic plasticity. *Curr. Biol.* 8:R151-3.

Stone, E. A., Cotecchia, S., Lin, Y., and Quartermain, D. (2002). Role of brain alpha 1B-adrenoceptors in modafinil-induced behavioral activity. *Synapse* 46, 269–270. doi: 10.1002/syn.10127

Sugden, M. C., Tordoff, A. F., Ilic, V., and Williamson, D. H. (1980). α-adrenergic stimulation of [1-14C]-oleate oxidation to 14CO2 in isolated rat hepatocytes. *FEBS Lett.* 120, 80–84. doi: 10.1016/0014-5793(80)81051-9

Szot, P., White, S. S., Greenup, J. L., Leverenz, J. B., Peskind, E. R., and Raskind, M. A. (2005). Alpha1-adrenoreceptor in human hippocampus: binding and receptor subtype mRNA expression. *Brain Res. Mol. Brain Res.* 139, 367–371. doi: 10.1016/j.molbrainres.2005.06.013

Szot, P., White, S. S., Greenup, J. L., Leverenz, J. B., Peskind, E. R., and Raskind, M. A. (2007). Changes in adrenoreceptors in the prefrontal cortex of subjects with dementia: evidence of compensatory changes. *Neuroscience* 146, 471–480. doi: 10.1016/j.neuroscience.2007.01.031

Tanaka, T., Yamamoto, J., Iwasaki, S., Asaba, H., Hamura, H., Ikeda, Y., et al. (2003). Activation of peroxisome proliferator-activated receptor δ induces fatty acid β-oxidation in skeletal muscle and attenuates metabolic syndrome. *Proc. Natl. Acad. Sci. U.S.A.* 100, 15924–15929. doi: 10.1073/pnas.0306981100

Tang, K. M., Wang, G. R., Lu, P., Karas, R. H., Aronovitz, M., Heximer, S. P., et al. (2003). Regulator of G-protein signaling-2 mediates vascular smooth muscle relaxation and blood pressure. *Nat. Med.* 9, 1506–1512. doi: 10.1038/nm958

Tanoue, A., Nasa, Y., Koshimizu, T., Shinoura, H., Oshikawa, S., Kawai, T., et al. (2002). The alpha(1D)-adrenergic receptor directly regulates arterial blood pressure via vasoconstriction. *J. Clin. Invest.* 109, 765–775. doi: 10.1172/jci200214001

Thomas, A. P., Martin-Requero, A., and Williamson, J. R. (1985). Interactions between insulin and alpha 1-adrenergic agents in the regulation of glycogen metabolism in isolated hepatocytes. *J. Biol. Chem.* 260, 5963–5973. doi: 10.1016/s0021-9258(18)88923-2

Thyrian, J. R., Hertel, J., Schulze, L. N., Dörr, M., Prüss, H., Hempel, P., et al. (2018). Prevalence and determinants of agonistic autoantibodies against α1-adrenergic receptors in patients screened positive for dementia: results from the population-based DelpHi-study. *J. Alzheimers Dis.* 64, 1091–1097. doi: 10.3233/jad-171096

Torkaman-Boutorabi, A., Danyali, F., Oryan, S., Ebrahimi-Ghiri, M., and Zarrindast, M. R. (2014). Hippocampal α-adrenoceptors involved in the effect of histamine on spatial learning. *Physiol. Behav.* 129, 17–24. doi: 10.1016/j.physbeh.2014.02.009

Townsend, S. A., Jung, A. S., Hoe, Y. S., Lefkowitz, R. Y., Khan, S. A., Lemmon, C. A., et al. (2004). Critical role for the alpha-1B adrenergic receptor at the sympathetic neuroeffector junction. *Hypertension* 44, 776–782. doi: 10.1161/01.hyp.0000145405.01113.0e

Trost, B. N., Weidmann, P., Riesen, W., Claessens, J., Streulens, Y., and Nelemans, F. (1987). Comparative effects of doxazosin and hydrochlorothiazide on serum lipids and blood pressure in essential hypertension. *Am. J. Cardiol.* 59, 99–104.

Tsuchida, A., Liu, Y., Liu, G. S., Cohen, M. V., and Downey, J. M. (1994). Alpha 1-adrenergic agonists precondition rabbit ischemic myocardium independent of adenosine by direct activation of protein kinase C. *Circ. Res.* 75, 576–585. doi: 10.1161/01.res.75.3.576

Turnbull, L., McCloskey, D. T., O'Connell, T. D., Simpson, P. C., and Baker, A. J. (2003). Alpha 1-adrenergic receptor responses in alpha 1AB-AR knockout mouse hearts suggest the presence of alpha 1D-AR. *Am. J. Physiol. Heart Circ. Physiol.* 284, H1104–H1109.

Unnerstall, J. R., Fernandez, I., and Orensanz, L. M. (1985). The alpha-adrenergic receptor: radiohistochemical analysis of functional characteristics and biochemical differences. *Pharmacol. Biochem. Behav.* 22, 859–874. doi: 10.1016/0091-3057(85)90538-6

Ussher, J. R., Wang, W., Gandhi, M., Keung, W., Samokhvalov, V., Oka, T., et al. (2012). Stimulation of glucose oxidation protects against acute myocardial infarction and reperfusion injury. *Cardiovasc. Res.* 94, 359–369. doi: 10.1093/cvr/cvs129

Van Asseldonk, B., Barkin, J., and Elterman, D. S. (2015). Medical therapy for benign prostatic hyperplasia: a review. *Can. J. Urol.* 22(Suppl. 1), 7–17.

Vanhoose, A. M., Emery, M., Jimenez, L., and Winder, D. G. (2002). ERK activation by G-protein-coupled receptors in mouse brain is receptor identity-specific. *J. Biol. Chem.* 277, 9049–9053. doi: 10.1074/jbc.m108309200

Vann, S. D., and Albasser, M. M. (2011). Hippocampus and neocortex: recognition and spatial memory. *Curr. Opin. Neurobiol.* 21, 1–6.

Vecchione, C., Fratta, L., Rizzoni, D., Notte, A., Poulet, R., Porteri, E., et al. (2002). Cardiovascular influences of alpha1b-adrenergic receptor defect in mice. *Circulation* 105, 1700–1707. doi: 10.1161/01.cir.0000012750.08480.55

Velásquez-Martinez, M. C., Vázquez-Torres, R., and Jiménez-Rivera, C. A. (2012). Activation of alpha1-adrenoceptors enhances glutamate release onto ventral tegmental area dopamine cells. *Neuroscience* 216, 18–30. doi: 10.1016/j.neuroscience.2012.03.056

Vieira, E., Liu, Y. J., and Gylfe, E. (2004). Involvement of alpha1 and beta-adrenoceptors in adrenaline stimulation of the glucagon-secreting mouse alpha-cell. *Naunyn. Schmiedebergs Arch. Pharmacol.* 369, 179–183. doi: 10.1007/s00210-003-0858-5

Villalba, N., Stankevicius, E., Garcia-Sacristán, A., Simonsen, U., and Prieto, D. (2007). Contribution of both Ca2+ entry and Ca2+ sensitization to the alpha1-adrenergic vasoconstriction of rat penile small arteries. *Am. J. Physiol. Heart Circ. Physiol.* 292, H1157–H1169.

Walden, P. D., Durkin, M. M., Lepor, H., Wetzel, J. M., Gluchowski, C., and Gustafson, E. L. (1997). Localization of mRNA and receptor binding sites for the alpha 1a-adrenoceptor subtype in the rat, monkey and human urinary bladder and prostate. *J. Urol.* 157, 1032–1038. doi: 10.1016/s0022-5347(01)65136-x

Wallukat, G., Jandrig, B., Becker, N. P., Wendler, J. J., Göttel, P., Müller, J., et al. (2020). Autoantibodies directed against α1-adrenergic receptor and endothelin receptor A in patients with prostate cancer. *Auto. Immun. Highlights* 11:13. doi: 10.1186/s13317-020-00136-y

Wang, B. H., Du, X. J., Autelitano, D. J., Milano, C. A., and Woodcock, E. A. (2000). Adverse effects of constitutively active alpha(1B)-adrenergic receptors after pressure overload in mouse hearts. *Am. J. Physiol. Heart Circ. Physiol.* 279, H1079–H1086.

Wang, J., Yang, L., Rezaie, A. R., and Li, J. (2011). Activated protein C protects against myocardial ischemic/reperfusion injury through AMP-activated protein kinase signaling. *J. Thromb. Haemost.* 9, 1308–1317. doi: 10.1111/j.1538-7836.2011.04331.x

Waugh, D. J. J., Gaivin, R. J., Zuscik, M. J., Gonzalez-Cabrera, P., Ross, S. A., Yun, J., et al. (2001). Phe308 and Phe312 in TM VII are major sites of α1-adrenergic receptor antagonist binding: imidazoline agonists bind like antagonists. *J. Biol. Chem.* 276, 25366–25371.

Weinberger, M. H. (1986). Antihypertensive therapy and lipids: Paradoxical influences on cardiovascular disease risk. *Am. J. Med.* 80(Suppl. 2A), 64–70. doi: 10.1016/0002-9343(86)90162-2

Wenner, M. I., Maker, G. L., Dawson, L. F., Drummond, P. D., and Mullaney, I. (2016). The potential of metabolomic analysis techniques for the characterisation of α1-adrenergic receptors in cultured N1E-115 mouse neuroblastoma cells. *Cytotechnology* 68, 1561–1575. doi: 10.1007/s10616-015-9915-4

Wenzel, K., Haase, H., Wallukat, G., Derer, W., Bartel, S., Homuth, V., et al. (2008). Potential relevance of a1-adrenergic receptor autoantibodies in refractory hypertension. *PLoS One* 3:e3742. doi: 10.1371/journal.pone.0003742

Wier, W. G., and Morgan, K. G. (2003). Alpha1-adrenergic signaling mechanisms in contraction of resistance arteries. *Rev. Physiol. Biochem. Pharmacol.* 150, 91–139. doi: 10.1007/s10254-003-0019-8

Willis, M. S., Ilaiwy, A., Montgomery, M. D., Simpson, P. C., and Jensen, B. C. (2016). The alpha-1A adrenergic receptor agonist A61603 reduces cardiac polyunsaturated fatty acid and endocannabinoid metabolites associated with inflammation in vivo. *Metabolomics* 12:155.

Winder-Rhodes, S. E., Chamberlain, S. R., Idris, M. I., Robbins, T. W., Sahakian, B. J., and Müller, U. (2010). Effects of modafinil and prazosin on cognitive and physiological functions in healthy volunteers. *J. Psychopharmacol. Oxf. Engl.* 24, 1649–1657. doi: 10.1177/0269881109105899

Wold, E. A., Chen, J., Cunningham, K. A., and Zhou, J. (2019). Allosteric modulation of class A GPCRs: targets, agents, and emerging concepts. *J. Med. Chem.* 62, 88–127. doi: 10.1021/acs.jmedchem.8b00875

Woo, S. H., and Lee, C. O. (1999). Role of PKC in the effects of alpha1-adrenergic stimulation on Ca2+ transients, contraction and Ca2+ current in guinea-pig ventricular myocytes. *Pflugers Arch.* 437, 335–344. doi: 10.1007/s004240050787

Wootten, D., Christopoulos, A., Marti-Solano, M., Babu, M. M., and Sexton, M. (2018). Mechanisms of signalling and biased agonism in G protein-coupled receptors. *Nat. Rev. Mol. Cell Biol.* 19, 638–653. doi: 10.1038/s41580-018-0049-3

Wu, J., and Li, L. (2016). Autoantibodies in Alzheimer's disease: potential biomarkers, pathogenic roles, and therapeutic implications. *J. Biomed. Res.* 30, 361–372.

Wu, X. S., and Wu, L. G. (2001). Protein kinase C increases the apparent affinity of the release machinery to Ca^{2+} by enhancing the release machinery downstream of the Ca^{2+} sensor. *J. Neurosci.* 21, 7928–7936. doi: 10.1523/JNEUROSCI.21-20-07928.2001

Xiao, L., and Jeffries, W. B. (1998). Kinetics of alkylation of cloned rat α1-adrenoceptor subtypes by chloroethylclonidine. *Eur. J. Pharmacol* 347, 319–327. doi: 10.1016/s0014-2999(98)00109-5

Xu, L., Anwyl, R., and Rowan, M. J. (1998). Spatial exploration induces a persistent reversal of long-term potentiation in rat hippocampus. *Nature* 394, 891–894. doi: 10.1038/29783

Yan, L., Tan, X., Chen, W., Zhu, H., Cao, J., and Liu, H. (2014). Enhanced vasoconstriction to α1 adrenoceptor autoantibody in spontaneously hypertensive rats. *Sci. China Life Sci.* 57, 681–689. doi: 10.1007/s11427-014-4672-8

Yeh, C. C., Fan, Y., Xu, Y., Yang, Y. L., Simpson, P. C., and Mann, M. J. (2017). Shift toward greater pathologic post-myocardial infarction remodeling with loss of the adaptive hypertrophic signaling of alpha1 adrenergic receptors in mice. *PLoS One* 12:e0188471. doi: 10.1371/journal.pone.0188471

Zhang, J., Ash, T., Huang, W., Smith, A., Huang, H., and Jensen, B. (2020). An essential protective role for cardiomyocyte alpha1A-adrenergic receptors in a mouse model of myocardial infarction. *Circ. Res.* 127:A408.

Zhang, Z., Cordeiro Matos, S., Jego, S., Adamantidis, A., and Seguela, P. (2013). Norepinephrine drives persistent activity in prefrontal cortex via synergistic alpha1 and alpha2 adrenoceptors. *PLoS One* 8:e66122. doi: 10.1371/journal.pone.0066122

Zhao, M., Hagler, H. K., and Muntz, K. H. (1996). Regulation of alpha 1-, beta 1-, and beta 2-adrenergic receptors in rat heart by norepinephrine. *Am. J. Physiol.* 271(5 Pt 2), H1762–H1768.

Zhao, X., Balaji, P., Pachon, R., Beniamen, D. M., Vatner, D. E., Graham, R. M., et al. (2015). Overexpression of cardiomyocyte α1A-adrenergic receptors attenuates postinfarct remodeling by inducing angiogenesis through heterocellular signaling. *Arterioscler. Thromb. Vasc. Biol.* 35, 2451–2459. doi: 10.1161/atvbaha.115.305919

Zhao, X., Park, J., Ho, D., Gao, S., Yan, L., Ge, H., et al. (2012). Cardiomyocyte overexpression of the α1A-adrenergic receptor in the rat phenocopies second but not first window preconditioning. *Am. J. Physiol. Heart Circ. Physiol.* 302, H1614–H1624.

Zhou, J., and Cunningham, K. A. (2019). Positive-allosteric modulation of the 5-HT2C receptor: implications for neuropsychopharmacology and neurotherapeutics. *Neuropsychopharmacology* 44, 230–231. doi: 10.1038/s41386-018-0190-x

Zhou, Z., Liao, Y., Li, L., Wei, F., Wang, B., Wei, Y., et al. (2008). Vascular damages in rats immunized by alpha1-adrenoceptor peptides. *Cell. Mol. Immunol.* 5, 349–356. doi: 10.1038/cmi.2008.43

Zhou, Z., Liao, Y. H., Wei, Y., Wei, F., Wang, B., Li, L., et al. (2005). Cardiac remodeling after long-term stimulation by antibodies against the alpha1-adrenergic receptor in rats. *Clin. Immunol.* 114, 164–173. doi: 10.1016/j.clim.2004.09.011

Zilles, K., Gross, G., Schleicher, A., Schildgen, S., Bauer, A., Bahro, M., et al. (1991). Regional and laminar distributions of alpha1-adrenoceptors and their subtypes in human and rat hippocampus. *Neuroscience* 40, 307–320. doi: 10.1016/0306-4522(91)90122-5

Zou, M. X., Roy, A. A., Zhao, Q., Kirshenbaum, L. A., Karmazyn, M., and Chidiac, P. (2006). RGS2 is upregulated by and attenuates the hypertrophic effect of alpha1-adrenergic activation in cultured ventricular myocytes. *Cell Signal.* 18, 1655–1663. doi: 10.1016/j.cellsig.2006.01.012

Zuscik, M. J., Chalothorn, D., Hellard, D., Deighan, C., McGee, A., Daly, C. J., et al. (2001). Hypotension, autonomic failure, and cardiac hypertrophy in transgenic mice overexpressing the alpha 1B-adrenergic receptor. *J. Biol. Chem.* 276, 13738–13743. doi: 10.1074/jbc.m008693200

Zuscik, M. J., Sands, S., Ross, S. A., Waugh, D. J., Gaivin, R. J., Morilak, D., et al. (2000). Overexpression of the alpha1B-adrenergic receptor causes apoptotic neurodegeneration: multiple system atrophy. *Nat. Med.* 6, 1388–1394. doi: 10.1038/82207

Conflict of Interest: The author declares that the research was conducted in the absence of any commercial or financial relationships that could be construed as a potential conflict of interest.

frontiers in Cell and Developmental Biology

ORIGINAL RESEARCH
published: 20 August 2021
doi: 10.3389/fcell.2021.710664

G-Protein-Coupled Estrogen Receptor-1 Positively Regulates the Growth Plate Chondrocyte Proliferation in Female Pubertal Mice

Ya-Shuan Chou[1,2], Shu-Chun Chuang[1,2], Chung-Hwan Chen[1,2,3,4,5,6,7], Mei-Ling Ho[1,2,8,9,10] and Je-Ken Chang[1,2,3,4,5]**

[1] Orthopaedic Research Center, Kaohsiung Medical University, Kaohsiung, Taiwan, [2] Regenerative Medicine and Cell Therapy Research Center, Kaohsiung Medical University, Kaohsiung, Taiwan, [3] Department of Orthopaedics, Kaohsiung Medical University Hospital, Kaohsiung Medical University, Kaohsiung, Taiwan, [4] Department of Orthopaedics, College of Medicine, Kaohsiung Medical University, Kaohsiung, Taiwan, [5] Department of Orthopaedics, Kaohsiung Municipal Ta-Tung Hospital, Kaohsiung, Taiwan, [6] Institute of Medical Science and Technology, National Sun Yat-sen University, Kaohsiung, Taiwan, [7] Department of Healthcare Administration and Medical Informatics, Kaohsiung Medical University, Kaohsiung, Taiwan, [8] Department of Physiology, College of Medicine, Kaohsiung Medical University, Kaohsiung, Taiwan, [9] Department of Marine Biotechnology and Resources, National Sun Yat-sen University, Kaohsiung, Taiwan, [10] Department of Medical Research, Kaohsiung Medical University Hospital, Kaohsiung Medical University, Kaohsiung, Taiwan

OPEN ACCESS

Edited by:
Sameer Mohammad, King Abdullah International Medical Research Center (KAIMRC), Saudi Arabia

Reviewed by:
Bin Guo, Jilin University, China
Ana Rufino, Chemistry and Technology Network (REQUIMTE), Portugal

***Correspondence:**
Mei-Ling Ho
homelin@kmu.edu.tw
Je-Ken Chang
jkchang@cc.kmu.edu.tw

Specialty section:
This article was submitted to Signaling, a section of the journal Frontiers in Cell and Developmental Biology

Received: *17 May 2021*
Accepted: *28 July 2021*
Published: *20 August 2021*

Citation:
Chou Y-S, Chuang S-C, Chen C-H, Ho M-L and Chang J-K (2021) G-Protein-Coupled Estrogen Receptor-1 Positively Regulates the Growth Plate Chondrocyte Proliferation in Female Pubertal Mice. Front. Cell Dev. Biol. 9:710664. doi: 10.3389/fcell.2021.710664

Estrogen enhances long bone longitudinal growth during early puberty. Growth plate chondrocytes are the main cells that contribute to long bone elongation. The role of G-protein-coupled estrogen receptor-1 (GPER-1) in regulating growth plate chondrocyte function remains unclear. In the present study, we generated chondrocyte-specific GPER-1 knockout (CKO) mice to investigate the effect of GPER-1 in growth plate chondrocytes. In control mice, GPER-1 was highly expressed in the growth plates of 4- and 8-week-old mice, with a gradual decline through 12 to 16 weeks. In CKO mice, the GPER-1 expression in growth plate chondrocytes was significantly lower than that in the control mice (80% decrease). The CKO mice also showed a decrease in body length (crown–rump length), body weight, and the length of tibias and femurs at 8 weeks. More importantly, the cell number and thickness of the proliferative zone of the growth plate, as well as the thickness of primary spongiosa and length of metaphysis plus diaphysis in tibias of CKO mice, were significantly decreased compared with those of the control mice. Furthermore, there was also a considerable reduction in the number of proliferating cell nuclear antigens and Ki67-stained proliferating chondrocytes in the tibia growth plate in the CKO mice. The chondrocyte proliferation mediated by GPER-1 was further demonstrated *via* treatment with a GPER-1 antagonist in cultured epiphyseal cartilage. This study demonstrates that GPER-1 positively regulates chondrocyte proliferation at the growth plate during early puberty and contributes to the longitudinal growth of long bones.

Keywords: G-protein-coupled estrogen receptor-1, chondrocyte-specific knockout mice, estrogen receptor, bone growth, long bone elongation

INTRODUCTION

Long bone longitudinal growth is mainly driven by chondrocyte proliferation at the growth plate during puberty. Estrogen is well-known to regulate longitudinal growth during puberty (Chagin and Savendahl, 2007a). More importantly, low estrogen levels stimulate bone growth in early puberty, whereas high estrogen levels induce growth plate closure at the end of puberty (Almeida et al., 2017). The molecular mechanisms involved in the change of estrogen levels and the differences of estrogen receptors (ERs) remain unclear. A membranous ER, G-protein-coupled estrogen receptor-1 (GPER-1), also called GPR30, was recently shown to mediate the non-genomic effects of estrogen (Revankar et al., 2005). GPER-1 has been indicated to be widely expressed in mouse and human tissues, such as the heart (Martensson et al., 2009; Patel et al., 2010), brain (Hazell et al., 2009), pancreas (Liu et al., 2009; Martensson et al., 2009; Kumar et al., 2011), uterus (Gao et al., 2011), bone (Chagin and Savendahl, 2007b; Heino et al., 2008), and cartilage (Chagin and Savendahl, 2007b; Ribeiro et al., 2020). More importantly, the expression level of GPER-1 in the human growth plate was found to decrease during pubertal progression, suggesting that GPER-1 might be involved in the modulation of pubertal bone growth (Chagin and Savendahl, 2007b). Although GPER-1 expression in the bone and cartilage has been investigated previously, the function of GPER-1 in bone growth remains unclear. Accordingly, in this study, we hypothesized that GPER-1 might regulate early growth plate development and affect long bone longitudinal growth.

In global *GPER-1* knockout mice, GPER-1 deficiency causes certain metabolic alterations as well as a reduction in body weight and bone growth, suggesting that GPER-1 might play a role in skeletal development (Martensson et al., 2009). In contrast, another study showed that the increase in body weight in female global *GPER-1* knockout mice was due to abnormal obesity (Haas et al., 2009). However, these studies using global *GPER-1* knockout mice did not specifically investigate the role of GPER-1 in growth plate chondrocytes and long bone longitudinal growth. Recently, the Cre/loxP system has been used to generate a tissue-specific *GPER-1* knockout mouse model, serving as an alternative experimental strategy and providing a more reliable phenotype. In this study, we developed a chondrocyte-specific *GPER-1* deficient (*Col2a1-Cre*; *GPER-1*$^{f/f}$, CKO) mouse model to investigate the role of GPER-1 in the growth plate chondrocytes of growing bones. The role of GPER-1 in the regulation of longitudinal bone growth during puberty, including bone length, growth plate thickness, and growth plate chondrocyte proliferation in long bones, was investigated using the animal model.

MATERIALS AND METHODS

Experimental Animals

All animal studies were approved by the Kaohsiung Medical University Animal Care and Use Committee (104166 and 107157). Four animals were housed per cage, maintained on a 12/12-h light/dark cycle at 23 ± 2°C, with food and water freely available (Altromin, DEU).

In female mice, the onset of puberty can occur as early as P26 (3.5 weeks old) (Bell, 2018), and the age of mature adult mice can range from 3 to 6 months (Flurkey et al., 2007). Therefore, according to previous reports, 2-, 4-, 8-, 12-, and 16-week-old mice represent the stages of early life, early-puberty, puberty, end-puberty, and post-puberty, respectively (van der Eerden et al., 2000; Li et al., 2012). The body weight of the mice was analyzed every week, and axial growth was measured through the crown–rump length before death. Mice were randomly killed at 2, 4, 8, 12, and 16 weeks old (n = 6–8 mice per group), at which point the tissues were isolated. Bone tissues were collected and fixed with a 10% formalin solution, decalcified in a 10% ethylenediaminetetraacetic acid solution, embedded in paraffin, and sectioned at a thickness of 5 μm.

Generation of *Col2a1-Cre*; *GPER-1*$^{f/f}$ Mice

The *GPER-1*^{tm1c} conventional GPER-1 mice were purchased from the Knockout Mouse Project (University of California-Davis, Davis, CA, United States). The *GPER-1*^{tm1c} mice were generated by crossing the *GPER-1*^{tm1a} mice with Flp mice, which ubiquitously express Flp recombinase. The flanking loxP sites within exon 3 were generated, expanded, and injected into the C57BL/6 blastocysts as part of the Knockout Mouse Project (Skarnes et al., 2011). The offspring were crossed with flippase-transgenic mice to remove the NeoR flanked by flippase recombinase target sequences. The hybrid mice were backcrossed with the C57BL/6 strain for 12 generations. The *GPER-1*^{tm1c} mice were generated and further maintained with a C57BL/6J background.

To generate the chondrocyte-specific (*Col2a1*-Cre) homozygous floxed GPER-1 transgenic (*Col2a1*-Cre; *GPER-1*$^{f/f}$) mice, the *GPER-1*^{tm1c} mice were crossed with *Col2a1*-Cre mice, which were purchased from the Jackson Laboratory (JAX stock #003554; Bar Harbor, ME, United States) (Ovchinnikov et al., 2000) to obtain the offspring *Col2a1*-Cre; *GPER-1*$^{+/f}$ mice. The resulting offspring were then intercrossed to breed chondrocyte-specific *GPER-1* knockout mice, *Col2a1*-Cre; *GPER-1*$^{f/f}$ mice (n = 28). To confirm the genotypes of these offspring, genomic DNA was obtained from the tails of the mice. Genotyping of the GPER-1 floxed allele was performed by polymerase chain reaction (PCR) using the forward and reverse primers 5′-GAA CCC ACA GCT CTC TTG TGT GC-3′ and 5′-GGA AAA CTA CTG TTT GTC GAG ACA GG-3′, which amplified a 507-bp fragment, whereas the GPER-1 wild-type allele produced a 322-bp fragment. Moreover, the *Col2a1*-Cre transgene was detected by PCR using the forward and reverse primers 5′-CTA AAC ATG CTT CAT CGT CGG TC-3′ and 5′-TCG GAT CAT CAG CTA CAC CAG AG-3′, which produced a 420-bp fragment. In this study, the *GPER-1*$^{f/f}$ mice without *Col2a1*-Cre were used as the control group (n = 34). All animals were generated in the National Laboratory Animal Center (Tainan, Taiwan).

Measurement of Serum Estrogen Levels

Blood samples were collected from the proestrus vena cava of 8-week-old mice (n = 4). To quantitatively detect estrogen in CKO or control mouse serum, a mouse estrogen enzyme-linked immunosorbent assay (ELISA) kit (EM1501, FineTest, Hubei, China) was used. First, 50 μl of standard or sample was added to each well that had been pre-coated with estrogen. Second, 50 μl biotin-detection antibody was added to each well of 96-well plate and was incubated for 45 min at 37°C. The antibody was removed and washed using wash buffer, and then, 100 μl SABC working solution was added to each well for 30 min at 37°C. After the working solution was removed, 90 μl of 3,3′,5,5′-tetramethylbenzidine substrate was added, and the solution was incubated for 15 min at 37°C. Finally, a stop solution was added, and the absorbance of the samples was measured using an ELISA reader at 450 nm. For the estrogen ELISA kit, a standard curve was generated to calculate the value of the tested sample in each assay. The testing sensitivity was 15.625 pg/ml, the concentration range was 15.625 to 1,000 pg/ml, and the mean ± SD deviation of the R^2 value was 0.99 ± 0.0047 for all assays. The intra-assay and inter-assay coefficients of variation (CV) were 6.79% (n = 9) and 9.08% (n = 3), respectively. The data corresponded with the criteria (intra-assay: CV < 8%, and inter-assay: CV < 10% from the protocol).

Micro-Computed Tomography Imaging System for Bone Structure Analysis

Three-dimensional (3-D) reconstruction of the specimens was performed using high-resolution micro-computed tomography (μ-CT) analysis (Skyscan 1076; Skyscan NV, Kontich, Belgium) to characterize bone formation at the ultrastructural level in more detail. Mice (n = 4–8) were anesthetized and scanned at an isotropic voxel resolution of 18 μm with a 0.5 mm aluminum filter, a 50-kV X-ray tube voltage, a 200 μA tube electric current, and a 520-ms scanning exposure time. The 3-D images were reconstructed for analysis using a scale of 0–0.065 (NRecon version 1.6.1.7; Skyscan NV, Kontich, Belgium). The 3-D morphometric parameters were computed using the direct 3-D approach, including the lengths of the tibia, femur, epiphysis, and metaphysis plus diaphysis, and thicknesses of the cortical bone, growth plate, and primary spongiosa (in millimeter). The region of interest from the 3-D reconstruction images was obtained and analyzed using CTAn software (CT-Analyser version 1.20.3.0; Skyscan NV, Kontich, Belgium). To measure the tibia length, we determined the distance between the proximal end of the tibia and the most distal end of the medial malleolus. To measure the femur length, we calculated the distance between the proximal end of the femoral head and the most distal end of the condyle. The cortex thickness of the diaphysis was measured using a cross-sectional view of the 3-D reconstruction image for a 2-mm segment at the mid-diaphysis. The thicknesses of the growth plate and the primary spongiosa were reported as the mean values measured from 30 sites in the mid-coronal section of each proximal tibia.

Safranin O/Fast Green Staining for the Observation of Growth Plate Histology

Sulfated glycosaminoglycan was stained with Safranin O/Fast Green (1% Safranin-O counter-stained with 0.75% hematoxylin and 1% Fast Green; Sigma-Aldrich, St Louis, MO, United States). The histological measurements (tissue section, n = 8) were performed at the central three-fourths of the growth plate sections using the Image J software (National Institutes of Health, Bethesda, MD, United States). The average cell numbers were calculated from three independent visual fields per growth plate. The average heights of the growth plate, resting zone, proliferative zone, and hypertrophic zone were the mean values measured from 15 sites in each growth plate.

Immunohistochemistry for Detecting Protein Expression in Growth Plate Cartilage

The fixed sections of the tibia, rib, and uterus were pretreated with the antigen retrieval solution suppressing all endogenous peroxidase activity and incubated with primary antibodies at 4°C overnight (n = 5). The following antibodies were used in this study: GPER-1 (Santa Cruz Biotechnology, Dallas, TX, United States), estrogen receptor-alpha (ERα) (Santa Cruz Biotechnology), type II collagen (Abcam, Cambridge, MA, United States), type X collagen (St John's laboratory, London, United Kingdom), proliferating cell nuclear antigen (PCNA) (Abcam), and Ki67 (Millipore, Burlington, MA, United States). Peroxidase-conjugated anti-mouse or anti-rabbit antibodies (Santa Cruz Biotechnology) were used as the secondary antibody and were visualized by 3,3′-diaminobenzidine staining. The tissues were stained with hematoxylin (Sigma-Aldrich, St Louis, MO, United States) to visualize the nuclei, and the images were observed and photographed using a microscope (Nikon, Japan). Immunohistochemistry (IHC) measurements were performed at the central three-fourths of the growth plate sections using the Image J software (National Institutes of Health, Bethesda, MD, United States). The number of 3,3′-diaminobenzidine-positive cells was calculated from three independent visual fields per growth plate. The thicknesses of the type X collagen-stained hypertrophic zone were the mean values measured from 15 sites on each growth plate.

Bromodeoxyuridine Assay to Assess Cell Proliferation in Cultured Epiphyseal Cartilage

G1 is a specific agonist, whereas G15 is a specific antagonist of GPER-1, both of which have no effect on classic ERs (Bologa et al., 2006; Dennis et al., 2009). G-1 (881639-98-1; Cayman Chemical, MI, United States) and G-15 (1161002-05-6; Cayman Chemical) were dissolved in dimethyl sulfoxide as a stock solution. Four-day-old neonatal rats were killed, and their tibias were harvested (n = 5). The samples were washed three times with antibiotics to avoid contamination, and part of the epiphyseal cartilage was harvested. The samples were cultured in BGJb medium containing 10% charcoal-striped serum (100-ml fetal bovine

serum treated with 0.5-g charcoal and 0.052-g dextran T-70 for 2 h at 37°C and then centrifuged at 12,000 rpm for 10 min), and 0.5% antibiotics.

The cultured cartilages were divided randomly into the control, G-1, and G15 treatment groups ($n \geq 5$). Approximately 6 days after treatment, 10 μM bromodeoxyuridine (BrdU) labeling solution (Abcam) was added to each group, and the cultured cartilages were further incubated for 24 h at 37°C. After BrdU treatment for 24 h, the samples were harvested and fixed with 10% neutral buffered formalin. The cultured cartilages were decalcified in 10% formic acid and embedded in paraffin, and 5 μm-thick sections were prepared and processed according to the instructions provided in the BrdU IHC Kit (ab125306; Abcam, Cambridge, MA, United States). The number of BrdU-positive cells was counted from three independent visual fields per cultured epiphyseal cartilage using Image J software (National Institutes of Health, Bethesda, MD, United States).

Statistical Analyses

Each experimental group was repeated with at least five mice, and these data are expressed as the mean ± standard deviation. Statistical analyses were performed using the SPSS 20 (Chicago, IL, United States) software. Data were visualized using box plots with the median as represented by the SigmaPlot version 12 (San Jose, CA, United States) software. All data points are displayed. For comparisons between two groups, the *P*-values were calculated using either the paired or the unpaired two-tailed Student's *t*-tests. The one-way analysis of variance evaluated statistical significance, and multiple comparisons were performed using Scheffé's method for three-group statistical analyses. *P*-values <0.05 were considered statistically significant.

RESULTS

Age-Related Changes of G-Protein-Coupled Estrogen Receptor-1 and Estrogen Receptor-Alpha Expressions in Tibia Growth Plates

The distribution of the GPER-1 protein was detected on the sections of the tibial growth plates from the female mice. The immunoreactivity of GPER-1 in growth plate chondrocytes was detected in 2-, 4-, 8-, 12-, and 16-week-old mice (**Figure 1A**). In 2-week-old mice, the growth plate chondrocytes showed minimal GPER-1 expression. In early puberty, the GPER-1 expression was significantly increased in 4-week-old mice compared with that in 2-week-old mice. In the growth plate chondrocytes of 4- and 8-week-old mice, 68.69 ± 5.90% and 60.61 ± 14.45% of the cells were GPER-1 positive, respectively. During the end-puberty stage in 12-week-old mice, GPER-1 expression decreased to 37.2 ± 5.68%. After sexual maturation in 16-week-old mice, the values decreased to less than 10%. The quantitative analysis of GPER-1-positive cells showed an age-related variation in the tibial growth plate of mice (**Figure 1B**).

Developmental changes in ERα expression were also observed in the tibia of female mice. In 2-week-old mice, minimal ERα expression was observed in the growth plate chondrocytes. During puberty, abundant cellular staining of ERα was observed in the growth plate (**Figure 1C**). ERα immunoreactivity was detected in the resting, proliferative, and hypertrophic chondrocytes of 4- to 16-week-old mice. However, ERα expression did not show significant age-related variation in these mice (**Figure 1D**).

Generation of the Chondrocyte-Specific *G-Protein-Coupled Estrogen Receptor-1* Knockout (CKO) Mice

To elucidate GPER-1-mediated chondrocyte functions, we generated a CKO mouse model with a floxed exon 3 at the *GPER-1* locus, which is the only coding exon of the *GPER-1* gene (**Figure 2A**). In the CKO mice, Cre was expressed only in chondrocytes, which expressed type II collagen. Genotyping was performed by PCR using tail genomic DNA (**Figure 2B**). Both the control and CKO groups had *GPER-1* floxed alleles (507 bp). Only CKO mice expressed Cre recombinase under the type II collagen-specific promoter (420 bp). There was no change in the serum estrogen levels between the control and CKO mice (**Figure 2C**). Furthermore, ERα expression in the tibia growth plates showed no significant difference between the control and CKO mice as verified *via* IHC staining (**Figure 2D**).

Chondrocyte-specific GPER-1 knockout mice had a reduced GPER-1 protein expression in chondrocytes but not in the cortical bone tissue or the uterus (**Figure 2E**). IHC of the growth plate cartilage, articular cartilage, and costal cartilage demonstrated GPER-1 immunoreactivity in type II collagen-positive cells in control mice, which were almost completely abolished in CKO mice. In the growth plate cartilage, the number of GPER-1 positive cells decreased by approximately 82% in CKO mice.

Phenotypical Changes in the Body Weight, Length, Bone Length, and Cortical Bone Thickness in Chondrocyte-Specific G-Protein-Coupled Estrogen Receptor-1 Knockout Mice

The CKO mice exhibited a short body phenotype compared with the control mice (**Figure 3A**). The CKO mice had decreased body weight (**Figure 3B**) as well as shorter body length (crown–rump length) at 4 and 8 weeks than the control mice (**Figure 3C**). The femoral length of CKO mice decreased by 2.84%, and the tibial length decreased by 2.32% in 8-week-old mice compared with that in the control mice, as determined *via* μ-CT analysis (**Figures 3D,E**). The cortex thickness was analyzed in the middle of the diaphysis, and there was no difference between the CKO and control mice (**Figures 3F,G**).

These findings indicated that the reduced body weight might be associated with a reduction in bone growth because both the axial and appendicular skeletons were significantly shortened in the 8-week-old CKO mice. The chondrocyte-specific GPER-1 deficiency may regulate endochondral ossification rather than

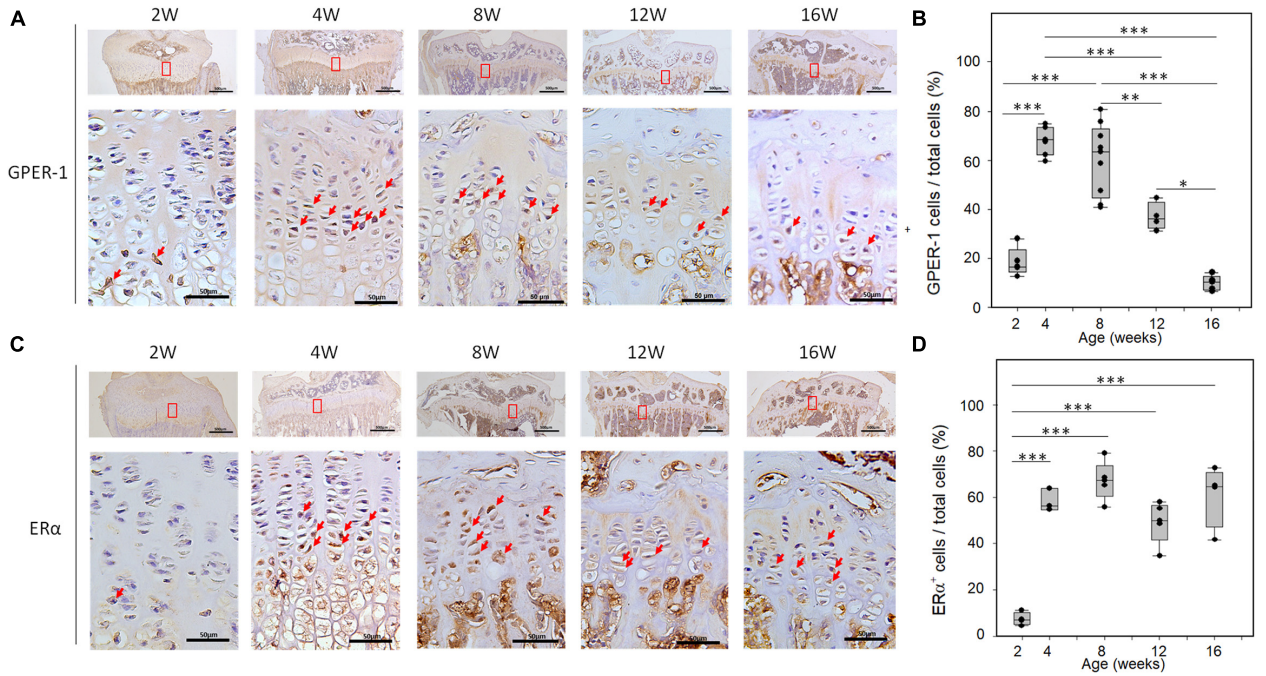

FIGURE 1 | Age-related changes of GPER-1 and ERα levels in tibia growth plates as determined *via* IHC staining. **(A,C)** Growth plate cartilage of tibias from 2-, 4-, 8-, 12-, and 16-week-old mice were stained for GPER-1 and ERα. Representative micrographs of growth plates at low (scale bars, 500 μm) and high (scale bars, 50 μm) magnification. **(B,D)** Image-J analysis of percentage of GPER-1- and Erα-positive cells from total number of hematoxylin-stained cells (total cells). Each group, $N = 5$. $^{*}P < 0.05$, $^{**}P < 0.01$, $^{***}P < 0.001$.

intramembranous ossification, as there were skeletal changes in bone length rather than cortical bone thickness.

Changes of Growth Plate Development in the Chondrocyte-Specific G-Protein-Coupled Estrogen Receptor-1 Knockout Mice

To analyze the effects of GPER-1 deficiency on tibial growth plate morphology, Safranin O/Fast Green staining for glycosaminoglycan was performed, which showed the structure of the growth plate in 8-week-old mice (**Figure 4A**). Histological analyses demonstrated that the cell numbers of growth plate were significantly decreased in the CKO mice compared with those in the control mice (**Figure 4B**). Morphometric analyses showed that the resting zones of the growth plate in the knockout mice had a similar size as seen in the control mice. In contrast, the thickness of the proliferative zones was decreased, and the hypertrophic zones were increased in the *GPER-1* knockout mice compared with those in the control mice (**Figure 4C**).

Histological analysis of type X collagen staining in the tibial growth plate cartilage showed a greater type X collagen distribution in the CKO mice compared with the control group (**Figure 4D**). We analyzed the hypertrophic region of the growth plate with the type X collagen expressed in the territorial matrix of hypertrophic chondrocytes. Morphometric analyses showed that GPER-1 deficiency increased the hypertrophic zone thickness (**Figure 4E**).

Hypertrophic chondrocytes are replaced by bone *via* apoptosis and remodel the metaphysis of the growing bone. The area containing a basophilic core of mineralized cartilage spicules and early ossification is termed the primary spongiosa. In 4-week-old mice, there was no significant difference in growth plate thickness between the control and knockout mice as determined *via* μ-CT analysis, but the thickness of the primary spongiosa was significantly reduced in CKO mice (**Figure 4F**). The epiphysis length showed no significant change between the control and CKO mice, but the lengths of the metaphysis plus diaphysis were significantly reduced in the 8-week-old CKO mice compared with that in the control (**Figure 4G**). These data indicated that the reduced bone length might be associated with a reduction in endochondral ossification because the primary spongiosa thickness and the lengths of metaphysis plus diaphysis were significantly reduced rather than that of the epiphysis.

Effects of Chondrocyte-Specific G-Protein-Coupled Estrogen Receptor-1 Deficiency on the Chondrocyte Proliferation at Tibia Growth Plates

To confirm whether the decreased growth plate thickness was due to suppressing chondrocyte proliferation in CKO mice, IHC analysis of PCNA and Ki67 was performed (**Figure 5**). The number of PCNA-positive cells per total cell in the growth plate was significantly reduced by GPER-1 deficiency in 4- and 8-week-old mice (**Figure 5A**). In 8-week-old mice, the number of

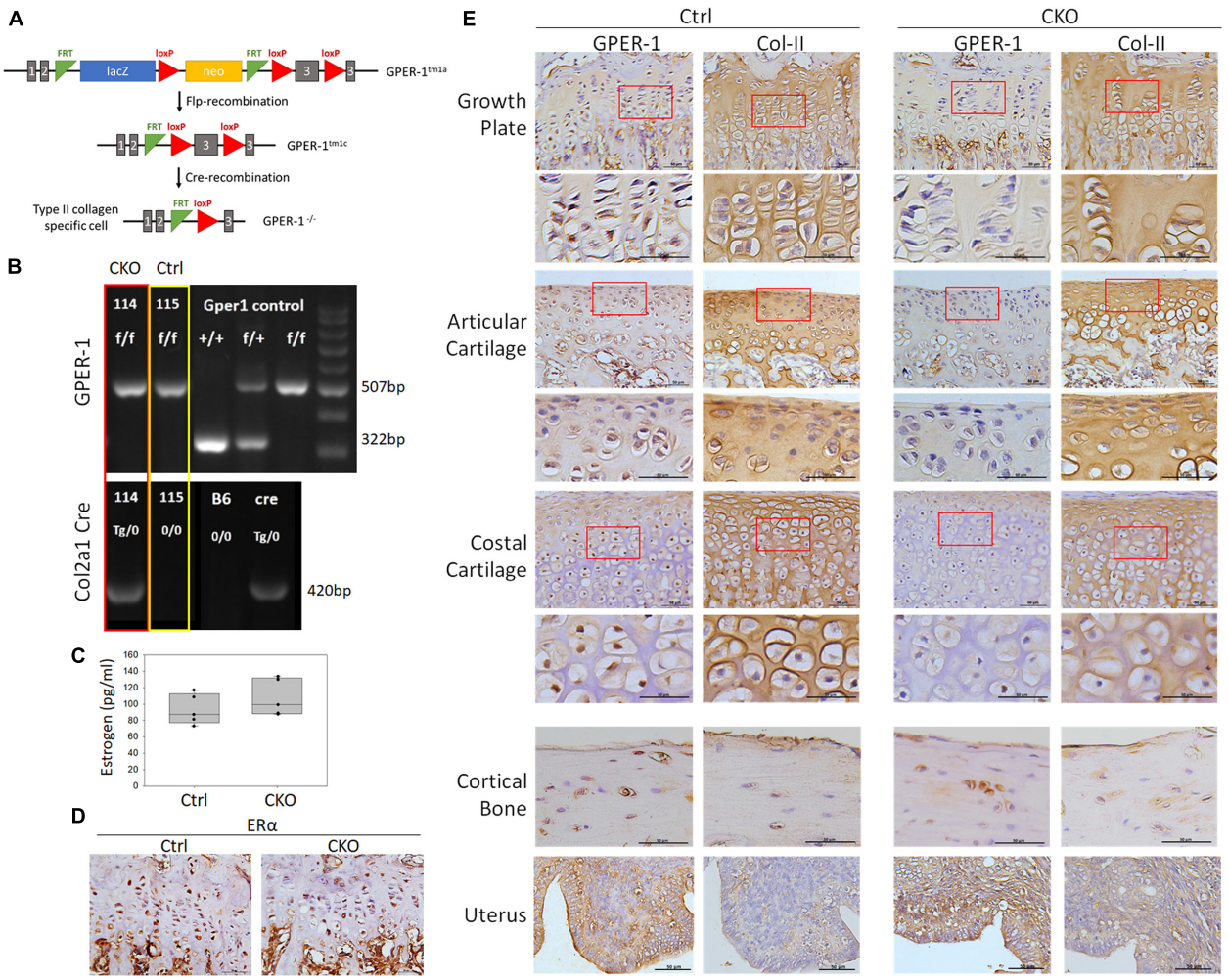

FIGURE 2 | Generation of chondrocyte-specific GPER-1 knockout (CKO) mice using Cre/loxP system. **(A)** Schematic diagram of producing *Col2a1-Cre*; *GPER-1*$^{f/f}$ mice. **(B)** Genotyping of *Col2a1-Cre* and *GPER-1* in control (Ctrl) and CKO mice. Genotyping of GPER-1 floxed allele amplified a 507-bp fragment, whereas GPER-1 wild-type allele produced a 322-bp fragment. *Col2a1-Cre* transgene produced a 420-bp fragment. Each group, *N* = 28–34. **(C)** Serum levels of estrogen showed no significant difference with GPER-1 deficiency. **(D)** IHC staining of ERα in tibia growth plates showed no significant difference between two groups. Scale bars, 50 μm. **(E)** GPER-1 and type II collagen (Col-II) were stained by IHC staining and analyzed in tibia growth plate, articular cartilage, costal cartilage, cortical bone, and uterus. Representative micrographs of growth plates at low and high magnification. Scale bars, 50 μm. Each group, *N* = 3–5.

Ki-67-positive cells also decreased in the CKO mice compared with that in the control group (**Figure 5B**). These data indicated that GPER-1 deficiency could reduce proliferative zone thickness and cell number which might be associated with the inhibition of chondrocyte proliferation.

Effects of G-Protein-Coupled Estrogen Receptor-1 Agonist and Antagonist Treatment on Chondrocyte Proliferation in the Cultured Epiphyseal Cartilage

To analyze whether blocking GPER-1 expression reduces chondrocyte proliferation in cultured epiphyseal cartilage of tibias, we treated the epiphyseal articular cartilages with the specific antagonist (G15) and agonist (G1) of GPER-1 (**Figure 6A**). The results revealed fewer BrdU-positive cells in the G15 treatment group and more BrdU-positive cells in the G1 treatment group compared with the control group (**Figures 6B,C**). These findings showed that GPER-1 antagonists reduced chondrocyte proliferation in cultured articular cartilages. On the other hand, GPER-1 promoted chondrocyte proliferation.

DISCUSSION

This study is the first to investigate the role of GPER-1 in growth plate chondrocytes and its subsequent effect on bone growth at puberty using a tissue-specific *GPER-1* knockout mouse model. We originally demonstrated that GPER-1 deficiency results in reducing the chondrocyte proliferation, cell number, and thickness of proliferation zone in the growth plates of tibias in pubertal female mice. The reduction in the lengths of primary

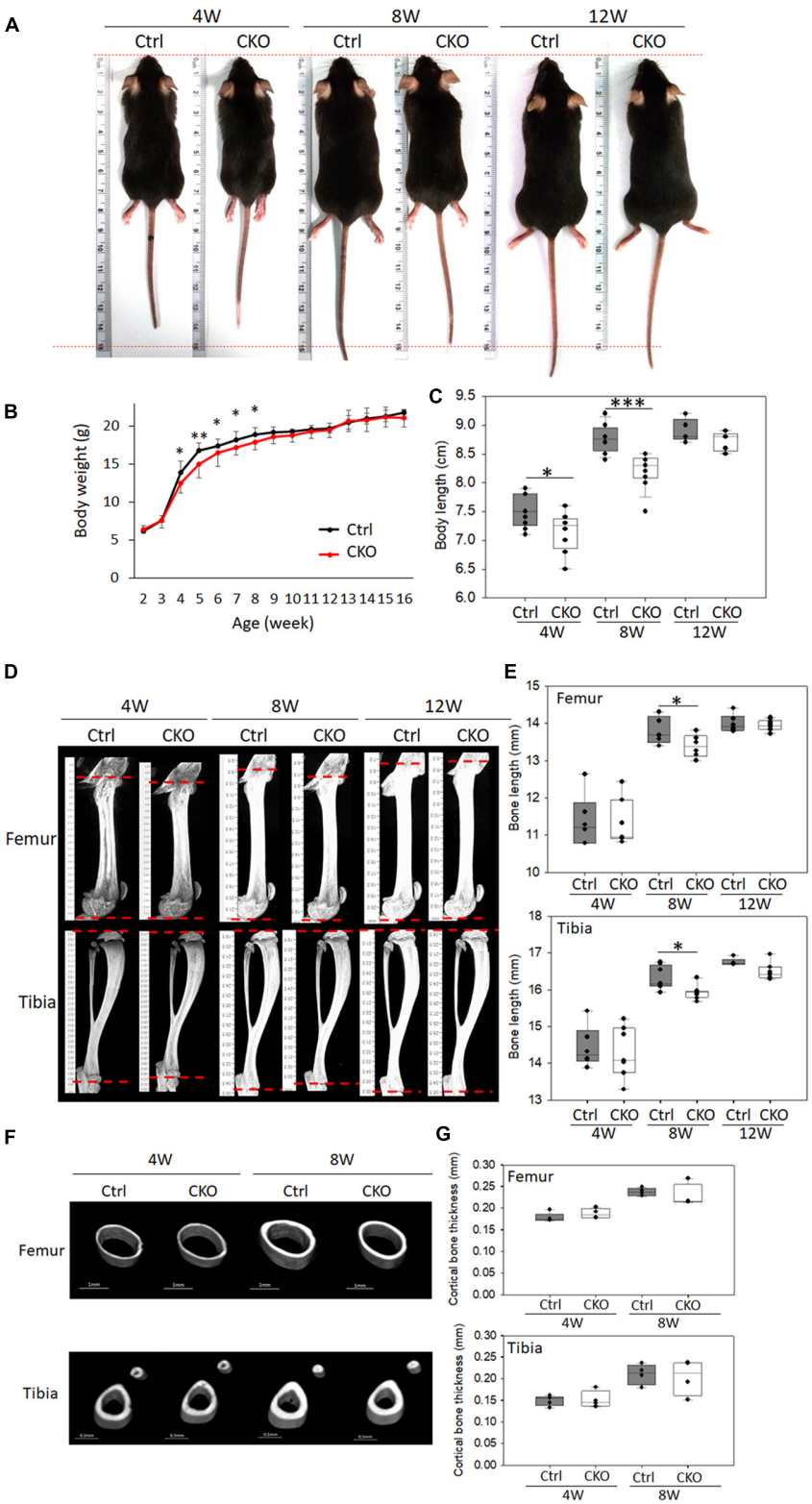

FIGURE 3 | Comparison of phenotypes between chondrocyte-specific GPER-1 knockout mice (CKO) and control mice (Ctrl). **(A)** General appearance of 4-, 8-, and 12-week-old female mice. **(B)** Body weight of CKO and Ctrl mice. **(C)** Body length (crown–rump length) of CKO and Ctrl mice. **(D,E)** Femur and tibia μ-CT images and length quantitation in 4-, 8-, and 12-week-old CKO and Ctrl mice. **(F,G)** Cortical bone thicknesses were analyzed *via* μ-CT. Each group, $N = 6–8$. $^{*}P < 0.05$, $^{**}P < 0.01$, $^{***}P < 0.001$.

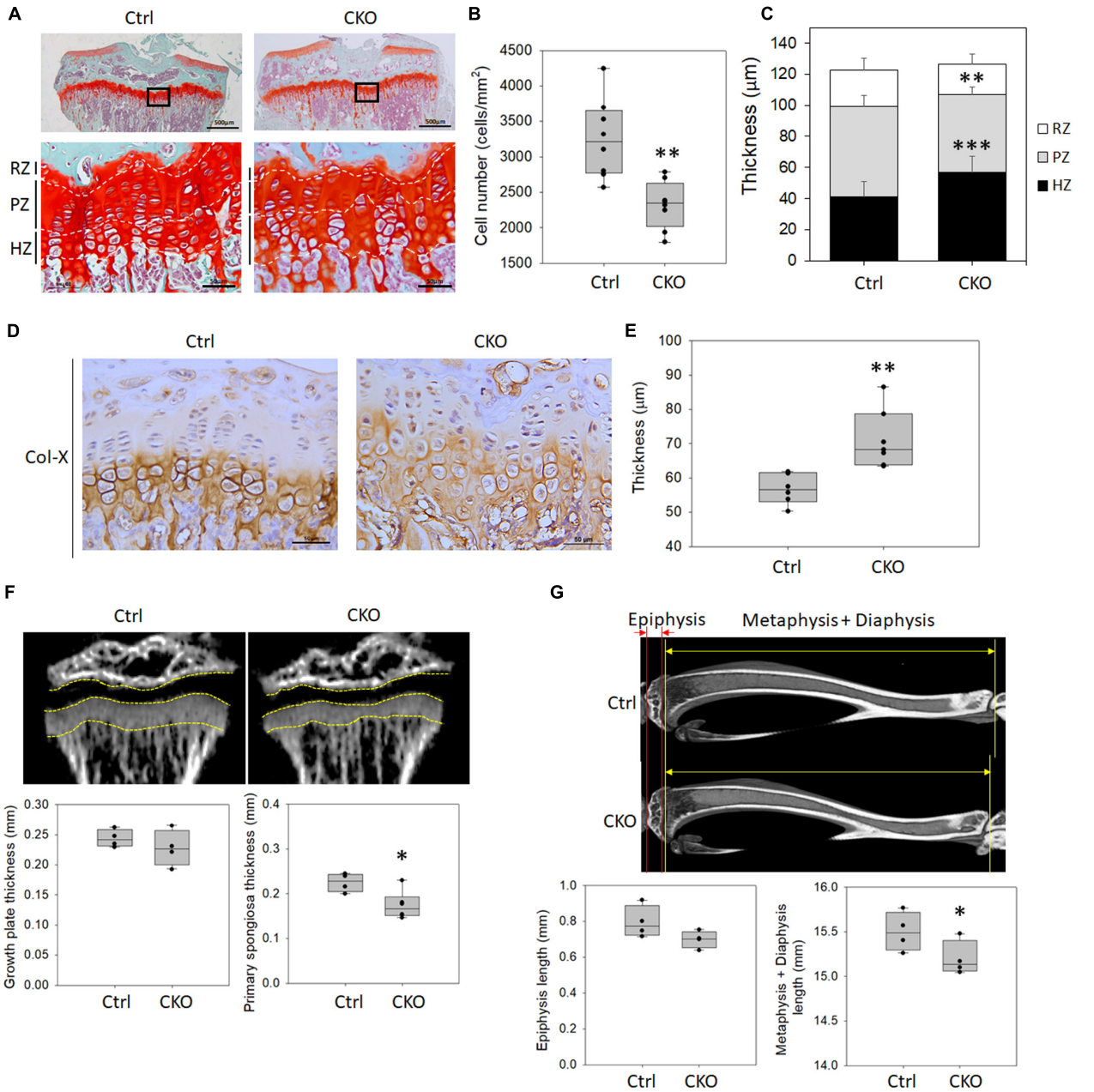

FIGURE 4 | Changes of growth plate development in chondrocyte-specific GPER-1 knockout (CKO) mice. **(A)** Tibial growth plates of 8-week-old female mice were stained with Safranin O/Fast Green staining. Representative micrographs of growth plates at low (scale bars, 500 μm) and high (scale bars, 50 μm) magnification. **(B)** Cell numbers were measured in CKO mice. **(C)** Thicknesses of resting zone, proliferation zone, and hyperopic zone were analyzed. **(D)** Hypertrophic zones of growth plates were stained *via* IHC to detect type X collagen (Col-X) in 8-week-old mice. Scale bars, 50 μm. **(E)** Thicknesses of type X collagen-stained hypertrophic zone were quantified. **(F)** Thicknesses of growth plate and primary spongiosa of 4-week-old mice were measured by μ-CT analysis. **(G)** Lengths of epiphysis and metaphysis plus diaphysis of 8-week-old mice were measured by μ-CT analysis. Each group, $N = 4–8$. $^{*}P < 0.05$, $^{**}P < 0.01$, $^{***}P < 0.001$. RZ: resting zone, PZ: proliferative zone, HZ: hypertrophic zone.

spongiosa, metaphysis, and diaphysis was also found in the tibias of CKO mice. Estrogen is known to be an important hormone in regulating long bone elongation during puberty. Circulatory levels of estrogen were thought to be a key factor in determining the growth and closure of the growth plate (Grumbach, 2004), however, the ERs that mediate this event remain unclear. In this study, our histological analysis found that the peak level of GPER-1 in growth plates was at early puberty, and then, it declined by age to extremely low levels at sexual maturation in the control mice. On the other hand, we also found that ERα expression has a marked increase at early puberty and is maintained until sexual maturation in female mice. This indicated that the existence

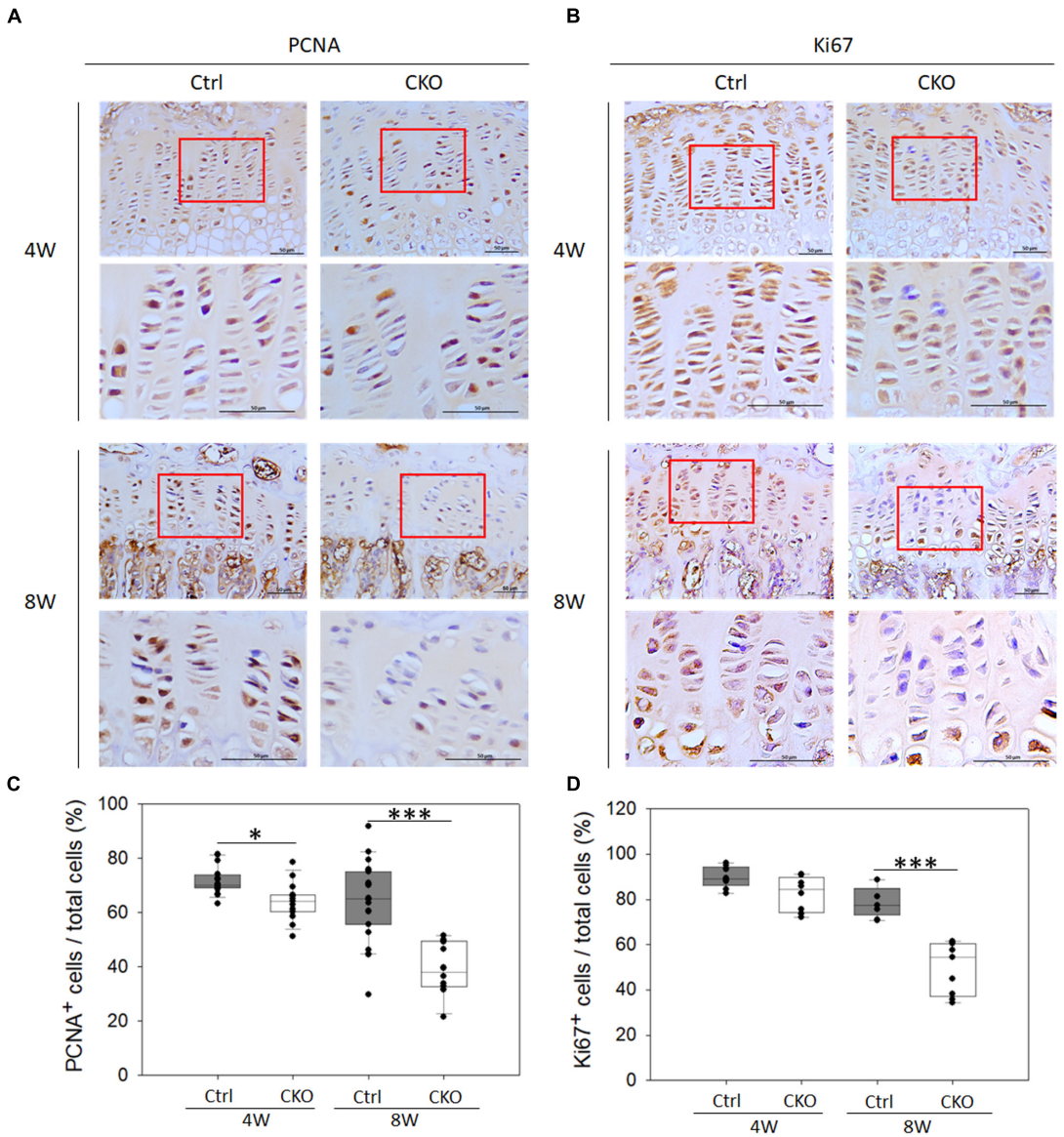

FIGURE 5 | Effects of chondrocyte-specific GPER-1 knockout (CKO) on chondrocyte proliferation in tibia growth plates. **(A,B)** IHC staining of PCNA and Ki67 in tibial growth plates in 4- and 8-week-old female mice. Representative micrographs of growth plates at low and high magnification. Scale bars, 50 μm. **(C,D)** Quantification of ratio of proliferative cells to total cells was shown as ratio of PCNA- and Ki67-positive cells to hematoxylin-stained cells (total cells). Each group, $N = 5$. $^{*}P < 0.05$, $^{***}P < 0.001$.

and amount of GPER-1 might play a role in mediating estrogen signals to regulate chondrocyte proliferation and subsequent bone elongation during pubertal bone growth.

According to previous reports, the 2-, 4-, 8-, 12-, and 16-week-old mice represent the stages of early life, early-puberty, puberty, end-puberty, and post-puberty, respectively (van der Eerden et al., 2000; Li et al., 2012; Bell, 2018). In this study, we found that the percentage of GPER-1-positive cells in growth plates increased from the age of 2 to 4 weeks in mice but declined gradually to extremely low levels until the age of 16 weeks (from 60.61 to 9.47%). On the other hand, unlike the huge change in GPER-1, the percentage of ERα-positive cells in growth plates showed no significant change during puberty (from 4 to 16 weeks old). Other studies had also indicated that the expression of ERα protein in the growth plate did not significantly decline during sexual maturation in rats (van der Eerden et al., 2002; Li et al., 2012). In the human growth plates, ERα distribution and the percentage of Erα-positive cells showed no significant changes from childhood to adolescence (Egerbacher et al., 2002; Nilsson et al., 2003). Previous reports and the findings from this study indicate that GPER-1 might be involved in the modulation of bone growth at puberty rather than post-puberty. The most important event of pubertal bone growth should be the growth plate-involved bone elongation, in which chondrocytes play the

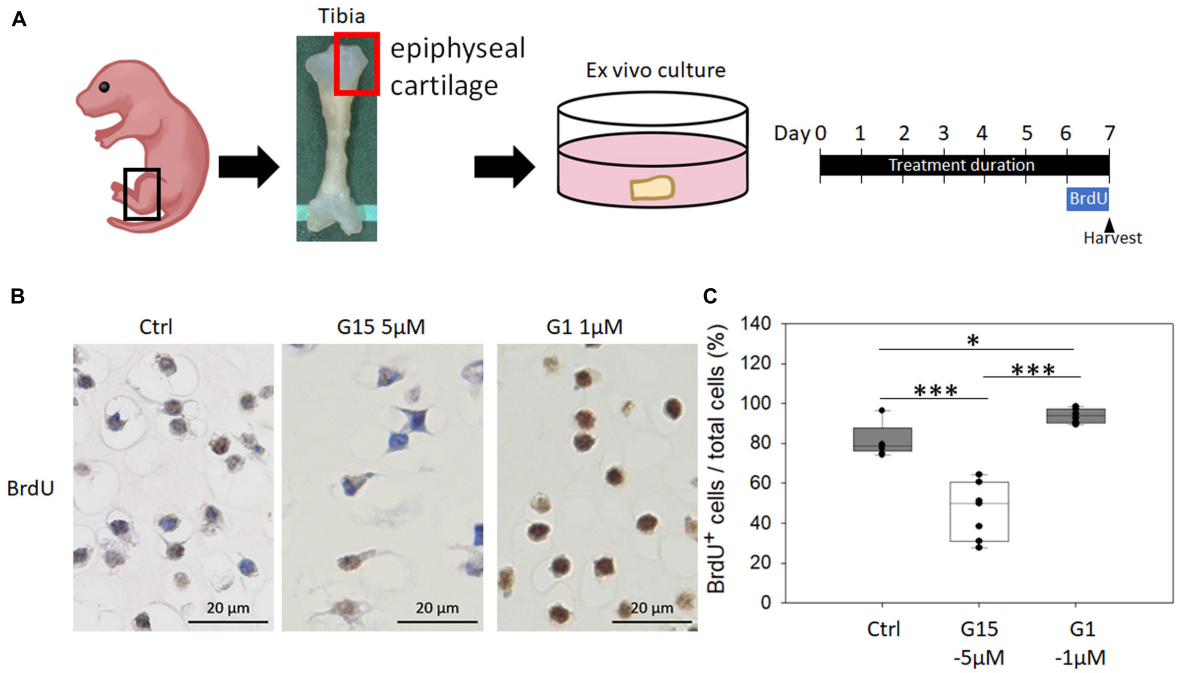

FIGURE 6 | Effects of GPER-1 agonist and antagonist treatment on chondrocyte proliferation in cultured epiphyseal cartilage. **(A)** Graphical depiction of procedures described using *ex vivo* epiphyseal cartilage. **(B,C)** Antagonist (G15) and agonist (G1) of GPER-1 were used to testing effect of GPER-1 mediation on cell proliferation by measuring number of BrdU-positive chondrocytes. Scale bars, 20 μm. Each group, $N = 5$. $^{*}P < 0.05$, $^{***}P < 0.001$.

most important role. Therefore, we used the CKO mice to study the role of GPER-1 in growth plate chondrocytes without affecting other cells in bones.

In this study, we generated novel CKO mice with floxed exon 3 of the *GPER-1* locus and the knockout of *GPER-1* in type II collagen-expressing tissue, resulting in chondrocyte-specific knockout (**Figure 2A**). We confirmed that GPER-1 was deficient in tissues expressing type II collagen, including the tibia growth plate, articular cartilage, and costal cartilage, in CKO mice (**Figure 2E**). Serum estrogen levels exhibited no difference between the CKO and control mice, which is similar to that found in female global *GPER-1* knockout mice in a previous study (Martensson et al., 2009). There have been several reports on the interaction between GPER-1 and nuclear ERs (Kang et al., 2010; Smith et al., 2016; Romano and Gorelick, 2018). A study indicated that GPER-1 might crosstalk with other ERs (Romano and Gorelick, 2018). Other studies on different cell lines found that a selective GPER-1 agonist inhibits nuclear ERs activity in human breast cancer cells (MCF-7) (Smith et al., 2016), whereas it was indicated to upregulate ERα expression in human breast cancer cells (SK-BR-3), human embryonic kidney cells (HEK293), and monkey kidney cells (COS7) (Kang et al., 2010). In this study, the ERα level in growth plate cartilages of CKO mice showed no difference between the control mice. This result indicates that the CKO system generated in this study specifically knocks out GPER-1 but is not interrupted by the estrogen ligand or the ERα crosstalk.

Longitudinal bone growth is through the process of endochondral bone formation. During this process, the growth plate chondrocytes undergo proliferation, hypertrophy, and eventually apoptosis. In this study, we found a decrease in the number of proliferative chondrocytes, length of proliferation zone of the growth plate, and length of the tibia in CKO mice. A previous study, using a global *GPER-1* knockout model with a deletion of a whole *GPER-1* open-reading frame, found that the lengths of femur and crown–rump were decreased in the female mice (Martensson et al., 2009). In contrast, a study on full *GPER-1* knockout male mice showed increased body length, bone mineral density, trabecular bone volume, and cortical bone thickness (Ford et al., 2011). These results indicated that a sexually dimorphic effect of GPER-1 might occur in global knockout mice. Additionally, in the global GPER-1 knockout model, systemic effects cannot be excluded, such as increased fat mass (Haas et al., 2009), increased blood pressure, and impaired glucose tolerance (Martensson et al., 2009). On the other hand, the tissue-specific GPER-1 knockout model can reduce the complexity of systemic interactions. In this study, using our CKO model, we demonstrated that CKO mice did not only have decreased bone length but also have decreased the number of Ki67- and PCNA-positive proliferative chondrocytes in the growth plate of 8-week-old pubertal female mice. These results emphasized that GPER-1 plays a crucial role in promoting the proliferation of growth plate chondrocytes and contributes to bone elongation during pubertal bone growth.

The length of the long bone is determined by increasing not only the height but also the timing of growth plates closure. In this study, we found that the number of GPER-1-positive chondrocytes was significantly lower in the post-puberty

compared with the puberty stage, suggesting the bone elongation might terminate in adult mice. In contrast to the results found in the pubertal mice, we demonstrated that the bone lengths in femurs and tibia were shorter but not statistically different in the post-puberty (12-week-old) CKO mice compared with those in the control mice (**Figures 3D,E**). A previous study also indicated that estrogen treatment on the 12-week-old ovariectomized female *GPER*-1 knockout mice did not affect both the longitudinal skeletal growth and growth plate height (Windahl et al., 2009). Another report indicated that treatment of GPER-1 agonist on the 12-week-old ovariectomized female mice did not affect tibia and femur growth (Iravani et al., 2019). These two reports indicated that GPER-1 did not affect growth plate thickness in adult mice. Together with the results from these previous and current studies, the level change of GPER-1 expression may determine bone elongation rather than that of receptor ligands, such as estrogen and GPER-1 agonist.

Although estrogen and its receptors are involved in bone growth, the physiological regulation of bone growth and remodeling at any stage in life is dynamic and complicated. In previous GPER-1 studies, some of the conflicting results for bone growth might be because of differences in age, sex, and genetic backgrounds of the various animal models (Martensson et al., 2009; Ford et al., 2011). Furthermore, hormone regulation of longitudinal bone growth through endochondral ossification is also complicated. In addition to estrogen, longitudinal bone growth is also regulated by the growth hormone and thyroid hormone (Nilsson et al., 1994). Because both ERα and GPER-1 are expressed in growth plate chondrocytes, it is difficult to distinguish the effect *via* ERα, ERβ, or GPER-1 using the natural ligand estradiol. Therefore, we performed an *ex vivo* study to investigate the influence of GPER-1 on the cultured epiphyseal cartilage from the tibia upon treatment with a GPER-1-specific agonist (G1) and antagonist (G15). The results revealed that G1 significantly enhanced chondrocyte proliferation, whereas G15 showed an inhibitory effect. These findings are consistent with those of a recent study demonstrating the role of GPER-1 in increasing chondrocyte proliferation (Fan et al., 2018). Furthermore, an *ex vivo* study, which excluded the effects of complicated systemic factors, revealed that GPER-1 directly promotes chondrocyte proliferation, further confirming the *in vivo* findings.

The limitation of this study is the lack of investigation regarding the underlying molecular mechanisms at the cellular level. In our previous study, GPER-1 was found to mediate bone marrow-derived mesenchymal stem cell proliferation *via* the cyclic adenosine 3′,5′-monophosphate/protein kinase A/phosphorylation of cyclic adenosine 3′,5′-monophosphate-response element-binding protein pathway upon treatment with a GPER-1 agonist (Chuang et al., 2020). Another study indicated that the GPER-1 agonist activated the phosphoinositide 3-kinase/Akt signaling pathway in the ATDC5 cell line (Fan et al., 2018), however, it failed to induce Akt or ERK1/2 phosphorylation in human adult articular chondrocytes (Ribeiro et al., 2020). These studies showed that different GPER-1 mediated signal pathways might occur in different types of cells. Accordingly, the intracellular regulatory mechanism of GPER-1 in grow plate chondrocytes is also worth investigating. In conclusion, chondrocyte-specific *GPER-1* knockout in female mice and subsequent treatment with a specific GPER-1 agonist or antagonist on the implant culture of epiphytical cartilage showed that GPER-1 plays an important role in facilitating the elongation of long bone by enhancing the growth plate chondrocyte proliferation in female pubertal mice.

DATA AVAILABILITY STATEMENT

The original contributions presented in the study are included in the article/**Supplementary Material**, further inquiries can be directed to the corresponding author/s.

ETHICS STATEMENT

The animal study was reviewed and approved by Kaohsiung Medical University Animal Care and Use Committee (104166 and 107157).

AUTHOR CONTRIBUTIONS

All authors listed have made a substantial, direct and intellectual contribution to the work, and approved it for publication.

FUNDING

This study was supported by grants from the Ministry of Science and Technology of Taiwan (107-2314-B-037-002 and 108-2314-B-037-058). We appreciate the support from members of the Orthopedic Research Center and the Regenerative Medicine and Cell Therapy Research Center (KMU-TC108A02), Kaohsiung Medical University.

SUPPLEMENTARY MATERIAL

The Supplementary Material for this article can be found online at: https://www.frontiersin.org/articles/10.3389/fcell.2021.710664/full#supplementary-material

REFERENCES

Almeida, M., Laurent, M. R., Dubois, V., Claessens, F., O'Brien, C. A., Bouillon, R., et al. (2017). Estrogens and androgens in skeletal physiology and pathophysiology. *Physiol. Rev.* 97, 135–187. doi: 10.1152/physrev.00033.2015

Bell, M. R. (2018). Comparing postnatal development of gonadal hormones and associated social behaviors in rats, mice, and humans. *Endocrinology* 159, 2596–2613. doi: 10.1210/en.2018-00220

Bologa, C. G., Revankar, C. M., Young, S. M., Edwards, B. S., Arterburn, J. B., Kiselyov, A. S., et al. (2006). Virtual and biomolecular screening converge

on a selective agonist for GPR30. *Nat. Chem. Biol.* 2, 207–212. doi: 10.1038/nchembio775

Chagin, A. S., and Savendahl, L. (2007a). Estrogens and growth: review. *Pediatr. Endocrinol. Rev.* 4, 329–334.

Chagin, A. S., and Savendahl, L. (2007b). GPR30 estrogen receptor expression in the growth plate declines as puberty progresses. *J. Clin. Endocrinol. Metab.* 92, 4873–4877. doi: 10.1210/jc.2007-0814

Chuang, S. C., Chen, C. H., Chou, Y. S., Ho, M. L., and Chang, J. K. (2020). G protein-coupled estrogen receptor mediates cell proliferation through the cAMP/PKA/CREB pathway in murine bone marrow mesenchymal stem cells. *Int. J. Mol. Sci.* 21:6490. doi: 10.3390/ijms21186490

Dennis, M. K., Burai, R., Ramesh, C., Petrie, W. K., Alcon, S. N., Nayak, T. K., et al. (2009). In vivo effects of a GPR30 antagonist. *Nat. Chem. Biol.* 5, 421–427. doi: 10.1038/nchembio.168

Egerbacher, M., Helmreich, M., Rossmanith, W., and Haeusler, G. (2002). Estrogen receptor-alpha and estrogen receptor-beta are present in the human growth plate in childhood and adolescence, in identical distribution. *Horm. Res.* 58, 99–103. doi: 10.1159/000064661

Fan, D. X., Yang, X. H., Li, Y. N., and Guo, L. (2018). 17beta-estradiol on the expression of G-protein coupled estrogen receptor (GPER/GPR30) mitophagy, and the PI3K/Akt signaling pathway in ATDC5 chondrocytes in vitro. *Med. Sci. Monit.* 24, 1936–1947. doi: 10.12659/msm.909365

Ford, J., Hajibeigi, A., Long, M., Hahner, L., Gore, C., Hsieh, J. T., et al. (2011). GPR30 deficiency causes increased bone mass, mineralization, and growth plate proliferative activity in male mice. *J. Bone Miner. Res.* 26, 298–307. doi: 10.1002/jbmr.209

Gao, F., Ma, X., Ostmann, A. B., and Das, S. K. (2011). GPR30 activation opposes estrogen-dependent uterine growth via inhibition of stromal ERK1/2 and estrogen receptor alpha (ERalpha) phosphorylation signals. *Endocrinology* 152, 1434–1447. doi: 10.1210/en.2010-1368

Grumbach, M. M. (2004). Mutations in the synthesis and action of estrogen: the critical role in the male of estrogen on pubertal growth, skeletal maturation, and bone mass. *Ann. N. Y. Acad. Sci.* 1038, 7–13. doi: 10.1196/annals.1315.008

Haas, E., Bhattacharya, I., Brailoiu, E., Damjanovic, M., Brailoiu, G. C., Gao, X., et al. (2009). Regulatory role of G protein-coupled estrogen receptor for vascular function and obesity. *Circ. Res.* 104, 288–291. doi: 10.1161/CIRCRESAHA.108.190892

Hazell, G. G., Yao, S. T., Roper, J. A., Prossnitz, E. R., O'Carroll, A. M., and Lolait, S. J. (2009). Localisation of GPR30, a novel G protein-coupled oestrogen receptor, suggests multiple functions in rodent brain and peripheral tissues. *J. Endocrinol.* 202, 223–236. doi: 10.1677/JOE-09-0066

Heino, T. J., Chagin, A. S., and Savendahl, L. (2008). The novel estrogen receptor G-protein-coupled receptor 30 is expressed in human bone. *J. Endocrinol.* 197, R1–R6. doi: 10.1677/JOE-07-0629

Iravani, M., Lagerquist, M. K., Karimian, E., Chagin, A. S., Ohlsson, C., and Savendahl, L. (2019). Effects of the selective GPER1 agonist G1 on bone growth. *Endocr. Connect.* 8, 1302–1309. doi: 10.1530/EC-19-0274

Kang, L., Zhang, X., Xie, Y., Tu, Y., Wang, D., Liu, Z., et al. (2010). Involvement of estrogen receptor variant ER-alpha36, not GPR30, in nongenomic estrogen signaling. *Mol. Endocrinol.* 24, 709–721. doi: 10.1210/me.2009-0317

Flurkey, K., Currer, J. M., and Harrison, D. E. (2007). *The Mouse in Biomedical Research. Mouse Models in Aging Research*, 2nd Edn, Vol. 3, Chap. 20. Cambridge: Academic Press, 637–672. doi: 10.1016/B978-012369454-6/50074-1

Kumar, R., Balhuizen, A., Amisten, S., Lundquist, I., and Salehi, A. (2011). Insulinotropic and antidiabetic effects of 17beta-estradiol and the GPR30 agonist G-1 on human pancreatic islets. *Endocrinology* 152, 2568–2579. doi: 10.1210/en.2010-1361

Li, X. F., Wang, S. J., Jiang, L. S., and Dai, L. Y. (2012). Gender- and region-specific variations of estrogen receptor alpha and beta expression in the growth plate of spine and limb during development and adulthood. *Histochem. Cell Biol.* 137, 79–95. doi: 10.1007/s00418-011-0877-0

Liu, S., Le May, C., Wong, W. P., Ward, R. D., Clegg, D. J., Marcelli, M., et al. (2009). Importance of extranuclear estrogen receptor-alpha and membrane G protein-coupled estrogen receptor in pancreatic islet survival. *Diabetes* 58, 2292–2302. doi: 10.2337/db09-0257

Martensson, U. E., Salehi, S. A., Windahl, S., Gomez, M. F., Sward, K., Daszkiewicz-Nilsson, J., et al. (2009). Deletion of the G protein-coupled receptor 30 impairs glucose tolerance, reduces bone growth, increases blood pressure, and eliminates estradiol-stimulated insulin release in female mice. *Endocrinology* 150, 687–698. doi: 10.1210/en.2008-0623

Nilsson, A., Ohlsson, C., Isaksson, O. G., Lindahl, A., and Isgaard, J. (1994). Hormonal regulation of longitudinal bone growth. *Eur. J. Clin. Nutr.* 48 Suppl 1, S150–S158. doi: 10.1007/BF02558817 discussion S158-160,

Nilsson, O., Chrysis, D., Pajulo, O., Boman, A., Holst, M., Rubinstein, J., et al. (2003). Localization of estrogen receptors-alpha and -beta and androgen receptor in the human growth plate at different pubertal stages. *J. Endocrinol.* 177, 319–326. doi: 10.1677/joe.0.1770319

Ovchinnikov, D. A., Deng, J. M., Ogunrinu, G., and Behringer, R. R. (2000). Col2a1-directed expression of Cre recombinase in differentiating chondrocytes in transgenic mice. *Genesis* 26, 145–146. doi: 10.1002/(sici)1526-968x(200002)26:2<145::aid-gene14>3.0.co;2-c

Patel, V. H., Chen, J., Ramanjaneya, M., Karteris, E., Zachariades, E., Thomas, P., et al. (2010). G-protein coupled estrogen receptor 1 expression in rat and human heart: protective role during ischaemic stress. *Int. J. Mol. Med.* 26, 193–199. doi: 10.3892/ijmm_00000452

Revankar, C. M., Cimino, D. F., Sklar, L. A., Arterburn, J. B., and Prossnitz, E. R. (2005). A transmembrane intracellular estrogen receptor mediates rapid cell signaling. *Science* 307, 1625–1630. doi: 10.1126/science.1106943

Ribeiro, M., Sousa, C., Rufino, A. T., Judas, F., and Mendes, A. F. (2020). Expression and function of the nonclassical estrogen receptor, GPR30, in human cartilage and chondrocytes. *J. Cell. Physiol.* 235, 8486–8494. doi: 10.1002/jcp.29691

Romano, S. N., and Gorelick, D. A. (2018). Crosstalk between nuclear and G protein-coupled estrogen receptors. *Gen. Comp. Endocrinol.* 261, 190–197. doi: 10.1016/j.ygcen.2017.04.013

Skarnes, W. C., Rosen, B., West, A. P., Koutsourakis, M., Bushell, W., Iyer, V., et al. (2011). A conditional knockout resource for the genome-wide study of mouse gene function. *Nature* 474, 337–342. doi: 10.1038/nature10163

Smith, L. C., Ralston-Hooper, K. J., Ferguson, P. L., and Sabo-Attwood, T. (2016). The G protein-coupled estrogen receptor agonist G-1 inhibits nuclear estrogen receptor activity and stimulates novel phosphoproteomic signatures. *Toxicol. Sci.* 151, 434–446. doi: 10.1093/toxsci/kfw057

van der Eerden, B. C., Gevers, E. F., Lowik, C. W., Karperien, M., and Wit, J. M. (2002). Expression of estrogen receptor alpha and beta in the epiphyseal plate of the rat. *Bone* 30, 478–485. doi: 10.1016/s8756-3282(01)00703-7

van der Eerden, B. C., Karperien, M., Gevers, E. F., Lowik, C. W., and Wit, J. M. (2000). Expression of Indian hedgehog, parathyroid hormone-related protein, and their receptors in the postnatal growth plate of the rat: evidence for a locally acting growth restraining feedback loop after birth. *J. Bone Miner. Res.* 15, 1045–1055. doi: 10.1359/jbmr.2000.15.6.1045

Windahl, S. H., Andersson, N., Chagin, A. S., Martensson, U. E., Carlsten, H., Olde, B., et al. (2009). The role of the G protein-coupled receptor GPR30 in the effects of estrogen in ovariectomized mice. *Am. J. Physiol. Endocrinol. Metab.* 296, E490–E496. doi: 10.1152/ajpendo.90691.2008

Conflict of Interest: The authors declare that the research was conducted in the absence of any commercial or financial relationships that could be construed as a potential conflict of interest.

Publisher's Note: All claims expressed in this article are solely those of the authors and do not necessarily represent those of their affiliated organizations, or those of the publisher, the editors and the reviewers. Any product that may be evaluated in this article, or claim that may be made by its manufacturer, is not guaranteed or endorsed by the publisher.

frontiers in Cell and Developmental Biology

REVIEW
published: 29 September 2021
doi: 10.3389/fcell.2021.703966

Distinct Identity of GLP-1R, GLP-2R, and GIPR Expressing Cells and Signaling Circuits Within the Gastrointestinal Tract

*Nadya M. Morrow[1,2], Antonio A. Hanson[1,2] and Erin E. Mulvihill[1,2,3,4]**

[1] Energy Substrate Laboratory, University of Ottawa Heart Institute, Ottawa, ON, Canada, [2] Department of Biochemistry, Microbiology and Immunology, University of Ottawa, Ottawa, ON, Canada, [3] Montreal Diabetes Research Center CRCHUM-Pavillion R, Montreal, QC, Canada, [4] Centre for Infection, Immunity and Inflammation, University of Ottawa, Ottawa, ON, Canada

Enteroendocrine cells directly integrate signals of nutrient content within the gut lumen with distant hormonal responses and nutrient disposal via the production and secretion of peptides, including glucose-dependent insulinotropic polypeptide (GIP), glucagon-like peptide 1 (GLP-1) and glucagon-like peptide 2 (GLP-2). Given their direct and indirect control of post-prandial nutrient uptake and demonstrated translational relevance for the treatment of type 2 diabetes, malabsorption and cardiometabolic disease, there is significant interest in the locally engaged circuits mediating these metabolic effects. Although several specific populations of cells in the intestine have been identified to express endocrine receptors, including intraepithelial lymphocytes (IELs) and αβ and γδ T-cells (*Glp1r*+) and smooth muscle cells (*Glp2r*+), the definitive cellular localization and co-expression, particularly in regards to the *Gipr* remain elusive. Here we review the current state of the literature and evaluate the identity of *Glp1r, Glp2r,* and *Gipr* expressing cells within preclinical and clinical models. Further elaboration of our understanding of the initiating G-protein coupled receptor (GPCR) circuits engaged locally within the intestine and how they become altered with high-fat diet feeding can offer insight into the dysregulation observed in obesity and diabetes.

Keywords: glucagon-like peptides, intestine, incretins, metabolism, glucose-dependent insulinotropic polypeptide

OPEN ACCESS

Edited by:
Sameer Mohammad, King Abdullah International Medical Research Center (KAIMRC), Saudi Arabia

Reviewed by:
Ankit Malik, University of Chicago, United States
Venkateswarlu Kanamarlapudi, Swansea University, United Kingdom

***Correspondence:**
Erin E. Mulvihill
emulvihi@uottawa.ca

Specialty section:
This article was submitted to Signaling, a section of the journal Frontiers in Cell and Developmental Biology

Received: *01 May 2021*
Accepted: *16 August 2021*
Published: *29 September 2021*

Citation:
Morrow NM, Hanson AA and Mulvihill EE (2021) Distinct Identity of GLP-1R, GLP-2R, and GIPR Expressing Cells and Signaling Circuits Within the Gastrointestinal Tract. Front. Cell Dev. Biol. 9:703966. doi: 10.3389/fcell.2021.703966

Abbreviations: 5-HT, serotonin receptor; ApoB48, apolipoprotein B48; ATP, adenosine triphosphate; AUC, area under curve; cAMP, cyclic adenosine monophosphate; ChAT, choline-acetyltransferase; CNS, central nervous system; DIRKO, double incretin receptor knockout; DPP4, dipeptidyl peptidase 4; DS, dextrane sulfate; EGFR, tyrosine kinase IGF1R/ErbB; eNOS, endothelial nitric oxide synthase; ER, endoplasmic reticulum; FABP5, fatty acid-binding protein 5; FFA, free fatty acid; FFAR1, free-fatty acid receptor 1; FFAR2, free-fatty acid receptor 2; FFAR4, free-fatty acid receptor 4; GAL_1, galinin receptor; Gcg, preproglucagon; GCGR, glucagon receptor; GIP, glucose-dependent insulinotropic polypeptide; GIPR, glucose-dependent insulinotropic polypeptide receptor; GLP-1, glucagon-like peptide 1; GLP-1R, glucagon-like peptide 1 receptor; GLP-2, glucagon-like peptide 2; GLP-2R, glucagon-like peptide 2 receptor; GPCR, G-protein coupled receptor; GPR119, G-protein coupled receptor 119; GPR93, G-protein coupled receptor 93; GPRC6A, G-protein coupled receptor family C group 6 subtype A; IEL, intraepithelial lymphocyte; IL-1β, interleukin 1 beta; IL-6, interleukin 6; KGF, keratinocyte growth factor; LCFA, long-chain fatty acid; LPL, lipoprotein lipase; LPS, lipopolysaccharide; nNOS, neuronal nitric oxide synthase; NOD, non-obese diabetic; OGTT, oral glucose tolerance test; PBS, phosphate-buffered saline; PC1/3, prohormone convertase 1/3; PC2, prohormone convertase 2; Pdx1, pancreatic and duodenal homeobox 1; Rfx6, regulatory factor X6; RYGB, Roux-en-Y gastric bypass; SCFA, short-chain fatty acid; SGLT1, sodium glucose co-transporter 1; SP, substance P; STAT, subtherapeutic antibody therapy; T2DM, type 2 diabetes mellitus; TG, triglyceride; TPN, total parenteral nutrition; TRL, triglyceride rich lipoprotein; VIP, vasoactive intestinal polypeptide; VSG, vertical sleeve gastrectomy; αSMA, smooth muscle actin.

INTRODUCTION

Extending between the stomach and the colon lies among the most significant hormone-producing and immunological organs responsible for nutrient digestion and absorption: the small intestine. Within the small intestine lumen, the surface area is ideally maximized to enhance nutrient absorption through villi and microvilli, which increase intestinal surface area by 30–600-fold (Kiela and Ghishan, 2016). A single layer of epithelial cells lines the surface of each villus to serve as the gateway for controlled nutrient absorption and a barrier to dietary antigens and diverse microorganisms (Turner, 2009). Absorptive enterocytes populate the villus tip and account for >80% of intestinal epithelial cells. The remaining mature cell types include mucin-producing goblet cells, antimicrobial defensins-producing Paneth cells, peptide-hormone-producing enteroendocrine cells, and cytokine-producing tuft cells which reside throughout the epithelium (Ensari and Marsh, 2018). Shallow invaginations surrounding each villus are intestinal crypts and the site of cell division: highly mitotic stem cells that give rise to progenitor cells, which in turn proliferate to become mature epithelial cells (Gehart and Clevers, 2019). The continuous supply of progenitor and new epithelial cells physically promotes the transit of the latter from the crypts up to the villus tip, where they populate the newly vacant area of previously shed apoptotic epithelial cells (Gehart and Clevers, 2019). Therefore, in addition to the maximized absorptive surface area, the constantly renewing barrier protects the internal environment from the harsh conditions of the intestinal lumen. This single epithelial layer sits on a basement membrane surrounding a connective tissue core called the lamina propria, which contains lymphocytes and innate immune cells (Ensari and Marsh, 2018). Each villus is supplied by an arteriole that forms a capillary network, a venule that drains into larger vessels at the crypts (Ensari and Marsh, 2018), and 1–2 lacteals, which are terminal lymphatic vessels of the mesenteric network. Pericytes coat villus blood vessels while smooth muscle cells coat lacteals. The lamina propria also contains connective tissue scaffolds, enteric nerves, fibroblasts, and smooth muscle cells (Bernier-Latmani and Petrova, 2017). The lamina propria is encapsulated by a myofibroblast shell that directly contacts the vascular network. From the villus tip to the muscularis mucosa, onto which villi are anchored, is considered the mucosal layer. The submucosal layer contains blood and lymphatic vessels and a plexus of parasympathetic nerves (Bernier-Latmani and Petrova, 2017), while the smooth muscle cell-rich muscularis propria allows for contractile peristalsis (Collins et al., 2021). The final outer layer of the intestine is the serosa, composed of loose connective tissue and squamous epithelial cells (Collins et al., 2021), which is continuous with the mesentery. The mesentery supports the intestine in the peritoneum and also contains blood vessels, nerves, and lymphatics (Argikar and Argikar, 2018). The coordination of barrier function with nutrient absorption and transit is governed by a complex integration of signals, including local enteroendocrine production of peptide hormones, which impacts both the dynamic and highly efficient process of nutrient assimilation.

In addition to its expression in the pancreas, proglucagon is also produced in enteroendocrine L cells throughout the small and large intestine (Jorsal et al., 2018). Here, posttranslational processing of the 160 amino acid proglucagon by prohormone convertase 1/3 (PC1/3) yields active peptides glicentin, glucagon-like peptide 1 (GLP-1), intervening peptide 2 (IP2), and glucagon-like peptide 2 (GLP-2) (Mojsov et al., 1986; Orskov et al., 1986). Evidence for gut-derived glucagon is observed in patients with a total pancreatectomy during a glucose tolerance test (Lund et al., 2016). GLP-1, first identified from amino acids 1–37 and 1–33 (Drucker et al., 1986), is active upon N-terminal truncation, where GLP-1(7–37) and GLP-1(7–36)amide are physiologically active with well-defined roles in promoting nutrient-stimulated insulin secretion (Drucker et al., 1987; Holst et al., 1987). The active form of GLP-2 in tissue and circulation is the complete 1–33 amino acid (Brubaker et al., 1997) upon C-terminal truncation of 2 amino acids (Orskov et al., 1989b) with a well-defined role of acting locally to promote nutrient uptake, barrier function and gut growth.

Glucose-dependent insulinotropic polypeptide (GIP) is a peptide hormone expressed and secreted by intestinal K enteroendocrine cells. GIP is derived from a 144 amino acid (rodent) (Higashimoto et al., 1992; Higashimoto and Liddle, 1993; Tseng et al., 1993) or 153 amino acid (human) (Takeda et al., 1987) precursor, proGIP. Most K cells express PC1/3, which cleaves proGIP at Arg65, resulting in the biologically active GIP(1–42) (Ugleholdt et al., 2006) and stored in secretory granules (∼450 nm) (Buchan et al., 1978). A small population of K cells express PC2 instead of PC1/3, resulting in GIP(1–31), which is amidated by peptidyl-glycine α-amidating monooxygenase, resulting in GIP(1–30) (Fujita et al., 2010). Initially discovered in 1973 for its role in inhibiting gastric acid secretion in excised canine stomach pouches, and later shown to not have this effect in humans (Meier et al., 2004a), GIP promotes nutrient-stimulated insulin secretion and increases glucagon secretion in the fasted state but not in patients with type 2 diabetes (Baggio and Drucker, 2007; Christensen et al., 2011).

The physiological concentrations of the peptide hormones GIP, GLP-1, and GLP-2, are tightly controlled by the nutrient-sensing abilities of their respective enteroendocrine cells. Additionally, the serine protease dipeptidyl peptidase 4 (DPP4) limits the bioavailability of GIP, GLP-1, and GLP-2 by cleaving the first two amino acids, rendering them inactive (Deacon et al., 1995a; Knudsen and Pridal, 1996; Hansen et al., 1999). In healthy humans, GIP has a circulating half-life of 7 min (Meier et al., 2004b), GLP-1 has a circulating half-life of 1–2 min (Deacon et al., 1995b), and GLP-2 has a circulating half-life of 7 min (Drucker et al., 1997; Hartmann et al., 2000). GIP concentrations are much greater than GLP-1 in the postprandial state (Meek et al., 2021). Prolonged activation of GLP-1, GLP-2, and GIP receptors is achieved through receptor agonists resistant to DPP4 cleavage or through compounds that inhibit DPP4 activity (Jeppesen et al., 2005; Baggio and Drucker, 2007).

This review highlights the biology and paracrine roles of GLP-1, GIP, and GLP-2 in integrating the response to food intake with the maintenance of the structure and function of the gut as it relates to nutrient absorption. We critically assess experiments

reporting the identification and role(s) of GPCRs: GIP receptor (GIPR), GLP-1 receptor (GLP-1R) and GLP-2 receptor (GLP-2R) in intestinal physiology. We also emphasize both preclinical and clinical studies identifying how agonists to these receptors transduce their metabolic actions. We limit our discussion to intestinal biology and the resulting metabolic phenotypes and refer readers interested in other aspects of the GLP-1R, GLP-2R and GIPR biology to access other excellent publications (Campbell, 2021; Ghislain and Poitout, 2021; Gribble and Reimann, 2021; McLean et al., 2021).

GUT HORMONAL RESPONSES TO NUTRIENTS

Enteroendocrine cells are highly sensitized to nutrient intake due to their polarized shape, direct contact with the lumen, and proximity to the vasculature for peptide secretion. Upon ligand-receptor binding and depolarization, hormone-containing granules fuse with the lateral and basal membrane for discharge into the villus capillaries (Paternoster and Falasca, 2018). This idealistic design favors rapid and precise peptide delivery in circulation to initiate signaling through their respective receptors to control metabolism. Additionally, enteroendocrine cells are equipped with GPCRs and transporters to sense the macronutrients and release the appropriate hormones (Spreckley and Murphy, 2015). These include: G-protein coupled receptor (GPCR) family C group 6 subtype A (GPRC6A), Taste Rs (amino acids), G-protein coupled receptor 93 (GPR93) (peptones), free-fatty acid receptor 2 (FFAR2), free-fatty acid receptor 3 (FFAR3), short-chain fatty acid (SCFA), free-fatty acid receptor 1 (FFAR1), free-fatty acid receptor 4 (FFAR4), long-chain fatty acid (LCFA) and G-protein coupled receptor 119 (GPR119) [oleoylethanolamide (oea)] are some of the macronutrient-sensing receptors present on enteroendocrine cells (Spreckley and Murphy, 2015). First, we begin with an overview of the regulation of the synthesis, secretion, and location of these peptides.

GIP Expression and Secretion

GIP mRNA (Tseng et al., 1993) and concentration (Bryant et al., 1983) are enriched in duodenal and jejunal mucosal tissues in rodents and humans compared to the distal ileum (**Figure 1**). Forty-eight hours of fasting in rats significantly decreases *Gip* mRNA (∼44%) in the proximal small intestine compared to rats maintained on a chow diet. At the same time, GIP peptide concentrations do not change with fasting or feeding (Higashimoto et al., 1995), suggesting that synthesis and secretion are relatively synchronized. K-cells in the proximal small intestine contain more GIP protein and secrete more GIP in response to intestinal lard oil perfusion than distal K cells (Iwasaki et al., 2015). *GIP* expression is significantly greater in both the small intestine and colon of patients with Type 2 diabetes than healthy individuals (Jorsal et al., 2018). Interestingly, in patients with type 2 diabetes, the density of PC1/3-positive cells decreases while both the expression and density of PC-2 positive cells increases (Jorsal et al., 2018). Nutrient stimulation of GIP secretion has also been reviewed here (Pais et al., 2016; Reimann et al., 2020).

In K cells, regulatory factor X6 (Rfx6) is a transcription factor that binds to the *Gip* promoter to increase *Gip* mRNA expression (Suzuki et al., 2013). Intestine-specific gene transfer experiments of pancreatic and duodenal homeobox-1 (*Pdx1*) siRNA in 8–10-week-old mice reveal that posteriori suppression of Pdx1 decreases K-cell number, intestinal GIP protein and mRNA expression, and GIP secretion in response to an oral glucose tolerance test (OGTT) (Ikeguchi et al., 2018). The number of K cells and their *Gip* mRNA content increases with age, which corresponds to the GIP hypersecretion observed in 1 year old mice compared to 3–4-month-old mice (Ikeguchi et al., 2018). Moreover, transcription factor *Pdx1*, but not *Rfx6* mRNA increases with age in K cells (Ikeguchi et al., 2018). Both dietary fat and carbohydrate stimulate GIP secretion (Pederson et al., 1975; Brown and Otte, 1979; McCullough et al., 1983). Intraduodenal perfusion of 20% Lipomul significantly increases duodenal *Gip* mRNA at 30 and 60 min compared to saline control (Tseng et al., 1993). Both glucose (4-fold) and fat (2.5-fold) ingestion increase *Gip* mRNA expression compared to chow-diet feeding (Higashimoto et al., 1995). High-fat feeding does not increase K-cell number in mice, instead, it increases GIP protein content and mRNA expression, which correlates to increased *Rfx6* and *Pdx1* mRNA expression (Suzuki et al., 2013). Therefore, through different mechanisms, both diet-induced obesity and aging act on the gut to increase GIP reserves for secretion into circulation.

Nutrient Stimulated GIP Secretion

GIP secretion increases more rapidly in response to simple, fast-absorbing carbohydrates compared to complex, slow-absorbing carbohydrates (Collier et al., 1984). Plasma GIP levels rise significantly higher upon oral fat consumption compared to glucose in mice (Shibue et al., 2015) and in humans (Yamane et al., 2012). Further, ingestion of a mixed carbohydrate and fat meal significantly increases plasma GIP levels compared to carbohydrates alone in healthy humans (Collier et al., 1984) but this increase is not as great as ingestion of fat alone in healthy humans (Creutzfeldt et al., 1978). GIP secretion in response to oral fat is greater in patients with obesity and glucose intolerance, and does not change with the addition of glucose to the meal (Creutzfeldt et al., 1978).

GIP concentrations in the bloodstream are the highest in hepatic portal plasma, however, lymph GIP concentrations are ∼3-fold higher upon the same stimulus (D'Alessio et al., 2007; Lu et al., 2008), indicating peptide transit from K cells to villus lacteals. Intraduodenal delivery of a bolus of dextrin and a bolus of Liposyn (20%) in rats each induce ∼800 and ∼400 pg/mL peaks, respectively, in lymph GIP concentrations at 60 min (Lu et al., 2008). However, the peak secretion rate occurs at 30 min for Liposyn (1,159 ± 393 pg/h) and at 60 min for dextrin (2,410 ± 566 pg/h). The combination of dextrin and Liposyn delivery significantly increases GIP secretion at 30 min (2,094 ± 241 pg/h) and at 60 min (8,027 ± 1,057 pg/h) compared to saline, dextrose alone, and Liposyn alone (Lu et al., 2008). These data suggest that glucose and lipids stimulate K cells

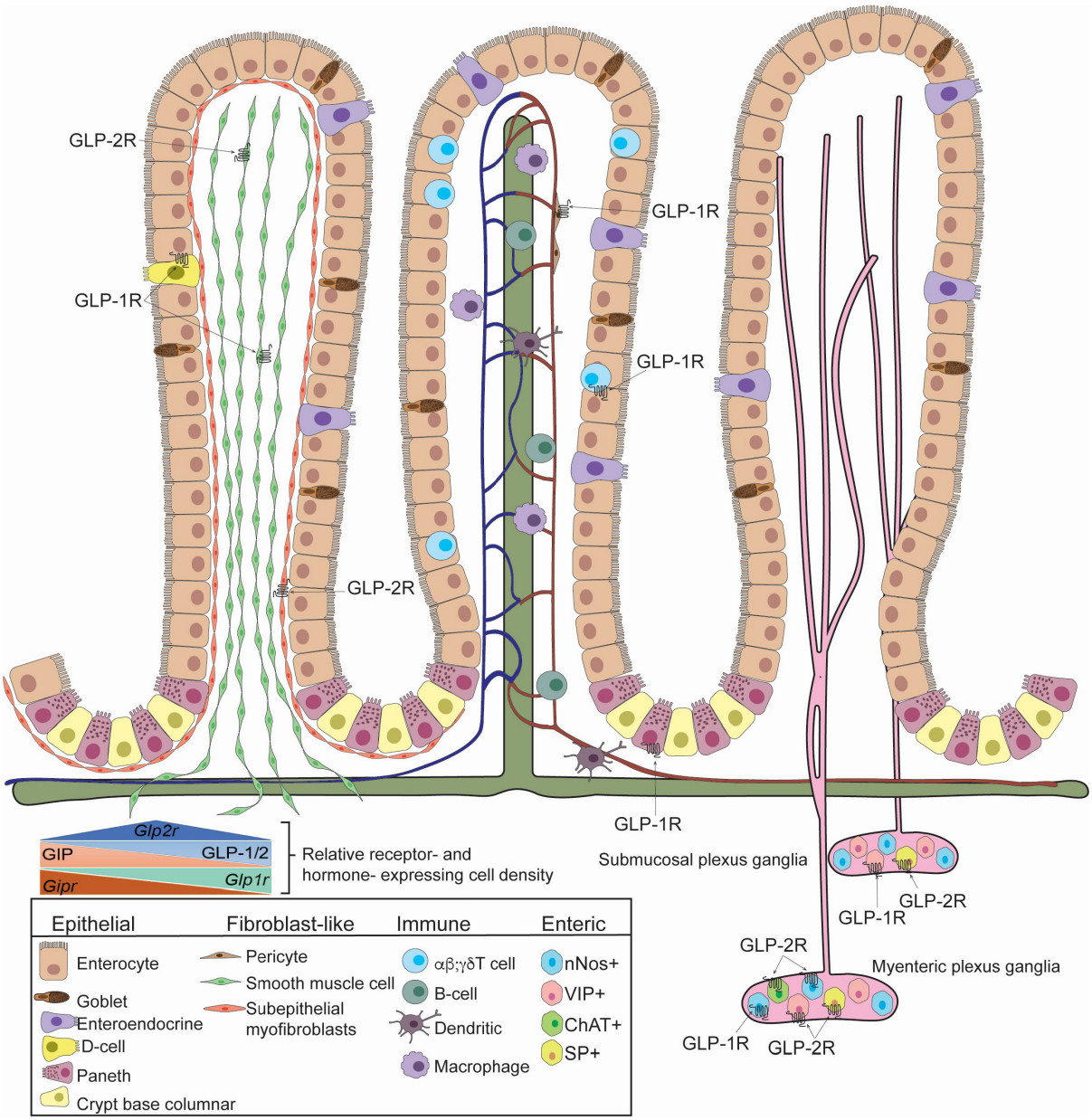

FIGURE 1 | GLP-1R and GLP-2R-expressing cells in the small intestine identified in mice. Villus architecture is organized as fibroblast-like cells **(Left)**, blood, lymph and immune cells **(Middle)**, enteric cells **(Right)**. GLP-1R is expressed in somatostatin-secreting enteroendocrine cells, smooth muscle cells, pericytes, Paneth cells, Tαβ cells, Tγδ cells, submucosal and myenteric neurons. GLP-1R is detected in neuronal nitric oxide (nNOS)+ neurons. GLP-2R is detected in smooth muscle cells, subepithelial myofibroblasts, submucosal and myenteric neurons. Specifically, GLP-2R is expressed in nNOS+ cells, vasoactive intestinal polypeptide (VIP)+ cells, choline-acetyltransferase (ChAT)+ cells, and substance P (SP)+ cells. The relative receptor- and hormone- expression cell density within the small intestine is depicted (inset). Studies highlighted here did not determine co-expression of GLP-1R and GLP-2R and specific identity of GIPR-expressing cells is unclear.

differently, therefore potentiating release when administered together. Indeed, preventing micelle formation via common bile duct ligation abolishes GIP secretion upon a lard gavage compared to sham controls, independent of meal transit (Shibue et al., 2015). As dietary fatty acids are assembled into lipoproteins in intestinal enterocytes for subsequent circulatory transport, blocking lipoprotein transit from endoplasmic reticulum (ER) to Golgi by Pluronic L-81 in rats robustly reduces (∼4.5-fold) lymph GIP levels and secretion rates in response to Liposyn to levels similar to saline controls (Lu et al., 2012). Therefore, GIP secretion from K cells in response to Liposyn requires post-Golgi chylomicron transit in enterocytes, not lipid absorption alone (Lu et al., 2012). GIP secretion increases in response to chylomicrons alone and the presence of glucose in both murine and human duodenal cultures in a dose-dependent fashion (Psichas et al., 2017). Glucose stimulation of chylomicron secretion is well

documented (Robertson et al., 2003; Stahel et al., 2019; Xiao et al., 2019) where glucose promotes chylomicron secretion from lipid stores in enterocytes (Stahel et al., 2019), which may provide additional stimulus for GIP secretion. Co-intraduodenal infusion of mixed nutrients (carbohydrate, dextrose) and lipid (20% Liposyn) in rats significantly increase GIP secretion in lymph to a greater extent than either nutrient at the same meal caloric value alone, suggesting a synergistic effect (Lu et al., 2008). Consistent with glucose-stimulated chylomicron secretion, lymph TG values are the same when Liposyn accounts for half of the meal calories (the other half being dextrose) compared to a full Liposyn meal (Lu et al., 2008). Experiments measuring glucose-stimulated GIP secretion after inhibiting chylomicron release (Pluronic 8–18) or basolateral hydrolysis of chylomicrons (poloxamer-407) may help delineate the exact contribution of each nutrient. Nevertheless, the requirement of chylomicron formation for GIP secretion from proximal K cells corresponds to a location-specific stimulus. Taken together, these studies demonstrate the complex integration of pathways governing GIP secretion and intestinal lipid metabolism.

The free fatty acid receptor GPR120 is enriched in proximal K cells while GPR40, GPR41, and GPR43 are significantly enriched in distal K cells (Iwasaki et al., 2015). GIP secretion is unaffected by FFA1 agonism (Am-1638) or antagonism (GW1100) in primary murine duodenal cultures (Psichas et al., 2017). GIP concentration in plasma over 120 min decreases by 75% in *Gpr120*$^{-/-}$ mice upon lard oil gavage compared to wild-type mice (Iwasaki et al., 2015). Correspondingly, intestinal perfusion experiments in *Gpr120*$^{-/-}$ mice reveal that GIP secretion is significantly reduced from both proximal and distal regions of the small intestine compared to wild-type controls (Iwasaki et al., 2015). Similarly, oral pretreatment with a GPR120 partial antagonist, grifolic acid methyl ether, reduces GIP secretion by 80% in response to lard oil gavage (Iwasaki et al., 2015). All GIP+ cells express fatty acid-binding protein 5 (FABP5) (Shibue et al., 2015). While whole-body elimination of FABP5 in mice does not impact GIP content or K cell number, these mice secrete significantly less GIP into plasma 60 min after a lard gavage compared to wild-type controls (Shibue et al., 2015). *Ex vivo* duodenal segments from *Fabp5*$^{-/-}$ mice secrete significantly less GIP in response to oleic acid with 4 v/v% bile in media than tissues isolated from wild-type mice (Shibue et al., 2015). These data suggest that micelle-facilitated fatty acid uptake via FABP5 in response to luminal lipids significantly contributes to meal-stimulated GIP secretion (Shibue et al., 2015) (**Figure 2**).

Glucose stimulates GIP secretion only when administered orally, therefore requiring apical exposure to K cells. Curiously, intraduodenal infusion of glucose in healthy men does not significantly increase plasma GIP levels from baseline (Herrmann et al., 1995), suggesting a transit time dependency for glucose-stimulated GIP secretion. Glucose injection in the upper intestine significantly increases plasma GIP levels while glucose injection in the colon does not (Moriya et al., 2009). Perfusion of glucose, sucrose, galactose, maltose, 3-*O*-methylglucose, and *a*- or *B*-methylglucoside significantly stimulate GIP secretion, while mannose, 6-deoxygalactose, 2-deoxyglucose, myoinositol, fructose or lactose do not (Sykes et al., 1980). Therefore, active transport by the sodium-dependent hexose pathway is required for GIP secretion (Sykes et al., 1980). Indeed, sodium glucose co-transporter 1 (SGLT1) receptor is expressed only on the apical side of K cells and oral gavage of SGLT1 substrate, a-methyl-D-glucopyranoside, stimulates GIP secretion (Moriya et al., 2009). The necessity for apical glucose transport is demonstrated in *Sglt1*$^{-/-}$ mice, where glucose-stimulated GIP secretion is eliminated and levels rise only to the same extent as observed in the saline control (Gorboulev et al., 2012). Genetic elimination of K_{ATP} channels (*Kir6.2*$^{-/-}$ mice) significantly increases glucose absorption and glucose-stimulated GIP secretion, through a compensatory increase in duodenal *Sglt1* mRNA expression (Ogata et al., 2014). Preventing glucose absorption with phloridizin abolishes glucose-stimulated GIP secretion in healthy wild-type (Sykes et al., 1980) and *Kir6.2*$^{-/-}$ mice (Ogata et al., 2014), even in the presence of *a*-methyl-D-glucopyranoside (Moriya et al., 2009). Similar to humans, mice and rats with diabetes secrete more GIP in response to oral glucose. Fructose transporter, GLUT5, is expressed on K-cells; however, fructose does not stimulate GIP secretion in healthy humans, rats, or mice (Kuhre et al., 2014; Seino et al., 2015). Fructose significantly increases GIP secretion in streptozotocin-treated, hyperglycemic mice in a K_{ATP}-dependent manner (Seino et al., 2015) and in *ob/ob* mice (Flatt et al., 1989). This is further supported by the inability of phlorizin to prevent glucose-induced GIP secretion in streptozotocin-treated, hyperglycemic mice, where complete blockage of GIP secretion is only achieved in these mice upon both phlorizin and K_{ATP} channel activation (diazoxide) (Ogata et al., 2014).

Non-nutrient promoters of GIP secretion include oral administration of $ZnCl_2$ to non-fasted mice, which increases GIP secretion 26% via K cell expression of GPR39 (Moran et al., 2019). Additionally, associated metabolic improvements with $ZnCl_2$ administration are lost in *Gipr*$^{-/-}$ mice (Moran et al., 2019). Galinin is a centrally and peripherally synthesized neuropeptide and its receptor (GAL_1) is expressed in K cells (Psichas et al., 2016). Both galinin and GAL_1 agonist (M617) significantly inhibit IBMX−stimulated GIP secretion from primary duodenal cultures (Psichas et al., 2016). Oral administration of progesterone significantly increases glucose-stimulated GIP secretion (5 min) in male wild-type and *Glp1r*$^{-/-}$*Gipr*$^{-/-}$ (double incretin receptor knockout; DIRKO) mice, but not in *Glp1r*$^{-/-}$ mice (Flock et al., 2013) (**Figure 2**).

GIP Secretion and the Microbiome

Glucose-dependent insulinotropic polypeptide levels are increased with subtherapeutic antibiotic therapy (STAT) (Cho et al., 2012) while other hormones are unaffected. It is suspected that levels are greater due to the increased abundance of Firmicutes and subsequent SCFA production (Martin et al., 2019), however, further studies to confirm this hypothesis are required.

Expression and Secretion of GLP-1 and GLP-2

GLP-1+ cells reside in crypts and the villus epithelium; their density increases distally with the highest abundance in the ileum

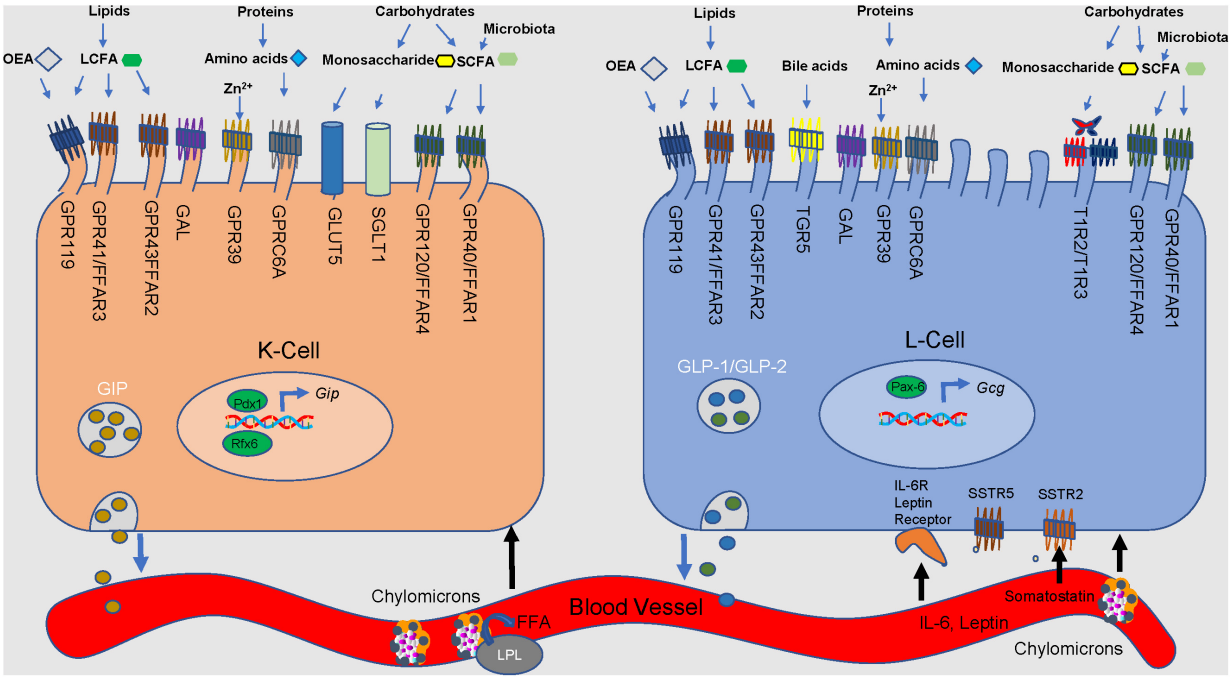

FIGURE 2 | Nutrient stimulation of GIP from K cells and GLP-1 and GLP-2 from L cells. Microvilli protrude from the apical side of the cell, extending toward the lumen. Incoming macronutrients from the lumen are detected and sensed by receptors present on the apical border. Carbohydrates are divided into monosaccharides and short-chain fatty-acids (SCFA). Glucose is transported through the sodium-glucose linked transporter (SGLT1). Glucose passes through the glucose transporter 2 (GLUT2) present on the basolateral membrane, and into the bloodstream. GLUT5 is responsible for sensing fructose. Present on only L cells, sweet receptors (T1R2/T1R3) also sense glucose. Short-chain fatty acids (SCFA) are derived from microbial fermentation, and are sensed by the free fatty acid receptors (GPR40/FFAR1 and GPR120/FFAR4). Long-chain fatty-acids are sensed by GPR43/FFAR2 and GPR41/FFAR3, along with G-protein coupled receptor 119 (GPR119). GPR119 is also a receptor for oleoylethanolamide (OEA). Amino acids are detected by GPR9C6A. GPR39 and Takeda G-protein coupled receptor 5 (TGR5) detect luminal zinc and bile acids, respectively. Galanin receptor (GAL) acts to inhibit both GLP-1 and GIP secretion. Lipoprotein lipase is involved in the production of LCFA and monoacylglycerols. Somatostatin receptors 2 and 5 (SSTR2&5) sense somatostatin from D cells. Regulatory factors x6 (Rfx6) and insulin promoter factor 1 (Pdx1) influence GIP expression and secretion.

in rodents (**Figure 1**) and the colon in humans (Eissele et al., 1992). Within L cells, GLP-1 is stored in granules (Eissele et al., 1992) in its active form (7–36 amide) in the small (Orskov et al., 1989a) and large intestine (Deacon et al., 1995b). Forty-eight hours of fasting in rats significantly reduces ileal *Gcg* mRNA (25–50%), which was associated with a 41–60% decrease in plasma bioactive GLP-2 (Nelson et al., 2008). Both plasma GLP-2 and ileal *Gcg* mRNA levels were restored upon 2 days of refeeding or 4 days of continuous intragastric, but not intravenous, refeeding with total parenteral nutrition (TPN) solution (32% energy from fat 68% energy from dextrose) (Nelson et al., 2008). Colonic L cells contain twice as much GLP-1 peptide than proximal intestine L cells (Reimann et al., 2008). Both colonic *GCG* expression and GLP-1+ cell density increase in patients with type 2 diabetes compared to healthy individuals (Jorsal et al., 2018). By contrast, while *PCSK1/3* mRNA increases in patients with diabetes compared to healthy individuals, the density of PC1/3-positive cells decreases (Jorsal et al., 2018), suggesting a posttranslational impact on GLP-1 availability. GLP-1+ cells are also found in the stomach fundus where concentrations are higher than in the antrum in both diet-induced obese rats and humans with obesity (Ribeiro-Parenti et al., 2021). In diet-induced obese mice, IBMX-stimulated GLP-1 release *ex vivo* is completely abrogated in the antrum (Ribeiro-Parenti et al., 2021). Interestingly, the remodeling of the gastric mucosa following Roux-en-Y gastric bypass (RYGB) bariatric surgery in humans is accompanied by a ∼2-fold increase in fundic GLP-1 positive cells; this increase is not observed in patients following vertical sleeve gastrectomy (VSG) surgery (Ribeiro-Parenti et al., 2021). This increase in fundic mucosal GLP-1 following RYGB but not VSG was consistent in diet-induced obese rats, where instead, VSG surgery induced a 50% increase in GLP-1+ cells in the antrum (Ribeiro-Parenti et al., 2021). This increase was associated with a 1.5-fold increase in portal plasma GLP-1 upon gastric glucose stimulation in diet-induced obese VSG rats compared to diet-induced obese sham controls, suggesting that antral GLP-1 producing cells contribute significantly to portal GLP-1 (Ribeiro-Parenti et al., 2021). However, further experiments preventing GLP-1 secretion from ileal L cells will be required to precisely assess the contribution from the stomach after surgery.

Nutrient Stimulated GLP-1 Secretion

In healthy men, oral ingestion of corn oil induces a 1,000% increase in the early phase of GLP-1 secretion, which does not return to baseline even after 120 min (Herrmann et al., 1995). In the same study, oral ingestion of a mixed meal containing

soybean oil, casein, and glucose induces a rapid ∼6-fold increase in GLP-1 levels, which is lower than corn oil alone and also leads to a return to baseline (Herrmann et al., 1995). Ileal luminal perfusion of a mixed meal in rats induces a rapid rise (2-fold) in portal plasma GLP-1 in 30 min (Herrmann et al., 1995). A 20% infusion of Intralipid in the perfused rat ileum, however, does not significantly increase portal plasma GLP-1 from baseline (Herrmann et al., 1995), suggesting that since orally ingested fatty acids do not reach the ileum, a direct sensing mechanism for this lipid composition does not exist in the ileum or that GLP-1 in this experiment bypasses portal circulation. By contrast, experiments directly administering corn oil into either duodenal or ileal luminal compartments in anesthetized rats demonstrate significantly increased plasma GLP-1 (obtained from carotid artery) to the same extent from baseline (Roberge and Brubaker, 1993). Taken together, these studies demonstrate that either higher fatty acid concentration, mechanical stimulation, or a specific blood sampling pool is required to detect this response from the distal gut. While not often measured, the GLP-1/GLP-2 ratio (detecting C-terminal of GLP-1 and N-terminal of GLP-2) remains consistent throughout an oral fat tolerance test, but interestingly significantly increases at 120 and 250 min during an OGTT in obese men (Matikainen et al., 2016). Additionally, in response to a meal, in patients with short bowel syndrome with a preserved colon (jejuno-colonic anastomosis), both baseline GLP-1 and GLP-2 are elevated with GLP-2 levels threefold greater than control patients (average concentration of 72 pmol/L), which persists throughout the post-prandial period (Jeppesen et al., 2000).

Lymph fistula experiments in rats reveal post-prandial levels in intestinal lymph are 5–6 times higher for GLP-1 compared to portal venous plasma (D'Alessio et al., 2007; Lu et al., 2007). Similarly, GLP-2 concentrations in the lymph are significantly higher (∼2-fold) than in blood at fasting and 2 h after (∼3-fold) duodenal infusion of perilla oil (Sato et al., 2013). The physiological advantage for lymph vs. blood secretion is not clear; however, DPP4 activity is significantly higher during fasting (20-fold) and post-meal (3-fold) in plasma than in lymph (D'Alessio et al., 2007). Intraduodenal infusion of Liposyn significantly increases lymph flow, lymph GLP-1 levels and secretion rates before increases in lymph TG and lymph free fatty acid (FFA) compared to saline control are observed (Lu et al., 2012). Pluronic L-81 impairs lymphatic transport of TG without inhibiting fatty acid absorption or TG assembly (Tso et al., 1981; Hayashi et al., 1990), therefore leading to the accumulation of large apical lipid droplets in enterocytes (Tso et al., 1981). The addition of pluronic L-81 to the Liposyn infusion significantly reduces lymph flow to rates observed in saline control. It completely abolishes TG and FFA concentrations and delays the peak in lymph GLP-1 concentrations from 30 to 120 min, with a 75% reduction in the rate at 30 min, but secretion was the same at 60 min (Lu et al., 2012). Overall, the addition of L-81 to Liposyn did not reduce the cumulative GLP-1 output to the same levels as saline controls, whereas GIP secretion was abolished (Lu et al., 2012).

In the presence of glucose, chylomicrons (10 and 100 μg/mL) significantly increase GLP-1 secretion from GLUTag cells, murine duodenal cultures, and human duodenal cultures (Psichas et al., 2017). Lipoprotein lipase (*Lpl*) is highly expressed in duodenal L cells and GLUTag cells; both the lipase inhibitor orlistat and siRNA-mediated knockdown of *Lpl* significantly inhibits chylomicron-induced GLP-1 secretion in GLUTag cells (Psichas et al., 2017). LPL-mediated hydrolysis of chylomicrons yields long chain fatty acids and monoacylglycerols, which are ligands for FFA1 and GPR119. Indeed, L cells express free acid receptors *Ffar1* and G-protein coupled receptor 119 (Psichas et al., 2017). FFA1 receptor signaling increases GLP-1 secretion with or without chylomicron treatment, as shown with FFA1 agonist (AM-1638), FFA1 antagonist (GW110), and siRNA-mediated knockdown experiments in GLUTag cells (Psichas et al., 2017). While GPR119 activation stimulates GLP-1 secretion in primary duodenal cultures, activation is not absolutely required for GLP-1 secretion as shown by L cell specific knockout (Psichas et al., 2017). Additionally, inhibiting both FFA1 and GPR119 at the same time does not impact GLP-1 secretion upon chylomicron treatment in primary duodenal cultures (Psichas et al., 2017). Also, orlistat does not significantly impact chylomicron-stimulated GLP-1 secretion in duodenal cultures, suggesting that LPL-mediated release of FFA1 and GPR119 ligands may be restricted to GLUTag cells (Psichas et al., 2017). However, in primary cultures, only the apical membrane of L cells are exposed to chylomicrons (Psichas et al., 2017). Therefore, basolateral LPL access to chylomicrons may be required.

In healthy men, oral glucose significantly increases plasma total GLP-1 [GLP-1(1–36) and GLP-1(7–36)] levels after 30 min; its rise is delayed compared to the rapid increase of circulating GIP (Herrmann et al., 1995). Compared to oral glucose, oral galactose and amino acids rapidly increase plasma GLP-1 levels (Herrmann et al., 1995). In healthy men, intraduodenal infusion of glucose induces a rapid 200% increase in GLP-1 that returns to baseline by 30 min (Herrmann et al., 1995). Ileal luminal perfusion of a 5% glucose dissolved in saline in rats induces a rapid rise (∼2-fold) in portal plasma GLP-1 in 30 min (Herrmann et al., 1995). This effect is lost when glucose is dissolved in distilled water (Herrmann et al., 1995). While significantly lower than portal GLP-1 secretion upon intraduodenally delivered glucose, delivering glucose directly to the stomach in anesthetized rats with a pylorus ligature induces a significant increase in portal GLP-1 [+133 pM vs. phosphate-buffered saline (PBS)] and gastric vein (+140 pM vs. PBS) at 15 min compared to PBS control, where ∼1/2 of this total GLP-1 in the gastric vein is the active peptide (Ribeiro-Parenti et al., 2021). Gastric mucosal cells produce proglucagon, GLP-1, and GLP-2 (Ribeiro-Parenti et al., 2021). Despite GLP-1 concentration being higher in the fundus than the antrum, its release *ex vivo* upon IBMX stimulation increases to the same extent in both the fundus and antrum, suggesting a significant contribution to both portal and gastric GLP-1 (Ribeiro-Parenti et al., 2021). Intraduodenal administration of sucrose, sucralose, and the artificial sweetener PALSWEET each significantly increase lymph GLP-2 output compared to saline control (Sato et al., 2013).

A paracrine relationship exists between GLP-1-secreting L cells and somatostatin-secreting D-cells (Jepsen et al., 2019). Additionally, the somatostatin receptor *Sstr5* expression is present in GLP-1-immunoreactive cells (Jepsen et al., 2019).

GLP-1 secretion in response to intraduodenal infusion of glucose increases with somatostatin receptor antagonism (SSTr2 and SSTr5) (Jepsen et al., 2019). Similarly, somatostatin secretion is dependent on GLP-1R activation as its secretion is inhibited upon GLP-1R antagonist (exendin-9) treatment (Jepsen et al., 2019). Taken together, this relationship is regulated by L cell and D cell expression of SSTr5 and GLP-1R, respectively. Additionally, these findings explain the increased endogenous GLP-1 release upon exendin-(9–39) treatment.

Hormonal Stimulation of GLP-1 Secretion

Plasma GLP-1 levels peak within 5–15 min of food ingestion, where certainly these nutrients do not reach the ileum to directly stimulate L cells (Borgstrom et al., 1957). A neuroendocrine loop exists in proximal-distal intestine to stimulate ileal L cells when dietary fat enters the duodenum (Roberge and Brubaker, 1993; Rocca and Brubaker, 1999). As previously mentioned, administration of corn oil to duodenal luminal compartments elicits the same plasma GLP-1 response compared to corn oil administration to ileal luminal compartments (Roberge and Brubaker, 1993). Despite the presence of L cells in the duodenum, they are not responsible for the GLP-1 release as removing the jejunum-ileum before infusing the duodenal compartment with fat prevents the observed increase of plasma GLP-1 (Roberge et al., 1996). Still, plasma GIP secretion in response to duodenal luminal administration occurs earlier than GLP-1 secretion (Roberge and Brubaker, 1993). Importantly, intravenous infusion of post-prandial levels of GIP increases plasma GLP-1 levels twofold, independent of blood glucose levels (Roberge and Brubaker, 1993), suggesting that GIP stimulates early GLP-1 secretion in response to duodenal luminal nutrients. Indeed, GLP-1 secretion is abolished upon corn oil infusion to the proximal duodenal compartment in vagotomized rats (Rocca and Brubaker, 1999). Electrical stimulation of the vagus nerve stimulates GLP-1 secretion, even in the absence of nutrients (Rocca and Brubaker, 1999). GIP can stimulate the first phase of GLP-1 secretion independent of the vagus nerve, but only when infused at suprapharmacological levels, as evidenced by the rapid rise and fall in plasma GLP-1 upon supraphysiological infusion of GIP in sham and vagotomized rats (Rocca and Brubaker, 1999). At physiological levels, infusion of GIP does not stimulate GLP-1 secretion in vagotomized rats compared to the peak observed at 10 min in the sham controls (Rocca and Brubaker, 1999). Curiously, ingestion of 200 mL of pure water increases late phase plasma GLP-1, while GIP secretion is unchanged (Herrmann et al., 1995), suggesting a GIP-independent and potentially mechanically-mediated increase in GLP-1.

Leptin increases GLP-1 secretion in fetal rat intestinal cells, GLUTag, and NCI-H716 human enteroendocrine cells, all of which express a functional leptin receptor in GLP-1+ cells (Anini and Brubaker, 2003). Leptin (1 mg/kg, *i.p.*) increases fasting GLP-1 secretion 1.8-fold compared to saline control, reaching 6 pmol/L at 120 min, which increases even further in leptin-deficient mice (*ob/ob*) (Anini and Brubaker, 2003). Therefore, leptin appears to induce the later phase of GLP-1 secretion compared to the early peak upon GIP treatment, which may be important for potentiating the leptin-stimulated reduction in food intake. Interestingly, leptin treatment significantly increases water intake in healthy rats (Sivitz et al., 1997), which may link the late-phase GLP-1 secretion induced by both leptin and water. Additionally, while high-fat fed mice with leptin resistance display increased GLP-1 content in the ileum and the colon, both fasting and glucose-stimulated GLP-1 secretion are significantly reduced in these mice (Anini and Brubaker, 2003), which may provide a link between leptin resistance in L cells and the reduced late phase (60–160 min) total and active GLP-1 secretion in patients with diabetes compared to healthy individuals (Vilsboll et al., 2001).

Similar to K cells, L cells also express the Galinin receptor, GAL_1, and its activation via Galinin treatment or GAL_1 agonist (M617) treatment prevents the accumulation of cyclic adenosine monophosphate (cAMP) in L cells within primary duodenal cultures in response to the adenylyl cyclase activator, forskolin and inhibits GLP-1 secretion from primary duodenal and ileal cultures (Psichas et al., 2016).

Inflammation and GLP-1 Secretion

Links between inflammation, the gut microbiota and GLP-1 secretion have also been reported (Everard et al., 2011; Greiner and Backhed, 2016; Wu et al., 2018; Covasa et al., 2019; Martchenko et al., 2020). Indeed, lipopolysaccharide (LPS) acutely induces GLP-1 secretion (Nguyen et al., 2014). This was demonstrated to be dose- and time-dependent, where LPS-induced increases in circulating IL-6 (30 min) preceded that of both total and active GLP-1 (120 min) (Kahles et al., 2014). LPS also stimulates the release of IL-1β, where the latter also increases plasma GLP-1 upon *i.p.* injection in mice to a greater extent than IL-6 injection (Kahles et al., 2014). However, loss of IL-1R signaling does not impact LPS-mediated GLP-1 secretion, as shown in $Il1r^{-/-}$ mice while neither LPS nor IL-1β stimulate GLP-1 secretion in $Il6^{-/-}$ mice (Kahles et al., 2014). Similarly, IL-6, but not LPS or IL-1β, increases GLP-1 secretion from GLUTag cells (Kahles et al., 2014). LPS induces GLP-1 secretion to the same extent in both the fasted and fed state, where not surprisingly, insulin is only increased in these mice during the fed state. While these data demonstrate the glucose-dependency for the insulinotropic role of GLP-1, they also reveal nutrient-independent GLP-1R signaling pathways (Kahles et al., 2014). Plasma total GLP-1 concentrations are significantly higher in patients with sepsis than non-septic ICU patients; these levels are positively associated with IL-6, C-reactive protein, and the association of GLP-1 with plasma insulin is lost (Kahles et al., 2014). Taken together, this study reveals an integral role for the gut in systemic inflammation in pathways that remain incompletely understood.

Hwang et al. (2015) demonstrate that the antibiotics, vancomycin and bacitracin decrease the abundance of both Bacteroidetes and Firmicutes, and increase Proteobacteria, which is associated with increased GLP-1 secretion and improved glucose tolerance and insulin resistance. *Coriobacteriaceae* are involved in the metabolism of bile acids. This family of bacteria are able to metabolize primary bile acids into secondary bile acids, which then bind to TGR5 and stimulate GLP-1 secretion (Allin et al., 2015). Fourteen weeks of HFD-feeding

supplemented with *Akkermansia muciniphila* significantly increases the ileal expression of *Gcg* and *Pcsk1,* and oral glucose-stimulated plasma GLP-1 compared to mice fed the HFD alone (Yoon et al., 2021). The cell-free supernatant from live *A. muciniphila* isolated from human feces significantly increases GLP-1 secretion from human enteroendocrine L cells (NCI-H716) in a dose-dependent manner and to a greater extent than the microbial products acetate and propionate (Yoon et al., 2021). Indeed, the authors identified, the protein P9 of the peptidase S41A family robustly increases GLP-1 secretion from human L cells *in vitro* and in mice after a single *i.p.* injection compared to saline control and injection of SCFA (Yoon et al., 2021). Mice fed a HFD supplemented with P9 display increased ileal *Gcg* and *Pcsk1* expression as well as compared to mice fed the HFD-alone (Yoon et al., 2021). HFD-fed mice supplemented with *A. muciniphila* also display increased ileal and colonic *Il-6* mRNA expression, and while IL-6 treatment in GLUTag cells does not stimulate GLP-1 secretion to the same extent as P9, co-treatment of IL-6 and P9 induces an additive effect (Yoon et al., 2021). Interestingly, P9 supplementation to a HFD does not increase plasma GLP-1 in $Il6^{-/-}$ mice (Yoon et al., 2021). A far lesser amount of studies have correlated populations of microbiota with GLP-2 secretion (Utzschneider et al., 2016). Already known to increase GLP-1 secretion, ingestion of *Lactobacillus reuteri* demonstrates increased GLP-2 secretion as well (Simon et al., 2015).

Exercise-Induced GLP-1 Secretion

Ninety minutes of exercise in mice induces a 2.5-fold increase in plasma active GLP-1, mediated by skeletal-muscle-derived IL-6, as shown by abolishing exercise-induced active GLP-1 levels in $Il6^{-/-}$ mice and by treating wild-type mice with an antibody to IL-6 (Ellingsgaard et al., 2011). Interestingly, injecting mice with 400 ng of recombinant mouse IL-6 twice daily for 7 days significantly increases fasting plasma active GLP-1, as well as ileal *Gcg* and *Pcsk1* mRNA, but not plasma GLP-2 (ELISA) or DPP4 activity (Ellingsgaard et al., 2011). Indeed, GLUTag cells express the IL-6 receptor, and IL-6 treatment increases GLP-1 secretion in a dose-dependent manner, where acute IL-6 treatment increases GLP-1 exocytosis in a JAK2-STAT3-dependent manner, and chronic IL-6 treatment increases GLP-1 content and glucose uptake in a sodium glucose transporter 1-dependent manner in the L cell (Ellingsgaard et al., 2011). Surprisingly, despite increasing *Gcg* mRNA, chronic IL-6 treatment does not increase plasma GLP-2 levels suggesting a difference in GLP-1 and GLP-2 transcript or protein stability.

RECEPTOR EXPRESSION WITHIN THE GASTROINTESTINAL TRACT

GPCRs initiate the cellular responses to nearly all hormones and neurotransmitters; they are grouped into six main classes (A to F) by sequence homology and function. GCPRs have 7 transmembrane helices, and in the cases of GIPR, GLP-1R and GLP-2R, signal via Gs-mediated cAMP production and downstream signaling cascades. They are all class B1 GPCRs, share significant sequence similarity (Usdin et al., 1993) and form secretin-VIP receptor family (Campbell and Scanes, 1992).

GIPR Expression

The human GIP receptor (GIPR) gene is ∼13.8 kb long containing 14 exons. The receptor is 466 amino acids in length, including a signal peptide and 7 transmembrane domains; the gene contains 14 exons (Yamada et al., 1995). The first 92 bp of the *GIPR* gene contains 88% sequence identity between rat and human; interestingly, neither promoter regions contains a TATA box (Boylan et al., 2006). MZF1/Sp1-C (−75), Sp1-B (−57), and Sp1-A (−45) transcription factor binding sites were identified using radiolabeled synthetic probes and confirmed with CHiP analysis (Boylan et al., 2006). Indeed, sequence deletion between −85 and −40 decreases promoter activity by 88% (Boylan et al., 2006).

The identification of cell-specific expression of *Gipr* in the gastrointestinal tract remains largely unsolved; however, clues are beginning to emerge. On a whole tissue level, *Gipr* mRNA is expressed in rat stomach, duodenum, and proximal small intestine (Usdin et al., 1993; Coon et al., 2013). *GIPR* mRNA expression is detected in neuroendocrine tumors isolated from the small bowel and colorectal tumors (Sherman et al., 2013; Koehler et al., 2015) (**Table 1**). GIPR is faintly detected at the protein level at multiple sizes (50, 55, 60, and 70 kDa) in jejunal mucosal cells compared to the strong signal at 50 kDa in pancreatic homogenates (Coon et al., 2013). In this same study, GIPR immunohistochemistry demonstrated positive staining beneath the basolateral surface of epithelial cells of the proximal jejunum (Coon et al., 2013). In the stomach, RNAseq of purified gastric somatostatin-producing D-cells from SST-Cre.ROSA26^{EYFP} mice reveal *Gipr* expression in these cells (Adriaenssens et al., 2015). A number of distinct neuronal populations also express the *Gipr* (Adriaenssens et al., 2019). Genetic elimination of *Gipr* in hematopoietic cell lineages, including endothelial cells ($Gipr^{Tie2-/-}$ mice) does not impact jejunal *Gipr* mRNA (Pujadas et al., 2020).

GLP-1R Expression in the Gut

The transcriptional start site of the GLP-1R does not contain a TATA- or a CAAT-box element, however, it contains 3 putative Sp1 binding sites (Lankat-Buttgereit and Goke, 1997). Within the 350 bp region, 74% of the sequence is GC nucleotides (Lankat-Buttgereit and Goke, 1997). *Glp1r* expression determined by RNAscope *in situ* hybridization reveals the highest expression in duodenal Brunner's glands and in stomach gland parietal cells (Wismann et al., 2017). Consistent with this use of a reporter mouse together with a number of validation approaches the GLP-1R was identified in chief cells, parietal cells and Brunner's glands (Andersen et al., 2021). A well-validated antibody to the GLP-1R (MAb 3F52) and corroborated with ^{125}I-labeled GLP-1 also demonstrated a strong signal in stomach parietal cells, basolateral epithelial cells in the duodenum, Brunner's glands and the myenteric nerve plexus (Pyke et al., 2014). *Glp1r* expression localizes to the basolateral side of enterocytes in the mucosal layer, and its abundance increases distally (Wismann et al., 2017). *Glp1r* mRNA is higher in mucosal cells from the ileum

TABLE 1 | Summary of methods used to identify GIPR expressing cells within the gastrointestinal tract.

Cell/organ	Species	Method of identification	References
Small bowel neuroendocrine tumors	Human	*GIPR* mRNA qRT-PCR analysis	Sherman et al., 2013
Human colorectal tumors	Human	*GIPR* mRNA qRT-PCR analysis	Koehler et al., 2015
Human hypothalamic cells (vascular, glial, neuronal cells)	Human	Single-cell RNA sequencing of GIPR+ cells	Adriaenssens et al., 2019
T-cells, myeloid cells, myeloid precursors	Mouse	*Gipr* mRNA RT-qRT-PCR analysis	Pujadas et al., 2020

and colon than in the non-epithelial fraction (Kedees et al., 2013). Conversely, *Glp1r* mRNA expression is highest in the jejunum within the epithelial fraction, followed by ileum then colon (Kedees et al., 2013). *Glp1r* is not detected in GLP-1+ cells (L cells) (Grigoryan et al., 2012); however, it is detected in chromogranin A+ enteroendocrine cells (Kedees et al., 2013; Andersen et al., 2021). *Glp1r* is also detected in Paneth cells, identified by lysozyme expression, in the jejunum and ileum crypts but not colon, distinct from proliferating Ki67+ cells (Kedees et al., 2013). *Glp1r* mRNA expression increases with age from 2 to 12 weeks in murine jejunum, ileum, and colon (Campos et al., 1994). Additionally, *Glp1r* expression in mice is detected in a subset of neurons of the myenteric and submucosal plexus (Andersen et al., 2021) that also express the neuron cytoplasmic protein 9.5 (PGP9.5) (Kedees et al., 2013) (**Table 2** and **Figure 1**).

Studies using the mouse *Glp1r* promoter to drive expression of a fluorescent reporter protein reveal *Glp1r* expression in the antral area of the stomach (near the gastric pylorus) as a fibrous signal that does not overlap with smooth muscle α-actin (αSMA) (Richards et al., 2014). *Glp1r* expression is also observed in the arteries and arterioles of the intestine and colocalizes with αSMA and the pericyte marker NG2 (Richards et al., 2014) (**Figure 1**). In this model, *Glp1r* fluorescence is absent from the epithelial layer. Instead, mRNA expression is detected in myenteric ganglia in the intestinal mucosa, which are excitable by GLP-1 treatment *ex vivo* (64% synaptic and 36% after-hyperpolarizing types) (**Figure 1** and **Table 2**). Indeed, 63% of *Glp1r*-fluorescent neurons in primary small intestinal cultures and 19% in colonic cultures are neuronal nitric oxide synthase (nNOS) positive markers for inhibitory motor neurons (Richards et al., 2014). GLP-1 receptors are expressed in the enteric nervous system and in the vagus nerve (Grasset et al., 2017), which allow for the activation of the gut-brain-periphery axis. As such, the presence of GLP-1R+ cell bodies in the enteric nervous system has been proposed to provide the signaling route to the central nervous system (CNS) required for distally secreted GLP-1. Consistent with *Glp1r* mRNA expression, immunofluorescence analyses in Glp1r.tdTomato reporter mice reveal GLP-1R expression in various enteroendocrine cells (**Table 1**), but not GLP-1+ cells (Andersen et al., 2021). Sequential collagenase digestion of the gut reveals *Glp1r* expression to be within the epithelial fraction instead of crypt, mesenchyme, or smooth muscle layer fractions (Yusta et al., 2015). Within the epithelial compartment of the small intestine, intraepithelial lymphocytes (IELs) (both the Tαβ and Tγδ subsets) express *Glp1r* (Yusta et al., 2015; He et al., 2019) (**Figure 1** and **Table 2**). Additionally, GLP-1R-expressing αβ and γδ T cells transit to the gut via integrin B7 (*Itgb7*) (He et al., 2019). Indeed, IELs encode a functional GLP-1R as exendin-4 treatment in sorted activated and non-activated IELs increases cAMP levels. However, GLP-1R in IELs is not required for IEL development or recruitment to the gut as their abundance does not change in response to GLP-1R agonist treatment or in $Glp1r^{-/-}$ mice (Yusta et al., 2015). These receptors are functional as mice receiving exendin-4 *i.v.* exhibit an 84% increase in *c-fos* mRNA expression in the ileal mucosa (Kedees et al., 2013). The increased c-fos expression occurs in neurons as it is abolished upon co-treatment with tetrodotoxin, a voltage-gated sodium current blocker. Additionally, exendin-4 treatment increases *c-fos* expression in in GLP-1R+ Paneth cells (**Figure 1**), which is abolished when exendin-(9–39) is administered prior to exendin-4 treatment (Kedees et al., 2013).

GLP-2R Expression in the Gut

The human GLP-2 receptor is localized to chromosome 17p13.3 and encodes a 550 amino acid G protein-coupled receptor, processed to become a 486 amino acid receptor (Munroe et al., 1999). The gene at chromosome 17p13.3 encoding for the human GLP-2 receptor is also very well conserved as the rat sequence is 80% of the same amino acid sequence (Shin et al., 2005). The GLP-2 receptor is 14 exons long and has seven transmembrane domains and, although similar in amino acid sequence to both the glucagon and GLP-1 receptor, only recognizes GLP-2 and not related members of the glucagon family (Drucker and Yusta, 2014).

GLP-2R is expressed in the gastric mucosa in a subpopulation of fundas gland cells (Li et al., 2017) (**Table 3**). In the rat jejunum, *Glp2r* expression as a percentage of the expression in intact intestine is 0.07, 33, 256, and 392% in the epithelium, mucosa, smooth muscle layer, and the intestine devoid of epithelium, respectively (Pedersen et al., 2015). GLP-2R transcripts are expressed in human colorectal tumors (Koehler et al., 2015) and GLP-2R protein is expressed in human colon neoplasms (Koehler et al., 2008) (**Table 3**). In rats, mice, marmosets and human intestinal tissue, GLP-2R localizes to cells residing immediately below the basolateral membrane of enterocytes, which are subepithelial myofibroblasts as marked by αSMA (Orskov et al., 2005) (**Figure 1** and **Table 3**). *Glp2r* expression is most abundant in the lamina propria of duodenal and jejunal villi (Wismann et al., 2017), where in the jejunum its expression within the lamina propria stromal cells predominate in the upper half of villi (Yusta et al., 2019) (**Figure 1**). The receptor's location in the lamina propria is consistent with evidence that suggests the link between GLP-2 to KGF, IGF-1, and ErbB, as these growth factors are produced and secreted from stromal cells found in the lamina propria (Yusta et al., 2019). GLP-2R protein in neonatal pigs colocalizes with chromogranin A+

TABLE 2 | Summary of methods used to identify GLP-1R expressing cells within the gastrointestinal tract.

Cell/organ	Species	Method of identification	References
Human colorectal tumors	Human	*GLP-1R* expression (qRT-PCR analysis of RNA).	Koehler et al., 2015
Intestinal intraepithelial lymphocyte (IEL)	Mouse	*Glp-1r* Real-time qRT-PCR (mRNA), immunohistochemistry (rabbit polyclonal anti-CD3 antibody and hematoxylin). Used GLP-1R$^{-/-}$ model. *Glp-1r* transcript identified in isolated RNA (qRT-PCR), southern blot detects *Glp-1r* PCR product.	Yusta et al., 2015
Synaptic type neurons	Mouse	GLP-1R fluorescent cell population. Whole cell current clamp.	Richards et al., 2014
After-hyperpolarizing type neurons	Mouse	GLP-1R fluorescent cell population. Whole cell current clamp.	Richards et al., 2014
Inhibitory motor neurons	Mouse	Immunostained for nNOS (marker mainly restricted to inhibitory motor neurons), most GLP-1R fluorescent neurons were nNOS+.	Richards et al., 2014
Intrinsic primary afferent neurons	Mouse	GLP-1R-fluorescent cells in culture stained for Calretinin (marker for intrinsic primary afferent neurons)	Richards et al., 2014
Vagal afferent neurons	Mouse	GLP-1R-fluorescent cells. Immunostained for RFP.	Richards et al., 2014
Intraepithelial lymphocytes	Mouse	*Glp1r.tdTomato* reporter mouse. ISH of GLP-1R and tdTomato expression. *Glp-1r* mRNA *in situ* hybridization.	Andersen et al., 2021
Neurotensin+ N-cells, Somatostatin+ D-cells, PYY+ L-cells, serotonin+ enterochromaffin cells (EC)	Mouse	*Glp1r.tdTomato* reporter mouse. ISH of GLP-1R and tdTomato expression. *Glp-1r* mRNA *in situ* hybridization.	Andersen et al., 2021
Mucus cells (antrum)	Mouse	*Glp1r.tdTomato* reporter mouse. ISH of GLP-1R and tdTomato expression. *Glp-1r* mRNA *in situ* hybridization.	Andersen et al., 2021
Parietal cells	Mouse	Td.Tomato-positive cells. ISH of GLP-1R and tdTomato expression. *Glp-1r* mRNA *in situ* hybridization.	Andersen et al., 2021
Chief cells	Mouse	Td.Tomato-positive cells. Immunohistochemistry.	Andersen et al., 2021
αβ, γδ T cells	Mouse	Expression of *Glp-1r* (mRNA).	He et al., 2019
Myenteric neurons	Mouse	*Glp1r*-CRE fluorescent reporter.	Richards et al., 2014
Neurons of the myenteric and submucosal plexus	Mouse	Expression of *Glp-1r* (mRNA). Immunohistochemistry.	Kedees et al., 2013
Brunner's gland (duo)	Mouse	Glp-1r.tdTomato signal. ISH of GLP-1R and tdTomato expression. *Glp-1r* mRNA *in situ* hybridization.	Andersen et al., 2021
Parietal cells Brunner's gland	Monkey	MAb 3F52.	Pyke et al., 2014
Parietal cells Brunner's glands	Mouse	RNAScope *in situ* hybridization.	Wismann et al., 2017
Myenteric nurons	Monkey	MAb 3F52	Pyke et al., 2014
Epithelial cells	Mouse	Expression of *Glp-1r* (mRNA). Immunohistochemistry.	Kedees et al., 2013
Basolateral epithelial cells	Monkey	MAb 3F52.	Pyke et al., 2014

enteroendocrine cells in the jejunal villus (∼58%) and crypt epithelium (60%) (Guan et al., 2006) (**Table 3**). A rat polyclonal antibody localized using immunohistochemistry the GLP-2R to vagal afferents, enteric neurons, enteroendocrine cells, and myenteric plexus nerve fibrils (Nelson et al., 2007). Isolated rat intestinal mucosal cells expressing *Glp2r* transcripts also expressed markers for enteroendocrine or neural cells (Walsh et al., 2003) (**Table 3**). Isolated Human GLP-2R protein also colocalizes to chromogranin A+ enteroendocrine cells in both the villus and crypt epithelium (Guan et al., 2006). Human GLP-2R protein colocalizes to 5-HT-containing cells in the epithelium, a neurotransmitter released by enteroendocrine cells (Guan et al., 2006). Human VIP+ enteric neurons in the submucosal plexus and myenteric plexus express the GLP-2R (Guan et al., 2006) (**Table 3**). In the mouse duodenal myenteric plexus, ∼18% of GLP-2R+ are nNOS+, 10% are vasoactive intestinal polypeptide

(VIP)+, ∼71% are choline-acetyltransferase (ChAT)+, and 27% are SP+ (Cinci et al., 2011) (**Figure 1** and **Table 3**). In the submucosal plexus, only SP+ cells were GLP-2R+ (Cinci et al., 2011) (**Figure 1** and **Table 3**). Human eNOS+ enteric neurons in the submucosa also express the GLP-2R, supporting a direct role for GLP-2-mediated increase in eNOS protein and NOS release through cAMP-dependent protein kinase A (Guan et al., 2006) (**Table 3**).

DISTINCT AND OVERLAPPING FUNCTIONAL ROLES OF GIPR, GLP-1R, AND GLP-2R

Regulation of Post-prandial Lipid Metabolism

Spearman correlations between GLP-1, GLP-2, GIP, and TG responses in plasma during an oral fat tolerance test in obese men reveal a small albeit significant positive correlation (*r*-squared values close to zero) between all three hormone area under curves (AUCs) for TG and apoB48 (Matikainen et al., 2016). In this study, these gut hormones display small contributions to explaining the variance in TG AUC, where instead fasting TG values serve as the largest contributor for explaining this variance (Matikainen et al., 2016). Still, the high concentrations of GLP-1, GLP-2, and GIP within the gut circulation relative to systemic circulation suggest that endogenous gut hormone action on chylomicron secretion may be local and underestimated.

GIP Receptor (GIPR)

Chronic reduction in GIP secretion reduces obesity and insulin resistance in high-fat fed mice (Nasteska et al., 2014). Interestingly, dietary fat absorption and intestinal-TG secretion are unchanged upon K cell destruction (Pedersen et al., 2013; Holst et al., 2016). Similarly, GIP infusion *i.v.* does not impact TG levels (Holst et al., 2016). Rather, GIP has been shown to increase circulating lipid clearance via an increase in adipose tissue blood flow. GIPR antagonist, GIP(3–30)NH2, and GIP co-infusion in lean individuals prevented a fivefold increase in adipose tissue blood flow induced by GIP infusion alone (Asmar et al., 2017). Additionally, both TG and glucose uptake decrease in response to GIP(3–30)NH2 alone and GIP co-infusion compared to GIP infusion alone (Asmar et al., 2017).

Co-administration of triton-WR1339 infusion and D-Ala2-GIP injection 20 min following oil gavage in mice significantly increases TG accumulation in plasma at 60 and 90 min, and ApoB-48 levels at 90 min compared to PBS control (Hsieh et al., 2010), suggesting a role for GIP in plasma TG independent of triglyceride rich lipoprotein (TRL) clearance. Additionally, selective deletion of *Gipr* in brown adipose tissue significantly increases both fasting (overnight) and fed (1h re-feed) TG levels of high-fat fed mice (Beaudry et al., 2019). Furthermore, acute lipid challenges in $Gipr^{BAT-/-}$ mice fed a high-fat diet for 8–10 weeks housed at room temperature reveal significantly increased TG excursion, an effect lost upon 28 weeks of high-fat feeding (Beaudry et al., 2019). GIP, in the presence of insulin, increases LPL gene expression in 3T3-L1 adipocytes via PKB/LKB1/AMPK signaling (Kim et al., 2007a) mediated by resistin (Kim et al., 2007b) and in human adipocytes by increasing TORC2 and phospho-CREB nuclear localization to bind to the CRE-II promoter region (Kim et al., 2010). GIP infusion significantly increases LPL activity in obese (*fa/fa*) and lean (*fa/-*) VDF Zucker rats (Kim et al., 2007a). Conversely, treatment of rats with the GIPR antagonist, rat GIP (3–30)NH2, does not modify food intake but significantly increases plasma TG and LPL compared with controls (Baldassano et al., 2019). Alternatively, D-Ala2-GIP treatment significantly reduces serum LPL activity in both chow- and high-fat diet-fed mice (Szalowska et al., 2011). However, the significance of endogenous GIP secretion as a dominant regulator of LPL secretion is uncertain. In humans, intravenous infusion of a somatostatin analog, octreotide, 30 min prior to carbohydrate meal (Hycal) significantly impairs insulin, GLP-1, and GIP secretion in both lean and obese women, yet post-heparin LPL activity (contributions from adipose, skeletal and cardiac tissue) is unchanged 1.5 h post-peak insulin in lean and obese women (Ranganath et al., 1999). Therefore, suppression of insulin, GIP, and GLP-1 does not impact plasma LPL activity following oral carbohydrate.

GLP-1R

High-fructose feeding for 10 days in hamsters significantly increases plasma TG and cholesterol levels (Hsieh et al., 2010), where only the former can be significantly decreased after 3 weeks of systemic DPP4 inhibition (sitagliptin). This treatment paradigm reduces post-prandial TRL-fraction TG levels and ApoB48 production (Hsieh et al., 2010). Acute sitagliptin administration to chow-fed mice significantly reduces plasma cholesterol and TG at 90 min post-triton infusion and oil gavage (Hsieh et al., 2010). Co-administration of triton by infusion and exendin-4 by injection 20 min following oil gavage in mice significantly decreases TRL-fraction TG accumulation at 90 min, and ApoB48 levels at 60 and 90 min, an effect significantly reversed by the co-administration of GLP-1R antagonist exendin(9–39) 20 min prior to gavage (Hsieh et al., 2010). While sitagliptin and exendin-4 significantly increase plasma insulin levels 5-min post injection, these levels are not significantly different from PBS control after 20 min, suggesting that the GLP-1 mediated reduction in intestinal-TG secretion is independent of the incretin effect. Indeed, the authors show that in co-administration of insulin injection and triton infusion 20 min post-olive oil gavage in mice does not significantly change the accumulation of TG in plasma (Hsieh et al., 2010). This effect is significant given the studies in humans where acute insulin treatment inhibits intestinal lipoprotein secretion in response to hourly meals, an effect partially lost upon concomitant Intralipid and heparin infusion (Pavlic et al., 2010), suggesting mediation by FFA. Exendin-4 decreases TG and cholesterol in the VLDL/chylomicron fraction of chow-fed hamsters while a GLP-1R antagonist increases ApoB48 accumulation 120 min-post oil in chow-fed hamsters (Hsieh et al., 2010). Despite similar gastric emptying rates between $Glp1r^{-/-}$ mice wild-type controls (Baggio et al., 2004), $Glp1r^{-/-}$ mice display significantly increased TG accumulation in plasma and the TRL fraction

TABLE 3 | Summary of methods used to identify GLP-2R expression throughout the gastrointestinal tract.

Cell/organ	Species	Method of identification	References
Human colorectal tumors	Human	*GLP-2R* mRNA transcripts expressed qRT-PCR.	Koehler et al., 2015
Human colon neoplasms	Human	Immunohistochemistry.	Koehler et al., 2008
Gastric chief cells	Human	GLP-2R Fluorescence ISH. GLP-2R by western blot.	Li et al., 2017
Myenteric plexus	Human	*In vitro* receptor autoradiography of human intestinal tissue.	Pedersen et al., 2015
Lamina propria stromal cells	Mouse	ISH with RNAscope, *Glp-2r* mRNA detected. GLP2R-driven LacZ expression.	Yusta et al., 2019
Vagal afferents	Rat	GLP-2R antibody localizing GLP-2R immunoreactivity. ISH.	Nelson et al., 2007
Intestinal muscularis	Mouse	*Glp-2r* mRNA transcripts by RT-PCR.	Shin et al., 2005
Jejunal enteroendocrine cells	Pig	*Glp-2r* mRNA transcripts by qRT-PCR of laser micro-dissected tissue. *In situ* hybridization. Immunostaining.	Guan et al., 2006
Subepithelial myofibroblasts	MouseRatMouse	*Glp-2r* mRNA expression by qRT-PCR. Immunohistochemistry (antibody 99077).	Orskov et al., 2005
Subepithelial myofibroblasts	MouseRatMouse	*Glp-2r* mRNA expression by qRT-PCR. Immunohistochemistry (antibody 99077).	Orskov et al., 2005
Isolated intestinal mucosal cells	Rat	GLP-2R mRNA transcripts by RT-PCR.	Walsh et al., 2003
Lamina propria of duodenal and jejunal villi, submucosal nerve plexuses	Mouse	RNAScope *in situ* hybridization.	Wismann et al., 2017
Smooth muscle layer, intestine devoid of epithelium, respectively	Rat	*Glp-2r* mRNA expression by qRT-PCR.	Pedersen et al., 2015

as well as TRL ApoB48 post-oil gavage (Hsieh et al., 2010). Furthermore, pulse-chase experiments in primary suspended villi from chow-fed hamsters reveal that exendin-4 does not change cellular ApoB48 levels, but significantly decreases ^{35}S-labeled ApoB48 secretion in the media (Hsieh et al., 2010).

Patients with type 2 diabetes treated with metformin and the GLP-1R agonist exenatide for 1 year display significantly reduced circulating TG, apoB48, and FFA following an early meal (50 g of fat, 75 g of carbohydrates, 35 g of protein). Interestingly, TG and apoB48 levels rapidly rise in the 2 h following the second meal in these patients to levels similar as pre-treatment responses (Bunck et al., 2010). In patients with recent-onset type 2 diabetes, subcutaneous injection of exenatide immediately prior to meal consumption (5,384 kJ) significantly reduces serum insulin at 2, 4, 6, and 8 h post-meal (Schwartz et al., 2010). Moreover, exenatide reduces post-meal serum TG and remnant lipoprotein TG at 2-, 4-, and 6-h post-meal, in particular preventing the 4-h peak in TG seen in placebo controls (Schwartz et al., 2010). Plasma remnant lipoprotein cholesterol is also significantly reduced 4 h post-meal in these patients (Schwartz et al., 2010). Similarly, exenatide significantly reduces serum apoB48 levels throughout the 8-h sampling period (Schwartz et al., 2010). Meal-induced increases in plasma apoCIII are also prevented by exenatide (Schwartz et al., 2010). Two weeks of exenatide treatment twice daily, 1 h before morning and evening meals, significantly reduces plasma TG following these meals (∼50% carbohydrate, 20% protein, and 30% fat) compared to placebo but TG levels rise to similar levels as placebo following the midday meal, where no changes in post-prandial FFA concentrations are observed (Schwartz et al., 2008). Exenatide treatment and co-infusion of d3-leucine 5 h after starting continuous infusion of lipid/carbohydrate formula in healthy fasted humans via nasoduodenal tube 2 h after starting a pancreatic clamp does not significantly affect plasma TG, FFA, or TRL-TG compared to placebo (Xiao et al., 2012). However, this treatment paradigm demonstrates the acute reduction in apoB48 concentrations in the TRL fraction for 10 h post-injection (−37%) compared to placebo controls with a significant decrease in apoB48 production rate, no change in fractional catabolic rate, and no changes in hepatic apoB100 levels were observed (Xiao et al., 2012). Still, the precise mechanisms through which GLP-1R signaling controls post-prandial lipid metabolism remain unclear.

Genetic elimination of *Itgb7* in mice decreases the expression of *Glp1r* on αβ and γδ T cells yet increases fasting plasma GLP-1, intestinal *Gcg* mRNA expression, and ileal L cell abundance (He et al., 2019). Interestingly, these mice display improved lipid tolerance (He et al., 2019). *In vitro* experiments reveal GLP-1 concentration in media after 24 h of co-incubation of GLUTag cells with αβ and γδ T cells negatively associate with the level of *Glp1r* expression in the latter cells (He et al., 2019). Moreover, high *Glp1r* expressing αβ and γδ T cells can further decrease GLP-1 concentration in media from GLUTag cells in the presence of exendin-4, suggesting that *Glp1r*-expressing αβ and γδ T cells act as a sink for local GLP-1 production (He et al., 2019). Additionally, this supports the increased circulating GLP-1 levels observed in $Glp1r^{-/-}$ mice (Lamont et al., 2012), albeit the intact receptor is required for improved post-prandial lipid tolerance. These results are replicated *ex vivo*, where media GLP-1 concentration from ileal tissue from $Itgb7^{-/-}$

mice is significantly higher than in the media from wild-type tissue, and this increase can be replicated in wild-type tissue upon GLP-1R antagonist (exendin-9) treatment (He et al., 2019). Overall, this additional pool of GLP-1 during fasting clearly plays an important role in GLP-1R-mediated control of circulating lipoproteins, suggesting that the circuit engaged occurs within the gut.

GLP-2R

Subcutaneous injection (15,000 μg) of GLP-2 5 h after the start of a liquid mixed macronutrient formula infusion through a nasoduodenal tube in healthy men significantly increases peak plasma TG and TRL-apoB48 at 1 h and area under the concentration curve for the first 3 h of treatment (Dash et al., 2014). GLP-2 does not increase TRL apoB48 by increasing the synthesis of new particles, nor does it decrease the clearance of TRL apoB48, rather, GLP-2 stimulates the release of pre-formed TRL apoB48 during the first hour of treatment (Dash et al., 2014). Similarly, GLP-2 treatment significantly increases plasma TG, TRL-TG, TRL retinyl palmitate, and retinyl palmitate in the chylomicron fraction for 2 h when administered 7 h after a meal containing retinyl palmitate (Dash et al., 2014).

Glp2r$^{-/-}$ mice display increased fasting and 10 min post-olive oil gavage plasma active GLP-1 compared to wild-type controls, despite similar fasting DPP4 activity levels in circulation (Fuchs et al., 2020). Accordingly, plasma-TG excursion following the olive oil gavage is not significantly different from wild-type controls, although trends for decreased secretion are observed (Fuchs et al., 2020). When administered 20 min after the oil gavage, GLP-2 increases TRL-TG and TRL-cholesterol 3.5- and 3-fold, respectively, in hamsters (Hsieh et al., 2009). Radiolabeled gavage experiments (^{3}H-triolein) reveal that GLP-2 increases the radiolabel incorporation into plasma TG at 60- and 90-min post-gavage with no differences observed in plasma cholesterol compared to control (Hsieh et al., 2009). Similar to hamsters, GLP-2 treatment significantly increases plasma TG concentration at 60- and 90-min post-oil gavage as well as TG and apoB48 accumulation in the chylomicron fraction of plasma in the presence of triton WR-1339 (blocking lipoprotein catabolism) (Hsieh et al., 2009). GLP-2 does not increase the protein expression of FATP4 or MTP, rather it significantly increases the expression of glycosylated CD36. CD36 localizes to the apical membrane of enterocytes found on the tips of jejunal villi (Hsieh et al., 2009). Assessing the requirement of CD36 for GLP-2-mediated increases in intestinal-TG secretion are complicated by the increased fatty acid absorption (as shown by appearance of radiolabel in plasma), TRL-TG and TRL-apoB48 secreted by *Cd36*$^{-/-}$ mice compared to wild-type controls (Hsieh et al., 2009). Still, GLP-2 does not increase TRL-TG or TRL-apoB48 secretion in *Cd36*$^{-/-}$ mice compared to saline control (Hsieh et al., 2009). ^{35}S-methionine pulse-chase experiments of jejunal fragments isolated hamsters 1 h after an olive oil gavage reveal that GLP-2 treatment *ex vivo* increases the secretion of the radiolabelled-apoB48 into the media with unchanged cellular concentrations. However, since the GLP-2 treatment *ex vivo* was for 45 min (Hsieh et al., 2009), and that GLP-2 treatment rapidly induces the mobilization of pre-formed chylomicrons by 1 h treatment in humans (Dash et al., 2014), this increase in apoB48 synthesis may be driven by clearing the preformed particles earlier than vehicle controls. Still, this experiment demonstrates that GLP-2R-expressing cell(s) mediating this indirect increase reside near enterocytes in these jejunal fragments. As previously mentioned, GLP-2 increases intestinal blood flow and stimulates the expression of intestinal endothelial nitric oxide synthase (eNOS) (Guan et al., 2003). Inhibiting nitric oxide synthase with L-NAME does not impact intestinal-TRL secretion in hamsters (Hsieh et al., 2015), likely due to the lymphatic fate of these particles. Still, preventing GLP-2-mediated increases in portal and intestinal blood flow via L-NAME, blocks the GLP-2-mediated increase in apoB48 in the TRL fraction of plasma (Hsieh et al., 2015). Mice lacking endothelial nitric oxide synthase (*eNOS*$^{-/-}$ mice) display normal radiolabel appearance into plasma as wild-type controls, however, GLP-2 treatment in these mice did not increase plasma ^{3}H compared to treatment in wild-type mice (Hsieh et al., 2015). ApoB48 in the TRL fraction is significantly lower in *eNOS*$^{-/-}$ mice compared to wild-type mice, independent of GLP-2 treatment (Hsieh et al., 2015). Additionally, jejunal TG mass is significantly greater in *eNOS*$^{-/-}$ mice compared to wild-type mice, again independent of GLP-2, suggesting that eNOS is involved in the release of stored TG as large chylomicrons rather than absorbed dietary TG and this is upregulated by exogenous GLP-2 (Hsieh et al., 2015). Indeed, GLP-2 treatment 5 h after 200 μL of intraduodenally administered olive oil significantly increases TRL-TG, which is inhibited by co-treatment with L-NAME. Similar to acute L-NAME treatment, L-NAME treatment alone 5 h post-oil does not change TRL-TG secretion compared to saline control (Hsieh et al., 2015), suggesting that GLP-2 may influence the partitioning of dietary fatty acids from lymph to portal circulation or that endogenous gut-hormone action by GLP-1R and/or GIPR maintains normal intestinal-TRL secretion. GLP-2 rapidly increases lymph flow and cumulative lymph volume in cannulated rats 300 min after an intraduodenal bolus of Intralipid 20% (Stahel et al., 2019). GLP-2 does not significantly change lymph TG concentration, TG output (mL TG per hour) or chylomicron size (TG:apoB48) compared to placebo control, rather it increases the cumulative increase in lymph TG in 60 min (Stahel et al., 2019).

Regulation of Intestinal Growth and Response Injury

GLP-1R

Interestingly, *Gcgr*$^{-/-}$ mice have increased circulating GLP-1 and GLP-2 (Gelling et al., 2003; Ali et al., 2011; Grigoryan et al., 2012). Unsurprisingly, *Gcgr*$^{-/-}$ mice have significantly increased small and large intestinal length and weight due to the elevated levels of gut-derived hormones (Koehler et al., 2015). Consistent with this, co-administration of the GLP-2R agonist h(Gly^{2})GLP-2 and exendin-4 increases small intestinal weight and length to a greater extent compared to the agonists administered alone (Koehler et al., 2015). However, using *Gcgr*$^{-/-}$:*Glp2r*$^{-/-}$ mice, the authors demonstrate that GLP-1R signaling can still increase small intestinal length and weight compared to wild

type, although not to the same extent as in *Gcgr*$^{-/-}$ mice (Koehler et al., 2015). However, despite these potent effects, increased large bowel weight and length in *Gcgr*$^{-/-}$ mice appears to be driven by GLP-1R signaling as these parameters are unchanged in *Gcgr*$^{-/-}$:*Glp2r*$^{-/-}$ mice (Koehler et al., 2015). Therefore, the trophic effects of GLP-1R signaling appear to target the distal gut (small intestinal length, large bowel length and weight) (Koehler et al., 2015). Indeed, exendin-4 and liraglutide treatment for 1 week increases small intestinal length and weight as well as large intestinal weight in wild-type mice but not in *Glp1r*$^{-/-}$ mice (Koehler et al., 2015). *Glp1r*$^{-/-}$ mice lose significantly more weight, exhibit significantly increased disease activity scores and greater colon damage than wild-type controls in response to DSS-induced colitis (Yusta et al., 2015). Unlike GLP-2, which increases crypt cell proliferation and villus elongation (Drucker and Yusta, 2014) exendin-4 treatment does not enhance crypt-cell proliferation, which was demonstrated by BrDU labeling and measuring crypt depth (Koehler et al., 2015). Instead, chronic treatment of exendin-4 increases crypt number in the proximal intestine and colon, leading to increased intestinal circumference and length (Koehler et al., 2015). The authors demonstrate that GLP-1R agonist treatment induces expression of tyrosine kinase IGF1R/ErbB (EGFR) pathways, however, agonist treatment can still increase intestinal growth in the absence of intestinal epithelial IGF1 receptor as well as EGF receptor signaling (Koehler et al., 2015). Acute, but not chronic, exendin-4 treatment increases *Fgf7* mRNA expression in the small intestine (Koehler et al., 2015). The intestinotrophic effects of exendin-4 are lost in *Fgf7*$^{-/-}$ mice, effects that were not observed upon GLP-2 treatment in these mice (Koehler et al., 2015). Despite the role of IELs in mediating intestinal mucosal repair through Fgf7/KGF (Boismenu and Havran, 1994), reconstituting *Glp1r*+ IELs into *Glp1r*$^{-/-}$ mice via bone marrow transplant does not rescue the intestinotrophic effects of exendin-4 in these mice (Koehler et al., 2015).

Plasma GLP-1 levels increase in response to intestinal injury or mucosal inflammation (Zietek and Rath, 2016). IELs protect the epithelial barrier by promoting pathogen clearance and lysing pathogen-infected cells (Cheroutre et al., 2011). Treatment with exendin-4 significantly attenuates proinflammatory cytokines IL-2, IL-17a, interferon γ, tumor necrosis factor-α mRNA and protein in IELs activated by immobilized anti-CD3 and soluble anti-CD28, an effect partially blocked by GLP-1R antagonist exendin (9–39) (Yusta et al., 2015). Colonic mRNA expression analysis in *Glp1r*$^{-/-}$ mice at baseline reveal significant reductions in trefoil factor (*Tff-1* and -2), transforming growth factor (*Tgf-b1* and *Tgf-3*), epidermal growth factor receptor (*Egfr*), keratinocyte growth factor (*Fgf7*), hepatocyte growth factor (*Hgf*) (epithelial protection and repair), *Il6, Il1b* (innate immune response), *Il12b* (inflammation) (Yusta et al., 2015). Upon dextrane sulfate (DS)-induced colitis, colonic *Tff2, Tff3, Tgfb1,* and *Tgfb3* mRNA levels are significantly lower in *Glp1r*$^{-/-}$ mice compared to wild-type controls (Yusta et al., 2015). By contrast, colonic *Tgfb2* and *Ifng* mRNA levels are significantly higher in *Glp1r*$^{-/-}$ mice compared to wild-type controls (Yusta et al., 2015). Genes involved in innate immunity and inflammation, which are lower in *Glp1r*$^{-/-}$ at baseline, increases in both WT and *Glp1r*$^{-/-}$ in DSS-induced colitis, but differences between genotypes are lost (Yusta et al., 2015). Bone marrow transplantation, and therefore re-establishment of wild-type IELs in the intestinal mucosa, from wild-type donor mice to wild-type and *Glp1r*$^{-/-}$ recipient mice, normalizes colonic gene expression in response to DSS-induced colitis (Yusta et al., 2015). Exendin-4 increases mRNA expression of *Il1b, Il6, Il22, Il12b, Tnfa, Ccl2, Cxcl1,* and *Cxcl2* (innate immunity), regenerating islet-derived protein 2, *RegIIIy* and *RegIIIB* (anti-microbial proteins), as well as *Il-5, Il-13* (pathogen clearance) within 4 h of administration, returning to baseline expression by 24 h (Yusta et al., 2015), suggesting that GLP-1R activation engages a cytoprotective response. Exendin-4 treatment following DSS-induced colitis does not prevent weight loss, colon length shortening, or improve colon damage score, however, reductions in colon weight are attributable to a reduction of edema (Yusta et al., 2015).

GLP-2R

The intestinotrophic effects of GLP-2 have been well-described since its initial characterization (Drucker et al., 1997). GLP-2 increases intestinal cell proliferation while inhibiting apoptosis, leading to increased villus height and expanding the absorptive mucosal surface (Drucker et al., 1997). GLP-2 decreases mucosal injury by stimulating intestinal growth; specifically, increasing villus height, crypt depth, improving nutrient absorption and nutritional status (Estall and Drucker, 2005). Mice fasted for 24 h exhibit small intestinal atrophy, a decrease in intestinal weight, a decrease in crypt-villus height, and an increase in villus apoptosis (Shin et al., 2005). Refeeding restored all parameters, while co-administration of GLP-2R antagonist, GLP-2^{3-33}, prevents adaptive changes to refeeding (Shin et al., 2005). Similarly, the restoration of jejunal mucosal mass, protein, and DNA 25–65% by *ad libitum* or intragastric infusion for 2–4 days is blunted with 2.5 or 50 μg/kg body weight GLP-2^{3-33}, but not 10 μg/kg body weight GLP-2^{3-33}, compared to the baseline fed group (Nelson et al., 2008). Mucosal growth following refeeding is associated with increased circulating GLP-2 and jejunal *Igf-1* mRNA expression. Interestingly, GLP-2^{3-33} at any dose prevents restoration of plasma IGF-I levels in response to refeeding (Nelson et al., 2008). There is evidence for both paracrine and neuronal mechanisms for GLP-2-mediated gut growth. GLP-2R+ myofibroblasts in the small intestine and colon contain keratinocyte growth factor (KGF), whereby immunoneutralization of KGF abolishes the trophic effects of GLP-2 treatment in the colon, but not the small intestine in mice (Orskov et al., 2005). Mechanistically, GLP-2 activates its receptors on subepithelial myofibroblasts, which in turn increase expression and secretion of IGF-1 (Dube et al., 2006). Gut growth coincides with increased IGF-1 and IGF-2, particularly in the mucosal and muscularis regions (Dube et al., 2006). GLP-2-mediated increases in IGF-1 activates the IGF-1 receptor on intestinal epithelial cells to stimulate proliferation (Rowland et al., 2011). Chronic GLP-2 treatment does not increase crypt-cell proliferation, and growth of the crypt-villus is reduced in intestinal epithelial-specific IGF knockout mice (Rowland et al., 2011).

Treatment of mice with DS-induced colitis (resembling human ulcerative colitis) with the human GLP-2 analog h(Gly^2)GLP, twice daily for 10 days, reverses weight loss independent on food intake, decreases interleukin-1 expression and increased colon length, crypt depth, and mucosal area compared to treatment with saline (Drucker et al., 1999). h(Gly^2)GLP-2 treatment also improves survival in drug-induced enteritis (non-steroidal anti-inflammatory drug - indomethacin) survival, reduces disease activity, decreases occurrence of intestinal ulcerations, and lowers cytokines and myeloperoxidase activity in mice (Boushey et al., 1999). In *Glp2r*$^{-/-}$ mice, levels of various Paneth cell genes are lower in the jejunum and ileum, some specifically in charge of defensin activity suggesting alterations in gut barrier function. The bacterial translocation and Paneth cell defect alter host-bacterial interactions within the intestine, further enhancing morbidity in *Glp2r*$^{-/-}$ mice (Lee et al., 2012). In the non-obese diabetic (NOD) mouse, a model of type 1 diabetes, treatment with h(Gly^2)GLP-2 once daily for 14 days, increases small intestine length and weight, while also improving jejunal transepithelial resistance compared to treatment with saline. NOD mice treated with a single injection of h(Gly^2)GLP-2 appear to have significantly decreased ion conductance in the jejunum (Hadjiyanni et al., 2009).

DISCUSSION

Agonism of GIPR, GLP-1R, and GLP-2R has a clear clinical impact on nutrient absorption and utilization; however, unraveling endogenous circuits' location in mediating this beneficial effect has been challenging. Clearly, gut hormones represent a signal produced by cells in direct contact with nutrients, bacteria and circulation. Evaluation of models of metabolic disease and aging describe resistance to signaling through established GLP-1R+ circuits (Grasset et al., 2017; Varin et al., 2020). It is currently unclear if the resistance to GLP-1 is primarily due to impaired receptor expression, reduced signaling in the gut-brain axis and/or intestinal dysbiosis. It is also unknown how much of resistance of endogenous signaling contributes to the heterogeneity observed in metabolic disease and the variable patient responses to pharmacological treatments including DPP4 inhibitors, GLP-1R agonists and bariatric surgery.

As co-agonists are developed and proposed to have greater glycemic and intestinotrophic effects, further understanding of the endogenous signaling and target cells can only improve tailoring and outcomes.

AUTHOR CONTRIBUTIONS

NM, AH, and EM: writing—original draft preparation and review and editing. EM: funding acquisition. All authors have read and agreed to the published version of the manuscript.

FUNDING

NM was the recipient of QEII-GSST and UOHI Cardiac Endowment Fellowship. This research was funded by the NSERC Discovery Grant to EM. EM was the recipient of a Diabetes Canada New Investigator Award, NSERC Discovery Grant RGPIN-2017-05996, and Diabetes Canada New Investigator NC-3-18-5425.

REFERENCES

Adriaenssens, A., Lam, B. Y., Billing, L., Skeffington, K., Sewing, S., Reimann, F., et al. (2015). A transcriptome-led exploration of molecular mechanisms regulating somatostatin-producing D-cells in the gastric epithelium. *Endocrinology* 156, 3924–3936. doi: 10.1210/en.2015-1301

Adriaenssens, A. E., Biggs, E. K., Darwish, T., Tadross, J., Sukthankar, T., Girish, M., et al. (2019). Glucose-dependent insulinotropic polypeptide receptor-expressing cells in the hypothalamus regulate food intake. *Cell Metab.* 30, 987–996.e6. doi: 10.1016/j.cmet.2019.07.013

Ali, S., Lamont, B. J., Charron, M. J., and Drucker, D. J. (2011). Dual elimination of the glucagon and GLP-1 receptors in mice reveals plasticity in the incretin axis. *J. Clin. Invest.* 121, 1917–1929. doi: 10.1172/JCI43615

Allin, K. H., Nielsen, T., and Pedersen, O. (2015). Mechanisms in endocrinology: Gut microbiota in patients with type 2 diabetes mellitus. *Eur. J. Endocrinol.* 172, R167–R177. doi: 10.1530/EJE-14-0874

Andersen, D. B., Grunddal, K. V., Pedersen, J., Kuhre, R. E., Lund, M. L., Holst, J. J., et al. (2021). Using a reporter mouse to map known and novel sites of GLP-1 receptor expression in peripheral tissues of male mice. *Endocrinology* 162:bqaa246. doi: 10.1210/endocr/bqaa246

Anini, Y., and Brubaker, P. L. (2003). Role of leptin in the regulation of glucagon-like peptide-1 secretion. *Diabetes* 52, 252–259. doi: 10.2337/diabetes.52.2.252

Argikar, A. A., and Argikar, U. A. (2018). The mesentery: an ADME perspective on a 'new' organ. *Drug Metab. Rev.* 50, 398–405. doi: 10.1080/03602532.2018.1484756

Asmar, M., Asmar, A., Simonsen, L., Gasbjerg, L. S., Sparre-Ulrich, A. H., Rosenkilde, M. M., et al. (2017). The gluco- and liporegulatory and vasodilatory effects of glucose-dependent insulinotropic polypeptide (GIP) are abolished by an antagonist of the human gip receptor. *Diabetes* 66, 2363–2371. doi: 10.2337/db17-0480

Baggio, L. L., and Drucker, D. J. (2007). Biology of incretins: GLP-1 and GIP. *Gastroenterology* 132, 2131–2157. doi: 10.1053/j.gastro.2007.03.054

Baggio, L. L., Huang, Q., Brown, T. J., and Drucker, D. J. (2004). A recombinant human glucagon-like peptide (GLP)-1-albumin protein (albugon) mimics peptidergic activation of GLP-1 receptor-dependent pathways coupled with satiety, gastrointestinal motility, and glucose homeostasis. *Diabetes* 53, 2492–2500. doi: 10.2337/diabetes.53.9.2492

Baldassano, S., Gasbjerg, L. S., Kizilkaya, H. S., Rosenkilde, M. M., Holst, J. J., and Hartmann, B. (2019). Increased body weight and fat mass after subchronic GIP receptor antagonist, but Not GLP-2 receptor antagonist, administration in rats. *Front. Endocrinol. (Lausanne)* 10:492. doi: 10.3389/fendo.2019.00492

Beaudry, J. L., Kaur, K. D., Varin, E. M., Baggio, L. L., Cao, X., Mulvihill, E. E., et al. (2019). Physiological roles of the GIP receptor in murine brown adipose tissue. *Mol. Metab.* 28, 14–25. doi: 10.1016/j.molmet.2019.08.006

Bernier-Latmani, J., and Petrova, T. V. (2017). Intestinal lymphatic vasculature: structure, mechanisms and functions. *Nat. Rev. Gastroenterol. Hepatol.* 14, 510–526. doi: 10.1038/nrgastro.2017.79

Boismenu, R., and Havran, W. L. (1994). Modulation of epithelial cell growth by intraepithelial gamma delta T cells. *Science* 266, 1253–1255. doi: 10.1126/science.7973709

Borgstrom, B., Dahlqvist, A., Lundh, G., and Sjovall, J. (1957). Studies of intestinal digestion and absorption in the human. *J. Clin. Invest.* 36, 1521–1536. doi: 10.1172/JCI103549

Boushey, R. P., Yusta, B., and Drucker, D. J. (1999). Glucagon-like peptide 2 decreases mortality and reduces the severity of indomethacin-induced murine

enteritis. *Am. J. Physiol.* 277, E937–E947. doi: 10.1152/ajpendo.1999.277.5.E937

Boylan, M. O., Jepeal, L. I., and Wolfe, M. M. (2006). Sp1/Sp3 binding is associated with cell-specific expression of the glucose-dependent insulinotropic polypeptide receptor gene. *Am. J. Physiol. Endocrinol. Metab.* 290, E1287–E1295. doi: 10.1152/ajpendo.00535.2005

Brown, J. C., and Otte, S. C. (1979). GIP and the entero-insular axis. *Clin. Endocrinol. Metab.* 8, 365–377. doi: 10.1016/s0300-595x(79)80047-x

Brubaker, P. L., Crivici, A., Izzo, A., Ehrlich, P., Tsai, C. H., and Drucker, D. J. (1997). Circulating and tissue forms of the intestinal growth factor, glucagon-like peptide-2. *Endocrinology* 138, 4837–4843. doi: 10.1210/endo.138.11.5482

Bryant, M. G., Bloom, S. R., Polak, J. M., Hobbs, S., Domschke, W., Domschke, S., et al. (1983). Measurement of gut hormonal peptides in biopsies from human stomach and proximal small intestine. *Gut* 24, 114–119. doi: 10.1136/gut.24.2.114

Buchan, A. M., Polak, J. M., Capella, C., Solcia, E., and Pearse, A. G. (1978). Electronimmunocytochemical evidence for the K cell localization of gastric inhibitory polypeptide (GIP) in man. *Histochemistry* 56, 37–44. doi: 10.1007/BF00492251

Bunck, M. C., Corner, A., Eliasson, B., Heine, R. J., Shaginian, R. M., Wu, Y., et al. (2010). One-year treatment with exenatide vs. insulin glargine: effects on postprandial glycemia, lipid profiles, and oxidative stress. *Atherosclerosis* 212, 223–229. doi: 10.1016/j.atherosclerosis.2010.04.024

Campbell, J. E. (2021). Targeting the GIPR for obesity: To agonize or antagonize? *Potential. Mech. Mol. Metab.* 46:101139. doi: 10.1016/j.molmet.2020.101139

Campbell, R. M., and Scanes, C. G. (1992). Evolution of the growth hormone-releasing factor (GRF) family of peptides. *Growth Regul.* 2, 175–191.

Campos, R. V., Lee, Y. C., and Drucker, D. J. (1994). Divergent tissue-specific and developmental expression of receptors for glucagon and glucagon-like peptide-1 in the mouse. *Endocrinology* 134, 2156–2164. doi: 10.1210/endo.134.5.8156917

Cheroutre, H., Lambolez, F., and Mucida, D. (2011). The light and dark sides of intestinal intraepithelial lymphocytes. *Nat. Rev. Immunol.* 11, 445–456. doi: 10.1038/nri3007

Cho, I., Yamanishi, S., Cox, L., Methe, B. A., Zavadil, J., Li, K., et al. (2012). Antibiotics in early life alter the murine colonic microbiome and adiposity. *Nature* 488, 621–626. doi: 10.1038/nature11400

Christensen, M., Vedtofte, L., Holst, J. J., Vilsboll, T., and Knop, F. K. (2011). Glucose-dependent insulinotropic polypeptide: a bifunctional glucose-dependent regulator of glucagon and insulin secretion in humans. *Diabetes* 60, 3103–3109. doi: 10.2337/db11-0979

Cinci, L., Faussone-Pellegrini, M. S., Rotondo, A., Mule, F., and Vannucchi, M. G. (2011). GLP-2 receptor expression in excitatory and inhibitory enteric neurons and its role in mouse duodenum contractility. *Neurogastroenterol. Motil.* 23, e383–e392. doi: 10.1111/j.1365-2982.2011.01750.x

Collier, G., McLean, A., and O'Dea, K. (1984). Effect of co-ingestion of fat on the metabolic responses to slowly and rapidly absorbed carbohydrates. *Diabetologia* 26, 50–54. doi: 10.1007/BF00252263

Collins, J. T., Nguyen, A., and Badireddy, M. (2021). *Anatomy, Abdomen and Pelvis, Small Intestine*. Treasure Island FL: StatPearls.

Coon, S. D., Schwartz, J. H., Rajendran, V. M., Jepeal, L., and Singh, S. K. (2013). Glucose-dependent insulinotropic polypeptide regulates dipeptide absorption in mouse jejunum. *Am. J. Physiol. Gastrointest. Liver Physiol.* 305, G678–G684. doi: 10.1152/ajpgi.00098.2013

Covasa, M., Stephens, R. W., Toderean, R., and Cobuz, C. (2019). Intestinal sensing by gut microbiota: targeting gut peptides. *Front. Endocrinol. (Lausanne)* 10:82. doi: 10.3389/fendo.2019.00082

Creutzfeldt, W., Ebert, R., Willms, B., Frerichs, H., and Brown, J. C. (1978). Gastric inhibitory polypeptide (GIP) and insulin in obesity: increased response to stimulation and defective feedback control of serum levels. *Diabetologia* 14, 15–24. doi: 10.1007/BF00429703

D'Alessio, D., Lu, W., Sun, W., Zheng, S., Yang, Q., Seeley, R., et al. (2007). Fasting and postprandial concentrations of GLP-1 in intestinal lymph and portal plasma: evidence for selective release of GLP-1 in the lymph system. *Am. J. Physiol. Regul. Integr. Comp. Physiol.* 293, R2163–R2169. doi: 10.1152/ajpregu.00911.2006

Dash, S., Xiao, C., Morgantini, C., Connelly, P. W., Patterson, B. W., and Lewis, G. F. (2014). Glucagon-like peptide-2 regulates release of chylomicrons from the intestine. *Gastroenterology* 147, 1275–1284 e4. doi: 10.1053/j.gastro.2014.08.037

Deacon, C. F., Johnsen, A. H., and Holst, J. J. (1995a). Degradation of glucagon-like peptide-1 by human plasma in vitro yields an N-terminally truncated peptide that is a major endogenous metabolite in vivo. *J. Clin. Endocrinol. Metab.* 80, 952–957. doi: 10.1210/jcem.80.3.7883856

Deacon, C. F., Johnsen, A. H., and Holst, J. J. (1995b). Human colon produces fully processed glucagon-like peptide-1 (7-36) amide. *FEBS Lett.* 372, 269–272. doi: 10.1016/0014-5793(95)00983-g

Drucker, D. J., Mojsov, S., and Habener, J. F. (1986). Cell-specific post-translational processing of preproglucagon expressed from a metallothionein-glucagon fusion gene. *J. Biol. Chem.* 261, 9637–9643.

Drucker, D. J., Philippe, J., Mojsov, S., Chick, W. L., and Habener, J. F. (1987). Glucagon-like peptide I stimulates insulin gene expression and increases cyclic AMP levels in a rat islet cell line. *Proc. Natl. Acad. Sci. U.S.A.* 84, 3434–3438. doi: 10.1073/pnas.84.10.3434

Drucker, D. J., Shi, Q., Crivici, A., Sumner-Smith, M., Tavares, W., Hill, M., et al. (1997). Regulation of the biological activity of glucagon-like peptide 2 in vivo by dipeptidyl peptidase IV. *Nat. Biotechnol.* 15, 673–677. doi: 10.1038/nbt0797-673

Drucker, D. J., and Yusta, B. (2014). Physiology and pharmacology of the enteroendocrine hormone glucagon-like peptide-2. *Annu. Rev. Physiol.* 76, 561–583. doi: 10.1146/annurev-physiol-021113-170317

Drucker, D. J., Yusta, B., Boushey, R. P., DeForest, L., and Brubaker, P. L. (1999). Human [Gly2]GLP-2 reduces the severity of colonic injury in a murine model of experimental colitis. *Am. J. Physiol.* 276, G79–G91. doi: 10.1152/ajpgi.1999.276.1.G79

Dube, P. E., Forse, C. L., Bahrami, J., and Brubaker, P. L. (2006). The essential role of insulin-like growth factor-1 in the intestinal tropic effects of glucagon-like peptide-2 in mice. *Gastroenterology* 131, 589–605. doi: 10.1053/j.gastro.2006.05.055

Eissele, R., Goke, R., Willemer, S., Harthus, H. P., Vermeer, H., Arnold, R., et al. (1992). Glucagon-like peptide-1 cells in the gastrointestinal tract and pancreas of rat, pig and man. *Eur. J. Clin. Invest.* 22, 283–291. doi: 10.1111/j.1365-2362.1992.tb01464.x

Ellingsgaard, H., Hauselmann, I., Schuler, B., Habib, A. M., Baggio, L. L., Meier, D. T., et al. (2011). Interleukin-6 enhances insulin secretion by increasing glucagon-like peptide-1 secretion from L cells and alpha cells. *Nat. Med.* 17, 1481–1489. doi: 10.1038/nm.2513

Ensari, A., and Marsh, M. N. (2018). Exploring the villus. *Gastroenterol. Hepatol. Bed Bench* 11, 181–190.

Estall, J. L., and Drucker, D. J. (2005). Tales beyond the crypt: glucagon-like peptide-2 and cytoprotection in the intestinal mucosa. *Endocrinology* 146, 19–21. doi: 10.1210/en.2004-1389

Everard, A., Lazarevic, V., Derrien, M., Girard, M., Muccioli, G. G., Neyrinck, A. M., et al. (2011). Responses of gut microbiota and glucose and lipid metabolism to prebiotics in genetic obese and diet-induced leptin-resistant mice. *Diabetes* 60, 2775–2786. doi: 10.2337/db11-0227

Flatt, P. R., Kwasowski, P., and Bailey, C. J. (1989). Stimulation of gastric inhibitory polypeptide release in ob/ob mice by oral administration of sugars and their analogues. *J. Nutr.* 119, 1300–1303. doi: 10.1093/jn/119.9.1300

Flock, G. B., Cao, X., Maziarz, M., and Drucker, D. J. (2013). Activation of enteroendocrine membrane progesterone receptors promotes incretin secretion and improves glucose tolerance in mice. *Diabetes* 62, 283–290. doi: 10.2337/db12-0601

Fuchs, S., Yusta, B., Baggio, L. L., Varin, E. M., Matthews, D., and Drucker, D. J. (2020). Loss of Glp2r signaling activates hepatic stellate cells and exacerbates diet-induced steatohepatitis in mice. *JCI Insight* 5:e136907. doi: 10.1172/jci.insight.136907

Fujita, Y., Asadi, A., Yang, G. K., Kwok, Y. N., and Kieffer, T. J. (2010). Differential processing of pro-glucose-dependent insulinotropic polypeptide in gut. *Am. J. Physiol. Gastrointest. Liver Physiol.* 298, G608–G614. doi: 10.1152/ajpgi.00024.2010

Gehart, H., and Clevers, H. (2019). Tales from the crypt: new insights into intestinal stem cells. *Nat. Rev. Gastroenterol. Hepatol.* 16, 19–34. doi: 10.1038/s41575-018-0081-y

Gelling, R. W., Du, X. Q., Dichmann, D. S., Romer, J., Huang, H., Cui, L., et al. (2003). Lower blood glucose, hyperglucagonemia, and pancreatic alpha cell

hyperplasia in glucagon receptor knockout mice. *Proc. Natl. Acad. Sci. U.S.A.* 100, 1438–1443. doi: 10.1073/pnas.0237106100

Ghislain, J., and Poitout, V. (2021). Targeting lipid GPCRs to treat type 2 diabetes mellitus - progress and challenges. *Nat. Rev. Endocrinol.* 17, 162–175. doi: 10.1038/s41574-020-00459-w

Gorboulev, V., Schurmann, A., Vallon, V., Kipp, H., Jaschke, A., Klessen, D., et al. (2012). Na(+)-D-glucose cotransporter SGLT1 is pivotal for intestinal glucose absorption and glucose-dependent incretin secretion. *Diabetes* 61, 187–196. doi: 10.2337/db11-1029

Grasset, E., Puel, A., Charpentier, J., Collet, X., Christensen, J. E., Terce, F., et al. (2017). A Specific gut microbiota dysbiosis of type 2 diabetic mice induces GLP-1 resistance through an enteric NO-dependent and gut-brain axis mechanism. *Cell Metab.* 25, 1075–1090 e5. doi: 10.1016/j.cmet.2017.04.013

Greiner, T. U., and Backhed, F. (2016). Microbial regulation of GLP-1 and L-cell biology. *Mol. Metab.* 5, 753–758. doi: 10.1016/j.molmet.2016.05.012

Gribble, F. M., and Reimann, F. (2021). Metabolic Messengers: glucagon-like peptide 1. *Nat. Metab.* 3, 142–148. doi: 10.1038/s42255-020-00327-x

Grigoryan, M., Kedees, M. H., Charron, M. J., Guz, Y., and Teitelman, G. (2012). Regulation of mouse intestinal L cell progenitors proliferation by the glucagon family of peptides. *Endocrinology* 153, 3076–3088. doi: 10.1210/en.2012-1120

Guan, X., Karpen, H. E., Stephens, J., Bukowski, J. T., Niu, S., Zhang, G., et al. (2006). GLP-2 receptor localizes to enteric neurons and endocrine cells expressing vasoactive peptides and mediates increased blood flow. *Gastroenterology* 130, 150–164. doi: 10.1053/j.gastro.2005.11.005

Guan, X., Stoll, B., Lu, X., Tappenden, K. A., Holst, J. J., Hartmann, B., et al. (2003). GLP-2-mediated up-regulation of intestinal blood flow and glucose uptake is nitric oxide-dependent in TPN-fed piglets 1. *Gastroenterology* 125, 136–147. doi: 10.1016/s0016-5085(03)00667-x

Hadjiyanni, I., Li, K. K., and Drucker, D. J. (2009). Glucagon-like peptide-2 reduces intestinal permeability but does not modify the onset of type 1 diabetes in the nonobese diabetic mouse. *Endocrinology* 150, 592–599. doi: 10.1210/en.2008-1228

Hansen, L., Deacon, C. F., Orskov, C., and Holst, J. J. (1999). Glucagon-like peptide-1-(7-36)amide is transformed to glucagon-like peptide-1-(9-36)amide by dipeptidyl peptidase IV in the capillaries supplying the L cells of the porcine intestine. *Endocrinology* 140, 5356–5363. doi: 10.1210/endo.140.11.7143

Hartmann, B., Harr, M. B., Jeppesen, P. B., Wojdemann, M., Deacon, C. F., Mortensen, P. B., et al. (2000). In vivo and in vitro degradation of glucagon-like peptide-2 in humans. *J. Clin. Endocrinol. Metab.* 85, 2884–2888. doi: 10.1210/jcem.85.8.6717

Hayashi, H., Nutting, D. F., Fujimoto, K., Cardelli, J. A., Black, D., and Tso, P. (1990). Transport of lipid and apolipoproteins A-I and A-IV in intestinal lymph of the rat. *J. Lipid Res.* 31, 1613–1625.

He, S., Kahles, F., Rattik, S., Nairz, M., McAlpine, C. S., Anzai, A., et al. (2019). Gut intraepithelial T cells calibrate metabolism and accelerate cardiovascular disease. *Nature* 566, 115–119. doi: 10.1038/s41586-018-0849-9

Herrmann, C., Goke, R., Richter, G., Fehmann, H. C., Arnold, R., and Goke, B. (1995). Glucagon-like peptide-1 and glucose-dependent insulin-releasing polypeptide plasma levels in response to nutrients. *Digestion* 56, 117–126. doi: 10.1159/000201231

Higashimoto, Y., and Liddle, R. A. (1993). Isolation and characterization of the gene encoding rat glucose-dependent insulinotropic peptide. *Biochem. Biophys. Res. Commun.* 193, 182–190. doi: 10.1006/bbrc.1993.1607

Higashimoto, Y., Opara, E. C., and Liddle, R. A. (1995). Dietary regulation of glucose-dependent insulinotropic peptide (GIP) gene expression in rat small intestine. *Comp. Biochem. Physiol. C Pharmacol. Toxicol. Endocrinol.* 110, 207–214. doi: 10.1016/0742-8413(94)00087-q

Higashimoto, Y., Simchock, J., and Liddle, R. A. (1992). Molecular cloning of rat glucose-dependent insulinotropic peptide (GIP). *Biochim. Biophys. Acta* 1132, 72–74. doi: 10.1016/0167-4781(92)90054-4

Holst, J. J., Orskov, C., Nielsen, O. V., and Schwartz, T. W. (1987). Truncated glucagon-like peptide I, an insulin-releasing hormone from the distal gut. *FEBS Lett.* 211, 169–174. doi: 10.1016/0014-5793(87)81430-8

Holst, J. J., Windelov, J. A., Boer, G. A., Pedersen, J., Svendsen, B., Christensen, M., et al. (2016). Searching for the physiological role of glucose-dependent insulinotropic polypeptide. *J. Diabetes Investig.* 7(Suppl 1), 8–12. doi: 10.1111/jdi.12488

Hsieh, J., Longuet, C., Baker, C. L., Qin, B., Federico, L. M., Drucker, D. J., et al. (2010). The glucagon-like peptide 1 receptor is essential for postprandial lipoprotein synthesis and secretion in hamsters and mice. *Diabetologia* 53, 552–561. doi: 10.1007/s00125-009-1611-5

Hsieh, J., Longuet, C., Maida, A., Bahrami, J., Xu, E., Baker, C. L., et al. (2009). Glucagon-like peptide-2 increases intestinal lipid absorption and chylomicron production via CD36. *Gastroenterology* 137, 997-1005, 1005.e1–4. doi: 10.1053/j.gastro.2009.05.051

Hsieh, J., Trajcevski, K. E., Farr, S. L., Baker, C. L., Lake, E. J., Taher, J., et al. (2015). Glucagon-like peptide 2 (GLP-2) stimulates postprandial chylomicron production and postabsorptive release of intestinal triglyceride storage pools via induction of nitric oxide signaling in male hamsters and mice. *Endocrinology* 156, 3538–3547. doi: 10.1210/EN.2015-1110

Hwang, I., Park, Y. J., Kim, Y. R., Kim, Y. N., Ka, S., Lee, H. Y., et al. (2015). Alteration of gut microbiota by vancomycin and bacitracin improves insulin resistance via glucagon-like peptide 1 in diet-induced obesity. *FASEB J.* 29, 2397–2411. doi: 10.1096/fj.14-265983

Ikeguchi, E., Harada, N., Kanemaru, Y., Sankoda, A., Yamane, S., Iwasaki, K., et al. (2018). Transcriptional factor Pdx1 is involved in age-related GIP hypersecretion in mice. *Am. J. Physiol. Gastrointest. Liver Physiol.* 315, G272–G282. doi: 10.1152/ajpgi.00054.2018

Iwasaki, K., Harada, N., Sasaki, K., Yamane, S., Iida, K., Suzuki, K., et al. (2015). Free fatty acid receptor GPR120 is highly expressed in enteroendocrine K cells of the upper small intestine and has a critical role in GIP secretion after fat ingestion. *Endocrinology* 156, 837–846. doi: 10.1210/en.2014-1653

Jeppesen, P. B., Hartmann, B., Thulesen, J., Hansen, B. S., Holst, J. J., Poulsen, S. S., et al. (2000). Elevated plasma glucagon-like peptide 1 and 2 concentrations in ileum resected short bowel patients with a preserved colon. *Gut* 47, 370–376. doi: 10.1136/gut.47.3.370

Jeppesen, P. B., Sanguinetti, E. L., Buchman, A., Howard, L., Scolapio, J. S., Ziegler, T. R., et al. (2005). Teduglutide (ALX-0600), a dipeptidyl peptidase IV resistant glucagon-like peptide 2 analogue, improves intestinal function in short bowel syndrome patients. *Gut* 54, 1224–1231. doi: 10.1136/gut.2004.061440

Jepsen, S. L., Grunddal, K. V., Wewer Albrechtsen, N. J., Engelstoft, M. S., Gabe, M. B. N., Jensen, E. P., et al. (2019). Paracrine crosstalk between intestinal L- and D-cells controls secretion of glucagon-like peptide-1 in mice. *Am. J. Physiol. Endocrinol. Metab.* 317, E1081–E1093. doi: 10.1152/ajpendo.00239.2019

Jorsal, T., Rhee, N. A., Pedersen, J., Wahlgren, C. D., Mortensen, B., Jepsen, S. L., et al. (2018). Enteroendocrine K and L cells in healthy and type 2 diabetic individuals. *Diabetologia* 61, 284–294. doi: 10.1007/s00125-017-4450-9

Kahles, F., Meyer, C., Mollmann, J., Diebold, S., Findeisen, H. M., Lebherz, C., et al. (2014). GLP-1 secretion is increased by inflammatory stimuli in an IL-6-dependent manner, leading to hyperinsulinemia and blood glucose lowering. *Diabetes* 63, 3221–3229. doi: 10.2337/db14-0100

Kedees, M. H., Guz, Y., Grigoryan, M., and Teitelman, G. (2013). Functional activity of murine intestinal mucosal cells is regulated by the glucagon-like peptide-1 receptor. *Peptides* 48, 36–44. doi: 10.1016/j.peptides.2013.07.022

Kiela, P. R., and Ghishan, F. K. (2016). Physiology of Intestinal Absorption and Secretion. *Best Pract. Res. Clin. Gastroenterol.* 30, 145–159. doi: 10.1016/j.bpg.2016.02.007

Kim, S. J., Nian, C., and McIntosh, C. H. (2007a). Activation of lipoprotein lipase by glucose-dependent insulinotropic polypeptide in adipocytes. A role for a protein kinase B, LKB1, and AMP-activated protein kinase cascade. *J. Biol. Chem.* 282, 8557–8567. doi: 10.1074/jbc.M609088200

Kim, S. J., Nian, C., and McIntosh, C. H. (2007b). Resistin is a key mediator of glucose-dependent insulinotropic polypeptide (GIP) stimulation of lipoprotein lipase (LPL) activity in adipocytes. *J. Biol. Chem.* 282, 34139–34147. doi: 10.1074/jbc.M704896200

Kim, S. J., Nian, C., and McIntosh, C. H. (2010). GIP increases human adipocyte LPL expression through CREB and TORC2-mediated trans-activation of the LPL gene. *J. Lipid Res.* 51, 3145–3157. doi: 10.1194/jlr.M006841

Knudsen, L. B., and Pridal, L. (1996). Glucagon-like peptide-1-(9-36) amide is a major metabolite of glucagon-like peptide-1-(7-36) amide after in vivo administration to dogs, and it acts as an antagonist on the pancreatic receptor. *Eur. J. Pharmacol.* 318, 429–435. doi: 10.1016/s0014-2999(96)00795-9

Koehler, J. A., Baggio, L. L., Yusta, B., Longuet, C., Rowland, K. J., Cao, X., et al. (2015). GLP-1R agonists promote normal and neoplastic intestinal growth through mechanisms requiring Fgf7. *Cell Metab.* 21, 379–391. doi: 10.1016/j.cmet.2015.02.005

Koehler, J. A., Harper, W., Barnard, M., Yusta, B., and Drucker, D. J. (2008). Glucagon-like peptide-2 does not modify the growth or survival of murine or human intestinal tumor cells. *Cancer Res.* 68, 7897–7904. doi: 10.1158/0008-5472.CAN-08-0029

Kuhre, R. E., Gribble, F. M., Hartmann, B., Reimann, F., Windelov, J. A., Rehfeld, J. F., et al. (2014). Fructose stimulates GLP-1 but not GIP secretion in mice, rats, and humans. *Am. J. Physiol. Gastrointest. Liver Physiol.* 306, G622–G630. doi: 10.1152/ajpgi.00372.2013

Lamont, B. J., Li, Y., Kwan, E., Brown, T. J., Gaisano, H., and Drucker, D. J. (2012). Pancreatic GLP-1 receptor activation is sufficient for incretin control of glucose metabolism in mice. *J. Clin. Invest.* 122, 388–402. doi: 10.1172/JCI42497

Lankat-Buttgereit, B., and Goke, B. (1997). Cloning and characterization of the 5′ flanking sequences (promoter region) of the human GLP-1 receptor gene. *Peptides* 18, 617–624. doi: 10.1016/s0196-9781(97)00001-6

Lee, S. J., Lee, J., Li, K. K., Holland, D., Maughan, H., Guttman, D. S., et al. (2012). Disruption of the murine Glp2r impairs Paneth cell function and increases susceptibility to small bowel enteritis. *Endocrinology* 153, 1141–1151. doi: 10.1210/en.2011-1954

Li, F., Lu, L., Peng, Y., Zhang, Y., Gao, J., Zhou, D., et al. (2017). Increased GLP2R expression in gastric chief cells of patients with severe obesity regardless of diabetes status. *Int. J. Obes. (Lond)* 41, 1303–1305. doi: 10.1038/ijo.2017.77

Lu, W. J., Yang, Q., Sun, W., Woods, S. C., D'Alessio, D., and Tso, P. (2007). The regulation of the lymphatic secretion of glucagon-like peptide-1 (GLP-1) by intestinal absorption of fat and carbohydrate. *Am. J. Physiol. Gastrointest. Liver Physiol.* 293, G963–G971. doi: 10.1152/ajpgi.00146.2007

Lu, W. J., Yang, Q., Sun, W., Woods, S. C., D'Alessio, D., and Tso, P. (2008). Using the lymph fistula rat model to study the potentiation of GIP secretion by the ingestion of fat and glucose. *Am. J. Physiol. Gastrointest. Liver Physiol.* 294, G1130–G1138. doi: 10.1152/ajpgi.00400.2007

Lu, W. J., Yang, Q., Yang, L., Lee, D., D'Alessio, D., and Tso, P. (2012). Chylomicron formation and secretion is required for lipid-stimulated release of incretins GLP-1 and GIP. *Lipids* 47, 571–580. doi: 10.1007/s11745-011-3650-1

Lund, A., Bagger, J. I., Wewer Albrechtsen, N. J., Christensen, M., Grondahl, M., Hartmann, B., et al. (2016). Evidence of extrapancreatic glucagon secretion in man. *Diabetes* 65, 585–597. doi: 10.2337/db15-1541

Markovic, M. A., and Brubaker, P. L. (2019). The roles of glucagon-like peptide-2 and the intestinal epithelial insulin-like growth factor-1 receptor in regulating microvillus length. *Sci. Rep.* 9:13010. doi: 10.1038/s41598-019-49510-5

Martchenko, S. E., Martchenko, A., Cox, B. J., Naismith, K., Waller, A., Gurges, P., et al. (2020). Circadian GLP-1 secretion in mice is dependent on the intestinal microbiome for maintenance of diurnal metabolic homeostasis. *Diabetes* 69, 2589–2602. doi: 10.2337/db20-0262

Martin, A. M., Sun, E. W., Rogers, G. B., and Keating, D. J. (2019). The influence of the gut microbiome on host metabolism through the regulation of gut hormone release. *Front. Physiol.* 10:428. doi: 10.3389/fphys.2019.00428

Matikainen, N., Bjornson, E., Soderlund, S., Boren, C., Eliasson, B., Pietilainen, K. H., et al. (2016). Minor contribution of endogenous GLP-1 and GLP-2 to postprandial lipemia in obese men. *PLoS One* 11:e0145890. doi: 10.1371/journal.pone.0145890

McCullough, A. J., Miller, L. J., Service, F. J., and Go, V. L. (1983). Effect of graded intraduodenal glucose infusions on the release and physiological action of gastric inhibitory polypeptide. *J. Clin. Endocrinol. Metab.* 56, 234–241. doi: 10.1210/jcem-56-2-234

McLean, B. A., Wong, C. K., Campbell, J. E., Hodson, D. J., Trapp, S., and Drucker, D. J. (2021). Revisiting the complexity of GLP-1 action from sites of synthesis to receptor activation. *Endocr. Rev.* 42, 101–132. doi: 10.1210/endrev/bnaa032

Meek, C. L., Lewis, H. B., Burling, K., Reimann, F., and Gribble, F. (2021). Expected values for gastrointestinal and pancreatic hormone concentrations in healthy volunteers in the fasting and postprandial state. *Ann. Clin. Biochem.* 58, 108–116. doi: 10.1177/0004563220975658

Meier, J. J., Goetze, O., Anstipp, J., Hagemann, D., Holst, J. J., Schmidt, W. E., et al. (2004a). Gastric inhibitory polypeptide does not inhibit gastric emptying in humans. *Am. J. Physiol. Endocrinol. Metab.* 286, E621–E625. doi: 10.1152/ajpendo.00499.2003

Meier, J. J., Nauck, M. A., Kranz, D., Holst, J. J., Deacon, C. F., Gaeckler, D., et al. (2004b). Secretion, degradation, and elimination of glucagon-like peptide 1 and gastric inhibitory polypeptide in patients with chronic renal insufficiency and healthy control subjects. *Diabetes* 53, 654–662. doi: 10.2337/diabetes.53.3.654

Mojsov, S., Heinrich, G., Wilson, I. B., Ravazzola, M., Orci, L., and Habener, J. F. (1986). Preproglucagon gene expression in pancreas and intestine diversifies at the level of post-translational processing. *J. Biol. Chem.* 261, 11880–11889.

Moran, B. M., Miskelly, M. G., Abdel-Wahab, Y. H. A., Flatt, P. R., and McKillop, A. M. (2019). Zinc-induced activation of GPR39 regulates glucose homeostasis through glucose-dependent insulinotropic polypeptide secretion from enteroendocrine K-cells. *Biol. Chem.* 400, 1023–1033. doi: 10.1515/hsz-2018-0393

Moriya, R., Shirakura, T., Ito, J., Mashiko, S., and Seo, T. (2009). Activation of sodium-glucose cotransporter 1 ameliorates hyperglycemia by mediating incretin secretion in mice. *Am. J. Physiol. Endocrinol. Metab.* 297, E1358–E1365. doi: 10.1152/ajpendo.00412.2009

Munroe, D. G., Gupta, A. K., Kooshesh, F., Vyas, T. B., Rizkalla, G., Wang, H., et al. (1999). Prototypic G protein-coupled receptor for the intestinotrophic factor glucagon-like peptide 2. *Proc. Natl. Acad. Sci. U.S.A.* 96, 1569–1573. doi: 10.1073/pnas.96.4.1569

Nasteska, D., Harada, N., Suzuki, K., Yamane, S., Hamasaki, A., Joo, E., et al. (2014). Chronic reduction of GIP secretion alleviates obesity and insulin resistance under high-fat diet conditions. *Diabetes* 63, 2332–2343. doi: 10.2337/db13-1563

Nelson, D. W., Murali, S. G., Liu, X., Koopmann, M. C., Holst, J. J., and Ney, D. M. (2008). Insulin-like growth factor I and glucagon-like peptide-2 responses to fasting followed by controlled or ad libitum refeeding in rats. *Am. J. Physiol. Regul. Integr. Comp. Physiol.* 294, R1175–R1184. doi: 10.1152/ajpregu.00238.2007

Nelson, D. W., Sharp, J. W., Brownfield, M. S., Raybould, H. E., and Ney, D. M. (2007). Localization and activation of glucagon-like peptide-2 receptors on vagal afferents in the rat. *Endocrinology* 148, 1954–1962. doi: 10.1210/en.2006-1232

Nguyen, A. T., Mandard, S., Dray, C., Deckert, V., Valet, P., Besnard, P., et al. (2014). Lipopolysaccharides-mediated increase in glucose-stimulated insulin secretion: involvement of the GLP-1 pathway. *Diabetes* 63, 471–482. doi: 10.2337/db13-0903

Ogata, H., Seino, Y., Harada, N., Iida, A., Suzuki, K., Izumoto, T., et al. (2014). KATP channel as well as SGLT1 participates in GIP secretion in the diabetic state. *J. Endocrinol.* 222, 191–200. doi: 10.1530/JOE-14-0161

Orskov, C., Bersani, M., Johnsen, A. H., Hojrup, P., and Holst, J. J. (1989a). Complete sequences of glucagon-like peptide-1 from human and pig small intestine. *J. Biol. Chem.* 264, 12826–12829.

Orskov, C., Buhl, T., Rabenhoj, L., Kofod, H., and Holst, J. J. (1989b). Carboxypeptidase-B-like processing of the C-terminus of glucagon-like peptide-2 in pig and human small intestine. *FEBS Lett.* 247, 193–196. doi: 10.1016/0014-5793(89)81332-8

Orskov, C., Hartmann, B., Poulsen, S. S., Thulesen, J., Hare, K. J., and Holst, J. J. (2005). GLP-2 stimulates colonic growth via KGF, released by subepithelial myofibroblasts with GLP-2 receptors. *Regul. Pept.* 124, 105–112. doi: 10.1016/j.regpep.2004.07.009

Orskov, C., Holst, J. J., Knuhtsen, S., Baldissera, F. G., Poulsen, S. S., and Nielsen, O. V. (1986). Glucagon-like peptides GLP-1 and GLP-2, predicted products of the glucagon gene, are secreted separately from pig small intestine but not pancreas. *Endocrinology* 119, 1467–1475. doi: 10.1210/endo-119-4-1467

Pais, R., Gribble, F. M., and Reimann, F. (2016). Stimulation of incretin secreting cells. *Ther. Adv. Endocrinol. Metab.* 7, 24–42. doi: 10.1177/2042018815618177

Paternoster, S., and Falasca, M. (2018). Dissecting the physiology and pathophysiology of glucagon-like peptide-1. *Front. Endocrinol. (Lausanne)* 9:584. doi: 10.3389/fendo.2018.00584

Pavlic, M., Xiao, C., Szeto, L., Patterson, B. W., and Lewis, G. F. (2010). Insulin acutely inhibits intestinal lipoprotein secretion in humans in part by suppressing plasma free fatty acids. *Diabetes* 59, 580–587. doi: 10.2337/db09-1297

Pedersen, J., Pedersen, N. B., Brix, S. W., Grunddal, K. V., Rosenkilde, M. M., Hartmann, B., et al. (2015). The glucagon-like peptide 2 receptor is expressed in

enteric neurons and not in the epithelium of the intestine. *Peptides* 67, 20–28. doi: 10.1016/j.peptides.2015.02.007

Pedersen, J., Ugleholdt, R. K., Jorgensen, S. M., Windelov, J. A., Grunddal, K. V., Schwartz, T. W., et al. (2013). Glucose metabolism is altered after loss of L cells and alpha-cells but not influenced by loss of K cells. *Am. J. Physiol. Endocrinol. Metab.* 304, E60–E73. doi: 10.1152/ajpendo.00547.2011

Pederson, R. A., Schubert, H. E., and Brown, J. C. (1975). Gastric inhibitory polypeptide. Its physiologic release and insulinotropic action in the dog. *Diabetes* 24, 1050–1056. doi: 10.2337/diab.24.12.1050

Psichas, A., Glass, L. L., Sharp, S. J., Reimann, F., and Gribble, F. M. (2016). Galanin inhibits GLP-1 and GIP secretion via the GAL1 receptor in enteroendocrine L and K cells. *Br. J. Pharmacol.* 173, 888–898. doi: 10.1111/bph.13407

Psichas, A., Larraufie, P. F., Goldspink, D. A., Gribble, F. M., and Reimann, F. (2017). Chylomicrons stimulate incretin secretion in mouse and human cells. *Diabetologia* 60, 2475–2485. doi: 10.1007/s00125-017-4420-2

Pujadas, G., Varin, E. M., Baggio, L. L., Mulvihill, E. E., Bang, K. W. A., Koehler, J. A., et al. (2020). The gut hormone receptor GIPR links energy availability to the control of hematopoiesis. *Mol Metab.* 39:101008. doi: 10.1016/j.molmet.2020.101008

Pyke, C., Heller, R. S., Kirk, R. K., Orskov, C., Reedtz-Runge, S., Kaastrup, P., et al. (2014). GLP-1 receptor localization in monkey and human tissue: novel distribution revealed with extensively validated monoclonal antibody. *Endocrinology* 155, 1280–1290. doi: 10.1210/en.2013-1934

Ranganath, L. R., Beety, J. M., and Morgan, L. M. (1999). Inhibition of insulin, glucose-dependent insulinotropic polypeptide (GIP) and glucagon-like peptide-1 (GLP-1) secretion by octreotide has no effect on post-heparin plasma lipoprotein lipase activity. *Horm. Metab. Res.* 31, 262–266. doi: 10.1055/s-2007-978729

Reimann, F., Diakogiannaki, E., Moss, C. E., and Gribble, F. M. (2020). Cellular mechanisms governing glucose-dependent insulinotropic polypeptide secretion. *Peptides* 125:170206. doi: 10.1016/j.peptides.2019.170206

Reimann, F., Habib, A. M., Tolhurst, G., Parker, H. E., Rogers, G. J., and Gribble, F. M. (2008). Glucose sensing in L cells: a primary cell study. *Cell Metab.* 8, 532–539. doi: 10.1016/j.cmet.2008.11.002

Ribeiro-Parenti, L., Jarry, A. C., Cavin, J. B., Willemetz, A., Le Beyec, J., Sannier, A., et al. (2021). Bariatric surgery induces a new gastric mucosa phenotype with increased functional glucagon-like peptide-1 expressing cells. *Nat. Commun.* 12:110. doi: 10.1038/s41467-020-20301-1

Richards, P., Parker, H. E., Adriaenssens, A. E., Hodgson, J. M., Cork, S. C., Trapp, S., et al. (2014). Identification and characterization of GLP-1 receptor-expressing cells using a new transgenic mouse model. *Diabetes* 63, 1224–1233. doi: 10.2337/db13-1440

Roberge, J. N., and Brubaker, P. L. (1993). Regulation of intestinal proglucagon-derived peptide secretion by glucose-dependent insulinotropic peptide in a novel enteroendocrine loop. *Endocrinology* 133, 233–240. doi: 10.1210/endo.133.1.8319572

Roberge, J. N., Gronau, K. A., and Brubaker, P. L. (1996). Gastrin-releasing peptide is a novel mediator of proximal nutrient-induced proglucagon-derived peptide secretion from the distal gut. *Endocrinology* 137, 2383–2388. doi: 10.1210/endo.137.6.8641190

Robertson, M. D., Parkes, M., Warren, B. F., Ferguson, D. J., Jackson, K. G., Jewell, D. P., et al. (2003). Mobilisation of enterocyte fat stores by oral glucose in humans. *Gut* 52, 834–839. doi: 10.1136/gut.52.6.834

Rocca, A. S., and Brubaker, P. L. (1999). Role of the vagus nerve in mediating proximal nutrient-induced glucagon-like peptide-1 secretion. *Endocrinology* 140, 1687–1694. doi: 10.1210/endo.140.4.6643

Rowland, K. J., Trivedi, S., Lee, D., Wan, K., Kulkarni, R. N., Holzenberger, M., et al. (2011). Loss of glucagon-like peptide-2-induced proliferation following intestinal epithelial insulin-like growth factor-1-receptor deletion. *Gastroenterology* 141, 2166–2175.e7. doi: 10.1053/j.gastro.2011.09.014

Sato, S., Hokari, R., Kurihara, C., Sato, H., Narimatsu, K., Hozumi, H., et al. (2013). Dietary lipids and sweeteners regulate glucagon-like peptide-2 secretion. *Am. J. Physiol. Gastrointest. Liver Physiol.* 304, G708–G714. doi: 10.1152/ajpgi.00282.2012

Schwartz, E. A., Koska, J., Mullin, M. P., Syoufi, I., Schwenke, D. C., and Reaven, P. D. (2010). Exenatide suppresses postprandial elevations in lipids and lipoproteins in individuals with impaired glucose tolerance and recent onset type 2 diabetes mellitus. *Atherosclerosis* 212, 217–222. doi: 10.1016/j.atherosclerosis.2010.05.028

Schwartz, S. L., Ratner, R. E., Kim, D. D., Qu, Y., Fechner, L. L., Lenox, S. M., et al. (2008). Effect of exenatide on 24-hour blood glucose profile compared with placebo in patients with type 2 diabetes: a randomized, double-blind, two-arm, parallel-group, placebo-controlled, 2-week study. *Clin. Ther.* 30, 858–867. doi: 10.1016/j.clinthera.2008.05.004

Seino, Y., Ogata, H., Maekawa, R., Izumoto, T., Iida, A., Harada, N., et al. (2015). Fructose induces glucose-dependent insulinotropic polypeptide, glucagon-like peptide-1 and insulin secretion: Role of adenosine triphosphate-sensitive K(+) channels. *J. Diabetes Investig.* 6, 522–526. doi: 10.1111/jdi.12356

Sherman, S. K., Carr, J. C., Wang, D., O'Dorisio, M. S., O'Dorisio, T. M., and Howe, J. R. (2013). Gastric inhibitory polypeptide receptor (GIPR) is a promising target for imaging and therapy in neuroendocrine tumors. *Surgery* 154, 1206–1213;discussion1214. doi: 10.1016/j.surg.2013.04.052

Shibue, K., Yamane, S., Harada, N., Hamasaki, A., Suzuki, K., Joo, E., et al. (2015). Fatty acid-binding protein 5 regulates diet-induced obesity via GIP secretion from enteroendocrine K cells in response to fat ingestion. *Am. J. Physiol. Endocrinol. Metab.* 308, E583–E591. doi: 10.1152/ajpendo.00543.2014

Shin, E. D., Estall, J. L., Izzo, A., Drucker, D. J., and Brubaker, P. L. (2005). Mucosal adaptation to enteral nutrients is dependent on the physiologic actions of glucagon-like peptide-2 in mice. *Gastroenterology* 128, 1340–1353. doi: 10.1053/j.gastro.2005.02.033

Simon, M. C., Strassburger, K., Nowotny, B., Kolb, H., Nowotny, P., Burkart, V., et al. (2015). Intake of Lactobacillus reuteri improves incretin and insulin secretion in glucose-tolerant humans: a proof of concept. *Diabetes Care* 38, 1827–1834. doi: 10.2337/dc14-2690

Sivitz, W. I., Walsh, S. A., Morgan, D. A., Thomas, M. J., and Haynes, W. G. (1997). Effects of leptin on insulin sensitivity in normal rats. *Endocrinology* 138, 3395–3401. doi: 10.1210/endo.138.8.5327

Spreckley, E., and Murphy, K. G. (2015). The L-cell in nutritional sensing and the regulation of appetite. *Front. Nutr.* 2:23. doi: 10.3389/fnut.2015.00023

Stahel, P., Xiao, C., Davis, X., Tso, P., and Lewis, G. F. (2019). Glucose and GLP-2 (Glucagon-Like Peptide-2) mobilize intestinal triglyceride by distinct mechanisms. *Arterioscler. Thromb. Vasc. Biol.* 39, 1565–1573. doi: 10.1161/ATVBAHA.119.313011

Suzuki, K., Harada, N., Yamane, S., Nakamura, Y., Sasaki, K., Nasteska, D., et al. (2013). Transcriptional regulatory factor X6 (Rfx6) increases gastric inhibitory polypeptide (GIP) expression in enteroendocrine K-cells and is involved in GIP hypersecretion in high fat diet-induced obesity. *J. Biol. Chem.* 288, 1929–1938. doi: 10.1074/jbc.M112.423137

Sykes, S., Morgan, L. M., English, J., and Marks, V. (1980). Evidence for preferential stimulation of gastric inhibitory polypeptide secretion in the rat by actively transported carbohydrates and their analogues. *J. Endocrinol.* 85, 201–207. doi: 10.1677/joe.0.0850201

Szalowska, E., Meijer, K., Kloosterhuis, N., Razaee, F., Priebe, M., and Vonk, R. J. (2011). Sub-chronic administration of stable GIP analog in mice decreases serum LPL activity and body weight. *Peptides* 32, 938–945. doi: 10.1016/j.peptides.2011.02.011

Takeda, J., Seino, Y., Tanaka, K., Fukumoto, H., Kayano, T., Takahashi, H., et al. (1987). Sequence of an intestinal cDNA encoding human gastric inhibitory polypeptide precursor. *Proc. Natl. Acad. Sci. U.S.A.* 84, 7005–7008. doi: 10.1073/pnas.84.20.7005

Tseng, C. C., Jarboe, L. A., Landau, S. B., Williams, E. K., and Wolfe, M. M. (1993). Glucose-dependent insulinotropic peptide: structure of the precursor and tissue-specific expression in rat. *Proc. Natl. Acad. Sci. U.S.A.* 90, 1992–1996. doi: 10.1073/pnas.90.5.1992

Tso, P., Balint, J. A., Bishop, M. B., and Rodgers, J. B. (1981). Acute inhibition of intestinal lipid transport by Pluronic L-81 in the rat. *Am. J. Physiol.* 241, G487–G497. doi: 10.1152/ajpgi.1981.241.6.G487

Turner, J. R. (2009). Intestinal mucosal barrier function in health and disease. *Nat. Rev. Immunol.* 9, 799–809. doi: 10.1038/nri2653

Ugleholdt, R., Poulsen, M. L., Holst, P. J., Irminger, J. C., Orskov, C., Pedersen, J., et al. (2006). Prohormone convertase 1/3 is essential for processing of the glucose-dependent insulinotropic polypeptide precursor. *J. Biol. Chem.* 281, 11050–11057. doi: 10.1074/jbc.M601203200

Usdin, T. B., Mezey, E., Button, D. C., Brownstein, M. J., and Bonner, T. I. (1993). Gastric inhibitory polypeptide receptor, a member of the secretin-vasoactive intestinal peptide receptor family, is widely distributed in peripheral organs and the brain. *Endocrinology* 133, 2861–2870. doi: 10.1210/endo.133.6.8243312

Utzschneider, K. M., Kratz, M., Damman, C. J., and Hullar, M. (2016). Mechanisms linking the gut microbiome and glucose metabolism. *J. Clin. Endocrinol. Metab.* 101, 1445–1454. doi: 10.1210/jc.2015-4251

Varin, E. M., Hanson, A. A., Beaudry, J. L., Nguyen, M. A., Cao, X., Baggio, L. L., et al. (2020).). Hematopoietic cell- versus enterocyte-derived dipeptidyl peptidase-4 differentially regulates triglyceride excursion in mice. *JCI Insight* 5:e140418. doi: 10.1172/jci.insight.140418

Vilsboll, T., Krarup, T., Deacon, C. F., Madsbad, S., and Holst, J. J. (2001). Reduced postprandial concentrations of intact biologically active glucagon-like peptide 1 in type 2 diabetic patients. *Diabetes* 50, 609–613. doi: 10.2337/diabetes.50.3.609

Walsh, N. A., Yusta, B., DaCambra, M. P., Anini, Y., Drucker, D. J., and Brubaker, P. L. (2003). Glucagon-like peptide-2 receptor activation in the rat intestinal mucosa. *Endocrinology* 144, 4385–4392. doi: 10.1210/en.2003-0309

Wismann, P., Barkholt, P., Secher, T., Vrang, N., Hansen, H. B., Jeppesen, P. B., et al. (2017). The endogenous preproglucagon system is not essential for gut growth homeostasis in mice. *Mol. Metab.* 6, 681–692. doi: 10.1016/j.molmet.2017.04.007

Wu, J., Ren, W., Li, L., Luo, M., Xu, K., Shen, J., et al. (2018). Effect of aging and glucagon-like peptide 2 on intestinal microbiota in SD rats. *Aging Dis.* 9, 566–577. doi: 10.14336/AD.2017.1001

Xiao, C., Bandsma, R. H., Dash, S., Szeto, L., and Lewis, G. F. (2012). Exenatide, a glucagon-like peptide-1 receptor agonist, acutely inhibits intestinal lipoprotein production in healthy humans. *Arterioscler Thromb. Vasc. Biol.* 32, 1513–1519. doi: 10.1161/ATVBAHA.112.246207

Xiao, C., Stahel, P., Carreiro, A. L., Hung, Y. H., Dash, S., Bookman, I., et al. (2019). Oral glucose mobilizes triglyceride stores from the human intestine. *Cell Mol. Gastroenterol. Hepatol.* 7, 313–337. doi: 10.1016/j.jcmgh.2018.10.002

Yamada, Y., Hayami, T., Nakamura, K., Kaisaki, P. J., Someya, Y., Wang, C. Z., et al. (1995). Human gastric inhibitory polypeptide receptor: cloning of the gene (GIPR) and cDNA. *Genomics* 29, 773–776. doi: 10.1006/geno.1995.9937

Yamane, S., Harada, N., Hamasaki, A., Muraoka, A., Joo, E., Suzuki, K., et al. (2012). Effects of glucose and meal ingestion on incretin secretion in Japanese subjects with normal glucose tolerance. *J. Diabetes Investig.* 3, 80–85. doi: 10.1111/j.2040-1124.2011.00143.x

Yoon, H. S., Cho, C. H., Yun, M. S., Jang, S. J., You, H. J., Kim, J. H., et al. (2021). Akkermansia muciniphila secretes a glucagon-like peptide-1-inducing protein that improves glucose homeostasis and ameliorates metabolic disease in mice. *Nat. Microbiol.* 6, 563–573. doi: 10.1038/s41564-021-00880-5

Yusta, B., Baggio, L. L., Koehler, J., Holland, D., Cao, X., Pinnell, L. J., et al. (2015). GLP-1R agonists modulate enteric immune responses through the intestinal intraepithelial lymphocyte GLP-1R. *Diabetes* 64, 2537–2549. doi: 10.2337/db14-1577

Yusta, B., Boushey, R. P., and Drucker, D. J. (2000). The glucagon-like peptide-2 receptor mediates direct inhibition of cellular apoptosis via a cAMP-dependent protein kinase-independent pathway. *J. Biol. Chem.* 275, 35345–35352. doi: 10.1074/jbc.M005510200

Yusta, B., Matthews, D., Koehler, J. A., Pujadas, G., Kaur, K. D., and Drucker, D. J. (2019). Localization of glucagon-like peptide-2 receptor expression in the mouse. *Endocrinology* 160, 1950–1963. doi: 10.1210/en.2019-00398

Zietek, T., and Rath, E. (2016). Inflammation meets metabolic disease: gut feeling mediated by GLP-1. *Front. Immunol.* 7:154. doi: 10.3389/fimmu.2016.00154

Conflict of Interest: The EM lab receives funding from the Merck IISP program for preclinical studies unrelated to this work.

The remaining authors declare that the research was conducted in the absence of any commercial or financial relationships that could be construed as a potential conflict of interest.

Publisher's Note: All claims expressed in this article are solely those of the authors and do not necessarily represent those of their affiliated organizations, or those of the publisher, the editors and the reviewers. Any product that may be evaluated in this article, or claim that may be made by its manufacturer, is not guaranteed or endorsed by the publisher.

frontiers in Cell and Developmental Biology

ORIGINAL RESEARCH
published: 25 October 2021
doi: 10.3389/fcell.2021.749607

Loss of Function Glucose-Dependent Insulinotropic Polypeptide Receptor Variants Are Associated With Alterations in BMI, Bone Strength and Cardiovascular Outcomes

Hüsün Sheyma Kizilkaya[1†], Kimmie Vestergaard Sørensen[2†], Camilla J. Kibsgaard[1], Laerke Smidt Gasbjerg[1], Alexander S. Hauser[3], Alexander Hovard Sparre-Ulrich[1,4], Niels Grarup[2‡] and Mette M. Rosenkilde[1*‡]*

[1] Department of Biomedical Sciences, Faculty of Health and Medical Sciences, University of Copenhagen, Copenhagen, Denmark, [2] Faculty of Health and Medical Sciences, Novo Nordisk Foundation Center for Basic Metabolic Research, University of Copenhagen, Copenhagen, Denmark, [3] Department of Drug Design and Pharmacology, University of Copenhagen, Copenhagen, Denmark, [4] Antag Therapeutics ApS, Copenhagen, Denmark

Glucose-dependent insulinotropic polypeptide (GIP) and its receptor (GIPR) are involved in multiple physiological systems related to glucose metabolism, bone homeostasis and fat deposition. Recent research has surprisingly indicated that both agonists and antagonists of GIPR may be useful in the treatment of obesity and type 2 diabetes, as both result in weight loss when combined with GLP-1 receptor activation. To understand the receptor signaling related with weight loss, we examined the pharmacological properties of two rare missense *GIPR* variants, R190Q (rs139215588) and E288G (rs143430880) linked to lower body mass index (BMI) in carriers. At the molecular and cellular level, both variants displayed reduced G protein coupling, impaired arrestin recruitment and internalization, despite maintained high GIP affinity. The physiological phenotyping revealed an overall impaired bone strength, increased systolic blood pressure, altered lipid profile, altered fat distribution combined with increased body impedance in human carriers, thereby substantiating the role of GIP in these physiological processes.

Keywords: glucose-dependent insulinotropic polypeptide receptor (GIPR), single nucleotide variants (SNVs), altered receptor signaling and internalization, gut-bone axis, bone mineral density, type 2 diabetes and adiposity, blood pressure, lipids

OPEN ACCESS

Edited by:
Sameer Mohammad, King Abdullah International Medical Research Center (KAIMRC), Saudi Arabia

Reviewed by:
Giulia Baldini, University of Arkansas for Medical Sciences, United States
Nigel Irwin, Ulster University, United Kingdom

****Correspondence:***
Niels Grarup
niels.grarup@sund.ku.dk
Mette M. Rosenkilde
rosenkilde@sund.ku.dk

† These authors have contributed equally to this work and share first authorship

‡ These authors have contributed equally to this work and share last authorship

Specialty section:
This article was submitted to Signaling, a section of the journal Frontiers in Cell and Developmental Biology

Received: *29 July 2021*
Accepted: *16 September 2021*
Published: *25 October 2021*

Citation:
Kizilkaya HS, Sørensen KV, Kibsgaard CJ, Gasbjerg LS, Hauser AS, Sparre-Ulrich AH, Grarup N and Rosenkilde MM (2021) Loss of Function Glucose-Dependent Insulinotropic Polypeptide Receptor Variants Are Associated With Alterations in BMI, Bone Strength and Cardiovascular Outcomes. Front. Cell Dev. Biol. 9:749607. doi: 10.3389/fcell.2021.749607

INTRODUCTION

Glucose-dependent insulinotropic polypeptide (GIP) is a gut-derived hormone that is secreted from the enteroendocrine K cells in the proximal part of the small intestinal in response to nutrient intake (Baggio and Drucker, 2007; Sonne et al., 2014). GIP, along with a related hormone, glucagon-like peptide-1 (GLP-1), constitute the incretin hormones that regulate postprandial glucose tolerance by stimulating insulin release from pancreatic β-cells (Gasbjerg et al., 2020a). In contrast to GLP-1, GIP has been demonstrated to enhance glucagon secretion in a glucose-dependent manner in healthy individuals, thus at low- and normal blood glucose levels GIP stimulates glucagon secretion from α-cells, but fails to do so at higher blood glucose levels

(Christensen et al., 2011, 2015). GIP has also been ascribed a role in mediating fat deposition (Asmar et al., 2016). The GIP receptor (GIPR) belongs to the class B1 G protein-coupled receptor (GPCR) superfamily and signals through $G\alpha_s$/adenylyl cyclase activation, leading to increased cyclic adenosine monophosphate (cAMP) concentrations (Holst, 2019).

The GIPR is not only expressed in pancreatic islet cells and adipocytes but has a wide expression profile including, but possibly not limited to, the heart, spleen, lung, central nervous system, and thyroid cells (Baggio and Drucker, 2007). Additionally, the GIP system is important for bone metabolism through GIPR expression on osteoblasts and osteoclasts (Bollag et al., 2000; Zhong et al., 2007; Skov-Jeppesen et al., 2021) through which GIP inhibits bone resorption as well as promotes bone formation (Tsukiyama et al., 2006; Zhong et al., 2007; Berlier et al., 2015; Skov-Jeppesen et al., 2019). Even though it is now getting recognized that GIP/GIPR is involved in bone metabolism, it is largely unknown how genetic alterations, influencing GIPR signaling, affect bone growth and resorption. The potential impact of the GIP-GIPR axis in other organ systems is similarly underinvestigated. A recent review emphasized the potential importance of GIP/GIPR in cardiovascular diseases, although details of the operation of this axis in humans are virtually unknown (Heimbürger et al., 2020).

GIP is associated with the pathophysiology of obesity and type 2 diabetes mellitus (T2D) and have therefore been the focus of therapeutic interest for many years. It is currently debated whether to use GIPR agonists or -antagonists in combination with GLP-1 agonists to treat obesity and T2D, as both combinations show promising results (Holst and Rosenkilde, 2020; Killion et al., 2020; Min et al., 2020). Clearly, there is a need to better understand the biology of the GIPR system to be able to exploit its pharmacological potential.

Genome-wide association studies (GWAS) have revealed that common variants in the *GIPR* are associated with obesity (Vogel et al., 2009; Speliotes et al., 2010) and impaired glucose- and bone mineral homeostasis (Sauber et al., 2010; Saxena et al., 2010; Torekov et al., 2014). With the exemption of rs1800437 causing the amino acid change E354Q, which leads to long-term functional impairment due to its distinct ligand binding kinetics, signaling and internalization profile (Kubota et al., 1996; Almind et al., 1998; Fortin et al., 2010; Mohammad et al., 2014; Gabe et al., 2019), the *GIPR* variants have not been functionally characterized. In a recent exome-wide association study designed to discover protein-altering variants associated with body mass index (BMI), two rare variants in *GIPR* were identified (Turcot et al., 2018). These missense variants result in amino acid changes, R190Q (rs139215588) and E288G (rs143430880). From gnomAD (Karczewski et al., 2020), the frequencies of R190Q and E288G in Europeans are 0.00093 and 0.0017, corresponding to ∼1 in 500 and ∼1 in 300 being heterozygous carriers, respectively. For each variant, heterozygote carriers of the rare allele had a ∼0.15 SD lower BMI compared to non-carriers, corresponding to an effect of ∼0.65 kg/m^2. Interestingly, one middle-aged woman carried both rare *GIPR* mutations in heterozygote form and she weighed ∼11 kg less than the average non-carrier of the same height (Turcot et al., 2018).

Here we combine molecular pharmacological phenotyping with the physiological consequences of carrying these two rare *GIPR* variants. First, we investigated experimentally the GIP receptor binding and activation properties of the two variants, and secondly, we linked our findings to human physiology by assessing summary data of previously published studies and online portals.

MATERIALS AND METHODS

Materials

The human GIPR that was inserted into pcDNA 3.1 plasmid (GenBank accession number: NM_000164) was synthesized and purchased from GenScript (Piscataway, NJ) along with the GIPR mutations: R190Q, E288G and the double mutant R190Q-E288G. For the real-time internalization assay, the N-terminally SNAP-tagged GIPR was synthesized and purchased from Cisbio (Codolet, France) and R190Q and E288G were introduced into the wild-type GIPR by site-directed mutagenesis according to quick-change protocol, using primers:

GCGGCCATTCTCAGCCAGGACCGTCTGC (forward for R190Q), GCAGACGGTCCTGGCTGAGAATGGCCGC (reverse for R190Q), CGCAGTGCTGGGGCCGCAACGA AGTCAAGGC (forward for E288G), GCCTTGACTTCG TTGCGGCCCCAGCACTGCG (reverse for E288G).

Human GIP(1-42) was purchased from Caslo ApS (Lyngby, Denmark). HEK293 and COS-7 cells were both purchased from ATTC (Manassas, VA). Cell medium for HEK293 was purchased from Thermo Fisher Scientific (Waltham, MA) and the cell medium for COS-7 cells were prepared in-house. Other chemicals were purchased from standard commercial sources.

Transfection and Tissue Culture

COS-7 cells were cultured at 10% CO_2 and 37°C in Dulbecco's Modified Eagle Medium (DMEM) 1885 supplemented with 10% fetal bovine serum (FBS), 2 mmol/L glutamine, 180 units/mL penicillin and 45 g/mL streptomycin. HEK293 cells were cultured at 10% CO_2 and 37°C in DMEM GlutaMAX^{TM}-I supplemented with 10% FBS, 180 units/mL penicillin and 45 g/mL streptomycin. Both cell lines were transfected using the calcium phosphate precipitation method (Jensen et al., 2008) for binding and cAMP assay. For β-arrestin 2 recruitment assay, the PEI-transfection method was used and the Lipofectamine transfection method was used for the internalization assay.

Transiently transfected COS-7 cells were used in homologous competition binding assay. HEK293 cells were used in cAMP accumulation, β-arrestin 2 recruitment and internalization experiments.

cAMP Experiments

HEK293 cells were transiently transfected with either wild-type GIPR, R190Q, E288G or the double mutation R190;E288G, and the cAMP measurements were done with an enzyme fragment complementation (EFC)-based assay (Hansen et al., 2016). In

brief, the cells were seeded in white 96-well plates at a density of 35.000 per well 1 day after the transfection. The following day, the cells were washed twice with HEPES-buffered saline (HBS) and incubated with HBS and 1 mM 3-isobutyl-1-methylxanthine (IBMX) for 30 min at 37°C. The cells were then stimulated with increasing concentrations of GIP(1-42) and incubated for additional 30 min at 37°C. The HitHunterTM cAMP XS assay (DiscoverX, Herlev, Denmark) was carried out according to manufacturer's instructions.

Homologous Competition Binding Assay

Transiently transfected COS-7 cells expressing either wild-type GIPR, R190Q, E288G or R190Q;E288G were seeded in a clear 96-well plate 1 day after transfection. The number of cells added per well was adjusted aiming for 5–10% specific binding of ^{125}I-GIP(1-42). The following day, the cells were assayed by competition binding for 3-h at 4°C using ∼15–40 pM of ^{125}I-GIP(1-42) and increasing concentrations of GIP(1-42) in binding buffer (50 mmol/L HEPES buffer, pH 7.2 supplemented with 0.5% bovine serum albumin (BSA). After incubation, the cells were washed in ice-cold binding buffer and lysed with 200 mmol/L NaOH with 1% SDS for 30 min. The samples were analyzed by the Wallac Wizard 1470 Gamma Counter.

β-Arrestin 2 Recruitment Assay

To measure β-arrestin 2 recruitment, HEK293 cells were transiently transfected with either wild-type GIPR, R190Q, E288G or R190Q;E288G and the donor Rluc8-Arrestin-3-Sp1, the acceptor mem-linker-citrine-SH3 and GPCR kinase 2 (GRK2) to facilitate β-arrestin 2 recruitment. Two days after transfection, the cells were washed with PBS and re-suspended in PBS with 5 mmol/L glucose. Subsequently, 85 μL of the cell suspension solution was transferred to its respective wells on a white 96-well isoplate followed by the addition of PBS with 5 μmol/L coelenterazine-h. After a 10 min incubation of the cells with coelenterazine-h, increasing concentration of endogenous GIP(1-42) were added and luminescence was measured by the Berthold Technologies Mithras Multilabel Reader (Rluc8 at 485 ± 40 nm and YFP at 530 ± 25 nm).

Real-Time Internalization Assay

HEK293 parental cells transiently expressing the SNAP-tag GIPR or the variant, SNAP-tag-R190Q or—E288G were seeded in white 384-well plate after transfection, at a density of 20.000 cells per well. The following day, the medium was removed and fresh medium was added to all wells. The next day, the assay was carried out by labeling all SNAP-tagged cells with 100 nmol/L Taglite SNAP-Lumi4-Tb (donor) in OptiMEM for 60 min at 37°C. Subsequently, the cells were washed 4 × with HBBS supplemented with 1 mM $CaCl_2$, 1 mM $MgCl_2$, 20 mM HEPES and 0.1% BSA (internalization buffer, pH 7.4). 50 μM pre-heated fluorescein-O'-acetic acid (acceptor) was added to all wells, except wells where only donor signal was measured. The 384-plates were incubated at 37°C for 5–10 min prior to ligand addition. Then, the cells were stimulated with increasing doses of GIP(1-42), that was pre-heated at 37°C, and donor signal and internalization rate were measured every 4 min for 90 min at 37°C in PerkinElmer^{TM} Envision 2014 multi-label Reader.

Analysis of Online High Quality Summary Statistics of R190Q and E288G

Frequencies of R190Q and E288G were from gnomAD v2.1.1 (Karczewski et al., 2020). We examined available summary data from published papers to determine the effect of *GIPR* R190Q and E288G on relevant phenotypes. Data on bone mineral density (BMD) and bone fracture risk have been contributed by Morris et al. (2019). The *p*-values P.NI and P.I were used, respectively, as recommended by the authors. The data was downloaded from http://www.gefos.org/?q=content/data-release-2018. The BMD and fracture risk summary data derive from analyses performed in UK Biobank (N_{BMD} = 426,824; fracture risk = 53,184 cases and 373,611 controls). Summary statistical data on body composition, obesity risk, physical activity, and cardiovascular events were derived from GeneATLAS (UK Biobank, *N* = 452,264) (Canela-Xandri et al., 2018). These summary data were downloaded from http://geneatlas.roslin.ed.ac.uk/. Summary data on circulating leptin levels (*N* = 57,232) have been contributed by Yaghootkar et al. (2020) via the NHGRI-EBI GWAS Catalog. The NHGRI-EBI GWAS Catalog is funded by NHGRI Grant Number 2U41HG007823, and delivered by collaboration between the NHGRI, EMBL-EBI and NCBI. Summary statistics were downloaded from the NHGRI-EBI GWAS Catalog (Buniello et al., 2019) for study GCST90007307 and GCST90007319 (Yaghootkar et al., 2020) on 15/12/2020 and 16/12/2020, respectively. Risk of T2D was assessed by summary statistical data (48,286 cases and 250,671 controls) contributed by Mahajan et al. (2018), and the data were downloaded from http://diagram-consortium.org/downloads.html. Results included two models either not including BMI as a covariate or adjusted for BMI (BMI adj.). The lipid levels association results were derived from summary data of an exome-wide meta-analysis (*N* = ∼350,000) contributed by Lu et al. (2017), and we downloaded the data from http://csg.sph.umich.edu/willer/public/lipids2017EastAsian/.

Blood pressure and hypertension were investigated based on summary data derived from a meta-analysis of rare variants associated with blood pressure measures in European individuals (*N* = 1,164,961) performed by Surendran et al. (2020). These summary data were downloaded from https://app.box.com/s/1ev9iakptips70k8t4cm8j347if0ef2u.

Data on myocardial infarction include summary statistics (*N* = 42,335 cases and 78,240 controls) contributed by the CARDIoGRAMplusC4D Consortium (Myocardial Infarction Genetics and CARDIoGRAM Exome Consortia Investigators, Stitziel et al., 2016). Data on coronary artery disease/myocardial infarction were contributed by the Myocardial Infarction Genetics and CARDIoGRAM Exome investigators and were downloaded from www.CARDIOGRAMPLUSC4D.ORG. Summary statistical data on SOFT coronary artery disease [fatal or non-fatal myocardial infarction, percutaneous transluminal coronary angioplasty or coronary artery bypass grafting, chronic ischemic heart disease, and angina; *N* = 71,602 cases and 260,875

controls (53,135 cases and 215,611 controls for the exome markers)] are derived from a meta-analysis of three GWAS, namely UK Biobank (interim release), CARDIoGRAMplusC4D 1000 Genomes-based, and the Myocardial Infarction Genetics and CARDIoGRAM Exome (Nelson et al., 2017). Data on coronary artery disease/myocardial infarction have been contributed by the CARDIoGRAMplusC4D and UK Biobank CardioMetabolic Consortium CHD working group who used the UK Biobank Resource (application number 9922). Data have been downloaded from www.CARDIOGRAMPLUSC4D.ORG. **Supplementary Table 1** provides further details about the different studies and cohorts. A *p*-value below 0.05 was considered as statistically significant in analyses of specific hypotheses, while a significance threshold of 10^{-4} was applied on the phenome-wide scan in UK Biobank data.

RESULTS

The Glucose-Dependent Insulinotropic Polypeptide Receptor Variants, R190Q and E288G, Show Markedly Reduced G Protein-Mediated Signaling Despite Maintained Glucose-Dependent Insulinotropic Polypeptide Binding

The residue R190 is placed in the second transmembrane (TM2) domain in position 67 of the GIPR, hence denoted $R190^{2.67}$ (Wooten nomenclature in superscript; Wootten et al., 2013), near the first extracellular loop (ECL1), whereas E288 residue is located in the second extracellular loop (ECL2) of the receptor (**Figure 1A**). It has previously been shown that the N-terminal part of GIP, interacts with $R190^{2.67}$ by forming a hydrogen bond (Smit et al., 2021; Zhao et al., 2021).

As $G\alpha_s$ is the main signaling pathway for the GIPR, we assessed the impact of these two mutations either separately or in combination. This was done by measuring intracellular cAMP accumulation in transiently transfected HEK293 cells in response to increasing concentrations of GIP. Both variants displayed reduced signaling capacity compared to wild-type GIPR with a markedly decreased (>250-fold) potency of GIP with EC_{50}-values of 10 nM for R190Q and 3.6 nM for E288Q, compared to the wild-type GIPR with an EC_{50}-value of 4.2 pM (**Table 1**). R190Q reached a maximal activation (E_{max}) of 75% of that of wild-type GIPR at 1 μM, whereas E288G reached 90%. The double mutant, R190Q-E288G resulted in a complete loss of activation through $G\alpha_s$ (**Figure 1B**).

To determine whether the reduced cAMP formation was due to impaired agonist binding, we performed homologs competition binding, using ^{125}I-GIP(1-42) as radio-ligand for the wildtype plus all three GIPR variants. Both single mutations displayed reduced binding capacity (B_{max}) with 30% of the wild-type GIPR for R190Q, and only 13% for E288G, while the double mutant exhibited minimal binding (< 1%) (**Figure 1D**). The binding affinities (K_D) of GIP were, however, not affected substantially as GIP bound with an affinity (K_D) of 5.0 nM and 3.9 nM for R190Q and E288G, respectively, while it bound the wild-type GIPR with an affinity of 2.7 nM (**Figure 1C**).

The Glucose-Dependent Insulinotropic Polypeptide Receptor Variants Display Impaired β-Arrestin 2 Recruitment and Internalization

Due to the maintained binding affinity but lower number of receptors expressed, we next set out to investigate β-arrestin 2 recruitment given its role in the desensitization and internalization of the GIPR (Gabe et al., 2018, 2020). All three variants displayed reduced ability to recruit β-arrestin 2 with an E_{max} of 9.0% for R190Q, 8.6% for E288G, and 12% for the double mutant compared to wild-type GIPR. There was, however, no major difference with respect to the potencies of the receptors' ability to recruit β-arrestin 2; R190Q had an EC_{50} of 0.76 nM while E288G had an EC_{50} value of 0.23 nM compared to wild-type GIPR with an EC_{50} of 0.88 nM. The double mutant, however, displayed an EC_{50}-value of 11 nM (**Figure 1E**). Thus, the overall maintained potency in β-arrestin 2 recruitment but lower E_{max} corresponded with the binding profiles of the variants.

We then performed real-time internalization experiments to determine whether the reduced β-arrestin recruitment influenced receptor internalization. Here, we used SNAP-tagged versions of the single mutant GIPR variants expressed transiently in HEK293 cells while the double mutant was omitted due to its low expression. Upon transfection with same amount of DNA of either wild-type SNAP-tagged GIPR or SNAP-tagged GIPR mutants, we observed a significantly lower receptor cell surface expression of 60% of wild-type GIPR for both single mutant variants (**Figure 1G**). This indicates that the reduced binding capacity of GIP to R190Q and E288G could partly be explained by the lower receptor cell surface expression. Since internalization measurements are dependent on receptor expression (Foster and Bräuner-Osborne, 2018), we next titrated receptor concentrations to obtain similar donor signal (i.e., similar cell surface expression) from the SNAP-tag in the different GIPR variants. For similar expression levels, we observed no internalization of either variant receptors (**Figure 1F**).

Taken together, the molecular pharmacological phenotype of the GIPR variants comprised diminished signaling through $G\alpha_s$, reduced β-arrestin 2 recruitment and impaired receptor internalization. The affinity of GIP was maintained for the GIPR variants but with lower binding capacity, which could be explained by the lower receptor cell surface expression.

The Glucose-Dependent Insulinotropic Polypeptide Receptor E288G Variant Reduces Bone Mineral Density

Since R190Q (rs139215588) and E288G (rs143430880) diminished receptor activation, we were interested in linking these functional consequences with phenotypes in humans. At first, we searched for the largest genetic studies to gather available results of the two *GIPR* variants. The present study therefore includes high quality data for R190Q and E288G

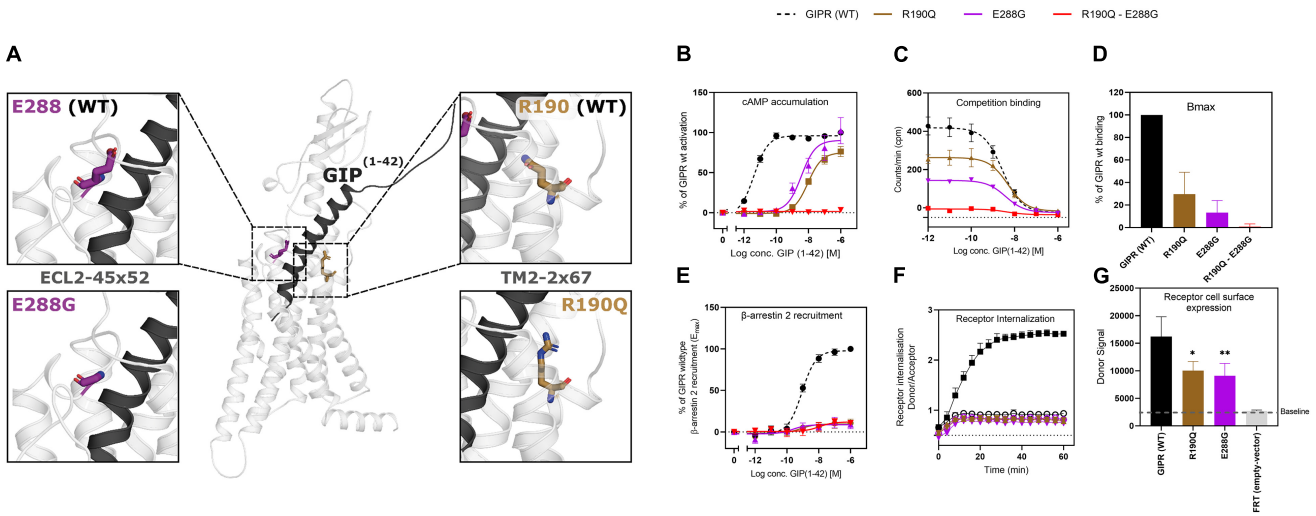

FIGURE 1 | Structural localization of R190Q and E288G on the wild-type GIPR and the molecular pharmacological phenotype of the variants. **(A)** Structural illustration of the wild-type GIPR and the position of the *GIPR* variants, R190Q and E288G. **(B)** Dose-response curve in cAMP accumulation of wild-type GIPR, R190Q, E288G and double mutant. **(C)** Dose-response curves of the homologous competition binding data with [^{125}I]GIP and unlabeled GIP at 4°C for 3 h of wildtype GIPR, R190Q, E288G and double mutant. **(D)** Corresponding B_{max} values. **(E)** Dose-response curve of β-arrestin 2 recruitment of wild-type GIPR, R190Q, E288G and double mutant. **(F)** Internalization of SNAP-GIPR, SNAP-R190Q and SNAP-E288G over time following stimulation with 1 μM GIP vs. baseline. **(G)** Receptor cell surface expression levels of SNAP-GIPR, SNAP-R190Q, SNAP-E288G, and FRT (empty-SNAP-vector). Data represent the mean ± SEM of minimum $n = 3$. Independent experiments are performed in either duplicate or triplicates. Statistical significance was assessed using an ordinary one-way ANOVA for receptor cell surface expression (*$p < 0.05$; **$p < 0.01$; as compared to wild-type response).

from these genetic studies, in which we evaluated each *GIPR* variant separately.

We started our physiological investigation by examining bone mineral density (BMD) and fracture risk in carriers of R190Q and E288G using summary data from a study in UK Biobank with a total sample size of 426,824 individuals (Morris et al., 2019). Interestingly, E288G was associated with lower BMD (Beta –0.056 SD, *p*-value = 0.002) and R190Q showed similar effect size (–0.057 SD), but this was not statistically significant (**Figure 2**). None of the two *GIPR* variants seemed to be associated with an overall risk of bone fracture (**Table 2**).

Both Body Mass Index-Lowering Glucose-Dependent Insulinotropic Polypeptide Receptor Variants Show Effects of Cardio-Metabolic Importance

Next, we examined the association with several traits of importance for cardio-metabolic health and disease. First, we evaluated the impact of R190Q and E288G on blood pressure in summary data from a newly published paper of rare genetic variations associating with blood pressure measures, which comprised > 800,000 individuals (Surendran et al., 2020). Both *GIPR* variants were associated with higher systolic blood pressure (R190Q: 0.045 SD; E288G: 0.049 SD), although the diastolic blood pressure was not significantly different between carriers and non-carriers (**Figure 2**). Furthermore, the E288G variant was associated with higher pulse pressure (**Figure 2**), while neither of the *GIPR* variants were associated with increased risk of hypertension (**Table 2**).

We next examined the lipid profile to gain further insight into how R190Q and E288G with impaired GIPR signaling affected lipid homeostasis. Here we used summary statistics from an exome-chip based meta-analysis of ∼350,000 individuals (Lu et al., 2017). Carriers of R190Q did not have altered lipid levels compared to non-carriers, whereas carriers of E288G had lower high-density lipoprotein (HDL) cholesterol levels (beta = –0.10 SD, *p*-value = 0.02), yet with no changes in low-density lipoprotein (LDL), triglycerides or total cholesterol (**Figure 2**). Despite the impact on cardiovascular parameters, neither one of the rare *GIPR* variants, R190Q and E288G, in the present study associated with overall risk of cardiovascular events as major cause of death (**Supplementary Table 2**) in summary data for the UK Biobank cohort (N = 452,264) (Canela-Xandri et al., 2018).

Alterations in circulating leptin levels could be a putative mechanism of body weight regulation, and we therefore evaluated whether the two *GIPR* variants had altered levels from a genetic study of circulating leptin in early adiposity ($N = 57,232$) (Yaghootkar et al., 2020). Only R190Q was significantly associated with lowered leptin levels, although this association was lost when adjusting for BMI (**Figure 2**).

We also explored how the *GIPR* variants affect risk of T2D in summary data from a study of coding variants in T2D (48,286 cases and 250,671 controls) (Mahajan et al., 2018). In a model not adjusted for BMI, none of the rare *GIPR* variants were associated with risk of T2D. In contrast, a BMI-adjusted model showed that carriers of E288G had a decreased risk of T2D compared to non-carriers (OR 0.76, *p*-value = 0.04) (**Table 2**).

TABLE 1 | Pharmacological data of *GIPR* variants, R190Q, E288G and the double mutant.

	Binding			cAMP accumulation			β -arrestin 2 recruitment		
	B_{max}	pIC_{50}	F_{mut}	E_{max}	pEC_{50}	F_{mut}	E_{max}	pEC_{50}	F_{mut}
Missense variant	**% of WT ± SEM**	**pIC_{50} ± SEM**	**(K_D mutation/K_D Wild-type)**	**% of WT ± SEM**	**$LogEC_{50}$ ± SEM**	**(EC_{50} mutation/EC_{50} Wild-type)**	**% of WT ± SEM**	**pEC_{50} ± SEM**	**(EC_{50} mutation/EC_{50} Wild-type)**
GIPR (WT)	100	8.6 ± 0.2		96 ± 1.4	11 ± 0.1		98 ± 2.7	9.1 ± 0.1	
R190Q	30 ± 11	8.3 ± 0.2	1.8	75 ± 2.8	8.0 ± 0.1	> 250	9.0 ± 2.5	9.1 ± 0.7	0.9
E288G	13 ± 6.1	8.4 ± 0.3	1.4	90 ± 6.2	8.4 ± 0.2	> 250	8.6 ± 2.5	9.6 ± 0.8	0.3
R190Q;E288G	0.70 ± 1.4	8.4 ± 0.5	1.5	NA	NA	NA	12 ± 2.8	8.0 ± 0.6	12.5

All data were fitted with three-parameter logistic curve to obtain pEC_{50} and E_{max}. pEC_{50} and pIC_{50} represent the negative logarithm of agonist concentration in molar that produces half the maximal response/inhibition. B_{max} is characterized as the maximum specific binding normalized to wild-type GIPR. E_{max} is characterized as the maximal response normalized to wild-type GIPR. F_{mut} is the fold change in potency, EC_{50} and in affinity, $K_{Dmutant}$, between mutants and wildtype receptor, calculated as $EC_{50\ mutant}$ / $EC_{50\ wildtype}$ and $K_{Dmutant}$ / $K_{Dwildtype}$. Data represent the mean ± SEM of at least three independent experiments performed in duplicate. NA, no activation observed.

Both Glucose-Dependent Insulinotropic Polypeptide Receptor Variants Associate With Multiple Adiposity-Related Measures

To further assess how the two *GIPR* variants, R190Q and E288G, impact adiposity, we evaluated adiposity-related traits using UK Biobank results from the GeneATLAS portal (N = 452,264) (Canela-Xandri et al., 2018). We found the same direction of association with BMI for R190Q and E288G (**Figure 3**), however, with a somewhat smaller effect size than previously reported (R190Q: –0.088 SD; E288G: –0.093 SD) (Turcot et al., 2018). Interestingly, carriers of either of the two *GIPR* variants had in general lower values of most adiposity-related measures compared to non-carriers; hence carriers had lower weight (R190Q: –0.091 SD; E288G: –0.092 SD), lower hip circumference (R190Q: –0.11 SD; E288G: –0.12 SD), lower waist circumference (R190Q: –0.056 SD; E288G: –0.063 SD), lower fat percentage (R190Q: –0.062 SD; E288G: –0.052 SD), lower fat mass (R190Q: –0.091 SD; E288G: –0.082 SD) and fat-free body mass (R190Q: –0.057 SD; E288G: –0.057 SD) (**Figure 3**). Furthermore, both variants were associated with a lower basic metabolic rate (R190Q: –0.064 SD; E288G: –0.063 SD). Despite these findings, none of the *GIPR* variant carriers significantly decreased risk of obesity (data not shown).

Finally, we investigated UK Biobank data by a phenome-wide study. Here, all above-mentioned findings at p-value $< 10^{-4}$ for both *GIPR* variants were related to adiposity (**Supplementary Tables 3**, **4**).

DISCUSSION

We show that two naturally occurring rare *GIPR* variants, R190Q and E288G (rs139215588 and rs143430880, respectively), result in impaired GIPR function at the molecular level which in turn seems to impact human physiology and pathophysiology regarding adiposity, bone health and the cardiovascular system (**Figure 4**).

The prevailing model for ligand-binding and receptor activation of class B1 receptors, including the GIPR, is that the extracellular domain (ECD) of the receptor recognizes the C-terminal of the endogenous peptide hormone that in turn allows the N-terminal part of the ligand to position itself into the transmembrane domain (TMD) (Schwartz and Frimurer, 2017). While several structure models exist for the closely related class B1 receptors, GLP-1R and glucagon receptor (Zhang et al., 2017, 2018), the structural data of the full length human GIPR are scarce, and only few studies have been conducted to describe GIPR residues of importance for receptor activation (Yaqub et al., 2010; Cordomí et al., 2015). However, the importance of the R190- and E288 residues for GIP binding and GIPR activation was recently discussed in a study that combined MD simulations and mutagenesis experiments (Smit et al., 2021). Here, it was shown that R190 is an important residue for GIPR activation as the N-terminal part of the GIP was described to form a hydrogen bond with this residue. A similar observation was made earlier

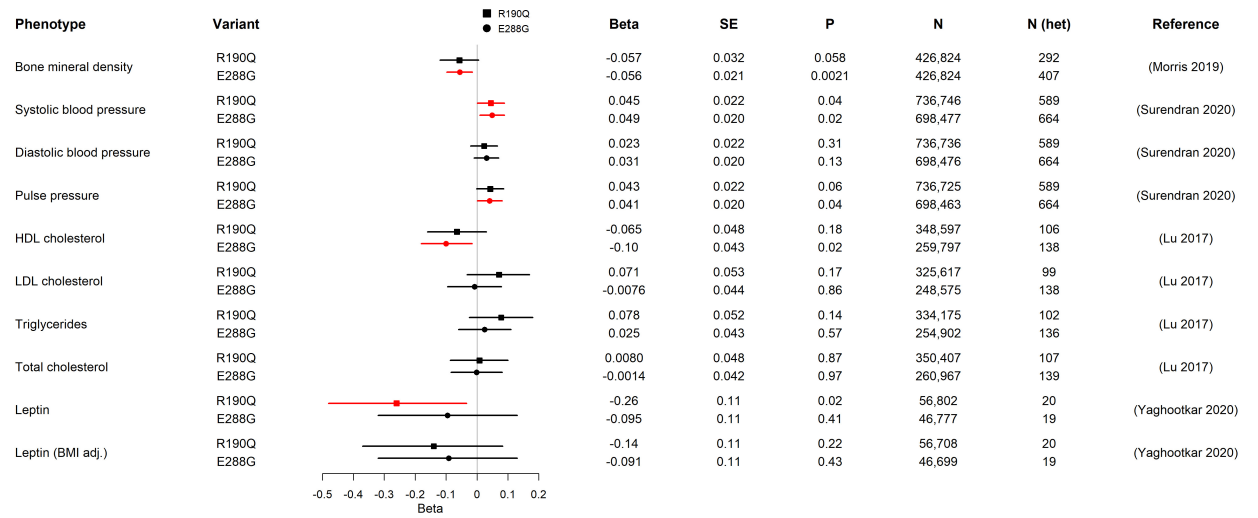

FIGURE 2 | Association of *GIPR* R190Q and E288G variants with quantitative cardio-metabolic traits in GWAS. For each variant, beta, standard error (SE), the *p*-value (P), sample size (N), estimate of heterozygous variant carriers (N het), and the publication of the study from which we have gathered data from are shown. The forest plot shows the beta in SD and the 95% confidence interval. Statistically significant results are shown in red. The number of heterozygous variant carriers (N het) was estimated from allele frequency and total number of individuals (N). HDL cholesterol, high-density lipoprotein cholesterol; LDL cholesterol, low-density lipoprotein cholesterol.

TABLE 2 | Association of *GIPR* variants, R190Q and E288G with relevant dichotomous phenotypes.

Trait	R190Q (rs139215588)					E288G (rs143430880)					References
	EAF	OR	95% CI	P	N	EAF	OR	95% CI	P	N	
Fracture risk	0.0014	1.001	0.80–1.25	0.99	426,795	0.0019	0.995	0.86–1.15	0.94	426,795	Morris et al., 2019
T2D	0.0015	1.19	0.84–1.69	0.56	298,957	0.0017	0.82	0.65–1.04	0.17	298,957	Mahajan et al., 2018
T2D, BMI adj.	0.0015	1.30	0.93–1.81	0.28	298,957	0.0017	0.76	0.60–0.96	0.04	298,957	Mahajan et al., 2018
	EAF	Z-score		P	N	EAF	Z-score		P	N	
Hypertension	0.0016	1.78		0.07	614,250	0.0087	1.71		0.09	548,903	Surendran et al., 2020

EAF, effect allele frequency; SE, standard error; P, p-value; N, sample size; OR, odds ratio; BMI adj., body mass index adjusted.

by Yaqub et al. (2010) who showed a decrease in cAMP signaling upon agonist binding. Moreover, a recent cryo-EM structure by Zhao et al. (2021) of the human GIPR in complex with GIP and a G_s-heterotrimer confirmed the formation of hydrogen bond between GIP and the R190 residue. The E288 residue appears to have a bigger impact on ligand binding (5.4-fold reduction in affinity and a B_{max} of 32% compared to wild-type) than on activation, when substituted with an alanine (Smit et al., 2021). This is in line with the results of the present study, as we also saw a limited maximum binding capacity of 13% in E288Q, as we would expect a mutation to glycine (in E288G) to remove all functionality like alanine does (in E288A). In addition, we also observed a > 250-fold reduction in the GIP potency in G protein signaling for E288Q compared to wild-type GIPR, and supra-physiological GIP levels were needed for near maximum receptor activation. Similar impairment in terms of cAMP production was also published very recently (Akbari et al., 2021). We, in addition, found that R190Q and E288G displayed a diminished arrestin recruitment that in return resulted in a lack of receptor internalization, consistent with the previously established arrestin dependency for GIPR internalization (Gabe et al., 2018). Altogether, the functional data indicate that both *GIPR* variants disrupt the conformational changes necessary for receptor activation and arrestin recruitment, and also reduce receptor cell surface expression, while still preserving the binding of GIP.

Circulating GIP is a multi-functional incretin hormone that acts on several targets, among which bone metabolism has been the focus of several recent studies. Rodents that lack GIPR have reduced bone size, bone mass, altered bone microarchitecture- and bone turnover (Xie et al., 2005; Gaudin-Audrain et al., 2013; Mieczkowska et al., 2013). Thus, GIP analogs have been shown to improve bone composition and strength in rodents (Mabilleau et al., 2014; Vyavahare et al., 2020), while a GIPR antagonist impairs bone remodeling in humans (Gasbjerg et al., 2020b; Helsted et al., 2020). In the present study, E288G carriers had a significantly lower BMD, yet neither of the two *GIPR* variants showed a significantly increased overall bone fracture risk, possibly due to low statistical power. The common *GIPR* variant, E354Q (rs1800437), showed similar effects of lowered BMD

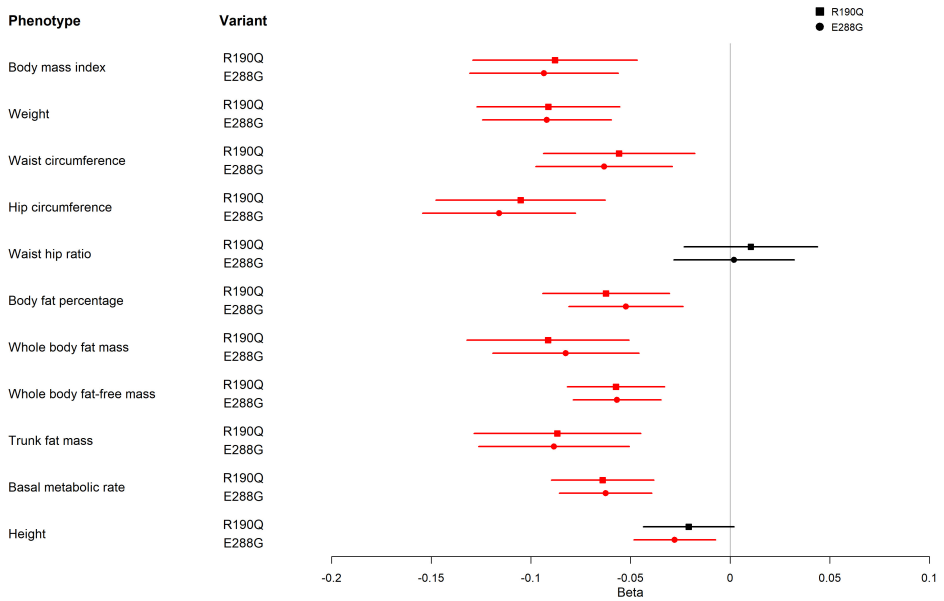

FIGURE 3 | Association of *GIPR* R190Q and E288G variants with adiposity-related measurements in UK Biobank. For each variant, beta, standard error (SE), and the *p*-value (P) are shown. All results are from an analysis of rank normalized phenotypes. The forest plot shows the beta in SD and the 95% confidence interval. Statistically significant results are shown in red. The analyses include 452,264 individuals. The effect allele frequencies of GIPR R190Q and E288G are 0.001557 and 0.001915, respectively, corresponding to 352 and 433 carriers of the variants, respectively.

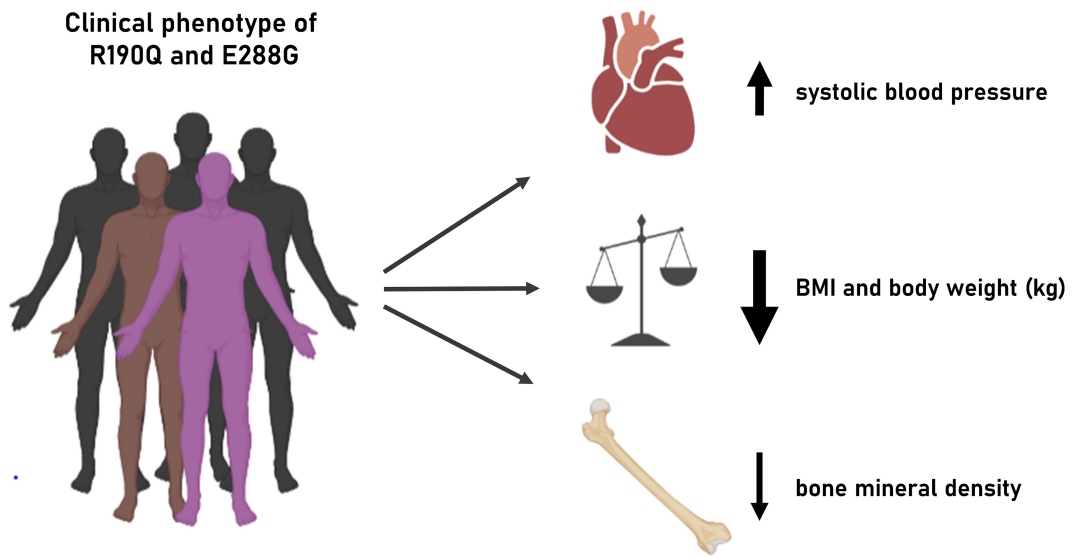

FIGURE 4 | Illustration of clinical phenotype of *GIPR* R190Q and E288G. Overview of the clinical phenotypes associated with the two *GIPR* variants presented in this study.

along with increased risk of non-vertebral fractures (Torekov et al., 2014). However, E354Q shows either a similar or slightly enhanced signaling pattern as wild-type GIPR with an increased rate of receptor internalization, possibly due to a longer residence time of GIP for this mutant (Almind et al., 1998; Fortin et al., 2010; Mohammad et al., 2014; Gabe et al., 2019). As a result of decreased recycling of the receptor to the cell surface, this ultimately may result in functional impairment of the *GIPR* variant, E354Q, thus exhibiting the same phenotypic trait as R190Q and E288G.

Previous studies have already established the importance of the GIP-GIPR axis in glucose regulation. For instance, GIPR-deficient mice showed lower glucose-stimulated insulin levels and higher levels of plasma glucose (Miyawaki et al., 1999), a risk factor for T2D (Garber, 2000). In the present study, we found that E288G associated with a 24% decreased risk of T2D,

whereas Turcot et al. (2018) did not detect this protective effect (Turcot et al., 2018), perhaps due to the lower sample size in the previous study [N ∼50,000 compared to ∼300,000 individuals (**Table 2**)]. Several GWAS have identified variants positioned in the *GIPR* locus, including the E354Q *GIPR* variant, to associate with increased 2-h glucose levels, decreased insulin secretion, insulin resistance and risk of T2D (Almind et al., 1998; Hu et al., 2010; Sauber et al., 2010; Saxena et al., 2010), further supporting the importance of the GIP-GIPR axis in glucose regulation.

Regarding the impact on the cardiovascular system, it was previously shown that GIP infusions decreased mean arterial blood pressure and increased resting heart rate (Wice et al., 2012). In fact, GIP infusions decreased diastolic blood pressure and increased heart rate during normoglycemia and hypoglycemia (Skov-Jeppesen et al., 2019; Heimbürger et al., 2020), whereas during hyperglycemia, the systolic blood pressure was increased as well (Gasbjerg et al., 2021). In our study, carriers of either *GIPR* variants had a higher systolic blood pressure and pulse pressure. Since a previous study showed no association between the two *GIPR* variants and systolic blood pressure (Turcot et al., 2018), the higher statistical power of the current study (N ∼700,000; **Figure 2**) compared to the study by Turcot et al. (2018) (N ∼135,000) may explain this discrepancy. Taken together, our results establish that GIPR signaling is important for the regulation of blood pressure in a manner dependent on the glycemic state.

Dysregulation of circulating lipids is also a risk factor of cardiovascular diseases. High circulating levels of GIP have shown beneficial effects on the lipid profile in humans (Møller et al., 2016), and treatment with GIPR/GLP-1R co-agonists have shown improvement of the lipid profile in patients with T2D (Frias et al., 2017, 2018). We found that carriers of E288G had significantly decreased HDL cholesterol levels without effect on other parameters of the lipid profile, suggesting that reduced GIPR signaling is involved in part of the cholesterol and lipid metabolism. These results are consistent with a previous study (Turcot et al., 2018), and the *GIPR* E354Q variant also showed a trend toward decreased HDL levels (Nitz et al., 2007). Even though carriers of R190Q and E288G have higher blood pressure and decreased HDL levels, they are not at higher risk of a cardiovascular event, and E354Q only nominally associated with cardiovascular disease (Nitz et al., 2007). Thus, reduced GIPR signaling does not seem to have fatal effects on the cardiovascular system, however, it is more likely that this study lacks statistical power to detect an effect on a clinical dichotomous phenotype even though association with a quantitative risk factor is detected. Similarly, we observe an association with BMD, yet no association with risk of fractures. Our observation that carriers of either *GIPR* variants had lower body fat mass and lean body mass than non-carriers corresponds with a previous association with lower BMI (Turcot et al., 2018), and was confirmed recently by whole-exome sequencing (Akbari et al., 2021). These results suggest that GIPR signaling contributes to regulation of body weight and body composition, and that reduced GIPR signaling is a potentially beneficial strategy against obesity. In support, obese *Gipr* knockout mice show lower body weight gain compared to wild-type mice, which may be explained by a lower fat mass, lean tissue mass and food intake, and an increased physical activity in these mice (Boer et al., 2021; Zhang et al., 2021). In the present study, we did not see an increased self-reported physical activity among carriers of R190Q or E288G. Furthermore, no increase was observed for the *GIPR* variant carriers regarding circulating leptin levels. In a previous study, obese *Gipr* knockout mice maintained leptin sensitivity compared to obese wild-type mice, and their leptin-induced anorectic effect was not inhibited by GIP infusion (Kaneko et al., 2019). If same scenario applies for humans, inadequate GIPR signaling, as for R190Q and E288G, may have beneficial effects in treatment of obesity. Further investigation in humans is needed to understand how GIPR signaling affects leptin sensitivity and long-term appetite control.

Although our results together with several studies of anti-GIPR antibodies (Gault et al., 2005; Killion et al., 2018; Min et al., 2020; Svendsen et al., 2020; Chen et al., 2021) could indicate that GIPR antagonists could protect from diet-induced obesity and improve glycemic and insulinotropic effects, other studies have shown the same for GIPR agonists (Nørregaard et al., 2018; Mroz et al., 2019; Samms et al., 2021). It is therefore still uncertain whether an agonist or an antagonist would be superior for the treatment of obesity. It is also worth noticing that the most prominent anti-obesity effect of GIPR agonists as well as antagonist is accomplished in combination with GLP-1R agonists (Killion et al., 2018, 2020; Nørregaard et al., 2018; Holst and Rosenkilde, 2020) indicating an important interplay between the two incretin hormones and their receptors.

CONCLUSION

In conclusion, our results suggest that reduced GIPR signaling can have both beneficial and disadvantageous effects on human physiology. Long-term use of GIPR antagonists may be of exceptional benefit in lowering adiposity for treatment of obesity and its comorbidities, such as T2D. In contrast, long-term use of a GIPR antagonist may, to some extent, negatively affect bone metabolism and the cardiovascular system, although the effects seem to be rather small. There are various additional *GIPR* missense variants detected in the human population, which could be explored for their potential impairment and/or altered signaling properties. This may provide a more complete picture of the physiological impact of GIPR signaling and how to best exploit its therapeutic potential.

DATA AVAILABILITY STATEMENT

The datasets presented in this study can be found in online repositories. The names of the repository/repositories and accession number(s) can be found in the article/**Supplementary Material**.

AUTHOR CONTRIBUTIONS

HK, KS, MR, and NG: study design, manuscript writing—original draft. HK, MR, AS-U, and CK: functional studies. KS

and NG: human genetic studies. AH: structural modeling. HK, KS, LG, AH, NG, and MR: manuscript writing—reviewing and editing. All authors revised the manuscript and approved the final version. All authors contributed to the article and approved the submitted version.

FUNDING

This work was supported by a scholarship to HK from the Danish Diabetes Academy, which was funded by the Novo Nordisk Foundation (Grant No. NNF17SA0031406) and a grant to MR from EFSD/Lilly European Diabetes Research Programme. KS and NG from The Novo Nordisk Foundation Center for Basic Metabolic Research were funded by an unrestricted donation to the University of Copenhagen by the Novo Nordisk Foundation (Grant No. NNF18CC0034900).

ACKNOWLEDGMENTS

We thank colleagues, Maibritt Sigvardt Baggesen for their assistance with performing the functional studies and thank all colleagues for their critical reading of the manuscript.

SUPPLEMENTARY MATERIAL

The Supplementary Material for this article can be found online at: https://www.frontiersin.org/articles/10.3389/fcell.2021.749607/full#supplementary-material

REFERENCES

Akbari, P., Gilani, A., Sosina, O., Kosmicki, J. A., Khrimian, L., Fang, Y.-Y., et al. (2021). Sequencing of 640,000 exomes identifies GPR75 variants associated with protection from obesity. *Science* 373:eabf8683. doi: 10.1126/science.abf8683

Almind, K., Ambye, L., Urhammer, S. A., Hansen, T., Echwald, S. M., Holst, J. J., et al. (1998). Discovery of amino acid variants in the human glucose-dependent insulinotropic polypeptide (GIP) receptor: the impact on the pancreatic beta cell responses and functional expression studies in Chinese hamster fibroblast cells. *Diabetologia* 41, 1194–1198. doi: 10.1007/s001250051051

Asmar, M., Arngrim, N., Simonsen, L., Asmar, A., Nordby, P., Holst, J. J., et al. (2016). The blunted effect of glucose-dependent insulinotropic polypeptide in subcutaneous abdominal adipose tissue in obese subjects is partly reversed by weight loss. *Nutr. Diabetes* 6:e208. doi: 10.1038/nutd.2016.15

Baggio, L. L., and Drucker, D. J. (2007). Biology of incretins: GLP-1 and GIP. *Gastroenterology* 132, 2131–2157. doi: 10.1053/j.gastro.2007.03.054

Berlier, J. L., Kharroubi, I., Zhang, J., Dalla Valle, A., Rigutto, S., Mathieu, M., et al. (2015). Glucose-Dependent insulinotropic peptide prevents serum deprivation-induced apoptosis in human bone marrow-derived mesenchymal stem cells and osteoblastic cells. *Stem Cell Rev. Rep.* 11, 841–851. doi: 10.1007/s12015-015-9616-6

Boer, G. A., Keenan, S. N., Miotto, P. M., Holst, J. J., and Watt, M. J. (2021). GIP receptor deletion in mice confers resistance to HFD-induced obesity via alterations in energy expenditure and adipose tissue lipid metabolism. *Am. J. Physiol. Endocrinol. Metab.* 320, E835–E845. doi: 10.1152/ajpendo.00646.2020

Bollag, R. J., Zhong, Q., Phillips, P., Min, L., Zhong, L., Cameron, R., et al. (2000). Osteoblast-derived cells express functional glucose-dependent insulinotropic peptide receptors. *Endocrinology* 141, 1228–1235. doi: 10.1210/endo.141.3.7366

Buniello, A., MacArthur, J. A. L., Cerezo, M., Harris, L. W., Hayhurst, J., Malangone, C., et al. (2019). The NHGRI-EBI GWAS Catalog of published genome-wide association studies, targeted arrays and summary statistics 2019. *Nucleic Acids Res.* 47, D1005–D1012. doi: 10.1093/nar/gky1120

Canela-Xandri, O., Rawlik, K., and Tenesa, A. (2018). An atlas of genetic associations in UK Biobank. *Nat. Genet.* 50, 1593–1599. doi: 10.1038/s41588-018-0248-z

Chen, J., Zheng, S., Hu, Y., Mou, X., and Wang, H. (2021). Chronic treatment with anti-GIPR mAb alone and combined with DPP-4 inhibitor correct obesity, dyslipidemia and nephropathy in rodent animals. *Life Sci.* 269:119038. doi: 10.1016/j.lfs.2021.119038

Christensen, M., Calanna, S., Sparre-Ulrich, A. H., Kristensen, P. L., Rosenkilde, M. M., Faber, J., et al. (2015). Glucose-dependent insulinotropic polypeptide augments glucagon responses to hypoglycemia in type 1 diabetes. *Diabetes* 64, 72–78. doi: 10.2337/db14-0440

Christensen, M., Vedtofte, L., Holst, J. J., Vilsbøll, T., and Knop, F. K. (2011). Glucose-dependent insulinotropic polypeptide: a bifunctional glucose-dependent regulator of glucagon and insulin secretion in humans. *Diabetes* 60, 3103–3109. doi: 10.2337/db11-0979

Cordomí, A., Ismail, S., Matsoukas, M. T., Escrieut, C., Gherardi, M. J., Pardo, L., et al. (2015). Functional elements of the gastric inhibitory polypeptide receptor: comparison between secretin- and rhodopsin-like G protein-coupled receptors. *Biochem. Pharmacol.* 96, 237–246. doi: 10.1016/j.bcp.2015.05.015

Fortin, J. P., Schroeder, J. C., Zhu, Y., Beinborn, M., and Kopin, A. S. (2010). Pharmacological characterization of human incretin receptor missense variants. *J. Pharmacol. Exp. Ther.* 332, 274–280. doi: 10.1124/jpet.109.160531

Foster, S. R., and Bräuner-Osborne, H. (2018). Investigating internalization and intracellular trafficking of GPCRs: new techniques and real-time experimental approaches. *Handb. Exp. Pharmacol.* 245, 41–61. doi: 10.1007/164_2017_57

Frias, J. P., Bastyr, E. J., Vignati, L., Tschöp, M. H., Schmitt, C., Owen, K., et al. (2017). The sustained effects of a dual GIP/GLP-1 receptor agonist, NNC0090-2746, in patients with Type 2 diabetes. *Cell Metab.* 26, 343–352.e2. doi: 10.1016/j.cmet.2017.07.011

Frias, J. P., Nauck, M. A., Van, J., Kutner, M. E., Cui, X., Benson, C., et al. (2018). Efficacy and safety of LY3298176, a novel dual GIP and GLP-1 receptor agonist, in patients with type 2 diabetes: a randomised, placebo-controlled and active comparator-controlled phase 2 trial. *Lancet (London, England)* 392, 2180–2193. doi: 10.1016/S0140-6736(18)32260-8

Gabe, M. B. N., Sparre-Ulrich, A. H., Pedersen, M. F., Gasbjerg, L. S., Inoue, A., Bräuner-Osborne, H., et al. (2018). Human GIP(3-30)NH2 inhibits G protein-dependent as well as G protein-independent signaling and is selective for the GIP receptor with high-affinity binding to primate but not rodent GIP receptors. *Biochem. Pharmacol.* 150, 97–107. doi: 10.1016/j.bcp.2018.01.040

Gabe, M. B. N., van der Velden, W. J. C., Gadgaard, S., Smit, F. X., Hartmann, B., Bräuner-Osborne, H., et al. (2019). Enhanced agonist residence time, internalization rate and signalling of the GIP receptor variant [E354Q] facilitate receptor desensitization and long-term impairment of the GIP system. *Basic Clin. Pharmacol. Toxicol.* 126(Suppl 6), 122–132. doi: 10.1111/bcpt.13289

Gabe, M. B. N., van der Velden, W. J. C., Smit, F. X., Gasbjerg, L. S., and Rosenkilde, M. M. (2020). Molecular interactions of full-length and truncated GIP peptides with the GIP receptor – A comprehensive review. *Peptides* 125:170224. doi: 10.1016/j.peptides.2019.170224

Garber, A. J. (2000). The importance of early insulin secretion and its impact on glycaemic regulation. *Int. J. Obes. Relat. Metab. Disord.* 24 Suppl 3, S32–S37. doi: 10.1038/sj.ijo.0801423

Gasbjerg, L. S., Bari, E. J., Stensen, S., Hoe, B., Lanng, A. R., Mathiesen, D. S., et al. (2021). Dose-dependent efficacy of the glucose-dependent insulinotropic polypeptide (GIP) receptor antagonist GIP(3-30)NH2 on GIP actions in humans. *Diabetes Obes. Metab.* 23, 68–74. doi: 10.1111/dom.14186

Gasbjerg, L. S., Bergmann, N. C., Stensen, S., Christensen, M. B., Rosenkilde, M. M., Holst, J. J., et al. (2020a). Evaluation of the incretin effect in humans using GIP

and GLP-1 receptor antagonists. *Peptides* 125:170183. doi: 10.1016/j.peptides.2019.170183

Gasbjerg, L. S., Hartmann, B., Christensen, M. B., Lanng, A. R., Vilsbøll, T., Jørgensen, N. R., et al. (2020b). GIP's effect on bone metabolism is reduced by the selective GIP receptor antagonist GIP(3-30)NH2. *Bone* 130:115079. doi: 10.1016/j.bone.2019.115079

Gaudin-Audrain, C., Irwin, N., Mansur, S., Flatt, P. R., Thorens, B., Baslé, M., et al. (2013). Glucose-dependent insulinotropic polypeptide receptor deficiency leads to modifications of trabecular bone volume and quality in mice. *Bone* 53, 221–230. doi: 10.1016/j.bone.2012.11.039

Gault, V. A., Irwin, N., Green, B. D., McCluskey, J. T., Greer, B., Bailey, C. J., et al. (2005). Chemical ablation of gastric inhibitory polypeptide receptor action by daily (Pro3)GIP administration improves glucose tolerance and ameliorates insulin resistance and abnormalities of islet structure in obesity-related diabetes. *Diabetes* 54, 2436–2446. doi: 10.2337/diabetes.54.8.2436

Hansen, L. S., Sparre-Ulrich, A. H., Christensen, M., Knop, F. K., Hartmann, B., Holst, J. J., et al. (2016). N-terminally and C-terminally truncated forms of glucose-dependent insulinotropic polypeptide are high-affinity competitive antagonists of the human GIP receptor. *Br. J. Pharmacol.* 173, 826–838. doi: 10.1111/bph.13384

Heimbürger, S. M., Bergmann, N. C., Augustin, R., Gasbjerg, L. S., Christensen, M. B., and Knop, F. K. (2020). Glucose-dependent insulinotropic polypeptide (GIP) and cardiovascular disease. *Peptides* 125:170174. doi: 10.1016/j.peptides.2019.170174

Helsted, M. M., Gasbjerg, L. S., Lanng, A. R., Bergmann, N. C., Stensen, S., Hartmann, B., et al. (2020). The role of endogenous GIP and GLP-1 in postprandial bone homeostasis. *Bone* 140:115553. doi: 10.1016/j.bone.2020.115553

Holst, J. J. (2019). The incretin system in healthy humans: the role of GIP and GLP-1. *Metabolism* 96, 46–55. doi: 10.1016/j.metabol.2019.04.014

Holst, J. J., and Rosenkilde, M. M. (2020). GIP as a therapeutic target in diabetes and obesity: insight from incretin co-agonists. *J. Clin. Endocrinol. Metab.* 105, e2710–e2716. doi: 10.1210/clinem/dgaa327

Hu, C., Zhang, R., Wang, C., Wang, J., Ma, X., Hou, X., et al. (2010). Variants from GIPR, TCF7L2, DGKB, MADD, CRY2, GLIS3, PROX1, SLC30A8 and IGF1 are associated with glucose metabolism in the Chinese. *PLoS One* 5:e15542. doi: 10.1371/journal.pone.0015542

Jensen, P. C., Thiele, S., Ulven, T., Schwartz, T. W., and Rosenkilde, M. M. (2008). Positive versus negative modulation of different endogenous chemokines for CC-chemokine receptor 1 by small molecule agonists through allosteric versus orthosteric binding. *J. Biol. Chem.* 283, 23121–23128. doi: 10.1074/jbc.M803458200

Kaneko, K., Fu, Y., Lin, H.-Y., Cordonier, E. L., Mo, Q., Gao, Y., et al. (2019). Gut-derived GIP activates central Rap1 to impair neural leptin sensitivity during overnutrition. *J. Clin. Invest.* 129, 3786–3791. doi: 10.1172/JCI126107

Karczewski, K. J., Francioli, L. C., Tiao, G., Cummings, B. B., Alföldi, J., Wang, Q., et al. (2020). The mutational constraint spectrum quantified from variation in 141,456 humans. *Nature* 581, 434–443. doi: 10.1038/s41586-020-2308-7

Killion, E. A., Chen, M., Falsey, J. R., Sivits, G., Hager, T., Atangan, L., et al. (2020). Chronic glucose-dependent insulinotropic polypeptide receptor (GIPR) agonism desensitizes adipocyte GIPR activity mimicking functional GIPR antagonism. *Nat. Commun.* 11:4981. doi: 10.1038/s41467-020-18751-8

Killion, E. A., Wang, J., Yie, J., Shi, S. D.-H., Bates, D., Min, X., et al. (2018). Anti-obesity effects of GIPR antagonists alone and in combination with GLP-1R agonists in preclinical models. *Sci. Transl. Med.* 10:eaat3392. doi: 10.1126/scitranslmed.aat3392

Kubota, A., Yamada, Y., Hayami, T., Yasuda, K., Someya, Y., Ihara, Y., et al. (1996). Identification of two missense mutations in the GIP receptor gene: a functional study and association analysis with NIDDM: no evidence of association with Japanese NIDDM subjects. *Diabetes* 45, 1701–1705. doi: 10.2337/diab.45.12.1701

Lu, X., Peloso, G. M., Liu, D. J., Wu, Y., Zhang, H., Zhou, W., et al. (2017). Exome chip meta-analysis identifies novel loci and East Asian-specific coding variants that contribute to lipid levels and coronary artery disease. *Nat. Genet.* 49, 1722–1730. doi: 10.1038/ng.3978

Mabilleau, G., Mieczkowska, A., Irwin, N., Simon, Y., Audran, M., Flatt, P. R., et al. (2014). Beneficial effects of a N-terminally modified GIP agonist on tissue-level bone material properties. *Bone* 63, 61–68. doi: 10.1016/j.bone.2014.02.013

Mahajan, A., Wessel, J., Willems, S. M., Zhao, W., Robertson, N. R., Chu, A. Y., et al. (2018). Refining the accuracy of validated target identification through coding variant fine-mapping in type 2 diabetes. *Nat. Genet.* 50, 559–571. doi: 10.1038/s41588-018-0084-1

Mieczkowska, A., Irwin, N., Flatt, P. R., Chappard, D., and Mabilleau, G. (2013). Glucose-dependent insulinotropic polypeptide (GIP) receptor deletion leads to reduced bone strength and quality. *Bone* 56, 337–342. doi: 10.1016/j.bone.2013.07.003

Min, X., Yie, J., Wang, J., Chung, B. C., Huang, C. S., Xu, H., et al. (2020). Molecular mechanism of an antagonistic antibody against glucose-dependent insulinotropic polypeptide receptor. *MAbs* 12, 1–12. doi: 10.1080/19420862.2019.1710047

Miyawaki, K., Yamada, Y., Yano, H., Niwa, H., Ban, N., Ihara, Y., et al. (1999). Glucose intolerance caused by a defect in the entero-insular axis: a study in gastric inhibitory polypeptide receptor knockout mice. *Proc. Natl. Acad. Sci. U.S.A.* 96, 14843–14847. doi: 10.1073/pnas.96.26.14843

Mohammad, S., Patel, R. T., Bruno, J., Panhwar, M. S., Wen, J., and McGraw, T. E. (2014). A naturally occurring GIP receptor variant undergoes enhanced agonist-induced desensitization, which impairs GIP control of adipose insulin sensitivity. *Mol. Cell. Biol.* 34, 3618–3629. doi: 10.1128/MCB.00256-14

Møller, C. L., Vistisen, D., Færch, K., Johansen, N. B., Witte, D. R., Jonsson, A., et al. (2016). Glucose-Dependent insulinotropic polypeptide is associated with lower low-density lipoprotein but unhealthy fat distribution, independent of insulin: the ADDITION-PRO study. *J. Clin. Endocrinol. Metab.* 101, 485–493. doi: 10.1210/jc.2015-3133

Morris, J. A., Kemp, J. P., Youlten, S. E., Laurent, L., Logan, J. G., Chai, R. C., et al. (2019). An atlas of genetic influences on osteoporosis in humans and mice. *Nat. Genet.* 51, 258–266. doi: 10.1038/s41588-018-0302-x

Mroz, P. A., Finan, B., Gelfanov, V., Yang, B., Tschöp, M. H., DiMarchi, R. D., et al. (2019). Optimized GIP analogs promote body weight lowering in mice through GIPR agonism not antagonism. *Mol. Metab.* 20, 51–62. doi: 10.1016/j.molmet.2018.12.001

Myocardial Infarction Genetics and CARDIoGRAM Exome Consortia Investigators, Stitziel, N. O., Stirrups, K. E., Masca, N. G. D., Erdmann, J., Ferrario, P. G., et al. (2016). Coding variation in ANGPTL4, LPL, and SVEP1 and the risk of coronary disease. *N. Engl. J. Med.* 374, 1134–1144. doi: 10.1056/NEJMoa1507652

Nelson, C. P., Goel, A., Butterworth, A. S., Kanoni, S., Webb, T. R., Marouli, E., et al. (2017). Association analyses based on false discovery rate implicate new loci for coronary artery disease. *Nat. Genet.* 49, 1385–1391. doi: 10.1038/ng.3913

Nitz, I., Fisher, E., Weikert, C., Burwinkel, B., Li, Y., Möhlig, M., et al. (2007). Association analyses of GIP and GIPR polymorphisms with traits of the metabolic syndrome. *Mol. Nutr. Food Res.* 51, 1046–1052. doi: 10.1002/mnfr.200700048

Nørregaard, P. K., Deryabina, M. A., Tofteng Shelton, P., Fog, J. U., Daugaard, J. R., Eriksson, P.-O., et al. (2018). A novel GIP analogue, ZP4165, enhances glucagon-like peptide-1-induced body weight loss and improves glycaemic control in rodents. *Diabetes. Obes. Metab.* 20, 60–68. doi: 10.1111/dom.13034

Samms, R. J., Sloop, K. W., Gribble, F. M., Reimann, F., and Adriaenssens, A. E. (2021). GIPR function in the central nervous system: implications and novel perspectives for GIP-based therapies in treating metabolic disorders. *Diabetes* 70, 1938–1944. doi: 10.2337/dbi21-0002

Sauber, J., Grothe, J., Behm, M., Scherag, A., Grallert, H., Illig, T., et al. (2010). Association of variants in gastric inhibitory polypeptide receptor gene with impaired glucose homeostasis in obese children and adolescents from Berlin. *Eur. J. Endocrinol.* 163, 259–264. doi: 10.1530/EJE-10-0444

Saxena, R., Hivert, M. F., Langenberg, C., Tanaka, T., Pankow, J. S., Vollenweider, P., et al. (2010). Genetic variation in GIPR influences the glucose and insulin responses to an oral glucose challenge. *Nat. Genet.* 42, 142–148. doi: 10.1038/ng.521

Schwartz, T. W., and Frimurer, T. M. (2017). Structural biology: full monty of family B GPCRs. *Nat. Chem. Biol.* 13, 819–821. doi: 10.1038/nchembio.2438

Skov-Jeppesen, K., Hepp, N., Oeke, J., Hansen, M. S., Jafari, A., Svane, M. S., et al. (2021). The antiresorptive effect of GIP, but not GLP-2, is preserved in patients with hypoparathyroidism—a randomized crossover study. *J. Bone Miner. Res.* 36, 1448–1458. doi: 10.1002/jbmr.4308

Skov-Jeppesen, K., Svane, M. S., Martinussen, C., Gabe, M. B. N., Gasbjerg, L. S., Veedfald, S., et al. (2019). GLP-2 and GIP exert separate effects on bone

turnover: a randomized, placebo-controlled, crossover study in healthy young men. *Bone* 125, 178–185. doi: 10.1016/j.bone.2019.05.014

Smit, F. X., van der Velden, W. J. C., Kizilkaya, H. S., Nørskov, A., Lückmann, M., Hansen, T. N., et al. (2021). Investigating GIPR (ant)agonism: a structural analysis of GIP and its receptor. *Structure* 29, 679–693.e6. doi: 10.1016/j.str.2021.04.001

Sonne, D. P., Rehfeld, J. F., Holst, J. J., Vilsbøll, T., and Knop, F. K. (2014). Postprandial gallbladder emptying in patients with type 2 diabetes: potential implications for bile-induced secretion of glucagon-like peptide 1. *Eur. J. Endocrinol.* 171, 407–419. doi: 10.1530/EJE-14-0309

Speliotes, E. K., Willer, C. J., Berndt, S. I., Monda, K. L., Thorleifsson, G., Jackson, A. U., et al. (2010). Association analyses of 249,796 individuals reveal 18 new loci associated with body mass index. *Nat. Genet.* 42, 937–948. doi: 10.1038/ng.686

Surendran, P., Feofanova, E. V., Lahrouchi, N., Ntalla, I., Karthikeyan, S., Cook, J., et al. (2020). Discovery of rare variants associated with blood pressure regulation through meta-analysis of 1.3 million individuals. *Nat. Genet.* 52, 1314–1332. doi: 10.1038/s41588-020-00713-x

Svendsen, B., Capozzi, M. E., Nui, J., Hannou, S. A., Finan, B., Naylor, J., et al. (2020). Pharmacological antagonism of the incretin system protects against diet-induced obesity. *Mol. Metab.* 32, 44–55. doi: 10.1016/j.molmet.2019.11.018

Torekov, S. S., Harsløf, T., Rejnmark, L., Eiken, P., Jensen, J. B., Herman, A. P., et al. (2014). A functional amino acid substitution in the glucose-dependent insulinotropic polypeptide receptor (GIPR) gene is associated with lower bone mineral density and increased fracture risk. *J. Clin. Endocrinol. Metab.* 99, 729–733. doi: 10.1210/jc.2013-3766

Tsukiyama, K., Yamada, Y., Yamada, C., Harada, N., Kawasaki, Y., Ogura, M., et al. (2006). Gastric inhibitory polypeptide as an endogenous factor promoting new bone formation after food ingestion. *Mol. Endocrinol.* 20, 1644–1651. doi: 10.1210/me.2005-0187

Turcot, V., Lu, Y., Highland, H. M., Schurmann, C., Justice, A. E., Fine, R. S., et al. (2018). Protein-altering variants associated with body mass index implicate pathways that control energy intake and expenditure in obesity. *Nat. Genet.* 50, 26–35. doi: 10.1038/s41588-017-0011-x

Vogel, C. I. G., Scherag, A., Brönner, G., Nguyen, T. T., Wang, H. J., Grallert, H., et al. (2009). Gastric inhibitory polypeptide receptor: association analyses for obesity of several polymorphisms in large study groups. *BMC Med. Genet.* 10:19. doi: 10.1186/1471-2350-10-19

Vyavahare, S. S., Mieczkowska, A., Flatt, P. R., Chappard, D., Irwin, N., and Mabilleau, G. (2020). GIP analogues augment bone strength by modulating bone composition in diet-induced obesity in mice. *Peptides* 125:170207. doi: 10.1016/j.peptides.2019.170207

Wice, B. M., Reeds, D. N., Tran, H. D., Crimmins, D. L., Patterson, B. W., Dunai, J., et al. (2012). Xenin-25 amplifies GIP-mediated insulin secretion in humans with normal and impaired glucose tolerance but not type 2 diabetes. *Diabetes* 61, 1793–1800. doi: 10.2337/db11-1451

Wootten, D., Simms, J., Miller, L. J., Christopoulos, A., and Sexton, P. M. (2013). Polar transmembrane interactions drive formation of ligand-specific and signal pathway-biased family B G protein-coupled receptor conformations. *Proc. Natl. Acad. Sci. U.S.A* 110, 5211–5216. doi: 10.1073/pnas.1221585110

Xie, D., Cheng, H., Hamrick, M., Zhong, Q., Ding, K. H., Correa, D., et al. (2005). Glucose-dependent insulinotropic polypeptide receptor knockout mice have altered bone turnover. *Bone* 37, 759–769. doi: 10.1016/j.bone.2005.06.021

Yaghootkar, H., Zhang, Y., Spracklen, C. N., Karaderi, T., Huang, L. O., Bradfield, J., et al. (2020). Genetic studies of leptin concentrations implicate leptin in the regulation of early adiposity. *Diabetes* 69, 2806–2818. doi: 10.2337/db20-0070

Yaqub, T., Tikhonova, I. G., Lättig, J., Magnan, R., Laval, M., Escrieut, C., et al. (2010). Identification of determinants of glucose-dependent insulinotropic polypeptide receptor that interact with N-terminal biologically active region of the natural ligand. *Mol. Pharmacol.* 77, 547–558. doi: 10.1124/mol.109.060111

Zhang, H., Qiao, A., Yang, L., Van Eps, N., Frederiksen, K. S., Yang, D., et al. (2018). Structure of the glucagon receptor in complex with a glucagon analogue. *Nature* 553, 106–110. doi: 10.1038/nature25153

Zhang, Q., Delessa, C. T., Augustin, R., Bakhti, M., Colldén, G., Drucker, D. J., et al. (2021). The glucose-dependent insulinotropic polypeptide (GIP) regulates body weight and food intake via CNS-GIPR signaling. *Cell Metab.* 33, 833–844.e5. doi: 10.1016/j.cmet.2021.01.015

Zhang, Y., Sun, B., Feng, D., Hu, H., Chu, M., Qu, Q., et al. (2017). Cryo-EM structure of the activated GLP-1 receptor in complex with a G protein. *Nature* 546, 248–253. doi: 10.1038/nature22394

Zhao, F., Zhang, C., Zhou, Q., Hang, K., Zou, X., Chen, Y., et al. (2021). Structural insights into hormone recognition by the human glucose-dependent insulinotropic polypeptide receptor. *Elife* 10:e68719. doi: 10.7554/eLife.68719.sa2

Zhong, Q., Itokawa, T., Sridhar, S., Ding, K.-H., Xie, D., Kang, B., et al. (2007). Effects of glucose-dependent insulinotropic peptide on osteoclast function. *Am. J. Physiol. Endocrinol. Metab.* 292, E543–E548. doi: 10.1152/ajpendo.00364.2006

Conflict of Interest: MR was co-founder of Antag Therapeutics and Bainan Biotech. AS-U was co-founder and CEO of Antag Therapeutics. LG was co-founder of Antag Therapeutics.

The remaining authors declare that the research was conducted in the absence of any commercial or financial relationships that could be construed as a potential conflict of interest.

Publisher's Note: All claims expressed in this article are solely those of the authors and do not necessarily represent those of their affiliated organizations, or those of the publisher, the editors and the reviewers. Any product that may be evaluated in this article, or claim that may be made by its manufacturer, is not guaranteed or endorsed by the publisher.

frontiers in Cell and Developmental Biology

ORIGINAL RESEARCH
published: 26 October 2021
doi: 10.3389/fcell.2021.753787

Identification and Functional Analysis of G Protein-Coupled Receptors in 20-Hydroxyecdysone Signaling From the *Helicoverpa armigera* Genome

*Yan-Li Li, Yan-Xue Li, Xiao-Pei Wang, Xin-Le Kang, Ke-Qin Guo, Du-Juan Dong, Jin-Xing Wang and Xiao-Fan Zhao**

Shandong Provincial Key Laboratory of Animal Cells and Developmental Biology, School of Life Sciences, Shandong University, Qingdao, China

G protein-coupled receptors (GPCRs) are the largest family of membrane receptors in animals and humans, which transmit various signals from the extracellular environment into cells. Studies have reported that several GPCRs transmit the same signal; however, the mechanism is unclear. In the present study, we identified all 122 classical GPCRs from the genome of *Helicoverpa armigera*, a lepidopteran pest species. Twenty-four GPCRs were identified as upregulated at the metamorphic stage by comparing the transcriptomes of the midgut at the metamorphic and feeding stages. Nine of them were confirmed to be upregulated at the metamorphic stage. RNA interference in larvae revealed the prolactin-releasing peptide receptor (PRRPR), smoothened (SMO), adipokinetic hormone receptor (AKHR), and 5-hydroxytryptamine receptor (HTR) are involved in steroid hormone 20-hydroxyecdysone (20E)-promoted pupation. Frizzled 7 (FZD7) is involved in growth, while tachykinin-like peptides receptor 86C (TKR86C) had no effect on growth and pupation. Via these GPCRs, 20E regulated the expression of different genes, respectively, including *Pten* (encoding phosphatidylinositol-3,4,5-trisphosphate 3-phosphatase), *FoxO* (encoding forkhead box O), *BrZ7* (encoding broad isoform Z7), *Kr-h1* (encoding Krüppel homolog 1), *Wnt* (encoding Wingless/Integrated) and *cMyc*, with hormone receptor 3 (HHR3) as their common regulating target. PRRPR was identified as a new 20E cell membrane receptor using a binding assay. These data suggested that 20E, via different GPCRs, regulates different gene expression to integrate growth and development.

Keywords: genome, GPCR, 20-hydroxyecdysone (20E), forkhead box O, *Pten*

OPEN ACCESS

Edited by:
Sameer Mohammad,
King Abdullah International Medical Research Center (KAIMRC), Saudi Arabia

Reviewed by:
Wen Liu,
Huazhong Agricultural University, China
Zhen Li,
China Agricultural University, China

****Correspondence:***
Xiao-Fan Zhao
xfzhao@sdu.edu.cn

Specialty section:
This article was submitted to Signaling, a section of the journal Frontiers in Cell and Developmental Biology

Received: *05 August 2021*
Accepted: *30 September 2021*
Published: *26 October 2021*

Citation:
Li Y-L, Li Y-X, Wang X-P, Kang X-L, Guo K-Q, Dong D-J, Wang J-X and Zhao X-F (2021) Identification and Functional Analysis of G Protein-Coupled Receptors in 20-Hydroxyecdysone Signaling From the Helicoverpa armigera Genome. Front. Cell Dev. Biol. 9:753787. doi: 10.3389/fcell.2021.753787

INTRODUCTION

G protein-coupled receptors (GPCRs) are present widely in animals and humans (Hanlon and Andrew, 2015). GPCRs sense and transmit external stimuli into cells to regulate a variety of physiological processes, including cognition, metabolism, inflammation, immunity, and cell proliferation (Rasmussen et al., 2011). There are more than 800 GPCRs encoded in the human genome (Fredriksson and Schioth, 2005), over 1,300 GPCRs in mice, 116 classical GPCRs, which can act as guanine nucleotide exchange factors (GEFs), in *Drosophila* (Hanlon and Andrew, 2015), and 276 in *Anopheles gambiae* (Hill et al., 2002). The importance of GPCRs in cellular signaling has

resulted in ∼34% of human drugs acting at GPCRs (Hauser et al., 2017). GPCRs are also suggested as targets for next generation pesticides (Audsley and Down, 2015). An interesting phenomenon in GPCRs-mediated signaling is that several GPCRs transmit the same signal of a ligand. For example, nine GPCRs function for adrenaline and five for dopamine (Hauser et al., 2017); however, the mechanism is unclear.

G protein-coupled receptors also transmit animal steroid hormone signals in the cell membrane. For example, GPCR 30 (GPR30/GPER) is an estrogen cell membrane receptor and transmits estrogen signals in mammals (Maggiolini and Picard, 2010). The dopamine/ecdysteroid receptor (DopEcR) transmits the non-genomic signal of insect molting hormone 20-hydroxyecdysone (20E) in *Drosophila* (Srivastava et al., 2005) and in *Helicoverpa armigera* (Kang et al., 2019). To date, several GPCRs have been proven to transmit 20E signals in *H. armigera* (Zhao, 2020), including ecdysone-responsible GPCR 1 (ErGPCR-1), ecdysone-responsible GPCR 2 (ErGPCR-2), and ecdysone-responsible GPCR 3 (ErGPCR-3) (Cai et al., 2014a; Wang et al., 2015; Kang et al., 2021). These data suggest that several GPCRs function as steroid hormone receptors; however, whether any other GPCRs transmit 20E signals, and the mechanism by which several GPCRs function in 20E signaling, are unclear.

Helicoverpa armigera is a widespread lepidopteran agricultural pest (Wu et al., 2008). We used *H. armigera* as the research model to identify the new GPCRs involved in 20E signaling and addressed the mechanism of their function in the 20E pathway. In all, 122 GPCRs were identified from the genome of *H. armigera*. Six GPCRs transmit 20E signal for hormone receptor 3 (*HHR3*) expression, a 20E-induced delayed early gene (Palli et al., 1997). 20E, via different GPCRs, regulates the expression of various genes, including *Pten* (encoding phosphatidylinositol-3,4,5-trisphosphate 3-phosphatase), *FoxO* (encoding transcription factor forkhead box O), which are known playing roles in 20E signaling (Cai et al., 2016), *BrZ7* (encoding broad isoform Z7), a transcription factor that promotes metamorphosis (Cai et al., 2014b), *Kr-h1* (encoding Krüppel homolog 1), the antimetamorphic effector induced by juvenile hormone (JH) (Belles, 2020), and *Wnt* (encoding Wingless/Integrated) and *cMyc*, which play significant roles in insect growth and development (Clevers, 2006; Kayukawa et al., 2012; Cai et al., 2014b), to integrate growth and metamorphosis. One GPCR, prolactin-releasing peptide receptor (PRRPR), was determined to bind 20E. Our study presents an example to explain the mechanism by which several GPCRs transmit the same signal.

RESULTS

Identification of *Helicoverpa armigera* G Protein-Coupled Receptors From the Genome

We searched for all GPCRs from the genome of *H. armigera* to identify classification of those GPCRs that are involved in 20E signaling. We found 122 genes encoding classical GPCRs in the *H. armigera* genome[1] using BLAST (Basic Local Alignment Search Tool) with *Drosophila* and *Bombyx mori* GPCRs, respectively. Having removed four GPCRs with large sequence differences, the sequences of 118 presumed GPCRs, named as they are in the genome, were used to create a phylogenetic tree. These GPCRs could be divided into three clades according to four major categories of GPCRs (Sadowski and Parish, 2003): Class A (89 sequences), class B (15 sequences) and class C or F (14 sequences) (**Figure 1** and **Supplementary Table 1**). Some GPCRs from *D. melanogaster* and *Homo sapiens* were used as landmarks of the classes, respectively. Fifteen GPCRs annotated to class A, B, C, or F in the genome were reclassified in different classes according to the sequences, which are marked with the related colors in each class in **Figure 1**. Twenty-five GPCRs that were not classified in the genome were gathered to different classes according to our phylogenetic analysis, which are marked in black in **Figure 1**. Four GPCRs known to transmit 20E signals in *H. armigera*, were classified as Class A (DopEcR) and class B (ErGPCR-1, ErGPCR-2, and ErGPCR-3).

Screening of the G Protein-Coupled Receptors in 20E Signaling

To screen for GPCRs involved in 20E signaling pathway, we compared the transcriptomes of the midgut at the feeding stage (6th–24 h) and the metamorphic molting stage (6th–72 h). Twenty-four GPCRs were found to be upregulated and seven were downregulated in the metamorphic stage (**Supplementary Figure 1**), suggesting that these twenty-four GPCRs are involved in metamorphosis. To examine the transcriptome analysis, 13 of the GPCRs (11 upregulated and 2 downregulated) from different classes were selected and examined for their developmental expression profiles in tissues using quantitative real-time reverse transcription PCR (qRT-PCR) to validate the result of the transcriptome analysis. Three GPCR genes, *PrRPR*, *Akhr* (encoding adipokinetic hormone receptor), and *Fzd7* (encoding frizzled 7), showed increased expression during metamorphosis (MM to P) in four detected tissues (**Figure 2**). Six GPCR genes, *Smo* (encoding smoothened), *Htr* (encoding 5-hydroxytryptamine receptor), *TkR86C* (encoding tachykinin-like peptides receptor 86C), *Fshr* (encoding follicle-stimulating hormone receptor), *Rya-R* (encoding the RYamide receptor), and *Npfr* (encoding neuropeptide F receptor) showed increased expression during metamorphosis in some tissues (**Figure 3**). Four GPCR genes, *Galr3* (encoding galanin receptor type 3), *GPCR4* (encoding the uncharacterized protein LOC110374861), *Opsin* (encoding red-sensitive opsin), and *Fzd4* (encoding frizzled 4) did not show increased expression during metamorphosis (**Supplementary Figure 2**). These results confirmed that the expression levels of nine GPCRs genes increased during metamorphosis, with or without tissue specificity, and might play roles in 20E-promoted metamorphosis.

[1]https://www.ncbi.nlm.nih.gov/Taxonomy/Browser/wwwtax.cgi?mode=Info&id=29058

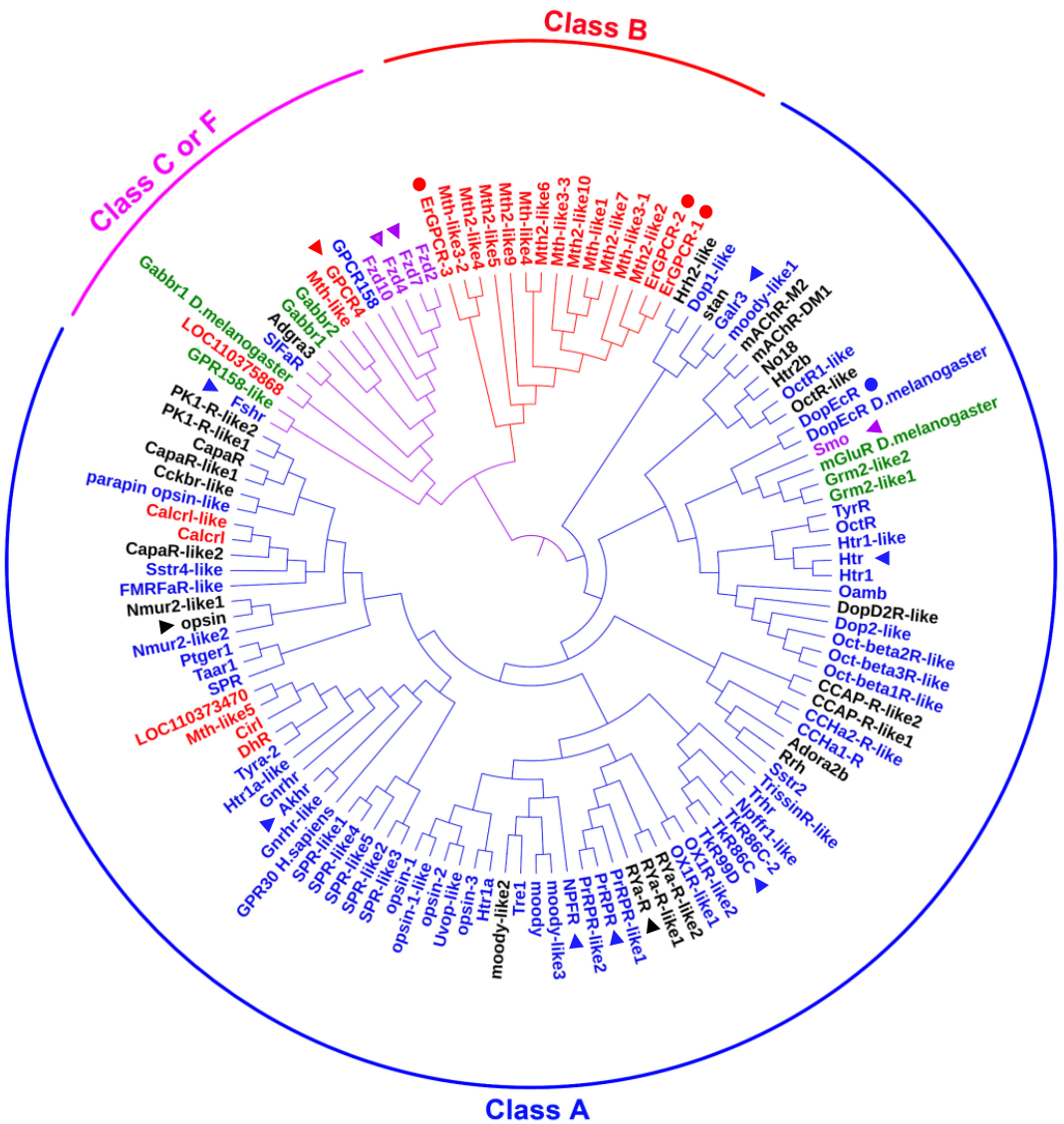

FIGURE 1 | The phylogenetic analysis of classical GPCRs of *H. armigera*. Names in blue indicate GPCRs belonging to class A that were identified in the genome. Names in red indicate GPCRs belonging to class B that were identified in the genome. Names in green indicate GPCRs belonging to class C that were identified in the genome. Names in purple indicate GPCRs belonging to class F that were identified in the genome. Names in black indicate GPCRs that have not been classified in the genome. GenBank numbers were shown in **Supplementary Table 1**. The triangle represents the GPCRs studied in this article, and the circle represents the GPCRs in 20E signaling studied previously.

G Protein-Coupled Receptors Have Different Functions in 20E Pathway

Among the nine GPCRs that showed increased expression during metamorphosis, three GPCRs-*Fshr*, *Rya-R*, and *Npfr* were not successfully knocked down in larvae using RNA interference (RNAi). Other six GPCRs, *PrRPR*, *Smo*, *Akhr*, *Htr*, *Fzd7*, and *TkR86C*, which showed increased expression during metamorphosis in all tissues or in some tissues, were knocked down in larvae using RNAi to examine their roles in 20E-promoted earlier pupation. In the *dsGFP* plus 20E treatment group, 91.1% of the larvae pupated in 111 h (timed from the 6th instar 6 h to pupae). However, knockdown of *PrRPR* caused 63.3% of the larvae delayed pupation for 36 h, and increased death, compared with *dsGFP* plus 20E (**Figures 4A–C**). In addition, the midgut did not show a red color, a sign of programmed cell death (Wang et al., 2007; Hakim et al., 2010), in the *dsPrRPR* plus 20E treatment group compared with that in the *dsGFP* plus 20E control (**Figure 4D**). Hematoxylin and eosin (HE) staining showed that the imaginal midgut formed after *dsGFP* control injection, indicating the occurrence of midgut remodeling. In contrast, the imaginal midgut did not form after *dsPrRPR* injection for 60 h (**Figure 4E**). Similar results were obtained after knockdown of *Smo*, *Akhr*, and *Htr*. Compared with the *dsGFP* + 20E group, 53–65% of larvae delayed pupation for

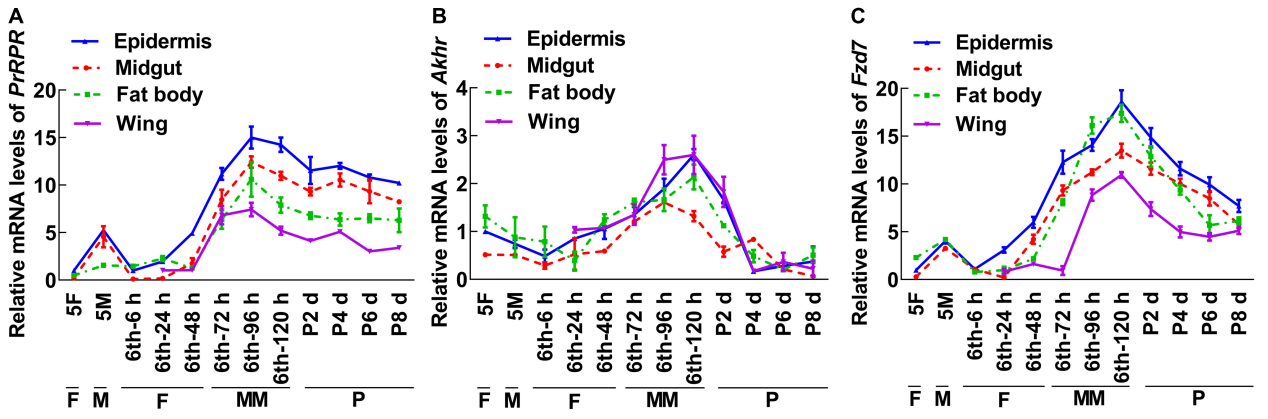

FIGURE 2 | qRT-PCR showing the upregulated GPCRs during metamorphosis in all four tissues. **(A–C)** The relative mRNA levels of *PrRPR*, *Akhr,* and *Fzd7*. *Actb* was used as a control. All the experiments were performed in triplicate, and the bars indicate the mean ± SD. 5F, fifth instar feeding larvae; 5M, fifth instar molting larvae; 6th–6 h to 6th–120 h, time stages of sixth instar larvae; P2 d–P8 d, 2 day to 8-day-old pupae; F, feeding; M, larval molting; MM, metamorphic molting; P, pupae stage.

24–43 h, and the midgut did not change to red or remodel on time (**Supplementary Figures 3–5**). These results suggested that these four GPCRs play roles in 20E-promoted pupation.

However, knockdown of *Fzd7* caused 57.8% of the larvae to form small pupae (**Figures 5A,B**). The pupal weight decreased to an average of 0.29 g compared with 0.43 g of the *dsGFP* injection control, with no significant difference in pupation time compared with the control group (**Figures 5C,D**). These results suggested that FZD7 is involved in larval growth. However, knockdown of *TkR86C* resulted in no abnormal phenotype (**Supplementary Figure 6**). The efficacy of RNAi was confirmed for these GPCRs, and except for *Smo* and *Fzd7*, which decreased after knockdown of *Htr*, no off target effects were detected for the other GPCRs (**Supplementary Figure 7**). These results showed that different GPCRs in the 20E signaling pathway play different roles in regulating growth and metamorphosis.

20E, via Different G Protein-Coupled Receptors, Regulates Gene Expression

The mechanism by which knockdown of the six GPCRs caused different outcomes was addressed by examining gene expression, including *HHR3*, *Pten*, *FoxO*, and *BrZ7*, which play roles in 20E-induced metamorphosis, *Kr-h1*, which plays role in JH signaling, *Wnt* and *cMyc*, which play roles in growth. qRT-PCR analysis showed that the expression levels of the six GPCR genes were upregulated by 20E in the midgut, confirming their responses to 20E induction. After knockdown of the six GPCR genes by RNAi in larvae, the mRNA levels of *HHR3* decreased, suggesting that these six GPCRs play roles in 20E signaling. However, the expression of *Pten* and *FoxO* decreased only after *PrRPR* and *Smo* knockdown (**Figures 6A,B**), but not after *Akhr*, *Htr*, *Fzd7*, and *TkR86C* knockdown (**Figures 6C–F**). Furthermore, *BrZ7* expression decreased after knockdown of *PrRPR* and *Smo*, *Kr-h1* expression increased after *Akhr* and *Htr* knockdown, and *Wnt* and *cMyc* decreased after knockdown of *Fzd7* (**Figure 7**). These results revealed that 20E, via different GPCRs, integrates insect pupation and growth by regulating the expression of various genes.

To support this conclusion, the previous reported GPCRs that transmit the 20E signal, ErGPCR-1, ErGPCR-2, ErGPCR-3, and DopEcR, were examined for their regulation of gene expression. The results showed that the expression of *HHR3* decreased after knockdown of *ErGPCR-1, ErGPCR-2*, *ErGPCR-3*, and *DopEcR*; however, *Pten* and *FoxO* expression decreased after *ErGPCR-1* knockdown, but not after *ErGPCR-2*, *ErGPCR-3*, or *DopEcR* knockdown (**Supplementary Figure 8A**), which confirmed that different GPCRs regulate the expression of different genes in the 20E pathway. The RNA interference efficiency of these four GPCRs was confirmed (**Supplementary Figures 8B–E**).

Prolactin-Releasing Peptide Receptor Binds 20E

To identify new GPCR functioning as cell membrane receptor of 20E, PRRPR and SMO were further analyzed for their binding 20E to determine their receptor roles in 20E signaling. Surflex-Dock (SFXC) in SYBYL X2.0 software (Certara, Princeton, NJ, United States) was used to dock 20E to PRRPR and SMO to predict the possibility of PRRPR and SMO binding 20E (**Figures 8A,B**). 20E forms hydrogen bonds with Ala-61, Gly-64, and Pro-316, of PRRPR, and Gln-314 and Glu-219 of SMO (**Figures 8C,D**). The scores for PRRPR and SMO binding to 20E were 2.96, and –0.78, respectively. These data predicted that PRRPR has a higher binding ability to 20E than SMO.

PRRPR-GFP and SMO-GFP were overexpressed in an *H. armigera* epidermal cell line (HaEpi) to address their binding to 20E. Green fluorescent protein (GFP) was overexpressed as a tag control. The overexpressed PRRPR-GFP and SMO-GFP were confirmed to be located in the cell membrane (**Figure 9A**). A binding assay using a 20-hydroxyecdysone enzyme immunoassay (20E-EIA) showed that the amount of

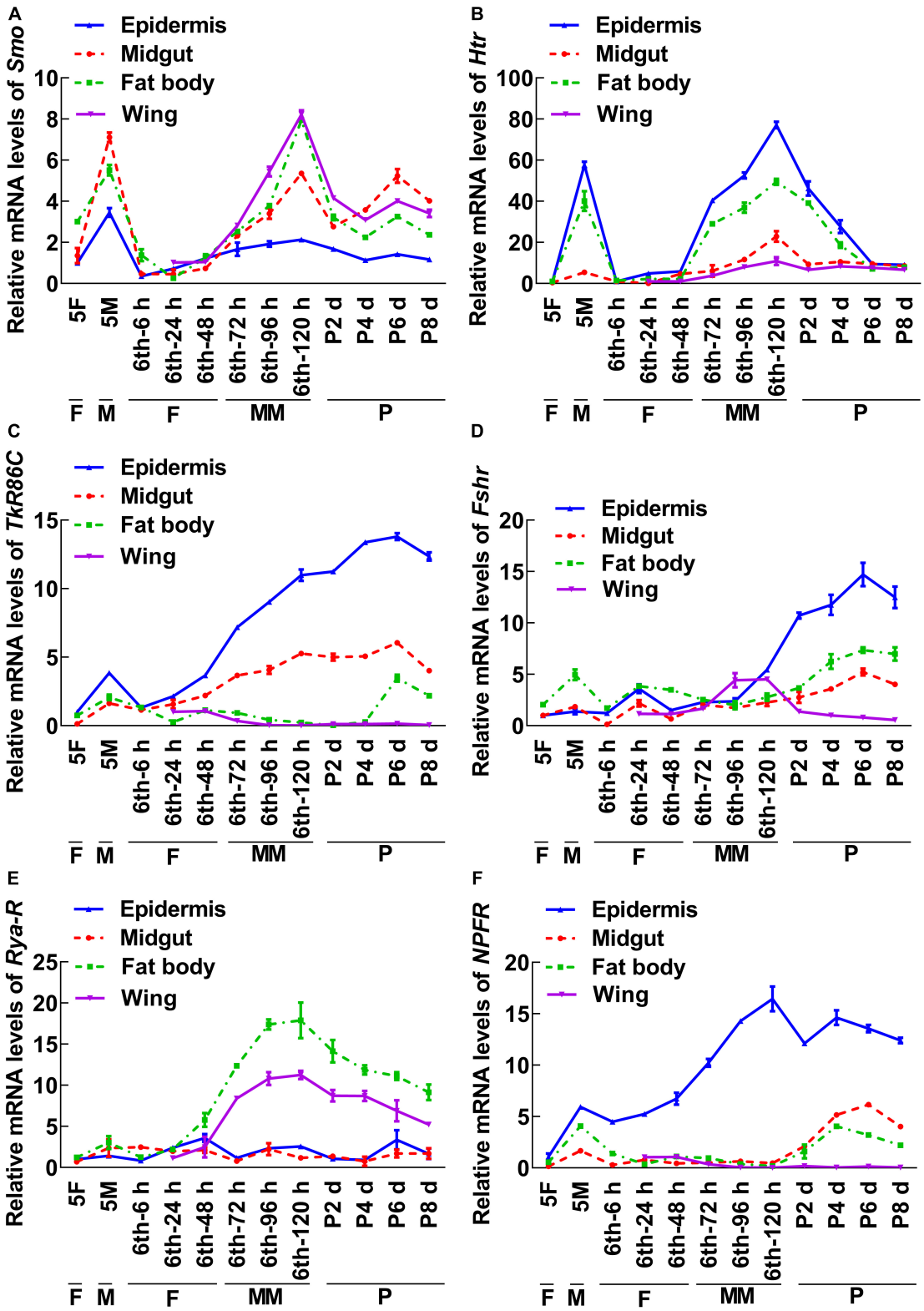

FIGURE 3 | qRT-PCR showing the upregulated GPCRs during metamorphosis with tissue differences. The mRNA levels of GPCRs in *H. armigera* larval tissues. **(A–F)** The relative mRNA levels of *Smo, Htr, TrR86C, Fshr, Rya-R*, and *NPFR*. *Actb* was used as the control. All the experiments were performed in triplicate and the bars indicate the mean ± SD.

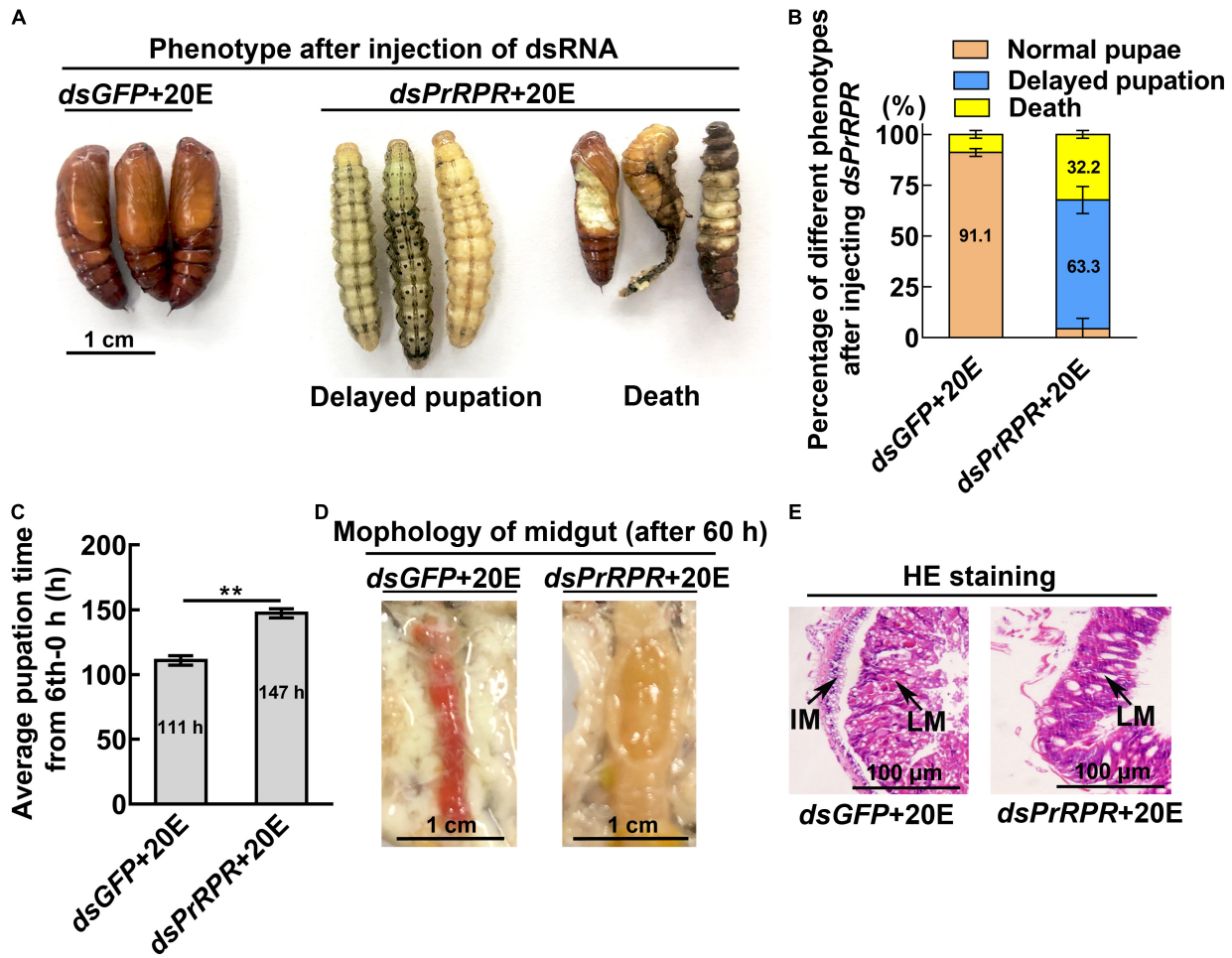

FIGURE 4 | Knockdown of *PrRPR* delayed larval-pupal transition. **(A)** Phenotypes after *dsPrRPR* or *dsGFP* injection (sixth instar 6 h larvae for the first dsRNA injection, thrice at 24 h intervals, 1 μg dsRNA/larva), and 20E treatment (500 ng/larva). Images were obtained at 120 h after the first dsRNA injection. Scale bar = 1 cm. **(B)** Percentages of the phenotypes in **(A)**. **(C)** Statistical analysis of pupation time from 6th instar 0 h larvae developing to pupae. **(D)** Morphology of the midgut 60 h after the first dsRNA injection. **(E)** HE-stained midgut after knockdown of *PrRPR*, observed at 60 h after the first dsRNA injection. LM, larval midgut; IM, imaginal midgut. HE staining showing the morphology of the midgut. The bars represent 100 μm. The experiments were performed in triplicate, and significant differences were calculated using Student's *t*-test (**$p < 0.01$). The bars indicate the mean ± SD.

20E bound by the cell membrane from the PRRPR-GFP-overexpressing cells increased significantly compared with that bound by the GFP-overexpressing cells. However, the amount of 20E bound by cell membranes from SMO-GFP overexpressing cells did not increase compared with that of the GFP-overexpressing cells (**Figure 9B**). These results suggested that PRRPR could bind 20E in the cell membrane.

A saturation-binding curve was constructed using 20E-EIA to further examine the affinity of GPCRs to 20E by calculating their dissociation constants (Kds). The saturable specific binding of cell membranes from cells overexpressing PRRPR-GFP to 20E had a Bmax of 2.096 ± 0.1037 nmol/mg protein and a Kd of 12.76 ± 2.192 nM. In comparison, the saturation binding of cell membranes from cells overexpressing GFP to 20E had a Bmax of 1.195 ± 0.1007 nmol/mg protein and a Kd of 30.2 ± 6.452 nM (cells overexpressing GFP still have other GPCRs on their cell membranes) (**Figure 9C**). The 20E-EIA assay is based on competition between the unlabeled 20E (20E bound to GPCR) and acetyl choline esterase (AChE)-labeled 20E (Tracer) for the limited-specific rabbit anti-20E antiserum; therefore, an inhibition or competitive curve was not detected. These data confirmed that the PRRPR-GFP could bind 20E.

DISCUSSION

This research identified and classified all classical GPCRs in the *H. armigera* genome. The GPCRs that function as 20E receptors were classified in classes A, B and class C or F. Further study revealed that different GPCRs showed different expression profiles and mediated the expression of different genes in 20E signaling. PRRPR was determined as a new GPCR cell membrane receptor. These data explained the mechanism by which several GPCRs are involved in the signaling of the same ligand.

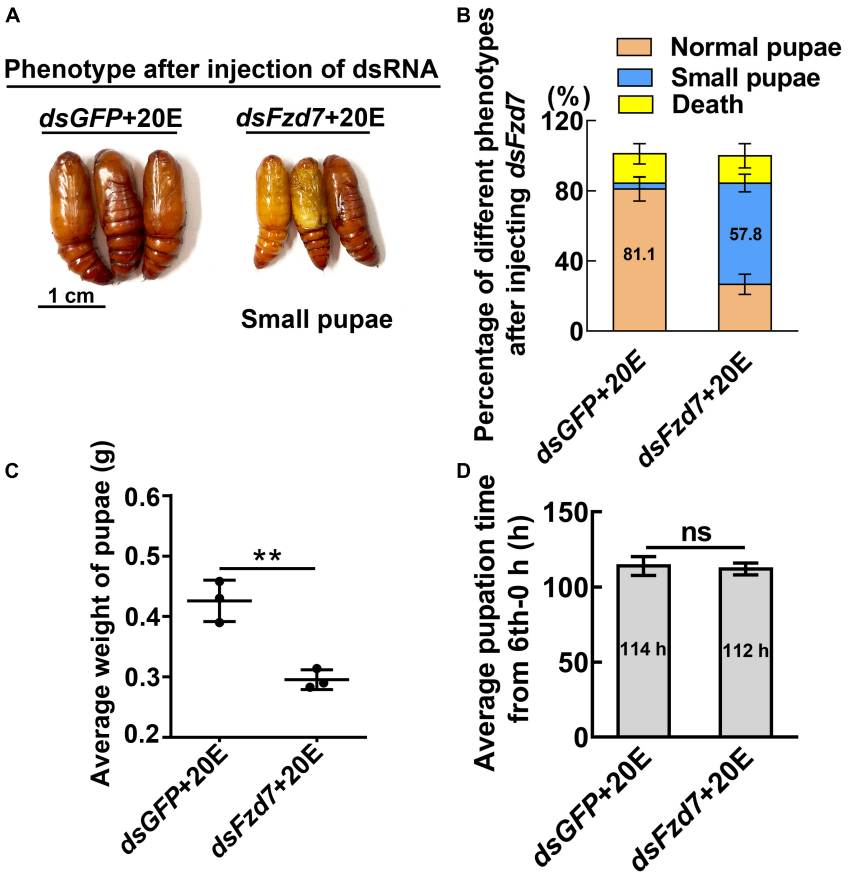

FIGURE 5 | Knockdown of *Fzd7* decreased body weight. **(A)** Phenotypes after *dsFzd7* or *dsGFP* injection (sixth instar 6 h larvae for the first dsRNA injection, thrice at 24 h intervals, 1 μg dsRNA/larva), and 20E treatment (500 ng/larva). Images were obtained at 120 h after the first dsRNA injection. Scale bar = 1 cm. **(B)** Percentages of the phenotypes in **(A)**. **(C)** Statistical analysis of average weight of a pupa at day one, by individually weight, after *Fzd7* knockdown by injection with *dsFzd7*. **(D)** Statistical analysis of pupation time from 6th instar 0 h larvae developing to pupae. The experiments were performed in triplicate, and significant differences were calculated using Student's *t*-test (**$p < 0.01$). The bars indicate the mean ± SD.

Identification and Classification of G Protein-Coupled Receptors in *Helicoverpa armigera* Genome

We identified 122 genes encoding classical GPCRs in the *H. armigera* genome. The GPCRs were classified into categories A, B, C, or F, which was relatively consistent with the classification of GPCRs in *Drosophila* (Hanlon and Andrew, 2015). Most of the GPCRs were classified consistently with their classification in the genome; however, some GPCRs were mixed in different classes in our study when using the full open reading frames (ORFs). We found 19 Mth-like GPCRs in the *H. armigera* genome, which is close to the 16 Mth-like GPCRs in *D. melanogaster* (Patel et al., 2012), but more than the 7 found in *Anopheles*, and the 2 found in *B. mori* (Fan et al., 2010). The Mth-like GPCRs play various roles in regulating the metabolism, aging, and self-balance to high temperature, hunger, dryness, and oxidative damage (Friedrich and Jones, 2016). In insects, Mth-like GPCRs are known to play roles in the setting of the endogenous circadian clocks (Mertens et al., 2007), regulation of fluid and ion secretion (Reagan, 1994), as well as the stress response and longevity (Lin et al., 1998).

20E, via Different G Protein-Coupled Receptors, Regulates Gene Expression

The involvement of several GPCRs in a same signal, such as 20E signaling, is an intriguing phenomenon. The differences among the GPCRs in 20E signaling have been explained by their induced downstream effects, including ErGPCR-1 inducing the Ca^{2+}-PKC signaling, while ErGPCR-2 inducing the GPCR-cAMP-PKA and GPCR-Ca^{2+}-PKC signaling, increasing 20E entry, and being internalized by 20E induction. DopEcR of *H. armigera* directly interacts with Gαs and Gαq under the induction of 20E to increase the levels of cAMP and Ca^{2+} (Zhao, 2020). ErGPCR-3 has very similar characteristics to ErGPCR-2 (Kang et al., 2021). Different GPCRs can cross react with different G proteins (Flock et al., 2017). Here, we further revealed that GPCRs have quite different expression profiles in tissues and at different developmental stages. Importantly, 20E, via different GPCRs, regulates the expression of various genes, including via PRRPR and SMO, which upregulate the expression of *Pten*, *FoxO*, and *BrZ7* to promote pupation. 20E, via AKHR and HTR, represses the expression of *Kr-h1* to promote pupation. 20E via FZD7

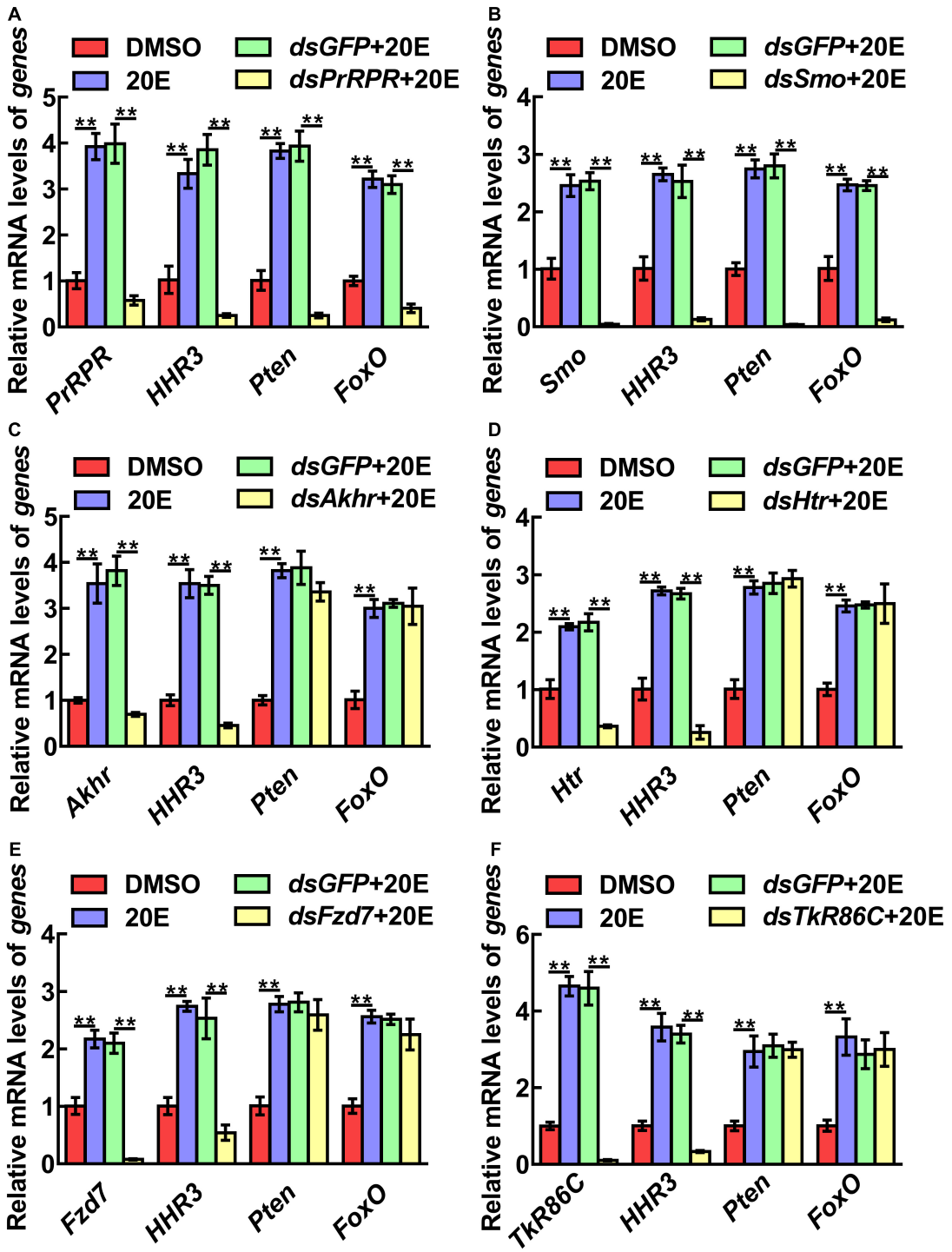

FIGURE 6 | qRT-PCR showing the relative mRNA levels of genes after knockdown GPCRs. **(A–F)** *PrRPR*, *Smo*, *Akhr*, *Htr*, *Fzd7*, and *TkR86C* knockdown and transcript levels of *HHR3*, *Pten* and *FoxO* in 6th–72 h larval midgut (1 μg *dsRNA*/larva). DMSO or 20E (500 ng/larva) were added for 12 h. DMSO was used as the solvent control. All the experiments were performed in triplicate, and significant differences were calculated using Student's *t*-test (**$p < 0.01$). The bars indicate the mean ± SD.

upregulates the expression of *Wnt* and *cMyc* to promote growth. 20E signaling also promotes wing disk development (Mirth et al., 2009). By the integration and competition of different signals induced by different ligands *in vivo*, 20E regulates pupation. These findings in 20E signaling first revealed the mechanism by which several GPCRs transmit the same signal

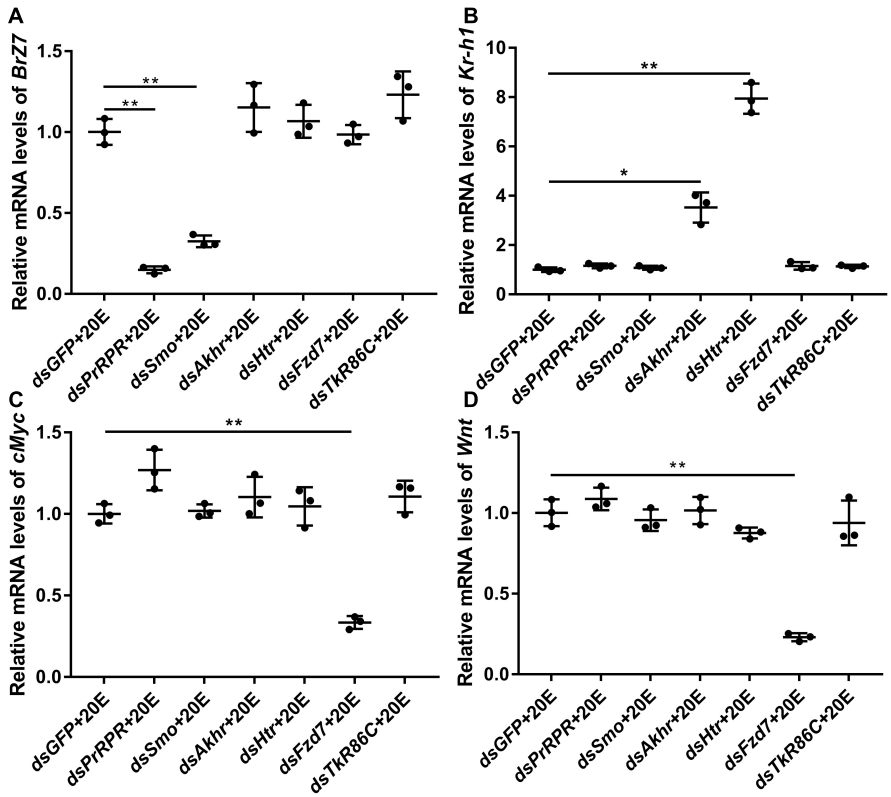

FIGURE 7 | qRT-PCR showing the relative mRNA levels of *BrZ7, Kr-h1, cMyc*, and *Wnt* after knocking down GPCRs. **(A–D)** The transcript levels of *BrZ7*, *Kr-h1*, *cMyc*, and *Wnt* in the larval midgut after knockdown of GPCRs *PrRPR*, *Smo*, *Akhr*, *Htr*, *Fzd7*, and *TkR86C* [sixth instar 6 h larvae for the first dsRNA injection, thrice at 24 h intervals, 1 μg dsRNA/larva; 20E (500 ng/larva) for 12 h]. DMSO was used as the solvent control. All the experiments were performed in triplicate, and significant differences were calculated using Student's *t*-test (*$p < 0.05$; **$p < 0.01$). The bars indicate the mean ± SD.

to regulate the expression of different genes in the network of the cells. In this work, we performed the screen based on the expression levels of GPCRs. There might be GPCRs transmit external signals in an expression-independent manner, which needs further study.

Our results suggested PRRPR, SMO, AKHR, HTR, FZD7, and TKR86C are involved in 20E-inducing *HHR3* expression, suggesting that they transmit 20E signals. In humans, PRRPR is a neuropeptide prolactin receptor (Dodd and Luckman, 2013). Human SMO participates in hedgehog signaling to guide cell differentiation, proliferation, and survival (Wu et al., 2017). FZD7 is the most important WNT receptor involved in cancer development and progression in mammals (King et al., 2012). In insects, AKHR binds AKH (adipokinetic hormone) to increase lipolysis, glycogenolysis, and trehalose production (Van der Horst et al., 2001; Bednarova et al., 2013; Baumbach et al., 2014). HTR (5-HT receptor) plays a key role in morphogenesis in the insect nervous system (Blenau and Thamm, 2011). TkR86C is the neurokinin K receptor in *D. melanogaster* that plays a role in neuromodulation in the central nervous system, participating in the processing of sensory information and the control of motor activities (Vanden Broeck et al., 1999). The role of TkR86C in insect needs further study. Here, we revealed a new function of these GPCRs in 20E signaling.

G Protein-Coupled Receptors Can Transmit 20E Signals Whether They Bind 20E or Not

It has been suggested that cells or cell membranes that overexpress GPCRs can bind steroid hormones in *Drosophila* (Srivastava et al., 2005) and mammals (Maggiolini and Picard, 2010). We found that PRRPR could bind 20E with the saturable specific binding Kd of 12.76 ± 2.192 nM. However, SMO could not bind 20E, although SMO transmits the 20E signal and is involved in 20E-induced pupation. In our previous study, we found that ErGPCR-1, ErGPCR-2, ErGPCR-3, and DopEcR can transmit 20E signals in *H. armigera*. ErGPCR-2, ErGPCR-3, and DopEcR can bind 20E, but ErGPCR-1 cannot (Kang et al., 2019, 2021). These data suggested that GPCRs transmit 20E signal with or without binding 20E. This might be because GPCRs loosely or dynamically bind their ligands (Nygaard et al., 2013; Strasser et al., 2017). Another possibility is that 20E competes with another ligand, such as dopamine, in *H. armigera* (Kang et al., 2019). GPCRs might also play

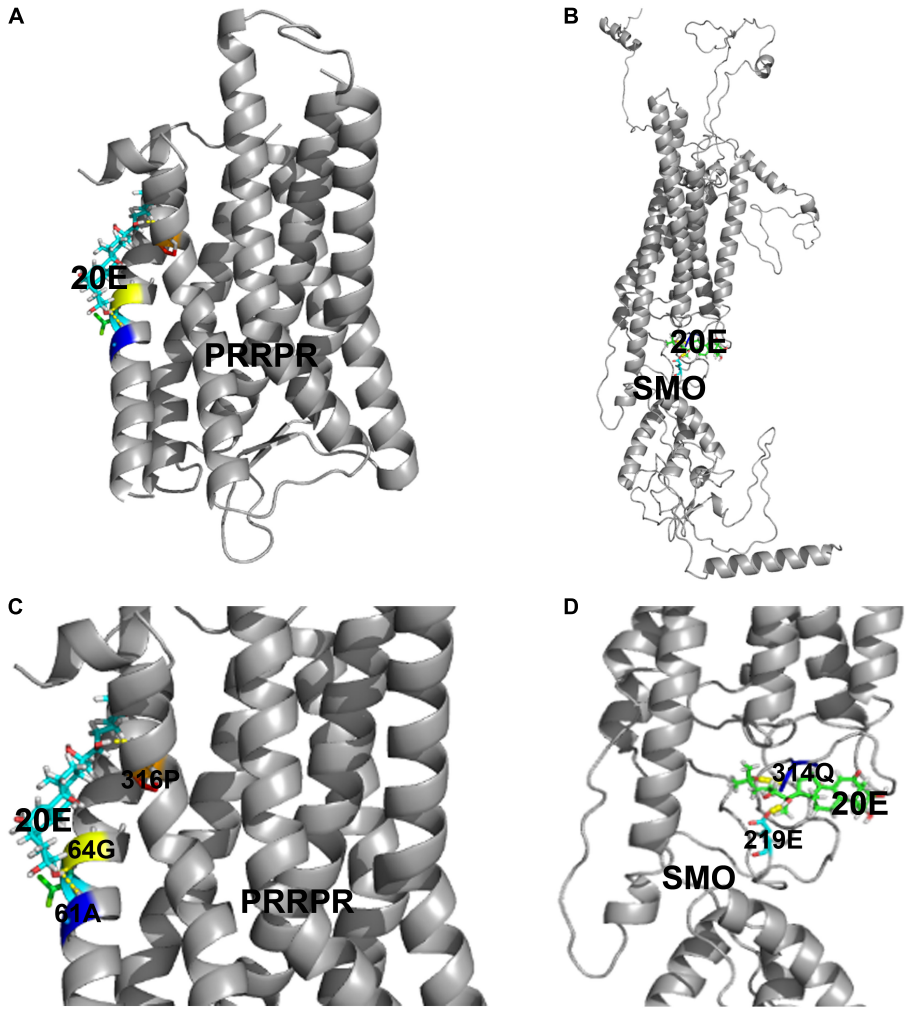

FIGURE 8 | Modeling of the ligand-binding complex of PRRPR and SMO. Prediction from the Surflex-Dock (SFXC) program from the SYBYL X2.0 software. **(A,B)** Whole structures of PRRPR and docked 20E, and SMO and docked 20E, respectively. **(C,D)** A closer view of the docking model pockets of PRRPR-20E and SMO-20E complexes. The amino acid residues with which 20E can form hydrogen bonds were shown in the figure.

roles in other pathways after upregulation by 20E, which requires further study.

G protein-coupled receptors share a seven transmembrane domain structural architecture (Latorraca et al., 2017). Except ErGPCR-1, ErGPCR-2, ErGPCR-3, and DopEcR have been reported to bind 20E. In addition to DopEcR in class A, ErGPCR-1, ErGPCR-2, and ErGPCR-3 belong to the Mth-like GPCRs in class B. An important feature of Mth-like GPCRs is the presence of 10 cysteine residues that form five disulfide bonds (West et al., 2001). The long N-terminal domains tend to recognize peptide ligands, such as hormones and neuropeptides (Cardoso et al., 2005, 2010), such as secretin; therefore, these GPCRs are also called secretin receptors (Cvejic et al., 2004; Ja et al., 2009). The relationship between the structure of GPCR and its binding 20E is unclear now. Up to date, several GPCRs can bind 20E, therefore, the upregulation of GPCR expression by 20E is likely a key factor to perform their functions. The mechanism that 20E upregulates GPCR expression differentially needs further studied. Mth-like GPCRs are not present in vertebrates, but are more abundant in arthropods (Patel et al., 2012; Araujo et al., 2013; de Mendoza et al., 2016), and thus represent targets for insecticides.

CONCLUSION

There are 122 classical GPCRs in the genome of *H. armigera*. The GPCRs that transmit 20E signal were classified in classes A, B and class C or F. Various GPCRs transmit 20E signals according to their different expression patterns in tissues and their increased expression during metamorphosis. 20E, via different GPCRs, regulates the expression of various genes, thus promoting pupation by integrating different signals *in vivo*. PRRPR binds 20E and is a newly identified 20E cell membrane receptor (**Figure 10**).

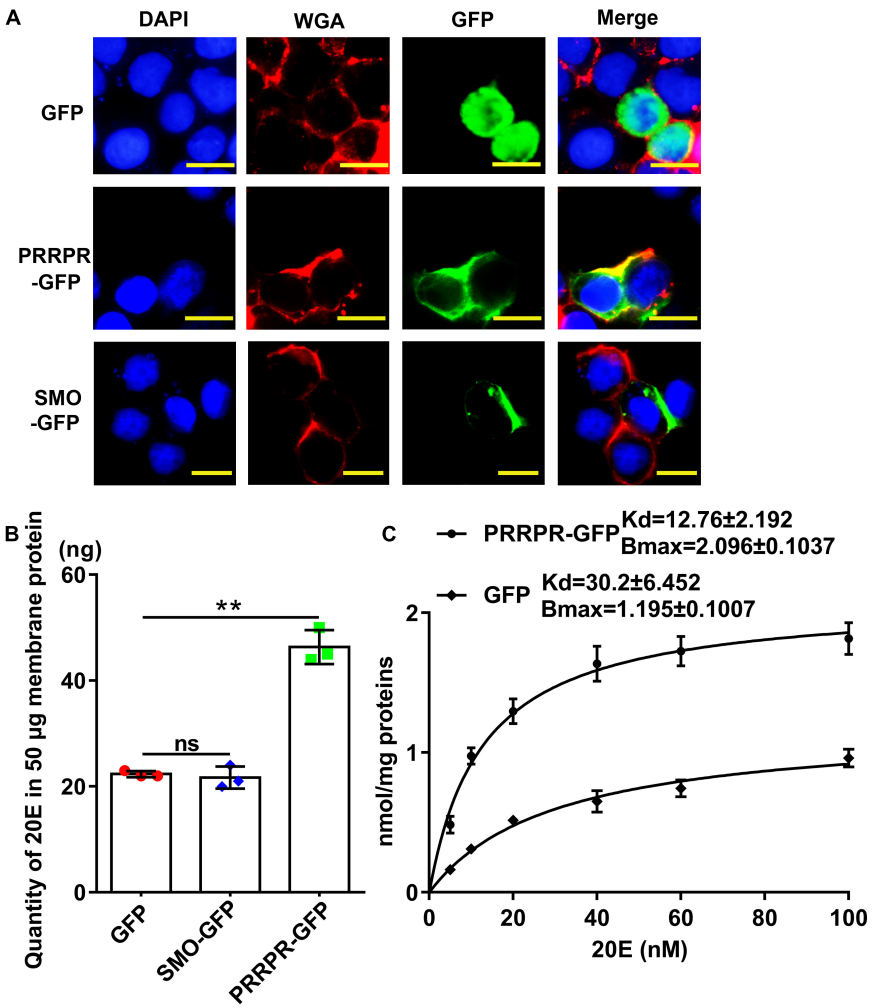

FIGURE 9 | Detection of 20E that was bound by the cell membrane proteins from HaEpi cells overexpressing GPCRs. **(A)** Cell membrane localization of overexpressed GFP, PRRPR, and SMO. Blue: Nuclei stained with DAPI. Red: Cell membrane was marked by WGA. Green: Fluorescence from GFP and various GPCRs fused with GFP. Scale bar = 20 μm. **(B)** Quantity of 20E bound by 50 μg of membrane proteins from HaEpi cells overexpressing GFP, PRRPR-GFP, or SMO-GFP. **(C)** Saturation binding curves of HaEpi cell membranes from cells overexpressing GFP, PRRPR-GFP, SMO-GFP to 20E. Error bars represent the SD of three replicates. Asterisks indicate significant differences according to Student's *t*-tests (**$p < 0.01$).

MATERIALS AND METHODS

Identification of G Protein-Coupled Receptors

Putative *H. armigera* GPCRs were identified in four steps: First, we downloaded all the GPCR protein sequences of *Drosophila* (Hanlon and Andrew, 2015) and *B. mori* (Fan et al., 2010). *B. mori* protein sequences were retrieved from the NCBI sequence repository[2]. We obtained 90 classical GPCRs from *B. mori*. *Drosophila* protein sequences were retrieved from FlyBase[3] and the NCBI database. We obtained 116 classical *Drosophila* GPCRs. Second, preliminary screening to obtain putative GPCRs of *H. armigera* was performed using NCBI BLAST based on downloaded *Drosophila* and *B. mori* GPCRs. We queried the *H. armigera* proteome[4] using each GPCR sequence from *Drosophila* and *B. mori* separately and selected the protein sequences with the highest scores. Third, the protein sequences with highest score were then used as query sequences one by one in a BLAST search against the proteome from *H. armigera* to obtain other GPCRs sequences that were not found in the previous step. Finally, we removed the repetitive sequences in the protein sequence obtained in the above steps. Then, NCBI conserved domain search service (CD search)[5] and SMART online software[6] were used to predict the structure of these protein sequences, and the GPCRs were seven-transmembrane domain proteins (7TMPs) were obtained.

[2]http://www.ncbi.nlm.nih.gov/

[3]http://www.flybase.org/

[4]https://www.ncbi.nlm.nih.gov/genome/?term=Helicoverpa+armigera

[5]https://www.ncbi.nlm.nih.gov/Structure/cdd/wrpsb.cgi

[6]http://smart.embl-heidelberg.de/smart/set_mode.cgi?NORMAL=1

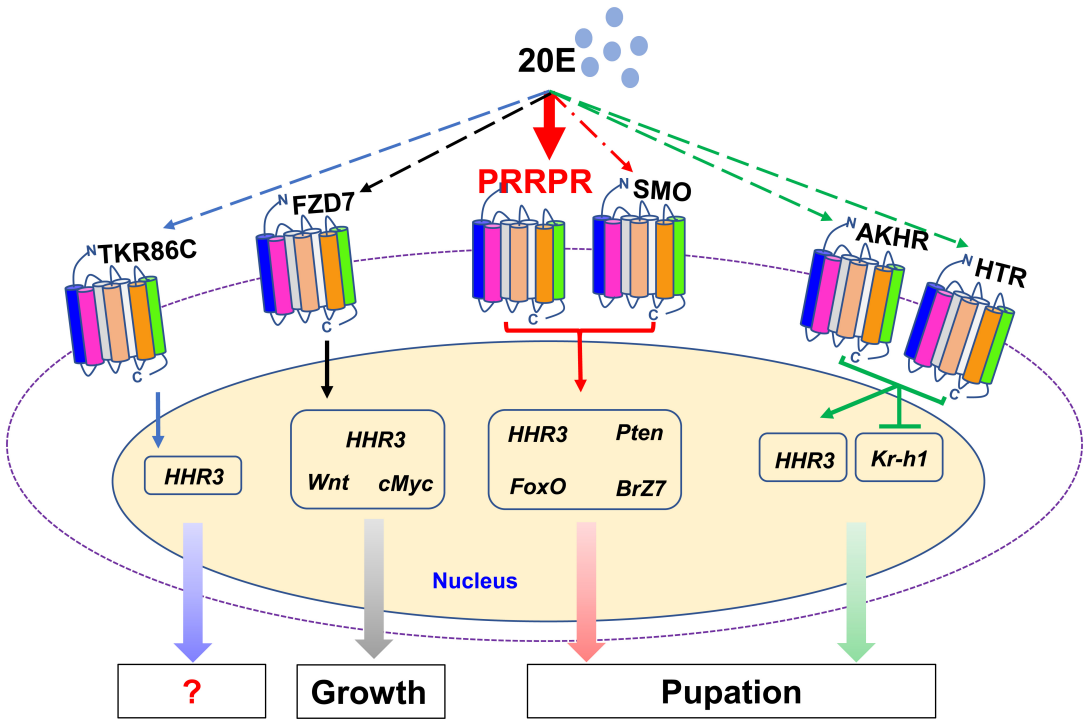

FIGURE 10 | 20E, through different GPCRs, regulates the expression of different genes to integrate growth and pupation. 20E through PRRPR, SMO, AKHR, HTR, FZD7, and TKR86C, regulates the expression of *HHR3*. 20E via PRRPR and SMO upregulates the expression of *Pten*, *FoxO*, and *BrZ7* to promote pupation. 20E, via AKHR and HTR, represses the expression of *Kr-h1* to promote pupation. 20E, via FZD7, upregulates the expression of *Wnt* and *cMyc* for growth.

GPCRs were identified from the transcriptomes of 6th–24 h larvae and 6th–72 h larvae. The transcriptomes were analyzed once without technique replicates. However, the samples were collected from several larvae to normalize the individual differences. The mRNA levels of GPCRs were examined after injection of 20E or Double-Stranded RNA (dsRNA) using qRT-PCR, with an equal amount of diluted DMSO as a solvent control.

Phylogenetics Analyses

The classification of *Drosophila* and *Homo sapiens* proteins in each GPCR family is clear and detailed. We classified the potential GPCRs in the *H. armigera* genome into various categories based on sequence homology. *Drosophila* and *Homo sapiens* GPCRs were used as guides, and the MEGA 6.0 software was used to construct phylogenetic trees using the Neighbor-Joining method with 1000 bootstraps (Tamura et al., 2013).

Insects

Helicoverpa armigera larvae were raised in the insect culture room at 25–27°C under a photoperiod of 14 h light/10 h dark. The larvae are reared on a previously described artificial diet (Zhao et al., 1998).

Quantitative Real-Time Reverse Transcription PCR

The total RNA was extracted using the Trizol reagent (TransGen Biotech, Beijing, China). cDNA was synthesized from the total RNA using a FastQuant RT Kit (Tiangen Biotech, Beijing, China). qRT-PCR was then carried out using the cDNA as the template in a CFX96 real-time system (Bio-Rad, Hercules, CA, United States) with 2 × SYBR qRT-PCR pre-mixture (TransGen Biotech). All the primers used are listed in **Supplementary Table 2**. *Actb* encodes a type of actin, which is a structural component of the cytoskeleton microfilaments. The *Actb* gene is highly conserved and highly expressed at the mRNA level (Butet et al., 2014). In many studies, including studies on different developmental stages and different tissues in *H. armigera* (Di et al., 2020), *Actb* is considered a suitable internal reference gene (Lu et al., 2013; Gao et al., 2017). *H. armigera Actb* (encoding beta actin; GenBank accession no. EU52707) was used as the internal standard. All data were from at least three biological replicates and were analyzed using the $2^{-\Delta\Delta CT}$ method ($\Delta\Delta CT = \Delta CT_{treatedsample} - \Delta CT_{control}$, $\Delta CT = CT_{gene} - CT_{Actb}$) (Livak and Schmittgen, 2001).

20E Induction in Larvae

The 20E powder (10 mg) was dissolved in 1 mL DMSO as a storage solution and diluted with phosphate-buffered saline (PBS; 140 mM NaCl, 10 mM sodium phosphate, pH 7.4) for experiment. 20E was injected into the hemocoel from the side of the larval abdomen. The control groups were treated with the equal amount of diluted DMSO.

Double-Stranded RNA Synthesis

RNA interference (RNAi) has been used for gene knockdown in many moths (Xu et al., 2016). The long dsRNA is broken down into smaller fragments *in vivo* (Zamore et al., 2000) and specifically and successfully inhibits the expression of target genes in worms (Fire et al., 1998). DNA fragments– 5′-583 bp-1037 bp-3′ of *Fzd7*, 5′-586 bp-1109 bp-3′ of *Htr*, 5′-43 bp-586 bp-3′ of *PrRPR*, 5′-1195 bp-1858 bp-3′ of *Smo*, 5′-641 bp-1045 bp-3′ of *Akhr*, 5′-65 bp-740 bp-3′ of *TkR86C*– were amplified as the template for dsRNA synthesis using the primers RNAiF and RNAiR. A T7 promoter sequence was added to the RNAi primers (**Supplementary Table 2**). The cDNA of the target gene was amplified using a single PCR reaction and was used as the template to synthesize dsRNA. The dsRNA was synthesized using MEGAscript RNAi kit (Ambion, Austin, TX, United States) according to the instruction manual. Next, the product was purified using the phenol-chloroform method. The quality of the synthesized dsRNA was quantified using a micro-spectrophotometer and detected using 1% agarose gel electrophoresis.

RNA Interference of Genes in Larvae

The dsRNA was diluted with PBS. The sixth instar 6 h larvae were placed on ice for 15 min until they did not move. A sterile micro syringe was used to inject 1 μg of dsRNA into the hemocoel from the side of the larval abdomen (taking care not to touch the midgut). dsRNAs were injected three times at 24 h intervals. The control groups were treated with the same amount of *dsGFP*. Each experimental group and control group contained 30 larvae and three independent biological replicates were performed. Total RNA was extracted using Trizol reagent (TransGen Biotech) and qRT-PCR was performed to detect the effects of RNAi at 24 h after the last injection.

Hematoxylin-Eosin Staining

The midgut dissected from the larva was washed with PBS, and then fixed in 4% paraformaldehyde at 4°C overnight. The fixed tissue was submitted to a professional company (Servicebio, Wuhan, China) for processing into glass slides and for Hematoxylin-Eosin (HE) staining.

Overexpression of Prolactin-Releasing Peptide Receptor and Smoothened in HaEpi Cells

The pIEx-4-GFP-His vector that was fused with a sequence encoding the green fluorescent protein (GFP) and used for experiments in the insect cell line. The open reading frames (ORFs) of *PrRPR* (GenBank accession no. XP_021184170.1) and *Smo* (GenBank accession no. XP_021189185.1) were amplified using primers (**Supplementary Table 1**) and inserted into the vector. Then, 5 μg of the recombinant plasmids were transfected into HaEpi cells using the QuickShuttle-enhanced transfection reagent (Biodragon Immunotech, Beijing, China). After 48 h of transfection, further experiments were conducted.

Immunocytochemistry

After PRRPR-GFP and SMO-GFP were overexpressed for 48 h, HaEpi cells were washed three times with 500 μL of Dulbecco's phosphate-buffered saline (DPBS; 137 mM NaCl, 2.7 mM KCl, 1.5 mM KH_2PO_4 and 8 mM Na_2HPO_4, pH 7.4), and fixed with PBS containing 4% paraformaldehyde for 10 min in the dark at room temperature. The fixed cells were washed three times for 3 min each. The plasma membrane was stained using wheat germ agglutinin (WGA; Sigma-Aldrich, St. Louis, MO, United States; 1 μg/mL in PBS) in the dark for 4 min and then washed with PBS six times. Nuclei were stained with 4′-6-diamidino-2-phenylindole dihydrochloride (DAPI; Sangon Biotech, Shanghai, China; 1 μg/mL in PBS) in the dark at room temperature for 10 min and then washed with PBS six times. Fluorescence was detected using an Olympus BX51 fluorescence microscope (Olympus, Tokyo, Japan). The negative control (GFP expression) was treated following the same method.

20-Hydroxyecdysone Enzyme Immunoassay

The 20-hydroxyecdysone enzyme immunoassay (20E-EIA) is based on the competition between unlabeled 20E (free 20E) and acetylcholinesterase (AChE)-labeled 20E (Tracer) for limited specific rabbit anti-20E antiserum. The rabbit anti-20E antiserum was combined with the mouse anti-rabbit monoclonal antibody coated-plate. Then, the plate was washed using the wash buffer included with the 20-Hydroxyecdysone Enzyme Immunoassay kit (20E-EIA kit) (Bertin Pharma, Paris, France) (2 mL of concentrated Wash Buffer #A17000 was diluted by 800 mL of UltraPure water then added 400 μL of Tween20 #A12000) to remove all unbound reagents. Then, tracer and free 20E in samples were added into the wells and the plates were incubated at 4°C overnight. After washing the plate five times with wash buffer, 200 μL Ellman's reagent (an enzymatic substrate for AChE and a chromogen) was added to the wells, and the plate was then incubated with an orbital shaker at 400 rpm in the dark at room temperature. AChE-labeled 20E acts on the substrate in Ellman's Reagent to form a yellow compound, which can strongly absorb light at 414 nm. The intensity of the color was detected using a spectrophotometer (Infinite M200PRO NanoQuant, Tecan, Grödig, Austria) at 414 nm. The optical density was proportional to the amount of tracer bound to the well and inversely proportional to the amount of 20E in the sample. The 20E standard curve generated by this method was used to determine the quantity of 20E bound to cell membrane proteins.

Detection of the 20E Quantity Bound by the Cell Membranes of HaEpi Cells

PRRPR-GFP and SMO-GFP were overexpressed in HaEpi cells in a 25 cm^2 cell culture bottle, respectively. After washing with DPBS twice, the cells were incubated in Grace's medium containing 1 μM 20E for 5 min at 27°C to allow 20E to bind to the cell membrane. The cells were then collected by centrifugation at 1,700 × *g* at 4°C for 5 min and the pellet was resuspended in 500 μL enzyme immunoassay (EIA) buffer (Bertin Pharma, Paris, France) and sonicated for 5 min. The pelleted cell membrane

debris was resuspended in 100 μL EIA buffer after centrifugation at 4°C at 48,000 × *g* for 1 h. Then, 50 μg of cell membrane proteins with fixed 20E in 50 μL EIA buffer was added with 450 μL EIA buffer and used to quantify 20E. The 20E-EIA kit was used to detect cell membrane bound-20E according to the manufacturer's instructions.

Statistical Analysis

Two-group datasets were analyzed using Student's *t*-test and in the figures, an asterisk represents a significant difference ($p < 0.05$) and two asterisks represent an extremely significant difference ($p < 0.01$). Analysis of variance (ANOVA) was used for multiple comparisons and in the figures, different lowercase letters indicate significant differences ($p < 0.05$), and the bars indicate the mean ± standard deviation (SD) of three biological replicates. The details are provided in the figure legends.

DATA AVAILABILITY STATEMENT

The datasets presented in this study can be found in online repositories. The names of the repository/repositories and accession number(s) can be found in the article/**Supplementary Material**.

AUTHOR CONTRIBUTIONS

Y-LL and X-FZ designed the experiments and wrote the manuscript. D-JD, J-XW, and X-FZ conceived the idea. Y-LL, Y-XL, X-PW, X-LK, and K-QG performed the experiments. Y-LL and Y-XL performed the data analyses. All the authors contributed to the article and approved the submitted version.

FUNDING

This project was supported by funding from the National Natural Science Foundation of China (http://www.nsfc.gov.cn/publish/portal0/default.htm) (Grant No. 31730083) to X-FZ. The funders had no role in study design, data collection and analysis, decision to publish, or preparation of the manuscript.

ACKNOWLEDGMENTS

We thank Caiyun Sun from State Key Laboratory of Microbial Technology, Shandong University for the assistance of using Infinite M200PRO NanoQuant.

SUPPLEMENTARY MATERIAL

The Supplementary Material for this article can be found online at: https://www.frontiersin.org/articles/10.3389/fcell.2021.753787/full#supplementary-material

REFERENCES

Araujo, A. R., Reis, M., Rocha, H., Aguiar, B., Morales-Hojas, R., Macedo-Ribeiro, S., et al. (2013). The *Drosophila melanogaster* methuselah gene: a novel gene with ancient functions. *PLoS One* 8:e63747. doi: 10.1371/journal.pone.0063747

Audsley, N., and Down, R. E. (2015). G protein-coupled receptors as targets for next generation pesticides. *Insect Biochem. Mol. Biol.* 67, 27–37. doi: 10.1016/j.ibmb.2015.07.014

Baumbach, J., Xu, Y., Hehlert, P., and Kuhnlein, R. P. (2014). Gαq, Gγ1 and Plc21C control *Drosophila* body fat storage. *J. Genet. Genomics* 41, 283–292. doi: 10.1016/j.jgg.2014.03.005

Bednarova, A., Kodrik, D., and Krishnan, N. (2013). Unique roles of glucagon and glucagon-like peptides: parallels in understanding the functions of adipokinetic hormones in stress responses in insects. *Comp. Biochem. Physiol. A Mol. Integr. Physiol.* 164, 91–100. doi: 10.1016/j.cbpa.2012.10.012

Belles, X. (2020). Kruppel homolog 1 and E93: the doorkeeper and the key to insect metamorphosis. *Arch. Insect Biochem. Physiol.* 103:e21609. doi: 10.1002/arch.21609

Blenau, W., and Thamm, M. (2011). Distribution of serotonin (5-HT) and its receptors in the insect brain with focus on the mushroom bodies: lessons from *Drosophila melanogaster* and *Apis mellifera*. *Arthropod. Struct. Dev.* 40, 381–394. doi: 10.1016/j.asd.2011.01.004

Butet, N., Solihin, D., Soewardi, K., and Saefuddin, A. (2014). Actin gene from blood cockle *Anadara granosa* as a potential housekeeping gene for gene expression analysis. *Emir. J. Food Agr.* 26, 730–736. doi: 10.9755/ejfa.v26i8.15765

Cai, M. J., Dong, D. J., Wang, Y., Liu, P. C., Liu, W., Wang, J. X., et al. (2014a). G protein-coupled receptor participates in 20-hydroxyecdysone signaling on the plasma membrane. *Cell Commun. Signal.* 12:9. doi: 10.1186/1478-811X-12-9

Cai, M. J., Liu, W., Pei, X. Y., Li, X. R., He, H. J., Wang, J. X., et al. (2014b). Juvenile hormone prevents 20-hydroxyecdysone-induced metamorphosis by regulating the phosphorylation of a newly identified broad protein. *J. Biol. Chem.* 289, 26630–26641. doi: 10.1074/jbc.M114.581876

Cai, M. J., Zhao, W. L., Jing, Y. P., Song, Q., Zhang, X. Q., Wang, J. X., et al. (2016). 20-Hydroxyecdysone activates Forkhead box O to promote proteolysis during *Helicoverpa armigera* molting. *Development* 143, 1005–1015. doi: 10.1242/dev.128694

Cardoso, J. C. R., Clark, M. S., Viera, F. A., Bridge, P. D., Gilles, A., and Power, D. M. (2005). The secretin G protein-coupled receptor family: teleost receptors. *J. Mol. Endocrinol.* 34, 753–765.

Cardoso, J. C. R., Vieira, F. A., Gomes, A. S., and Power, D. M. (2010). The serendipitous origin of chordate secretin peptide family members. *BMC Evol. Biol.* 10:135. doi: 10.1186/1471-2148-10-135

Clevers, H. (2006). Wnt/beta-catenin signaling in development and disease. *Cell* 127, 469–480. doi: 10.1016/j.cell.2006.10.018

Cvejic, S., Zhu, Z., Felice, S. J., Berman, Y., and Huang, X. Y. (2004). The endogenous ligand stunted of the GPCR Methuselah extends lifespan in *Drosophila*. *Nat. Cell Biol.* 6, 540–546. doi: 10.1038/ncb1133

de Mendoza, A., Jones, J. W., and Friedrich, M. (2016). Methuselah/Methuselah-like G protein-coupled receptors constitute an ancient metazoan gene family. *Sci Rep.* 6:21801. doi: 10.1038/srep21801

Di, Y.-Q., Han, X.-L., Kang, X.-L., Wang, D., Chen, C.-H., Wang, J.-X., et al. (2020). Autophagy triggers CTSD (cathepsin D) maturation and localization inside cells to promote apoptosis. *Autophagy* 17, 1170–1192. doi: 10.1080/15548627.2020.1752497

Dodd, G. T., and Luckman, S. M. (2013). Physiological Roles of GPR10 and PrRP signaling. *Front. Endocrinol. (Lausanne)* 4:20. doi: 10.3389/fendo.2013.00020

Fan, Y., Sun, P., Wang, Y., He, X., Deng, X., Chen, X., et al. (2010). The G protein-coupled receptors in the silkworm, *Bombyx mori*. *Insect Biochem. Mol. Biol.* 40, 581–591. doi: 10.1016/j.ibmb.2010.05.005

Fire, A., Xu, S., Montgomery, M. K., Kostas, S. A., Driver, S. E., and Mello, C. C. (1998). Potent and specific genetic interference by double-stranded RNA in *Caenorhabditis elegans*. *Nature* 391, 806–811. doi: 10.1038/35888

Flock, T., Hauser, A. S., Lund, N., Gloriam, D. E., Balaji, S., and Babu, M. M. (2017). Selectivity determinants of GPCR-G-protein binding. *Nature* 545, 317–322. doi: 10.1038/nature22070

Fredriksson, R., and Schioth, H. B. (2005). The repertoire of G protein-coupled receptors in fully sequenced genomes. *Mol. Pharmacol.* 67, 1414–1425. doi: 10.1124/mol.104.009001

Friedrich, M., and Jones, J. W. (2016). Gene ages, nomenclatures, and functional diversification of the methuselah/methuselah-like GPCR family in *Drosophila* and *Tribolium*. *J. Exp. Zool. B Mol. Dev. Evol.* 326, 453–463. doi: 10.1002/jez.b.22721

Gao, X. K., Zhang, S., Luo, J. Y., Wang, C. Y., Lu, L. M., Zhang, L. J., et al. (2017). Identification and validation of reference genes for gene expression analysis in *Aphidius gifuensis* (Hymenoptera: Aphidiidae). *PLoS One* 12:e0188477. doi: 10.1371/journal.pone.0188477

Hakim, R. S., Baldwin, K., and Smagghe, G. (2010). Regulation of midgut growth, development, and metamorphosis. *Annu. Rev. Entomol.* 55, 593–608. doi: 10.1146/annurev-ento-112408-085450

Hanlon, C. D., and Andrew, D. J. (2015). Outside-in signaling–a brief review of GPCR signaling with a focus on the *Drosophila* GPCR family. *J. Cell Sci.* 128, 3533–3542. doi: 10.1242/jcs.175158

Hauser, A. S., Attwood, M. M., Rask-Andersen, M., Schioth, H. B., and Gloriam, D. E. (2017). Trends in GPCR drug discovery: new agents, targets and indications. *Nat. Rev. Drug Discov.* 16, 829–842. doi: 10.1038/nrd.2017.178

Hill, C. A., Fox, A. N., Pitts, R. J., Kent, L. B., Tan, P. L., Chrystal, M. A., et al. (2002). G protein-coupled receptors in *Anopheles gambiae*. *Science* 298, 176–178. doi: 10.1126/science.1076196

Ja, W. W., Carvalho, G. B., Madrigal, M., Roberts, R. W., and Benzer, S. (2009). The *Drosophila* G protein-coupled receptor, Methuselah, exhibits a promiscuous response to peptides. *Protein Sci.* 18, 2203–2208. doi: 10.1002/pro.221

Kang, X. L., Li, Y. X., Li, Y. L., Wang, J. X., and Zhao, X. F. (2021). The homotetramerization of a GPCR transmits the 20-hydroxyecdysone signal and increases its entry into cells for insect metamorphosis. *Development* 148:dev196667. doi: 10.1242/dev.196667

Kang, X. L., Zhang, J. Y., Wang, D., Zhao, Y. M., Han, X. L., Wang, J. X., et al. (2019). The steroid hormone 20-hydroxyecdysone binds to dopamine receptor to repress lepidopteran insect feeding and promote pupation. *PLoS Genet.* 15:e1008331. doi: 10.1371/journal.pgen.1008331

Kayukawa, T., Minakuchi, C., Namiki, T., Togawa, T., Yoshiyama, M., Kamimura, M., et al. (2012). Transcriptional regulation of juvenile hormone-mediated induction of Kruppel homolog 1, a repressor of insect metamorphosis. *Proc. Natl. Acad. Sci. U.S.A.* 109, 11729–11734. doi: 10.1073/pnas.1204951109

King, T. D., Zhang, W., Suto, M. J., and Li, Y. H. (2012). Frizzled7 as an emerging target for cancer therapy. *Cell Signal.* 24, 846–851.

Latorraca, N. R., Venkatakrishnan, A. J., and Dror, R. O. (2017). GPCR dynamics: structures in motion. *Chem. Rev.* 117, 139–155. doi: 10.1021/acs.chemrev.6b00177

Lin, Y. J., Seroude, L., and Benzer, S. (1998). Extended life-span and stress resistance in the *Drosophila* mutant methuselah. *Science* 282, 943–946. doi: 10.1126/science.282.5390.943

Livak, K. J., and Schmittgen, T. D. (2001). Analysis of relative gene expression data using real-time quantitative PCR and the 2(-Delta Delta C(T)) Method. *Methods* 25, 402–408. doi: 10.1006/meth.2001.1262

Lu, Y., Yuan, M., Gao, X., Kang, T., Zhan, S., Wan, H., et al. (2013). Identification and validation of reference genes for gene expression analysis using quantitative PCR in *Spodoptera litura* (Lepidoptera: Noctuidae). *PLoS One* 8:e68059. doi: 10.1371/journal.pone.0068059

Maggiolini, M., and Picard, D. (2010). The unfolding stories of GPR30, a new membrane-bound estrogen receptor. *J. Endocrinol.* 204, 105–114. doi: 10.1677/JOE-09-0242

Mertens, I., Husson, S. J., Janssen, T., Lindemans, M., and Schoofs, L. (2007). PACAP and PDF signaling in the regulation of mammalian and insect circadian rhythms. *Peptides* 28, 1775–1783. doi: 10.1016/j.peptides.2007.05.005

Mirth, C. K., Truman, J. W., and Riddiford, L. M. (2009). The ecdysone receptor controls the post-critical weight switch to nutrition-independent differentiation in *Drosophila* wing imaginal discs. *Development* 136, 2345–2353. doi: 10.1242/dev.032672

Nygaard, R., Zou, Y., Dror, R. O., Mildorf, T. J., Arlow, D. H., Manglik, A., et al. (2013). The dynamic process of beta(2)-adrenergic receptor activation. *Cell* 152, 532–542. doi: 10.1016/j.cell.2013.01.008

Palli, S. R., Ladd, T. R., and Retnakaran, A. (1997). Cloning and characterization of a new isoform of *Choristoneura* hormone receptor 3 from the spruce budworm. *Arch. Insect Biochem. Physiol.* 35, 33–44. doi: 10.1002/(SICI)1520-6327199735:1/2<33::AID-ARCH4>3.0.CO;2-Y

Patel, M. V., Hallal, D. A., Jones, J. W., Bronner, D. N., Zein, R., Caravas, J., et al. (2012). Dramatic expansion and developmental expression diversification of the methuselah gene family during recent *Drosophila* evolution. *J. Exp. Zool. B Mol. Dev. Evol.* 318, 368–387. doi: 10.1002/jez.b.22453

Rasmussen, S. G., DeVree, B. T., Zou, Y., Kruse, A. C., Chung, K. Y., Kobilka, T. S., et al. (2011). Crystal structure of the beta2 adrenergic receptor-Gs protein complex. *Nature* 477, 549–555. doi: 10.1038/nature10361

Reagan, J. D. (1994). Expression cloning of an insect diuretic hormone receptor. A member of the calcitonin/secretin receptor family. *J. Biol. Chem.* 269, 9–12.

Sadowski, M. I., and Parish, J. H. (2003). Automated generation and refinement of protein signatures: case study with G protein-coupled receptors. *Bioinformatics* 19, 727–734. doi: 10.1093/bioinformatics/btg075

Srivastava, D. P., Yu, E. J., Kennedy, K., Chatwin, H., Reale, V., Hamon, M., et al. (2005). Rapid, nongenomic responses to ecdysteroids and catecholamines mediated by a novel *Drosophila* G protein-coupled receptor. *J. Neurosci.* 25, 6145–6155. doi: 10.1523/JNEUROSCI.1005-05.2005

Strasser, A., Wittmann, H. J., and Seifert, R. (2017). Binding kinetics and pathways of ligands to GPCRs. *Trends Pharmacol. Sci.* 38, 717–732. doi: 10.1016/j.tips.2017.05.005

Tamura, K., Stecher, G., Peterson, D., Filipski, A., and Kumar, S. (2013). MEGA6: molecular evolutionary genetics analysis version 6.0. *Mol. Biol. Evol.* 30, 2725–2729. doi: 10.1093/molbev/mst197

Van der Horst, D. J., Van Marrewijk, W. J., and Diederen, J. H. (2001). Adipokinetic hormones of insect: release, signal transduction, and responses. *Int. Rev. Cytol.* 211, 179–240. doi: 10.1016/s0074-7696(01)11019-3

Vanden Broeck, J., Torfs, H., Poels, J., Van Poyer, W., Swinnen, E., Ferket, K., et al. (1999). Tachykinin-like peptides and their receptors – A review. *Ann. N. Y. Acad. Sci.* 897, 374–387. doi: 10.1111/j.1749-6632.1999.tb07907.x

Wang, D., Zhao, W. L., Cai, M. J., Wang, J. X., and Zhao, X. F. (2015). G protein-coupled receptor controls steroid hormone signaling in cell membrane. *Sci. Rep.* 5:8675. doi: 10.1038/srep08675

Wang, J. L., Jiang, X. J., Wang, Q., Hou, L. J., Xu, D. W., Wang, J. X., et al. (2007). Identification and expression profile of a putative basement membrane protein gene in the midgut of *Helicoverpa armigera*. *BMC Dev. Biol.* 7:76. doi: 10.1186/1471-213X-7-76

West, A. P. Jr., Llamas, L. L., Snow, P. M., Benzer, S., and Bjorkman, P. J. (2001). Crystal structure of the ectodomain of Methuselah, a *Drosophila* G protein-coupled receptor associated with extended lifespan. *Proc. Natl. Acad. Sci. U.S.A.* 98, 3744–3749. doi: 10.1073/pnas.051625298

Wu, F., Zhang, Y., Sun, B., McMahon, A. P., and Wang, Y. (2017). Hedgehog signaling: from basic biology to cancer therapy. *Cell Chem. Biol.* 24, 252–280. doi: 10.1016/j.chembiol.2017.02.010

Wu, K. M., Lu, Y. H., Feng, H. Q., Jiang, Y. Y., and Zhao, J. Z. (2008). Suppression of cotton bollworm in multiple crops in china in areas with Bt toxin-containing cotton. *Science* 321, 1676–1678. doi: 10.1126/science.1160550

Xu, J., Wang, X. F., Chen, P., Liu, F. T., Zheng, S. C., Ye, H., et al. (2016). RNA interference in moths: mechanisms, applications, and progress. *Genes (Basel)* 7:88. doi: 10.3390/genes7100088

Zamore, P., Tuschl, T., Sharp, P., and Bartel, D. (2000). RNAi: double-stranded RNA directs the ATP-dependent cleavage of mRNA at 21 to 23 nucleotide intervals. *Cell* 101, 25–33. doi: 10.1016/s0092-8674(00)80620-0

Zhao, X. F. (2020). G protein-coupled receptors function as cell membrane receptors for the steroid hormone 20-hydroxyecdysone. *Cell Commun. Signal.* 18:146.

Zhao, X. F., Wang, J. X., and Wang, Y. C. (1998). Purification and characterization of a cysteine proteinase from eggs of the cotton boll worm, *Helicoverpa armigera*. *Insect Biochem. Mol. Biol.* 28, 259–264. doi: 10.1016/S0965-1748(98)00015-0

Conflict of Interest: The authors declare that the research was conducted in the absence of any commercial or financial relationships that could be construed as a potential conflict of interest.

Publisher's Note: All claims expressed in this article are solely those of the authors and do not necessarily represent those of their affiliated organizations, or those of the publisher, the editors and the reviewers. Any product that may be evaluated in this article, or claim that may be made by its manufacturer, is not guaranteed or endorsed by the publisher.

frontiers in Cell and Developmental Biology

ORIGINAL RESEARCH
published: 28 October 2021
doi: 10.3389/fcell.2021.727576

The Novel Positive Allosteric Modulator of the $GABA_B$ Receptor, KK-92A, Suppresses Alcohol Self-Administration and Cue-Induced Reinstatement of Alcohol Seeking in Rats

Paola Maccioni[1†], Katarzyna Kaczanowska[2†], Harshani Lawrence[3], Sang Yun[3], Jessica Bratzu[1], Gian Luigi Gessa[1], Patricia McDonald[4‡] and Giancarlo Colombo[1*‡]*

[1] Neuroscience Institute, Section of Cagliari, National Research Council of Italy, Monserrato, Italy, [2] Department of Chemistry, The Scripps Research Institute, La Jolla, CA, United States, [3] Chemical Biology Core, Moffitt Cancer Center, Tampa, FL, United States, [4] Department of Cancer Physiology, Moffitt Cancer Center, Tampa, FL, United States

OPEN ACCESS

Edited by:
Manveen Kaur Gupta, Case Western Reserve University, United States

Reviewed by:
Nicholas Everett, The University of Sydney, Australia
Jesse Schank, University of Georgia, United States

***Correspondence:**
Giancarlo Colombo
giancarlo.colombo@cnr.it
Patricia McDonald
Patsy.McDonald@moffitt.org

[†] These authors have contributed equally to this work and share first authorship

[‡] These authors have contributed equally to this work and share senior authorship

Specialty section:
This article was submitted to Signaling, a section of the journal Frontiers in Cell and Developmental Biology

Received: *18 June 2021*
Accepted: *07 October 2021*
Published: *28 October 2021*

Citation:
Maccioni P, Kaczanowska K, Lawrence H, Yun S, Bratzu J, Gessa GL, McDonald P and Colombo G (2021) The Novel Positive Allosteric Modulator of the $GABA_B$ Receptor, KK-92A, Suppresses Alcohol Self-Administration and Cue-Induced Reinstatement of Alcohol Seeking in Rats. Front. Cell Dev. Biol. 9:727576. doi: 10.3389/fcell.2021.727576

Positive allosteric modulators (PAMs) of the $GABA_B$ receptor ($GABA_B$ PAMs) are of interest in the addiction field due to their ability to suppress several behaviors motivated by drugs of abuse. KK-92A is a novel $GABA_B$ PAM found to attenuate intravenous self-administration of nicotine and reinstatement of nicotine seeking in rats. This present study was aimed at extending to alcohol the anti-addictive properties of KK-92A. To this end, Sardinian alcohol-preferring rats were trained to lever-respond for oral alcohol (15% v/v) or sucrose (0.7% w/v) under the fixed ratio (FR) 5 (FR5) schedule of reinforcement. Once lever-responding behavior had stabilized, rats were exposed to tests with acutely administered KK-92A under FR5 and progressive ratio schedules of reinforcement and cue-induced reinstatement of previously extinguished alcohol seeking. KK-92A effect on spontaneous locomotor activity was also evaluated. Treatment with 10 and 20 mg/kg KK-92A suppressed lever-responding for alcohol, amount of self-administered alcohol, and breakpoint for alcohol. Treatment with 20 mg/kg KK-92A reduced sucrose self-administration. Combination of *per se* ineffective doses of KK-92A (2.5 mg/kg) and the $GABA_B$ receptor agonist, baclofen (1 mg/kg), reduced alcohol self-administration. Treatment with 5, 10, and 20 mg/kg KK-92A suppressed reinstatement of alcohol seeking. Only treatment with 80 mg/kg KK-92A affected spontaneous locomotor activity. These results demonstrate the ability of KK-92A to inhibit alcohol-motivated behaviors in rodents and confirm that these effects are common to the entire class of $GABA_B$ PAMs. The remarkable efficacy of KK-92A is discussed in terms of its ago-allosteric properties.

Keywords: KK-92A, positive allosteric modulator, $GABA_B$ receptor, alcohol self-administration, cue-induced reinstatement of alcohol seeking, rats

INTRODUCTION

Positive allosteric modulation of the $GABA_B$ receptor has emerged as an important molecular mechanism to effectively control several alcohol-motivated behaviors. Accordingly, all positive allosteric modulators (PAMs) of the $GABA_B$ receptor ($GABA_B$ PAMs) tested to date (namely: CGP7930, GS39783, BHF177, *rac*-BHFF, ADX71441, COR659, CMPPE, ORM-27669, and ASP8062) have invariably been reported to reduce excessive alcohol drinking (Orrù et al., 2005; Loi et al., 2013; Hwa et al., 2014; Ferlenghi et al., 2020), binge-like drinking (Hwa et al., 2014; Linsenbardt and Boehm, 2014; Colombo et al., 2015; de Miguel et al., 2019), relapse-like drinking (Vengeliene et al., 2018), operant oral alcohol self-administration (Liang et al., 2006; Maccioni et al., 2007, 2008b, 2009, 2010, 2012, 2015, 2017, 2018, 2019a,b; Augier et al., 2017; Lorrai et al., 2019; Ferlenghi et al., 2020; Haile et al., 2021), cue- and stress-induced reinstatement of alcohol seeking (Augier et al., 2017; Vengeliene et al., 2018; Maccioni et al., 2019a,b), alcohol-induced hyperlocomotion (Kruse et al., 2012), and alcohol-induced conditioned place preference (de Miguel et al., 2019) in rats and mice (for review, see Maccioni and Colombo, 2019; Holtyn and Weerts, 2020).

The pharmacological profile of $GABA_B$ PAMs possess numerous advantages, particularly when compared to that of the orthosteric agonist of the $GABA_B$ receptor, baclofen. Focusing on alcohol-motivated behaviors, the reducing effects of $GABA_B$ PAMs occurred at doses largely lower than those inducing sedation and muscle relaxation (Maccioni et al., 2010, 2017; Linsenbardt and Boehm, 2014; Vengeliene et al., 2018; de Miguel et al., 2019) and devoid of any effect on natural rewards (e.g., water, regular or palatable food) (Orrù et al., 2005; Maccioni et al., 2007, 2008b, 2009, 2010, 2012, 2015, 2019b; Loi et al., 2013; Hwa et al., 2014; Colombo et al., 2015; see however Augier et al., 2017). Additionally, no tolerance developed on continuing treatment (Loi et al., 2013; Maccioni et al., 2015, 2019a; Vengeliene et al., 2018). These favorable features (with undoubted translational value) likely reside in the use-dependent mechanism of action of $GABA_B$ PAMs. At variance with baclofen that stimulates each $GABA_B$ receptor it encounters, $GABA_B$ PAMs only potentiate the receptor activation induced by endogenous GABA, thus limiting their action when and where endogenous GABA is released (see Urwyler, 2011, 2016), resulting *in vivo* in a larger separation between the expected pharmacological effects and putative off-target side-effects. Additionally, the absence of persistent receptor activation (typical, on the other hand, of receptor agonists) results in a low propensity to induce receptor desensitization, explaining why repeated treatment with $GABA_B$ PAMs is associated with limited development of tolerance (see Urwyler, 2011, 2016). Together, these data indicate $GABA_B$ PAMs as active molecules having an improved therapeutic potential over baclofen.

KK-92A [(4-(cycloheptylamino)-5-(4-(trifluoromethyl)phenyl)pyrimidin-2-yl)methanol] is the final product of a recent project of medicinal chemistry and pharmacology aimed at identifying novel $GABA_B$ PAMs starting from the chemical structure of the $GABA_B$ PAM, BHF177 (Li et al., 2017). Among the approximately 100 analogs that had been synthesized, KK-92A was identified as the preferred compound because of its (i) high potency and selectivity as a $GABA_B$ PAM in multiple *in vitro* cell-based assays, (ii) high bioavailability in the brain, and (iii) remarkable *in vivo* efficacy (specifically, the selective reducing effect on intravenous self-administration of nicotine and cue-induced reinstatement of nicotine seeking in rats) (Li et al., 2017). The in-depth investigation of its *in vitro* pharmacological profile (Li et al., 2017) makes KK-92A one of the best characterized $GABA_B$ PAMs available to date and a powerful tool for further investigations of their *in vivo* actions and therapeutic potential.

Accordingly, the present study was designed to investigate whether the reducing effects of $GABA_B$ PAMs on alcohol-motivated behaviors are shared by KK-92A. To this end, acutely administered KK-92A was tested in three different, validated experimental procedures of alcohol seeking and drinking: operant oral alcohol self-administration under the fixed ratio (FR) (Experiment 1A) and progressive ratio (PR) (Experiment 2) schedules of reinforcement, that provide a measure of the reinforcing and motivational properties of alcohol, respectively (see Markou et al., 1993), and cue-induced reinstatement of alcohol seeking, that models human loss of control over alcohol and relapse into heavy alcohol drinking (see Martin-Fardon and Weiss, 2013) (Experiment 3). Selectivity of KK-92A effect on alcohol self-administration was evaluated testing acutely administered KK-92A on sucrose self-administration under the FR schedule of reinforcement (Experiment 1B). The present study also included investigation of the effect of acute treatment with the combination of *per se* ineffective doses of KK-92A and baclofen on alcohol self-administration under the FR schedule of reinforcement (Experiment 1C), with the intent of assessing whether treatment with KK-92A potentiated the reducing effect of baclofen on the reinforcing properties of alcohol. In an attempt to exclude the possibility that the effects of KK-92A on the above alcohol- and sucrose-motivated behaviors were due to sedative and motor-incoordinating effects of KK-92A (a not unlikely event when testing a drug that targets GABA neurotransmission), Experiment 4 evaluated the effect of acute treatment with KK-92A on spontaneous locomotor activity. The effect of acute treatment with KK-92A on blood alcohol levels (BALs) was also assessed (Experiment 5).

All experiments were conducted using the Sardinian alcohol-preferring (sP) rats, one of the few rat lines selectively bred for high alcohol preference and consumption (see Colombo et al., 2006; Bell et al., 2012). sP rats meet all the fundamental requirements posed when defining an animal model of alcohol use disorder (AUD) (see Colombo et al., 2006; Bell et al., 2012). Notably, in relation to the aims of the present study, several previous studies indicated that alcohol self-administration and cue-induced reinstatement of alcohol seeking in sP rats were highly sensitive to positive allosteric modulation of the $GABA_B$ receptor (Maccioni et al., 2007, 2008b, 2009, 2010, 2012, 2015, 2017, 2018, 2019a,b; Lorrai et al., 2019; Ferlenghi et al., 2020).

MATERIALS AND METHODS

The experimental procedures employed in the present study fully complied with European Directive no. 2010/63/EU and

subsequent Italian Legislative Decree no. 26, March 4, 2014, on the "Protection of animals used for scientific purposes."

Animals

Female sP rats (bred in our laboratory at Neuroscience Institute, Section of Cagliari, National Research Council of Italy, Italy) were used. Rats were 50-days-old at the start of each experiment, from 110th to 112th generation, and alcohol-naive at the start of each experiment. Rats were housed three per cage in standard plastic cages with wood chip bedding. The animal facility was under an inverted 12:12-h light-dark cycle (lights on at 7:00 p.m.), at a constant temperature of 22 ± 2°C and relative humidity of approximately 60%. Standard rat chow and tap water were always available in the homecage, except as noted below. Rats were extensively habituated to handling, intraperitoneal injections, and intragastric infusions (the latter limited to rats allocated to Experiment 5).

Female rats were preferred over male rats as their body weight is more stable and much lower than adult male sP rats, resulting in the several practical advantages described elsewhere (Lorrai et al., 2019). Importantly, sensitivity of alcohol self-administration to pharmacological manipulation is highly similar in female and male sP rats: as an example, acute treatment with the $GABA_B$ PAM, GS39783, reduced alcohol self-administration under the FR schedule with comparable potency and efficacy in female and male sP rats (Lorrai et al., 2019).

To avoid any possibility of ovarian hormones influencing alcohol and sucrose self-administration (Experiments 1A-C and 2), reinstatement of alcohol seeking (Experiment 3), and alcohol metabolism (Experiment 5), rats were ovariectomized. Ovariectomy was performed when rats were 45 days old and according to the procedure described in detail elsewhere (Lorrai et al., 2019). A recovery period of 5 days following surgery occurred before the start of the alcohol-drinking phase (see below). For reasons of uniformity and consistency among the five experiments, ovariectomy was also performed in rats allocated to Experiment 4 (spontaneous locomotor activity).

Each single experiment used an independent set of rats.

Drugs

KK-92A was synthesized in gram-scale with >99% purity (as determined by HPLC) in the Chemical Biology Core laboratory at Moffitt Cancer Center, FL, United States, according to the procedure described in detail by Li et al. (2017). The chemical analysis (^{1}H and ^{13}C NMR, HPLC-MS) of in-house synthesized KK-92A matched the reported data (see **Supplementary Material** for structure and chemical analysis). KK-92A was dissolved in a mixture containing dimethyl sulfoxide, polysorbate 80, and distilled water (ratio of the mixture components: 5:10:85) for *in vivo* assessment. In all experiments, KK-92A was administered acutely and intraperitoneally (i.p.; injection volume: 2 ml/kg) 30 min before (a) start of self-administration (Experiments 1A-C and 2), reinstatement (Experiment 3), and locomotor-activity (Experiment 4) sessions and (b) alcohol administration (Experiment 5). In Experiments 1A, 1B, 2, 3, and 5, KK-92A was tested at doses of 0, 5, 10, and 20 mg/kg; this dose range was chosen to be identical to that previously tested on nicotine self-administration and reinstatement of nicotine seeking in Wistar rats (Li et al., 2017). In Experiment 1C, KK-92A was tested at the doses of 0 and 2.5 mg/kg; the latter was chosen on the basis of preliminary data suggesting that it was totally ineffective, when given alone, on alcohol self-administration in sP rats (this laboratory, unpublished results). In Experiment 4, KK-92A was tested at the doses of 0, 20, 40, and 80 mg/kg; this larger dose range was chosen to identify possible sedative and motor-incoordinating effects.

Baclofen (Novartis, Basel, Switzerland) was dissolved in saline and injected i.p. (injection volume: 2 ml/kg) at the doses of 0 and 1 mg/kg 30 min before the start of the test session of Experiment 1C. Pretreatment time and route of administration were identical to those used in previous studies testing baclofen on alcohol self-administration in sP rats (Maccioni et al.2005, 2008, 2012; 2015). Dosage was selected as being totally ineffective, when given alone, on alcohol self-administration in sP rats (Maccioni et al., 2012, 2015).

Alcohol or Sucrose Self-Administration and Cue-Induced Reinstatement of Alcohol Seeking

Apparatus

Self-administration, extinction responding, and reinstatement sessions were conducted in modular chambers (Med Associates, St. Albans, VT, United States) described in detail elsewhere (e.g., Maccioni et al., 2015). Briefly, each chamber was equipped with two retractable response levers (connected to two syringe pumps located outside the chamber), one dual-cup liquid receptacle, two stimulus lights (mounted above each lever), and one tone generator.

In self-administration sessions, achievement of the response requirement (RR) had the following consequences: activation of alcohol (or sucrose) or water pumps, delivery of 0.1 ml fluid, illumination of the stimulus light for the time period of fluid delivery, and activation of the tone generator.

Experimental Procedure

Training and maintenance phases of alcohol or sucrose self-administration

In alcohol self-administration experiments, rats were initially exposed to the homecage 2-bottle "alcohol (10% v/v) vs. water" choice regimen with unlimited access for 24 h/day over 10 consecutive days, according to the procedure described in detail elsewhere (e.g., Maccioni et al., 2015). Subsequently, rats were introduced into the operant chambers and trained to lever-respond for alcohol. Self-administration sessions lasted 30 min (with the sole exception of the very first session, that lasted 120 min) and were conducted 5 days per week. Rats were water-deprived exclusively during the 12 h prior to the first session in the operant chamber. Rats were initially exposed to an FR1 schedule of reinforcement for 10% alcohol (v/v) for four sessions. FR was then progressively increased to FR5 over four sessions. In sessions 9 and 10, the alcohol solution was presented at a final concentration of 15% (v/v). Rats were then exposed to four sessions during which the water lever alone or alcohol lever alone

was available every other day; water and alcohol were available on FR1 and FR5, respectively. From then onward, both levers were concomitantly available (maintenance phase) for a total of 20 sessions conducted with FR5 and FR1 on the alcohol and water lever, respectively. On completion of the maintenance phase, rats displaying the most stable responding behavior were selected for use in Experiments 1A, 1C, 2, and 3.

In the sucrose self-administration experiment, rats were trained to lever-respond for a sucrose solution. Self-administration sessions lasted 30 min (with the sole exception of the very first session, that lasted 120 min) and were conducted 5 days per week. Rats were water-deprived exclusively during the 12 h prior to the first session in the operant chamber. Rats were initially exposed to an FR1 schedule of reinforcement for 2% (w/v) sucrose solution (in water) for four sessions. FR was then progressively increased to FR5 over four sessions. Sucrose concentration was reduced to 0.7% (w/v) over six sessions. This sucrose concentration was selected on the basis of previous results (e.g., Maccioni et al., 2010) in order to establish a lever-responding behavior comparable to that usually performed by sP rats to obtain 15% alcohol under FR5. Rats were then exposed to four sessions during which the water lever alone or the sucrose lever alone was available every other day; water and sucrose were available on FR1 and FR5, respectively. From then onward, both levers were concomitantly available (maintenance phase) for a total of 20 sessions conducted with FR5 and FR1 on the sucrose and water lever, respectively. On completion of the maintenance phase, the rats displaying the most stable responding behavior were selected for use in Experiment 1B.

Testing under the fixed ratio schedule

Experiment 1A evaluated the effect of acute treatment with different doses of KK-92A on alcohol self-administration under the FR5 (alcohol) and FR1 (water) schedule of reinforcement. This experiment employed a total of n = 48 rats (selected as described above from an original set of n = 56), divided into four groups of n = 12 matched for the number of responses on the alcohol lever over the last three sessions of the maintenance phase.

Experiment 1B evaluated the effect of acute treatment with different doses of KK-92A on sucrose self-administration under the FR5 (sucrose) and FR1 (water) schedule of reinforcement. This experiment employed a total of n = 44 rats (from an original set of n = 50), divided into four groups of n = 11 matched for the number of responses on the sucrose lever over the last three sessions of the maintenance phase.

Experiment 1C evaluated the effect of the combination of *per se* ineffective doses of KK-92A and baclofen on alcohol self-administration under the FR5 (alcohol) and FR1 (water) schedule of reinforcement. This experiment employed a total of n = 48 rats (from an original set of n = 56), divided into four groups of n = 12 matched for the number of responses on the alcohol lever over the last three sessions of the maintenance phase. The following four treatment combinations were tested: 0 mg/kg KK-92A + 0 mg/kg baclofen; 0 mg/kg KK-92A + 1 mg/kg baclofen; 2.5 mg/kg KK-92A + 0 mg/kg baclofen; 2.5 mg/kg KK-92A + 1 mg/kg baclofen.

In all three experiments, the test session occurred the day after completion of the maintenance phase, lasted 30 min, and was identical to those of the maintenance phase [FR5 and FR1 on the alcohol (or sucrose) and water lever, respectively].

Measured variables were: (a) number of responses on each lever; (b) amount of self-administered alcohol (expressed in g/kg pure alcohol) or sucrose solution (expressed in ml/kg), estimated from the number of earned reinforcers assuming that each reinforcer was entirely consumed. In Experiment 1A, latency (expressed in s) to the first alcohol reinforcer was also measured; rats that completely avoided responding on the lever were assigned the value 1,800 s (i.e., the entire length of the test session). Data on number of responses on each lever and amount of self-administered alcohol (or sucrose solution) were statistically evaluated by 1-way ANOVA with repeated measures, followed by Tukey's test for *post hoc* comparisons. Data on latency to the first alcohol reinforcer were statistically evaluated by Kruskal-Wallis test, followed by Dunn's for *post hoc* comparison.

Testing under the progressive ratio schedule

Experiment 2 evaluated the effect of acute treatment with different doses of KK-92A on alcohol self-administration under the PR schedule of reinforcement. This experiment employed a total of n = 48 rats (from an original set of n = 56), divided into four groups of n = 12 matched for the number of responses on the alcohol lever over the last three sessions of the maintenance phase. The test session occurred the day after completion of the maintenance phase and lasted 60 min. In the test session, RR on the alcohol lever was increased progressively over the session according to a procedure slightly adapted from that described by Richardson and Roberts (1996); namely, RR was increased as follows: 5, 9, 12, 15, 20, 25, 32, 40, 50, 62, 77, 95, 118, 145, 178, 219, etc. The water lever was inactive.

Measured variables were: (a) number of responses on each lever; (b) breakpoint for alcohol, defined as the lowest RR not achieved by the rat; (c) latency (expressed in s) to the first reinforcer (rats that completely avoided responding on the lever were assigned the value 3,600 s, i.e., the entire length of the test session). Data from each variable were statistically evaluated by 1-way ANOVA with repeated measures, followed by Tukey's test for *post hoc* comparisons.

Testing under the reinstatement of alcohol-seeking protocol

Experiment 3 evaluated the effect of acute treatment with different doses of KK-92A on cue-induced reinstatement of alcohol seeking. To this end, immediately after completion of the maintenance phase, rats underwent an extinction-responding phase made up of consecutive (no weekend interruption) daily sessions (lasting 60 min) characterized by unavailability of alcohol and water; specifically, syringe pumps, stimulus lights, and tone generator were off, and lever-responding was unreinforced. An extinction criterion was set at $\leq$12 responses on the alcohol lever per session for two consecutive sessions (Maccioni et al., 2019b).

This experiment employed a total of n = 30 rats (from an original set of n = 40), divided into four groups of n = 7–8 matched for the number of responses on the alcohol lever over

the first three sessions of the extinction-responding phase. The day after achievement of the extinction criterion, each rat was exposed to a single 60-min reinstatement (test) session, during which a stimulus complex—previously associated to availability of alcohol—was presented for 10 times within 20 s. This stimulus complex was composed of tone, turning on of the stimulus lights, and availability, every other time, of 0.1 ml alcohol (15% v/v) in the liquid receptacle (for a total number of 5 presentations). Immediately after the last presentation of the stimulus complex, both levers were inserted inside the chamber and lever-responding (still unreinforced) was recorded.

The measured variable was the number of responses on alcohol lever during the reinstatement session. Data were statistically evaluated by 2-way [phase (extinction/reinstatement); treatment (KK-92A dose)] ANOVA with repeated measures on the factor "phase," followed by Bonferroni's test for *post hoc* comparisons. An additional analysis evaluated the number of sessions of the extinction responding phase needed to achieve the extinction criterion; these data were analyzed by 1-way ANOVA and log-rank (Mantel-Cox) test.

Locomotor Activity

Apparatus

Locomotor activity (ambulation) was measured in Plexiglass test cages [480 × 480 × 400 (h) mm] by a computer-operated, photocell-equipped apparatus (Motil, TSE, Bad Homburg, Germany). Photocells were 40-mm spaced. Test cages were located in a sound-proof, dimly lit room adjacent to the housing room.

Experimental Procedure

Experiment 4 evaluated the effect of acute treatment with different doses of KK-92A on spontaneous locomotor activity. Rats were initially exposed to the homecage 2-bottle "alcohol (10% v/v) vs. water" choice regimen with unlimited access for 24 h/day throughout 10 consecutive days. Subsequently, rats were trained to lever-respond for alcohol using the same procedure described above. Consequently, the "alcohol" history of these rats was identical to that of the rats used in Experiments 1A, 1C, 2, 3, and 5.

This experiment employed a total of n = 39 rats, divided into four groups of n = 9–10 matched for body weight and number of responses on the alcohol lever over the last three sessions of the maintenance phase. The locomotor-activity test was conducted the day after completion of the maintenance phase and lasted 30 min. Rats were unfamiliar to the motility cage, in order to provide relatively high baseline levels of spontaneous locomotor activity (i.e., a desirable condition to amplify the possible suppressing effect of the tested drug) (see Kelley, 1993).

The measured variable was the number of motility counts (photocell breaks), recorded automatically by the apparatus. Data were divided into six 5-min time intervals and statistically analyzed by a 2-way (KK-92A dose; time) ANOVA with repeated measures on the factor "time," followed by Tukey's test for *post hoc* comparisons. The total (cumulated) number of motility counts over the entire session was statistically evaluated by 1-way ANOVA, followed by Tukey's test for *post hoc* comparisons.

Blood Alcohol Levels

Apparatus

Blood samples were analyzed by means of an enzymatic system [GL5 Analyzer (Analox Instruments, London, United Kingdom)] based on measurement of oxygen consumption in the alcohol-acetaldehyde reaction.

Experimental Procedure

Experiment 5 evaluated the effect of acute treatment with different doses of KK-92A on BALs. Rats were initially exposed to the homecage 2-bottle "alcohol (10% v/v) vs. water" choice regimen with unlimited access for 24 h/day throughout 10 consecutive days. Subsequently, rats were trained to lever-respond for alcohol using the same procedure described above. Consequently, the "alcohol" history of these rats was identical to that of the rats used in Experiments 1A, 1C, 2, 3, and 4.

This experiment employed a total of n = 40 rats, divided into four groups on n = 10 matched for body weight and number of responses on the alcohol lever over the last three sessions of the maintenance phase. The experiment was conducted the day after completion of the maintenance phase. Food pellets were removed 4 h before the experiment, to ensure that rats had empty stomachs at the time of alcohol infusion. Thirty min after treatment with KK-92A, rats were treated intragastrically with 1 g/kg alcohol (15% v/v). Blood samples (50 μL) were collected from the tip of the tail of each rat at 30, 60, 120, and 240 min after alcohol administration.

The measured variable was BALs (expressed in mg%). Data on BAL time-course were statistically evaluated by 2-way (KK-92A dose; time) ANOVA with repeated measures on the factor "time," followed by Tukey's test for *post hoc* comparisons. Data on the area under the curve of BAL time-course [expressed as (h*μg/ml)] were statistically evaluated by 1-way ANOVA, followed by Tukey's test for *post hoc* comparisons.

RESULTS

Experiment 1A: Testing KK-92A on Alcohol Self-Administration Under the FR5 Schedule

Acute treatment with KK-92A suppressed, in a dose-related manner, the number of lever-responses for alcohol [$F(3, 44) = 27.39$, $P < 0.0001$] in female sP rats exposed to the FR5 schedule of reinforcement (**Figure 1A**). *Post hoc* test indicated that statistical significance was reached by treatment with 10 ($P < 0.0001$) and 20 ($P < 0.0001$) mg/kg KK-92A. The magnitude of the suppressing effect of 10 and 20 mg/kg KK-92A on number of lever-responses for alcohol averaged approximately 60 and 95%, respectively. Suppression in number of lever-responses for alcohol resulted in a proportional decrease in the amount of self-administered alcohol [$F(3, 44) = 26.42$, $P < 0.0001$] (**Figure 1B**). At *post hoc* test, statistical significance was reached by treatment with 10 ($P < 0.0001$) and 20 ($P < 0.0001$) mg/kg KK-92A. Acute treatment with KK-92A increased latency to the first alcohol reinforcer [$F(3, 44) = 17.85$, $P < 0.0005$] (**Figure 1C**). *Post hoc*

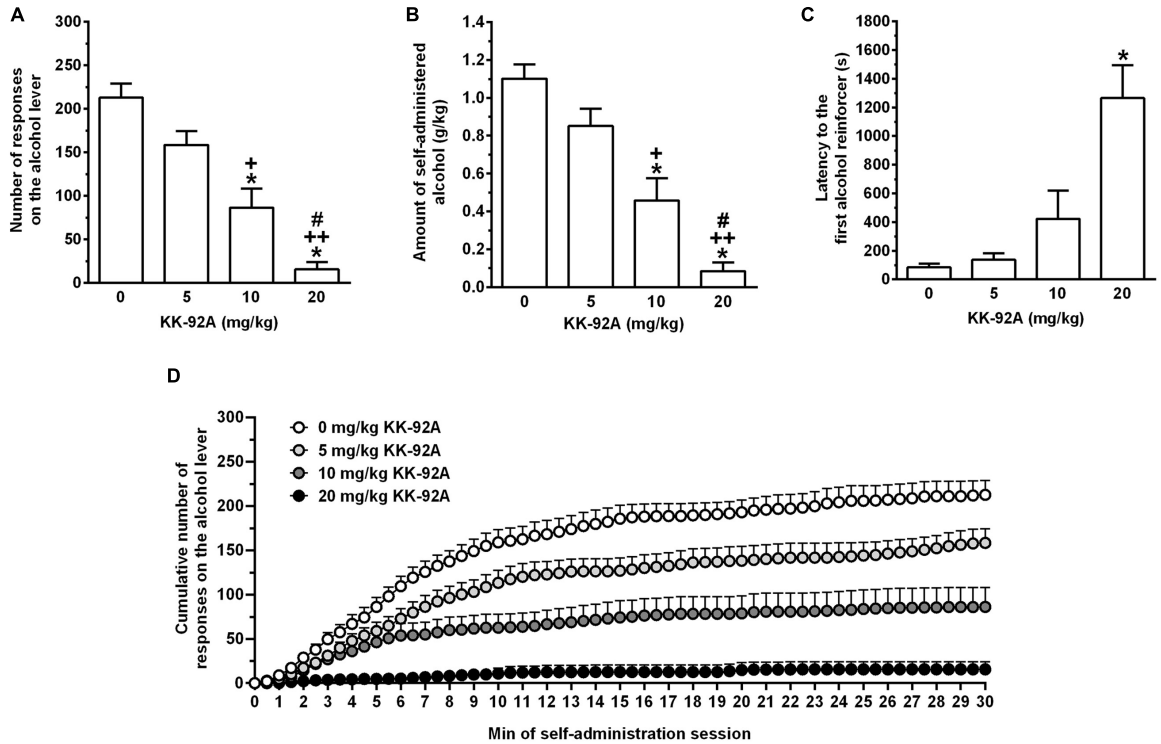

FIGURE 1 | Effect of acute treatment with the positive allosteric modulator of the $GABA_B$ receptor, KK-92A, on number of lever-responses for alcohol **(A)**, amount of self-administered alcohol **(B)**, latency to the first reinforcer on the alcohol lever **(C)**, and cumulative response patterns of alcohol self-administration **(D)** in female Sardinian alcohol-preferring rats. Rats were initially trained to lever-respond for oral alcohol (15% v/v in water) [Fixed Ratio (FR) 5 (FR5)] and water (FR1) in daily 30-min self-administration sessions. Once lever-responding had stabilized, rats were tested with KK-92A under the same FR schedule of reinforcement. KK-92A was administered intraperitoneally 30 min before the start of the self-administration session. In panel **(D)**, the self-administration session was divided into 30 intervals of 1 min each. Each bar or point is the mean ± SEM of $n = 12$ rats. $^{*}P < 0.0001$ in comparison to the rat group treated with 0 mg/kg KK-92A [Tukey's test in panels **(A,B)**; Dunn's test in panel **(C)**]; $^{+}P < 0.05$ and $^{++}P < 0.0001$ in comparison to the rat group treated with 5 mg/kg KK-92A (Tukey's test); $^{\#}P < 0.05$ in comparison to the rat group treated with 10 mg/kg KK-92A (Tukey's test).

test indicated that statistical significance was reached only by treatment with 20 mg/kg KK-92A ($P < 0.0005$). After treatment with 20 mg/kg KK-92A, latency to the first alcohol reinforcer was increased by approximately 15 times.

Lever-responding for water was negligible (averaging < 3 per session in all rat groups) and not altered by drug treatment (data not shown).

Experiment 1B: Testing KK-92A on Sucrose Self-Administration Under the FR5 Schedule

Acute treatment with KK-92A reduced, in a dose-related manner, the number of lever-responses for sucrose solution [$F(3, 40) = 4.44$, $P < 0.01$] in female sP rats exposed to the FR5 schedule of reinforcement (**Figure 2A**). *Post hoc* test indicated that statistical significance was reached only by treatment with 20 mg/kg KK-92A ($P < 0.05$). The magnitude of the suppressing effect of 20 mg/kg KK-92A on number of lever-responses for sucrose solution averaged approximately 60%. Reduction in number of lever-responses for sucrose solution resulted in a proportional decrease in the amount of self-administered sucrose solution [$F(3, 40) = 4.27$, $P < 0.05$] (**Figure 2B**). At *post hoc* test, statistical significance was reached only by treatment with 20 mg/kg KK-92A ($P < 0.05$).

Lever-responding for water was negligible (averaging < 2 per session in all rat groups) and not altered by treatment with KK-92A (data not shown).

Experiment 1C: Testing the Combination of KK-92A and Baclofen on Alcohol Self-Administration Under the FR5 Schedule

Acute treatment with the combination of KK-92A and baclofen reduced the number of lever-responses for alcohol [$F(3, 44) = 4.23$, $P < 0.05$] in female sP rats exposed to the FR5 schedule of reinforcement (**Figure 3A**). Neither KK-92A nor baclofen, when administered alone (or, more precisely, together with the vehicle of the other drug), altered the number of lever-responses for alcohol. Conversely, treatment with the combination of KK-92A and baclofen resulted in an approximately 30% reduction, in comparison to all other three rat groups ($P < 0.05$), in number of lever-responses for alcohol. Reduction in number of lever-responses for alcohol resulted in a proportional decrease

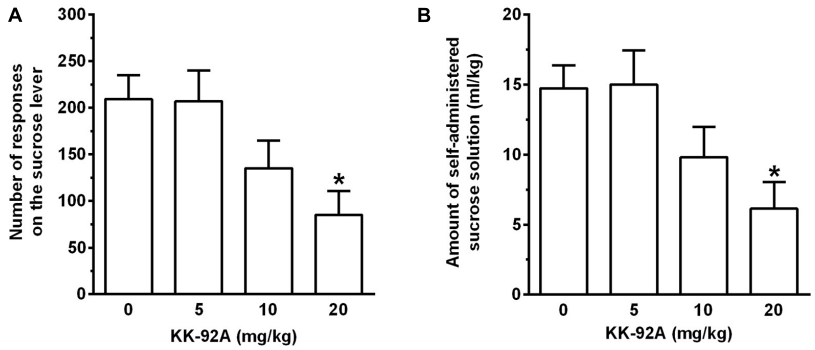

FIGURE 2 | Effect of acute treatment with the positive allosteric modulator of the $GABA_B$ receptor, KK-92A, on number of lever-responses for sucrose solution **(A)** and amount of self-administered sucrose solution **(B)** in female Sardinian alcohol-preferring rats. Rats were initially trained to lever-respond for sucrose solution (0.7% w/v in water) [Fixed Ratio (FR) 5 (FR5)] and water (FR1) in daily 30-min self-administration sessions. Once lever-responding had stabilized, rats were tested with KK-92A under the same FR schedule of reinforcement. KK-92A was administered intraperitoneally 30 min before the start of the self-administration session. Each bar is the mean ± SEM of n = 11 rats. *$P < 0.05$ in comparison to the rat group treated with 0 mg/kg KK-92A (Tukey's test).

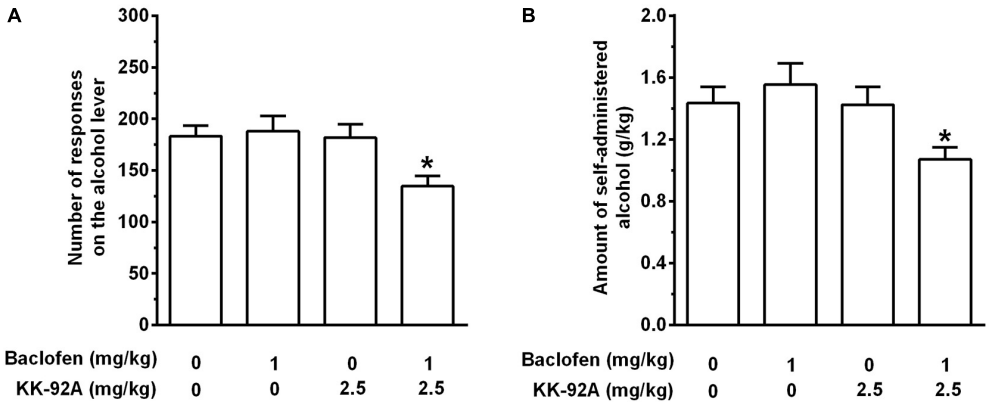

FIGURE 3 | Effect of acute treatment with the combination of *per se* ineffective doses of the positive allosteric modulator of the $GABA_B$ receptor, KK-92A, and the $GABA_B$ receptor agonist, baclofen, on number of lever-responses for alcohol **(A)** and amount of self-administered alcohol **(B)** in female Sardinian alcohol-preferring rats. Rats were initially trained to lever-respond for oral alcohol (15% v/v in water) [Fixed Ratio (FR) 5 (FR5)] and water (FR1) in daily 30-min self-administration sessions. Once lever-responding had stabilized, rats were tested with all treatment combinations under the same FR schedule of reinforcement. KK-92A and baclofen were administered intraperitoneally 30 min before the start of the self-administration session. Each bar is the mean ± SEM of n = 12 rats. *$P < 0.05$ in comparison to all other rat groups (Tukey's test).

in the amount of self-administered alcohol [$F(3, 44) = 3.56$, $P < 0.05$] (**Figure 3B**). Neither KK-92A nor baclofen, when administered alone, altered the amount of self-administered alcohol. Conversely, treatment with the combination of KK-92A and baclofen resulted in an approximately 25% reduction, in comparison to all other three rat groups ($P < 0.05$), in amount of self-administered alcohol.

Lever-responding for water was negligible (averaging < 2 per session in all rat groups) and not altered by treatment with KK-92A (data not shown).

Experiment 2: Testing KK-92A on Alcohol Self-Administration Under the Progressive Ratio Schedule

Acute treatment with KK-92A reduced, in a dose-related manner, the number of lever-responses for alcohol [$F(3, 44) = 11.46$, $P < 0.0001$] in female sP rats exposed to the PR schedule of reinforcement (**Figure 4A**). *Post hoc* test indicated that statistical significance was reached by treatment with 10 ($P < 0.0005$) and 20 ($P < 0.0001$) mg/kg KK-92A. The magnitude of the suppressing effect of 10 and 20 mg/kg KK-92A on number of lever-responses for alcohol averaged approximately 65 and 75%, respectively. Acute treatment with KK-92A also reduced, in a dose-related manner, breakpoint for alcohol [$F(3, 44) = 9.72$, $P < 0.0001$] (**Figure 4B**). *Post hoc* test indicated that statistical significance was reached by treatment with 10 ($P < 0.001$) and 20 ($P < 0.0001$) mg/kg KK-92A. The magnitude of the suppressing effect of 10 and 20 mg/kg KK-92A on breakpoint for alcohol averaged approximately 55 and 65%, respectively. Acute treatment with KK-92A markedly increased latency to the first reinforcer [$F(3, 44) = 7.29$, $P < 0.0005$] (**Figure 4C**). *Post hoc* test indicated that statistical significance was reached only by treatment with 20 mg/kg KK-92A ($P < 0.001$). After treatment

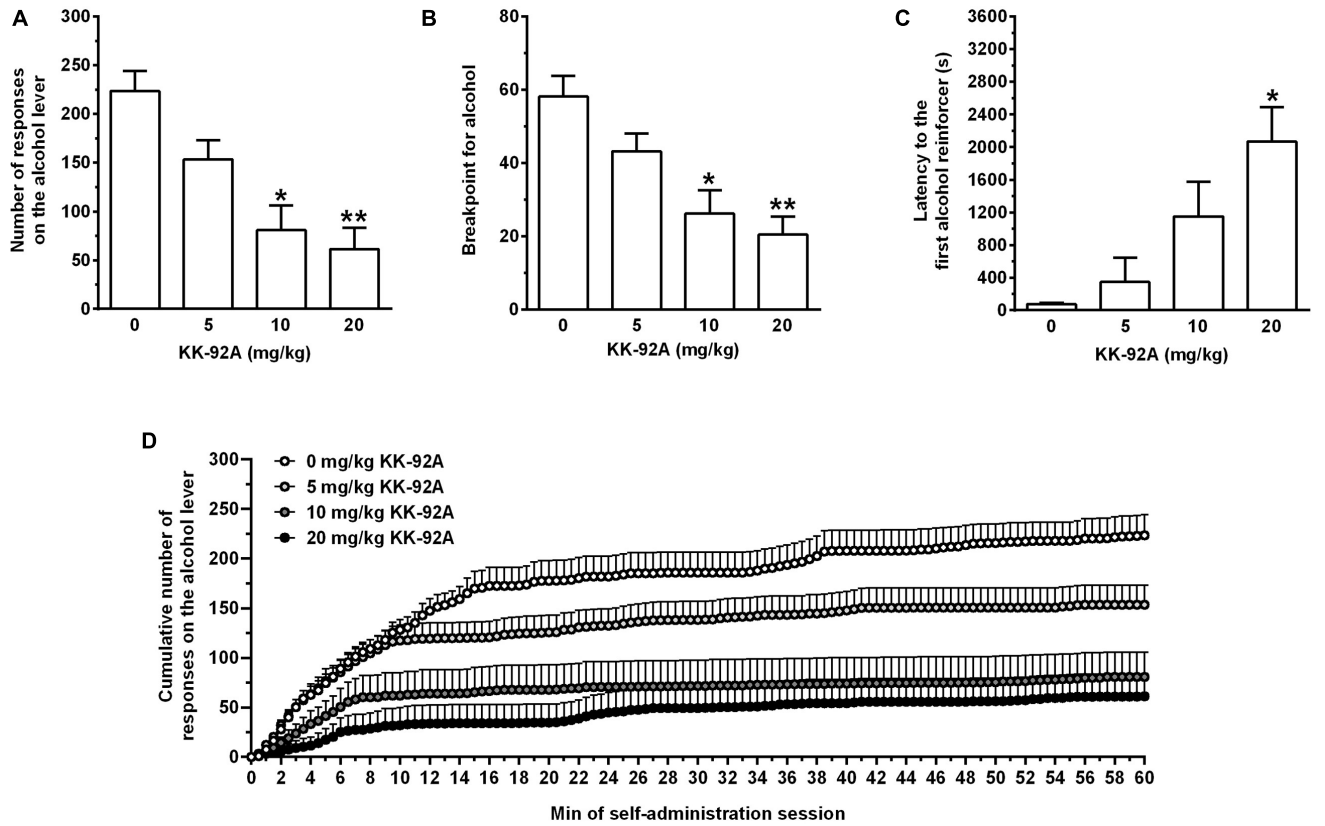

FIGURE 4 | Effect of acute treatment with the positive allosteric modulator of the $GABA_B$ receptor, KK-92A, on number of lever-responses for alcohol **(A)**, breakpoint for alcohol **(B)**, latency to the first response on the alcohol lever **(C)**, and cumulative response patterns of alcohol self-administration **(D)** in female Sardinian alcohol-preferring rats. Rats were initially trained to lever-respond for oral alcohol (15% v/v, in water) [Fixed Ratio (FR) 5 (FR5)] and water (FR1) in daily 30-min self-administration sessions. Once lever-responding had stabilized, rats were tested with KK-92A under a progressive ratio schedule of reinforcement, in which the response requirement (RR) was increased progressively over a 60-min session. Breakpoint was defined as the lowest RR not achieved by the rat. KK-92A was administered intraperitoneally 30 min before the start of the self-administration session. In panel **(D)**, the self-administration session was divided into 60 intervals of 1 min each. Each bar or point is the mean ± SEM of $n = 12$ rats. $^*P < 0.001$ and $^{**}P < 0.0001$ in comparison to the rat group treated with 0 mg/kg KK-92A (Tukey's test).

with 20 mg/kg KK-92A, latency to the first alcohol reinforcer was increased by approximately 28 times.

Responding on the inactive lever was modest (averaging < 11 per session in all rat groups) and not altered by treatment with KK-92A (data not shown).

Experiment 3: Testing KK-92A on Cue-Induced Reinstatement of Alcohol Seeking

Regarding the extinction-responding phase, Log-rank (Mantel-Cox) test indicated that the profile of lever-responding did not differ among the four groups of female sP rats subsequently treated with 0, 5, 10, and 20 mg/kg KK-92A and then exposed to the reinstatement session ($\chi^2 = 1.197$, $P > 0.05$) (**Figure 5A**). Additionally, the four rat groups did not differ in number of extinction-responding sessions needed to achieve the extinction criterion [10.6 ± 1.3, 9.7 ± 0.7, 8.9 ± 0.5, and 9.3 ± 2.1 (mean ± SEM) in rats subsequently treated with 0, 5, 10, and 20 mg/kg KK-92A, respectively; $F(3, 26) = 0.78$, $P > 0.05$].

Regarding the reinstatement session, ANOVA indicated significant effects of presentation of the alcohol-associated stimulus complex [$F(1, 26) = 8.33$, $P < 0.01$] and treatment with KK-92A [$F(3, 26) = 11.14$, $P < 0.0001$], and a significant interaction [$F(3, 26) = 9.32$, $P < 0.0005$], on number of responses on the alcohol lever. Number of lever-responses during the last session of the extinction-responding phase was virtually identical in the four rat groups subsequently treated with 0, 5, 10, and 20 mg/kg KK-92A (**Figure 5B**). In the reinstatement session, presentation of the alcohol-associated stimulus complex reinstated lever-responding in the vehicle-treated rat group: the number of lever-responses averaged indeed 26.9 ± 4.2 and was approximately four times higher than that recorded in the same rat group during the last session of the extinction-responding phase ($P < 0.0001$) (**Figure 5B**). Acute treatment with KK-92A suppressed, in a dose-related manner, lever-responding in the reinstatement session; *post hoc* test indicated that statistical

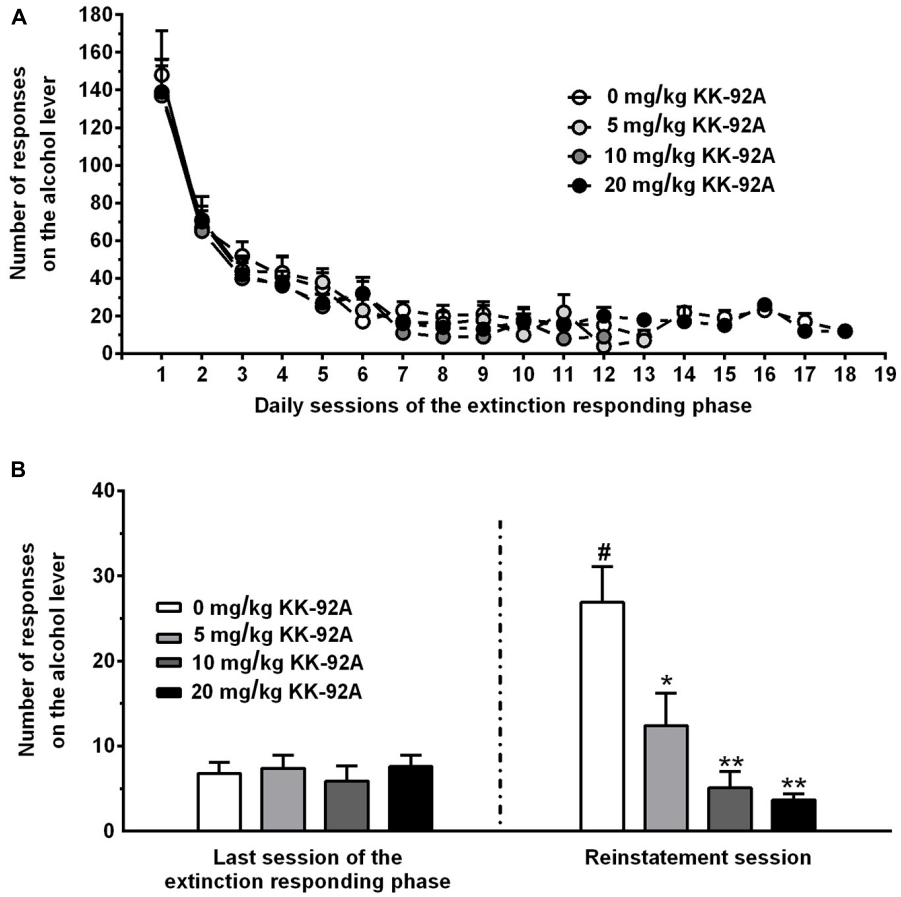

FIGURE 5 | Effect of acute treatment with the positive allosteric modulator of the $GABA_B$ receptor, KK-92A, on cue-induced reinstatement of alcohol-seeking behavior in female Sardinian alcohol-preferring rats. Rats were initially trained to lever-respond for oral alcohol (15% v/v, in water) [Fixed Ratio (FR) 5 (FR5)] and water (FR1) in daily 30-min self-administration sessions. Once lever-responding had stabilized, rats were exposed to an extinction responding phase **(A)** during which lever-responding was unreinforced. The reinstatement session occurred once each single rat had achieved the extinction criterion (≤12 responses on the alcohol lever per session for 2 consecutive sessions). In the reinstatement session **(B)**, unreinforced lever-responding was resumed by the repeated presentation of a complex of visual, auditory, gustatory, and olfactory stimuli previously associated with alcohol availability. The reinstatement session lasted 60 min. KK-92A was administered intraperitoneally 30 min before the start of the reinstatement session. In panel **(A)**, each point is the mean ± SEM of an *n* value varying from 7 to 8 in the first extinction-responding sessions to 2 in some of the last extinction-responding sessions (note that in some of these last sessions the sample size of the 20 mg/kg KK-92A-treated rat group was limited to $n = 1$). In panel **(B)**, each bar is the mean ± SEM of $n = 7$–8 rats. $^{\#}P < 0.0001$ in comparison to the same rat group in the last session of the extinction-responding phase (Bonferroni's test); $^{*}P < 0.0005$ and $^{**}P < 0.0001$ in comparison to the rat group treated with 0 mg/kg KK-92A in the reinstatement session (Tukey's test).

significance was reached by treatment with all three doses [5 ($P < 0.0005$), 10 ($P < 0.0001$), and 20 ($P < 0.0001$) mg/kg KK-92A]. The magnitude of the suppressing effect of 5, 10, and 20 mg/kg KK-92A on lever-responding averaged approximately 55, 80, and 85%, respectively (**Figure 5B**).

Experiment 4: Testing KK-92A on Spontaneous Locomotor Activity

Time-Course Data

Acute treatment with KK-92A reduced the number of motility counts in female sP rats [$F_{dose}(3, 35) = 5.81$, $P < 0.005$; $F_{time}(5, 175) = 35.39$, $P < 0.0001$; $F_{interaction}(15, 175) = 2.91$, $P < 0.0005$] (**Figure 6A**). *Post hoc* test indicated that the reducing effect of KK-92A was limited to (i) the two highest doses tested (40 and 80 mg/kg) at the first time interval (0–5 min) and (ii) the dose of 80 mg/kg at the second time interval (6–10 min). Conversely, the number of motility counts was never affected by treatment with 20 mg/kg KK-92A (i.e., the highest dose tested in Experiments 1–3).

Cumulated Data and Calculation of the Therapeutic Index

Acute treatment with KK-92A reduced, in a dose-related manner, the total number of motility counts recorded over the 30-min session in female sP rats [$F(3, 35) = 5.85$, $P < 0.005$] (**Figure 6B**). *Post hoc* test indicated that statistical significance was reached only by treatment with 80 mg/kg KK-92A ($P < 0.05$), with a tendency toward a reduction after treatment with 40 mg/kg KK-92A. Conversely, the total number of motility

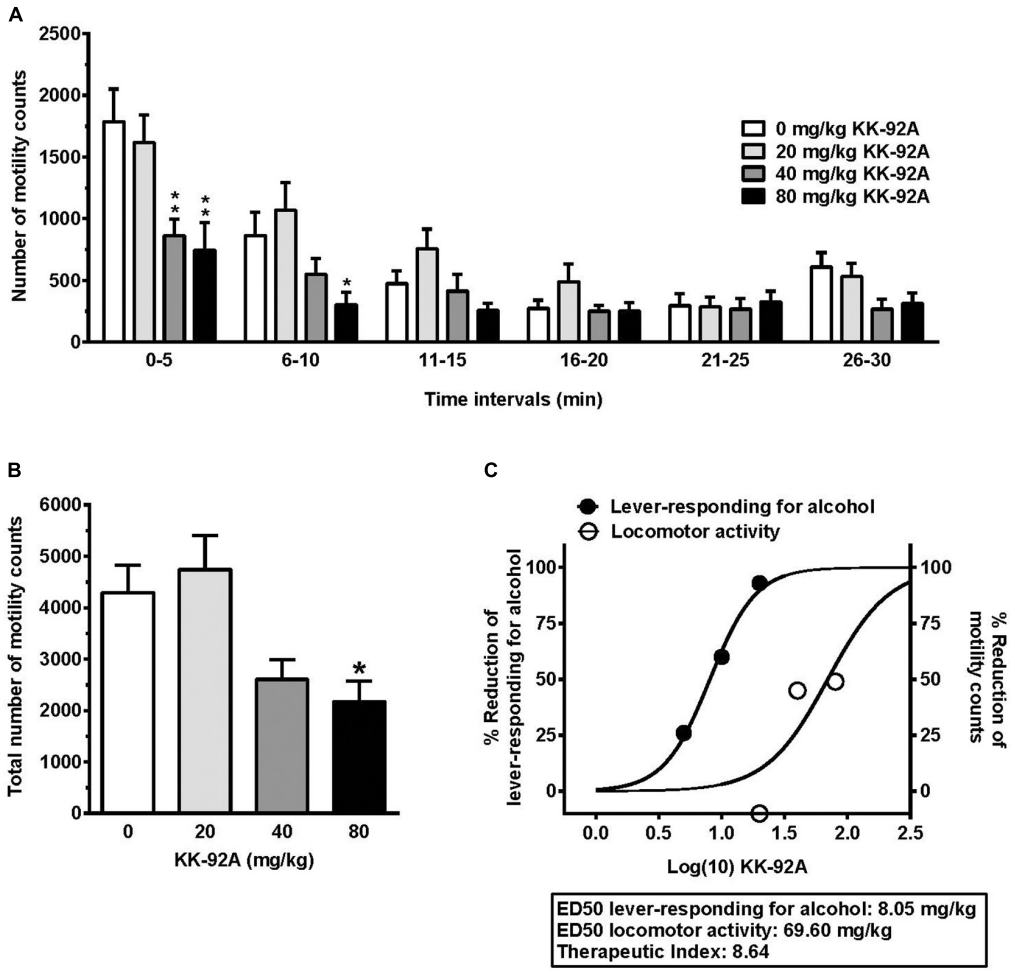

FIGURE 6 | Effect of acute treatment with the positive allosteric modulator of the $GABA_B$ receptor, KK-92A, on spontaneous locomotor activity in female Sardinian alcohol-preferring rats **(A,B)** and dose-response curves and calculated ED_{50}s for KK-92A-induced hypomotility and reducing effect on alcohol self-administration **(C)**. Rats were initially trained to lever-respond for oral alcohol (15% v/v, in water) [Fixed Ratio (FR) 5 (FR5)] and water (FR1) in daily 30-min self-administration sessions. Once lever-responding had stabilized, rats were exposed to the locomotor-activity session. Specifically, rats were exposed to a computer-operated, photocell-equipped cage, to which they were unfamiliar. KK-92A was administered intraperitoneally 30 min before the start of the locomotor-activity session. The locomotor-activity session lasted 30 min. The measured variable was the total number of counts (photocell breaks) recorded automatically by the apparatus. In panel **(A)**, data are expressed as mean ± SEM of number of motility counts in six 5-min time intervals in $n = 9$–10 rats; $^*P < 0.05$ and $^{**}P < 0.0001$ in comparison to the rat group treated with 0 mg/kg KK-92A (Tukey's test). In panel **(B)**, data are expressed as mean ± SEM of total number of motility counts over the entire locomotor-activity session in $n = 9$–10 rats; $^*P < 0.05$ in comparison to the rat group treated with 0 mg/kg KK-92A (Tukey's test). Data depicted in panel **(C)** are plotted as (i)% reduction in spontaneous locomotor activity [data from panel **(B)**] and (ii)% reduction in lever-responding for alcohol under the FR5 schedule of reinforcement (data from **Figure 1A**). EC_{50}s were calculated by 4-parameter (top *plateau*, bottom *plateau*, middle or $logEC_{50}$, and slope) logistic non-linear regression from sigmoidal dose-response curves using GraphPad 6 (GraphPad Software; La Jolla, CA, United States); bottom and top constraint equal to 0 and 100%, respectively, was used for curve fitting. Therapeutic index (TI) was calculated according to the following formula: "Hypomotility" ED_{50}/"Reduction of lever-responding for alcohol" ED_{50}.

counts recorded in the rat group treated with 20 mg/kg KK-92A was virtually identical to that recorded in vehicle-treated rats.

Data on KK-92A-induced hypomotility, together with those on KK-92A-induced suppression of alcohol self-administration under the FR5 schedule of reinforcement (Experiment 1A; **Figure 1A**), were used to establish a therapeutic index (TI) for KK-92A (**Figure 6C**). TI was calculated according to the following formula: "Hypomotility" ED_{50}/"Reduction of lever-responding for alcohol" ED_{50} (for details on ED_{50} calculation, see the legend of **Figure 6**); accordingly, TI for KK-92A resulted to be equal to 8.64.

Experiment 5: Testing KK-92A on Blood Alcohol Levels

Acute pretreatment with KK-92A reduced, in a dose-related manner, BALs produced in female sP rats by acute, intragastric administration of 1 g/kg alcohol [$F_{dose}(3, 36) = 9.93$, $P < 0.0001$; $F_{time}(2.20, 79, 93) = 45.34$, $P < 0.0001$; $F_{interaction}(9, 108) = 7.48$,

$P < 0.0001$] (**Figure 7A**). *Post hoc* test indicated that the reducing effect of KK-92A on BALs was (i) limited to the first two recording times (30- and 60-min) and (ii) of larger magnitude (˜70%) in the rat group treated with 20 mg/kg KK-92A at the 30-min recording time.

In close agreement with the above results, acute pretreatment with KK-92A also reduced the area under the curve of BAL time-course [$F(3, 36) = 5.22$, $P < 0.005$] (**Figure 7B**). *Post hoc* test indicated that statistical significance was reached by treatment with 10 ($P < 0.05$) and 20 ($P < 0.005$) mg/kg KK-92A. The magnitude of the reducing effect of 10 and 20 mg/kg KK-92A on the area under the curve of BAL time-course averaged approximately 30 and 40%, respectively.

DISCUSSION

In agreement with the working hypothesis of this study, data from Experiments 1A, 2, and 3 indicate that acute treatment with the $GABA_B$ PAM, KK-92A, effectively reduced operant oral alcohol self-administration and cue-induced reinstatement of alcohol-seeking behavior in selectively bred alcohol-preferring sP rats. At the two highest doses (10 and 20 mg/kg) the reducing effect of KK-92A emerged as a virtually complete suppression of lever-responding for alcohol, amount of self-administered alcohol, breakpoint for alcohol, and reinstatement of alcohol seeking. In Experiments 1A and 2, latency to achieving the first alcohol reinforcer was considerably prolonged by treatment with 20 mg/kg KK-92A, suggesting that this dose of KK-92A suppressed the urge to seek for and consume alcohol. Analysis of cumulative response patterns from Experiments 1A (**Figure 1D**) and 2 (**Figure 4D**) provides additional insights on KK-92A action: in comparison to vehicle treatment, administration of all three doses of KK-92A resulted in (i) less steep curves (suggestive of a reduced frequency in lever-responding for alcohol), and (ii) lower *plateau* values (suggesting that fewer ratios were completed before lever-responding for alcohol ended). In Experiment 1A, the complete flatness of cumulative response pattern over the first 10 min of the session, observed after treatment with 20 mg/kg KK-92A, suggests that this dose of KK-92A abolished the typical "front-loading" of alcohol-drinking pattern of sP rats exposed to alcohol self-administration sessions under the FR schedule of reinforcement.

Acute treatment with KK-92A also decreased operant self-administration of a sucrose solution, the reinforcing properties of which were comparable to those of alcohol (number of lever-responses for alcohol and sucrose solution were indeed highly similar in vehicle-treated rats of Experiments 1A and 1B). KK-92A was however less potent and effective in reducing sucrose than alcohol self-administration: in the "sucrose" experiment, (i) reduction in lever-responding for sucrose solution was induced only by treatment with 20 mg/kg KK-92A and (ii) magnitude of the reducing effect of 20 mg/kg KK-92A on lever-responding for sucrose solution was limited to approximately 60% (compared to the approximately 95% suppression recorded in the "alcohol" experiment).

The limited selectivity of KK-92A effect on alcohol self-administration was somewhat unexpected for the following two main reasons. First, most of the $GABA_B$ PAMs tested to date have been reported to reduce alcohol self-administration with no effect on self-administration of highly palatable sucrose, saccharin, sweetened-milk, or chocolate solutions (e.g., Filip et al., 2007; Maccioni et al. 2007, 2008b, 2009, 2010, 2012, 2015, 2019b; Leite-Morris, 2013; see however Augier et al., 2017; Maccioni et al., 2017, 2019a). Second, treatment with the same doses of KK-92A tested in the present study resulted to be totally ineffective on operant self-administration of regular food pellets in rats (Li et al., 2017). Together, these data are suggestive of a peculiar ability of KK-92A to affect the reinforcing properties of highly palatable foods; this hypothesis is currently under experimental

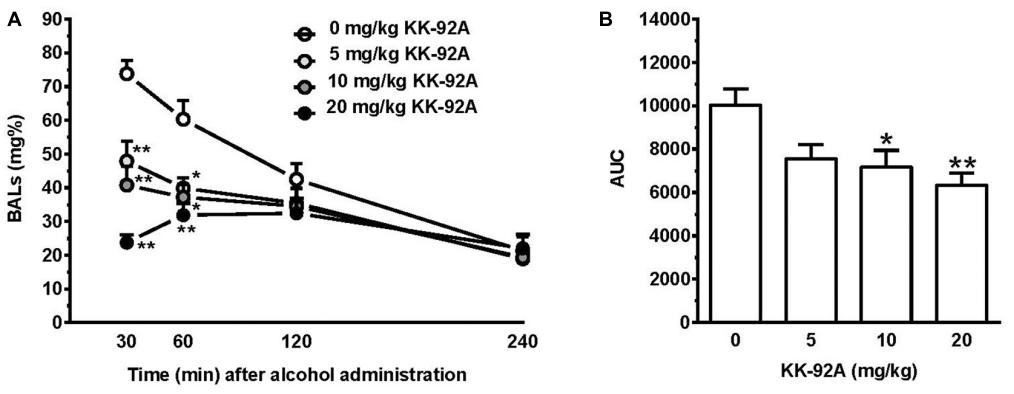

FIGURE 7 | Effect of acute pretreatment with the positive allosteric modulator of the $GABA_B$ receptor, KK-92A, on blood alcohol levels (BALs) in female Sardinian alcohol-preferring rats. Rats were initially trained to lever-respond for oral alcohol (15% v/v, in water) [Fixed Ratio (FR) 5 (FR5)] and water (FR1) in daily 30-min self-administration sessions. Once lever-responding had stabilized, KK-92A was administered intraperitoneally 30 min before the intragastric administration of 1 g/kg alcohol (15%, v/v). Blood samples were collected from the tip of the rat tail at 30, 60, 120, and 240 min after alcohol administration and analyzed by means of an enzymatic system. In panel **(A)**, BALs were expressed in mg%. Each point is the mean ± SEM of $n = 10$ rats. $^*P < 0.05$ and $^{**}P < 0.01$ in comparison to the rat group treated with 0 mg/kg KK-92A at the corresponding time (Tukey's test). In panel **(B)**, data on the area under the curve of BAL time-course are expressed as (h*μg/ml). Each bar is the mean ± SEM of $n = 10$ rats. $^*P < 0.05$ and $^{**}P < 0.005$ in comparison to the rat group treated with 0 mg/kg KK-92A (Tukey's test).

evaluation in our laboratories. These further analyses will also include investigation on whether treatment with KK-92A may alter palatability of sweet foods.

The suppressing effect of KK-92A on these alcohol- and sucrose-related behaviors was likely not influenced by any concurrent sedative or motor-incoordinating effect, which might have disrupted the regular rate of lever-responding. Data from Experiment 4 indicate indeed that hypolocomotion occurred at doses of KK-92A higher than those found to suppress alcohol and sucrose self-administration and reinstatement of alcohol seeking. More specifically, comparison of data from Experiments 1A and 4 resulted in a TI higher than 8, suggestive of a relatively large separation between the doses of KK-92A inducing the "desired" pharmacological effects (i.e., reduction of lever-responding for alcohol) and those inducing the "unwanted" adverse effects (i.e., sedation and reduced spontaneous locomotion).

Results of Experiments 1A, 2, and 3 extend to KK-92A a series of previous experimental data on the ability of the $GABA_B$ PAMs, CGP7930, GS39783, BHF177, *rac*-BHFF, ADX71441, COR659, CMPPE, ORM-27669, and ASP8062, to decrease the reinforcing and motivational properties of alcohol and abolish cue-induced reinstatement of alcohol seeking in rats and mice (for references, see section "Introduction"). To our understanding, this extension should not be intended as just the mere generalization of previous data to a further $GABA_B$ PAM; it is rather the demonstration that *all* $GABA_B$ PAMs, most chemically unrelated to each other (see Mugnaini and Corelli, 2016; Nieto et al., 2021), produce highly similar effects on different alcohol-motivated behaviors in rodents, suggesting that reduction of alcohol seeking and drinking is a major feature of the pharmacological profile of the entire class of $GABA_B$ PAMs. This conclusion, together with the notion that all these experimental data were collected using animal models with demonstrated predictive validity for specific aspects of human AUD, confer to $GABA_B$ PAMs a promising therapeutic potential for AUD. Notably, ASP8062 has already been tested in two different Phase 1 clinical trials, proving to be safe, well-tolerated, and with good CNS penetration in healthy subjects (Walzer et al., 2020, 2021). ASP8062 is currently under investigation in a Phase 1 clinical trial to assess its potential interaction with alcohol in healthy subjects (ClinicalTrials.gov, 2019). ASP8062 might therefore be the first $GABA_B$ PAM available to test whether the large and consistent body of preclinical evidence on the *anti*-alcohol effects of $GABA_B$ PAMs translates to AUD patients.

The results of Experiment 1C indicate that treatment with a *per se* ineffective dose of KK-92A (2.5 mg/kg) potentiated the effect of baclofen (also given at a *per se* ineffective dose: 1 g/kg) on alcohol self-administration. Combination of KK-92A and baclofen produced indeed a 25–30% reduction, in comparison to all other treatment combinations, in number of responses on the alcohol lever and amount of self-administered alcohol. These results provide further confirmation that $GABA_B$ PAMs augment *in vivo* the pharmacological activation of $GABA_B$ binding site (see Urwyler, 2016; Nieto et al., 2021). They are also in agreement with two previous sets of data on the ability of the combination of (i) sub-threshold doses of CGP7930 (10 mg/kg, i.p.) and baclofen (2 mg/kg, i.p.) to reduce alcohol self-administration in selectively bred alcohol-preferring Indiana P rats (Liang et al., 2006), and (ii) *per se* ineffective doses of GS39783 (5 mg/kg, i.p.) or *rac*-BHFF (5 mg/kg, i.p.) and baclofen (1 mg/kg, i.p.) to reduce alcohol self-administration in sP rats (Maccioni et al., 2015). The results of these "combination" experiments (Liang et al., 2006; Maccioni et al., 2015; present study) apparently possess translational interest, as they suggest that treatment with low doses of a $GABA_B$ PAM would potentiate the suppressing effect of baclofen on alcohol craving and consumption; this would permit to lower baclofen dose, maintaining its therapeutic effects unaltered while likely limiting its side-effects.

The results of the present study extend to alcohol previous data on the ability of KK-92A to ameliorate different nicotine-motivated behaviors in rats. More specifically, our US laboratory recently demonstrated that acute treatment with KK-92A (0, 5, 10, and 20 mg/kg; i.p.) decreased the number of nicotine infusions and breakpoint for nicotine in rats trained to self-administer nicotine intravenously under both FR and PR schedules of reinforcement (Li et al., 2017); acute treatment with KK-92A (0, 10, and 20 mg/kg; i.p.) also inhibited cue-induced reinstatement of nicotine seeking (Li et al., 2017). Notably, KK-92A effects were selective for nicotine, as no dose of KK-92A altered—even minimally—self-administration of and reinstatement of seeking behavior for regular food pellets (Li et al., 2017).

Inhibition of behaviors sustained by different drugs of abuse appears to be another remarkable, shared feature of the entire $GABA_B$-PAM class. Indeed, and in addition to the above "nicotine" data on KK-92A (Li et al., 2017), it has been reported that treatment with CGP7930, GS39783, BHF177, *rac*-BHFF, CMPPE, and COR659 attenuated (i) operant intravenous self-administration of cocaine (Smith et al., 2004; Filip et al., 2007) and nicotine (Paterson et al., 2008; Vlachou et al., 2011), (ii) cocaine-primed and cue-induced reinstatement of cocaine seeking (Filip and Frankowska, 2007; Vengeliene et al., 2018), (iii) cue-induced reinstatement of nicotine seeking (Vlachou et al., 2011), (iv) context-driven seeking for cocaine (Halbout et al., 2011), (v) the lowering effect of cocaine (Slattery et al., 2005) and nicotine (Paterson et al., 2008) on threshold for intracranial self-stimulation, (vi) conditioned place preference induced by cocaine (de Miguel et al., 2019), amphetamine (Halbout et al., 2011), methamphetamine (Voigt et al., 2011), and nicotine (Mombereau et al., 2007), and (vii) locomotor activity stimulated by cocaine (Lhuillier et al., 2007; de Miguel et al., 2019; Lobina et al., 2021), amphetamine (Wierońska et al., 2011; Lobina et al., 2021), nicotine (Lobina et al., 2011, 2021), and morphine (Lobina et al., 2021) in rats and mice (for review, see Frankowska et al., 2016; Li and Slesinger, 2021).

In the majority of studies testing $GABA_B$ PAMs on alcohol self-administration in rats and mice, and undeniably in all studies conducted in our Italian laboratory with sP rats, the magnitude of the decreasing effect of $GABA_B$ PAMs on lever-responding for alcohol never exceeded 40–50%, featuring a reduction—rather than a suppression—of the reinforcing and motivational properties of alcohol (e.g., Maccioni et al., 2007, 2008b, 2009, 2019b). This relatively limited efficacy has been explained by the use-dependent mechanism of

action of $GABA_B$ PAMs: $GABA_B$ PAMs potentiate endogenously released GABA, being ineffective in activating $GABA_B$ receptors *per se* (see Urwyler, 2011, 2016). Therefore, their action depends on GABA concentration in the synaptic cleft, and the halving of a given *in vivo* effect, rather than its suppression, is likely the maximal behavioral consequence of $GABA_B$ PAM-induced potentiation of extracellular GABA. Conversely, the effect of KK-92A on alcohol self-administration emerged as a marked suppression, as clearly depicted by the approximately 95% reduction in lever-responding for alcohol induced by treatment with 20 mg/kg KK-92A in Experiment 1A (**Figure 1A**). A possible explanation for this high efficacy may reside in the peculiar ago-allosteric profile of KK-92A. Recent *in vitro* assays demonstrated indeed that, beside potentiating GABA-induced cellular responses ($GABA_B$-PAM activity), KK-92A also displayed distinct, intrinsic agonistic activity, activating the $GABA_B$ receptor in the absence of GABA (Li et al., 2017). The suppressing effect of KK-92A on alcohol self-administration may therefore be the sum of two converging actions at the $GABA_B$ receptor: (i) agonistic activity, resembling the suppressing effect of the prototypic $GABA_B$ receptor agonist, baclofen, on alcohol-related behaviors (see Colombo and Gessa, 2018); (ii) positive allosteric modulation. The agonistic component of KK-92A might also be responsible for the reducing effect of KK-92A on sucrose self-administration, replicating the ability of baclofen to affect sucrose self-administration in rats at the same doses that reduced alcohol self-administration (e.g., Anstrom et al., 2003; Janak and Gill, 2003; Maccioni et al., 2005, 2008b; Echeverry-Alzate et al., 2021).

Reinstatement of alcohol seeking apparently deserves a separate mention. Indeed, the few studies conducted to date to test the effects of $GABA_B$ PAMs on cue- and stress-induced reinstatement of alcohol seeking have reported that treatment with ADX71441 (Augier et al., 2017), CMPPE (Vengeliene et al., 2018; Maccioni et al., 2019b), and COR659 (Maccioni et al., 2019a) completely suppressed, rather than merely reducing, lever-responding in the reinstatement session. The suppressing effect of KK-92A on cue-induced reinstatement of alcohol seeking, observed in Experiment 3, is entirely consistent with these literature data. Together, these results may be interpreted to suggest that reinstatement of alcohol seeking is highly sensitive to positive allosteric modulation of the $GABA_B$ receptor, theoretically highlighting $GABA_B$ PAMs as a drug of choice for treating craving for alcohol, loss of control over alcohol, and relapse episodes into heavy drinking. These data also suggest the relevant role of $GABA_B$ receptor in the neural substrate mediating the reinstatement of alcohol seeking behavior, as previously suggested by the suppressing effect of baclofen on cue-induced reinstatement of alcohol seeking in rats (Maccioni et al., 2008a; Vengeliene et al., 2018).

Data from Experiment 5 indicate that pretreatment with all three doses of KK-92A reduced BALs generated by the acute intragastric administration of 1 g/kg alcohol. This effect was evident over the first hour after alcohol administration (corresponding to 90 min after KK-92A injection), while it vanished at the subsequent recording times, likely paralleling the progressive reduction of KK-92A plasma levels and efficacy. To our knowledge, only two previous studies investigated the effect of $GABA_B$ PAMs on alcohol metabolism: (i) acute, intragastric administration of *rac*-BHFF suppressed BALs produced in sP rats by the acute intragastric administration of 1 g/kg alcohol (Maccioni et al., 2010); (ii) neither acute nor repeated intraperitoneal injection of GS39783 altered BALs produced in DBA/2J mice by acute or repeated administration of 2 g/kg alcohol (Kruse et al., 2012). Among the several methodological differences of these three studies (Maccioni et al., 2010; Kruse et al., 2012; present study), the route of alcohol administration might offer a key to explain the observed discrepancies. Since the two studies reporting a reduction in BALs used the intragastric route of alcohol administration, it is reasonable to hypothesize that positive allosteric modulation of $GABA_B$ receptors located in the gastrointestinal tract (Nakajima et al., 1996; Castelli et al., 1999) interfered with gastric emptying and/or intestinal motility, possibly altering alcohol absorption and metabolism.

The suppressing effect of KK-92A on alcohol self-administration (Experiment 1A) is somewhat difficult to reconcile with its effect on BALs (Experiment 5). Treatment with a drug reducing BALs is indeed expected to result in an increase, rather than a decrease, in alcohol seeking and drinking, as rats should increase their lever-responding for alcohol and amount of self-administered alcohol to possibly achieve the usual brain concentrations of alcohol and perceive the subsequent psychopharmacological effects. KK-92A-induced suppression of alcohol self-administration under the FR schedule of reinforcement and reduction of BALs appear to be opposite effects, with the former overtaking the latter: the central effects of KK-92A on the reinforcing and motivational properties of alcohol impacted the rat behavior to a greater extent than its peripheral effects on alcohol absorption and metabolism. Conversely, there was no apparent relationship between the central and peripheral effects of KK-92A in the results of Experiments 2 and 3, in which lever-responding resulted in modest and pharmacologically irrelevant intake (PR schedule of reinforcement) or even absence (reinstatement of alcohol seeking) of self-administered alcohol, ruling out that KK-92A action on alcohol absorption and metabolism could have influenced the rat behavior.

The experiments conducted in the present study used ovariectomized female sP rats. The choice of (small) female, instead of (heavy) male, rats was dictated by several practical advantages, described in detail elsewhere (Lorrai et al., 2019); here we mention solely the aptness of commercially available operant chambers, usually too narrow to accommodate animals as large as adult male sP rats. Ovariectomy was performed to avoid any possible influence of ovarian hormones on the several alcohol- and sucrose-related behaviors investigated in this study as well as on alcohol metabolism. While this has surely been an advantageous simplification of the experimental design of this first investigation, additional studies are now needed to assess and compare KK-92A effects in male and intact (non-ovariectomized) female sP rats. The results of these studies will be of relevance also in terms of the possible translatability of these findings to AUD patients.

The few studies to date that have investigated the neural substrates mediating the suppressing effects of $GABA_B$ PAMs on alcohol-related behaviors suggested a role for the mesolimbic dopamine "reward" system. More specifically, it has been proposed that activation of $GABA_B$ receptors located in the ventral tegmental area (VTA) likely hyperpolarizes the mesolimbic dopamine neurons, thus preventing their alcohol-induced stimulation and dopamine release in the nucleus accumbens, and decreasing the rewarding and reinforcing properties of alcohol (see Phillips and Reed, 2014; Colombo and Gessa, 2018; Maccioni and Colombo, 2019). This conclusion is supported by data demonstrating that intra-VTA microinjection of CGP7930, GS39783, and BHF177 effectively decreased alcohol self-administration (Maccioni et al., 2018), alcohol seeking (Leite-Morris et al., 2009; Leite-Morris, 2013), and accumbal dopamine release stimulated by cues predictive of alcohol availability (Leite-Morris, 2013) in rats. It is reasonable to hypothesize that this mechanism also applies to the suppressing effects of KK-92A on alcohol-motivated behaviors observed in the present study. An additional, possible mechanism of action is based on the recent observation that alcohol-dependent rats had reduced amygdalar levels of the GABA transporter GAT3 and, subsequently, high concentrations of extracellular GABA (Augier et al., 2018). It has been proposed that activation of amygdalar presynaptic $GABA_B$ receptors by baclofen—and $GABA_B$ PAMs, we add—would inhibit GABA release, reducing extracellular GABA levels, restoring the enhanced tonic inhibition of amygdala and, in the end, decreasing alcohol drinking (Spanagel, 2018; Marti-Prats et al., 2021).

In conclusion, the results of the present study demonstrate that treatment with non-sedative doses of the novel, selective $GABA_B$ PAM, KK-92A, potently and effectively suppressed operant oral alcohol self-administration and cue-induced reinstatement of alcohol seeking in alcohol-preferring sP rats. Treatment with KK-92A also potentiated the reducing effect of baclofen on alcohol self-administration. These data extend to KK-92A a large and entirely consistent body of experimental evidence on the ability of $GABA_B$ PAMs to decrease several alcohol-motivated behaviors in rodents, strengthening the notion that amelioration of alcohol-motivated behaviors is a major feature of the entire class of $GABA_B$ PAMs. Additionally, these data extend to alcohol previous experimental data on the ability of KK-92A to decrease nicotine self-administration and cue-induced reinstatement of nicotine seeking in rats (Li et al., 2017), widening the *anti*-addictive profile of KK-92A.

DATA AVAILABILITY STATEMENT

All raw data of this article will be made available on request by the corresponding authors, without undue reservation.

ETHICS STATEMENT

The experimental procedures employed in the present study fully complied with European Directive No. 2010/63/EU and subsequent Italian Legislative Decree No. 26, March 4, 2014, on the "Protection of animals used for scientific purposes."

AUTHOR CONTRIBUTIONS

GC, PMa, and PMc conceived the study. GC and PMa designed the experimental approach. KK, HL, and SY synthesized and performed the compound analysis of KK-92A. PMa and JB performed the *in vivo* experiments. PMa analyzed the *in vivo* data. GC, GG, and PMc wrote the manuscript. All authors contributed to the article and approved the submitted version.

FUNDING

We thank the National Cancer Institute grant P30-CA076292 for Moffitt Cancer Center (in part funding the Chemical Biology Core). HL acknowledges support by the National Cancer Institute grant R50CA211447.

ACKNOWLEDGMENTS

We are grateful to Carla Acciaro for animal breeding and care.

SUPPLEMENTARY MATERIAL

The Supplementary Material for this article can be found online at: https://www.frontiersin.org/articles/10.3389/fcell.2021.727576/full#supplementary-material

Supplementary Figure 1 | Structure and compound analysis of KK-92A. KK-92A was synthesized in gram-scale with >99% purity (as determined by HPLC) according to the procedure described in detail by Li et al. (2017). The chemical analysis (^1H and ^{13}C NMR, HPLC-MS) of in-house synthesized KK-92A matched the reported data.

REFERENCES

Anstrom, K. K., Cromwell, H. C., Markowski, T., and Woodward, D. J. (2003). Effect of baclofen on alcohol and sucrose self-administration in rats. *Alcohol. Clin. Exp. Res.* 27, 900–990. doi: 10.1097/01.ALC.0000071744.78580.78

Augier, E., Barbier, E., Dulman, R. S., Licheri, V., Augier, G., Domi, E., et al. (2018). A molecular mechanism for choosing alcohol over an alternative reward. *Science* 360, 1321–1326. doi: 10.1126/science.aao1157

Augier, E., Dulman, R. S., Damadzic, R., Pilling, A., Hamilton, J. P., and Heilig, M. (2017). The $GABA_B$ positive allosteric modulator ADX71441 attenuates alcohol self-administration and relapse to alcohol seeking in rats. *Neuropsychopharmacology* 42, 1789–1799. doi: 10.1038/npp.2017.53

Bell, R. L., Sable, H. J. K., Colombo, G., Hyytiä, P., Rodd, Z. A., and Lumeng, L. (2012). Animal models for medications development targeting alcohol abuse using selectively bred rat lines: neurobiological and pharmacological validity. *Pharmacol. Biochem. Behav.* 103, 119–155. doi: 10.1016/j.pbb.2012.07.007

Castelli, M. P., Inganni, A., Stefanini, E., and Gessa, G. L. (1999). Distribution of $GABA_B$ receptor mRNAs in the rat brain and peripheral organs. *Life Sci.* 64, 1321–1328. doi: 10.1016/s0024-3205(99)00067-3

ClinicalTrials.gov (2019). *A study to assess potential interaction between ASP8062 and alcohol in healthy adult subjects, NCT04003402*. Deerfield: Astellas Pharma Global Development, Inc.

Colombo, G., and Gessa, G. L. (2018). Suppressing effect of baclofen on multiple alcohol-related behaviors in laboratory animals. *Front. Psychiatry* 9:475. doi: 10.3389/fpsyt.2018.00475

Colombo, G., Lobina, C., Carai, M. A. M., and Gessa, G. L. (2006). Phenotypic characterization of genetically selected Sardinian alcohol-preferring (sP) and -non preferring (sNP) rats. *Addict. Biol.* 11, 324–338. doi: 10.1111/j.1369-1600.2006.00031.x

Colombo, G., Lobina, C., Maccioni, P., Carai, M. A. M., Lorrai, I., Zaru, A., et al. (2015). Anxiety-like behaviors at the end of the nocturnal period in sP rats with a "history" of unpredictable, limited access to alcohol. *Alcohol* 49, 707–712. doi: 10.1016/j.alcohol.2015.04.010

de Miguel, E., Vekovischeva, O., Kuokkanen, K., Vesajoki, M., Paasikoski, N., Kaskinoro, J., et al. (2019). $GABA_B$ receptor positive allosteric modulators with different efficacies affect neuroadaptation to and self-administration of alcohol and cocaine. *Addict. Biol.* 24, 1191–1203. doi: 10.1111/adb.12688

Echeverry-Alzate, V., Jeanblanc, J., Sauton, P., Bloch, V., Labat, L., Soichot, M., et al. (2021). Is R(+)-Baclofen the best option for the future of Baclofen in alcohol dependence pharmacotherapy? Insights from the preclinical side. *Addict. Biol.* 26:e12892. doi: 10.1111/adb.12892

Ferlenghi, F., Maccioni, P., Mugnaini, C., Brizzi, A., Fara, F., Mostallino, R., et al. (2020). The $GABA_B$ receptor positive allosteric modulator COR659: in vitro metabolism, in vivo pharmacokinetics in rats, synthesis and pharmacological characterization of metabolically protected derivatives. *Eur. J. Pharm. Sci.* 155:105544. doi: 10.1016/j.ejps.2020.105544

Filip, M., and Frankowska, M. (2007). Effects of $GABA_B$ receptor agents on cocaine priming, discrete contextual cue and food induced relapses. *Eur. J. Pharmacol.* 571, 166–173. doi: 10.1016/j.ejphar.2007.05.069

Filip, M., Frankowska, M., and Przegaliński, E. (2007). Effects of $GABA_B$ receptor antagonist, agonists and allosteric positive modulator on the cocaine-induced self-administration and drug discrimination. *Eur. J. Pharmacol.* 574, 148–157. doi: 10.1016/j.ejphar.2007.07.048

Frankowska, M., Przegaliński, E., and Filip, M. (2016). ""Targeting the $GABA_B$ receptor for the treatment of substance use disorder"," in *$GABA_B$ Receptor; The Receptors 29*, ed. G. Colombo (Cham: Springer International Publishing), 263–286. doi: 10.1007/978-3-319-46044-4_14

Haile, C. N., Carper, B. A., Nolen, T. L., and Kosten, T. A. (2021). The $GABA_B$ receptor positive allosteric modulator ASP8062 reduces operant alcohol self-administration in male and female Sprague Dawley rats. *Psychopharmacology* 238, 2587–2600. doi: 10.1007/s00213-021-05881-0

Halbout, B., Quarta, D., Valerio, E., Heidbreder, C. A., and Hutcheson, D. M. (2011). The GABA-B positive modulator GS39783 decreases psychostimulant conditioned-reinforcement and conditioned-reward. *Addict. Biol.* 16, 416–427. doi: 10.1111/j.1369-1600.2010.00278.x

Holtyn, A. F., and Weerts, E. M. (2020). $GABA_B$ receptors and alcohol use disorders: Preclinical studies. *Curr. Top. Behav. Neurosci.* 2020:178. doi: 10.1007/7854_2020_178

Hwa, L. S., Kalinichev, M., Haddouk, H., Poli, S., and Miczek, K. A. (2014). Reduction of excessive alcohol drinking by a novel $GABA_B$ receptor positive allosteric modulator ADX71441 in mice. *Psychopharmacology* 231, 333–343. doi: 10.1007/s00213-013-3245-z

Janak, P. H., and Gill, T. M. (2003). Comparison of the effects of allopregnanolone with direct GABAergic agonists on ethanol self-administration with and without concurrently available sucrose. *Alcohol* 30, 1–7. doi: 10.1016/s0741-8329(03)00068-5

Kelley, A. E. (1993). "Locomotor activity and exploration," in *Behavioural Neuroscience: A Practical Approach*, Vol. II, ed. A. Sahgal (Oxford, UK: Oxford University Press), 1–21.

Kruse, L. C., Linsenbardt, D. N., and Boehm, S. L. (2012). Positive allosteric modulation of the $GABA_B$ receptor by GS39783 attenuates the locomotor stimulant actions of ethanol and potentiates the induction of locomotor sensitization. *Alcohol* 46, 455–462. doi: 10.1016/j.alcohol.2012.03.004

Leite-Morris, K. A. (2013). Neurochemistry and neuropharmacology of the GABA-B receptor in a rodent model of alcohol binge drinking. *Alcohol. Clin. Exp. Res.* 37:255.

Leite-Morris, K. A., Kerestes, H. B., and Colombo, G. (2009). Intra-ventral tegmental area injection of the GABA B receptor positive allosteric modulator GS39783 inhibits ethanol seeking behavior in rats. *Alcohol. Clin. Exp. Res.* 33:226.

Lhuillier, L., Mombereau, C., Cryan, J. F., and Kaupmann, K. (2007). $GABA_B$ receptor-positive modulation decreases selective molecular and behavioral effects of cocaine. *Neuropsychopharmacology* 32, 388–398. doi: 10.1038/sj.npp.1301102

Li, X., and Slesinger, P. A. (2021). $GABA_B$ receptors and drug addiction: Psychostimulants and other drugs of abuse. *Curr. Top. Behav. Neurosci.* 2021:187. doi: 10.1007/7854_2020_187

Li, X., Sturchler, E., Kaczanowska, K., Cameron, M., Finn, M. G., Griffin, P., et al. (2017). KK-92A, a novel $GABA_B$ receptor positive allosteric modulator, attenuates nicotine self-administration and cue-induced nicotine seeking in rats. *Psychopharmacology* 234, 1633–1644. doi: 10.1007/s00213-017-4594-9

Liang, J. H., Chen, F., Krstew, E., Cowen, M. S., Carroll, F. Y., Crawford, D., et al. (2006). The $GABA_B$ receptor allosteric modulator CGP7930, like baclofen, reduces operant self-administration of ethanol in alcohol-preferring rats. *Neuropharmacology* 50, 632–639. doi: 10.1016/j.neuropharm.2005.11.011

Linsenbardt, D. N., and Boehm, S. L. (2014). Alterations in the rate of binge ethanol consumption: implications for preclinical studies in mice. *Addict. Biol.* 19, 812–825. doi: 10.1111/adb.12052

Lobina, C., Carai, M. A. M., Froestl, W., Mugnaini, C., Pasquini, S., Corelli, F., et al. (2011). Activation of the $GABA_B$ receptor prevents nicotine-induced locomotor stimulation in mice. *Front. Psychiatry* 2:76. doi: 10.3389/fpsyt.2011.00076

Lobina, C., Maccioni, P., Lorrai, I., Zaru, A., Collu, M., Carai, M. A. M., et al. (2021). Suppressing effect of the novel positive allosteric modulator of the $GABA_B$ receptor, COR659, on locomotor hyperactivity induced by different drugs of abuse. *Behav. Brain Res.* 400:113045. doi: 10.1016/j.bbr.2020.113045

Loi, B., Maccioni, P., Lobina, C., Carai, M. A. M., Gessa, G. L., Thomas, A. W., et al. (2013). Reduction of alcohol intake by the positive allosteric modulator of the $GABA_B$ receptor, *rac*-BHFF, in alcohol-preferring rats. *Alcohol* 47, 69–73. doi: 10.1016/j.alcohol.2012.11.002

Lorrai, I., Contini, A., Gessa, G. L., Mugnaini, C., Corelli, F., Colombo, G., et al. (2019). Operant, oral alcohol self-administration: Sex differences in Sardinian alcohol-preferring rats. *Alcohol* 79, 147–162. doi: 10.1016/j.alcohol.2019.04.003

Maccioni, P., Serra, S., Vacca, G., Orrù, A., Pes, D., Agabio, R., et al. (2005). Baclofen-induced reduction of alcohol reinforcement in alcohol-preferring rats. *Alcohol* 36, 161–168. doi: 10.1016/j.alcohol.2005.08.003

Maccioni, P., Pes, D., Orrù, A., Froestl, W., Gessa, G. L., Carai, M. A. M., et al. (2007). Reducing effect of the positive allosteric modulator of the $GABA_B$ receptor, GS39783, on alcohol self-administration in alcohol-preferring rats. *Psychopharmacology* 193, 171–178. doi: 10.1007/s00213-007-0776-1

Maccioni, P., Fantini, N., Froestl, W., Carai, M. A. M., Gessa, G. L., and Colombo, G. (2008b). Specific reduction of alcohol's motivational properties by the positive allosteric modulator of the $GABA_B$ receptor, GS39783 – Comparison with the effect of the $GABA_B$ receptor direct agonist, baclofen. *Alcohol. Clin. Exp. Res.* 32, 1558–1564. doi: 10.1111/j.1530-0277.2008.00725.x

Maccioni, P., Bienkowski, P., Carai, M. A. M., Gessa, G. L., and Colombo, G. (2008a). Baclofen attenuates cue-induced reinstatement of alcohol-seeking behavior in Sardinian alcohol-preferring (sP) rats. *Drug Alcohol Depend.* 95, 284–287. doi: 10.1016/j.drugalcdep.2008.02.006

Maccioni, P., Carai, M. A. M., Kaupmann, K., Guery, S., Froestl, W., Leite-Morris, K. A., et al. (2009). Reduction of alcohol's reinforcing and motivational properties by the positive allosteric modulator of the $GABA_B$ receptor, BHF177, in alcohol-preferring rats. *Alcohol. Clin. Exp. Res.* 33, 1749–1756. doi: 10.1111/j.1530-0277.2009.01012.x

Maccioni, P., Thomas, A. W., Carai, M. A. M., Gessa, G. L., Malherbe, P., and Colombo, G. (2010). The positive allosteric modulator of the $GABA_B$ receptor, *rac*-BHFF, suppresses alcohol self-administration. *Drug Alcohol Depend.* 109, 96–103. doi: 10.1016/j.drugalcdep.2009.12.019

Maccioni, P., Zaru, A., Loi, B., Lobina, C., Carai, M. A. M., Gessa, G. L., et al. (2012). Comparison of the effect of the $GABA_B$ receptor agonist, baclofen, and the positive allosteric modulator of the $GABA_B$ receptor, GS39783, on alcohol self-administration in three different lines of alcohol-preferring rats. *Alcohol. Clin. Exp. Res.* 36, 1748–1766. doi: 10.1111/j.1530-0277.2012.01782.x

Maccioni, P., Vargiolu, D., Thomas, A. W., Malherbe, P., Mugnaini, C., Corelli, F., et al. (2015). Inhibition of alcohol self-administration by positive allosteric

modulators of the $GABA_B$ receptor in rats: Lack of tolerance and potentiation of baclofen. *Psychopharmacology* 232, 1831–1841. doi: 10.1007/s00213-014-3815-8

Maccioni, P., Colombo, G., Lorrai, I., Zaru, A., Carai, M. A. M., Gessa, G. L., et al. (2017). Suppressing effect of COR659 on alcohol, sucrose, and chocolate self-administration in rats: Involvement of the $GABA_B$ and cannabinoid CB_1 receptors. *Psychopharmacology* 234, 2525–2543. doi: 10.1007/s00213-017-4644-3

Maccioni, P., Lorrai, I., Contini, A., Leite-Morris, K., and Colombo, G. (2018). Microinjection of baclofen and CGP7930 into the ventral tegmental area suppresses alcohol self-administration in alcohol-preferring rats. *Neuropharmacology* 136, 146–158. doi: 10.1016/j.neuropharm.2017.10.012

Maccioni, P., and Colombo, G. (2019). Potential of $GABA_B$ receptor positive allosteric modulators in the treatment of alcohol use disorder. *CNS Drugs* 33, 107–123. doi: 10.1007/s40263-018-0596-3

Maccioni, P., Colombo, G., Lorrai, I., Fara, F., Carai, M. A. M., Gessa, G. L., et al. (2019a). Anti-addictive properties of COR659 – Additional pharmacological evidence and comparison with a series of novel analogues. *Alcohol* 75, 55–66. doi: 10.1016/j.alcohol.2018.05.007

Maccioni, P., Fara, F., Lorrai, I., Acciaro, C., Mugnaini, C., Corelli, F., et al. (2019b). Suppressing effect of CMPPE, a new positive allosteric modulator of the $GABA_B$ receptor, on alcohol self-administration and reinstatement of alcohol seeking in rats. *Alcohol* 75, 79–87. doi: 10.1016/j.alcohol.2018.05.015

Markou, A., Weiss, F., Gold, L. H., Caine, S. B., Schulteis, G., and Koob, G. F. (1993). Animal models of drug craving. *Psychopharmacology* 112, 163–182. doi: 10.1007/BF02244907

Martin-Fardon, R., and Weiss, F. (2013). Modeling relapse in animals. *Curr. Top. Behav. Neurosci.* 13, 403–432. doi: 10.1007/7854_2012_202

Marti-Prats, L., Belin-Rauscent, A., Fouyssac, M., Puaud, M., Cocker, P. J., Everitt, B. J., et al. (2021). Baclofen decreases compulsive alcohol drinking in rats characterized by reduced levels of GAT-3 in the central amygdala. *Addict. Biol.* 26:e13011. doi: 10.1111/adb.13011

Mombereau, C., Lhuillier, L., Kaupmann, K., and Cryan, J. F. (2007). $GABA_B$ receptor-positive modulation-induced blockade of the rewarding properties of nicotine is associated with a reduction in nucleus accumbens ΔFosB accumulation. *J. Pharmacol. Exp. Ther.* 321, 172–177. doi: 10.1124/jpet.106.116228

Mugnaini, C., and Corelli, F. (2016). "Chemistry of $GABA_B$ receptor ligands: Focus on positive allosteric modulators," in *$GABA_B$ Receptor; The Receptors 29*, ed. G. Colombo (Cham: Springer International Publishing), 33–52. doi: 10.1007/978-3-319-46044-4_3

Nakajima, K., Tooyama, I., Kuriyama, K., and Kimura, H. (1996). Immunoistochemical demonstration of $GABA_B$ receptors in the rat gastrointestinal tract. *Neurochem. Res.* 21, 211–215. doi: 10.1007/BF02529137

Nieto, A., Bailey, T., Kaczanowska, K., and McDonald, P. (2021). $GABA_B$ receptor chemistry and pharmacology: Agonists, antagonists, and allosteric modulators. *Curr. Top. Behav. Neurosci.* 2021:232. doi: 10.1007/7854_2021_232

Orrù, A., Lai, P., Lobina, C., Maccioni, P., Piras, P., Scanu, L., et al. (2005). Reducing effect of the positive allosteric modulators of the $GABA_B$ receptor, CGP7930 and GS39783, on alcohol intake in alcohol-preferring rats. *Eur. J. Pharmacol.* 525, 105–111. doi: 10.1016/j.ejphar.2005.10.005

Paterson, N. E., Vlachou, S., Guery, S., Kaupmann, K., Froestl, W., and Markou, A. (2008). Positive modulation of $GABA_B$ receptors decreased nicotine self-administration and counteracted nicotine-induced enhancement of brain reward function in rats. *J. Pharmacol. Exp. Ther.* 326, 306–314. doi: 10.1124/jpet.108.139204

Phillips, T. J., and Reed, C. (2014). Targeting $GABA_B$ receptors for anti-abuse drug discovery. *Expert Opin. Drug Discov.* 9, 1307–1317. doi: 10.1517/17460441.2014.956076

Richardson, N. R., and Roberts, D. C. (1996). Progressive ratio schedules in drug self-administration studies in rats: a method to evaluate reinforcing efficacy. *J. Neurosci. Methods* 66, 1–11. doi: 10.1016/0165-0270(95)00153-0

Slattery, D. A., Markou, A., Froestl, W., and Cryan, J. F. (2005). The $GABA_B$ receptor-positive modulator GS39783 and the $GABA_B$ receptor agonist baclofen attenuate the reward-facilitating effects of cocaine: intracranial self-stimulation studies in the rat. *Neuropsychopharmacology* 30, 2065–2072. doi: 10.1038/sj.npp.1300734

Smith, M. A., Yancey, D. L., Morgan, D., Liu, Y., Froestl, W., and Roberts, D. C. (2004). Effects of positive allosteric modulators of the $GABA_B$ receptor on cocaine self-administration in rats. *Psychopharmacology* 173, 105–111. doi: 10.1007/s00213-003-1706-5

Spanagel, R. (2018). Aberrant choice behavior in alcoholism. *Science* 360, 1298–1299. doi: 10.1126/science.aau0668

Urwyler, S. (2011). Allosteric modulation of family C G-protein-coupled receptors: from molecular insights to therapeutic perspectives. *Pharmacol. Rev.* 63, 59–126. doi: 10.1124/pr.109.002501

Urwyler, S. (2016). ""Allosteric modulators: the new generation of $GABA_B$ receptor ligands"," in *$GABA_B$ Receptor; The Receptors 29*, ed. G. Colombo (Cham: Springer International Publishing), 357–375. doi: 10.1007/978-3-319-46044-4_18

Vengeliene, V., Takahashi, T. T., Dravolina, O. A., Belozertseva, I., Zvartau, E., Bespalov, A. Y., et al. (2018). Efficacy and side effects of baclofen and the novel $GABA_B$ receptor positive allosteric modulator CMPPE in animal models for alcohol and cocaine addiction. *Psychopharmacology* 235, 1955–1965. doi: 10.1007/s00213-018-4893-9

Vlachou, S., Guery, S., Froestl, W., Banerjee, D., Benedict, J., Finn, M. G., et al. (2011). Repeated administration of the $GABA_B$ receptor positive modulator BHF177 decreased nicotine self-administration, and acute administration decreased cue-induced reinstatement of nicotine seeking in rats. *Psychopharmacology* 215, 117–128. doi: 10.1007/s00213-010-2119-x

Voigt, R. M., Herrold, A. A., Riddle, J. L., and Napier, T. C. (2011). Administration of $GABA_B$ receptor positive allosteric modulators inhibit the expression of previously established methamphetamine-induced conditioned place preference. *Behav. Brain Res.* 216, 419–423. doi: 10.1016/j.bbr.2010.08.034

Walzer, M., Marek, G. J., Wu, R., Nagata, M., and Han, D. (2020). Single- and multiple-dose safety, tolerability, and pharmacokinetic profiles of ASP8062: Results from 2 phase 1 studies. *Clin. Pharmacol. Drug Dev.* 9, 297–306. doi: 10.1002/cpdd.766

Walzer, M., Wu, R., Ahmad, M., Freeman, J., Zammit, G., and Marek, G. J. (2021). A randomized phase 1 single-dose polysomnography study of ASP8062, a $GABA_B$ receptor positive allosteric modulator. *Psychopharmacology* 238, 867–876. doi: 10.1007/s00213-020-05738-y

Wierońska, J. M., Kusek, M., Tokarski, K., Wabno, J., Froestl, W., and Pilc, A. (2011). The $GABA_B$ receptor agonist CGP44532 and the positive modulator GS39783 reverse some behavioural changes related to positive syndromes of psychosis in mice. *Br. J. Pharmacol.* 163, 1034–1047. doi: 10.1111/j.1476-5381.2011.01301.x

Conflict of Interest: The authors declare that the research was conducted in the absence of any commercial or financial relationships that could be construed as a potential conflict of interest.

Publisher's Note: All claims expressed in this article are solely those of the authors and do not necessarily represent those of their affiliated organizations, or those of the publisher, the editors and the reviewers. Any product that may be evaluated in this article, or claim that may be made by its manufacturer, is not guaranteed or endorsed by the publisher.

Advantages of publishing in Frontiers

OPEN ACCESS
Articles are free to read for greatest visibility and readership

FAST PUBLICATION
Around 90 days from submission to decision

HIGH QUALITY PEER-REVIEW
Rigorous, collaborative, and constructive peer-review

TRANSPARENT PEER-REVIEW
Editors and reviewers acknowledged by name on published articles

Frontiers
Avenue du Tribunal-Fédéral 34
1005 Lausanne | Switzerland

Visit us: www.frontiersin.org
Contact us: frontiersin.org/about/contact

REPRODUCIBILITY OF RESEARCH
Support open data and methods to enhance research reproducibility

DIGITAL PUBLISHING
Articles designed for optimal readership across devices

FOLLOW US
@frontiersin

IMPACT METRICS
Advanced article metrics track visibility across digital media

EXTENSIVE PROMOTION
Marketing and promotion of impactful research

LOOP RESEARCH NETWORK
Our network increases your article's readership